LBL-15300 c.2

RECEIVED
LAWRENCE
BERKELEY LABORATORY

FEB 1 1984

LIBRARY AND
DOCUMENTS SECTION

# Annual Report
## FY 1982

# Energy & Environment Division

March 1983

TWO-WEEK LOAN COPY

*This is a Library Circulating Copy which may be borrowed for two weeks. For a personal retention copy, call Tech. Info. Division, Ext. 6782.*

Lawrence Berkeley Laboratory
University of California, Berkeley

LBL-15300 c.2

Prepared for the U.S. Department of Energy under Contract DE-AC03-76SF00098

## DISCLAIMER

This document was prepared as an account of work sponsored by the United States Government. While this document is believed to contain correct information, neither the United States Government nor any agency thereof, nor the Regents of the University of California, nor any of their employees, makes any warranty, express or implied, or assumes any legal responsibility for the accuracy, completeness, or usefulness of any information, apparatus, product, or process disclosed, or represents that its use would not infringe privately owned rights. Reference herein to any specific commercial product, process, or service by its trade name, trademark, manufacturer, or otherwise, does not necessarily constitute or imply its endorsement, recommendation, or favoring by the United States Government or any agency thereof, or the Regents of the University of California. The views and opinions of authors expressed herein do not necessarily state or reflect those of the United States Government or any agency thereof or the Regents of the University of California.

LBL-15300

# ENERGY & ENVIRONMENT DIVISION*

# ANNUAL REPORT

# FY 1982

Elton J. Cairns
Head, Energy & Environment Division
and
Associate Director, LBL

Report Coordinator
Maya Osowitt

*Renamed Applied Science Division as of July 1, 1983

Energy and Environment Division
Lawrence Berkeley Laboratory
University of California
Berkeley, California 94720

Prepared for the U.S. Department of Energy under Contract No. DE-AC03-76SF00098

# FOREWORD

The mission of the Energy & Environment Division is to research the complex energy issues that confront our nation. The research base is broad and is organized into five major programs: Chemical Process Research and Development, Solar Energy, Energy Efficient Buildings, Environmental Research, and Energy Analysis. The goal of these programs is to make key contributions to the solution of the critical problem of providing environmentally acceptable energy options for the future. Although researchers in each program use special expertise to conduct their studies, they are increasingly joining forces with the staff of other programs in the Division to investigate particular aspects of related problems. For example, the Windows and Daylighting Group in the Energy Efficient Buildings Program and the Passive Analysis and Design Group in the Solar Energy Program are jointly studying the effects of natural lighting on building energy efficiencies.

The Chemical Process R&D Program is investigating four major research areas: (1) bioconversion of cellulose to liquid fuel, (2) production of synthetic fuels from fossil fuels, (3) electrochemical energy storage, and (4) environmental protection from the hazards of synthetic-fuel production. The strong commonality of these research areas is the application of the principles of transport of mass and energy, chemical kinetics, thermodynamics, physical chemistry, and organic chemistry to develop approaches for solution of various aspects of energy-related problems.

The objective of the Solar Energy Program is to advance the development and application of solar energy as a supplement to traditional, nonrenewable energy resources, thus decreasing the rate at which these resources are depleted. The Solar Program consists of a number of applied and basic research projects, including (1) active solar cooling of buildings, (2) passive solar heating and cooling, (3) the conversion of solar energy to electricity, e.g., by means of the Small Particle Heat Exchange Receiver (SPHER), and (4) the photochemical conversion of sunlight to energy.

The efficient use of energy in buildings is the emphasis of the Energy Efficient Buildings Program (EEB), which comprises the following related groups: (1) Building Envelopes, (2) Efficient Windows and Daylighting, (3) Efficient Artificial Lighting, (4) Ventilation and Indoor Air Quality, (5) Building Energy Simulation using the DOE-2 computer model, and (6) Building Energy Data Compilation and Analysis.

The objective of the Environmental Research Program is to study the hazardous effects of energy generation and use. The program is divided into seven major research areas that encompass transport and transformation, impacts, characterization, and abatement. These major areas are (1) Atmospheric Aerosol Research, (2) Laser Spectroscopy, (3) Combustion Research, (4) Oil Shale Research, (5) Lake Ecotoxicology and Acid Rain, (6) Instrumentation Survey, and (7) Trace Element Analysis.

The Energy Analysis Program assesses economic and public policy and their relevance to the critical issues affecting national and regional energy supply and demand. The Program is organized into four study areas: (1) building energy use, (2) energy and peak demand forecasts, (3) international energy demand, and (4) energy supply. All of the research emphasizes the importance of energy policy relevance, quantitative analysis (often based on computer models), development of analysis tools, the potential for keeping the public informed, and the interdisciplinary nature of the research.

The Energy & Environment Division has close ties with several departments at the University of California, Berkeley, in particular the Mechanical Engineering and Chemical Engineering departments and the multidisciplinary Energy Resources Group.

# LAWRENCE BERKELEY LABORATORY
# UNIVERSITY OF CALIFORNIA
# ENERGY & ENVIRONMENT DIVISION

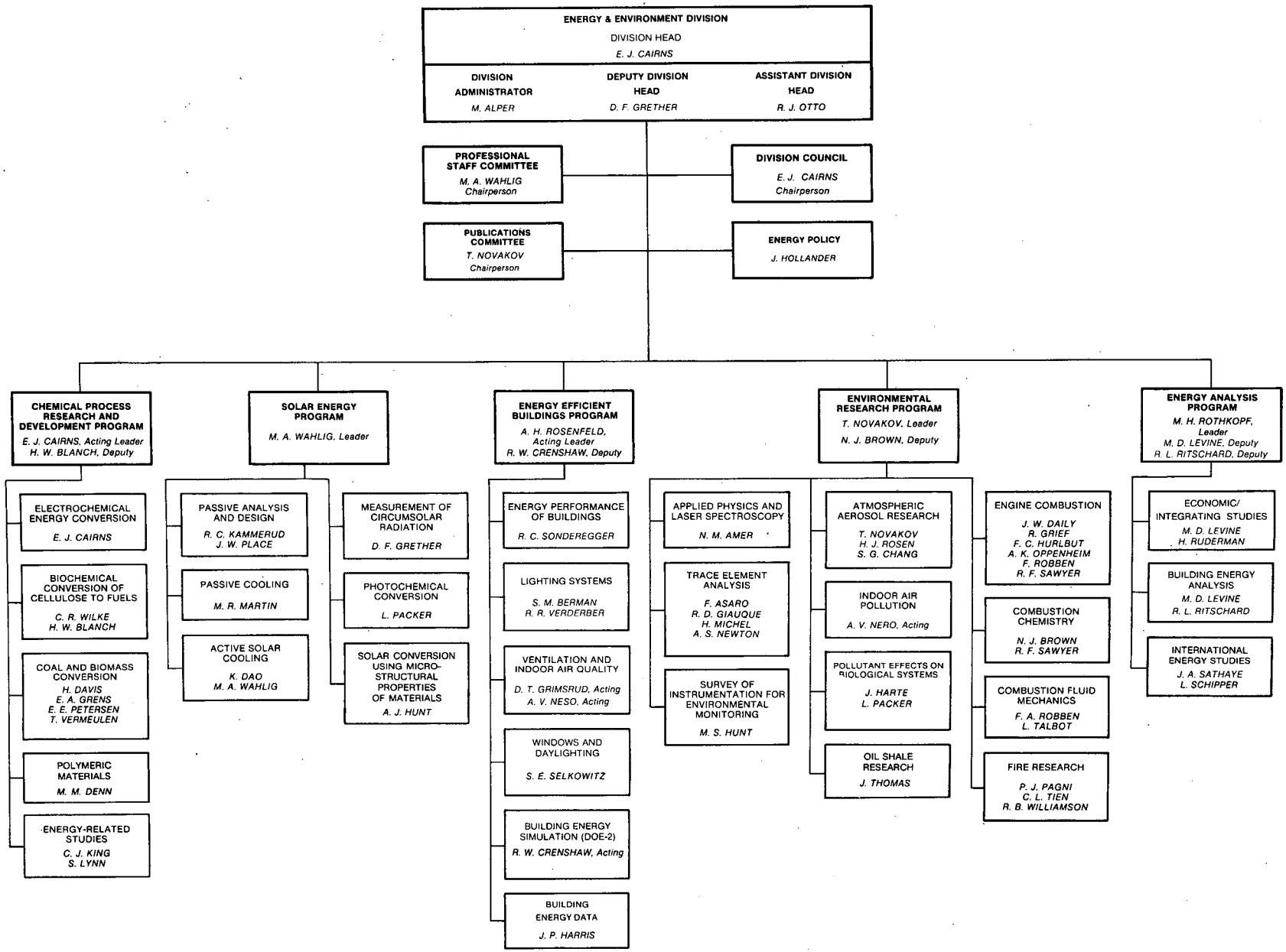

# ENERGY & ENVIRONMENT DIVISION

## PERSONNEL

**Elton J. Cairns**

**Division Head**

**Donald F. Grether**

**Deputy Division Head**

**Mark Alper**

**Division Administrator**

**Roland J. Otto**

**Assistant Division Head**

## DIVISION OFFICE STAFF

**Bron Hafner**
**Rebecca McEven**
**Sandra Mocco**
**Christine Nakata**
**Sally Nasman**
**Maya Osowitt**
**Maria Ossa**
**Susan Peterson**
**Judy Reyes-Ortiz**
**Janet Smith**
**Angela Smothers**
**Zenaida Yuson**
**Sharran Zeleke**

# CHEMICAL PROCESS RESEARCH AND DEVELOPMENT PROGRAM STAFF

Elton Cairns, Program Leader
Harvey Blanch, Deputy Program Leader

Myra Baker
James Bixby
Kathy Boyer
Patricia Bronnenberg
Garth Burns
Joni Buttke
Robert Chung
Gregg Cremer*
Hubert Davis
Robert Demyanovich
Morton Denn
Jesse Dobson
Michael Eames
Betsy Elzufon
Sabri Ergun
Mark Featherstone
Carlos Figueroa
Richard Fish
James Flatt
Alan Foss
Raymond Gansley
Robert Goldberg
Edward Grens
Donald Hanson
Neil Hendy
Mark Isaacson
Cihan Karatas
Marc Katz
Eileen Keefe
C. Judson King
John Komlenic
Phillip Lessner
Gary Lipscomb
Scott Lynn
John MacGlashan
Patricia MacKenzie
Frank McLarnon
Brian Maiorella
Anthony Mancusco
Kenneth Miller
Donald Mohr
Robert Moore
Curtis Munson
Thomas Murphy
Stuart Naftel
James Nichols
Steven Oblath
Timothy Oolman
Stephan Orichowsky
Michael Pedersen
Javier Perez
David Robinson
Larry Schaleger
Aldo Sciamanna
John Senetar
Mohindar Singh
Kathy Streibel
Raja Tannous
Rodney Thompson
Arne Thormodsen*
Theodore Vermeulen
Bruce Vickroy
James Walter
David Watt
Dale Wiley
Charles Wilke
Brian Wines
Harry Wong
Nasser Yaghoubzadeh
Rafael Zamora

*Materials and Molecular Research Division Staff

# SOLAR ENERGY PROGRAM STAFF

Michael A. Wahlig, Program Leader
Donald F. Grether, Deputy Program Leader

Emmanuel Altmayer
Brandt Andersson
Harry Angerman
Richard Armer
Cynthia Ashley
Fred Bauman
Paul Berdahl
William Carroll
Eduardo Ceballos
Stephen Choi
Craig Conner
J. Pascal Coutier
M. Benay Curtis
Kim Dao
Donald Elmer
David Evans
David Faiman
Ian Fry
Marc Fontoynont
Ashok Gadgil
Ron Glas
Leif Hansen
Mary Hart
Brenda Hatfield
Albert Heitz
Jeffrey Herz
Arlon Hunt
Ronald Kammerud
Stephen Kanzler
Eric Lam
Marlo Martin
Rolf Mehlhorn
Atila Mertol
Mark Nansteel
Lester Packer
J. Wayne Place
Cindy Polansky
Alex Quintanilla
John Randolph
Joseph Rasson
Fenwick Salter
Laurie Sampietro
Lauri Sariola
Gail Schiller
Laurant Simonesco
Charlotte Standish
Mehdi Tavana
John Thornton
Mashuri Warren
Cecelia Webster
Thomas Webster
Donald Worth
Hayward Zwerling

# ENERGY EFFICIENT BUILDINGS PROGRAM STAFF

## ADMINISTRATION

Richard Crenshaw*
Brigitte Fitzsimmons
Debbie Giallombardo
Mary Hart
Jeana McCreary
Moya Melody
Arthur Rosenfeld†
Lynne Sherman

## ENERGY PERFORMANCE OF BUILDINGS

Jim Adams
David Anderson
Richard Beerman
Peter Cleary
Richard Diamond
Darryl Dickerhoff
John Dickinson
Jim Dixon
Jean-Yves Garnier
Ronnie Lipschutz
David Grimsrud‡
Mark Modera
Vivian Kendon
Max Sherman
Brian Smith
Robert Sonderegger‡
Carol Stoker
James Kurck

## BUILDING VENTILATION AND INDOOR AIR QUALITY

Richard Allen
Michael Apte
Keith Archer
Andrew Carruthers
Jim Dillworth
Suzanne Doyle
Alfred Hodgson
William Fisk
Kristin Geisling
John Girman
David Grimsrud‡
Craig Hollowell‡§
Buck Koonce
Vera Martin
Barbara Moed
Nancy Morrison
William Nazaroff
Anthony Nero‡
Francis Offermann
Yoshiko Otonari
Brian Pederson
Kenneth Revzan
Alan Robb
Greg Traynor

## BUILDING ENERGY SIMULATION

Fred Buhl
Richard Curtis
Kathy Ellington
Ender Erdem
James Hirsch
Karen Olson
Frederick Winkelmann

## WINDOWS AND DAYLIGHTING AND LIGHTING SYSTEMS RESEARCH

Sam Berman‡
Stephen Choi
Robert Clear
Craig Connors
Dennis DiBartolomeo
Jean Ferrari
Richard Johnson
Mahnut Karayel
Jeff Kessel
Jong Jin Kim
Joseph Klems
Carl Lampert
Clifford Lee
David MacGowan
James McLane
Eli Naor
Mojtaba Navvab
Eliyahu Ne'eman
Mike Rubin
Francis Rubinstein
Joel Ryan
Stephen Selkowitz
Mark Spitzglas
Paul Stuart
Rudy Verderber
Michael Wilde
Ruth Williams

## BUILDINGS ENERGY DATA

Carl Blumstein||
Françoise Flouquet||
Betsy Gardiner
Charles Goldman
Jeff Harris||
Wolfgang Lührsen||
Virginia Magnus
Alan Meier
Brian O'Regan
Jesse Ribot
Arthur Rosenfeld‡
Tony Usibelli
Barbara Wagner
Leonard Wall||

---

*Deputy Program Leader
†Program Leader
‡Group Leader
§Deceased
||Visiting Researcher

# ENVIRONMENTAL RESEARCH PROGRAM STAFF

## ATMOSPHERIC AEROSOL RESEARCH

William Benner
Ray Dod
Max Dunn
Lara Gundel
Anthony Hansen
Samuel Markowitz
Michael McKinney
Tihomir Novakov*†
Roland Otto
Hal Rosen
Richard Schmidt
Linda Wroth

## APPLIED PHYSICS AND LASER SPECTROSCOPY RESEARCH

Nabil Amer†
Neil Bergstrom
Mark Cooper
Robert Gerlach
Akio Hitachi
Ralph Johnson
Stanley Kohn
Marjorie Olmstead
Andrew Skumanich
Douglas Wake
Zafer Yasa

## OIL SHALE RESEARCH

Jeremy Cantor
Christian Daughton‡
Gloria Gill
Dick Goodman‡
Bill Hall
Gloria Harris-Winston
Joe Healy
Al Hodgson
David Jenkins‡
Bonnie Jones
Eric Ko
Greg Langlois
Linda Maio
Kumar Mehta‡
T.N. Narasimhan
Peter Persoff
Martin Pollard
Joe Ratigan
Rick Sakaji
Bob Selleck‡
Jerry Thomas†
Neil Thomsen
Karen Yu

## COMBUSTION RESEARCH

Diana Brehob
Nancy Brown
Cam Carter
Minna Chan
Daih-Yeou Chen
Robert Cheng
Alexandre Chorin
Patrick Coico
Enrique Cuellar
John Daily
Derek Dunn-Rankin
Fred Fisher‡
Gloria Gill
Cecile Grant
Ralph Greif
John Hart
Jean Hertzberg*
David Hirvo
Kenneth Hom
Frank Hurlbut
Bruce Ingraham
Claire Johnson‡
Bill Kleiser‡
John LaFond
Donald Lucas
John Metcalf
Kenneth Metchette
Mehdi Namazian‡
Izak Namer
Terry Ng
Antoni Oppenheim
Patrick Pagni
Gary Parsons
Richard Peterson
William Pitz
Ola Rashed
Frank Robben
Robert Sawyer
Robert Schefer
Lily Shen‡
Pauline Sherman§
Horton Stewart‡
Lawrence Talbot
Chang Tien
Steve Vosen
R. Brady Williamson
Joan Woodard§

## SCRUBBER CHEMISTRY RESEARCH

Shih-Ger Chang†
David Littlejohn
Elizabeth Griffiths
Thuy Hoang
Scott Lynn
Robert Demyanovich

## LAKE ECOTOXICOLOGY

Charles Blanchard
John Harte†
Don Levy
Gregory Lockett
Harvey Michaels
Joan Oldfather
John Rees
Ellen Saegebarth
Richard Schneider
Kathy Tonnessen

## TRACE ELEMENT ANALYSIS

Frank Asaro
Charles Case
Robert Giauque
Ralph McLaughlin
Helen Michel
Anthony Nero
Mary Quinby-Hunt
Alexandre Quintanilha
Linda Sindelar

---

Program Leader, †Group Leader, ‡University of California, Berkeley, §Participating Guest

# ENERGY ANALYSIS PROGRAM STAFF

Mark Levine, Acting Program Leader
Ronald Ritschard, Acting Deputy Program Leader

Dariush Arasteh
Richard Boschen
Betty Bratton
L. Chang
W. Chern
*P.P. Craig
*J.C. Cramer
*de Piedade, A. Canha
Dorothy Dickey
*T.M. Dietz
Andre Ghirardi
Steve Gold
*B. Hackett
Vickie Horan
Chean Yok Hsui
Joe Huang
John Ingersoll
Edward Kahn
Andrea Ketoff
Daniel Kowalszyk
James McMahon
Stephen Meyers
Susie Ng
Susan Rosse
Henry Ruderman
Jayant Sathaye
Mark Seedall
Susan Schaffer
Lee Schipper
Nancy Schorn
Renee Slonek
*D. Tseng
Isaac Turiel
Dorothy Turner
Gleb Verzhbinsky
Edward Vine
Debbie Wilson
Winifred Yen

*Affiliated Staff

# CONTENTS

## CHEMICAL PROCESS RESEARCH AND DEVELOPMENT PROGRAM


INTRODUCTION ..... 1-1

*Chemical Liquefaction of Biomass*

THE DIRECT LIQUEFACTION OF BIOMASS
H.G. Davis, C. Figueroa, R. Gansley, L. Schaleger, and D. Watt ..... 1-2

*Fuels from Biomass by Biochemical Processes*

BIOCONVERSION OF CELLULOSE
H.W. Blanch, C.R. Wilke, A.F. Sciamanna, K. Murphy, D. Wiley, and H. Wong ..... 1-6

PRODUCTION OF SUGARS FROM CELLULOSE
C.R. Wilke, H.W. Blanch, N. Hendy, B. Maiorella, A. Mancuso, K. Murphy, S. Orichowskyj, and A. Sciamanna ..... 1-11

*Oil Shale and Petroleum-Related Research*

HOMOGENEOUS CATALYTIC HYDROGENATION: REGIOSPECIFIC REDUCTIONS OF POLYNUCLEAR AROMATIC AND HETEROAROMATIC NITROGEN COMPOUNDS CATALYZED BY TRANSITION-METAL CARBONYL HYDRIDES
R.H. Fish, A.D. Thormodsen, G.A. Cremer, T. Vermeulen, and H. Heinemann ..... 1-19

MOLECULAR CHARACTERIZATION AND FINGERPRINTING OF VANADYL PORPHYRIN AND NON-PORPHYRIN COMPOUNDS FOUND IN VARIOUS HEAVY CRUDE PETROLEUMS AND THEIR ASPHALTENES
R.H. Fish, J.J. Komlenic, B. Wines, and T. Vermeulen ..... 1-24

SYNTHESIS, STRUCTURAL ELUCIDATION, AND STEREOCHEMISTRY OF FIVE-COORDINATE ORGANOARSENIC CATECHOLATES
R.H. Fish and R.S. Tannous ..... 1-31

ORGANOMETALLIC GEOCHEMISTRY: ISOLATION AND IDENTIFICATION OF ORGANOARSENIC COMPOUNDS FROM GREEN RIVER FORMATION OIL SHALE
R.H. Fish, R.S. Tannous, W. Walker, C.S. Weiss, and F.E. Brinckman ..... 1-34

*Coal-Related Research*

PROCESSING OF CONDENSATE WATERS FROM COAL GASIFICATION
C.J. King, J. MacGlashan, D. Mohr, P. Mackenzie, R. Thompson, and J. Bixby ..... 1-38

*Electrochemical Energy Storage Research*

TECHNOLOGY BASE RESEARCH PROJECT FOR ELECTROCHEMICAL ENERGY STORAGE
E.J. Cairns and F.R. McLarnon ..... 1-43

BATTERY ELECTRODE STUDIES
E.J. Cairns, F.R. McLarnon, J.H. Flatt, M. Isaacson, M.H. Katz, P. Lessner, K.G. Miller, and J.T. Nichols ..... 1-45

## SOLAR ENERGY PROGRAM

INTRODUCTION ..... 2-1

PASSIVE RESEARCH AND DEVELOPMENT
R.C. Kammerud, J.W. Place, M.R. Martin, P.H. Berdahl, B. Andersson, F.S. Bauman, W.L. Carroll, A.J. Gadgil, A. Mertol, E. Ceballos, T.L. Webster, M.W. Nansteel, C.C. Conner, J.P. Coutier, M. Fontoynont, and E.F. Altmayer ..... 2-3

ACTIVE SOLAR COOLING
M. Wahlig, K. Dao, M. Warren, J. Rasson, R. Armer, A. Heitz, and F. Salter ..... 2-13

MOLECULAR ASPECTS OF LIGHT-ENERGY CONVERSION BY BACTERIORHODOPSIN
L. Packer, A.T. Quintanilha, R.J. Mehlhorn, H. Zwerling, J. Herz, E. Lam, W. Baird, and I. Fry ..... 2-19

LBL BUILDING 71 COOLING PROJECT
F. Salter ..... 2-24

SOLAR ENERGY SYSTEMS USING THE MICROSTRUCTURE OF MATERIALS
A. Hunt, D. Evans, L. Hansen, L. Sariola, L. Simionesco, and D. Worth ..... 2-25

## ENERGY EFFICIENT BUILDINGS PROGRAM

INTRODUCTION ..... 3-1

ENERGY PERFORMANCE OF BUILDINGS (EPB)
R.C. Sonderegger, J.W. Adams, P.G. Cleary, R.C. Diamond, D.J. Dickerhoff, J.B. Dickinson, J.D. Dixon, J.Y. Garnier, D.T. Grimsrud, R.D. Lipschutz, M.P. Modera, M.H. Sherman, and B.V. Smith ..... 3-4

BUILDING VENTILATION AND INDOOR AIR QUALITY
D.T. Grimsrud, A.V. Nero, Jr., J.R. Allen, M.G. Apte, K.M. Archer, A. Carruthers, J.F. Dillworth, S.M. Doyle, J. Eisenberg, P. Fischer, W.J. Fisk, K.L. Geisling, J.R. Girman, A.T. Hodgson, C.D. Hollowell, J.F. Koonce, Jr., V.M. Martin, B.A. Moed, W.W. Nazaroff, F.J. Offermann, Y. Otonari, B.S. Pedersen, B. Remijn, K.L. Revzan, A.W. Robb, R. Robison, R.G. Sextro, and G.W. Traynor ..... 3-12

WINDOWS AND DAYLIGHTING
S.E. Selkowitz, S.U. Choi, D.L. DiBartolomeo, R.L. Johnson, J.D. Kessel, J.H. Klems, C.M. Lampert, M. Navvab, E. Ne'eman, M.D. Rubin, J. Ryan, and G.M. Wilde ..... 3-22

LIGHTING SYSTEMS RESEARCH
S.M. Berman, R.R. Verderber, R.D. Clear, O.C. Morse, F.M. Rubinstein, and R.K. Sun ..... 3-35

BUILDINGS ENERGY DATA
J.P. Harris, B.L. Gardiner, C.A. Goldman, W. Luhrsen, V. Magnus, A.K. Meier, B.C. O'Regan, J.C. Ribot, A.H. Rosenfeld, A. Usibelli, B.S. Wagner, and L.W. Wall ..... 3-41

BUILDING ENERGY SIMULATION GROUP
J.J. Hirsch, W.F. Buhl, R.B. Curtis, A.E. Erdem, K.H. Olson and F.C. Winkelmann ..... 3-56

PUBLICATIONS LIST ..... 3-65

## ENVIRONMENTAL RESEARCH PROGRAM

INTRODUCTION ..... 4–1

*Atmospheric Aerosol Research*

EVIDENCE FOR PRIMARY OXIDANTS OF $SO_2$
W. H. Benner, P. M. McKinney, and T. Novakov ..... 4–3

S(IV) OXIDATION BY AMBIENT PARTICULATE MATTER
W. H. Benner and T. Novakov ..... 4–5

REAL-TIME MEASUREMENT OF THE ABSORPTION COEFFICIENT OF AEROSOL PARTICLES
A.D.A. Hansen, H.J. Rosen, and T. Novakov ..... 4–7

THE RELATIONSHIP BETWEEN OPTICAL ATTENUATION AND BLACK CARBON CONCENTRATION FOR CARBONACEOUS PARTICLES
L.A. Gundel, R.L. Dod, H.J. Rosen, and T. Novakov ..... 4–10

GRAPHITIC-CARBON-TO-LEAD RATIO AS A TRACER FOR SOURCES OF THE ARCTIC AEROSOL
H.J. Rosen, A.D.A. Hansen, and T. Novakov ..... 4–13

THE OXYGEN CONTENT OF AMBIENT PARTICULATE MATTER
W.H. Benner, C. Chuang, A.D.A. Hansen, and T. Novakov ..... 4–16

QUALITATIVE AND QUANTITATIVE ASPECTS OF EVOLVED GAS ANALYSIS
L.A. Gundel, R.L. Dod, and T. Novakov ..... 4–18

DETERMINATION OF NON-AMMONIUM, NON-NITRATE NITROGEN IN ATMOSPHERIC AEROSOL PARTICLES
R.L. Dod, L.A. Gundel, and T. Novakov ..... 4–24

INVESTIGATION OF THE RELATIONSHIP OF PARTICULATE NITROGEN AND SULFATE
R.L. Dod, W.H. Benner, and T. Novakov ..... 4–26

A COMPUTER-BASED CONTROL AND DATA ACQUISITION SYSTEM FOR EVOLVED GAS ANALYSIS
A.D.A. Hansen, W.H. Benner, and T. Novakov ..... 4–27

*Applied Physics and Laser Spectroscopy Research*
N.M. Amer, M.S. Cooper, R.W. Gerlach, A. Hitachi, W. Imler, M.A. Olmstead, A. Skumanich, D.R. Wake, D. Wei, and Z.A. Yasa
LASER PHOTOTHERMAL MEASUREMENTS AND CHARACTERIZATION ..... 4-30
AMORPHOUS PHOTOVOLTAIC SEMICONDUCTORS ..... 4-32
NOVEL LASER SYSTEMS ..... 4-37

*Oil Shale Research*

OIL SHALE WASTEWATER TREATMENT: EFFECT OF OZONATION AND UV IRRADIATION ON BIOREFRACTORY ORGANIC SOLUTES
B.M. Jones, G.W. Langlois, R.H. Sakaji, J.F. Thomas, and C.G. Daughton ..... 4-44

*Combustion Research*

THEORETICAL AND EXPERIMENTAL STUDIES OF REACTIONS IMPORTANT IN COMBUSTION
N. J. Brown, J.A. Miller, and O.M. Rashed ..... 4-52

NUMERICAL MODELING OF TURBULENT COMBUSTION
A.F. Ghoniem, A.J. Chorin, and A.K. Oppenheim ..... 4-55

CONTROLLED COMBUSTION
N.J. Brown, C.D. Carter, K. Hom, F.C. Hurlbut, D. Lucas, A.K. Oppenheim, R.B. Peterson, R.F. Sawyer, and H.E. Stewart ..... 4-59

HEAT AND MASS TRANSFER WITH COMBUSTION
R. Greif, J. Woodard, S. Vosen, and C. Yen ..... 4-63

FLAME PROPAGATION
D. Dunn-Rankin and R.F. Sawyer ..... 4-65

MEASUREMENT OF COMBUSTION-GENERATED POLLUTANT SPECIES
N.J. Brown, E. Cuellar, and D. Lucas ..... 4-66

COMBUSTION IN A TURBULENT BOUNDARY LAYER
R.K. Cheng, F. Robben, and L. Talbot ..... 4-70

TURBULENT BURNING VELOCITY IN PREMIXED TURBULENT FLAMES
R.K. Cheng, T.T. Ng, F. Robben, and L. Talbot ..... 4-73

PLASMA IGNITION STUDIES
A.K. Oppenheim, J. Cavolowsky, C. Edwards, K. Hom, and H.E. Stewart ..... 4-75

STRUCTURE OF A V-SHAPED TURBULENT FLAME
M. Namazian, J. Hertzberg, L. Talbot, and F. Robben ..... 4-77

TESTS AND CRITERIA FOR FIRE PROTECTION OF CABLE PENETRATIONS AND ELECTRICAL CABINETS
R.B. Williamson, F.L. Fisher, and F.W. Mowrer ..... 4-80

*Scrubber Chemistry Research*

THE EFFECTS OF METAL CHELATES ON WET FLUE GAS SCRUBBING CHEMISTRY
S.G. Chang, D. Littlejohn, and S. Lynn ..... 4-84

THE REACTION OF FERROUS NITROSYL COMPLEXES WITH SULFITE AND BISULFITE IONS
D. Littlejohn, E. Griffiths, and S.G. Chang ..... 4-89

IDENTIFICATION OF SPECIES IN A WET FLUE GAS DESULFURIZATION AND DENITRIFICATION SYSTEM BY LASER RAMAN SPECTROSCOPY
D. Littlejohn and S.G. Chang ..... 4-93

*Lake Ecotoxicology Research*

REALISM AND REPLICABILITY OF FRESHWATER LENTIC MICROCOSMS AS A FUNCTION OF WATER AGITATION
J. Harte, D.J. Levy, G.P. Lockett, J.M. Oldfather, J.T. Reese, E.I. Saegebarth, and R.A. Schneider ..... 4–98

ACID PRECIPITATION AND SURFACE-WATER VULNERABILITY ON THE WESTERN SLOPE OF THE HIGH COLORADO ROCKIES
J. Harte, G.P. Lockett, R.A. Schneider, H. Michaels, and C. Blanchard ..... 4–100

*Trace Element Analysis*

SURVEY OF INSTRUMENTATION FOR ENVIRONMENTAL MONITORING
M. Quinby-Hunt, R. McLaughlin, A. Quintanilha, G. Morton, and C. Case ..... 4–106

CURRENT STATUS OF THE IMPACT THEORY OF MASS EXTINCTION
H.V. Michel, F. Asaro, W. Alvarez, and L.W. Alvarez ..... 4–107

## ENERGY ANALYSIS PROGRAM

INTRODUCTION ..... 5-1

*Building Energy Analysis*

RESIDENTIAL ENERGY CONSERVATION: DEVELOPING A GUIDE FOR HOMEBUILDERS
R.L. Ritschard, Y.J. Huang, J.G. Ingersoll, M.D. Levine, R.A. Boschen, L. Chang, C. Hsui, and D. Wilson ..... 5-4

THE EFFECT OF WINDOW SIZE AND ORIENTATION ON HEATING AND COOLING LOADS IN RESIDENTIAL HOUSES
Y.J. Huang and R.L. Ritschard ..... 5-7

CLIMATE ANALYSIS IN SUPPORT OF THE HOMEBUILDERS' GUIDE
Y.J. Huang ..... 5-9

DETERMINATION OF THE SEASONAL COEFFICIENT OF PERFORMANCE OF CONVENTIONAL AIR SOURCE HEAT PUMPS IN RESIDENTIAL BUILDINGS
J.G. Ingersoll and D.K. Arasteh ..... 5-15

ENERGY EFFICIENCY IN CHINESE BUILDINGS
Y.J. Huang, A. Canha de Piedade, A.H. Rosenfeld, and D. Tseng ..... 5-18

OCCUPANT BEHAVIOR AND RESIDENTIAL ENERGY USE
P.P. Craig, J.C. Cramer, T.M. Dietz, B. Hackett, D.J. Kowalczyk, M.D. Levine, and E.L. Vine ..... 5-20

ENERGY CONSERVATION IN PUBLIC HOUSING
R.L. Ritschard and D.F. Dickey ..... 5-25

SIMPLIFIED ENERGY ANALYSIS METHODOLOGY FOR COMMERCIAL BUILDINGS
I. Turiel, R.A. Boschen, M. Seedall, and M.D. Levine ..... 5-29

*Economic Studies*

ESTIMATES OF RESIDENTIAL ENERGY SAVINGS FROM PROPOSED FEDERAL POLICIES FOR APPLIANCES
J.E. McMahon and M.D. Levine ..... 5-34

COST/EFFICIENCY TRADEOFFS IN THE RESIDENTIAL APPLIANCE MARKETPLACE
J.E. McMahon and M.D. Levine ..... 5-37

HEAT-PUMP ENERGY DEMAND ANALYSIS
H. Ruderman, J.A. Sathaye, and S. Ng ..... 5-40

UTILITY CONSERVATION PROGRAMS: THEORY AND PRACTICE
E.J. Kahn ..... 5-43

RESIDENTIAL HOURLY AND PEAK DEMAND MODEL: DESCRIPTION AND VALIDATION
G. Verzhbinsky, E.L. Vine, and M.D. Levine ..... 5-45

*International Research*

INTERNATIONAL PROGRESS IN RESIDENTIAL ENERGY EFFICIENCY
L.J. Schipper, A.N. Ketoff, S.P. Meyers, S. Rosse, and W. Chern ..... 5-49

# CHEMICAL PROCESS RESEARCH AND DEVELOPMENT PROGRAM

## INTRODUCTION

The Chemical Process Research and Development Program has four main projects applying chemistry and chemical engineering to problems in the production of unconventional new fuels, their environmental impact, and energy storage. These projects are:

(a) Production of synthetic fuels, predominantly by coal liquefaction
(b) Processing of effluent gases and liquids resulting from such synthetic-fuel production, to provide acceptable waste or recycle streams
(c) Production of liquid fuels from biomass
(d) Electrochemical energy storage.

Each of these projects focuses on transport-process principles, chemical kinetics, thermodynamics, separation processes, and organic and physical chemistry.

The first project is the liquefaction of coal. Selective hydrogenation achieves a substantial conversion of coal to liquid at moderate temperatures. Homogeneous metal-organic catalysts have interesting selectivities with respect to their ability to promote different types of hydrogenation and cracking involved in liquefaction. Another aspect of this work involves examining metal impurities in fossil fuels, especially crude petroleum and shale oil. These impurities have been shown to be metallo-organic compounds. Their isolation and identification is necessary if means are to be devised to separate them from the fossil fuels. One approach is to use metal-organic complexing to separate these impurities.

The second project involves the development of novel and improved methods for processing synfuel condensate waters to make them suitable for recycle, thereby minimizing process-water requirements. The main emphasis is on physiochemical methods, particularly solvent extraction and stripping, to remove organics. Identification of the contaminating organics is difficult, but necessary to permit development of appropriate solvents for their removal. LBL studies have successfully examined simultaneous solvent extraction in removal of ammonia and acid gases by stripping.

The conversion of biomass to liquid fuels has been an area of considerable research and development within the Chemical Process Program over the past several years. Two main approaches have been taken. The first is the liquefaction of biomass and peat. A bench-scale continuous liquefaction unit has been developed to evaluate the process steps and to determine the relevant engineering parameters and optimal conditions for reduction of the biomass with synthesis gas or $H_2$-CO mixtures. Catalytic hydrogenation has been used to increase the value of the product oils. The second approach is the biological conversion of wood and agricultural residues to ethanol. An enzymatic hydrolysis of these cellulosic materials has been developed to yield monomeric hexose and pentose sugars. These can be subsequently fermented to produce ethanol. Various high-rate fermentation processes have been developed, and novel processes for ethanol recovery that are less energy intensive than conventional processes are being examined.

The electrochemical energy storage program provides research to develop advanced battery systems for electric vehicle and stationary energy storage applications. General problem areas include identification of new electrochemical couples for advanced batteries, determination of technical feasibility of the new couples, improvements in battery components and materials, establishment of engineering principles applicable to electrochemical energy storage and conversion, and the assessment of fuel-cell technology for transportation. Major emphasis is on applied research that will lead to superior performance and lower life-cycle costs.

## THE DIRECT LIQUEFACTION OF BIOMASS*

*H.G. Davis, C. Figueroa, R. Gansley, L.L. Schaleger, and D. Watt*

The usual objective of synthetic liquid fuel programs has been the production of high-quality distillate fuels. This has not been the case with biomass (primarily wood) liquefaction. Here the product that arises most readily is a heavy, bituminous material, pumpable as a liquid but generally suitable only as boiler fuel. Because of a high content of oxygenated compounds, there have been fears (not always warranted) about its stability and corrosiveness.

The advantages of this "crude" product over raw biomass as a fuel lie in its effective densification (improvement in heating value per unit weight and per unit volume), dewatering, and conversion into a form that can be stored and pumped as a liquid. However, we currently question whether this product is valuable enough to justify commercial development.

Revamping the liquefaction program to focus on the goal of a distillate fuel has been difficult for both technical and economic reasons, but as the Biomass Group's FY 1982 program progressed, elements of a possible process appeared. Besides discussing our success in defining the limitations and possibilities of previously tested liquefaction processes, we will present the new approach, primarily as a basis for future effort.

### ACCOMPLISHMENTS DURING FY 1982

In FY 1982, our continuous liquefaction unit (CLU) was operated successfully to obtain operating conditions and product-yield distributions for the LBL, or water-slurry, liquefaction process. By comparing these results with those for the PERC, or wet-oil recycle, process, we established the strengths and failings of the two approaches. As the year progressed, however, we were more and more impressed with the disadvantages of both processes. We also explored the use of solvolysis (dissolution of wood by appropriate solvents), studied since 1979.[1-5] We outlined a process based on this approach and studied some of its key elements through batch experiments.

Our ability of characterize the products of liquefaction improved considerably. We modified the SESC technique[6] of sequential elution, which we adapted to biomass oils in 1981, to improve speed and reproducibility.[7] It is proving to be a useful tool for following product changes that result from changes in operations. We have also applied various forms of high-performance liquid chromatography (HPLC) to improve our characterization of water-soluble products, molecular-weight distributions, and other features.

### Comparison of CLU and PERC Operations

The operation of the CLU and its results have been described in detail in several publications.[8-10] We give here only a brief summary of the findings, comparing them with those for the wet-oil recycle process.

(1) At best—from Douglas fir wood with product oils having oxygen contents of 15-16%— the yield distribution by the water-slurry process is as follows: oil, 40% by weight; water-soluble organics (about half carboxylic acids or their anions), 25 wt.%; $CO_2$ and water, 35 wt.%. If char forms, the oil yield is reduced further. On the basis of data from the Albany process development unit (PDU), the oil-recycle or PERC process can result in 53% oil, 8% water solubles, and 39% $CO_2$ + water. The differences are the result of the high recycle of product oil, especially product-water solubles, and of the high ratio of oil to water in the PERC process.

(2) Aspen is a better raw material or substrate than Douglas fir. Oil yields can be about

*This work was supported by the Assistant Secretary for Conservation and Solar Energy, Office of Solar Applications for Industry, Biomass Energy Systems Division of the U.S. Department of Energy under Contract No. DE-AC03-76SF00098 and was funded through Battelle Pacific Northwest Laboratory, Lead Laboratory for the U.S. Department of Energy, Biomass Energy Systems Division, Thermochemical Conservation Program under Contract No. DE-AC06-76RL01830.

10% higher and water-soluble organic yields about 10% lower. The oil product is more fluid and contains less oxygen at comparable severities (e.g., 13 wt.% vs. 16 wt.%.

(3) Little or no reducing gas is consumed in the water-slurry process—again in contrast to the PDU-PERC result. Hence the gas can be CO, $H_2$, synthesis gas (syngas), or probably an inert gas like nitrogen. CO-steam liquefaction is largely pyrolysis under a pressure of steam and a reducing gas.

(4) In the range studied (initial aqueous slurry ~6 to 9), pH made little difference in product distribution, except to affect the yield of formic acid.

(5) About 350-360°C with about 20 minutes reaction time is a good operating range. Above 360°C, there is a danger of slurries going dry as the critical temperature and pressure of water are approached.

The CLU has now been modified so that slurry pyrolysis, catalytic hydrogenation with either a trickle bed or a CSTR, or a modification of the original CO-steam can be studied as needed.

## Observations on LBL and PERC Processes

Our observations on the state of the existing processes come from our own CLU studies (single-pass water-slurry or LBL process) and from a careful review of the Albany, Oregon, PDU (wet-oil recycle or PERC) operation. (The PDU was operated for DOE by Rust Engineering.) Data on Rust Engineering's[11,12] Test-Run 12 (TR-12), supplemented by additional data from Rust, were statistically analyzed. We were able to reach credible atom balances for a range of reaction severities.

The results of this study verify Rust Engineering's experimental oil yield of 53%. They indicate that, over the full range of temperatures used by Rust, yields and consumption vary as follows:

- oil—53 wt.% to 51 wt.%
- $H_2O$—7% to 8%
- CO reacted—0.3 mol/100 lbs wood feed to 0.6 mol
- Water-soluble organics—9% to 7%
- CO shifted to $CO_2$—~1.2 mol/100 lbs wood feed, independent of temperature, but dependent on CO/wood ratio.

This yield distribution is better than that we found with the water-slurry process. The cost of obtaining this improvement, however, is great. These costly steps are required:

- Grinding of wood feed to flour
- Drying of wood
- High recycle of product oil (in TR-12, on the order of 19 parts recycled for each part new oil generated).
- High recycle of water and water-soluble organics.
- Substantial usage of CO (0.5 mol/100 lbs feed = 179 scf/100 lbs $\cong$ 1300 scf/barrel oil produced).
- Shift reaction that converts ~3100 scf/bbl CO to hydrogen.

Our general conclusion is that the oil-recycle process is operable on the basis of the TR-12 results, and that the water-slurry process probably can be made operable on the basis of our CLU work. But economic or commercial feasibility of either route cannot be achieved without great and far from obvious improvements. TR-12 demonstrated the operability of several necessary components of an ultimate process—notably the ability to heat the oil-wood mix to 360-370°C in a direct-fired preheater and the stability of the oil during recycle. But a much better process than either PERC or LBL is needed.

## Characterization of Products

Methods developed during FY 1981 were applied throughout the year to characterize our products and follow changes in variables.

The SESC (sequential elution by solvent chromatography)[13] procedure was especially valuable. A substantial improvement in its speed and reproducibility was obtained by applying the recently developed "flash chromatography" technique. By this method, a whole, crude biomass oil product is divided into 8 (sometimes 9) fractions, mainly according to polarity. The reproducibility of the modified procedure is shown by the results of Table 1. In a recent publication,[7] we give detailed discussion of the method and the results found with our products.

Several high-performance liquid chromatography (HPLC) techniques were developed or improved dur-

Table 1. SESC fractionation of TR-7 oil.

| Fraction | | Amount (%) | Std. Dev. |
|---|---|---|---|
| F1,2 | 15% Benzene-hexanes | 3.5 ± 0.4 | |
| F3 | Chloroform | 16.8 ± 2.3 | |
| F4 | 6% Ether-chloroform | 44.1 ± 3.7 | |
| F5 | 4% Ethanol-ether | 21.2 ± 3.0 | |
| F6 | Methanol | 6.5 ± 1.3 | |
| F7 | 4% Ethanol-$CHCl_3$ | 1.0 ± 0.4 | |
| F8 | 4% EtOH-THF | 2.5 ± 1.7 | |
| F9 | HOAc | 4.2 ± 0.6 | |

ing the year. With size-exclusion chromatography (HPSEC), we obtained molecular-weight distributions of our product samples. With ion-exchange chromatography (HPIEC), we obtained quantitative yields of the light carboxylic acids and ions. Using Douglas fir as substrate, we found that one such acid, glycolic, was the largest single product of the reaction.

## Proposed Use of Solvolysis

We have developed[14] a conceptual schematic of a process based on solvolysis (Fig. 1). Biomass feed, with only incidental drying or grinding, is heated with a phenolic recycle oil at about 240°C. Separated water, if any, is removed by decantation, and the solvolysis product—effectively a solution of the biomass in recycle oil—is catalytically hydrogenated, or otherwise partially depolymerized at temperatures around 360°C.

The final product is distilled, at atmospheric pressure if possible, or under some variation (≥50 mm pressure). The overhead material is the product. This is further stabilized by hydrogenation to remove reactive oxygen groups like carboxyl and olefinic double bonds. If necessary for the end use, phenol hydroxyl is converted to ether by alkylation.

The kettle product is the recycle solvolytic agent. If insolubles (chars) are formed in the process, the kettle liquid must be drawn off and used as fuel or gasifier feed.

Preliminary experiments have been carried out with several forms of biomass.[14] They indicate that lower-boiling material is indeed formed during hydrogenation, oxygen content is reduced, and the product remains a solvolytic agent. But a large amount of research needs to be done.

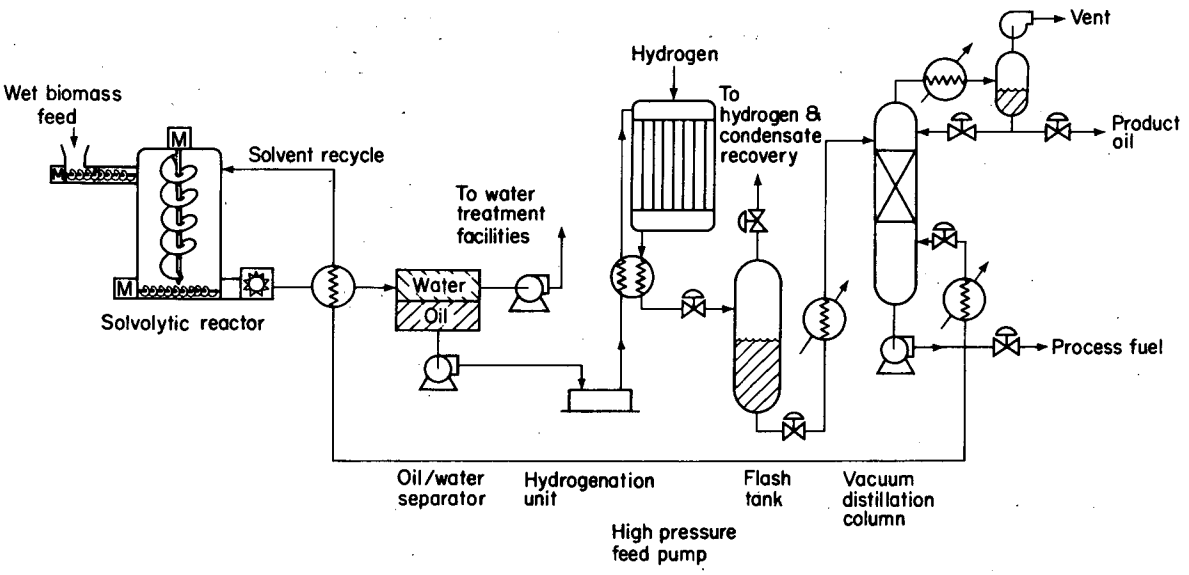


Figure 1. Schematic of solvolysis/ hydrogenation process. (XBL 827-7096)

## PLANNED ACTIVITIES FOR FY 1983

(1) We will institute basic studies of the chemistry of solvolysis, using such model feeds as wood components (cellulose, xylan, lignin), lignin monomers, glucose, etc. Phenol will be used as a model solvolytic agent, but recycle oils must also be studied.

(2) The chemistry of catalytic hydrogenation of (a) crude solvolytic product and (b) distillate from the product of primary hydrogenation will be studied. Commercial hydrogenation and hydrocracking catalysts will be tried as well as cheap homemade catalysts like precipitated, high-surface-area iron sulfide.

(3) Basic studies of the roles of the water-gas shift reaction and of formate ion and formate esters in the chemistry of reduction by carbon monoxide will be performed.

(4) The possible role of supercritical solvents in solvolysis, liquefaction, or product separation will be investigated. This should include fundamental phase-rule studies with model compounds.

(5) The organic chemistry of upgrading the distillate product, e.g., of alkylation with fuel-grade methanol or ethanol, will be studied.

## REFERENCES


1. Yu, S.-M. (1982), *Solvolytic Liquefaction of Wood under Mild Conditions*, Ph.D. Dissertation, Lawrence Berkeley Laboratory Report LBL-14096.
2. Seth, M., et al. (1981), "Catalytic Liquefaction of Biomass," in *Chemical Process Research and Development Program, FY 1980*, Lawrence Berkeley Laboratory Report LBL-10319.
3. Yu, G., Vermeulen, T., and Davis, H. (1982), "The Solvolysis of Douglas Fir Wood in Acidified Organic Solvents," in *Chemical Process Research and Development Program, FY 1981*, Lawrence Berkeley Laboratory Report LBL-11983.
4. Davis, H.G., Schaleger, L.L., and Yaghoubzadeh, N. (1982), "Chemistry and Mechanisms of Wood Liquefaction," in *Energy and Environment Division Annual Report, FY 1981*, Lawrence Berkeley Laboratory Report LBL-13500.
5. Davis, H.G., et al. (1981), *Research and Development Activities on Direct Liquefaction Technology*, April-June 1981 Quarterly Report, Lawrence Berkeley Laboratory Report LBID-426.
6. Schaleger, L.L., and Davis, H.G. (1982), "Progress in the Characterization of the Products of Direct Liquefaction of Douglas Fir," presented at the Workshop/Review Meeting on Biomass Liquefaction Research, National Research Council of Canada, Saskatoon, Saskatchewan, February 16–17, 1982, Lawrence Berkeley Laboratory Report LBL-14017.
7. Davis, H.G., et al. (1982), "The Products of Direct Liquefaction of Biomass," presented at the International Conference on Fundamentals of Thermochemical Biomass Conversion, Estes Park, Colorado, October 18–22, 1982, Lawrence Berkeley Laboratory Report LBL-15143.
8. Figueroa, C., Schaleger, L.L., and Davis, H. G. (1981), "LBL Continuous Bench-Scale Liquefaction Unit, Operation and Results," presented at the 6th Annual Conference on Energy from Biomass and Wastes, Lake Buena Vista, Florida, January 25–29, 1982, Lawrence Berkeley Laboratory Report LBL-13709.
9. Davis, H.G., Figueroa, C., Kloden, D., and Schaleger, L.L. (1982), *Research and Development Activities on Direct Liquefaction Technology*, October-December 1981 Quarterly Report, Lawrence Berkeley Laboratory Report LBID-470.
10. Davis, H.G., Figueroa, C., and L.L. Schaleger (1982), "Research and Development Activities on Direct Liquefaction Technology," presented at the 14th Biomass Thermal Chemical Conversion Contractors Meeting, Arlington, Virginia, June 23–24, 1982, Lawrence Berkeley Laboratory Report LBL-14595.
11. Thigpen, P., and Berry, W. (1982), "Liquid Fuels from Wood by Continuous Operation of the Albany, Oregon Liquefaction Facility," presented at the 6th Annual Conference on Energy from Biomass Wastes, Lake Buena Vista, Florida, January 25–29, 1982.
12. Berry W., and Thigpen, P. (1981), "Operation of the Biomass Liquefaction Facility, Albany, Oregon," in *Proceedings of the 13th Biomass Thermochemical Conversion Contractors' Meeting*, Arlington, Virgina, October 1981.

13. Farcasiu, M. (1977), "Fractional and Structural Characterization of Coal Liquids," *Fuel 56*, p. 9.
14. Davis, H.G., et al. (1982), *Research and Development Activities on Direct Liquefaction Technology,* July-September 1982 Quarterly Report, Lawrence Berkeley Laboratory Report LBID-638.

# FUELS FROM BIOMASS BY BIOCHEMICAL PROCESSES

## BIOCONVERSION OF CELLULOSE*

*H.W. Blanch, C.R. Wilke, A.F. Sciamanna, K. Murphy, D. Wiley, and H. Wong*

### STUDIES OF THE MECHANISM AND KINETICS OF CELLULOSE HYDROLYSIS

Most studies of enzyme kinetics have been concerned with homogeneous systems: the action of soluble enzymes on soluble substrates. The minority of studies focusing on heterogeneous systems have largely been confined to the action of insoluble (immobilized) enzymes on soluble substrates. Much less research has looked at soluble enzymes on insoluble substrates. The enzymatic hydrolysis of cellulose falls in this latter area. Its interest is thus both practical (for its applications in saccharification technology) and theoretical (as an investigation into this lesser-known area of enzyme kinetics).

The kinetics of enzymatic hydrolysis of cellulose depends on the structural features of cellulose, the nature of the enzyme system, and the interaction of substrate and enzyme. Structural features pertinent to the development of a model for cellulose hydrolysis include particle size and degree of crystallinity. These influence both the surface available for enzyme binding and the rate of reaction, since amorphous regions are degraded readily, while hydrolysis of crystalline regions proceeds only slowly. The nature of the cellulase system is described by the relative amounts of the constituent enzymes—endoglucanases, exoglucohydrolases, cellobiohydrolases and β-glucosidases. The interaction of substrate and enzymes includes adsorption, reaction, and product-inhibition phenomena. Development of a mechanistic model incorporating all three groups of factors is the objective of this work.

#### Accomplishments During FY 1982

The scheme for the purification of components of the cellulase complex obtained from *Trichoderma reesei* has been modified (Fig. 1). In this scheme, changes were made in the composition of eluting buffers to optimize the separation, and steps were added to remove salts that interfered with separation. Results of the ion-exchange step (the second step of the purification scheme shown in Fig. 1) appear in

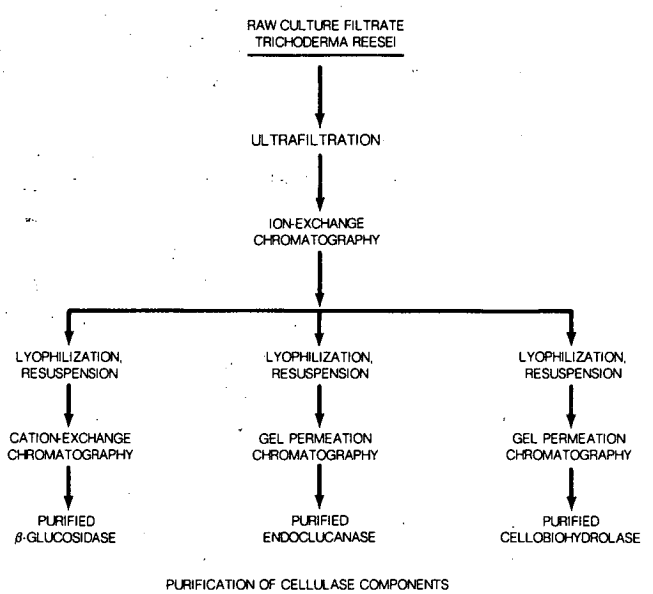


Figure 1. Purification of cellulase components. (XBL 8111-12529B)

*This work was supported by the Director of Energy Research, Office of Basic Energy Sciences, Division of Chemical Science of the Department of Energy under Contract No. DE-AC03-76SF00098.

Fig. 2. Gel permeation chromatography of the cellobiohydrolase has demonstrated that this component was purified to homogeneity.

## Planned Activities for FY 1983

Determination of Langmuir isotherms for the adsorption of purified endoglucanase and purified cellobiohydrolase, separately and in varying proportions, is the first step in developing a model to describe the interaction of these enzymes from *T. reesei*.

Kinetic and inhibition constants for the action of β-glucosidase and association constants for glucose-endoglucanase and cellobiose-cellobiohydrolase will be obtained from kinetic studies on the action of β-glucosidase in the presence of variable amounts of cellobiohydrolase, endoglucanase, cellobiose, and glucose. This will characterize the homogeneous reactions in enzymatic hydrolysis of cellulose and, in conjunction with adsorption data, will comprise the kinetic model being devised.

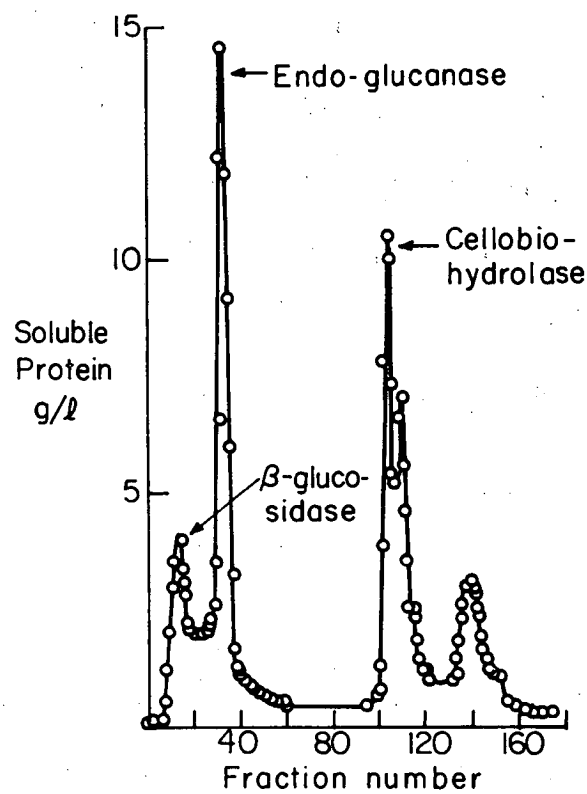


Figure 2. Ion-exchange chromatography of cellulase components. (XBL 8111-12529A)

# FUNDAMENTAL STUDIES OF HIGH-PRODUCTIVITY FERMENTATIONS: YEAST NUTRITION

A basic study of nutrient requirements for yeast fermentation of sugars to ethanol is important because nutrients are a significant part of ethanol production costs and because complex sources such molasses and corn-steep liquor provide many of the minerals, the growth factors, and the major effects of ethanol-producing processes in media.

Up to now, little effort has been devoted to defining the active components of these complex sources in yeast fermentation and to defining their optimal ratios for a balanced medium. A balanced medium will eliminate the cost of excess components and prevent their inhibitory effects on build-up in recycle processes with selective ethanol removal. Batch and continuous fermentations are therefore being carried out with synthetic and semisynthetic media to define quantitatively how all major media components are used for cell growth and ethanol production.

## Accomplishments During FY 1982

The most important growth factors were identified in batch fermentation, and continuous cultures were used to determine the optimum levels of all medium components in ethanol fermentation. The case considered was a medium with only 10–15 g/l glucose to eliminate the effects of ethanol inhibition and glucose inhibition on the medium requirements.

A novel procedure extending developments by Nateles and Battat[1] was employed. Each medium component is made the limiting substrate in terms of cell and ethanol yields. The limiting nutrient is first determined by observing which component, when injected as a concentrated pulse directly into the fermentor, produces a transient increase in cell mass or ethanol. The yields of cell mass and ethanol with respect to the limiting nutrient can then be determined from the known continuous or steady-state feed rate of the limiting nutrient and from the known productivity rates of cell mass and ethanol prior to the injection. When this limiting nutrient is found, its concentration in the feed reservoir, which has been feeding at a steady-state dilution rate, is increased so that the nutrient is no longer yield-limiting up to a given level of cell mass and ethanol. This component

can then be eliminated from further testing while the next component in the chain is made yield-limiting.

The minimal medium (no vitamins added) showed low cell and ethanol productivities with only about one-third of the available glucose consumed. Biotin added as a pulse gave a very positive response; when added continuously to the feed, it increased cell and ethanol productivities about three times.

Pantothenic acid was the next growth factor to show a positive pulse response after the biotin requirement was met. In fact, previous studies had shown that unless the biotin requirement was met first, pantothenic acid and pyridoxine did not show positive responses, which implies that biotin is needed for a critical reaction before pantothenic acid or pyridoxine can be utilized in subsequent reactions. The addition of pantothenic acid to the feed medium increased ethanol and cell production to the point where the glucose was almost entirely consumed so that the glucose itself became the limiting substrate.

Pyridoxine produced positive pulse and steady-state responses. A combination of thiamine, inositol, nicotinic acid, and p-aminobenzoic acid was pulsed into the fermentor with a positive response. After steady state was re-established, thiamine was pulsed with a positive response. However, the steady-state response to thiamine addition to the feed showed no significant change. Subsequent injections of the rest of the combination—inositol, nicotinic acid, and p-aminobenzoic acid—to the fermentor also showed no response. Yeast extract then gave a positive pulse response, indicating there were still nutrient limitations.

To observe the growth-limiting concentrations of the nutrient minerals, the medium was diluted to 10 g/l glucose and to two-thirds of the previous minimal and growth-factor concentrations for this glucose level. An injection of a mineral mixture gave a positive response, as did a subsequent injection of $(NH_4)_2SO_4$, which indicated that it was the limiting component responsible for the earlier positive response. The steady-state response for $(NH_4)_2SO_4$ addition to the feed showed a significant cell increase but a smaller ethanol increase.

With a recycle process that can produce high cell densities, high specific ethanol productivity will result in high total productivity. However, the cost of ethanol production will be largely determined by its yield with respect to its sugar substrate. Sugar should therefore be made the limiting substrate. This requires that the usage or, inversely, the yield of ethanol with respect to all other medium components must be known so that they will not become limiting.

### Planned Activities for FY 1983

Future work will be directed at scale-up of the low-glucose, low-ethanol conditions to higher glucose (100 g/l) and correspondingly higher ethanol. As a basis for comparison, yeast extract as a general nutrient source will be studied at varying concentrations. Then the effects of varying individual mineral and vitamin concentrations in a highly synthetic medium and in a semisynthetic medium with an inexpensive complex component—for example, corn-steep liquor—will also be investigated. Finally, when we have determined the usage requirement of each medium component from studies of synthetic or highly synthetic media, the best composition of the inexpensive complex component of the medium, and all costs, we will then determine the optimum blend of components for the medium through a linear program. This program can be used to give the economically optimum medium as prices change for various components.

## MODELS OF YEAST GROWTH, ETHANOL PRODUCTION, AND OXYGEN UPTAKE UNDER FERMENTATION CONDITIONS

Under aerobic conditions, yeast demand for oxygen can be determined from the overall reaction for aerobic growth given by Harrison[2]:

$$\begin{array}{ccccccc} 0.55556\ C_6H_{12}O_4 & + & 0.30017\ NH_3 & + & 1.45729\ O_2 & \rightarrow & \\ 100.00\ g & & 5.10\ g & & 46.63\ g & & \\ 0.30017\ C_6H_{10}O_3N & + & 2.28276\ H_2O & + & 1.53234\ CO_2 & & \\ 43.23\ g & & 41.08\ g & & 67.42\ g & & \end{array} \quad (1)$$

Almost all of the oxygen consumed by this reaction goes into the catabolic function of respiration as the terminal electron acceptors in oxidative phosphorylation. This use of oxygen for respiration is well understood and large enough to be easily measured.

However, oxygen is also required for less well understood biosynthesis under both aerobic and fer-

mentative conditions. It has been shown repeatedly that complete anaerobiosis results in very low cell and ethanol productivity.[3,4] Adding both ergosterol and unsaturated fatty acids to the medium gives relatively high cell yields even under anaerobiosis.[2] This suggests that oxygen is required for the synthesis of ergosterol and unsaturated fatty acids. Both are important components of yeast lipid, the bulk of which is required for cell membranes. However, the biosynthesis requirement for oxygen is very low and difficult to measure. It is even ignored by Harrison[2] in his overall reaction for fermentation:

$$\begin{array}{ccccc} 0.55556\ C_6H_{12}O_6 & + & 0.01214\ NH_3 & \rightarrow & \\ 100.00\ g & & 0.21\ g & & \\ 0.01214\ C_6H_{10}O_3N & + & 0.05697\ C_3H_8O_3 & & \\ 1.748\ g & & 5.241\ g & & \\ +\ 0.01204\ C_4H_6O_4 & + & 0.00071\ C_4H_{10}O & & (2) \\ 1.42\ g & & 0.05\ g & & \\ +\ 0.01164\ H_2O & + & 1.03076\ CO_2 & & \\ 0.21\ g & & 45.32\ g & & \\ +\ 1.00380\ C_2H_6O & & & & \\ 46.17\ g & & & & \end{array}$$

The objective of this research was to determine the fermentative oxygen requirement and its relationship to cell and ethanol productivities.

## Accomplishments During FY 1982

All yeast fermentations are linear combinations of the approximate reactions (1) and (2) of Harrison. Thus it is possible to calculate the fermentative oxygen demand by measuring the total oxygen uptake and subtracting out the oxygen uptake from aerobic growth. The relative extent of aerobic growth to fermentation can be determined from the respiratory quotient, which is the ratio of the carbon dioxide evolution rate to the oxygen consumption rate.

Using a continuous culture, we determined the carbon dioxide evolution rate by measuring the total gas outlet rate from the fermentor and by measuring its $CO_2$ composition by gas chromatography. The oxygen consumption rate was measured by the dynamic method described by Taguchi and Humphrey.[5] This method requires measuring the dissolved oxygen concentration (D.O.) in the fermentor as a function of time with a dissolved oxygen probe. After a steady-state D.O. is reached, the gas inlet containing the $O_2$ source is turned off. The slope of the D.O. decline gives the $O_2$ consumption rate. A typical trace is shown in Fig. 3. The initial steady D.O. level is varied by changing the agitation rate.

The yeast metabolism is assumed to be still predominantly fermentative even with the D.O. raised, mainly because of glucose repression of respiration and also because of the short time exposure to the higher D.O. level in some cases. According to Suomalainen, Nurminen, and Oura,[6] glucose concentrations over 50-100 mg/l result in a mainly or partly fermentative metabolism, even with intense aeration. Ferdouse et al.[7] observed that mitochondria and aerobic cytochromes appeared in yeast between 3 to 6 hours after the transition from anaerobiosis to aerobiosis in the presence of only 0.02 to 1.66 m*M* glucose.

The maximum possible specific oxygen consumption rate for a given specific growth rate is $q_{O_2}$ max. However, it is achieved only when the dissolved oxygen concentration is high enough to provide sufficient driving force for transport or for reaction, whichever is rate-limiting. The linear relationship in Fig. 4 between $q_{O_2}$ max and the dilution rate implies that a constant quantity of oxygen is used per unit yeast

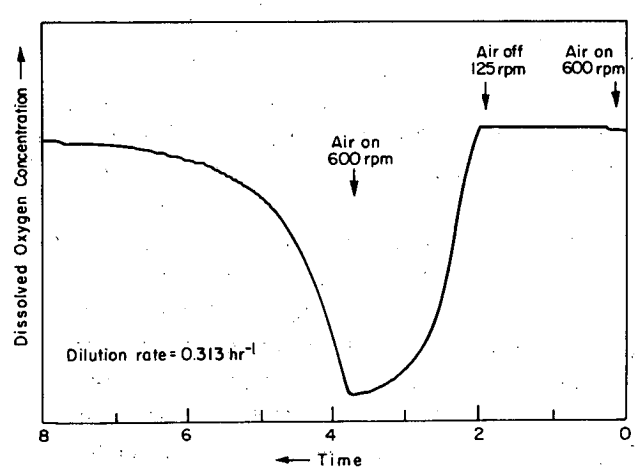


Figure 3. Typical dissolved oxygen trace for $q_{O_2}$ and $K_La$. (XBL 822-5278)

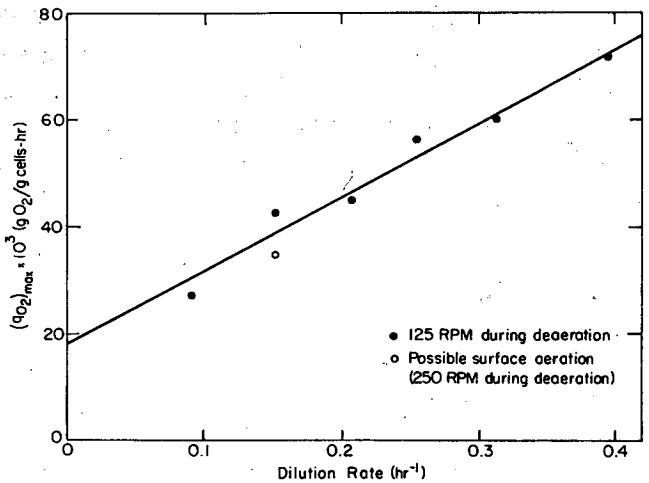


Figure 4. Maximum specific oxygen consumption versus dilution rate. (XBL 822-5286)

mass. This relationship can best be quantified as follows:

$$q_{O_2} \max (hr^{-1}) = 0.0175 + 0.140 \times \text{dilution rate } (hr^{-1})$$

The slope of this equation implies that 0.140 g $O_2$/g cells is the maximum required for growth for dilution rates up to 0.39 $hr^{-1}$. The intercept gives the maintenance requirement of 0.0175 g $O_2$/g cells/hr.

## Planned Activities for FY 1983

*Other Models of Yeast Growth and Ethanol Production*

Future work will be directed at explaining the unaccounted-for use of oxygen during fermentation and investigating the transport mechanism for oxygen into the cells. Preliminary calculations indicate passive diffusion is sufficient to satisfy oxygen requirements for the fermentative conditions used.

In addition to studying the effects of oxygen uptake, the effects of varying dissolved oxygen tension will be studied to determine if there is an optimum value for maximum ethanol productivity and yield. The dissolved oxygen range to be studied will be from below the detectable limits of current probes to the toxic levels much above atmospheric conditions. As a method for determining dissolved oxygen from measurements of the gas-phase oxygen concentration, fermentor mass transfer characteristics for oxygen will be studied. In particular, the effects of $CO_2$ on the degree of mixing in the gas phase will be examined.

Other environmental effects to be studied further are the inhibition of glucose, ethanol, and carbon dioxide. Glucose inhibition will be studied in batch culture with initial concentrations from 100 g/l to 400 g/l. The ethanol inhibition study will first check Bazua's model[8]; the inhibition effects of the previously minimal medium supplemented with biotin, pantothenic acid, pyridoxine, and thiamine will then be determined. The effect of carbon dioxide will be examined at concentrations from about 10% to about 90% by volume in the fermentor headspace.

*By-Product Inhibition in Cell Recycle and Vacuum Fermentation*

Inhibition by secondary fermentation products may limit the ultimate productivity of glucose in ethanol fermentation processes.[9] New processes are under development whereby ethanol is selectively removed from the fermenting broth to eliminate ethanol inhibition effects, but these processes can concentrate minor secondary products to the point where they become toxic to the yeast. Vacuum fermentation selectively concentrates nonvolatile products in the fermentation broth; membrane fermentation systems may concentrate large molecules that are sterically blocked from membrane transport; and extractive fermentation systems, employing nonpolar solvents, may concentrate small organic acids. Production rates and inhibition levels in continuous fermentation with *Saccharomyces cerevisiae* have been determined for many by-products, including acetaldehyde; glycerol; formic, lactic, and acetic acids; 1-propanol; 2-methyl-1-butanediol; and 2,3-butanediol, to assess their potential effects on new fermentation processes. Mechanisms for the various inhibition effects observed were proposed. These mechanisms will be described in forthcoming publications.

## REFERENCES

1. Mateles, R.J., and Battat, E. (1974), "Continuous Culture Used for Media Optimization," *Appl. Microbiol. 28*(6), p. 901–905.

2. Harrison, J.S. (1971), "Yeast Production" in *Progress in Industrial Microbiology 10,* D.J.D. Hockenhull, Ed., Churchill Livingstone, Edinburgh, p. 129–177.
3. Haukeli, A.D., and Lie, S. (1971), "Experimental Conditions Affecting Yeast Growth," *J. Inst. Brew. 77,* p. 253–258.
4. Cysewski, G.R., and Wilke, C.R. (1976), "Fermentation Kinetics and Process Economics for the Production of Ethanol," Ph.D. Thesis, Department of Chemical Engineering, University of California, Berkeley.
5. Taguchi, H., and Humphrey, A. (1966), "Dynamic Measurement of the Volumetric Oxygen Transfer Coefficient in Fermentation Systems," *J. Ferm. Tech. 44*(12), p. 881–889.
6. Suomalainen, H., Nurminen, T., and Oura, E. (1973), "Aspects of Cytology and Metabolism of Yeast," in *Progress in Industrial Microbiology 12,* D.J.D. Hockenhull, Ed., Churchill Livingstone, Edinburgh, p. 109.
7. Ferdouse, M., et al. (1972), "Quantitative Studies of the Development of *S. cerevisiae* Mitochondria," *Biotechnol. Bioeng. 14,* p. 1007–1026.
8. Bazua, C.D., and Wilke, C.R. (1977), "Ethanol Effects on the Kinetics of a Continuous Fermentation with *Saccharomyces cerevisiae,*" *Biotechnol. Bioeng. Symp. No. 7,* p. 105–118.
9. Maiorella, B., Blanch, H.W., and Wilke, C.R. (1981), "By-Product Inhibition Effects on Ethanol Fermentation by *Saccharomyces cerevisiae,*" presented at the American Chemical Society Annual Meeting, New York City, August 17, 1981, Lawrence Berkeley Laboratory Report LBL-13343.

# PRODUCTION OF SUGARS FROM CELLULOSE*

*C.R. Wilke, H.W. Blanch, N. Hendy, B. Maiorella, A. Mancuso, K. Murphy, S. Orichowskyj, and A.Sciamanna*

This research has focused on the hydrolysis of lignocellulosic materials to sugars and their subsequent fermentation to ethanol and other fuel-grade chemicals. Applied studies have examined the kinetics of enzymatic hydrolysis of cellulose and hemicellulose fractions for optimal sugar production; the physical and chemical nature of the raw materials; the optimal production and recovery of enzymes; and the use of new organisms for converting polymeric pentosans and hexosans to sugars. Optimization of the continuous ethanol removal and recovery process, as well as alternative methods of fermentation to ethanol, have also been studied. In all this work, the economic impact of each process change is evaluated.

## ACCOMPLISHMENTS DURING FY 1982

### Process Development Studies

*Enzymatic Hydrolysis of Corn Stover*

The hydrolysis of acid-treated corn stover with cellulase from *Trichoderma reesei* Rut-C30 was

*This work was supported by the Assistant Secretary for Conservation and Solar Energy of the U.S. Department of Energy under Contract No. DE-AC03-76SF00098 and by the Solar Energy Research Institute under Contract No. DR-0-9058-1.

evaluated.[1] Experiments were conducted with substrate concentrations of 5% to 25% by weight, enzyme activities of 0.5–7 International Units (IU) per milliliter, and residence times of 28–48 hours. The maximum conversion of available carbohydrates to fermentable sugars was 55% at a cellulase activity of 25–30 IU/g. Optimum cellobiase activity for minimum cellobiose production was approximately 1.8 cellobiase units to 1 filter paper activity (FPA) unit.

Hydrolysis experiments with steam-exploded corn stover, however, led to a maximum conversion of 80%, significantly higher than the results obtained for acid-treated substrate. In addition, steam-exploded corn stover was shown to be a suitable carbon source for growth of *T. reesei* in submerged cultures.

Computer-aided process evaluations were conducted for several processing alternatives, including steam explosion or dilute-acid pretreatment; equilibrium solid-liquid contacting or ultrafiltration for enzyme recovery; and batch, continuous, or continuous with cell-recycle culture for enzyme production. With dilute-acid-pretreated materials, glucose may be produced for 12–22 cents per pound at corn stover costs ranging from $0 to $30 per ton. This constitutes a 33% reduction over previous processing schemes employing cellulase from *T. reesei* QM9414. Enzyme production is the single most expensive processing step, accounting for 40% of processing costs. Preliminary evaluation of processing with steam-exploded corn stover leads to a glucose cost of 10–15 cents/pound for corn stover costing $0–$30 ton, with further improvement possible. The dominance of raw-material costs, however, tends to dampen the effect of process improvements on the cost of manufacturing ethanol.

*Economic Evaluation of Alternative Fermentation Processes*

A computer package (FERMEC) was developed, this being a comprehensive library of routines for the design and evaluation of alternative fermentation schemes. These schemes are compared on identical bases, using a single kinetic model of fermentation (based on the data of Bazua[2]) and identical economic assumptions. The entire fermentation plant, including feed preparation, fermentation, distillation, stillage processing, and feed and product storage is designed and costed (Fig. 1).

With this computer package, optimized designs were developed for batch, simple-continuous, series-continuous, plug flow, tower, cell-recycle, immobilized-cell fermentations, and fermentations coupled with selective ethanol removal processes. A high fermentor-cell density is most important for

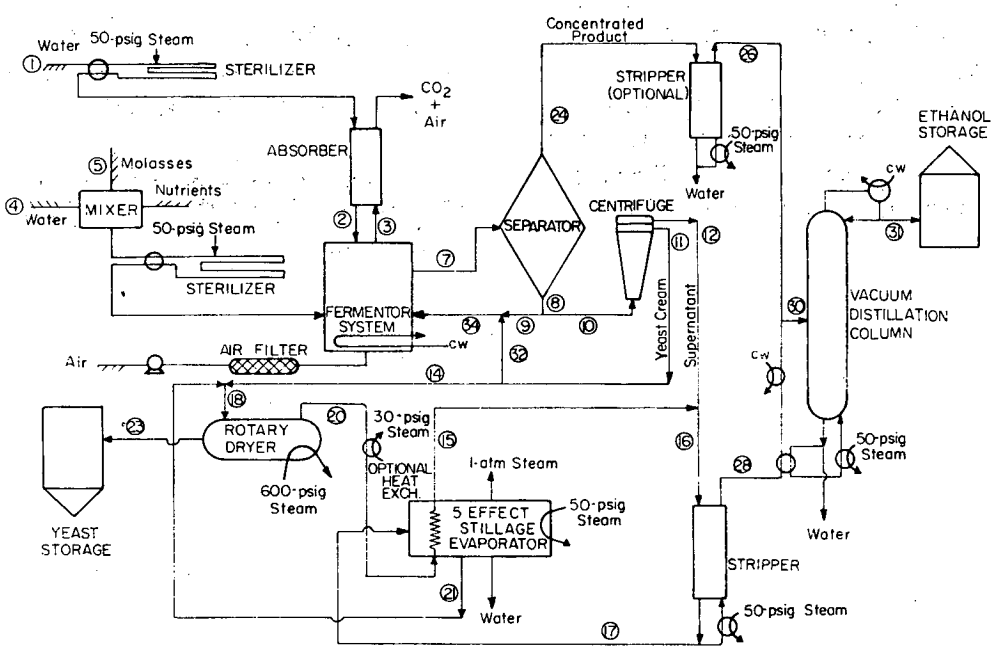


Figure 1. Flow model of fermentation plant for ethanol production. (XBL 825-5695)

achieving reduced costs. Excluding the selective ethanol removal processes, the recycle and tower fermentor processes are the most favorable, with similar economics. For ethanol produced from molasses containing approximately 50% fermentable sugars and priced at $85/ton, with a credit for yeast of 11.4 cents/kg and a 15% after-tax return on investment, the minimum charge is 48.2 cents/l, compared to 52.8 cents/l for the optimum conventional batch design.

For a selective ethanol removal process with a high separation factor (such as flash fermentation), the charge for ethanol, excluding the separator cost, is reduced to 42.9 cents/l, for a saving of 5.4 cents/l, the maximum achievable with a separator of the specified characteristics. This results not primarily from a reduction in fermentation or distillation costs, but from a reduction in the cost of auxiliaries such as stillage handling. If a dilute sugar source (such as glucose hydrolyzate) is used instead of molasses, then the cost of feed concentration offsets these savings.

With the FERMEC package, we evaluated possible fermentation cost savings from the use of genetically modified fermentation organisms. The yeast microorganism *Saccharomyces cerevisiae* (ar anamensis), grown in continuous culture with centrifuge recycle, was taken as a base case. We then used the economic model to assess the cost savings if each of four kinetic parameters could be raised by 15% through organism improvement techniques.

The results indicate that the greatest cost savings would be achieved by developing high-yielding, ethanol-tolerant organisms. A very high fermentation rate is of only secondary significance. The bacterium *Zymomonus mobilis* should be of particular interest because of its high product yield (approaching 0.49 g/g).

Documentation of the FERMEC package for use by other groups in evaluating alternative fermentation processes is nearing completion.

*Evaluation of the High-Pressure Hydrogen Chloride Process*

Saturating wood particles with HCl gas under pressure before subjecting the wood to dilute-acid hydrolysis was found to be an effective pretreatment—the glucose yield was doubled. The HCl gas makes the wood more susceptible to hydrolysis, which is otherwise inhibited by the tight lattice structure of cellulose.

The saturation was most effectively performed in a fluidized-bed reactor, with pure HCl gas fluidizing equal volumes of ground wood and inert particles, as shown in Fig. 2. The fluidized bed effectively dissipated the large amount of heat released upon HCl absorption into the wood. Batch reaction times of one hour at 314.7 psia gave glucose yields of 80% and xylose yields of 95% after dilute-acid hydrolysis. A noncatalytic gas-solid reaction model, with gas diffusion into the solid as the rate-limiting step, was found to describe this HCl-wood reaction.

Hydrogen chloride formed a stable adduct with the lignin residue in the wood, in a ratio of 3.33 moles

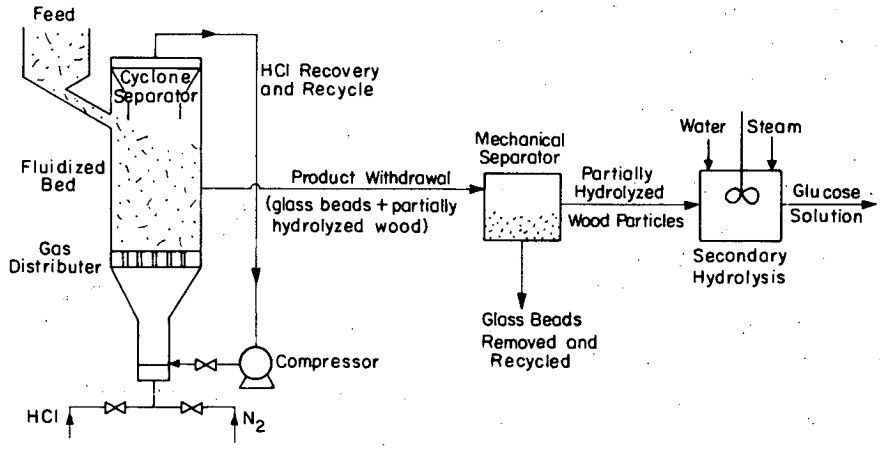


Figure 2. Flow diagram for proposed fluidized bed process. (XBL 812-5299)

per mole of lignin monomer. This resulted in a loss of 0.1453 pounds of HCl per pound of wood. The adduct was broken upon the addition of water.

A process design and economic evaluation for a plant producing 214 tons per day of glucose from ground and air-dried poplar wood (*Populus tristi*) gave an estimated glucose cost of 15.1 cents per pound. This would correspond to $2.54 per gallon of ethanol if the glucose were fermented. Key factors contributing to the cost of glucose production were unrecovered HCl, which contributed 5.70 cents per pound of glucose, and the cost of wood, which, at $25 per ton, contributed 4.17 cents per pound.

## Microbiological and Enzymatic Studies

### *Production of Cellulase Enzyme from High-Yielding Mutants*

Economic studies of enzymatic hydrolysis of biomass have indicated that enzyme production alone accounts for some 40% of the cost of glucose production from cellulosic material. To reduce the cost of enzymes, corn-steep liquor (CSL) has been investigated and found to be an adequate replacement for the more expensive proteose peptone. CSL at 0.5% w/v adequately replaces 1 g/l proteose peptone.

Two-stage continuous fermentation to increase cellulase production was also studied. This process uses two vessels; for both, the optimum pH was O and the optimum temperature was 28°C, and the incoming medium contained 20 g/l Solka Floc (finely ground, bleached white spruce). Maximum productivity was obtained at a dilution rate of 0.046 $hr^{-1}$ in the first stage and 0.028 $hr^{-1}$ in the second stage. This resulted in an exit stream containing 3.3 IU/ml of filter paper activity (FPA) at a productivity of 58 IU/l-hr. The first stage, viewed separately, produced 2.1 IU/ml FPA at a productivity of almost 100 IU/l-hr. The results are summarized in Fig. 3.

"Fed-batch" cultivation of the high-yielding fungus *T. reesei* Rut-C30 resulted in great improvements in cellulase productivity as well as enzyme activity. This mode of cultivation allows the use of high substrate concentration without leading to the repression effects and the agitation and aeration difficulties encountered with batch fermentation. The experiments were started as a conventional batch process with an initial Solka Floc concentration of 20 g/l. After 48 hours, Solka Floc was regularly added without exceeding a concentration of 20 g/l. In this manner, the total effective Solka Floc concentration was raised to as high as 150 g/l. Up to this limit, a proportional increase in cellulase production resulted. A maximum of 30.4 IU/ml FPA was achieved (the highest activity yet reported for this strain), with 47.6 g/l soluble protein at a high titre productivity of 206 IU/l-hr and a maximum productivity of 177 IU/l-hr. Further experiments will examine the upper limit of substrate concentration and the optimal conditions for enzyme production and activity by this very efficient cultivation procedure.

### *Hydrolysis Reactor Development*

*Enzyme Recovery in Cellulose Hydrolysis.* The adsorption of cellulase enzymes on unconverted cellulosic solids represents a large loss of enzyme, and hence increased glucose production costs. Alternative means to enhance the recovery of Rut-C30 cellulase enzyme from corn-stover hydrolysis were investigated.

In one, several nitrogenous salts were introduced to the hydrolysis to maximize the fraction of enzyme remaining in solution.[4] Urea was then added to the enzyme solution at a concentration of 1 *M*, resulting in 65% retention of enzyme in the hydrolyzate, with about 35% remaining on the extracted residue, compared to the usually observed 50 to 60% retained on the unextracted residue. For subsequent fermentation of the hydrolyzate, it is necessary to concentrate the sugar solution, which results in 5-7 *M* urea levels. However, at urea concentrations greater than 0.75 *M*, metabolic activities of *Saccharomyces cerevisiae*

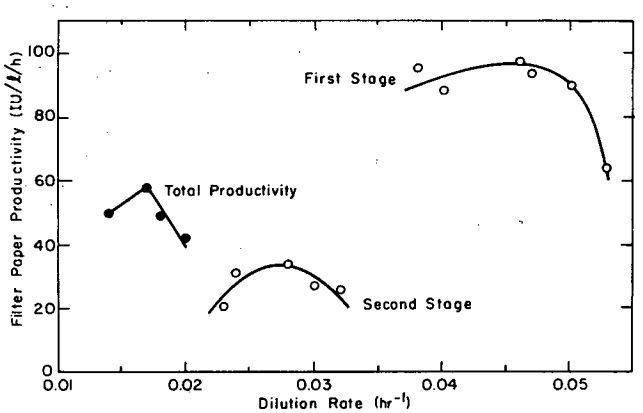


Figure 3. Two-stage continuous cultivation of *T. reesei* Rut-C30 on 20 g/l Solka Floc. (XBL 823-5436)

were greatly inhibited. Therefore, addition of urea to the hydrolysis is not feasible. No economical means of removing the urea prior to fermentation was found.

Among other alternatives investigated, countercurrent contacting of the solids results in an estimated 27% recovery of the enzyme entering the hydrolysis. A solids wash with concentrated urea solution recovers an estimated 35% of the enzyme entering the hydrolysis from the solids alone. Ultrafiltration was also evaluated. Because of losses attributed to the ultrafiltration units, the maximum enzyme recovery is estimated to be 56%. This alternative is marginally uneconomical because of excessive consumption of urea. Replacing the ultrafiltration units with precipitation of enzyme by acetone results in greater costs.

It is concluded that the most economical alternative for enzyme recovery is countercurrent contacting of the hydrolyzate with fresh solids. This is discussed further below.

*Cellulase Recovery by Countercurrent Adsorption.* This study evaluated countercurrent adsorption as a means of recovering enzyme from hydrolyzate.[5] Results from adsorption studies and hydrolysis experiments were used to design a system for enzymatic hydrolysis of steam-exploded corn stover that operated with two stages of countercurrent adsorption. Steam-exploded corn stover was selected because of the high conversions obtained (as much as 94%) through enzymatic hydrolysis. Enzyme concentration determinations included refinement of the assays for filter paper, crystalline, amorphous, and cellobiase activities, as all of the enzymatic assays are inaccurate when a high concentration of background sugars is present. To overcome this problem, acetone precipitation can be used to separate enzyme from sugars. Standard curves were constructed for the recovery of enzyme after acetone precipitation.

Studies to determine the effect of temperature and solids concentration on enzyme adsorption were performed. The initial enzyme-to-substrate ratio was 25 filter paper units (FPU) per gram solid. Adsorptions at 5.0 wt.% were observed at 15, 25, 35, and 45°C. In all four cases, adsorption decreased considerably within 5 to 10 minutes. At 30 to 45 minutes, 35% of the original filter paper activity remained in solution, regardless of temperature. Adsorption is greatest at low temperatures and low enzyme loadings. Enzyme is adsorbed quickly; most of the adsorption is complete within 5 minutes. Steam explosion is superior to Wiley milling followed by acid treatment in increasing the susceptibility of the substrate to enzyme attack.

Adsorption of filter-paper activity, activity towards cotton, activity towards carboxymethylcellulose, and cellobiase activity onto steam-exploded corn stover were measured and modeled by a Langmuir isotherm. The enzyme responsible for activity toward cotton is adsorbed to the greatest extent. Adsorption of cellobiase is weak.

Glucose yields as high as 94% are achieved by enzymatic hydrolysis of steam-exploded corn stover. High conversions permit release of enzyme so that it may be recovered from the liquid. The glucose yield decreases with increasing solids concentration because of product inhibition by glucose and cellobiose.

A 10 wt.% suspension of steam-exploded corn stover was hydrolyzed with an enzyme loading of 25 FPU/g at 45°C for 24 hours. Enzyme in the hydrolyzate was recovered by two stages of countercurrent adsorption, with each stage operated at 25°C for 45 minutes. The make-up enzyme requirement, measured as filter paper activity, was 35% of that required for the control experiment (batch hydrolysis without enzyme recovery). Compared to the control experiment, the release of filter paper activity and the rate of sugar production was considerably slower. This is attributed to poor recovery of cellobiase.

A preliminary economic evaluation showed that the enzyme production cost can be reduced by 61% if enzyme is recovered by countercurrent adsorption. This includes the cost of operating the countercurrent adsorption system.

### *Xylose Fermentation*

*Xylose Utilization by Bacillus Macerans.* The ability of *B. macerans* to ferment pentoses to ethanol was examined.[6] The organism was grown in a continuous-flow stirred-tank fermentor. In continuous culture at steady state, ethanol and acetic acid and acetone were produced. The organism was found to have a relatively high maximum specific growth rate. This maximum was higher than previously reported for *B. macerans* organisms.

However, *B. macerans* had difficulty attaining and maintaining a steady state when grown in continuous culture. A perturbation of the conditions in the fermentor, such as a step-change to a higher dilution rate, as shown in Fig. 4, or injection of a small amount of xylose into the fermentor, would cause growth to stop. Several days were required for the fermentor to return to normal.

A possible explanation for this behavior is an interaction between the magnitude of the transmembrane pH gradient, the metabolic rate, and protonated acetic acid inhibition. At a constant external pH, a decreasing metabolic rate would cause the pH gradient to decrease; this would increase acetic acid inhibition, in turn causing the metabolic rate to decline further. This was enhanced by the strong dependence of cell yield on metabolic rate. A small decrease in metabolic rate would cause a large decrease in specific growth rate because cell yield would decrease. A satisfactory mathematical model of the growth and metabolism of *B. macerans* was constructed to test this hypothesis of an interaction between metabolic rate, pH gradient, and acetic acid inhibition.

Although *B. macerans* grows rapidly and produces ethanol from pentoses, its instability and transient behavior in continuous culture render it unsuitable for use in a commercial process.

*Xylose Fermentation by Clostridium thermohydrosulfuricum.* The economic feasibility of fermenting xylose to ethanol with *Clostridium thermohydrosulfuricum* was examined. Initial experiments aimed at determining basic fermentation kinetics, as shown in Fig. 5. The maximum specific growth rate and specific ethanol productivity was found to be 0.32 $hr^{-1}$ and 0.31 g/l-hr, respectively, while the yield of ethanol from xylose was 0.33 g ethanol/g xylose. By-products of the fermentation include lactate and acetate.

These organisms are very sensitive to ethanol. Growth inhibition of 50% ws observed in the presence of 0.5 w/v% ethanol. To improve the organism's tolerance, an adapted strain, capable of growing at a rate of 0.29 $hr^{-1}$ in 3.5 w/v% ethanol, has been developed. Unfortunately, the adapted organism produces ethanol at a reduced yield of only 0.20 g/g xylose.

Recent research has focused on increasing the

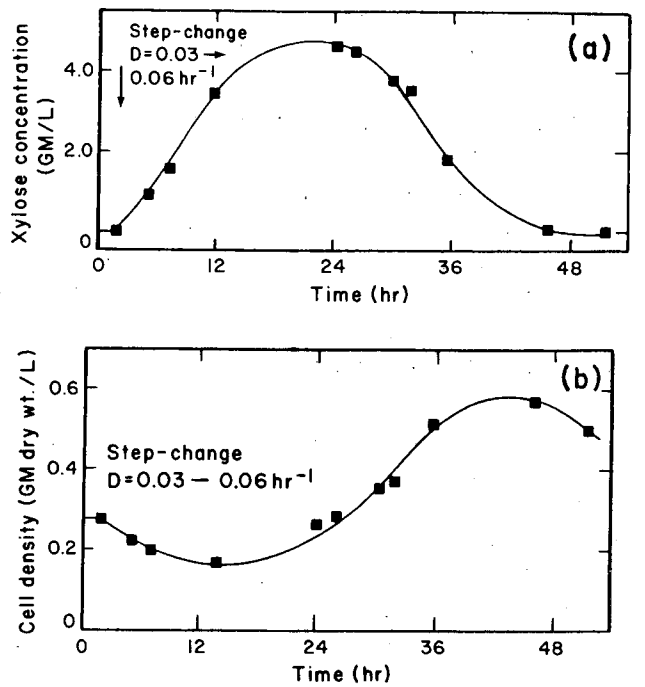


Figure 4. (a) Xylose concentration during a transient induced by a step-change in dilution rate from 0.03 to 0.06 $hr^{-1}$. Inlet xylose concentration was 11.6 g/l. (b) Cell density during a transient induced by a step-change in dilution rate from 0.03 to 0.06 $hr^{-1}$. Inlet xylose concentration was 11.6 g/l. [(a) XBL 819-1823; (b) XBL 819-1819]

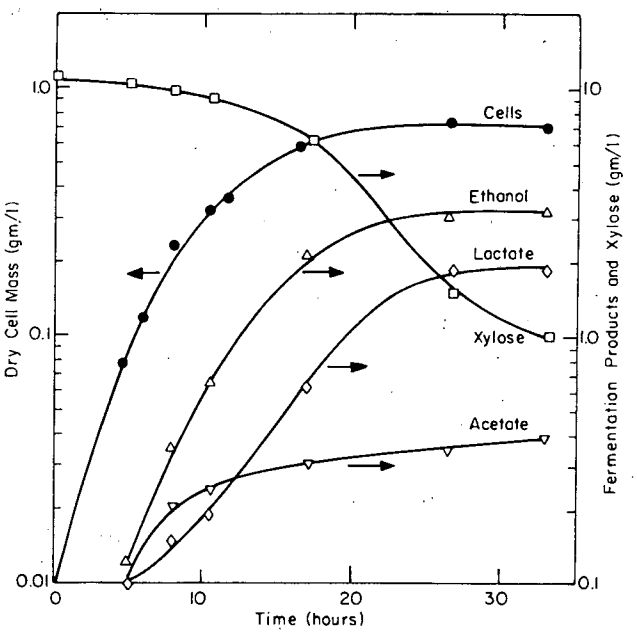


Figure 5. Fermentation profile of *Clostridium thermohydrosulfuricum.* (XBL 823-5405)

yield of ethanol produced by this ethanol-tolerant strain of *C. thermohydrosulfuricum* (strain UC-40). the effect of pH and by-product concentrations on ethanol yield has been examined. In addition, mutants producing relatively less by-product acids than UC-40 have been isolated.

*C. thermohydrosulfuricum* was grown at various pH's ranging from 6.0 to 7.9. The growth rate was highest (0.48 $hr^{-1}$) at pH 7.2. The yield of ethanol (0.22 g/g xylose fermented) was not a strong function of pH. Specific ethanol productivity had a maximum value of 0.36 $hr^{-1}$ over a pH range of 6.0 to 6.8.

Adding acetate and lactate to the growth medium shifted the distribution of end products formed by strain UC-40. Low concentrations (1 to 3%) of acetate completely suppressed acetate formation; the yield of ethanol was increased by 20%, while the yield of lactate was unaffected. Lactate formation was inhibited by including lactate (2 to 3%) in the medium; a corresponding increase in acetate formation but no ethanol formation was observed.

Ethyl methane sulfonate was used to induce mutants with lower lactate yields than strain UC-40. Strain UC-40-L1 produced 60% less lactate and 20% more ethanol than UC-40. Unfortunately, this strain was not very stable and reverted after approximately 35 generations. Another strain (UC-40-L2), one producing 57% less lactate, has also been isolated. This isolate appears to be more stable than UC-40-L1 and is currently being characterized.

## Fermentation and Separation Processes

### *Ethanol Distillation Technology*

The DISTILL computer package for the design and evaluation of alternative ethanol/water distillation processes has been completed and used to determine the minimum ethanol/water separation cost for an efficient two-stage vacuum distillation process.

At high-feed ethanol concentrations, the distillation energy requirement for 95 wt.% "azeotropic" ethanol production is set by an azeotrope-associated pinch. This pinch limitation is reduced at low pressure. The ETOH equilibrium package, using a modified temperature-dependent UNIQUAC equilibrium model based on over 2,000 data points, allows accurate distillation design, including evaluation of reduction of the pinch limitation at low pressure. The minimum external reflux ratio to distill a concentrated feed is reduced from 3.3 at one atmosphere to 1.8 at 100 mmHg pressure. The savings at 100 mmHg can be realized only after a feed of at least 13.2 wt.% ethanol is used.

The two-stage vapor reuse method overcomes this feed limitation. Dilute beers are fed first to an atmospheric pressure stripper. The concentrated stripper product is then fed to the vacuum distillation. High energy efficiency is maintained by reusing the stripper heat, condensing the stripper vapor in the vacuum distillation reboiler to drive this second distillation step.

The cost of this process has been assessed for base-case cost assumptions of steam at $3.15/1000 pounds, cooling water at 22.6 cents/1000 gal, labor (including supervision) at $12.6/man-hour, 18-year depreciation, and a 15% after-tax return on investment. For very dilute feeds (1 wt.% ethanol), the charge for distillation is high (7.5 cents/l). At typical (6 wt.%) feed concentrations, the distillation cost is reduced (2.2 cents/l). Beyond 9 wt.% ethanol, the pinch limitation (even at reduced pressure) is controlling and the distillation cost to produce 95% wt.% product is constant (1.8 cents/l). The steam requirement for an optimized typical 6 wt.% feed case is 1.61 kg/l of product.

The sensitivity of these costs to changes in the cost of steam and cooling water and to changes in required return on investment were also studied.

Finally, the vapor-reuse methods were extended to develop a five-column distillation process with acetaldehyde and fuel-oil removal to produce anhydrous ethanol. Capital costs are increased (for the added columns), but by careful staging of distillation-column pressures, no added energy is required to produce anhydrous ethanol as compared to 95 wt.% ethanol.

### *Solvent Extraction for Ethanol Recovery*

Solvent extraction represents a process for ethanol recovery that can allow significant energy savings compared to distillation, especially when the ethanol is to be recovered from a fairly dilute process stream. The advantage of extraction is in avoiding the vaporization of large quantities of water that occurs during distillation. The key to achieving this, however, lies either in using a solvent with a high separation factor (the ratio of ethanol to water distribution coefficients)

or in selectively removing the ethanol from the extractant stream.

Progress has been made toward the first goal with the experimental finding that high-molecular-weight aldehydes have better distribution coefficients and separation factors than any compounds tested previously. While the use of aldehydes in a commercial process is questionable because of their reactivity (including oxidation and aldol condensation), their desirable properties suggest that solvents with similar functional groups but less reactivity should be investigated. Interestingly, the effect of temperature on the ethanol distribution coefficient for aldehydes is opposite that for similar acids or alcohols. That is, the coefficient decreases with increasing temperature in the case of aldehydes, while it increases in the other cases.

The UNIFAC model for activity coefficient calculation has been applied to the ethanol-water-solvent systems, using the liquid-liquid equilibrium parameters suggested by Magnussen et al.[7] Although the results are not quantitatively correct, they are qualitatively correct in all cases tested. This holds the promise of a valuable method of screening solvents and ranking them in order of distribution coefficients and separation factors. Such an approach could significantly reduce the amount of experimental work necessary to identify good extraction solvents.

To synthesize an extraction process, a flexible computer simulation package is being prepared that incorporates economic analysis. The executive program is working, and a series of subroutines to model extraction, stripping, absorption, heat exchange, and other unit operations is being developed. The result will allow extraction optimization with regard to solvent, operating temperature, and process configuration.

## PLANNED ACTIVITIES FOR FY 1983

Mutation and selection studies on *Clostridium thermohydrosulfuricum* will be continued, with the objective of finding mutants suitable for ethanol production in the flash-fermentation apparatus. Once suitable strains are found, the efficiency of this device for xylose utilization will be examined, both experimentally and economically.

## REFERENCES


1. Perez, J., Wilke, C.R., and Blanch, H.W. (1981), *Enzymatic Hydrolysis of Corn Stover Process Development and Evaluation,* Lawrence Berkeley Laboratory Report LBL-14223.
2. Bazua, C.D., and Wilke, C.R. (1977), "Ethanol Effects on the Kinetics of a Continuous Fermentation with *Saccharomyces cerevisiae,*" *Biotechnol. Bioeng. Symp. 7,* p. 105.
3. Blanch, H.W., Antonopolis, R., Freitas, R., Sciamanna, A., and Wilke, C.R. (1982), "High Pressure HCl Conversion of Cellulose to Glucose," submitted to *Biotechnol. Bioeng.*
4. Dove, G.B., Wilke, C.R., and Blanch, H.W. (1982), "Process Development Studies: the Enhanced Recovery of Cellulase in Cellulose Hydrolysis," submitted to *Biotechnol. Bioeng.*
5. Orichowskyj, S., Wilke, C.R., and Blanch, H.W. (1982), *Recovery of Cellulase Enzymes by Countercurrent Adsorption,* Lawrence Berkeley Laboratory report LBL-15153.
6. Delfino, T., Blanch, H.W., and Wilke, C.R. (1981), *The Fermentation of Xylose by Bacillus macerans,* Lawrence Berkeley Laboratory Report LBL-14648.
7. Magnussen, T., Rasmussen, P., and Fredenslund, A. (1981), "UNIFAC Parameter Table for Predicting Liquid-Liquid Equilibria," *Ind. Eng. Chem. Proc. Des. Dev. 20,* p. 331.

# HOMOGENEOUS CATALYTIC HYDROGENATION: REGIOSPECIFIC REDUCTIONS OF POLYNUCLEAR AROMATIC AND HETEROAROMATIC NITROGEN COMPOUNDS CATALYZED BY TRANSITION-METAL CARBONYL HYDRIDES*

*R.H. Fish, A.D. Thormodsen, G.A. Cremer, T. Vermeulen, and H. Heinemann*

Synthetic fuel products derived from coal or oil shale require additional hydroprocessing to minimize their nitrogen and sulfur content; the selective hydrogenation of polynuclear heteroaromatics therefore becomes critical.[1–3] To this end, it is extremely important to have a basic understanding of which polynuclear aromatic and heteroaromatic compounds are hydrogenated in these complex fossil-fuel matrices.

Recently, Pettit and his co-workers[4–6] elegantly demonstrated the use of carbon monoxide and water as an alternative reducing agent to hydrogen in the hydroformylation of olefins and the reduction of nitroarenes. These reactions were catalyzed by transition metal carbonyl compounds [$M_x(CO)_y$] and are thought to proceed via the formation of transition metal carbonyl hydrides (e.g., $H_2M_x(CO)_y$), by nucleophilic attack of water or base on coordinated carbon monoxide.[7–9] Other methods of generating transition metal carbonyl hydrides from the corresponding carbonyls have used carbon monoxide and hydrogen and hydrogen alone as reagents.[10]

We therefore thought that the rather facile generation of transition metal carbonyl hydrides under water-gas shift (CO, $H_2O$, base) and synthesis gas (CO, $H_2$, 1:1) conditions as well as strictly hydrogenation conditions ($H_2$ alone) made these reagents very attractive for the purpose of testing their regioselectivities in the reductions of polynuclear aromatics and polynuclear heteroaromatic nitrogen compounds. Additionally, it is well known that homogeneous catalytic reductions proceed at lower temperatures and pressures, and, in fact, give the higher regioselectivities we were seeking when compared to their heterogeneous counterparts.[11,12]

## ACCOMPLISHMENTS DURING FY 1982

Figure 1 shows the polynuclear aromatic and polynuclear heteroaromatic nitrogen compounds (**1-8**) that we used as model synthetic fuel compounds.

We reacted a wide variety of transition metal carbonyl compounds with compounds **1-3** under water-gas shift (wgs) and synthesis gas (sg) conditions[13] and found that only $Fe(CO)_5$, $Mn_2(CO)_8(Bu_3P)_2$, and $Co_2CO_6(\Phi_3P)_2$ produced reduction products. For example, **1** was reduced to 9,10-dihydroanthracene (**9**) under wgs conditions with these carbonyls in rather poor yields of 8%, 13%, and 3% respectively,

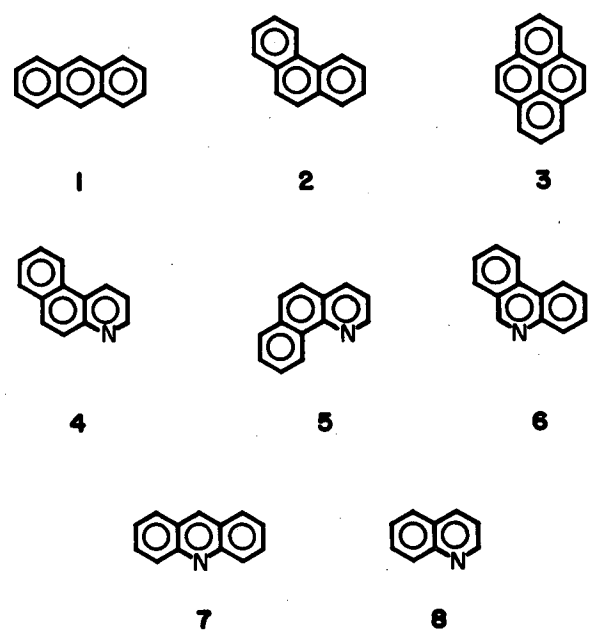


Figure 1. Model synthetic fuel compounds used in the catalytic hydrogenations with transition-metal carbonyl hydrides: **1**, anthracene; **2**, phenanthrene; **3**, pyrene; **4**, 5,6-benzoquinoline; **5**, 7,8-benzoquinoline; **6**, phenanthridine; **7**, acridine; and **8**, quinoline. (XBL 821-7773)

*This work was jointly supported by the Director, Office of Energy Research, Office of Basic Energy Sciences, Chemical Sciences Division, and the Assistant Secretary of Fossil Energy, Office of Coal Research, Liquefaction Division of the U.S. Department of Energy through the Pittsburgh Energy Technology Center under Contract No. DE-AC03-76SF00098.

while substrates **2** and **3** were totally unreactive.

In view of these discoveries, we decided to learn more about this reaction, using $Mn_2(CO)_8(Bu_3P)_2$ as the catalyst. The reaction of carbon monoxide and deuterium oxide ($D_2O$) with **1** provided only 9,10-dideuteroanthracene (**10**),[14] and this result strongly indicates that the hydrogen comes exclusively from water.

To elucidate the stereochemistry of the anthracene reaction, we reacted an analog of **1**, 9,10-dimethylanthracene (**11**) with $Mn_2(CO)_8(Bu_3P)_2$ under wgs conditions (180°, 5 hrs, 350 psi CO, 0.2 *M* KOH in THF, substrate-catalyst ratio = 20) to provide a 30% yield of *cis* and *trans* 9,10-dihydro-9,10-dimethylanthracene (**12** and **13**), in a ratio of 53%:47%.[15] A similar result was recently reported by Sweany et al.,[16] for the reaction of **10** and $HMn(CO)_5$ and by Taylor and Orchin[17] with $HCo(CO)_4$ under sg conditions (CO, $H_2$ 1:1, ~200°).

We also found that, under sg conditions ($CO/H_2$ = 1),[13] better yields of reduced polynuclear aromatic products could be obtained using $Mn_2(CO)_8(Bu_3P)_2$ as the catalyst and compounds **1–3** as substrates. Thus, reaction of **1** with $Mn_2(CO)_8(Bu_3P)_2$ provided **9** in 30% yield, while reaction with **2** gave no product and **3** produced 4,5-dihydropyrene (**14**), in a 3% yield.

From these results, it is evident that bent polynuclear aromatic compounds are extremely unreactive under either wgs or sg conditions when compared to **1**, a linear polynuclear aromatic compound.[18,19]

As previously stated, it is important to study the polynuclear heteroaromatic nitrogen compounds under various homogeneous hydrogenation conditions because they are prevalent in all coal and oil shale products. Despite this importance, few studies of their reactivity under either wgs or sg conditions or, for that matter, under strictly hydrogenation conditions, have been published. For example, Laine et al.[20] reported on the hydrogenation of the mononuclear heterocyclic compound pyridine under wgs conditions with $Rh_6(CO)_{16}$ as catalyst, and Derencsenyi and Vermeulen[19] reported that, under sg conditions, quinoline, **8**, was regioselectively reduced to 1,2,3,4-tetrahydroquinoline, using $Mn_2(C0)_8(Bu_3P)_2$ as a catalyst. Furthermore, Jardine and McQuillin[21] have reported that **8** was again reduced to 1,2,3,4-tetrahydroquinoline, when $RhCl_2Py_2(dmf)BH_4$ was used as the catalyst.

As seen in Table 1, we found a greater reactivity for the polynuclear heterocyclic nitrogen compounds, **4-8**, under either wgs or sg conditions, compared to their carbon analogs; e.g., acridine, **7**, is more reactive than anthracene, **1**. It is also important to note the high regioselectivity of compounds **4–8**—only the nitrogen ring was hydrogenated. This regioselectivity

Table 1. Reductions of polynuclear heteroaromatic nitrogen compounds **4–8**, under water-gas shift[a] (wgs) and syngas (sg) conditions[b] with transition metal carbonyls as catalysts.

| Substrate | Catalyst | Sub/Cat ratio | Temp. (°C) | Time (hr) | Conditions | Products (%)[d] |
|---|---|---|---|---|---|---|
| **4** | $Mn_2(CO)_8(Bu_3P)_2$ | 20 | 200 | 2 | sg | 1,2,3,4-tetrahydro-5,6-benzo-quinoline (7) |
| **4** | $Mn_2(CO)_8(Bu_3P)_2$ | 20 | 200 | 5 | wgs | 1,2,3,4-tetrahydro-5,6-benzo-quinoline (4) |
| **4** | $Fe(CO)_4(Bu_3P)$ | 10 | 180 | 5 | wgs | 1,2,3,4, tetrahydro-5,6-benzo-quinoline (1) |
| **4** | $Co_2(CO)_6(\Phi_3P)_2$ | 20 | 200 | 2 | sg | 1,2,3,4-tetrahydro-5,6-benzo-quinoline (8) |
| **5** | $Mn_2(CO)_8(Bu_3P)_2$ | 20 | 200 | 2 | sg | 1,2,3,4-tetrahydro-7,8-benzo-quinoline (2) |
| **5** | $Mn_2(CO)_8(Bu_3P)_2$ | 20 | 200 | 2 | wgs | No product |
| **6** | $Mn_2(CO)_8(Bu_3P)_2$ | 20 | 200 | 2 | wgs | 9,10-dihydro-phenanthridine (1) |
| **6** | $Mn_2(CO)_8(Bu_3P)_2$ | 20 | 200 | 2 | sg | 9,10-dihydro-phenanthridine (11) |
| **6** | $Co_2(CO)_6(\Phi_3P)_2$ | 20 | 200 | 2 | sg | 9,10-dihydro-phenanthridine (21) |
| **7** | $Fe(CO)_5$[c] | 10 | 180 | 2 | wgs | 9,10-dihydro-acridine (100) |
| **7** | $Mn_2(CO)_8(Bu_3P)_2$ | 10 | 200 | 2 | wgs | 9,10-dihydro-acridine (38) |
| **7** | $Mn_2(CO)_8(Bu_3P)_2$ | 20 | 200 | 2 | sg | 9,10-dihydro-acridine (100) |
| **7** | $Co_2(CO)_6(\Phi_3P)_2$ | 20 | 200 | 2 | sg | 9,10-dihydro-acridine (100) |
| **8** | $Fe(CO)_5$ | 10 | 180 | 2 | wgs | 1,2,3,4-tetrahydro-quinoline (0) |
| **8** | $Mn_2(CO)_8(Bu_3P)_2$ | 20 | 200 | 5 | wgs | 1,2,3,4-tetrahydro-quinoline (4) |
| **8** | $Mn_2(CO)_8(Bu_3P)_2$ | 20 | 200 | 5 | sg | 1,2,3,4-tetrahydro-quinoline (33) |
| **8** | $Co_2(CO)_6(\Phi_3P)_2$ | 20 | 200 | 1 | sg | 1,2,3,4-tetrahydro-quinoline (70) |

[a]Reaction run in THF (12 ml) with 0.2 *M* KOH (3 ml), 350 psi CO.

[b]350 psi $H_2$ and 350 psi CO in THF (15 ml).

[c]800 psi CO.

[d]Determined by capillary GC using a digital integrator (HP 5880A). Isolated by column chromatography (Florisil) and identified by GC-MS and NMR spectroscopy (250 MHz, $^1H$).

might be explained by the lowered aromaticity of the nitrogen-containing ring versus that of their carbon analogs, which would provide a lower activation energy for hydrogenation.[22]

That Fe, Mn, and Co carbonyls did provide reduced product under wgs conditions, while other transition metal carbonyls did not, may indicate that the former compounds are very poor shift catalysts.[23] Moreover, Mn and Co catalysts were also able to hydrogenate the substrates studied under sg conditions, while the other transition metal carbonyls were unreactive under these conditions.

We examined the reaction parameters and found that reduced product dramatically increased when carbon monoxide was removed from the reactions catalyzed by ruthenium carbonyls.

In initial experiments, we used $Ru(Cl)_2(CO)_2(\Phi_3P)_2$ as a catalyst. Interestingly, with this catalyst, both hydrogen and base were needed to reduce compound **1**.[24] No reaction occurred in the presence of carbon monoxide or in the absence of base. The reduction of **1** was highly regiospecific and gave exclusively 1,2,3,4-tetrahydroanthracene, **15**, in 30% yield.[25] A control experiment was performed to establish that 9,10-dihydroanthracene, **9**, was not the initial product formed; this product rearranged to compound **15**. We reacted **9** under similar reaction conditions and found that it did not produce compound **15**; hence, no rearrangement occurred.

Compounds **2** and **3** were unreactive under the reaction conditions, consistent with the previous finding that bent aromatic compounds are extremely unreactive versus the linear aromatics such as **1**. The polynuclear heteroaromatic nitrogen compounds, **4–8**, were reacted under similar conditions to produce poor to moderate yields of reduced product (Table 2). However, we found that the removal of base (KOH) in the reactions of **4–6** and **8** (but not **7**) with $Ru(Cl)_2(CO)_2(\Phi_3P)_2$ as catalyst provided an increase in the yields of all reduced products (Table 2). For example, compound **5** provided no reduced product with base present, while affording a 72% yield of 1,2,3,4-tetrahydro-7,8-benzoquinoline, **16**, in the absence of base. Additionally, as with compound **1**, carbon monoxide totally inhibited reduced product formation in the reactions of **4–8** with $Ru(Cl)_2(CO)_2(\Phi_3P)_2$ as catalyst. Interestingly, compound **8**, with $H_2$ and base, provided a small amount (5%) of the reduced aromatic ring compound 5,6,7,8-tetrahydroquinoline, which was not produced when base was omitted.

Table 2. Reductions of compounds **1–8** with $Ru(Cl)_2(CO)_2(\Phi_3P)_2$ and $H_4Ru_4(CO)_{12}$ as catalysts.

| Substrate | Catalyst | Products (%)[b] |
|---|---|---|
| **1** | $Ru(Cl)_2(CO)_2(\Phi_3P)_2$[a] | 1,2,3,4-tetrahydroanthracene (30) |
| **1** | $Ru(Cl)_2(CO)_2(\Phi_3P)_2$[c] | no product |
| **2** | $Ru(Cl)_2(CO)_2(\Phi_3P)_2$[a,c] | no product |
| **3** | $Ru(Cl)_2(CO)_2(\Phi_3P)_2$[a,c] | no product |
| **4** | $Ru(Cl)_2(CO)_2(\Phi_3P)_2$[a] | 1,2,3,4-tetrahydro-7,8-benzoquinoline (10) |
| **4** | $Ru(Cl)_2(CO)_2(\Phi_3P)_2$[c] | 1,2,3,4-tetrahydro-7,8-benzoquinoline (92) |
| **5** | $Ru(Cl)_2(CO)_2(\Phi_3P)_2$[a] | 1,2,3,4-tetrahydro-7,8-benzoquinoline (0) |
| **5** | $Ru(Cl)_2(CO)_2(\Phi_3P)_2$[c] | 1,2,3,4-tetrahydro-7,8-benzoquinoline (72) |
| **6** | $Ru(Cl)_2(CO)_2(\Phi_3P)_2$[a] | 9,10-dihydrophenanthridine (5) |
| **6** | $Ru(Cl)_2(CO)_2(\Phi_3P)_2$[c] | 9,10-dihydrophenanthridine (15) |
| **7** | $Ru(Cl)_2(CO)_2(\Phi_3P)_2$[a] | 9,10-dihydroacridine (100) |
| **7** | $Ru(Cl)_2(CO)_2(\Phi_3P)_2$[c] | 9,10-dihydroacridine (74) |
| **8** | $Ru(Cl)_2(CO)_2(\Phi_3P)_2$[a] | 1,2,3,4-tetrahydroquinoline (42)<br>5,6,7,8-tetrahydroquinoline (5) |
| **8** | $Ru(Cl)_2(CO)_2(\Phi_3P)_2$[c] | 1,2,3,4-tetrahydroquinoline (100) |
| **4** | $H_4Ru_4(CO)_{12}$[d] | 1,2,3,4-tetrahydro-5,6-benzoquinoline (75) |
| **5** | $H_4Ru_4(CO)_{12}$[d] | 1,2,3,4-tetrahydro-5,6-benzoquinoline (8) |
| **6** | $H_4Ru_4(CO)_{12}$[d] | 9,10-dihydrophenanthridine (15) |
| **7** | $H_4Ru_4(CO)_{12}$[d] | 9,10-dihydroacridine (100) |
| **8** | $H_4Ru_4(CO)_{12}$[d] | 1,2,3,4-tetrahydroquinoline (100) |

[a]Experiments were performed in a 45 ml Parr mini-reactor containing 1 m*M* of substrate, 0.1 m*M* $Ru(Cl)_2(CO)_2(\Phi_3P)_2$ in THF (12 ml), 0.2 *M* KOH (3 ml), 180°C, 350 psi $H_2$ for 5 hr, **1–7**, 2 hr, **8**.

[b]Analyzed by gas chromatography on a 12 m × 0.1 mm i.d. fused silica capillary column (OV101) using an HP-5880A instrument with flame ionization and digital integration. The percent product conversion was obtained by integration of product and any starting material remaining and normalizing to 100%. Products were isolated by column chromatography (Florisil) and identified by GC-MS and NMR spectroscopy ($^1H$, 250 mHz).

[c]180°C, THF (12 ml), 0.1 m*M* $Ru(Cl)_2(CO)_2(\Phi_3P)_2$, 1 m*M* substrate, 350 psi $H_2$ for 2 hr.

[d]Experiments were performed in a 45 ml Parr mini-reactor containing 1 m*M* of substrate, 0.1 m*M* $H_4Ru_4(CO)_{12}$ (10:1 substrate-to-catalyst ratio) in 15 ml of cyclohexane with 350 psi $H_2$ for 2 hr at 150°C.

In concurrent experiments, we discovered that tetrahydridotetraruthenium dodecacarbonyl, $H_4Ru_4(CO)_{12}$, was also an excellent catalyst for the hydrogenation of compounds **4–8** but was inactive for the reductions of compounds **1–3** under the conditions studied.[26,27] It was not, however, the initial

catalyst used; rather, we employed the catalytic activity of triruthenium dodecacarbonyl, $Ru_3(CO)_{12}$. We found that, under our reaction conditions, $H_4Ru_4(CO)_{12}$ readily formed (IR and MS analysis) by reaction of $Ru_3(CO)_{12}$ with hydrogen gas (Eq. 1)[27]:

$$4Ru_3(CO)_{12} + 6H_2 \rightarrow 3H_4Ru_4(CO)_{12} + 12CO \quad (1)$$

Under the latter reaction conditions, reduction of **4–8** was evident; however, catalytic activity increased dramatically if $H_4Ru_4(CO)_{12}$ was formed prior to substrate addition. In this process, CO was flushed from the system. Evidently, even a small partial pressure of CO [~10 psi CO was generated in the formation of $H_4Ru_4(CO)_{12}$ from $Ru_3(CO)_{12}$] was sufficient to inhibit substrate coordination to ruthenium and greatly reduced product yield. For example, $Ru_3(CO)_{12}$ provided a 7% yield of 1,2,3,4-tetrahydro,-5,6-benzoquinoline (**17**) from **4**, while $H_4Ru_4(CO)_{12}$ produced the same product in 75% yield.

Tetrahydridotetraruthenium dodecacarbonyl has been previously described as a hydrogenation catalyst for olefins, carboxylic acids and ketones,[28,29] but, to our knowledge, never for polynuclear heteroaromatic nitrogen compounds.[30] As with $Ru(Cl)_2(CO)_2(\Phi_3P)_2$, the results of these catalytic hydrogenations with $H_4Ru_4(CO)_{12}$ indicate high regioselectivity for the nitrogen heterocyclic ring.

## PLANNED ACTIVITIES FOR FY 1983

This study has provided evidence for the individual reactivity of a number of model synthetic fuel compounds under homogeneous catalytic hydrogenation conditions. However, their relative reactivities need to be ascertained, especially in mixtures of these compounds and in the presence of other polynuclear heterocyclics (e.g., sulfur and oxygen heterocycles). Also, work on the many mechanistic details, as well as expansion to the reactivities of polynuclear heterocyclic compounds of oxygen and sulfur, and the activity of heterogenized forms of the reported catalysts, is being pursued.[31]

Finally, our results point to the possible usefulness of these homogeneous catalysts and others in future synthetic fuel processes concerned with ultimately removing nitrogen from the nitrogen-containing ring in polynuclear heterocyclic nitrogen compounds.[32] The reported catalysts may also find some important uses in synthetic organic chemistry.[33]

## REFERENCES


1. Whitehurst, D.D., Ed. (1980), *Coal Liquefaction Fundamentals,* ACS Symposium Series 139, American Chemical Society, Washington, D.C.
2. Larsen, J.W., Ed. (1978), *Organic Chemistry of Coal,* ACS Symposium Series 7, American Chemical Society, Washington, D.C.
3. Yen, T.F., and Chillingarian, G.V., Eds. (1976), *Development of Petroleum Science,* Vol. 5, "Oil Shale," Elsevier Scientific Publishing Co., Amsterdam.
4. Kang, H.C., et al. (1977), "Reductions with Carbon Monoxide and Water in Place of Hydrogen. 1. Hydroformylation Reaction and Water Gas Shift Reaction," *J. Amer. Soc. 99,* p. 8923 and references therein.
5. Cann, K., et al. (1978), "Catalytic Reductions Using Carbon Monoxide and Water in Place of Hydrogen. 2. Reduction of Aromatic Nitro Compounds to Amines," *J. Amer. Chem. Soc.* 100, p. 3969.
6. Cole, T., et al. (1980), "Hydrogeneous Catalyst for Utilization of Synthesis Gas as a Reducing Agent," *J. Amer. Chem. Soc. 102,* p. 6182.
7. Grice, N., Kao, S.C., and Pettit, R. (1979), "Chemical Properties of Metallocarboxylic Acids of Transition Metals," *J. Amer. Chem. Soc. 101,* p. 1627.
8. Darensbourg, D.J., Baldwin, B.J., and Froelich, J.A. (1980), "Phase-Transfer-Catalyzed Nucleophilic Reactions of Hydroxide Ions at Metal-Bound Carbon Monoxide Centers," *J. Amer. Chem. Soc. 102,* p. 4688.
9. Ford, P.C. (1981), "The Water-Gas Shift Reaction: Homogeneous Catalysis by Ruthenium and Other Metal Carbonyls," *Accts. Chem. Res. 14,* p. 31.
10. Kaesz, H.D., and Saillant, R.B. (1972), "Hydride Complexes of the Transition Metals," *Chem. Rev. 72,* p. 231, and references therein.
11. James, B.J. (1973), *Homogeneous Hydrogenation,* John Wiley and Sons Inc., New York (1973).

12. Parshall, G.W. (1980), "Organometallic Chemistry in Homogeneous Catalysis," *Science 2098,* p. 1221.
13. Fish, R.H., Thormodsen, A.D., and Cremer, G.A. (1982), "Homogeneous Catalytic Hydrogenations, 2: Regiospecific Reductions of Polynuclear Aromatic and Polynuclear Heteroaromatic Nitrogen Compounds Catalyzed by Transition-Metal Carbonyl Hydrides," *J. Amer. Chem. Soc. 104,* p. 5234. Lawrence Berkeley Laboratory Reports LBL-13734 and LBL-13735.
14. GC-EI mass spectral analysis showed *m/e* 182 (100%), consistent with two deuterium atoms being incorporated into compound **1** *(m/e* 178).
15. The *cis* and *trans* isomers of 9,10-dihydro-9,10-dimethylanthracene (**12, 13**) could be cleanly separated on a 12 m × 0.1 mm i.d., fused silica capillary column (OV 101) using a HP 5880A instrument with flame ionization detection (temperature programming 60°–200°C, 10°/min).
16. Sweany, R., Butler, S.C., and Halpern, J. (1981), "The Hydrogenation of 9,10-Dimethylanthracene by Hydridopentacarbonyl Management (I.). Evidence for a Free Mechanism," *J. Org. Chem. 213,* p. 487.
17. Taylor, P.D. and Orchin, M.J. (1972), "Hydrogenation of 9,10-Dimethylanthracene with Cobalthydride Carbonyl," *J. Org. Chem. 37,* p. 3913.
18. Friedman, S., et al. (1959), "Selective Hydrogenation of Polynuclear Aromatic Hydrocarbons," *J. Org. Chem. 24,* p. 1287.
19. Derencsenyi, T.T., and Vermeulen, T. (1979), *Kinetics and Mechanism of Metal-Carbonyl-Catalyzed Hydrogenation of Aromatic Hydrocarbon Models for Coal Constituents* (Ph.D. dissertation of T.T.D.), Lawrence Berkeley Laboratory Report LBL-9777; also (1980), *Chem. Abs. 93,* no. 188929.
20. Laine, R.M., Thomas, D.W., and Cary, L.W. (1979), "Catalytic Reactions of Pyridine with Carbon Monoxide and Water. Reduction of Carbon Monoxide to Hydrocarbon. Applications of the Water-Gas Shift Reaction," *J. Org. Chem. 44,* p. 4964.
21. Jardine, I. and McQuillin, F.J. (1970), *Chem. Comm.,* 626.
22. Dewar, M.J.S. (1969), *The Molecular Orbital Theory of Organic Chemistry,* McGraw-Hill, New York.
23. For example, we found that $Mn_2(CO)_8(Bu_3P)_2$ did not produce $CO_2$ and $H_2$ to any significant extent in the absence of substrates **1–8** under wgs conditions (350 psi CO, 0.2 *M* KOH, 200° for 5 hr gave 10 psi $H_2$). Selected gas analysis under wgs conditions gave a qualitative order of wgs activity as follows: $Rh_6(CO)_{16} > Ru_3(CO)_{12} > Cr(CO)_6 > Mo(CO)_6 > W(CO)_6 > Fe(CO)_5 > Mn_2(CO)_{12} > Co_2(CO)_8$.
24. $Ru(Cl)_2(CO)_2(\Phi_3P)_2$ has been described as a homogeneous hydrogenation catalyst ($H_2$) for aliphatic and aromatic aldehydes [Strohmeier, W. and Weigelt, L. (1978), *J. Organometal. Chem. 145,* 189]; however, no references to its use as a homogeneous catalyst for polynuclear aromatic or heteroaromatic compounds have been found.
25. A similar regioselectivity was obtained with **1** and a ruthenium anion hydride under strictly $H_2$ conditions. See Grey, R.A., Pez, P.G., and Wallo, A. (1980), "Selective Homogeneous Catalytic Hydrogenation of Polynuclear Aromatics," *J. Amer. Chem. Soc. 102,* p. 5948, and references therein.
26. Piacenti, F., Bianchi, M., Frediani, P., and Benedetti, E. (1971), "Preparation and Reactivity of Some Ruthenium Carbonyl Hydrides," *Inorgan. Chem. 10,* p. 2759.
27. Knox, S.A.R., Keopke, J.W., Andrews, M.A., and Kaesz, H.D. (1975), "Synthesis of Hydrido- and Deuterio-Carbonyl Cluster Complexes of Ruthenium, Iron-Ruthenium, and Osmium from Metal Carbonyls and Hydrogen at Atmospheric Pressure," *J. Amer. Chem. Soc. 97,* p. 3943.
28. Valle, M., Osella, D., and Vaglio, D. (1976), *Inorg. Chem. Acta. 20,* p. 213, and references therein.
29. Bianchi, M., et al. (1980), "Homogeneous Catalytic Hydrogenation of Free Carboxylic Acids in the Presence of Cluster Ruthenium Carbonyl Hydrides," *J. Organometal. Chem. 188,* p. 109.
30. Infrared analysis of the yellow-colored reaction solutions of compounds **4–8** clearly shows $H_4Ru_4(CO)_{12}$ still present after reaction. More

important, no "heterogeneous" component was found after reaction at 150°C for the $H_4Ru_4(CO)_{12}$ catalyzed hydrogenations. The infrared analysis does not unequivocally demonstrate that $H_4Ru_4(CO)_{12}$ is the actual active catalyst, as pointed out by a referee, and we are presently running these reactions in a spectroclave (high-pressure RI cell) to clarify this point.

31. A preliminary account was presented at the 182nd National American Chemical Society Meeting, August 23-28, 1981, New York (Abstract Inorg. 49), and at the Pacific Conference on Chemistry and Spectroscopy, Anaheim, CA, October 19-21, 1981 (Abstract 188).
32. Laine, R.M., Thomas, D.W., and Cary, L.W. (1982), "Modeling Heterogeneous Catalysts with Homogeneous Catalysts. 2. Modeling Catalytic Hydrodenitrogenation," *J. Amer. Chem. Soc. 104*, p. 1763.

# MOLECULAR CHARACTERIZATION AND FINGERPRINTING OF VANADYL PORPHYRIN AND NON-PORPHYRIN COMPOUNDS FOUND IN VARIOUS HEAVY CRUDE PETROLEUMS AND THEIR ASPHALTENES*

*R.H. Fish, J.J. Komlenic, B. Wines, and T. Vermeulen*

As reserves of light crude oil throughout the world decrease, and as the nation switches to a more diversified and self-sufficient energy base, the processing of heavy crude petroleums and residuals will become increasingly important. In the past, primarily because of uneconomical catalyst poisoning effects associated with naturally occurring trace metal compounds in these oils, processing of such heavy crude feedstocks has been limited.[1-8] Although the concentrations of these trace metals—primarily vanadium and, to a lesser extent, nickel—are small, usually at the parts per million level, their harmful effects—both to the processing catalyst and, potentially, to the environment—are severe.

To design processes capable of efficiently removing vanadium and nickel from heavy crude oils before processing, it is essential to characterize or speciate the vanadium- and nickel-bearing compounds present. Such knowledge will be valuable in several ways. The information will help us to:

(1) design selective separation, removal, and recovery processes[9,10];
(2) explore for and process suitable heavy crude-oil feedstocks;
(3) identify oils in future pollution abatement efforts; and
(4) derive important geochemical information about the origin and biogenesis of heavy crude petroleum deposits.[11]

## ACCOMPLISHMENTS DURING FY 1982

### Speciation Using HPLC–GFAA

The automatic coupling of a high-performance liquid chromatograph to a graphite furnace atomic absorption spectrometer (HPLC–GFAA) is a promising means of speciating unidentified vanadyl compounds in heavy crude oils. This coupling of instruments provides continuous, on-line, element-specific detection of HPLC effluent peaks and combines the versatility, speed, and efficiency of HPLC with the selectivity and sensitivity of GFAA detection. This coupled system has been described elsewhere.[12-13]

### Model Vanadyl Porphyrin and Non-Porphyrin Compounds

Speciation using the HPLC–GFAA technique requires a large collection of model compounds in order to compare and characterize the elution behavior of unidentified components.[14,15]

Figure 1 shows VOEtio, VODPEP, and VORhodo porphyrin compounds that have been identified in heavy crude oils, as well as model vanadyl porphyrins and non-porphyrins used in this study. Porphyrin compounds consist of a 16-member ring containing

*This work was supported by the Assistant Secretary for Fossil Energy and the Division of Oil, Gas and Shale Technology, and the Bartlesville Energy Technology Center of the U.S. Department of Energy under Contract No. DE-AC03-76SF00098.

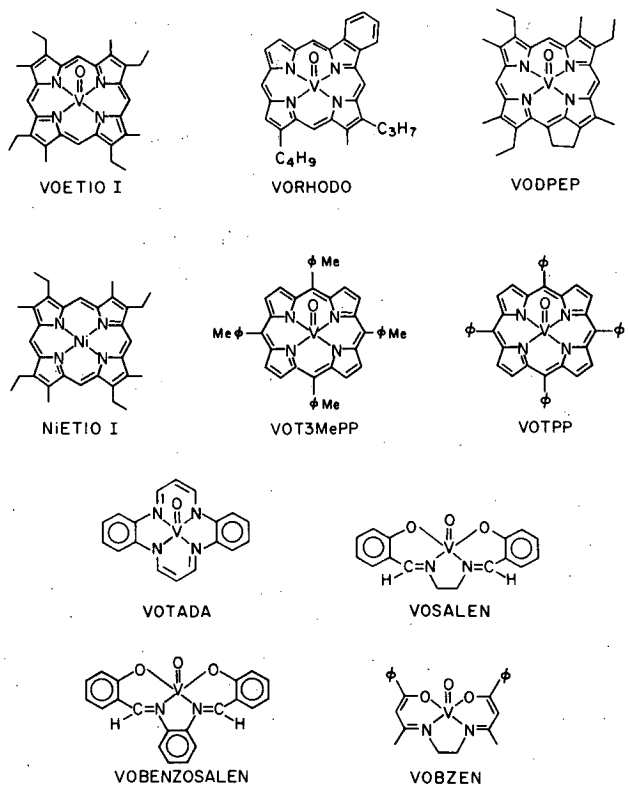


Figure 1. Model vanadyl porphyrin and non-porphyrin compounds. (XBL 8211-3357)

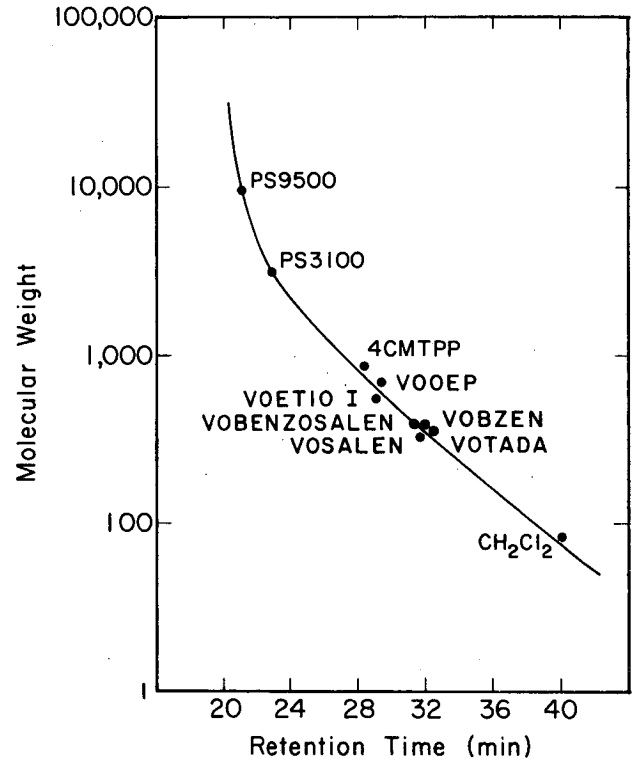


Figure 2. Log plot of molecular weight versus retention time for the 50/100 Å column combination. (XBL 826-10469)

four nitrogen donor atoms located in four conjugated pyrole groups. When a vanadyl ion is incorporated into this structure, these systems are extremely stable. VOT3MePP and VOTPP represent synthetic (not occurring in nature) vanadyl porphyrins that, because of the added conjugation of the peripherally attached phenyl rings, are stable in strong acid solutions.

Vanadyl non-porphyrins constitute a much broader class of compounds, with ring sizes varying from 12 to 16 members and with nitrogen, oxygen, and sulfur, in a variety of combinations, constituting the donating atoms. Although they give characteristic absorbances in the UV region of the spectrum, absorbance in the visible region is possible, depending on the extent of ring conjugation. Unlike vanadyl porphyrins, most vanadyl non-porphyrins decompose readily in dilute acid solutions. VOBenzosalen, VOSalen, VOTADA, and VOBZEN represent vanadyl non-porphyrin compounds that have yet to be identified in heavy crude petroleums.

The SEC calibration plot for the 50/100 Å column combination, which gives a linear working range of 100 to 3000 daltons, is shown in Fig. 2. Vanadyl porphyrin and non-porphyrin compounds have again been used as calibration standards, to minimize error when assigning molecular weights to components in the petroleum samples. Polystyrene standards of 3100 and 9500 daltons have been used to calibrate the high molecular weight ranges, since no vanadyl compounds at these ranges were available.

The 50/100 Å SEC–HPLC–GFAA data for the separation of several of the standards is shown in Fig. 3 (a). The polystyrene standards were monitored at 254 nm, the vanadyl porphyrins and the metal-free porphyrin at 400 nm, and the vanadyl non-porphyrin compounds at 320 nm. The lower portion of Fig. 3 (a) shows the GFAA vanadium histograms. The added 100 Å column provides increased resolution of molecules with molecular weights greater than 900 daltons, allowing for accurate determination from 100 to slightly greater than 2000 daltons. All quantitative calculations in this study have therefore been based on the 50/100 Å column combination.

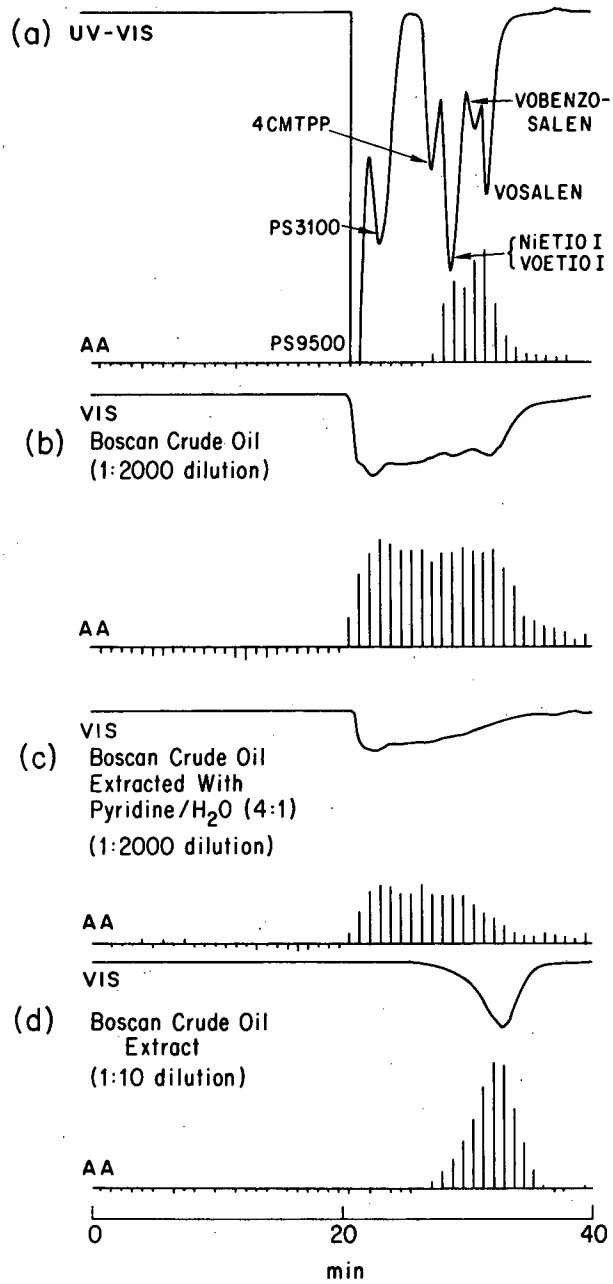


Figure 3. Combined 50/100 Å column SEC–HPLC–GFAA data for (a) standards, (b) Boscan crude oil, (c) crude oil after extraction, and (d) crude oil extract.

(XBL 826-10466)

The results shown in Fig. 2 were used to classify vanadyl compounds in the heavy crude oils by assigning them to one of four molecular-weight categories. In the first two categories, compounds with molecular weights of less than 400 daltons were classified as low-molecular-weight vanadyl non-porphyrins, and those between 400 and 900 daltons as vanadyl porphyrins, according to the definitions of these compound classes. With molecular weights above 900 daltons, vanadyl porphyrins cannot be present because of the increased ring conjugation that would be necessary. Instead, compounds with molecular weights between 900 and 2000 daltons were classified as high-molecular-weight vanadyl compounds, and, above 2000 daltons, as very high molecular weight vanadyl compounds. These latter two categories could include both low-molecular-weight vanadyl porphyrins and non-porphyrins intercalated into the asphaltenes, and high-molecular-weight vanadyl porphyrin and non-porphyrin compounds existing as asphaltenes.

Although vanadyl porphyrin compounds are not normally associated with molecular weights greater than 900 daltons, complexation to the asphaltene fraction of the oil could drastically increase their apparent molecular weight and change their physical and chemical properties. Likewise, low-molecular-weight vanadyl non-porphyrins could be incorporated into the asphaltene fraction of the oil by H–H interaction or hydrogen bonding, drastically altering their stability and other spectroscopic properties.

Figures 3 (b), (c), and (d) show the 50/100 Å column combination data for Boscan crude oil, the oil after extraction, and the extract, respectively. The upper portion of Fig. 3 (b) shows the visible absorbance, measured at 408 nm, while the lower portion gives the vanadium histogrammic output. The histogrammic peaks show vanadium in Boscan crude eluting at retention times from 20 to 40 minutes, corresponding to molecular weights ranging from more than 10,000 to 100 daltons. Interestingly, the HPLC–GFAA output shows that Boscan crude contains nearly equivalent percentages of vanadyl compounds in all four molecular-weight categories.

Figure 3 (c) shows vanadyl compounds being removed from the entire molecular-weight range of the crude oil. However, as evidenced in Fig. 3 (d), only vanadyl compounds with retention times greater than 28 minutes and centered at 32 minutes, corresponding to a molecular weight of 350 daltons, exist in the extract. Thus, although vanadyl compounds have been extracted from molecular weights greater than 900 daltons, only low-molecular-weight (less than 400 daltons) vanadyl porphyrin and non-

porphyrin compounds are present in the extract.

On the basis of the accuracy of the calibration data in Fig. 2, most of the vanadyl compounds in the extract can be classified as vanadyl non-porphyrins. The absence of high-molecular-weight vanadyl compounds from the extracts indicates that pyridine did not remove them from the oil. This raises important questions regarding the chemical nature of the non-extractable vanadyl compounds remaining in the asphaltenes.

Comparisons of the four oils, based on the SEC–HPLC–GFAA fingerprints from selective solvent extraction experiments, reveal several important features. Although the vanadium concentration varies widely, each oil contains a nearly similar percentage of all four molecular-weight categories. Geochemically, this is important, because it suggests that a similar mechanism of incorporation and competition for ligand sites occurs for the four oils. Also, vanadyl compounds remaining after extraction are evenly distributed between the two higher molecular-weight classes. This suggests that these heavier vanadyl compounds are similarly complexed. Of the three oils studied, only Prudhoe Bay crude shows any high-molecular-weight vanadyl compounds present in the extracts; this may be accounted for by a difference in the biogenesis and maturation of this relatively ancient petroleum.

Molecular-weight data for the four oils, based on the 50/100 Å SEC column combination, are summarized in Table 1. This table shows the vanadium concentrations (ppm) and percentage distributions for

Table 1. Molecular-weight distributions of vanadyl compounds present in heavy crude oils, oils after extraction, and the extracts, as determined by 50/100 Å SEC-HPLC-GFAA analysis.

| Source | Molecular Weight | >2000 | <2000 >900 | <900 >400 | <400 | >2000 | <2000 >900 | <900 >400 | <400 |
|---|---|---|---|---|---|---|---|---|---|
| | | Boscan | | | | Cerro Negro | | | |
| Heavy crude oil | V (ppm) | 307.[a] | 229. | 257. | 315. | 175. | 123. | 114. | 148. |
| | V(%) | 27.9[b] | 20.0 | 23.4 | 28.7 | 31.3 | 21.9 | 20.4 | 26.4 |
| Oil after extraction | V (ppm) | 176. | 128. | 127. | 109. | 106. | 93.0 | 55.7 | 25.2 |
| | V (%) | 32.6 | 23.7 | 23.6 | 20.1 | 37.9 | 33.2 | 19.9 | 9.0 |
| Removed | V(ppm) | 131. | 92. | 130. | 206. | 69.0 | 30.0 | 58.3 | 123. |
| | V (%) | 42.3 | 41.8 | 50.7 | 65.4 | 39.4 | 24.4 | 51.1 | 83.0 |
| Extract | V (ppm) | — | 6.0 | 136.0 | 418. | — | — | 74.0 | 206. |
| | V (%) | — | 1.1 | 24.3 | 74.6 | — | — | 26.4 | 73.6 |
| | | Wilmington | | | | Prudhoe Bay | | | |
| Heavy crude oil | V (ppm) | 13.8 | 11.1 | 9.3 | 14.3 | 5.8 | 5.3 | 4.3 | 3.3 |
| | V (%) | 28.5 | 22.9 | 19.1 | 29.5 | 31.1 | 28.6 | 22.9 | 17.4 |
| Oil after extraction | V (ppm) | 2.6 | 1.8 | 1.1 | 0.9 | 3.2 | 2.8 | 2.1 | 1.1 |
| | V (%) | 40.2 | 28.3 | 16.8 | 14.7 | 34.6 | 30.6 | 22.9 | 11.9 |
| Removed | V (ppm) | 11.2 | 9.3 | 8.2 | 13.4 | 2.6 | 2.5 | 2.2 | 2.2 |
| | V (%) | 81.1 | 83.8 | 88.2 | 93.7 | 44.8 | 47.2 | 51.1 | 66.7 |
| Extract | V (ppm) | 0.3 | 0.8 | 7.5 | 33.5 | 0.5 | 0.5 | 3.1 | 5.4 |
| | V (%) | 0.8 | 1.9 | 17.8 | 79.5 | 5.0 | 5.0 | 32.9 | 57.1 |

[a]Concentration of metal present at molecular weights greater than 2000 daltons.

[b]Percentage of total metal present at molecular weights greater than 2000 daltons.

the whole crudes, the oils after extraction, and the extracts in terms of the four molecular weight categories. The vanadium percentages were calculated using the 50/100 Å SEC calibration data from Fig. 2 and the digitally recorded histogrammic outputs. From Fig. 2, the retention times for eluting species in each molecular-weight category were ascertained. The histogrammic vanadium outputs in each category were then summed and divided by the total histogrammic output for each oil, as summed over all four molecular-weight categories.

The vanadium concentrations (in ppm) were then calculated by multiplying each percentage by the total amount of vanadium present in the heavy crude oils and in the oils after five extractions. The vanadium concentrations for the extracts were calculated from the amount of vanadium removed by extraction from each oil. Values for vanadium removal were calculated by subtracting vanadium concentrations after extraction from those concentrations before extraction for each molecular-weight category; the corresponding percentages were calculated by dividing the vanadium concentration for each molecular-weight category by the total vanadium extracted from each crude oil.

Although the total amount of vanadium in Boscan, Cerro Negro, and Wilmington crude oils varies substantially, the percentages of vanadyl compounds present in each molecular-weight category are very similar. As Table 1 indicates, they have nearly equal percentages of vanadyl compounds in the heaviest and lightest classes (greater than 2000 and less than 400 daltons) and also contain nearly equivalent percentages of vanadyl compounds in the intermediate classes. These three oils have approximately 10% less vanadium in the two intermediate molecular-weight fractions than in both the heaviest and lightest fractions. Prudhoe Bay crude, however, has increasing percentages of vanadyl compounds as molecular weight increases over all four fractions.

As Table 1 shows for the crude oils after extraction, the percentages of vanadyl compounds with molecular weights greater than 2000 daltons increased for all four oils. The increases ranged from 11% for Prudhoe Bay oil to 41% for Wilmington oil, for an average increase of 22%. The percentages of vanadyl compounds between 900 and 2000 daltons also increased, from 7% for Prudhoe Bay to 52% for Cerro Negro, for an average increase of 25%. The percentages of vanadyl compounds with molecular weights between 400 and 900 daltons decreased by 2 and 12% for Cerro Negro and Wilmington oils, but remained equal for Prudhoe Bay and increased by 1% for Boscan. The percentages of vanadyl compounds of less than 400 daltons decreased for all four oils, from 30% for Boscan to 66% for Cerro Negro, an average decrease of 44%.

Table 1 also shows the weight percentages of vanadyl compounds removed from the four molecular-weight categories for each oil. While the oils show a trend toward increased removal at decreased molecular weights (especially for less than 400 daltons), Wilmington crude oil shows significantly more vanadium removal over all four fractions.

That extraction of vanadyl compounds from the low-molecular-weight categories was greater than that from the high-weight categories is not surprising. Vanadyl porphyrin and non-porphyrin compounds in the low-molecular-weight, malthene fraction of the crude oils occur freely suspended and are therefore more likely to form ligational complexes. Vanadyl compounds in the high-molecular-weight, asphaltene fraction can be strongly complexed to the asphaltenes, making removal more difficult and sometimes impossible.

Finally, Table 1 shows the amounts and percentages of vanadyls in the four weight categories for each crude-oil extract. These data indicate that most of the vanadyl compounds in each extract exist at molecular weights of less than 400 daltons. Cerro Negro extract contains no vanadyl compounds above 900 daltons. Of the other extracts, only Prudhoe Bay has significant amounts of vanadyl compounds at molecular weights greater than 900 daltons.

This finding is important because it reveals that, although vanadyl porphyrin compounds are present in the extracts, they account for only 18 to 33% of the total vanadium present. The majority of the vanadyl compounds in the extracts are low-molecular-weight vanadyl non-porphyrin compounds. Demetallation of the pyridine extracts conceivably prohibits identification of these compounds because of their instability in dilute acid solutions.

This lack of high-molecular-weight vanadyl compounds in three of the four extracts suggests that, if distinct species are in fact present, removal of these highly conjugated molecules with coordinating solvents will be difficult.

## SEC–HPLC–GFAA Analysis of Heavy Crude Asphaltenes

The asphaltenes in the heavy crude oils contain a significant percentage of the vanadium, and thus examination of their content for vanadyl porphyrin and non-porphyrin compounds by HPLC–SEC–GFAA analysis would be critical. Additionally, extraction of the asphaltenes with a pyridine/$H_2O$ solution would be helpful in learning more about non-porphyrin vanadyl compounds complexed to the macromolecular structure of the asphaltenic fraction.

During this year, work has continued with the asphaltenes of Boscan, Cerro Negro, Wilmington, and Prudhoe Bay heavy crude oils. Separation is achieved by agitating samples in 10 volumes of pentane at about 300 motions per minute for 24 hours. Separations have also been made using heptane as the solvent, but these samples have not yet been analyzed. The asphaltenes are separated from the pentane solubles with a 0.45 micron Millipore filter, washed with pentane, and stored under nitrogen. X-ray fluorescence analysis for vanadium has been performed and compared with earlier results for whole crude oils (Table 2). A significant percentage of the vanadium in the oils is contained in the asphaltenes. The percentage of vanadium in the asphaltenes is not directly proportional to the amount of asphaltenes present in an oil; and although the asphaltenes represent less than 3% of the weight of a crude, they still account for almost half of the vanadium present.

Samples of the asphaltenes are redissolved in methylene chloride and analyzed by HPLC–SEC–GFAA using 50Å and 100Å SEC columns in series with element-specific vanadium detection at 318.4 nm. The visible detector was set at 408 nm to detect the soret bands of vanadyl porphyrins. The extraction and analysis were repeated three times for each oil. Figure 4 shows a typical SEC result. The asphaltenes were separated into the four molecular-

Table 2. Concentrations of vanadium in heavy crude oils and asphaltenes.

| Sample | ppm V in crude oil | ppm V in asphaltene | Wt.% of asphaltene in crude | Wt.% of total V in asphaltene |
|---|---|---|---|---|
| Boscan | 1100 | 4310 | 25 | 98 |
| Cerro Negro | 560 | 1680 | 20 | 60 |
| Wilmington | 49 | 422 | 6.2 | 53 |
| Prudhoe Bay | 19 | 280 | 2.9 | 43 |

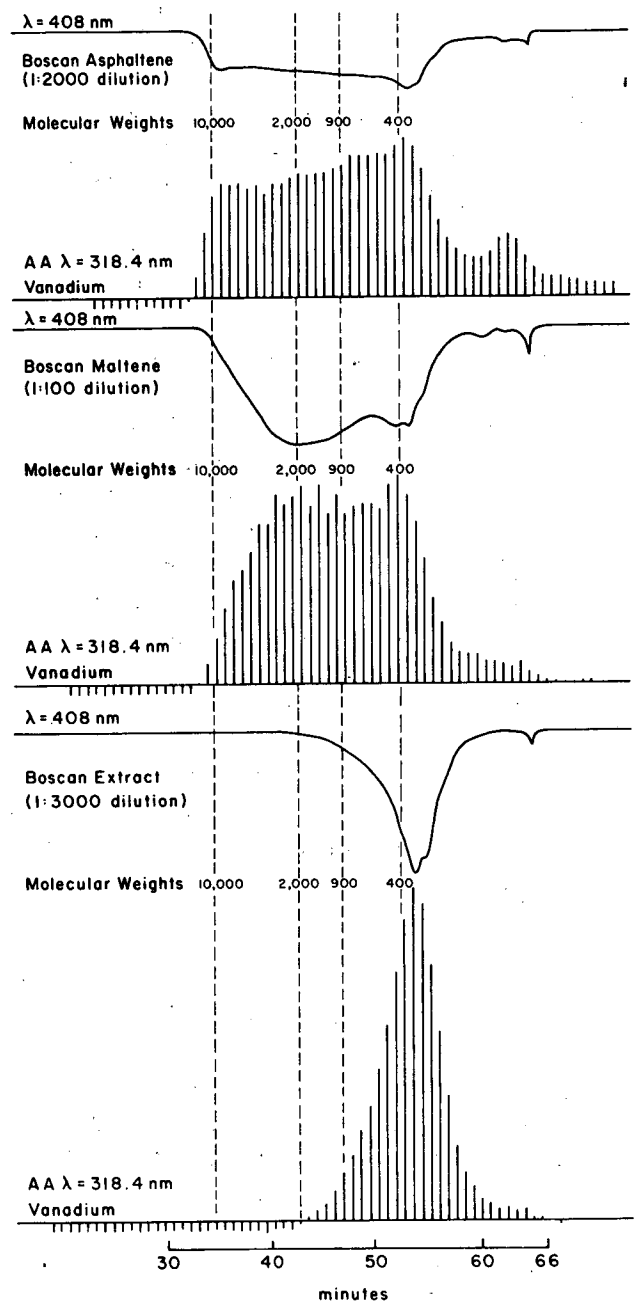


Figure 4. Combined 50/100/1000 Å column SEC–HPLC–GFAA analysis of Boscan asphaltene, malthene, and asphaltene extracts. (XBL 8210-3112)

weight fractions used before: greater than 2000, between 2000 and 900, between 900 and 400, and less than 400. The third fraction is assumed to be rich in vanadyl porphyrins. It can be shown that the percentage of vanadium in the 900-to-400 fraction is much lower for the asphaltenes. This does not mean that fewer porphyrins are in the asphaltenes, but rather that the asphaltenic porphyrins are incorporated into larger complexes, because there is intense visible absorption in the highest molecular-weight fraction.

The pentane-soluble, malthene fractions of the oils were vacuum-distilled to remove the pentane and then dissolved in methylene chloride for HPLC–SEC–GFAA analysis. Figure 4 shows a typical vanadium distribution for the malthene of Boscan heavy crude oil. By comparing the asphaltenes and malthenes with their whole oils, it can be observed that, in general, the asphaltenes are richer in the high-molecular-weight vanadium compounds, while the malthenes are richer in the two middle fractions. The heavier vanadium concentrations in the very highest and very lowest fractions of the asphaltenes conform well with the concept of asphaltenes as large molecules with smaller molecules encapsulated within them. It is also interesting to note that Boscan crude, which has the highest asphaltenic vanadium concentration of the four oils studied, has an asphaltenic vanadium distribution very similar to the vanadium distribution of the whole crude oil.

The four oils can also be divided into two groups: high-asphaltene oils, including Boscan and Cerro Negro, and low-asphaltene oils, including Wilmington and Prudhoe Bay. The high-asphaltene oils have similar molecular-weight distributions of vanadium in their asphaltenes and whole oils and have similar percentages of vanadium in the highest and lowest molecular-weight ranges of the asphaltenes. The low-asphaltene oils have more extreme variations in vanadium distribution between the asphaltenes and the whole oils, and their vanadium concentrations are significantly greater in the heaviest range than in the lightest. This feature is especially pronounced in the lowest-asphaltene oil, Prudhoe Bay, which has 57% of its vanadium in the greater-than-2000 range and only 17% in the less-than-400 range.

We have also attempted to isolate vanadyl porphyrins from the asphaltenes. Following a procedure similar to that used by other researchers, the asphaltenes were dissolved in xylene and extracted with a pyridine-water solution. The extracts have a strong absorbance at 408 nm, typical for vanadyl porphyrins. Of the four crude oils, only Boscan and Cerro Negro gave extracts with sufficiently large vanadium concentrations to make GFAA analysis possible. Analysis using the HPLC–SEC–GFAA combination showed that a substantial portion of the vanadium present in these two extracts had a molecular weight too small for porphyrins (Table 3). Further analysis with a second HPLC system equipped with an amino-cyano column and a rapid scanning UV–VIS detector has established the presence of several vanadyl non-porphyrin compounds in the pyridine-water extract. Future work will characterize these compounds.

Table 3. Vanadium distribution in pyridine-water extracts of asphaltenes (percent of total V in four classes of molecular weights).

| Sample | Molecular Weight | | | |
|---|---|---|---|---|
| | >2000 | <2000 >900 | <900 >400 | <400 |
| Boscan Extract | 4 | 18 | 39 | 39 |
| Cerro Negro Extract 4 | 20 | 36 | 40 | — |
| Boscan Filtrate | 54 | 24 | 12 | 10 |

## PLANNED ACTIVITIES FOR 1983

We will continue to work on the speciation of vanadyl non-porphyrin compounds in heavy crude petroleums and their asphaltenes; we expect the resulting knowledge may lead to rational removal methods and contribute to understanding catalyst poisoning phenomena.

## REFERENCES


1. Silbernagel, B.G., (1979), *J. Catalysis 56*, p. 315.
2. Silbernagel, B.G., Riley, K.L. (1980), in *Catalyst Deactivation*, B. Delmon and G.F. Froment, Eds., Elsevier Scientific Publishing Co., p. 313.
3. Sie, S.T. (1980), in *Catalyst Deactivation*, B. Delmon and G.F. Froment, Eds., Elsevier Scientific Publishing Co., p. 545.

4. Rahbe, G., Pachano, J., Krasuk, J.H., and Rodriquez, O. (1978), *J. Japan Petrol. Inst. 21*, p. 2.
5. Hung, C., and Wei, J. (1980), *Ind. Eng. Chem. Process Des. Dev. 19*, p. 250.
6. Hung, C., and Wei, J. (1980), *Ind. Eng. Chem. Process Des. Dev. 19*, p. 257.
7. Morales, A., and Galiasso, R. (1982), *Fuel 61*, p. 13.
8. Fish, R., and Tannous, R.S., (1982), *Organometallics 1*, p. 1238.
9. Bottino, Finocchiaro, P., Libertini, E., Reale, A., and Recca, A. (1980), *Inorg. Nucl. Chem. Letters 16*, p. 417.
10. Hodgson, G.W. (1973), *Ann. N.Y. Acad. Sci. 206, p. 417.*
11. Hodgson, G.W., (1973), *Ann. N.Y. Acad. Sci. 206, p. 670.*
12. Andrae, M.O., Klumpp, D. (1979), *Environ. Sci. Technol. 13*, p. 738.
13. Brinckman, F.E., Bellama, J.M., Eds. (1978), *Organometals and Organometalloids: Occurrence and Fate in the Environment,* ACS Symposium Series 82, American Chemical Society, Washington, D.C.
14. Fish, R.H., Jewett, K.L., and Brinckman, F.E. (1982), *Environ. Sci., and Tech. 16*, p. 174, and references therein.
15. Brinckman, F.E., and Fish, R.H., Eds. (1981), *Environmental Speciation and Monitoring Needs for Trace Metal-Containing Substances from Energy-Related Processes,* National Bureau of Standards Special Publication 618.

## SYNTHESIS, STRUCTURAL ELUCIDATION, AND STEREOCHEMISTRY OF FIVE-COORDINATE ORGANOARSENIC CATECHOLATES*

*R.H. Fish and R.S. Tannous*

Recently, we have been investigating the speciation or molecular characterization of organoarsenic compounds thought to be present in oil shale kerogen and the products of its pyrolysis, including the retort waters.[1,2] These studies led to the identification, for the first time, of methyl and phenylarsonic acids in these precursors and products.

We have since initiated studies to find innovative methods of removing these compounds and other organometallics from fossil fuel products. In this regard, we have been experimenting with a method that utilizes substituted catechols as potential ligands that could be placed in a polymeric matrix for the future removal of organoarsenic compounds from the above mentioned products.

Surprisingly, we found very few references on the reactions of catechols with alkyl or arylarsonic acids[3-8] and none on similar reactions with substituted catechols.[9]

### ACCOMPLISHMENTS DURING FY 1982

Chart 1 shows the catechols, **1–4**, that we used in the reactions with methyl and phenylarsonic acid, **5** and **6**. Compound **1** reacts with either **5** or **6** to provide a mixture of *cis* and *trans* five-coordinate organoarsenic catecholates **7–10** (Eq. 1).

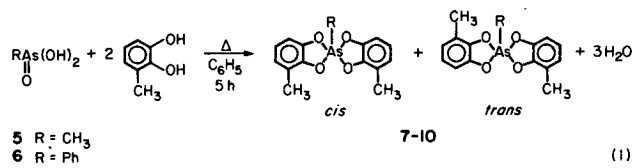


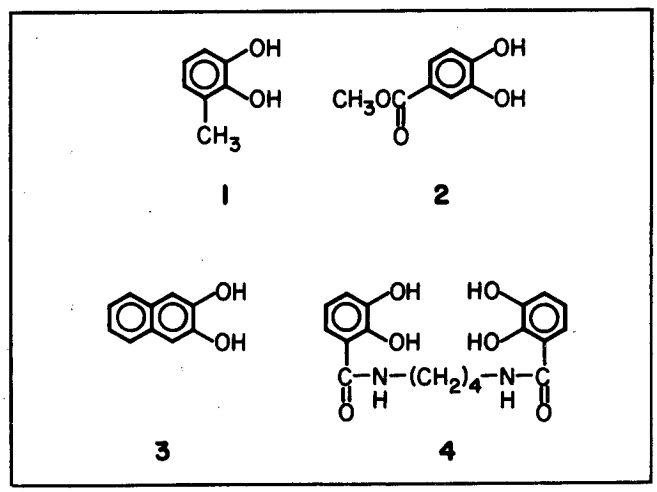


Chart 1. Catechols used in the synthesis of five-coordinate organoarsenic catecholates. (XBL 823-8458)

*This work was supported by the Assistant Secretary for Fossil Energy and the Division of Oil, Gas and Shale Technology, and the Bartlesville Energy Technology Center of the U.S. Department of Energy under contract No. DE-AC03-76SF00098.

Compounds **7–10** were characterized by a combination of nuclear magnetic resonance spectroscopy (NMR), mass spectrometry (MS), infrared spectroscopy (IR), and elemental analysis.[10] The 250 MHz $^1H$ NMR spectrum provided definitive evidence that compound **1** reacted with either **5** or **6** to give a mixture of *cis* and *trans* isomers (**7, 8** R = $CH_3$ and **9, 10** R = Ph). Thus, compounds **7** and **8** showed two methyl resonances (catecholate ring) at 2.21 and 2.19 ppm (benzene-$d_6$, TMS) and two methyl resonances for groups bonded to arsenic at 1.33 and 1.32 ppm in the ratio of 53:47.

The corresponding *cis* and *trans* compounds, **9** and **10**, where R = Ph, had methyl resonances at 2.26 and 2.12 ppm (benzene-$d_6$, TMS) in the ratio of 90:10. The complexity of the phenyl region at 250 MHz did not allow the catecholate protons and phenylarsenic protons to be separated, and thus the $^1H$ NMR spectrum was obtained at 400 MHz. The 400 MHz $^1H$ NMR spectrum of **9, 10** (benzene-$d_6$, TMS) showed resonances at 7.81 (doublet, J = 8.3 Hz); 6.83 (multiplet) and 6.74 ppm (overlapping triplets J = 8.3 Hz) for the phenylarsenic protons in the ratio of 2:1:2. The catecholate protons were found at 6.56 (doublet of doublets, $J_{ortho}$ = 7.8 Hz, $J_{meta}$ = 1.4 Hz); 6.65 (overlapping triplets, J = 7.8 Hz), 6.93 (triplet, J = 7.8 Hz) and the methyl groups at 2.24 ppm (singlet) in the ratio of 2:2:2:6. The complexity of the phenyl region, where protons on the phenyl group attached to arsenic appeared to be all non-equivalent, provided tentative evidence for the *cis* isomer, **9**, rather than the *trans* isomer, **10**, as the major product in this reaction.

In order to unequivocally ascertain the stereochemistry of the major isomer, as **9** (*cis*) or **10** (*trans*), we obtained a single-crystal x-ray analysis.[11] Figure 1 shows an ORTEP drawing of the major isomer, **9,** with the methyl groups clearly *cis* to each other and the geometry around the arsenic essentially rectangular-pyramidal (95%), while the axial phenyl group is twisted so that it lies in the same plane as oxygen 2 and oxygen 3. The angle between the carbons 1 through 6 on the phenyl group attached to arsenic and the oxygen-arsenic-oxygen plane is 4.7°. (See Table 1 for other pertinent bond angles and lengths.[12–14]) Recently, Day et al.[15] reported on the crystal structure of a product from the reaction of phenylarsenic acid and catechol.[6] This five-coordinate organoarsenic catecholate was also found to have a rectangular pyramidal geometry around arsenic.[15] Our study represents the first stereochemical assignment to be made on a five-coordinate organoarsenic catecholate and has implications for the mechanism of formation of these compounds.

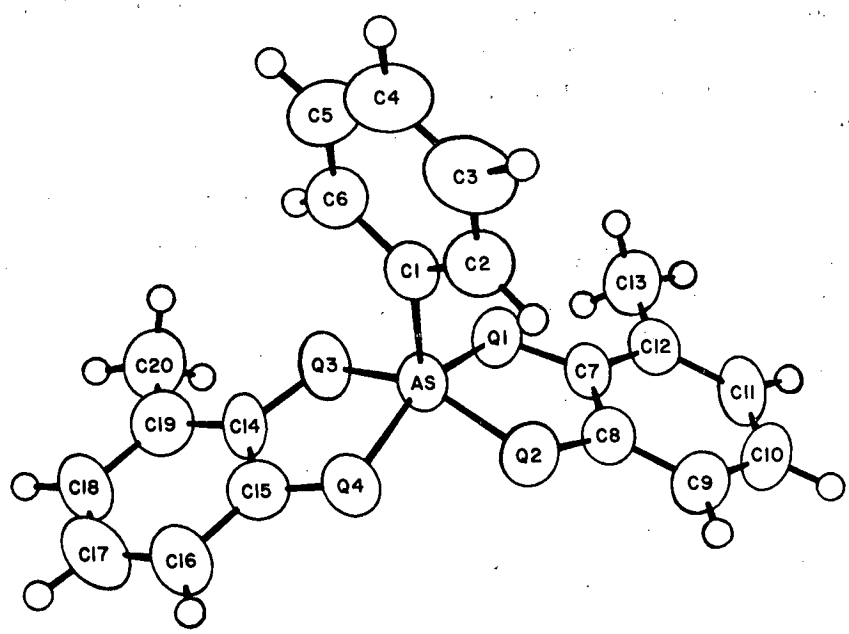


Figure 1. ORTEP diagram of *cis* $(3\text{-}CH_3\text{-}C_6H_3O_2)_2\ AsC_6H_5$, compound **9**, showing 50% probability ellipsoids. (XBL 823-8156A)

Table 1. Selected bond lengths and angles for *cis* $(3\text{-}CH_3\text{-}C_6H_3O_2)_2AsC_6H_5$, **9**.[a]

| Atoms | Bond Length | Atoms | Angle, Deg. |
|---|---|---|---|
| $As\text{-}O_1$ | 1.806 (1) | $O_1\text{-}As\text{-}O_2$ | 87.93 ( 7) |
| $As\text{-}O_2$ | 1.799 (2) | $O_1\text{-}As\text{-}O_3$ | 85.43 ( 7) |
| $As\text{-}O_3$ | 1.784 (2) | $O_1\text{-}As\text{-}O_4$ | 150.84 ( 9) |
| $As\text{-}O_4$ | 1.825 (2) | $O_2\text{-}As\text{-}O_3$ | 149.85 ( 9) |
| $As\text{-}C_1$ | 1.899 (2) | $O_2\text{-}As\text{-}O_4$ | 82.71 ( 8) |
| $C_7\text{-}O_1$ | 1.365 (3) | $O_3\text{-}As\text{-}O_4$ | 88.95 ( 9) |
| $C_8\text{-}O_2$ | 1.370 (3) | $O_1\text{-}As\text{-}C_1$ | 105.5 ( 8) |
| $C_{14}\text{-}O_3$ | 1.413 (3) | $O_2\text{-}As\text{-}C_1$ | 104.99 ( 9) |
| $C_{15}\text{-}O_4$ | 1.345 (3) | $O_3\text{-}As\text{-}C_1$ | 105.12 ( 9) |
| $C_{12}\text{-}C_{13}$ | 1.474 (4) | $O_4\text{-}As\text{-}C_1$ | 103.59 ( 9) |
| $C_{19}\text{-}C_{20}$ | 1.410 (4) | $As\text{-}O_1\text{-}C_7$ | 111.12 (13) |

[a]Estimated standard deviations in parentheses.

Compound **2** reacted with **5** to provide a compound, **11**, with a single methylarsenic resonance at 1.92 ppm ($^1H$, 250 MHz, DMSO-$d_6$, TMS) and a single methoxyl resonance at 3.78 ppm; this is indicative of one isomer, which we presume to have *cis* stereochemistry as in **9**. Compound **2** also reacts with **6** to provide a mixture of compounds, **12** and **13**, with two methoxyl signals ($^1H$, 250 MHz, DMSO-$d_6$, TMS) at 3.76 and 3.74 ppm in the ratio of 95:5. Again, as with **11**, we presume *cis* stereochemistry for the major isomer.

Compound **3**, a benzo-substituted catechol, reacted with **5** and with **6** to give the five-coordinate organoarsenic compounds **14** and **15** respectively. While no stereochemistry is involved in the formation of either **14** or **15**, it is important to note that substitution on the naphthyl ring is certainly possible for future attachment of this type of compound to a polymeric backbone. The pertinent $^1H$ NMR data (250 MHz, DMSO-$d_6$, TMS) provided an upfield shift, as with the NMR spectra of compounds **7–13**, for the catechol ring protons of **14** and **15** when compared to **3**. Thus, **14** had the catechol protons (singlet) at 7.09 ppm, **15** at 7.10 ppm, and **3** at 7.12 ppm, which indicates the influence of arsenic atoms on the shift of protons on catechol rings to higher fields. A similar NMR result was obtained by McArdle et al.[16] for some gallium and rhodium catecholate complexes.

Our final ligand of interest, **4**,[17] was important to study, since it represented a model for a recently reported polymer of potential use for our future applications.[18] We chose **4** (4-LICAM) after making Dreiding models that clearly showed the central cavity capable of accommodating an arsenic atom (~3.58 to 3.63 Å, Fig. 1). Reaction of **4**, with either **5** or **6** provided the intramolecular five-coordinate organoarsenic derivatives **16** and **17** (Eq. 2).

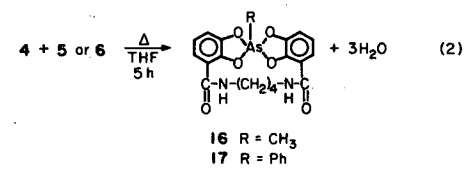


The 250 MHz $^1H$ NMR and 70 eV MS (solid probe) data were consistent with the structures assigned. Notably, the mass spectra provided the parent ion and an ion resulting from a loss of the catechol group with a carbonyl attached. This was followed by a fragmentation of the $\text{-}CH_2CH_2\text{-}NH$ groupings. For example, with **17**, the MS ions of interest were: *m/e* 508 ($M^{+\cdot}$); 373 ($M\text{-}C_7H_{13}N_2O_3$); 331 ($M\text{-}C_9H_8NO_3$); and 287 ($M\text{-}C_{11}H_{13}N_2O_3$).

A typical procedure for the preparation of a five-coordinate organoarsenic catecholate derivative is that for **9**, as follows.

In a 50 ml flask, equipped with condenser, drying tube, and Dean-Stark trap for water removal, was placed 1.29 g (10.42 m*M*) of phenylarsonic acid and 1.05 g (5.21 mM) 3-methylcatechol (freshly sublimed) in 30 ml of benzene. The reaction mixture was refluxed for 5 h. The benzene was removed on a rotary evaporator and the compound recrystallized from carbon tetrachloride/methanol and dried under vacuum to give 1.88 g (91% yield) of **9** (melting point, 134-135°C). Calculated for $C_{20}H_{17}O_4As$: C, 60.6; H, 4.3. Found: C, 60.39; H, 4.46; electron impact mass spectrometry (70 eV, solid probe), *m/e* 396 ($M^{+\cdot}$), 274, 197, 151, 106.[19,20]

We have used this procedure to derivatize both methyl and phenylarsonic acid, **5** and **6**, that had been isolated from a Green River oil shale kerogen by

extraction with methanol. Since **7** and **9** can be chromatographed on a 30 m fused silica capillary column (OV101), the use of GC-MS will enhance the utility of these organoarsonic acid derivatives for other applications.

## PLANNED ACTIVITIES FOR 1983

In future experiments, we hope to place several of our catechol derivatives in polymeric backbones to see if they retain their reactivity with organoarsonic acids.

## REFERENCES


1. Fish, R.H., Brinckman, F.E., and Jewett, K.L. (1982), *Environ. Sci. Technol. 16*, p. 174.
2. Weiss, C.S., Brinckman, F.E., and Fish, R.H. (1981), in *Proceedings on Environmental Speciation of Trace Metal-Containing Compounds in Energy-Related Processes*, May 18–20, Gaithersburg, Maryland. National Bureau of Standards Special Publication 618, p. 197.
3. Salmi, E.J., Merivuori, K., and Laaksonen, E. (1946), *Kemistilehti Suomen 19B*, 102 (Chem. Abs., *41*, 5440a).
4. Bacher, J.H., and Van Oosten, R.P. (1940), *Rec. Trav. Chem. 59*, p. 41.
5. Englund, B. (1926), *Chem. Ber. 59*, p. 2669.
6. Sau, A.C. and Holmes, R.R. (1980), *J. Organometal. Chem. 217*, p. 157.
7. Wieber, M., Eichhorn, B., and Gotz, J. (1973), *Chem. Ber. 106*, p. 2738.
8. Maroni, P., et al. (1976), *Tetrahedron Letters*, 1193.
9. Fish, R.H., and Weitl, F.L., (1981), in *Proceedings of the Tenth International Conference on Organometallic Chemistry, Toronto, Canada, August 9–14, 1981*, Abstract 1D12, p. 62.
10. All new compounds we report had elemental analyses (C, H, N) within ±0.5% of theory. The EIMS, IR, and NMR spectra for all compounds supported their structures.
11. A full account of the structural parameters for **9** will be given in a future paper.
12. Goldwhite, H. and, Teller, R.G. (1978), *J. Amer. Chem. Soc. 100*, p. 5357.
13. Wunderlich, H. (1978), *Acta Cryst. B 34*, p. 1000.)
14. Holmes, R.R. and Deiters, J. (1977), *J. Am. Chem. Soc. 99*, p. 3318.
15. Day, R.O. et al. (1982), *J. Am. Chem. Soc. 104*, p. 2127.
16. McArdle, J.V., Sofen, S.R., Cooper, S.R., and Raymond, K.N. (1978), *Inorg. Chem. 17*, p. 3075.
17. The series of LICAM derivatives of increasing methylene chains, **2-6**, were prepared according to the procedures of Dr. F.L. Weitl; see e.g., Weitl, F.L., and Raymond, K.N. (1980), *J. Amer. Chem. Soc. 102*, p. 2289.
18. Dawson, M.I., Chan, R.L.-S., Cloudsdale, I.S., and Harris, W.R. (1981), *Tetrahedron Letters 22*, p. 2739.
19. Fish, R.H., Tannous, R.S., Weiss, C.S., and Brinckman, F.E. (1983), *J. Chem. Soc. Chem. Commun.* (in press).
20. Fish, R.H., and Tannous, R.S. (1982), *Organometallics 1*, p. 1238.


# ORGANOMETALLIC GEOCHEMISTRY: ISOLATION AND IDENTIFICATION OF ORGANOARSENIC COMPOUNDS FROM GREEN RIVER FORMATION OIL SHALE*


*R.H. Fish, R.S. Tannous, W. Walker, C.S. Weiss,† and F.E. Brinckman†*


The molecular characterization of naturally occurring organometallic compounds in fossil fuel precursors is becoming a significant area of research because of the importance of these compounds in emerging synthetic fuel processes and their impact on the environment.[1]

Recently, using a high-performance liquid chromatograph coupled to a graphite-furnace atomic absorption spectrometer as an element-selective detector


*This work was supported by the Assistant Secretary for Fossil Energy and the Division of Oil, Gas and Shale Technology, and the Bartlesville Energy Technology Center of the U.S. Department of Energy under Contract No. DE-AC03-76SF00098. A portion of the NBS study was supported by the NBS Office of Standard Reference Materials. C.S.W. was a National Research Council–National Bureau of Standards Postdoctoral Research Associate (1980–1982).



†Chemical and Biodegradation Processes Group, Center for Materials Science, National Bureau of Standards, Washington, DC 20234.

(HPLC-GFAA), we identified methyl- and phenylarsonic acids as well as arsenate in oil-shale retort waters.[2] We also have analyzed the oils produced by shale pyrolysis and have found that the same organoarsonic acids occur, but in association with iron-containing macromolecules with molecular weights in the range of 2000 to 4000 daltons.[3,4]

In order to discern whether these compounds were natural products in the precursor of the shale oil and the retort waters or were formed during pyrolysis, we examined a sample of Green River Formation oil shale. Oil shale from the Green River Formation is a fine-grained sedimentary rock that contains appreciable quantities of organic material. It consists of three fractions—kerogen, bitumen, and an inert substance. Kerogen and bitumen, which constitutes the organic material, are regarded as biogeochemical fossil products, emanating largely from lipid fractions of ancient algae and forming the ubiquitous oil-source matrix in shales.[5]

## ACCOMPLISHMENTS DURING FY 1982

The Green River Formation oil shale sample (10 g) was crushed and Soxhlet-extracted with 500 ml of methanol for 48 hours. This effectively removed about 20% of its total arsenic. [The Green River oil shale sample from Anvil Points, Colorado (NBS Standard Reference Material) was found to contain approximately 20 ppm of total arsenic.] Following evaporation (25 ml) and filtration, we speciated the extract by HPLC, using a Dionex anion exchange column with 0.2 *M* ammonium carbonate in water/methanol (85:15) as the eluting solvent. The arsenic compounds were detected via automatic GFAA analysis at 197.3 nm.[1,2]

Figure 1 gives the arsenic-specific chromatogram of the compounds we identified as methylarsonic acid, phenylarsonic acid, and arsenate, based on retention times of the authentic arsenic compounds.[2] One or more unknown neutral organoarsenic compounds also eluted with the solvent front.

We recently studied the reactions of methyl- and phenylarsonic acids with substituted catechols and established that they provide five-coordinate organoarsenic catecholates.[6] Since many of these organoarsenic catecholates can be gas-chromatographed on fused silica capillary columns and characterized by electron impact mass spectros-

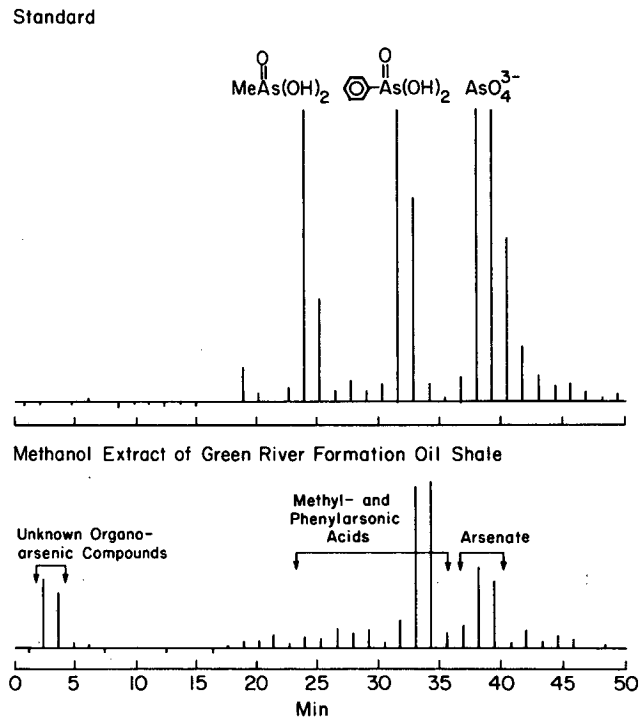


Figure 1. HPLC-GFAA analysis of Green River Formation oil shale extracted with refluxing methanol. AA detection of arsenic was at 193.7 nm. For HPLC, a Dionex anion-exchange column with 0.2 *M* $(NH_4)_2CO_3$ in aqueous methanol as the eluting solvent was used. Bracketed areas were isolated by preparative HPLC. (XBL 8210-3116)

copy (GC–EIMS), we decided to apply this technique to unequivocally identify the methyl- and phenylarsonic acids in the oil shale extract.

The methanol extract was purified by preparative HPLC (the area from 22 to 35 min was collected, see Fig. 1), lyophilized, and dissolved in benzene. To this solution was added excess 3-methylcatechol, and the reaction mixture was refluxed for 5 h and worked up to remove the excess 3-methylcatechol. A concentrated sample was subjected to GC-EIMS analysis to provide spectra and scan numbers (retention times) identical to the known samples of the 3-methylcatecholates of both methyl- and phenylarsonic acids.

Figure 2(A) shows the reconstructed ion chromatogram of the two standards, 3-methylcatecholates of methyl- and phenylarsonic acids; the single-ion chromatograms show pertinent fragments of interest at *m/e* 197 and 212 for the methylarsonic acid derivative [Fig. 2(B),(C)] and *m/e* 197 and 274 for

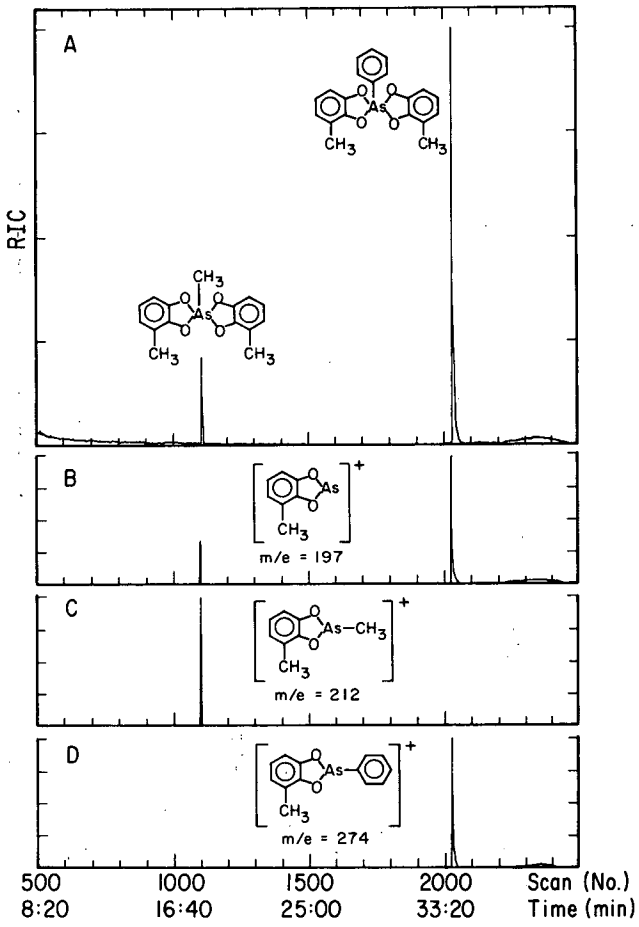


Figure 2. GC-EIMS analysis of the 3-methylcatecholates of methyl- and phenylarsonic acids. (A) Reconstructed ion chromatogram of known methyl- and phenylarsonic acid derivatives of 3-methylcatechol. (B) Selected ion chromatogram showing *m/e* 197 for each derivative. (C) Selected ion chromatogram for methylarsonic acid-3-methylcatecholate at *m/e* 212. (D) Selected ion chromatogram for phenylarsonic acid-3-methylcatecholate at *m/e* 274. (XBL 828-10938A)

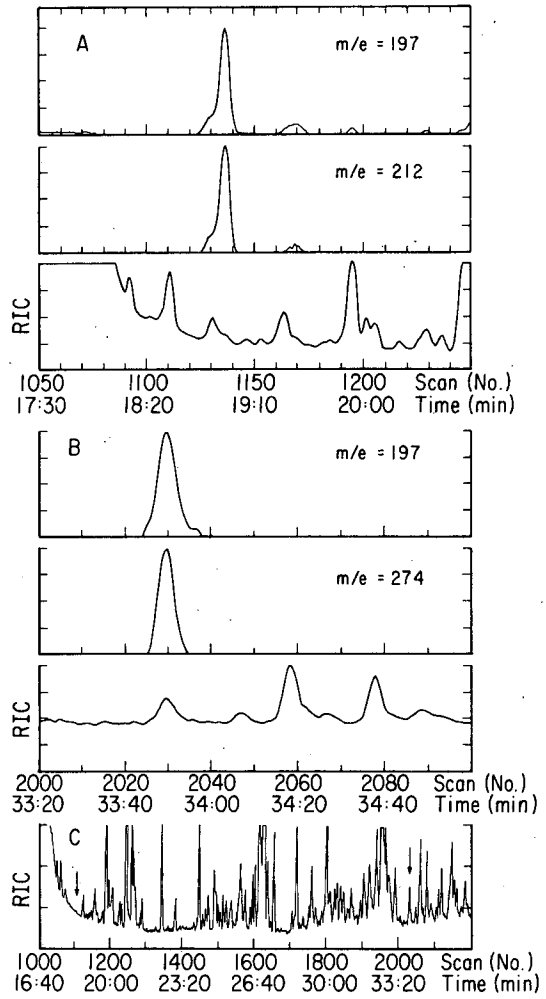


Figure 3. GC-EIMS analysis of the derivatized, HPLC-purified methanol extract. (A) Ion chromatograms near scan 1137 for *m/e* 197 and *m/e* 212, confirming identification of 3-methylcatecholate of methylarsonic acid in (C). (B) Ion chromatograms near scan 2030 for *m/e* 197 and *m/e* 274, confirming identification of 3-methylcatecholate of phenylarsonic acid in (C). (C) Reconstructed ion chromatogram of HPLC-purified methanol extract; arrow on left designates methylarsonic acid-3-methyl catecholate, and arrow on right designates phenylarsonic acid-3-methyl catecholate. (XBL 828-10939A)

the phenylarsonic acid derivative [Fig. 2(B),(D)]. Figure 3(C) shows the region we purified by HPLC containing the organoarsonic acids, which were derivatized, and the expanded sections of this chromatogram containing the organoarsenic catecholates with the important ions, *m/e* 197, 212, and 274, clearly evident for the 3-methylcatecholates of methylarsonic [Fig. 3(A)] and phenylarsonic [Fig. 3(B)] acids. Additionally, the inorganic anion, arsenate ($AsO_4^{3-}$), was verified in a similar fashion (preparative HPLC of the region from 35.5 to 41 min) by preparation of the *tris* (trimethylsilyl-) derivative of the ammonium salt of arsenate and analyzing the purified extract by GC-EIMS for ions at *m/e* 207, 343, and 358.[7] The organoarsenic compound or compounds that elute with the solvent front (Fig. 1) have not yet been identified, and work is in progress to determine the structure.[7]

## PLANNED ACTIVITIES FOR FY 1983

We believe these identifications of the organoarsonic acids to be the first such molecular characterizations of trace organometallic compounds to be reported for any fossil fuel precursors and that they initiate a new field, organometallic geochemistry, that has heretofore been totally unexplored.

Our findings imply that these organoarsonic acids are natural products and hence have a biogeochemical origin in the oil shale fossilization process. It is also interesting to note that no examples of biophenylation have been reported, whereas biomethylation of arsenic compounds is well-known.[8] How the phenylarsonic acid forms will have to be answered by examining oil shale precursors such as freshwater algal mats and other biogeochemical samples. We plan to proceed with this aspect in FY 1983.

Finally, the fact that these organoarsonic acids are released upon oil shale pyrolysis has important implications for synthetic fuel processes in which the role of organometallic compounds in poisoning process catalysts and in contributing to environmental problems is paramount.[9]

## REFERENCES


1. Brinckman, F.E. and Fish, R.H., Eds. (1981), *Environmental Speciation and Monitoring Needs for Trace Metal-Containing Substances from Energy-Related Processes,* NBS Special Publication 618, National Bureau of Standards, Washington, D.C.
2. Fish, R.H., Jewett, K.L., and Brinckman, F.E. (1982), *Environ. Sci. and Tech. 16,* p. 174, and references therein.
3. Brinckman, F.E., Weiss, C.S., and Fish, R.H. (1983), in *Chemical and Geochemical Aspects of Fossil Energy Extraction,* T.F. Yen, Ed., Ann Arbor Science, Ann Arbor, MI, chap. 13, p. 197.
4. Weiss, C.S., Parks, E.J., and Brinckman, F.E., (1982), in *Arsenic: Industrial, Biomedical, and Environmental Perspectives,* W.H. Lederer and R.J. Fensterheim, Eds., Van Rostrand-Reinhold Co., New York.
5. Yen, T.F., and Chilingarian, G.V., Eds. (1976), *Developments in Petroleum Science,* vol. 5, Elsevier, Amsterdam.
6. Fish, R.H. and Tannous, R.S. (1982), *Organometallics 1,* p. 1238.
7. Butts, W.C., and Rainey, W.T., Jr., (1979), *Anal. Chem. 43,* p. 538.
8. McBride, B.C., Merilees, H., Cullen, W.R., and Pickett, W. (1968), in *Organometals and Organometalloids: Occurrence and Fate in the Environment,* F.E. Brinckman and J.M. Bellama, Eds., ACS Symposium Series 82, American Chemical Society, Washington, D.C., p. 94.
9. Fish, R.H., Tannous, R.S., Walker, W., Weiss, C.S., and Brinckman, F.E. (1983), *J. Chem. Soc. Chem. Comm.* (in press). Lawrence Berkeley Laboratory report LBL-15060.

# PROCESSING OF CONDENSATE WATERS FROM COAL GASIFICATION*

*C.J. King, J. MacGlashan, D. Mohr, P. Mackenzie, R. Thompson, and J. Bixby*

Large volumes of condensate water are formed when effluents from coal-gasification reactors are cooled. These waters contain large concentrations of dissolved acid gases and ammonia, as well as substantial amounts of dissolved polar organics, notably phenols and related compounds. For water economy and environmental protection, it is desirable to recycle these waters to the gasification process. The principle objective of this project is to develop workable, reliable, and economical physicochemical processing methods that will enable such condensate waters to be recycled. Particular attention is being given to solvent-extraction and energy-efficient stripping processes, and to combinations of these.

Work to date has focused upon four areas:

(1) analyses of individual components contributing to the measured Chemical Oxygen Demand (COD);

(2) extraction with both conventional and novel solvents to allow more complete reduction of COD and/or lower energy consumption;

(3) interpretation of rates of stripping of ammonia and acid gases from condensate waters; and

(4) innovative combinations of extraction and stripping that have the potential to reduce substantially the energy required to remove ammonia and isolate it as a salable product.

Results through 1981 are described in the Annual Reports for FY 1979 through 1981.

*This work was supported by the Assistant Secretary for the Environment, Office of Environmental Compliance and Overview, Division of Environmental and Safety Engineering, Environmental Control Technology Branch of the U.S. Department of Energy under Contract No. DE-AC03-76SF00098.

## ACCOMPLISHMENTS DURING FY 1982

### Analyses of Condensate Waters

In the preceding year (FY 1981), three condensate-water samples were obtained from the slagging fixed-bed gasifier at the Grand Forks Energy Technology Center (GFETC) and analyzed (see FY 1981 Annual Report). During FY 1982, a fourth sample (RA-120) was obtained, also from GFETC. This sample was analyzed by a reversed-phase, gradient-elution, high-performance liquid chromatography (HPLC) technique. This technique can detect very polar, hydrophilic compounds that are not recovered by the methylene chloride extraction step in many gas-chromatography/mass-spectrometry (GC/MS) analytical procedures. Qualitative identification of individual HPLC fractions was accomplished by GC/MS and co-chromatography tests with known compounds. The procedures for condensate-water sampling and for qualitative and quantitative analysis have been described previously.[1]

Table 1 shows the results of chemical analyses of the four condensate-water samples received so far from GFETC. The compounds are divided into three categories—monohydric phenols and their derivatives (nos. 1–5), dihydric phenols (nos. 6–9), and hydantoin compounds (nos. 10–12). The hydantoin compounds are very polar and have low distribution coefficients ($K_D$) into common solvents. The structure of dimethyl hydantoin is shown in the FY 1981 Annual Report.[2]

The concentrations of compounds 1–9 in the RA-120 sample did not change significantly from the initial measurement to a sample age of 65 days. The concentration of dimethyl hydantoin measured in RA-120 increased with time from 70 ppm at 0.7 days to 165 ppm and 110 days, with intermediate values of 110 ppm and 150 ppm at 10 and 30 days, respectively. These observations are similar to the time-dependent behavior of the samples discussed in the FY 1981 report.

The most important differences between the samples are the high concentration of dihydric phenols (components 6–9) in the first two samples (RA-78 and RA-97), and the high concentration of dimethyl

Table 1. HPLC analyses of GFETC gasifier condensate waters (all concentrations expressed in ppm, w/w).

| Date of sample: | 6/20/80 | 6/10/81 | 9/30/81 | 4/20/82 |
|---|---|---|---|---|
| GFETC run no: | RA-78 | RA-97 | RA-106 | RA-120 |
| Sample age at analysis (days): | 200 | 40 | 1.7 | 0.7 |
| Components: | | | | |
| 1. Phenol | 5028 | 7405 | 3528 | 4370 |
| 2. Cresols | 3238 | 4267 | 2422 | 2565 |
| 3. $C_2$ Monohydric phenols | 456 | 473 | 434 | 400 |
| 4. o-Methoxy phenol | 259 | 448 | 165 | 260 |
| 5. p-Hydroxy acetophenone | 48 | 33 | 3 | ND |
| 6. Pyrocatechol | 973 | 848 | 38 | 2 |
| 7. 4-Methyl catechol | 613 | 497 | 21 | ND |
| 8. Resorcinol | 62 | 28 | 2 | ND |
| 9. Hydroquinone | 33 | 25 | 1 | ND |
| 10. 5,5-Dimethyl hydantoin ($C_5H_8O_2N_2$) | 1755 | 294 | 293 | 70 |
| 11. 5-Methyl hydantoic acid ($C_4H_6O_2N_2$) | 99 | 128 | ND | 35 |
| 12. 5-Methyl hydantoin ($C_4H_6O_2N_2$) | 136 | 41 | ND | 10 |
| Measured COD | 35,810 | 46,650 | 23,510 | 24,740 |
| Fractions of measured COD accounted for by: | | | | |
| Components 1–5 | 0.621 | 0.661 | 0.685 | 0.797 |
| Components 6–9 | 0.092 | 0.059 | 0.005 | 0.0001 |
| Components 10–12 | 0.112 | 0.014 | 0.019 | 0.004 |
| All identified components | 0.825 | 0.734 | 0.709 | 0.801 |

ND = not detected

hydantoin in RA-97. These differences may be due to changes in the operation of the coal-gasification process.

As reported in Table 1, the identified compounds account for 71 to 83% of the measured COD in these condensate-water samples.

## Extraction of Condensate Waters

Additional information about the chemical nature of the organic compounds in these samples can be obtained by various solvent-extraction procedures. This information can also be used to evaluate the performance of industrial solvent-extraction processes.

Methylisobutyl ketone (MIBK) is an attractive solvent for an industrial condensate-water treatment process because it gives high equilibrium distribution coefficients compared to other conventional solvents, and because it can be regenerated easily by distillation. Two sequential batch extractions with MIBK at a solvent-to-water volume ratio of 1:1 in each stage removed 92.5% of the COD from the RA-120 sample at a sample age of 0.7 days. This degree of COD removal could be accomplished in a countercurrent extraction process with an economically feasible solvent-to-water ratio.

Two other solvents were studied—tributyl phosphate (TBP) and 25 wt% trioctyl phosphine oxide (TOPO) dissolved in MIBK. TBP is a stronger Lewis base than MIBK, and TOPO is a stronger Lewis base than TBP. Batch extractions with a solvent-to-water volume ratio of 1:1 removed the following fractions of the COD from the RA-120 sample at a sample age of 11 days: MIBK, 0.881; TOPO/MIBK, 0.915; TBP, 0.920. Each solvent removed nearly all of the compounds 1–9 in Table 1. The COD that remains after extraction is therefore due to compounds that have not yet been identified. These remaining organic compounds are very polar and hydrophilic. Since the stronger Lewis-base solvents remove more of them, some of them may be Lewis acids. Ultrafiltration experiments using a membrane with a nominal molecular-weight cut-off of 1000 showed that none of the solutes remaining after MIBK extraction were retained by the membrane.

The portion of the COD removed from the RA-120 sample by a single extraction with MIBK decreased from 88.5% at a sample age of 0.7 days to 86.4% at a sample age of 190 days. The portion of the COD removed by two sequential MIBK extractions decreased from 92.5% to 88.4% over the same interval. This indicates that chemical reactions occurred during storage. It also demonstrates the importance of testing proposed treatment processes with fresh condensate-water samples.

Repeated extractions with MIBK from the RA-120 sample at 190 days showed that about 10% of the COD had a vanishingly small $K_D$ into this solvent. Residual dissolved MIBK was removed from the raffinate water after extraction by nitrogen stripping under conditions shown to leave no appreciable

amount of the solvent in the water. This stripping was to prevent dissolved MIBK from contributing to the COD analysis.

A technique for measuring organic nitrogen has recently been applied to the RA-120 sample. In this procedure, NaOH was added to the condensate water, and most of the ammonia was stripped out of the solution with 4 moles $N_2$ per mole $H_2O$ at 25°C. The difference between Kjeldahl nitrogen and ammonia nitrogen was then interpreted to be nitrogen contained in organic compounds. At an age of 190 days, the RA-120 sample contained about 250 mg N/l of organic nitrogen. After repeated extractions with MIBK, about 150 mg N/l remained in solution. This organic nitrogen has a very small $K_D$ into MIBK and was not removed by MIBK or methylene chloride at high pH. Therefore much of the poorly extracted COD may be due to very polar, nitrogen-containing compounds.

## Extraction of Phenols with Trioctyl Phosphine Oxide (TOPO)

Measurements of equilibrium distribution coefficients ($K_D$) for extraction of phenol, resorcinol, and pyrogallol from water into solvent mixtures of TOPO and diisobutyl ketone (DIBK) have been completed. The results and their interpretation in terms of complexation equilibria are presented elsewhere.[3]

We have found that regeneration of TOPO solutions by back-extraction into strong aqueous bases is complicated by emulsification. Also, the variation of $K_D$ with temperature[3] appears to be insufficient for a regeneration process based upon back-extraction into water at higher temperature. Regeneration by distillation is more likely to be cost-effective. Since DIBK has a lower boiling point than phenol, a higher ketone, isobutyl helptyl ketone (IBHK), was tested as a diluent for TOPO. Although the normal boiling point of phenol (181°C) is less than that of IBHK (218°C), it was found that complexation of phenol with TOPO substantially reduces the volatility of phenol under distillative regeneration conditions. For a solvent composed of 25% w/w TOPO in IBHK, measured values of the relative volatility of phenol to IBHK were only 0.85 and 1.11 at TOPO/phenol molar ratios of 1.0 and 0.5, respectively. Diluents with still higher boiling points appear to be required if phenol is to be regenerated from TOPO by distillation.

## Combined Stripping and Extraction for Removal and Isolation of Ammonia

As explained in the FY 1981 report, it may be possible to reduce the steam requirements for stripping ammonia and acid gases (carbon dioxide and hydrogen sulfide) from water by carrying out stripping and solvent extraction simultaneously. The energy used for this combined process plus that for solvent regeneration may be less than that for stripping alone. The process would also isolate the ammonia from the acid gases.

Before FY 1982, we had determined that (1) ammonia rather than the acid gas should be extracted, (2) a liquid ion exchanger is needed to achieve a high degree of ammonia removal, (3) the rate of acid gas removal by stripping in the presence of such a solvent is substantially faster than by stripping in the absence of a solvent, and (4) certain liquid ion exchangers can be regenerated by stripping at a temperature greater than that of the original combined stripping and extraction.

Several difficulties arise with liquid ion exchangers, however. Since they are ionic, they tend to be surface-active and to have a fairly high solubility in an aqueous phase, particularly in the salt form. This can result in poor phase separation and excessive extractant losses. In addition, they can degrade thermally at elevated temperatures, which would lead to additional costs for replenishing the extractant.

Work carried out in FY 1982 addressed the problems of extractant purity, alternative liquid ion exchangers, degree of ammonia extraction, phase separation, extractant losses, and regenerability.

Previously, the principal extractant studied had been di-2-ethylhexyl phosphoric acid (D2EHPA). The commercial product contains about 2% mono-2-ethylhexyl phosphoric acid, which is water soluble. In a continuous process, this impurity would wash out of the organic phase fairly quickly. To obtain meaningful results for the degree of extraction, extractant losses, etc., the commercial D2EHPA was purified by a copper-salt precipitation method[4] for measurements that began in FY 1982.

Other extractants examined were dinonylnaphthalene-sulfonic acid (DNNSA) and octylphenyl phosphoric acid (OPAP). DNNSA had been shown previously to degrade irreversibly when attempts were made to regenerate it. OPAP comes as a mixture of

mono- and di-acids, so it was washed before use to remove the di-acid. It gave results comparable to D2EHPA for ammonia extractability and phase separation, but, being a stronger acid, it is much more soluble in the aqueous phase than D2EHPA. Thus D2EHPA is still the most promising extractant examined thus far.

Since D2EHPA is a viscous liquid, it is dissolved in an organic diluent before use. The nature of this diluent can affect the degree of extraction, phase separation, extractant losses, and regenerability.

The degree of ammonia extraction by D2EHPA is greater in an inert diluent, such as an aliphatic hydrocarbon, than in an aromatic, such as toluene. This is probably due to the interaction of the $\pi$ electrons of the aromatic with D2EHPA, which reduces the availability of D2EHPA for ammonia extraction. Under identical conditions, using Norpar 12 (King Industries) ($C_{11}$ to $C_{13}$ paraffins) as diluent, 96% of the ammonia is extracted from an aqueous solution, while only 94% is extracted when the diluent is toluene.

Using a mixed diluent of toluene plus a modifier with D2EHPA allows us to take advantage of the chemical nature of a modifier that might be too viscous to use alone, but much depends on the acidity or basicity of the modifier. If the modifier is a stronger base than ammonia, such as a secondary or tertiary amine, ammonia extraction is markedly decreased. TOPO, a weaker base, which therefore does not compete as successfully for the D2EHPA as the amines do, has only a slightly detrimental effect on extraction.

Use of 1,1,2,2-tetrachloreothane, which has acidic protons, as a modifier with D2EHPA and toluene does not affect the degree of extraction much. Adding carboxylic acids, especially straight-chain ones such as 1-decanoic acid, as modifiers with D2EHPA and toluene greatly enhances the extraction of ammonia, although the carboxylic acids themselves do not extract ammonia significantly.

Sterically unhindered alcohols and phenols added as modifiers also exhibit this enhancement. For instance, under otherwise identical conditions, a diluent composed of 12.2% (by volume) 1-octanol in toluene results in 96.2% extraction of ammonia by D2EHPA, while a diluent composed of 12.2% (vol) 2-ethyl-1-hexanol in toluene yields only 93.6% extraction. Likewise, a diluent composed of 18.8% (vol) nonylphenol in toluene used with D2EHPA extracts 98.9% of the ammonia, while 18.8% (vol) 4-sec-butyl-2-($\alpha$-methylbenzyl) phenol in toluene as a diluent with D2EHPA extracts only 93.7%. These results are to be compared with 94% for toluene alone as the diluent.

To illustrate this point about alcohols further, the following percents of ammonia extracted were found for D2EHPA mixed with a diluent of toluene plus increasing amounts of 1-decanol: Zero percent decanol, 94% extracted; 1.8% (vol) decanol, 95.4% extracted; 12% (vol) decanol, 96.3% extracted; 50% decanol, 97% extracted; and 100% decanol, 98.5% extracted. Commercially available isodecyl alcohol behaves similarly to 1-decanol. The -OH group may be solvating the ammonia-D2EHPA complex in the organic phase and therefore lowering its activity.

Another problem in this system, poor phase separation, manifests itself as a white emulsion at the interface. We therefore attempted to reduce the surfactant nature of the organic phase. Since the ammonium salt of D2EHPA is highly surface-active, operating under conditions of low conversion of the D2EHPA to the salt form improved the phase separation. Modifiers that interact with the ammonium salt of D2EHPA also can decrease its interfacial activity. Hence, adding the unhindered carboxylic acids, alcohols, and phenols as modifiers to a toluene diluent greatly improves phase separation, especially at high modifier concentrations. Of particular interest are the excellent separations attained with a diluent composed of only 1.8% (vol) 1-decanoic acid in toluene and with another diluent containing 50% (vol) isodecyl alcohol in a commercial aromatic diluent (Chevron Solvent 25), both at an aqueous-to-organic phase ratio of 0.185.

Extractant losses from the organic phase to the aqueous phase are also affected by the nature of the organic diluent. These losses were quantified as follows: A solution of D2EHPA at 0.2 *M* in a given diluent was contacted with an aqueous solution containing 0.58 *M* ammonia, at an aqueous-to-organic phase ratio of 0.185. The concentration of phosphorus-containing compounds in the resulting aqueous phase was measured by a standard decomposition and precipitation method.[5]

Replacing an aliphatic diluent with an aromatic reduces extractant losses by about 50%, because the aromatic can better solvate the D2EHPA and its ammonium salt. By using modifiers in toluene that reduce the extraction of ammonia, less of the

ammonium salt of D2EHPA was formed, and the extractant loss was also reduced. Presumably, this is because the ammonium salt of D2EHPA is more soluble in water than is D2EHPA itself.

Sterically unhindered carboxylic acids, alcohols, and phenols added as modifiers to toluene also significantly reduce extractant losses to the aqueous phase. The strong interaction between the -OH group on these compounds and the ammonia-D2EHPA complex is probably responsible. For instance, using 50% isodecyl alcohol in the aromatic diluent, Chevron Solvent 25 reduces the extractant losses by 90% from those measured using an aliphatic diluent (Norpar 12). Under practical operating conditions, the extractant losses can thereby be reduced to less than $1.90/1000 gallons of water treated.

These results point to 50% isodecyl alcohol in an aromatic solvent as a good choice of diluent for D2EHPA, at least with respect to phase separation and extractant losses. So far, only one attempt has been made to regenerate such a solvent system. It was easily regenerated at 160°C, but some evidence of thermal decomposition was noted. Regeneration, therefore, will probably have to be carried out at a lower temperature. This may require a diluent that gives a lower extraction efficiency for ammonia, since the ammonia will then not be as tightly held and will therefore be more readily liberated from the solvent. A trade-off may exist between costs for extractant losses and steam requirements for regeneration.

## PLANNED ACTIVITIES FOR FY 1983

Analyses of condensate waters will continue, with the objective of identifying the remaining unknown components contributing to the COD. The initial focus will be on organic nitrogen compounds and amphoteric ionizing compounds. Solvent-extraction measurements will be continued to provide chemical information on the condensate-water constituents, and to provide effective solvent-extraction processes for removal of the compounds that have been identified.

Higher-boiling diluents for TOPO will be sought, most likely from among commercially available ketones, aromatics, alcohols, and naphthalenes, with aliphatic solvents being added to the diluent when needed to alter density or viscosity. Equilibrium data for the extraction of phenol will be obtained for mixtures of TOPO with diluents which appear promising from the standpoint of solvent-regeneration properties.

In the experiments directed toward simultaneous extraction of ammonia and stripping of acid gases, regeneration rates will be measured for mixtures of TOPO with diluents composed of aromatics and -OH-containing compounds, with the aim of identifying the most attractive diluent mixture on the bases of regenerability, low extractant losses through solubility or poor settling, and low thermal degradation. Equilibrium data will be quantified for the more attractive extractant/diluent combinations, and tests will be made with samples of real condensate waters.

## REFERENCES


1. Mohr, D.H., Jr., and King, C.J. (1981), "Identification and Removal of the Organic Compounds in Coal-Conversion Condensate Waters," presented at the Workshop on Processing of Wastewaters from Synthetic Fuels Processes, U.S. Department of Energy, Germantown, Maryland, June 24–25, 1981. Lawrence Berkeley Laboratory report LBL-13584 Revised.
2. King, C.J., et al. (1982), "Processing of Condensate Waters from Coal Conversion," in *Energy and Environment Division Annual Report, FY 1981*, p. 1-35.
3. MacGlashan, J.D., and King, C.J. (1982), *Extraction of Phenols From Water*, Lawrence Berkeley Laboratory report LBL-13963.
4. McDowell, W.J., Perdue, P.T., and Case, G.N. (1976), "Purification of di(2-ethylhexyl)phosphoric Acid," *J. Inorg. Nucl. Chem. 38*, p. 2127–29.
5. Pregl, F., and Grant, J. (1951). *Quantitative Organic Microanalysis*, The Blakiston Company, Philadelphia, Pennsylvania, p. 140–146.

# TECHNOLOGY BASE RESEARCH PROJECT FOR ELECTROCHEMICAL ENERGY STORAGE*

*E.J. Cairns and F.R. McLarnon*

The Lawrence Berkeley Laboratory (LBL) is lead center for management of the Technology Base Research (TBR) Project. During FY 1982, this project consolidated the research activities of several smaller programs in the electrochemical branch of DOE's Energy Storage Division. The general aim of the TBR Project is to provide an applied research base supporting the development of batteries and electrochemical systems that exhibit superior performance and acceptable life-cycle costs. The intended applications include electric vehicles and stationary energy storage and conversion. A major goal is to identify electrochemical technologies having the greatest potential to satisfy performance and economic requirements and transfer them to DOE's Exploratory Technology Development and Testing project and/or private industry for further development and scale-up.

The TBR Project includes four major elements: electrochemical systems, supporting research, electrochemical processes, and fuel cell research. (Fuel cell research is managed by the Los Alamos National Laboratory.) The generic research topics included in each of these elements are listed in Table 1.

The LBL scientists who participate in the program are E.J. Cairns and F.R. McLarnon of the Energy and Environment Division, and L.C. DeJonghe, J.W. Evans, R.H. Muller, J.S. Newman, P.N. Ross, and C.W. Tobias of the Materials and Molecular Research Division.

*This work was supported by the Assistant Secretary for Conservation and Renewable Energy, Office of Energy Systems Research, Energy Storage Division of the U.S. Department of Energy under Contract No. DE-AC03-76SF00098.

Table 1. Topics covered by the Technology Base Research Project for electrochemical energy storage.

I. ELECTROCHEMICAL SYSTEMS
- New Rechargeable Electrochemical Cells
- Metal/Air Cells

II. SUPPORTING RESEARCH

A. Engineering-Science Research
- Electrode Morphological Studies, Chemical/Structural Analysis
- Transport Phenomena, Electrocatalysis, Electrode Kinetics, and Cell Thermodynamics
- Modeling of Electrochemical Cells and Battery Systems
- Advanced Physiochemical Methods for Electrochemical Research

B. Materials Research
- Ceramic, Molten-Salt, Glass, and Polymeric Electrolytes
- Novel Electrode Structures
- New Fabrication Techniques for Components
- Battery Separators

III. ELECTROCHEMICAL PROCESSES
- Corrosion Problems in Electrochemical Storage Devices
- Characterization of Multi-Phase[a] Electrochemical Systems
- Electroorganic Synthesis
- Thermally-Regenerative Cells

IV. FUEL CELL RESEARCH
- New Components for Fuel Cells
- New Electrolytes
- Electrocatalysis

[a]Gas-solid-liquid.

## ACCOMPLISHMENTS DURING FY 1982

LBL monitored 40 subcontracts during FY 1982 and conducted a vigorous in-house research program. The in-house work, "Electrochemical Energy Storage," is summarized in the next article and in the *Materials and Molecular Research Division 1982 Annual Report* (LBL-15150). Progress in the subcontracted work, divided according to the four major elements of Table 1, can be briefly described as follows:

### Electrochemical Systems Research

(1) A multicell phototype Al/air system was successfully tested at Lawrence Livermore National Laboratory.

(2) A new project to investigate the use of sulfolane-based organic electrolytes in ambient-temperature rechargeable lithium batteries was initiated at EIC Laboratories, Inc.

### Supporting Research

(1) SRI International has nearly completed a program to measure the electrochemical kinetic parameters of rechargeable alkaline Zn, Fe, and NiOOH electrodes.

(2) A new effort to adapt a "transformation toughening" procedure to the manufacture of ceramic electrolytes was initiated at Rockwell International, Inc. Tetragonal $ZrO_2$ is incorporated into beta alumina ($\beta''$-$Al_2O_3$) electrolytes in high-temperature Na/S cells.

(3) Several less-promising research and development projects have been phased out of the TBR Project:

(a) Three projects (conducted by SRI International, EIC Laboratories, and Giner, Inc.), focusing on photoelectrochemical storage cells, identified significant material corrosion problems and/or very low current densities.

(b) NASICON ($Na_{1+x}Zr_2Si_xP_{3-x}O_{12}$, $0 < x < 3$) was shown by LBL and Ceramatec, Inc. to be unstable in molten sodium at 300°C; this material is therefore unsuitable for use in Na/S cells.

(c) An attempt by the University of Southampton (England) to employ Raman spectroscopy to identify reaction products at metal/electrolyte interfaces suffered from very low signal-to-noise ratios.

(d) Measurements of composition profiles in LiAl/LiCl-KC1/FeS cells at Oak Ridge National Laboratory lacked sufficient accuracy to confirm or refute proposed mathematical models.

(e) The Energy Research Corporation had previously shown that adding certain oxides to ZnO material employed in Zn/KOH/NiOH cells could reduce the solubility and increase the conductivity of the ZnO, which could thereby lead to improvements in cell performance and lifetime. However, subsequent work showed that these additions lowered the electrochemical activity of the ZnO.

(f) A study of transition-metal-coated porous titanium electrodes for redox batteries by the University of Akron failed to identify cost-effective catalyst/substrate combinations.

### Electrochemical Processes

(1) A four-year joint project conducted by Diamond Shamrock Corporation and Case Western Reserve University was successfully completed. A primary objective was the development of a high-performance oxygen electrode for chlorine/caustic cells, thus reducing cell operating voltage 1.0 V below that in conventional cells. Diamond Shamrock Corporation has now commercialized this technology.

(2) A new effort to explore the use of transition-metal macrocyclic compounds as catalysts for air electrodes was initiated at Case Western Reserve University.

(3) All research and development activities related

to electrolytic technology have been phased out of the TBR Project, including the following topics:

(a) Transport processes in membranes employed in chlorine/caustic cells.
(b) Transport phenomena and electrolyte impurity effects in magnesium reduction cells.
(c) Mathematical modeling of processes in aluminum reduction cells.
(d) Use of biomass materials to reduce cell voltages in electrolysis and electrowinning cells.

### Fuel Cells

Los Alamos National laboratory has prepared a plan for a "Fuel Cells for Transportation" Program. This document identifies and evaluates several candidate fuel cell technologies potentially suitable for use in vehicles.

## PLANNED ACTIVITIES FOR FY 1983

Major new initiatives include the following:

(1) A prime contractor for research and development of Al/air cells will be selected.
(2) Fuel cell research projects focusing on new electrocatalysts and solid polymer electrolytes will be initiated.
(3) Industrial participation in lithium-alloy/metal-disulfide research and development activities will be solicited.
(4) Research to identify new separators for alkaline zinc cells will be initiated.
(5) Additional studies of polymeric and/or liquid electrolytes for ambient-temperature rechargeable lithium batteries will begin.
(6) Carbon corrosion phenomena in air electrodes will be examined, as will corrosion problems in high-temperature cells employing sulfur electrodes.
(7) Work on thermally regenerative electrochemical systems will be initiated.

# BATTERY ELECTRODE STUDIES*†

*E.J. Cairns, F.R. McLarnon, J.H. Flatt, M. Isaacson, M.H. Katz, P. Lessner, K.G. Miller, and T.J. Nichols*

The purpose of this research is to study the behavior of electrodes used in secondary batteries and to investigate practical means for improving their performance and lifetime. Systems of current interest include ambient-temperature rechargeable cells with zinc electrodes [Zn/NiOOH, Zn/AgO, Zn/$Cl_2$, Zn/$Br_2$, Zn/air, and Zn/$Fe(CN)_6^{-3}$] and rechargeable molten-salt cells (Li-Al/FeS, Li-Al/$FeS_2$, Li-Si/FeS, Li-Si/$FeS_2$, and Na/$\beta''$-$Al_2O_3$/NaCl-$AlCl_3$-$SCl_4$). The approach used in this investigation is to study life- and performance-limiting phenomena under realistic cell operating conditions.

## ACCOMPLISHMENTS DURING FY 1982

Investigations have centered on the zinc electrode, which exhibits satisfactory performance in rechargeable alkaline cells (Zn/NiOOH, Zn/air, Zn/$Fe(CN)_6^{-3}$, Zn/AgO) but has an inadequate cycle life. Its short lifetime and continual loss of capacity are closely related to a phenomenon known as shape change, the redistribution of active material over the face of the electrode as the cell is cycled.

### Computer Control of Electrochemical Experiments with Application to Zinc/Nickel Oxide Cells

(by M.H. Katz, E.J. Cairns, and F.R. McLarnon)

A computer-controlled test system has been designed and constructed to allow the simultaneous and continuous cycling of 16 or more electrochemical cells. The system offers resolution and stability

*This work was supported by the Assistant Secretary for Conservation and Renewable Energy, Office of Energy Systems Research, Energy Storage Division of the U.S. Department of Energy under Contract No. DE-AC03-76SF00098.

†This project is part of a larger effort, "Electrochemical Energy Storage," described in the *Materials and Molecular Research Division 1982 Annual Report* (LBL-15150).

within 0.025% of full scale, and response times are typically 1 millisecond. A wide variety of charge and discharge regimes, including pulsed charge and power discharge profiles, are implemented through various computer algorithms. The software configuration allows two programs to execute concurrently in the computer memory and to communicate with each other through a set of codified messages. This arrangement permits flexible interaction with all experiments and provides on-line data reduction and display.

The test system has been employed to investigate the effects of constant-current and various pulsed-current charging modes on the cycle life and capacity retention of Zn/NiOOH cells cycled at 100% depth-of-discharge. Test results included cell voltages, potentials of the NiOOH and Zn electrodes versus Hg/HgO reference electrodes, coulombs, watt-hours, average voltages, and associated efficiencies. Postmortem tests included Zn electrode x-ray studies.

A pulse profile of 30 ms-on/90 ms-off, with a 15 $mA/cm^2$ peak current density, improved the operating conditions of the cells by minimizing the overpotentials on the Zn and NiOOH electrodes. In contrast to all other charge profiles tested, it eliminated cell shorting (for at least 100 cycles) and slowed the loss of ZnO reserve, thereby preventing a rapid decline in cell capacity.

## Active Materials Redistribution Rates: Effect of Alkaline Electrolytes Having Reduced Zinc Oxide Solubility

(by J.T. Nichols, E.J. Cairns, and F.R. McLarnon)

A series of electrolytes formulated with low hydroxide-ion concentration has been tested in 1.35 Ah tri-electrode Zn/NiOOH cells to assess their ability to reduce zinc redistribution rates. A 3.5 *M* $OH^-$ electrolyte and a 3.5 *M* $OH^-$–3.4 *M* $F^-$ electrolyte were tested along with a borate electrolyte. The electrolytes were chosen to exhibit ZnO solubility approximately one-fourth that of the standard 30% KOH–1% LiOH electrolyte. A 6-hour charge rate and a 2½-hour discharge rate were employed for the 62-by-70 mm zinc oxide, Teflon-bonded electrodes to which 2% PbO was added to reduce hydrogen evolution rates. Zinc redistribution rates were found to be lower for electrolytes with reduced ZnO solubility, and zinc penetration of the separator was non-existent, even when overpotentials approached 130 mV when charging the Zn electrode in the borate electrolyte and 290 mV in the fluoride electrolyte. The 3.5 *M* $OH^-$ electrolyte demonstrated reduced zinc penetration, and the cells with standard electrolyte shorted from zinc penetration through the face of the separator. The high overpotentials were found to exist when substantial amounts of ZnO remained in the electrode. Less than 2% inactive zinc was found in the zinc electrodes cycled in the fluoride and borate electrolytes, and a similar low amount was present in electrodes cycled in the 3.5 *M* and 7.4 *M* $OH^-$ electrolytes.

## Mathematical Modeling

(by K. Miller, E.J. Cairns, and F.R. McLarnon)

The zinc electrode in Zn/NiOOH cells exhibits failure upon cycling, and the purpose of this work is to develop a comprehensive model that describes this behavior. Suggested causes of failure include passivation by a zinc oxide film[1,2] and shape change, the redistribution of zinc across the face of the electrode due to the high solubility of zinc-bearing species.[3-5] Models have already been written to describe the variation of current density and species concentrations in directions parallel to[4] and perpendicular to[1] the electrode surface. The present work combines both features to provide a two-dimensional, time-dependent model. The equations for the model are being developed, and an existing model[6] is being coupled with more rigorous chemical analyses to determine mechanisms of electrode failure.

Other activities include experiments to determine parameters needed for modeling efforts. Microscopy will also be performed on cycled zinc electrodes to determine the character of the zinc deposit on the current collector.

## Effect of Mixed Electrolytes on the Performance and Cycle Life of Zn/NiOOH Cells

(by M. Isaacson, E.J. Cairns, and F.R. McLarnon)

The high solubility of the zincate ion in Zn/NiOOH battery electrolytes contributes to its limited cycle life.[3,4] The solubility of the zincate ion may be decreased by adding a less polar solvent, such as an alcohol, to the electrolyte while maintaining a high KOH concentration. These additions may improve the

cycle life of Zn/NiOOH cells.

ZnO solubilities were measured in KOH-water-methanol and KOH-water-ethanol electrolytes to determine the extent of the Zn species solubility suppression. The data for 30% KOH-water-methanol electrolyte showed:

(1) The solubility was a maximum for 30% KOH–70% water.
(2) The solubility decreased by 75% for a 30% KOH–40% water–30% methanol electrolyte.
(3) The solubility decreased by 90% for a 30% KOH–20% water–50% methanol electrolyte.

Cell cycling to determine the effect of the alcohol additions on cycle life and cell performance are planned.

## Study of Model Zinc Electrode Pores

(by J. H. Flatt, E.J. Cairns, and F.R. McLarnon)

An electrochemical cell has been developed to study the behavior of a model zinc electrode pore in alkaline electrolyte. The cell design (Fig. 1) permits in-situ microscopic observation of the electrode surface, and multiple zinc reference microelectrodes provide simultaneous measurements of local electrochemical potentials. The reference microelectrodes are fabricated by using semiconductor processing techniques, including vacuum metal deposition and photolithography. The effect of varying pore diameters, electrolyte formulations, and electrode–area/electrolyte–volume ratios on zinc electrode discharge behavior will be studied. Experiments are in progress.

## Engineering Analysis of Photoelectrochemical Cells

(by P. Lessner, E. J. Cairns, and F. R. McLarnon)

Photoelectrochemical cells offer a convenient and efficient method to convert solar energy to electrical energy. We are modeling systems that include a photoelectrode, a catalytically active (in the dark) counterelectrode, and a redox couple.

Current work aims to identify catalytically active counterelectrodes for various redox couples, in particular the $S^{2-}/S_x^{2-}$/NaOH system because of its ability to stabilize several photoelectrodes. Literature references[7] and our preliminary work show that insoluble

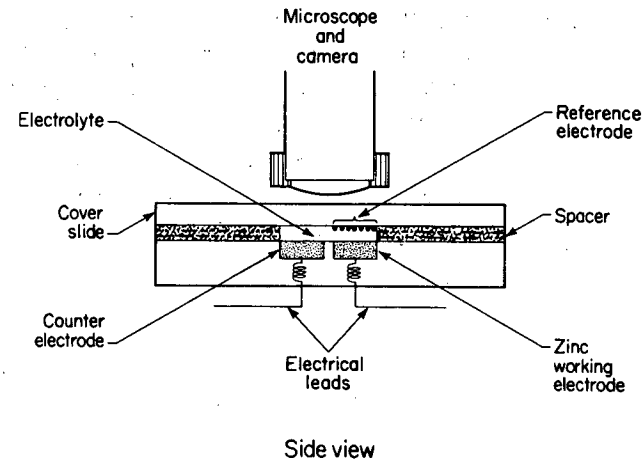


Figure 1. Electrochemical cell for studying the behavior of a model zinc electrode pore in alkaline electrolyte.
(XBL 831-27)

sulfur may foul these electrodes when operated in the anodic direction.

Future work will include an assessment of desirable qualities of electrolytes and an analysis of the effect of cell geometry and optical variables on photoelectrochemical cell performance.

## PLANNED ACTIVITIES FOR 1983

Planned efforts for each on-going project are described in the previous sections. New projects include the study of phase equilibria in molten lithium polysulfide electrolytes, the examination of novel electrolytes for use in Li/S cells, the study of corrosion-resistant current collector materials for use in sulfur electrodes, and an assessment of superacid electrolytes for fuel cells.

## REFERENCES

1. Sunu, W.T., and Bennion, D.N. (1980), "Transient and Failure Analysis of the Porous Zinc Electrode. I. Theoretical," *J. Electrochem. Soc. 127*, p. 2007.
2. Sunu, W.G. and Bennion, D.N. (1980), "Transient and Failure Analysis of the Porous Zinc Electrode. II. Experimental," *J. Electrochem. Soc. 127*, p. 2017.
3. McBreen, J. (1972), "Zinc Electrode Shape Change in Secondary Cells," *J. Electrochem. Soc. 119*, p. 1620.

4. Choi, K.W., Bennion, D.N., and Newman, J. (1976), "Engineering Analysis of Shape Change in Zinc Secondary Electrodes. I. Theoretical," *J. Electrochem. Soc. 123,* p. 1616.
5. Choi, K.W., et al. (1976), "Engineering Analysis of Shape Change in Zinc Secondary Electrodes. II. Experimental," *J. Electrochem. Soc. 123,* p. 1628.
6. Sunu, W.G. (1980), *Transient and Failure Analyses of Porous Zinc Electrodes,* Ph.D. dissertation, School of Engineering, University of California, Los Angeles.
7. Hodes, G., et al. (1980), "Electrocatalytic Electrodes for Polysulfide Redox System," *J. Electrochem. Soc. 127,* p. 544.

# SOLAR ENERGY PROGRAM

## INTRODUCTION

During FY 1982, the Solar Energy Program at Lawrence Berkeley Laboratory (LBL) continued to focus on research that will extend the technology base for a broad range of solar energy applications, and on exploration into new approaches to solar energy conversion.

Passive approaches to heating, cooling, and lighting of buildings have been a major topic of research. In these technologies, architectural design, construction materials, and natural energy flows between the interior and exterior environment are used to control a building's interior climate and reduce the use of non-renewable energy. In FY 1982, LBL's work in passive solar included heat transfer research, systems analysis, and materials studies. In the heat transfer area, two projects were pursued. In the first, experimental and analytic studies of natural convection processes that take place within buildings and between the interior of a building and the environment were performed. The purpose was to quantify the rates for natural ventilation, interzone heat transfer, and heat transfer to and from storage masses within a building. In the second project, data from spectral infrared sky measurements taken in previous years were analyzed in order to develop correlations between sky temperature and other environmental parameters. The ultimate purpose of this work was to determine the potential for radiative cooling of buildings in various parts of the country.

In the area of systems analysis, computer models of convective and other basic heat transfer processes were developed, verified, and incorporated into building energy analysis computer programs. The resulting computer models were then used to examine the energy consumption impacts of using passive heating, cooling, and lighting design strategies in commercial buildings. A broad-based technology assessment of passive cooling strategies was completed. The purpose was to quantify the relative merits of the various cooling techniques. Daylighting was also an integral part of our building energy systems analyses. Experimental measurements of illumination levels in scale models of daylit buildings are used in conjunction with dynamic simulations to quantify the impacts of the daylighting system on the energy consumed for electric lighting and auxiliary heating and cooling. The result is a true measure of the energy benefits of daylighting designs.

Finally, a new passive research project was initiated near the end of FY 1982. Innovative materials that can replace or supplement conventional glazing materials and provide large reductions in building energy use are being identified. Laboratory samples will be prepared and evaluated in future years.

LBL is also engaged in research on the active solar cooling of buildings. Thermodynamic cycles that have the potential for increasing the efficiency of solar-fired absorption air conditioners by at least a factor of two, compared to the current state-of-the-art, are being studied. An air conditioner based on one of these advanced cycles, the double-effect regenerative absorption cycle, has been designed, fabricated, and installed in a new laboratory test facility. Lab testing will be carried out during FY 1983. In parallel with the experimental work, analysis of the performance and economics of solar cooling systems has been performed. This analysis will help to establish realistic cost and performance goals for all solar cooling systems under development in the national DOE program.

Installation of a 25-ton-capacity solar absorption air conditioning system in LBL Building 71 as part of the Solar Federal Buildings Program will afford LBL engineers the opportunity to gain first-hand experience with one of the new solar cooling units developed in the DOE solar R&D program. The installation of this system was well under way by the end of FY 1982 and will be completed by mid-FY 1983.

In both the active solar cooling area and the passive area, LBL staff are providing technical support to DOE Headquarters and the DOE San Francisco Operations Office in developing program plans, evaluating reports and proposals, and technical monitoring of R&D activities by other contractors.

A new materials-oriented research program to explore advanced processes for solar energy utilization was established this year. The program evolved from an ongoing project to develop a new concept in high-temperature gas receivers based on the use of suspensions of very small (submicron) absorbing particles as radiant heat exchangers. The three primary elements of this research program are: solar heating and chemistry of small particle suspensions, porous optical materials for insulating glazings, and solar collection and control using diffractive optics. The underlying phenomenon in each case is based on the optical effects induced by the microstructural properties of materials.

One of the more basic research projects involves biological energy conversion techniques using one of the simplest and most stable biological energy converters known: the pigmented protein bacteriorhodopsin. This research project is attempting to elucidate how the molecular structure of this protein uses sunlight to produce an electrical proton current across bacterial and artificial membranes. Such understanding should ultimately lead to the production of novel photoelectric cells and solar batteries.

# PASSIVE RESEARCH AND DEVELOPMENT*

*R.C. Kammerud, J.W. Place, M.R. Martin, P.H. Berdahl, B. Andersson, F.S. Bauman, W.L. Carroll, A.J. Gadgil, A. Mertol, E. Ceballos, T.L. Webster, M.W. Nansteel, C.C. Conner, J.P. Coutier, M. Fontoynont, and E. F. Altmayer*

The amount of conventional fuel used to heat, cool, and light buildings is determined by (1) the interaction of the building with its environment, (2) the thermal gains associated with the activities occurring within the structure, (3) the thermal storage characteristics of the building, and (4) the operating characteristics of the equipment used to convert conventional fuels to end-use energy. Traditionally, the building design process has not adequately accounted for the combined influence of these four factors on building energy consumption. To do so requires that the designer have access to techniques for properly controlling the interactions of the building with the environment and for managing the energy flows within the structure.

Passive heating, cooling, and lighting strategies integrate the energy control and management schemes into the building design. The design parameters are selected so that they enhance and control the coupling of the building to the environment, thereby reducing the requirements for auxiliary heating, cooling, and lighting energy. In this context, the Passive Program at Lawrence Berkeley Laboratory is directed at theoretical and experimental investigations of the energy performance implications of passive design strategies, with emphasis on passive and hybrid cooling and natural lighting of commercial buildings. The specific objectives of the program are the following:

1. Develop analytic descriptions of the energy processes that occur within a building and between a building and the environment.
2. Develop and evaluate advanced passive/radiative cooling systems.
3. Evaluate the effectiveness of passive systems in reducing energy consumption for space heating, space cooling, and lighting.

*This research was supported by the Assistant Secretary for Conservation and Renewable Energy, Office of Solar Heat Technologies, Passive and Hybrid Solar Energy Division, of the U.S. Department of Energy under Contract DE-AC03-76SF00098.

The strategy used to meet these objectives consists of coordinated experimental and theoretical tasks leading to advanced energy analysis capabilities that can be used in passive system design and evaluation. The emphasis to date has been on the development and testing of techniques for predicting (1) the "resource" for passive systems and (2) a building's response to that resource. Here, the term "resource" implies the naturally occurring potentials of the environment to provide heating, lighting, and cooling. These potentials are being investigated in projects in the following areas: convection, radiative cooling, natural lighting, and passive building energy analysis. Accomplishments and plans in each of these areas are described below.

## ACCOMPLISHMENTS DURING FY 1982

### Convection Research

This project consists of both experimental and analytic studies of convective heat transfer both within a building and between the building and the environment. The objective is to develop technically sound and highly generalized predictive capabilities for (1) heat transfer between room surfaces and room air, (2) heat transfer through openings between rooms or zones, and (3) natural ventilation† of buildings with outside air. The analytic work attempts to develop and apply detailed numerical models for convection phenomena in order to develop simplified descriptive algorithms to represent the heat transfer process. Detailed experimental studies have provided the data needed for validation of the numerical analysis program.

Convection research conducted in FY 1982 focused on heat transfer within rooms via natural convection. A numerical analysis technique, validated against earlier LBL experiments and analysis,[1,2] was used to develop an extensive data base on heat transfer, air temperature, and air velocities for natural convection in a two-dimensional room (shown schematically in Fig. 1). The numerical data on heat transfer between the surfaces of the enclosure and the room air were analyzed to extract a correlation between surface temperature and surface heat flux for a range of

†Natural ventilation is defined here as controlled exchange of air between the interior and exterior of a building when ambient conditions are such that energy benefits can be realized. In contrast, infiltration is defined as the uncontrolled exchange of air with the environment, which is generally not energy advantageous.

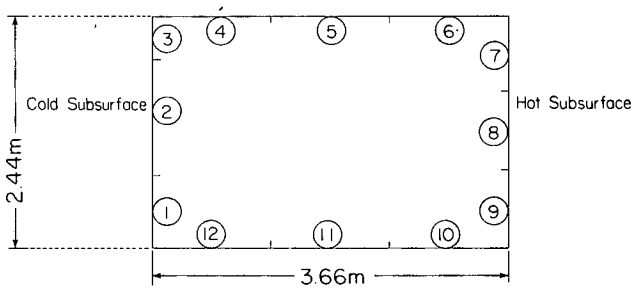


Figure 1. Schematic diagram of room used to develop convection correlation; circled numbers identify individual subsurfaces, with hot and cold subsurfaces at opposite ends of the room, as indicated. (XBL 8212-12514)

enclosure boundary conditions. These boundary conditions consisted of a hot surface on one wall, a cold surface on the opposite wall, and a constant intermediate temperature on all remaining surfaces in the room. The analysis was done for surfaces 1, 2, 7, and 8, which typically contribute on the order of 90% of the total heat transfer into or out of the room air, as described in Ref. 3. For these active surfaces, the correlation for the heat flux from the room surface to the room air, $q_i$, is shown below.

$$q_i = 2.40(T_i - T_i') \tag{1}$$

with

$$T_i' = K_1 T_H \left[\frac{A_H}{A}\right]^{3/4} + K_2 T_C \left[\frac{A_C}{A}\right]^{3/4} + K_3 T_I \left[\frac{A_I}{A}\right]^{3/4} + K_4 T_H + K_5 T_C \tag{2}$$

where $T_i$ is the temperature (°C) of surface $i$; $T_i'$ is the correlated temperature (°C) of air adjacent to surface $i$; $T_H$, $T_C$, and $T_I$ are the temperatures (°C) of the hot, cold, and inactive surfaces, respectively; $A_H$ and $A_C$, are the areas ($m^2$) of the hot and cold surfaces, respectively; $A_I$ is the total area of all inactive surfaces; and $A$ is the total surface area ($m^2$) of the room. The coefficients, $K_1$, $K_2$, $K_3$, $K_4$, and $K_5$ were obtained by fitting the numerically generated heat-transfer data base and are shown in Table 1. The constants shown in Table 1 are substituted into Eq. (2) and together with Eq. (1), produce a general correlation for the convective heat flux from the air to subsurface 1, 2, 7, or 8.

Table 1. Correlation constants.

| Subsurface Number | $K_1$ | $K_2$ | $K_3$ | $K_4$ | $K_5$ |
|---|---|---|---|---|---|
| 1 | 0.372 | 0.285 | 0.449 | 0 | 0.497 |
| 2 | 0.740 | 0.567 | 0.893 | 0 | 0 |
| 7 | 0.285 | 0.372 | 0.449 | 0.497 | 0 |
| 8 | 0.567 | 0.740 | 0.893 | 0 | 0 |

This correlation predicts convective heat transfer from room surfaces much more successfully than the existing correlations recommended by the American Society of Heating, Refrigeration, and Air-Conditioning Engineers (ASHRAE). Comparisons of predictions from the LBL and ASHRAE correlations with the observed heat fluxes from the numerical simulations are shown in Figs. 2a and 2b.

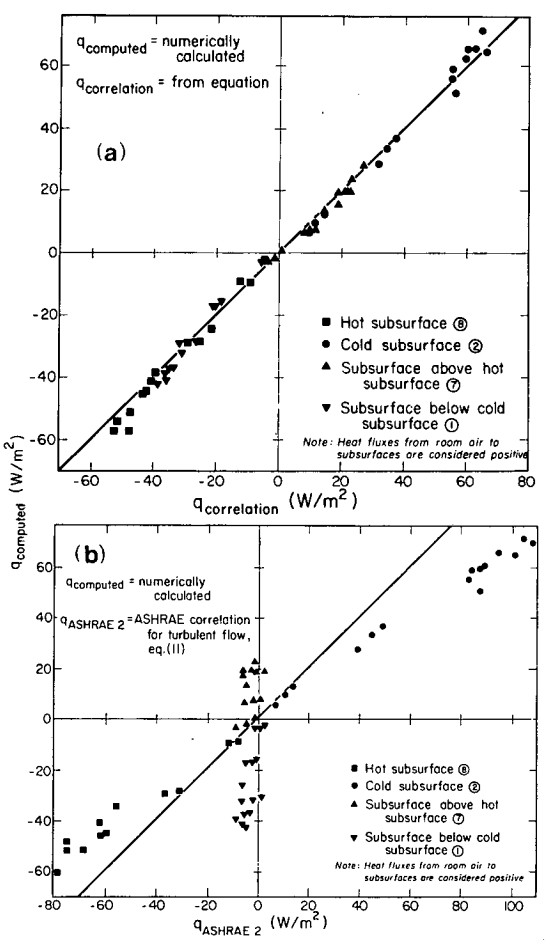


Figure 2. Heat-flux predictions from the LBL correlation (a) and the turbulent ASHRAE correlation (b) are compared with the numerically calculated results. Positions of the four subsurfaces are shown in Figure 1.

[(a) XBL 828-1081; (b) XBL 828-1085]

During FY 1982, experimental work on interzone convection in a two-dimensional enclosure separated by an adiabatic or a conducting partition was also concluded.[4] The experimental data for the two-zone configurations studied have been used to define a preliminary interzone convection heat transfer algorithm and will be used to further validate the convection numerical analysis computer program.

## Radiative Cooling

Infrared radiative cooling systems consist of a radiator surface exposed to the sky and a means for transporting heat from the building's interior to the radiator surface. The objective of this project is to quantify the environmental resource for radiative cooling in order to predict cooling system performance. The resource can be characterized in terms of the apparent sky emissivity for long-wavelength infrared radiation. To obtain a useful measure of sky radiance, radiometers were deployed in 1980 to collect data at six locations in the United States. The measurements taken included the spectral composition of the sky radiance as a function of zenith angle and local climate variables, such as dry-bulb and dew point temperatures.[5]

Raw data from the six locations were subjected to a detailed screening process to produce a final set of results consisting of measured values for a total of 57 months (6 locations) during 1979 and 1980 (an average of almost 10 months for each of the six locations); these results have been analyzed and expressed in terms of average monthly sky emissivities, since these quantities do not vary strongly with daily temperature fluctuations. Radiometer measurements taken through six infrared filters having the transmission characteristics shown in Fig. 3 are expressed as equivalent sky emissivities for the respective channels.

A set of graphs showing the equivalent spectral sky emissivity for several zenith angles is plotted as a function of total sky emissivity for the 8- to 14-micrometer channel under clear sky conditions in Fig. 4. Each letter plotted represents the monthly average emissivity for a single month of data taken at one of the six radiometer sites. Similar sets of graphs have been published for measurements made in each of the filter channels, and for both clear sky and all sky conditions.[6]

An empirical equation has been developed to correlate the large number of resulting data points with the total sky emissivity.[5,6,7] The spectral and angular component of clear sky radiation, $\epsilon_s(\lambda,\theta)$, is expressed in terms of the measured quantities $t(\lambda)/t$ and $b$ in the equation

$$\epsilon_s(\lambda,\theta) = 1 - (1-\epsilon_s)[t(\lambda)/t]e^{b(1.7 - 1/\cos\theta)} \quad (3)$$

Here, $\theta$ is the zenith angle, $\epsilon_s$ is the total sky emissivity, and $t(\lambda)/t$ is a normalized spectral transmission function for the clear atmosphere. The curved lines drawn through the data points in Fig. 4 represent best fits to the data, using $\theta$ = °C and $\theta$ = 60° measured values. The clear sky spectral and angular emissivities obtained from the six rather diverse U.S. locations can be expressed as a function of the total sky emissivity and do not exhibit marked regional variations. Systematic but small effects can be observed when the data taken under all sky conditions are plotted in a similar manner, due to the effect of cloud cover on the apparent sky emissivity.

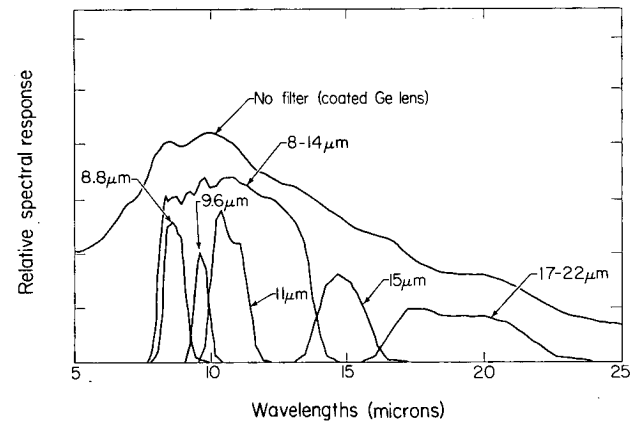


Figure 3. Radiometer spectral sensitivity with each of the six filters in place and the sensitivity with no filter.

(XBL 827-1610y)

## Commercial Building Energy Analysis

This project consists of (1) the development and experimental verification of computer programs that predict the energy consumption of passive commercial buildings and (2) the application of these programs to study the energy impacts of integrating various passive strategies with other energy systems in commercial buildings.

During FY 1982, research in this area centered on assessing the potential energy impacts of passive cooling technologies in nonresidential buildings.[8] The purpose was to identify those combinations of

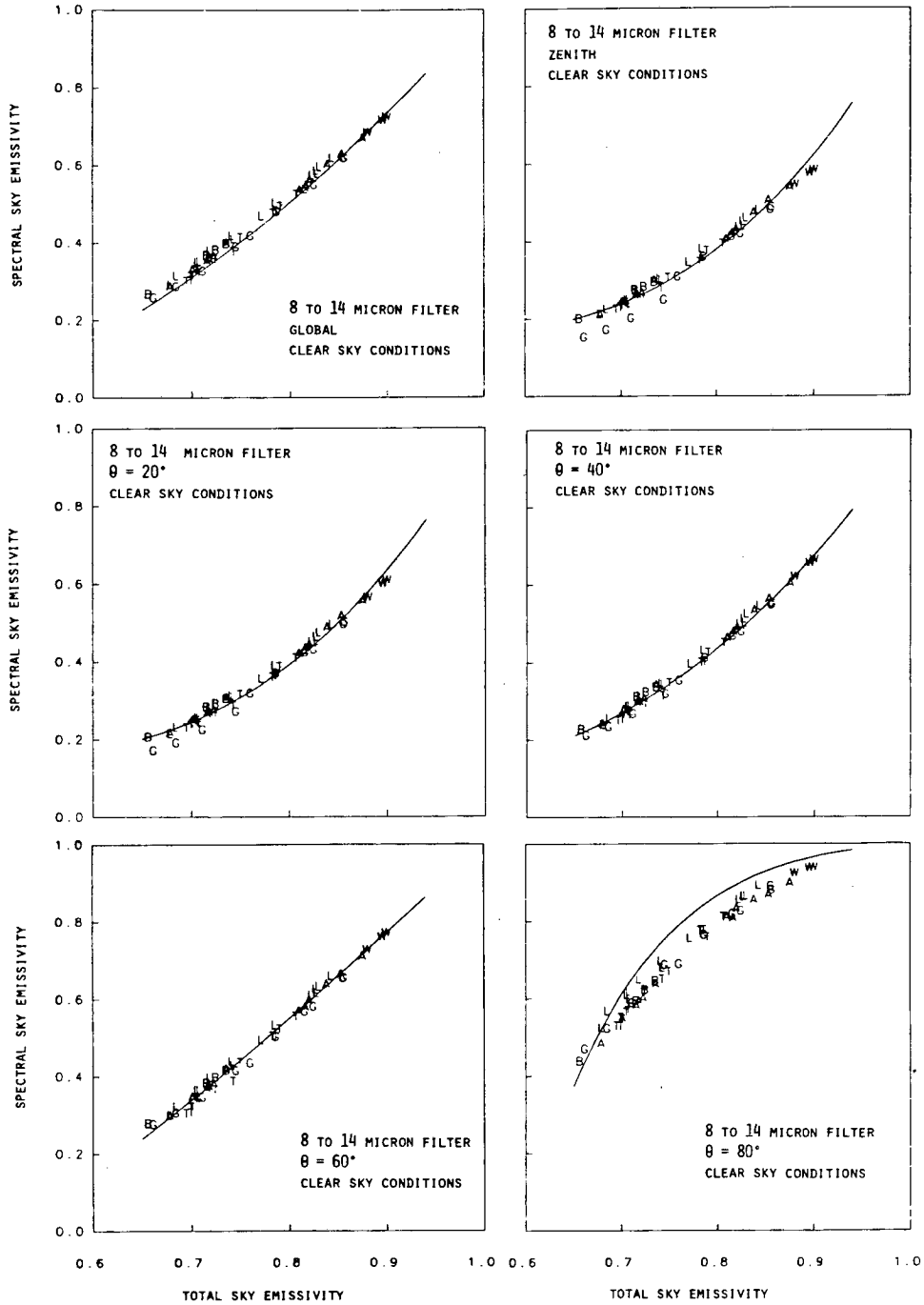


Figure 4. Measured monthly values of the 8- to 14-micron sky emissivities for clear skies, as functions of the total sky emissivity. Global values and measurements at zenith (0°), 20°, 40°, 60°, and 80° are shown. The global values are averages of the angular measurements, weighted with the cosine of the zenith angle. The 8- to 14-micron sky emissivity can be predicted from these results if the total sky emissivity is known. (XBL 831-7908)

passive cooling technologies, building types, and climates most likely to produce significant reductions in energy use; the passive technologies investigated were daylighting, ventilation, and dehumidification. This work was carried out jointly with personnel from the Los Alamos National Laboratory, who added an analysis of evaporative cooling to the assessment and who conducted economic analyses to establish preliminary indicators of economic feasibility.

Using BLAST[9] (and DOE-2 for evaporative cooling), energy consumption reductions were simulated for individual technologies as applied to specific buildings in specific climates. One-story (10,000-ft$^2$) and ten-story (100,000-ft$^2$) office buildings were selected for this assessment because they represent a large fraction of the floor area and energy consumption of the nonresidential sector and are relatively easily characterized. Eleven regions were selected to represent the range of climatic conditions for cooling in the United States. These regions were chosen using a climate aggregation methodology based on a similarity analysis of climate characteristics.[10] The energy performance of a base-case building was simulated first, then the building-simulation assumptions were changed to reflect the implementation of each passive cooling technology, and the building's energy performance was re-simulated.

*Base-Case Results*

The energy analyses of the base-case building provided a number of interesting results. Figure 5 shows total site energy consumption in kBtu/ft$^2$ yr for the one- and ten-story buildings. Requirements for both heating and cooling in such buildings are more climate-sensitive than previously thought: for the climates analyzed, the heating component varies by a factor of ten, and cooling by a factor of two. Results for the ten-story building show a similar pattern.

Lighting dominates electric consumption in all climate regions examined, ranging from roughly 60% to 75% of total electric consumption. Cooling, however, is the major source for peak power demand; significant reductions in peak power are reflected in reductions in both HVAC equipment size and utility capacity. The ratio of the peak power to total consumption tends to be higher in northern climates,

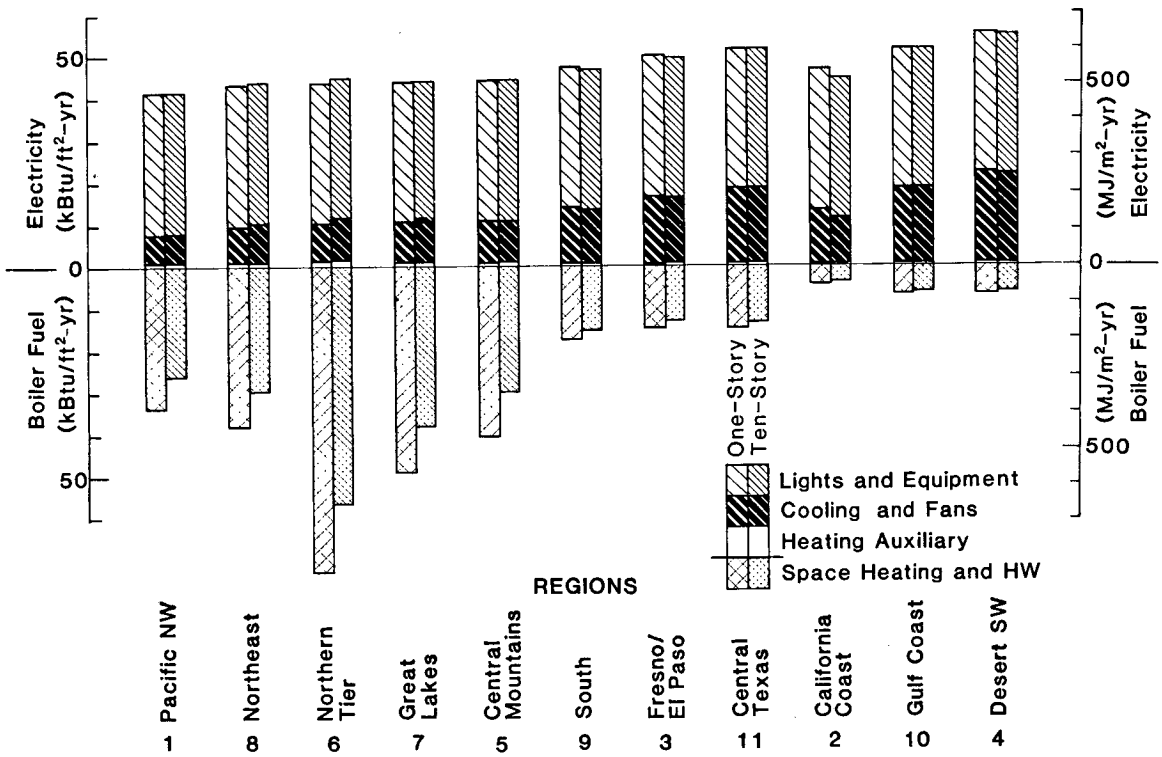


Figure 5. Annual electricity and fossil-fuel consumption of one- and ten-story office buildings, as computer-simulated for eleven regions and various end uses. These base-case designs are typical of current construction practice. The eleven regions span the range of climates in the continental U.S.

(XBL 827-7009)

suggesting that the most promising strategies there will be those having the biggest influence on peak power.

Total electricity costs for office buildings (including consumption and demand charges) far outweigh heating-fuel costs. In particular, demand charges represent a significant fraction of total electricity costs in most regions, although they vary widely. The overall importance of demand charges and their sensitivity to the application of passive cooling technologies are significant findings of the assessment. Further, the regional variation in energy costs does not correlate closely with the regional variation in energy use, showing the importance of local utility rate structures.

*Passive Cooling Technology Results*

Table 2 summarizes the energy and operating cost improvements for each technology. The range shown represents results for eleven climate regions representative of the continental United States. Results are for individual, newly constructed buildings. A discussion of the highlights of the results for each passive cooling technology follows.

- *Natural Lighting.* A realistically simulated natural lighting system for a one-story building produced energy consumption reductions and energy cost savings substantially greater than those of all other technologies investigated. The potential benefits of daylighting suggest that it should be one of the highest building-research priorities.
- *Evaporative Cooling.* Simulated energy performance results for the realistically designed systems showed modest savings in all climates, with the direct/indirect system showing a greater potential than the traditional direct evaporative coolers. The greatest savings occurred in the drier climates of the Southwest. Cost-savings patterns across climates were somewhat different than the energy-savings patterns due to variations in utility rate structures.
- *Nighttime Ventilation.* Simulation results for a thermodynamically ideal night ventilation system in a thermally massive building showed significant performance improvements in most climates investigated. Thermal mass was primarily responsible for substantial reduction in cooling demand and modest reductions in heating consumption. There is a strong possibility that this strategy could be effectively combined with other strategies such as day ventilation.
- *Daytime Ventilation.* Simulation of an idealized daytime ventilation system produced substantial reductions in space cooling loads, which in turn produced savings in cooling energy and total electricity consumption; the savings are similar in magnitude to those for the night ventilation strategy. The base-case building to which the daytime ventilation strategy was added in order to determine potential savings already used an economizer, so that the savings from daytime ventilation are in addition to those from economizer operation. Total energy cost-savings patterns across climates did not correlate in a simple manner with the energy-savings patterns; the relationship between energy cost savings and energy consumption savings across climates did not correlate with building size.
- *Dehumidification.* As a cooling strategy, this showed only limited potential for office buildings. Performance improvement was small in most of the climate regions analyzed and only modest in those few regions in which the best improvement was seen. The dehumidification system analyzed used the most favorable assumptions possible to characterize performance of the technology; only if occupant comfort requirements are modified will the potentials of dehumidification be enhanced over those summarized in Table 2.

Table 2. Summary of electricity consumption and cost reductions (in percents) for the passive cooling strategies examined in the technology assessment.

| | Electricity Use | | Electricity Cost | |
|---|---|---|---|---|
| Strategy | Cooling | Lighting | Consumption | Demand |
| Daylighting | 30 to 40 | 40 to 50 | about 40 | 20 to 35 |
| Nighttime Ventilation | 20 to 54 | 0 | 5 to 10 | 0 to 10 |
| Daytime Ventilation | 7 to 45 | 0 | +3 to 14 | 0 to 35 |
| Evaporation | 9 to 44 | 0 | 1 to 7 | 0 to 12 |
| Dehumidification | 2 to 21 | 0 | 0 to 7 | 0 to 16 |

## Natural Lighting

Natural lighting research within the Passive Program is closely connected to the energy analysis activities described above, but as a separate project it is more interdisciplinary in nature and addresses broader issues. The work focuses on examining the energy impacts of natural lighting within the context of the total energy requirements of the building. Experimental measurements are made on scale models to determine the radiation gains through glazing and the distribution of daylight within the building. These data are used with the energy analysis computer program BLAST to calculate the reduction in lighting electricity needed when the sunlight available is used to control electric lighting. The energy analysis program also performs a thermal analysis to predict the energy consumption for heating and cooling and the peak electric demand. The objective is to characterize the total energy impact of various solar aperture features, with an emphasis on generating design information for solar-aperture systems.[11]

An outdoor facility was set up at LBL to test the illumination behavior of a range of building configurations and daylighting apertures under actual solar conditions, using experimental scale models. During experiments, a model is mounted on a heliodon, a device that allows rapid reorientation of the model relative to the direction of beam sunlight. Within a few hours, enough data can be taken to effectively simulate clear-sky illumination effects for every possible combination of building orientation, hour of day, time of year, and geographic latitude in the United States. A pyranometer, pyrheliometer, and an array of photometers monitor radiation and illumination both external and internal to the scale model. A digital data acquisition system allows rapid scanning of the sensors to assure efficiency of measurement and simultaneity within a given set of sensor readings. The functional relationship between external-sensor data and internal-sensor data is put into BLAST to calculate the energy impacts of the daylighting system.

In FY 1982, energy analyses were performed on a prototypical single-story office building with tilted, south-facing glazing mounted in roof monitors. These simulations were performed using Typical Meteorological Year (TMY)[12] weather data for New York, Atlanta, and Los Angeles. Figure 6a shows the predicted annual lighting electricity consumption at the site vs. aperture ratio, defined as the ratio of the total area of glazing in the roof monitors to the total floor area in the building. For small aperture ratios (0 to 2.5%), the electric consumption decreases rapidly with each additional increment of aperture area. At larger aperture ratios (above 2.5%), the electric consumption is less sensitive to aperture area, indicating the diminishing number of hours during which additional sunlight can have a beneficial impact. The curves tend to asymptotically approach a lower limit, which is imposed by the electric lighting controllers and by the daily 12-hour lighting schedule, which includes many sunless hours. The reductions in lighting electricity were greater in Atlanta than New York because Atlanta has more available sunlight, particularly during the winter, when short days and cloudy conditions seriously limit the effectiveness of daylighting in New York. The greatest reductions in lighting electricity were observed in Los Angeles, which has almost exactly the same latitude as Atlanta, but clearer weather.

The annual energy consumption for cooling electricity at the site is plotted vs. aperture ratio in Fig. 6b. For small aperture ratios, cooling electricity consumption decreased with increasing aperture ratio for all three locations; this is the result of the higher luminous efficacy of sunlight in comparison to electric lighting. For larger aperture ratios, the solar gains become larger than required to provide lighting, and the cooling benefits of daylighting are negated.

The annual energy consumption of boiler fuel for heating is plotted vs. aperture ratio in Fig. 6c. For small aperture ratios, boiler fuel consumption increases with increasing aperture ratio because of the replacement of electric light with sunlight of lower heat content. This apparently negative effect is of little consequence, since the effect is small and boiler fuel is a much cheaper and more efficient source of heat than dissipating electric power in lamps. For large aperture ratios, the excess solar gains dominate the effect of the sunlight's higher luminous efficacy, and the boiler fuel consumption decreases with increasing aperture ratio. Figures 6a, b, and c suggest that movable insulation could produce significant reductions in energy consumption for lighting, cooling, and heating, if the insulation were controlled to limit summer gains to the level needed for illumination and controlled to maximize winter gains.

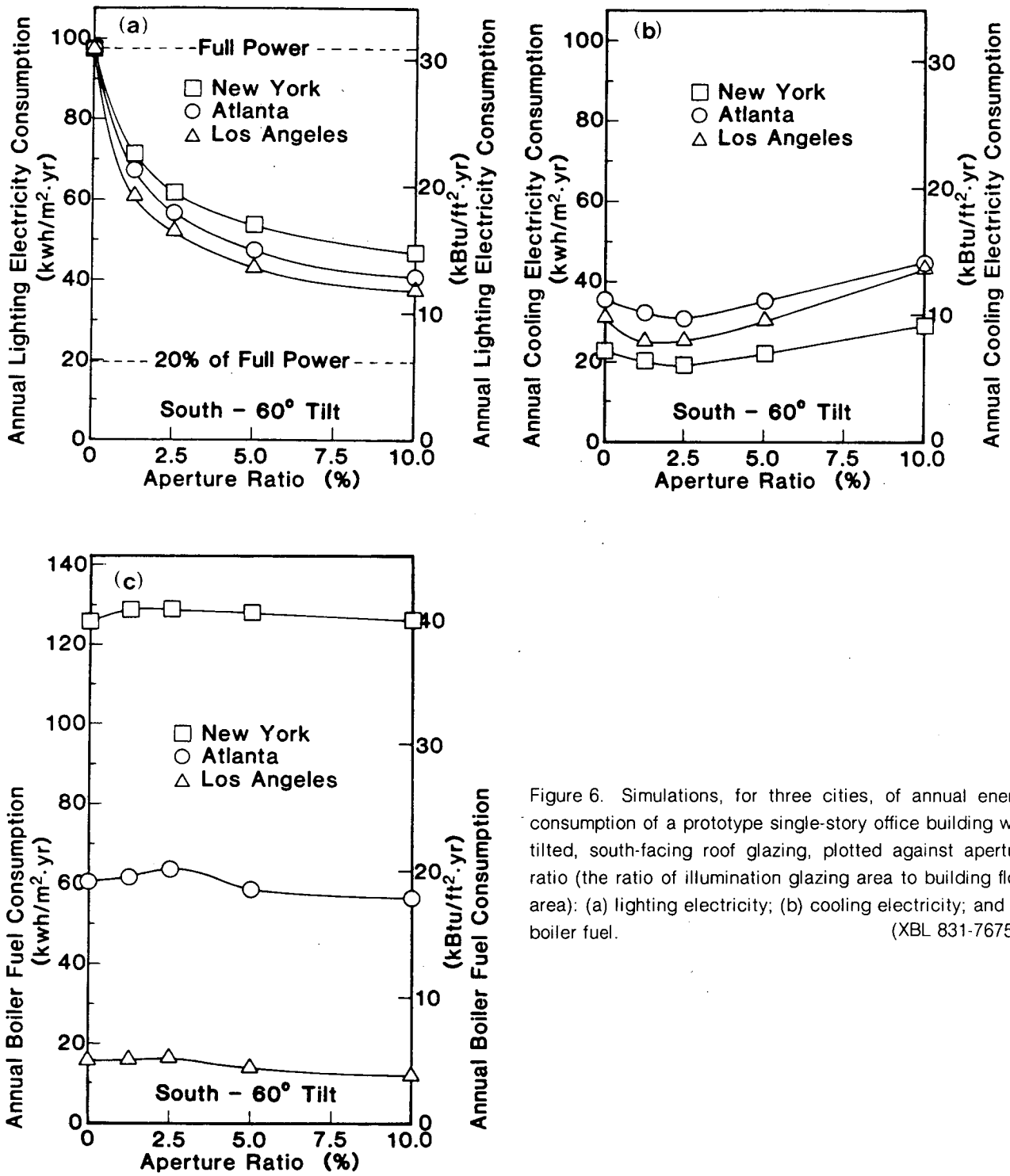


Figure 6. Simulations, for three cities, of annual energy consumption of a prototype single-story office building with tilted, south-facing roof glazing, plotted against aperture ratio (the ratio of illumination glazing area to building floor area): (a) lighting electricity; (b) cooling electricity; and (c) boiler fuel. (XBL 831-7675A)

Figure 7 shows the annual operating costs that have been computed for each location, using local billing policies for gas and electricity, including peak demand charges. For all three locations, costs decrease rapidly with increasing glazing area, up to an aperture ratio between 2% and 3%. Beyond an aperture ratio of 3%, increases in cooling electricity dominate decreases in lighting electricity, and the costs increase gradually with aperture area.

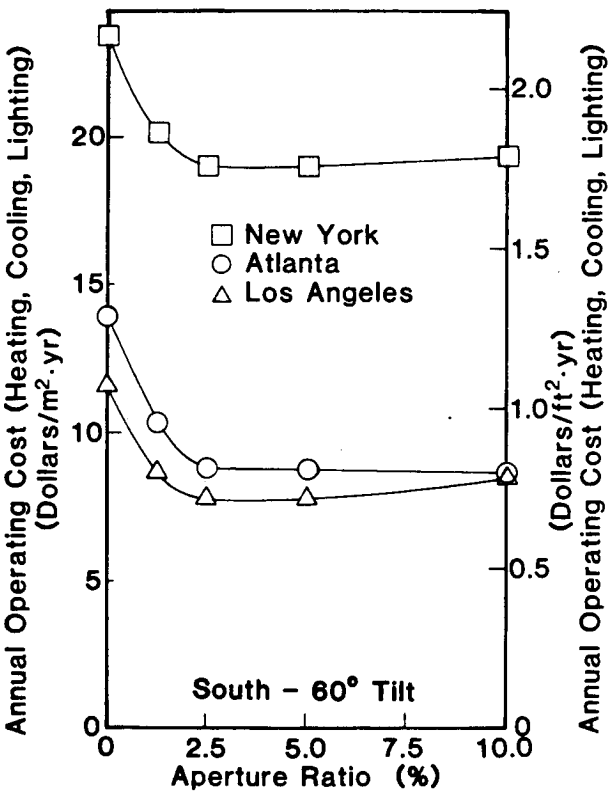


Figure 7. Annual operating costs for the prototype building of Fig. 6, computed for the same three cities and plotted against aperture ratio. (XBL 831-7675B)

## PLANNED ACTIVITIES FOR FY 1983

### Convection Research

The numerical simulations will be used for further studies of natural convection heat transfer from interior surfaces, and results will be used to produce correlations applicable to enclosure configurations and surface temperature distributions other than those studied in FY 1982. This work is expected to lead to a set of correlations applicable to geometric and thermal configurations of major interest, and will improve substantially the predictions of thermal loads in buildings. Turbulence model verification against data from wind tunnel tests conducted by the Florida Solar Energy Center in conjunction with Colorado State University is also expected to be completed in this period.

Construction of a full-scale, fully instrumented Multichamber Infiltration and Ventilation Efficiency (MIVE) facility is planned in FY 1983, in collaboration with two other groups in the E&E Division at LBL. Experimental research on interzone air flow driven by natural convection, wind infiltration, and/or mechanical ventilation systems will be conducted in the MIVE facility, using state-of-the-art instrumentation. Data from this facility will be used to further validate the convection analysis computer program, thereby enhancing confidence in the heat transfer correlations being developed.

### Radiative Cooling

The sky emissivity measurements will be used to develop a computer algorithm for predicting the average monthly sky temperature depression below the ambient air temperature. This algorithm, including the effects of cloud emissivity, will be used with average hourly weather data from TMY weather tapes to construct contour maps of the United States showing the monthly sky temperature depression. In addition, histograms will be developed to show the distribution of this quantity over the hours of the day for each month.

Substantial effort will be devoted to the conceptualization of radiative cooling assemblies and to the evaluation of their thermal performance. In particular, the need for new materials such as wavelength selective radiators and infrared transparent glazings will be assessed and performance goals established.

### Commercial Building Energy Analysis

A number of additional research pursuits are planned for FY 1983. We intend to: (1) extend the technology assessment analyses to include additional building types and passive cooling technologies (specifically, radiative-cooling and earth-contact strategies); (2) conduct parametric simulation analyses to determine the sensitivity of commercial building energy performance to selected design and use parameters and determine correlations between energy performance and climate; (3) continue investi-

gation of daylighting, ventilation, and evaporation technology analyses with increased focus on synergistic combinations, system integration, and thermal comfort issues; (4) conduct a detailed simulation-based reanalysis of selected buildings that were designed and constructed under the DOE-sponsored passive commercial buildings program.

## Natural Lighting

The natural lighting studies carried out in FY 1982 will be extended to examine the effect of variations in the input parameters, in order to determine the sensitivity of the energy consumption and cost predictions to various assumptions in the analysis. Among the factors to be examined are: thermal comfort controls, glazing characteristics, internal surface treatments, and dirt accumulation on the glazing. These studies will help define (1) the validity of the work done to date and (2) areas of emphasis in refining the design of daylighting systems. In addition to these sensitivity studies, the roof aperture work will be extended to other glazing tilts and orientations, as well as combinations of glazing orientations, and it will also consider more sophisticated techniques such as special glazing materials, reflector enhancements, and movable shading and insulation elements.

## REFERENCES


1. Bauman, F.S., Gadgil, A.J., Kammerud, R.C., Altmayer, E.F., and Nansteel, M.W. (1983), "Convective Heat Transfer in Buildings: Recent Research Results," to be published in *ASHRAE Transactions 89,* 1, Lawrence Berkeley Laboratory Report LBL-13883.
2. Gadgil, A.J., Bauman, F.S., and Kammerud, R.C. (1982), "Natural Convection in Passive Solar Buildings: Experiments, Analysis, and Results," *Passive Solar Journal 1,* 1, Lawrence Berkeley Laboratory Report LBL-9297 Revised.
3. Altmayer, E.F., Gadgil, A.J., Bauman, F.S., and Kammerud, R.C. (1982), "Correlations for Convective Heat Transfer from Room Surfaces," submitted for presentation to ASHRAE Semiannual Meeting, Washington, D.C., 26-30 June 1983, Lawrence Berkeley Laboratory Report LBL-14893.
4. Nansteel, M.W. (1982), *Natural Convection in Enclosures,* Ph.D. Thesis, Department of Mechanical Engineering, University of California, Berkeley.
5. Martin, M.R. and Berdahl, P.H. (1982), *Summary of Results of Spectral and Angular Sky Radiation Measurement Program,* Lawrence Berkeley Laboratory Report LBL-14913.
6. Martin, M.R. and Berdahl, P.H. (1983), "Results of Spectral and Angular Sky Radiation Measurement Program," to be published.
7. Berdahl, P.H., Martin, M.R., and Sakkal, F. (1983), "Thermal Performance of Radiative Cooling Panels," to be published in *Intl. J. Heat & Mass Transfer.*
8. Carroll, W.L., Webster, T.L., Mertol, A., Andersson, B., Kammerud, R.C., Place, J.W., Martin, M.R., Peterson, J., Mangeng, C., Roach, F., Whiddon, W.I., and Hart, G.K. (1982), *Passive Cooling Technology Assessment:* Synthesis Report, Lawrence Berkeley Laboratory Report LBL-15184.
9. BLAST (Building Loads Analysis and System Thermodynamics) is trademarked by the Construction Engineering Research Laboratory, U.S. Department of the Army, Champaign, Illinois.
10. Andersson, B.A., Carroll, W.L., and Martin, M.R. (1982), "Aggregation of U.S. Population Centers into Climate Regions," in *Proceedings,* 7th National Passive Solar Conference, 30 August - 1 September 1982, Knoxville, Tennessee, Lawrence Berkeley Laboratory Report LBL-14351.
11. Place, J.W., Fontoynont, M., Conner, C.C., Kammerud, R.C., Andersson, B.A., Bauman, F., Carroll, W.L., Howard, T.C., Mertol, A., and Webster, T.L. (1982), "Daylight Strategies," presented at Passive and Hybrid Solar Energy Update Meeting, 15-17 September 1982, Washington, D.C., Lawrence Berkeley Laboratory Report LBL-14946.
12. "Typical Meteorological Year User's Manual: Hourly Solar Radiation — Surface Meteorological Observations," TD-9734, National Climatic Center, April 1981.

# ACTIVE SOLAR COOLING*

*M. Wahlig, K. Dao, M. Warren, J. Rasson, R. Armer, A. Heitz,† and F. Salter*

This project has three major tasks: (1) research on improved absorption cycles for active solar cooling and heating, (2) systems and economic analysis of active solar cooling and heating systems to establish cost and performance goals for the national research program, and (3) technical support activities for the active solar cooling program.

## Absorption Chiller Research

The objective of the research activity on absorption cycles is to achieve a significantly higher conversion efficiency than is possible using other approaches for solar cooling and heating of buildings. Being essentially heat pumps, absorption-cycle chillers can be used for heating as well as cooling, if the refrigerant fluid does not freeze in the outdoor coil during heating applications. We restrict our fluid choices to those for which this heating option is available.

The absorption-cycle research program consists of four phases, each successive phase leading closer to the final machine. The first phase was successfully completed some time ago.[1] By modifying a conventional gas-fired ammonia/water absorption chiller, we demonstrated the capability of our analysis techniques to predict accurately the performance of single-effect absorption-cycle chillers under operating conditions appropriate for solar-powered cooling.

In the second phase, a completely new solar single-effect chiller[2] was designed, fabricated, and tested, using the experience gained during the first phase. This new ammonia/water chiller had several unique features for recouping thermal and mechanical energy. The report on this phase is essentially completed and should be available in March 1983.

In the third phase, we are investigating the performance improvement obtained by adding a unique second effect to the single-effect chiller tested in the second phase. The basic concept of the resulting double-effect regenerative cycle (or cycle 2R) has been described previously.[3] This 2R chiller has been designed,[4] fabricated, and assembled; the debugging and testing will be carried out during FY 1983.

During the fourth phase of the research, investigations will be carried out of a new concept in refrigeration absorption cycles, having still higher efficiency while requiring less heat-exchanger area, for a potentially lower cost. The basic concept of this single-effect regenerative cycle (which we call cycle 1R) has also been described previously.[5] The success of the cycle 1R chiller depends on our experience in developing the cycle 2R chiller. Locating a refrigerant-absorbent fluid pair with suitable properties at 300°F or higher should further increase the efficiency of the 1R chiller.

## Systems and Economics Analysis

The objectives of the systems and economics analyses are: to establish cost goals for active solar cooling and heating technologies based on the present value of future energy savings; to assess the current state of solar absorption and Rankine cooling technologies; to analyze the results of computer simulations to determine where improvements can and must be made in thermal and electrical performance; and to make recommendations on research needs to develop cost-effective active solar cooling technology.

## Technical Support Activities

Our technical support activities provide assistance in the active solar cooling program area to the DOE San Francisco Operations Office (SAN) Conservation and Solar Division and to the DOE Headquarters (HQ) Active Heating and Cooling Division, Office of Solar Heat Technologies. These activities include program planning; technical monitoring and evaluation of ongoing projects, including site visits and review of progress reports; coordination of review of unsolicited proposals; assistance in the preparation and evaluation of responses to program solicitations; and coordination of related activities by other organizations.

# ACCOMPLISHMENTS DURING FY 1982

## Absorption Chiller Research

*Conclusions of Research on the Single-Effect Chiller*

Detailed analysis of the experimental data from the single-effect chiller tested in 1981 has been com-

*This work was supported by the Assistant Secretary for Conservation and Renewable Energy, Office of Solar Heat Technologies, Active Heating and Cooling Division of the U.S. Department of Energy under Contract No. DE-AC03-76SF00098.

†Head of Heitz Energy Engineering, Inc.

pleted. The evaluation of the chiller and the resulting recommendations have been incorporated in a report that should be available in March 1983.

Conclusions presented in the report include the following:

1. The amount of heat available in the hot ammonia vapor generated should be recuperated in the preheater to increase the coefficient of performance (COP) by about 15% compared to conventional chiller designs.
2. The amount of work available in the high-pressure strong absorbent returning to the absorber should be recuperated in a piston driver to reduce parasitic pumping power (for solar-driven operating conditions) from about 150 watts/ton to 50 watts/ton.
3. For ammonia-water solutions in sensible, boiling, and absorption heat-exchange processes, conventional correlations using Nusselt, Reynolds, Prandtl, and friction factors can be used to predict (with an acceptable accuracy of ±20%) the overall heat-transfer coefficients and pressure-drop characteristics of the components. For two-phase flow regimes, the Lockhart-Martinelli and Shah correlations are applicable.
4. Detailed operating characteristics of the chiller can be accurately (±5%) predicted by computer simulation. The computer simulation proposed in the report produces results that match all experimental runs to within:

   ±2°F for all absolute temperatures
   ±5% for all differential temperatures
   ±5 psi for all absolute pressures
   ±10% for all differential pressures
   ±2% for all mass flow rates
   ±5% for all amounts of heat exchanged.

   These errors are also of the same order as the experimental errors. Computer simulations can thus definitely be used as a design tool for the next generation of single-effect absorption chillers, even though heat-transfer and pressure-drop characteristics can be validated only to ±20% error.
5. Control of the chiller should be studied carefully to further improve chiller performance. In particular:
   - The condenser/absorber fan speed should be controlled to match the cooling load for reduced parasitic power.
   - The liquid-ammonia expansion valve should be modulated to match the leaving chilled-water temperature at reduced cooling load.
   - The leaving chilled-water temperature should be allowed to rise when the input hot-water temperature is low, at least partially satisfying the load and thereby assisting the back-up cooling unit.

   In other words, although the proper strategy for controlling the chiller should be an integral part of the solar cooling system, it has yet to be fully thought out. An increase of about 30% in seasonal output of the chiller should be obtainable with good control strategy.

*The 2R Chiller*

The fabrication and installation of the 2R chiller have been completed. Figure 1 is a photograph of

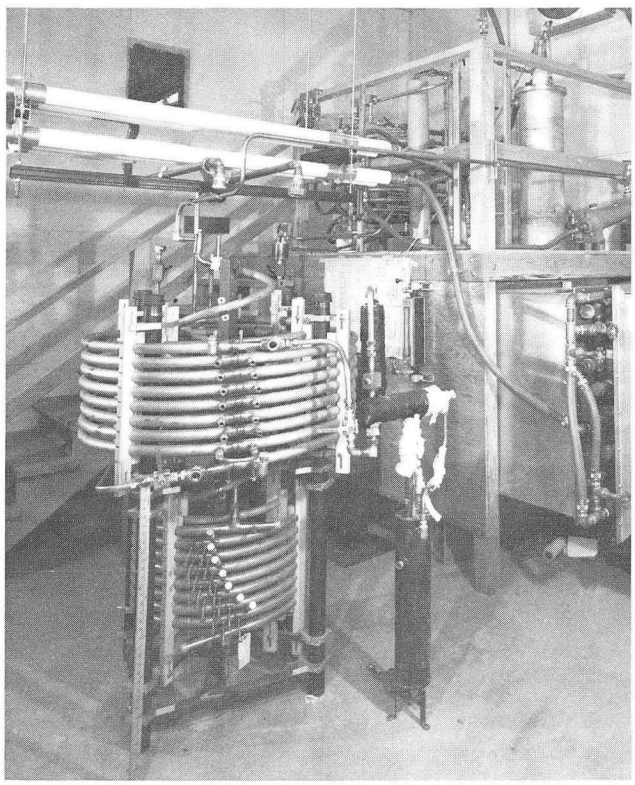

Figure 1. The cycle 2R absorption chiller being assembled in the LBL Experimental Chiller Test Facility.
(CBB 826-5078)

the installation in the laboratory test facility. Debugging was started at the end of FY 1982. The single-effect subcycle of the 2R chiller will be tested first, and modified as necessary until it runs reliably and efficiently, before the regenerative effect of the 2R cycle is tested. This should eliminate an appreciable fraction of the potential operating problems before testing the 2R chiller as a whole.

*Candidate Fluids for the Cycle 1R Chiller*

Under DOE contract and LBL guidance, SRI International conducted a literature search during FY 1981 and followed up with experimental measurements of the properties of absorbent and refrigerant fluids previously identified by LBL to be candidates for high-temperature (260 to 360°F) operation of a cycle 1R chiller. These measurements were completed during FY 1982, and the suitability of these fluids for cycle 1R operation will be evaluated during FY 1983.

## Systems and Economics Analysis

Principal accomplishments during FY 1982 include analyzing the electrical and thermal energy performance of both commercial and residential absorption and Rankine cooling systems, establishing quantitative cost goals and estimates of advanced solar and conventional system costs, developing research recommendations for the most promising cooling technologies, and refining the cost goal methodology to include the effects of taxes and depreciation.

The thermal and electrical characteristics of absorption and Rankine solar-fired cooling systems have been evaluated[6-8] for a number of system concepts, including single- and double-effect absorption systems, and Rankine turbines driving a mechanical compressor with and without electric power generation. Three heat rejection options were considered: air cooling, evaporative cooling, and use of a wet cooling tower. Both commercial systems (25 tons of cooling for a seven-zone light commercial office building) and residential systems (3 tons of cooling for a single-story residence) were evaluated. The systems analysis is based on recent computer simulations[9] in four cities representative of different climate regions: Miami, warm and humid; Phoenix, hot and dry; Fort Worth, warm and humid with mild winters; and Washington, D.C., warm in summer and cold in winter.

If solar cooling is to become a viable technology in the marketplace, the costs of today's systems must be reduced and the electrical and thermal performance must be improved. Four measures can and must be applied:

(1) Improve the thermal performance of the systems;
(2) Improve the electrical performance by reducing the parasitic power consumption;
(3) Decrease the costs of the major system components; and
(4) Achieve system integration to reduce the number of components in the system.

*Thermal Performance Improvement*

The thermal performance of active solar cooling systems can be improved by increasing the thermal coefficient of performance (COP) of the absorption-cycle or Rankine-cycle chillers, thereby reducing the solar heat input, collector area, and heat-rejection requirements for meeting a given fraction of the cooling load. The efficiency of the collector system can also be improved.

Advanced evacuated tube collectors with parabolic concentrating reflectors will have improved performance at the high temperatures needed for many active solar cooling applications. The operating performance of systems can be improved by application of control strategies such as variable flow-rate control in the collector loop, chilled-water reset, capacity modulation, spin down, and applying microcomputer control techniques. The thermal performance of the system can also be improved by applying storage strategies to obtain better matching between resource and load.

Advanced absorption chillers presently under development, if successful, will operate at higher temperatures with improved performance; these include the double-effect lithium bromide-water chiller with COP = 1.1 at 260°F and the water-ammonia regenerative chillers with COP = 1.25 at 280°F ("2R") and with COP = 1.55 at 280°F ("1R").

The thermal performance of Rankine-cycle systems can be improved by operation at higher temperatures and by development of more efficient expanders (e.g., turbines) and compressors. A Rankine cooling system with minimal storage and electric power generation with utility interface can obtain better utilization of the solar resource than a system without power generation.

*Electrical Performance Improvement*

A crucial issue in the development of cost-effective solar-fired absorption and Rankine cooling systems is

the reduction of parasitic power consumption. The electric energy consumption of the chiller system consists of energy to run the collector loop; energy to run the heat-rejection loop; energy to run the chilled-water loop; and energy to run the internal chiller pumps (e.g., the feed pump for a Rankine chiller, or the solution and refrigerant pumps for an absorption chiller). The electrical energy consumption can be reduced by proper design and sizing of pumps, piping, and heat exchangers.

For Rankine-cycle systems with electricity generation, the mechanical and electrical losses can be kept to a minimum by means of high-speed direct coupling of turbine and generator and by the use of unloading or pressure reduction to minimize windage losses (friction of the turbine or compressor spinning without power or load).

The electrical energy required to reject heat to the environment depends on the type of sink used (wet cooling tower, air-cooled dry coil, or wet-coil evaporative cooler); the amount of air movement; and the fluid pumping power required. The wet cooling tower is efficient in approaching ambient wet-bulb temperatures with minimum fan power, but fluid pumping energy is required. In many applications, an air-cooled condenser is preferred; however, the air-coil fluid cooler requires movement of a larger volume of air than does a wet cooling tower to remove the same amount of heat. The evaporatively cooled direct condenser coil achieves a good approach to the wet-bulb temperature and has the lowest combined fan and fluid pumping power requirement.

Because almost twice the heat must be rejected by a solar-fired cooling system compared to a conventional electric-powered system for the same efficiency of heat rejection, roughly twice the fan energy will be required. Improving the thermal performance of the solar-driven chillers clearly helps to reduce the limitation that heat rejection places on the energy savings for active solar cooling systems.

*Cost Reduction*

For active solar cooling to be a viable technology, the costs of the major components must be reduced. Absorption- or Rankine-chiller costs can be reduced by volume production and careful packaging. System control costs can be reduced by applying integrated microcomputer control with fewer sensors. The cost of high-performance evacuated-tube or linear-trough concentrating collectors must be reduced to about $9/ft$^2$, if the value of solar heat collected is to be competitive with natural gas. For operation at lower temperatures, the cost of plastic-laminated-film flat-plate collectors must be reduced to about $5/ft$^2$.

*System Integration*

A high degree of integration must be achieved in active solar cooling systems to eliminate duplication of function and to minimize the number and size of components. Careful packaging of equipment can minimize the number of pumps and valves and reduce the piping runs to a minimum. Careful integration of the control of system functions can minimize the number of sensors required and maximize reliability. Using a direct-fire backup of an absorption chiller in both the cooling and heating modes will efficiently use natural gas as a backup fuel.

*Incremental System Costs and Cost Goals*

In FY 1982, work continued on refining the cost-goal methodology[10] based on the discounted present value of future energy savings and the assumption of a 20-year system life and 20-year, 9-year, and 5-year payback periods. Estimates were made of the energy savings, incremental cost goals, and incremental system costs. Table 1 summarizes the estimated system costs and the projected cost goals based on the Science Applications, Inc. (SAI) simulation analysis for high-temperature (300°F) second-generation Rankine turbine systems.

Table 1. Comparison of system costs and year 2000 cost goals (in 1981 $) for variations of a high-temperature (300°F), second-generation Rankine turbine system in Phoenix.

| Evap. Temp./ Cond. Type | Area ($m^2$) | System Incremental Cost[a] ($) | Incremental Cost Goal 20-yr payback ($) | 9-yr payback ($) | 5-yr payback ($) |
|---|---|---|---|---|---|
| 45°F/evap | 232 | 78 066 | 98 949 | 50 353 | 26 370 |
| 55°F/evap | 232 | 78 066 | 109 034 | 55 486 | 29 057 |
| 55°F/water | 232 | 78 066 | 94 082 | 47 877 | 25 073 |
| 55°F/air | 232 | 78 066 | 78 886 | 39 126 | 20 490 |

[a]Costs of evaporatively cooled and air-cooled units should be comparable to those of the water-cooled units.

Evaporatively cooled condenser systems outperform both water-cooled (wet-cooling-tower) and air-cooled systems. Where possible, evaporative cooling should be used for heat rejection. Estimates of the costs of evaporatively cooled condensers should be made. The systems that operate at an evaporator tempera-

ture of 55°F save more energy than those operating at 45°F. The high-temperature advanced Rankine turbine systems should pay back in less than 20 years in the year 2000.

### Technical Support Activities

*Solar Cooling Program Planning*

The following are among the major planning activities carried out during FY 1982:

- Prepared documents on key accomplishments, present status, and future directions of the active solar cooling research and development program.
- Participated in major program planning and review meetings for the DOE Active Heating and Cooling Division, including plans for FY 1982, FY 1983, and future years.
- Made presentations on the overall DOE solar absorption and Rankine cooling program.

*Technical Monitoring*

The following are some of the major FY 1982 activities by LBL in providing technical monitoring and evaluation of solar cooling projects by outside (non-LBL) contractors:

- Conducted 23 site visits and project reviews covering 14 DOE contractors.
- Reviewed six final reports and topical reports and three follow-on proposals.
- Interacted with many of the solar cooling contractors at SAN and LBL meetings with individual contractors; in addition, numerous technical discussions with contractors took place by phone and by mail.
- Prepared and sent to DOE/SAN monthly summary reports on all the DOE solar absorption and Rankine cooling projects and related projects.

*Proposals for New Work*

One unsolicited proposal review was conducted by LBL during FY 1982, with the resulting recommendation for action being forwarded to DOE/SAN.

*Coordinating Activities*

The following coordinating activities were carried out during FY 1982:

- Worked in support of DOE/SAN and ETEC (Energy Technology Engineering Center) to coordinate the technical monitoring of eight solar-cooling Operational Test Sites, including numerous meetings, site field visits, and reporting.
- Participated in the redirection of the U.S.-Mexican solar-refrigeration project, through a joint meeting in Mexico City of U.S. and Mexican technical experts, followed by first steps in the execution of the resulting joint project plan.
- Participated, as a member of the Heat Pump Integration Task Force, chaired by John Ryan of DOE/HQ, which effort culminated during FY 1982 in a report and presentation on promising future directions for an integrated program in absorption and chemical heat pumps.
- Participated in Organic Rankine-Cycle Coordination Meeting hosted by the Jet Propulsion Laboratory.
- Held frequent discussions with SERI (Solar Energy Research Institute) staff members responsible for technical support of the solar desiccant cooling program, to coordinate reports and presentations on the overall solar cooling program (including absorption, Rankine, and desiccant elements).
- Held discussions with ORNL staff for the purpose of coordinating the absorption-heat-pump activities supported by DOE/Conservation (for which ORNL has technical support responsibility) with the absorption-cooling activities supported by DOE/Solar.
- Participated in several meetings per month at SAN to coordinate LBL's technical support with SAN's program management responsibilities for the solar cooling program.

## PLANNED ACTIVITIES FOR FY 1983

### Absorption Chiller Research

Testing of the 2R chiller will continue throughout most or all of FY 1983. Anticipated problems include:

- Instability of operation because of unequal flow distribution into the successive absorption stages.
- Low effective generator temperature because of fluctuating vapor flow rates into the absorption channels of the generator.
- Low effectiveness of the recuperator

because of incomplete absorption in the low-pressure channel of the recuperator.

All of these problems should be correctable using suitable flow-control devices. For the moment, it is intended to test the 2R chiller with the simplest flow-control devices, namely, simple, properly sized orifices.

If testing of the 2R chiller is successful, as predicted, design of the 1R chiller would be started late in FY 1983.

### Systems and Economics Analysis

Systems and economics analysis of advanced active solar cooling systems will continue in FY 1983 in cooperation with the Active Program Research Requirements assessment. Work will focus on detailed analysis of absorption and Rankine solar cooling systems and on defining technical issues that must be addressed. We plan continued development of in-house capabilities for systems simulation and analysis of active cooling systems, including evaluation of the impact of chiller control strategies on system performance and energy savings.

### Technical Support Activities

The technical support activities in FY 1983 will be similar to those carried out during FY 1982. Program planning will continue to be an important task as the respective future roles of the Administration and of Congress in setting program directions become clarified. The major documentation task of describing the accomplishments of the national solar heating and cooling program since its inception, which was to have been written during FY 1982, has been delayed and is now expected to be completed during FY 1983.

Site visits to solar cooling contractors and review of topical and final reports will continue. A number of existing projects are expected to conclude during FY 1983. At the same time, several expected program solicitations during FY 1983 should result in several new active cooling projects. LBL will be involved in helping to draft technical scope statements for these solicitations and in technical review of the proposals received. In addition, reviews of unsolicited proposals will continue to be conducted as received.

Coordination activities with other organizations involved in similar programs will continue to be pursued with high priority. The importance of this coordination increases as the total resources available to the DOE/Solar and DOE/Conservation programs decrease.

## REFERENCES


1. Dao, K., Simmons, M., Wolgast, R., and Wahlig, M. (1977), *Performance of an Experimental Solar-Driven Absorption Air Conditioner,* Lawrence Berkeley Laboratory Report LBL-5911.
2. Dao, K., Wolgast, R., and Wahlig, M. (1979), *Development of Solar-Driven Absorption Air Conditioners and Heat Pumps,* Lawrence Berkeley Laboratory Report LBL-9630, p.15.
3. Kao, K. (1978), *Conceptual Design of an Advanced Absorption Cycle:* The Double-Effect Regenerative Absorption Refrigeration Cycle, Lawrence Berkeley Laboratory Report LBL-8405.
4. Dao, K., Wahlig, M., and Wali, E. (1980), *Development of Solar Driven Absorption Air Conditioners,* Lawrence Berkeley Laboratory Report LBL-11175, p.3-27.
5. Dao, K. (1978), *A New Absorption Cycle:* The Single-Effect Regenerative Absorption Refrigeration Cycle, Lawrence Berkeley Laboratory Report LBL-6879.
6. Warren, M.L. (1982), *Active Program Research Requirements for Water and Air Cooled Closed Cycle Commercial Absorption Systems,* LBID-651.
7. Warren, M.L. (1982), *Active Program Research Requirements for Commercial Solar Rankine Cooling Systems,* LBID-650.
8. Warren, M.L. (1982), *Active Program Research Requirements for Residential Solar Absorption and Rankine Cooling Systems,* LBID-652.
9. Choi, M., Morehouse, J. (1982), *Analysis of Commercial and Residential Solar Absorption and Rankine Cooling Systems,* Science Applications, Inc., Draft Final Report for Contract No. DE-AC03-81SF11573.
10. Warren, M.L., and Wahlig, M.A. (1982), *Cost and Performance Goal Methodology for Active Solar Cooling Systems,* LBL-12753.

# MOLECULAR ASPECTS OF LIGHT-ENERGY CONVERSION BY BACTERIORHODOPSIN*

*L. Packer, A.T. Quintanilha, R.J. Mehlhorn, H. Zwerling, J. Herz, E. Lam, W. Baird, and I. Fry*

Cells have developed several mechanisms for transducing and storing energy: some use them for harnessing solar energy. In the last few years, we have studied one of the simplest and most stable biological solar-energy converters known: bacteriorhodopsin (bR); Fig. 1 shows its structure. This pigmented protein catalyst can be found in the cell membrane of *Halobacterium halobium*, a bacterium that requires high concentrations of salt to survive. Our research program is attempting to determine the molecular details of how this protein utilizes light from the sun to produce an electrical current across the bacterial membranes. We anticipate that such understanding will ultimately lead to the production of novel photoelectric cells and solar batteries.

*This work was supported by the Office of Energy Research, Office of Basic Energy Sciences, Division of Biological Energy Research of the U.S. Department of Energy under Contract No. DE-AC03-76SF00098.

Light generates an electric (proton) current across the bR-containing "purple membrane" patch found in the cell membrane of these bacteria. We are attempting to elucidate how the molecular structure of bR gives this protein the capacity of converting visible-light energy into a proton current.

The purple membrane is made up exclusively of bR and lipids: the retinal chromophore in bR is attached to a lysine (amino acid) in the protein by a protonated Schiff's base linkage. Following a flash of light, the chromophore undergoes a photocycle in which several intermediates have been identified by their distinct absorption bands. Resonance Raman studies have shown that the appearance of one of these intermediates (designated $M_{412}$) is accompanied by the deprotonation of the retinal's Schiff's base linkage to the protein. Since, in the presence of light, bR functions as a proton ($H^+$) pump, it is commonly believed that the chromophore could be directly involved in the proton-pumping activity.

Whether or not other protonatable amino acid residues found in bR are involved in the mechanism of proton pumping across this protein is currently being investigated by a few groups around the world,

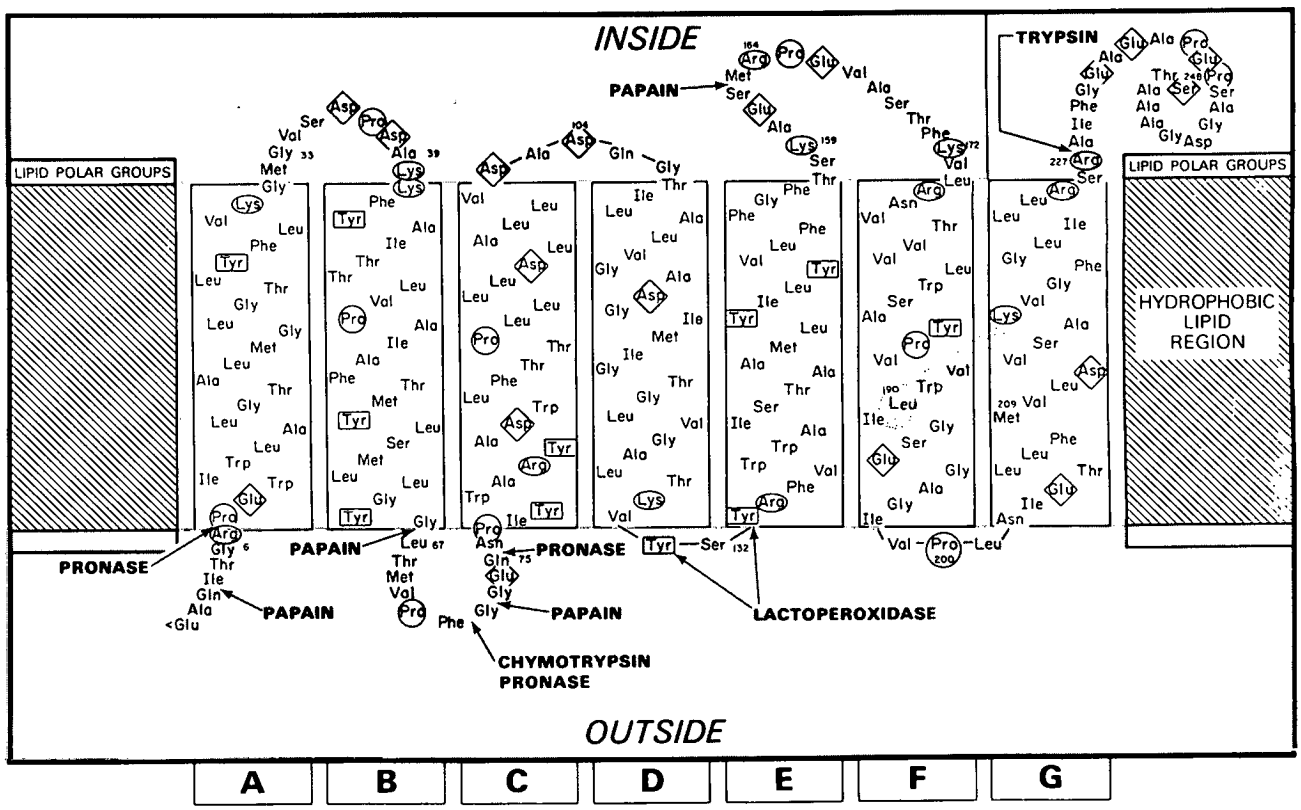


Figure 1. Amino acid sequence and membrane localization of bacteriorhodopsin.
(CBB 831-149)

including ours. Such information would be extremely important in any attempt to correlate the molecular events that occur during the photocycle, and would in fact be essential in the development of molecular models of photochemical conversion.

## ACCOMPLISHMENTS DURING FY 1982

### White Membrane Studies

Last year, we reported[1] that we were initiating studies with a mutant species of halobacteria which forms a membrane patch that apparently contains the apoprotein portion of bR but totally lacks retinal. Upon addition of all-*trans* retinal, this white mutant ($R_1$mW) of *H. Halobium* can reconstitute the functions of bR in intact cells.[2] The "white membrane patch" isolated from these cells forms a chromophore with $\lambda_{max}$ of about 568 nm after reconstitution with stoichiometric amounts of retinal.

Under acid conditions, bacteriorhodopsin is known to undergo a transformation to a species absorbing with a $\lambda_{max}$ of about 600 nm. This may involve carboxyl groups of amino acids. Difference spectra of the formation of this species show a positive maximum at 640 nm. The formation of this acid species is favored by low ionic strength, low pH, and high temperature. One of the intermediates of the photocycle ($O_{640}$) has been proposed to be similar, if not identical, to the acid-induced species, since it displays the same dependence on pH and temperature. Our recent studies suggest that the acid-induced species observed in reconstituted white membranes is similar, if not identical, to that of purple membranes; however, they also indicate that the pK of the transition is significantly higher in the reconstituted white membranes.[3]

The flash-induced absorbance increase at 640 nm in both purple and reconstituted white membranes was compared at different temperatures. Both preparations show stabilization of the O intermediate at higher temperature, thus confirming that the O intermediate of the reconstituted white membranes is similar to that of purple membranes. However, the 640 nm absorbance increase is larger in the reconstituted white membranes under the various temperatures studied, suggesting that the O intermediate is stabilized in the reconstituted white membranes.

It is known that the acid-stabilized species contains a higher percentage of 13-*cis* retinal and that low pH facilitates the light-dark adaptation rate of bR in native purple membranes. The dark-adapted form contains a much greater percentage of 13-*cis* retinal compared to the light-adapted form. Our results, however, show[3] that the rate of dark adaptation is considerably enhanced in reconstituted white membranes with a $t_{1/2}$ of about 2 minutes compared to 60 minutes for native purple membranes.

Thus, the results of these investigations show that certain properties of reconstituted white membrane patches differ from those of native purple membranes. These differences might be caused by stabilization of the 13-*cis* conformation of retinal in the reconstituted white membranes. In any case, it seems unlikely that they arise from differences in amino acid composition of bacteriorhodopsin in the mutant since the $R_1$mW strain of *H. halobium* is a spontaneous mutation that involves synthesis of retinal. In agreement with our suggestions at the time,[3] the studies described below provide further evidence that the differences might be due to changes in the lipid-protein interactions in the two systems.

### Protein Chemistry Studies†

Using the technique of SDS polyachrylamide gel electrophoresis, we compared native purple membrane preparations with white membrane preparations. When the gels were run for white membrane patches, we found that only one major protein peak was obtained whose speed of migration on the gel coincided with that of the single band found in the native purple membranes.

To determine if this apoprotein in white membrane closely resembled the bR protein molecule, we resorted to the technique of peptide mapping, previously used by the Cambridge group. Delipidated white membrane and purple membrane proteins were succinylated with $^{14}$C-succinic anhydride before specific enzymic cleavage. The peptides were chromatographed, and the characteristic patterns were analyzed by radioautography. Bacteriorhodopsin's characteristic pattern showed a close resemblance to the radioautographs obtained for similarly treated white membrane preparations. These results strongly suggest that the apoprotein in the white membrane patches is not substantially altered from the native protein.

†Collaboration with Prof. R. Perham, Department of Biochemistry, University of Cambridge, United Kingdom.

## Lipid and Lipid-Protein Interactions‡

We were able to show that the $^{31}P$ nuclear magnetic resonance pattern of white patches is similar at pH 7.0 to purple membrane patches, but differs from them at low and high pH. A lamellar hexagonal transition occurs in both membrane preparations at pH 2.0 in purple membranes and at pH 4.0 in white membranes. This correlates well with functional photocycle studies of white and purple membranes observed earlier, where the pHs of the $O_{640}$ photocycle intermediates differ by some 2 pH units in the acid range.[3] In the high pH range (pH > 8.5), the $^{31}P$ NMR spectrum exhibited a transition not observed in purple membranes. Again, this correlates well with changes in the visible spectrum of the chromoprotein of reconstituted white membrane patches at high pH not seen in purple membranes.

Infrared studies were made by means of a special technique for the preparation of wet thin-film specimens. The IR spectrum of the white membrane preparations is a function of temperature and pH. Again, the pattern found in white membranes was different from the native purple membrane in the region of the IR spectrum where phospholipid structural features should be observed. Preliminary infrared results of white membranes also show a change in the amide band below pH 5.0, indicating a lipid-protein transition at higher pH than in purple membrane patches.

Extraction of the lipids of the white membrane patches with organic solvents and spotting them on thin layer chromatographic plates further revealed that the pattern of the lipid composition in the white membranes substantially differs from that in the purple membranes.

We conclude from these studies that the differences observed in reconstituted white membranes from native purple membranes under different conditions of temperature and pH probably arise as a result of differences in lipids and lipid-protein interactions.

## Circular Dichroism and Optical Absorption Spectral Studies§

White membranes show no optical activity in areas of the circular dichroism (CD) spectrum where contributions from retinyl-protein and chromoprotein-chromoprotein interactions would be expected. After reconstitution of white membranes, however, many of the distinctive features of the CD pattern due to retinyl-protein and chromoprotein-chromoprotein interactions developed. These included the formation of a negative exciton coupling band ascribed to chromophore interactions in the visible region. In the ultraviolet region, a sharp CD band at 265 nm was induced upon reconstitution of the white membrane.[4,5] This band was present only as a small shoulder in unreconstituted white membranes. The optical activity in this region is likely due to interaction of retinal with aromatic amino acid bands in the protein. The generation of this CD band in bleached purple membrane was not conclusively shown previously because of poorer resolution of this feature.

## Chemical Modification Studies

### *Tyrosine*

Last year,[1] we reported studies carried out at low temperatures[6] which showed that at least two (and perhaps more) tyrosine residues have some role in the blue shift in $\lambda_{max}$ for iodinated bR. We concluded that a few tyrosine residues may be important in determining the color of native bR.

We have continued studies in the modification of tyrosines by using tetranitromethane (TNM).

Bacteriorhodopsin was modified by TNM at pH 8.0 by the method of Lemke and Oesterhelt. This results in a nitrotyrosine peak at about 360 nm and a blue shift in the chromophore. Under these conditions, the only nitrotyrosine residue that could not be reduced by dithionite was tyrosine-26, even though the blue shift remained, and we concluded that nitration of tyrosine-26 probably causes the blue shift. We found that the blue shift occurred only when light is present during modification.[7,8] Our results also suggest that modification of another tyrosine residue requires the presence of light at pH 5.5. Since normal nitration by TNM proceeds with the tyrosinate form of tyrosine, and since low pH did not inhibit this blue shift, the tyrosine residue modified must have an unusual pKa or else a different mechanism of reaction may be involved. That this reaction is totally light-dependent at pH 5.5, however, suggests that a complex of TNM with this special tyrosine might be a cause of this

‡Collaboration with Prof. D. Chapman, Biophysical Chemistry Department, Royal Free Hospital School of Medicine, University of London.

§Collaboration with Drs. N. Dencher and M. Heyn, Biophysical Chemistry Department, Biozentrum, University of Basel, Basel, Switzerland.

light-dependency: model system studies[9,10] show that, in the presence of light, TNM reacts with undissociated phenols. Chymotrypsin cleavage of the protein indicated that the residue modified was on the $C_1$ fragment (residues 72-248). Our method therefore allows a more specific modification of tyrosine using low pH and light.

*Carboxyl*

Two years ago[11] we reported results on the modification of the carboxyl group using carbodiimide. These studies have been extended.

Carboxyl groups on bR, in purple membranes, were covalently spin-labeled with Tempamine, using N-(ethoxycarbonyl)-2-ethoxy-1,2-dihydroquinoline as a highly specific coupling agent.[11,13] Spin-labeled bR (2 spins/mole) retained photocycling and proton pumping functions. Accessibility to paramagnetic broadening agents, $Fe(CN)_6^{-3}$ and $Ni^{+2}$, demonstrated the existence of two distinct spin populations in purple membranes: a highly mobile surface group quenched at low concentrations of these agents and buried immobilized groups whose ESR (electron spin resonance) signal remained at high quencher concentration. Treatment with denaturing agents greatly increased the mobility and quenching of these buried residues. A series of stearic acid spin labels bound to purple membranes was used to define the depth of paramagnetic interactions. $Fe(CN)_6^{-3}$ interactions were limited to surfaces whereas $Ni^{+2}$ and $Cu^{+2}$ effects extended into hydrophobic domains. A double modification procedure in which surface groups were first blocked selectively spin-labeled only a buried carboxyl group having a strongly immobilized signal. Comparison of the quenching behavior of stearic acids with this doubly modified sample indicated that one carboxyl residue is buried about 20 Å from the membrane surface. Cleavage of the carboxyl-terminal tail with trypsin increased the mobility of the spectrum, showing that this tail is moderately immobilized in the native structure. These data are consistent with tertiary-structure bR models that place carboxyls within hydrophobic domains of the protein-membrane matrix.

## Secondary Structure Modeling of Bacteriorhodopsin**

Computer models for possible helix and $\beta$-pleated sheet secondary structures for the membrane-bound portions of the primary amino acid sequence of bR were constructed on the NASA-Ames molecular modeling system.[13,14] Models were analyzed to determine the positions of charged groups and identify the structures which cause these groups to extend in a common direction. The complete bR monomer was constructed by assigning secondary structures to the seven rods of the three-dimensional data according to the several schemes favored by current experimental evidence. For each model, secondary structures were chosen that could be rotationally oriented to exclude the projection of charged side chains into the lipid environment and pair opposing charges internally.

Diffraction amplitudes for two-dimensional projections of these models were calculated and compared with the 3.7 Å projection found experimentally to see whether the theoretically preferred orientations gave a better fit than other orientations and whether models with our choice of secondary structures gave a better fit than models composed only of $\alpha$-II helices.

Further refinement of helix position was carried out using the interactive structural refinement procedure, and the best model has been selected. One of the favored models is shown in Fig. 2. Energy minimiza-

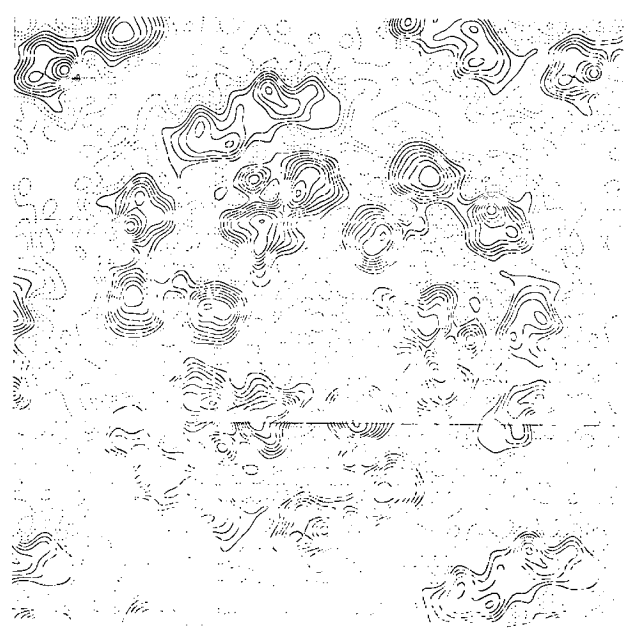

Figure 2. Computer simulated model of part of the bR molecule. (XBL 824-9354)

**Collaboration with Dr. R. MacElroy, NASA-Ames Research Center, Moffitt Field, California.

tion techniques will subsequently be used to explore the details of helix packing and side-chain positioning.

## PLANNED ACTIVITIES FOR FY 1983

Collaborative work with Dr. Perham's group in Cambridge and Dr. Chapman's group in London will continue to focus on basic aspects of lipid composition and structure as well as lipid-protein and protein-protein interactions. These studies may help us to elucidate the differences between the reconstituted white membrane and the purple membrane.

White membranes will be used for chemical modification studies in attempts to identify those amino groups that are important for reconstituting the photo-cycling and $H^+$ pumping activity of the protein. These studies, in conjunction with spin labeling, will provide us with a deeper understanding of the general topography of the protein, which of course will be extremely important for any attempts at theoretical structural modeling of the system.

We will extend our flash photolysis system into the ultraviolet range in order to look at some of the reactions that involve protonation and deprotonation of aromatic residues in the protein. Our time resolution will also be improved so that earlier events in the photocycle become accessible to study.

Computer simulation studies will be pursued in collaboration with Dr. R. MacElroy. These studies will make use of the results obtained by chemical modification of the protein in terms of defining the overall topography of the system.

Our well-characterized chemically modified samples will be used for FTIR studies that will be conducted in collaboration with Drs. K. Rothschild and D. Chapman. These studies will concentrate on the overall conformational changes that accompany the photocycle as they may be resolved in time.

Photoelectric properties of both native and chemically modified samples will be explored in collaboration with the laboratories of Dr. Keszthelyi in Szeged, Hungary,[16] and Dr. Fahr in Berlin. We hope to be able to clarify the electrical events that accompany the translocation of protons across these proteins.

## REFERENCES


1. Energy and Environment Division (1982), *Annual Report FY 1981*, Lawrence Berkeley Laboratory Report LBL-13500, p. 2-16.
2. Fry, I., et al., "Reconstitution of Light-Induced Ion Transport and Electrical Potentials by All-*Trans* Retinal in Membrane Vesicles of *Halobacterium halobium*," in preparation.
3. Lam, E., et al. (1982), "Comparison of the $O_{640}$ Photo-Intermediate and the Acid-Induced Species in Membrane Patches from *Halobacteria halobium* $S_9$ and $R_1$mW Strains," *FEBS Lett. 146*, pp.. 106-110.
4. Fry, I., et al., "Structure of White Membrane Patches from *Halobacterium halobium* $R_1$mW Before and After Reconstitution of Bacteriorhodopsin with All-*Trans* Retinal Measured by Circular Dichroism," in preparation.
5. Packer, L., et al., "Circular Dichroism Studies of Tyrosine-Modified Bacteriorhodopsin," in preparation.
6. Iwawa, T., et al. (1983), "The Photoreaction of Tyrosine-Iodinated Bacteriorhodopsin at Low Temperatures," *Bioscience Reports* (in press).
7. Katsura, T., et al. (1982), "Light-Dependent Modification of Bacteriorhodopsin by Tetranitromethane. Interaction of a Tyrosine and a Tryptophan Residue with Bound Retinal," *Biochem. Internatl. 5*, pp. 445-456.
8. Katsura, T., et al. (1983), "Specific Modification of a Tyrosine Residue Involved in the Interaction Between Bacteriorhodopsin and Retinal," *FEBS Lett.*, in press.
9. Seltzer, S., Lam.E., and Packer, L. (1982), "Photonitration of Phenols by Tetranitromethane under Visible Light," *J. Amer. Chem. Soc.* (in press).
10. Lam, E., Seltzer, S., and Packer, L. (1983), "Light-Dependent Modification of Bacteriorhodopsin with Tetranitromethane," to be presented at Biophysical Society meeting, San Diego, February 13-16, 1983.
11. Energy and Environment Division (1981), *Annual Report FY 1980*, Lawrence Berkeley Laboratory Report LBL-1190, p. 2-15.
12. Herz, J.M., Mehlhorn, R.J., and Packer, L. (1983), "Topography and Mobility of Spin-Labeled Carboxyl Residues in Bacteriorhodopsin," to be presented at Biophysical Society meeting, San Diego, February 13-16, 1983.
13. Herz, J.M., Mehlhorn, R.J., and Packer, L., "Topographic Studies of Spin-Labeled Bacteriorhodopsin: Evidence for Buried Carboxyl

Residues and Immobilization of the C-Terminal Tail," submitted for publication.
14. Zwerling, H., et al. (1982), "A Computer Technique for Structural Studies of Bacteriorhodopsin," in *Methods in Enzymology* (L. Packer, ed.), Vol. 88, Academic Press, New York, pp. 772-784.
15. Baird, W., et al. (1983), "Secondary Structure Modeling of Bacteriorhodopsin," to be presented at Biophysical Society meeting, San Diego, February 13-16, 1983.
16. Packer, L., et al. (1982), "Electrical Signals in the Photocycle of Tyrosine Modified Bacteriorhodopsin," *Biochem. Intl. 5*, pp. 437-443.

## LBL BUILDING 71 SOLAR COOLING PROJECT*

*F. Salter*

This active solar cooling project is part of the Department of Energy (DOE) Solar in Federal Buildings Program. The purposes of this program are to demonstrate the Federal Government's confidence in the solar industry and to stimulate growth and technical improvements in solar technology through the installation and demonstration of a variety of commercially applicable solar energy systems in buildings owned or occupied by the Federal Government. The program provides technical and financial assistance through interagency agreements to Federal agencies for design, acquisition, construction, and installation of solar heating and cooling equipment projects.

The LBL Plant Engineering Department is responsible for project engineering and contract administration. LBL's duties include: preparing the project proposal, preliminary engineering, conceptual design, design criteria, selection of an outside architect/engineer for final engineering and preparation of plans and specifications, engineering and administrative support for the architect/engineer, periodic review of the final design, administration of the bid process and subcontract negotiations, construction supervision, acceptance testing, and field testing of the system. The LBL Active Solar Research Group provides technical assistance and review of the project.

Overall administration is provided by the San Francisco Operations Office of the Department of Energy (DOE/SAN). DOE/SAN has subcontracted technical management of the project to Energy Technology Engineering Center (ETEC).

The Solar Cooling System will provide substitute capacity for the existing Building 71 chilled water system by installing the new chiller next to and in parallel with the existing electric chillers, which will be retained for back-up. The system will consist of roof-mounted collectors, storage tanks, a nominal 25-ton capacity lithium bromide chiller package and associated pumps, piping, insulation, valves and fittings, controls, and instrumentation. The chiller package will be supplied by Arkla and will be field-tested in the Solar Cooling System. Because more than 25 tons of cooling are continuously required at Building 71, the solar chiller will operate at full load for an average 6 hours per day.

Table 1 summarizes the design parameters of the cooling system. In addition, the collector array will utilize Energy Design HP250 evacuated-tube solar collectors to accomplish the 250°F maximum design temperature. The collector design emphasizes simplicity and durability to minimize maintenance. This is essential, as access to the collectors will be restricted during operation of the Building 71 accelerator because of roof radiation. Fluid will be contained in continuous copper tubing so that glass-tube breakage

Table 1. Parameters of LBL Building 71 solar cooling project.

| | |
|---|---|
| Chiller Capacity | 22 tons |
| Chiller COP | 0.73 |
| Average Operation | 6 hr/day (at 22-ton loading) |
| Generator Entering Water Temp. | 185°F (adjustable 170°F to 200°F) |
| Exiting Chilled Water Temp. | 45°F |
| Entering Condenser Water Temp. | 80°F |
| Maximum Storage Temp. | 250°F |
| Collector Area | 5400 $ft^2$ (gross area) |
| Collector Type | evacuated tube collector |
| Storage Tank | 2500 gallons |
| Thermal Ballast Tank | 500 gallons |
| Expansion Tank | 500 gallons |

*This work was supported by the Assistant Secretary for Conservation and Renewable Energy, Office of Solar Heat Technologies, Active Heating and Cooling Division of the U.S. Department of Energy under Contract No. DE-AC03-76SF00098.

will not disrupt system operation, and tube replacement can be scheduled for periods when the accelerator is not operating. Further reliability is accomplished by using high-quality "Pyrex-type" evacuated tubes that are less prone to breakage. The collectors have no cover glass, making tube replacement easier.

## ACCOMPLISHMENTS DURING FY 1982

The Final Design Review was held at LBL in December 1981. The project went to bid in early March 1982, and bids were opened on April 7, 1982. Additional funds were obtained to permit installation of the full project, and construction was started on June 7, 1982. The following construction had been accomplished by the end of FY 1982:

- The chiller package was modified, acquired, and placed in the mechanical room.
- The supporting steel framework for the solar collector was in place on the Building 71 roof.
- Most associated roofing work was complete.
- The concrete pad for the storage tanks was in place.
- Part of the electrical work was completed.

## PLANNED ACTIVITIES FOR FY 1983

The solar collectors and the storage tanks are scheduled to be received in December 1982. The Building 71 accelerator will be shut down for the month of January 1983, and installation of the collectors and above-roof piping is scheduled for this period.

All project construction is scheduled for completion by March 1983. ETEC will provide acceptance testing shortly thereafter, in the latter part of March 1983. The Final Report should be completed in April 1983.

LBL will review system performance periodically thereafter, using Btu meters placed in the solar collector loop, the generator loop, and the chilled water loop.

# SOLAR ENERGY SYSTEMS USING THE MICROSTRUCTURE OF MATERIALS*

*A. Hunt, D. Evans, L. Hansen, L. Sariola, L. Simionesco, and D. Worth*

## INTRODUCTION

The goal of this program is to explore new avenues in the collection and control of sunlight and its conversion to other energy forms through the use of the microstructure of matter. The optical behavior (reflectivity, color, transmission, etc.) of bulk matter undergoes profound changes when the dimensions of the material approach that of the wavelength of light. This optical behavior may be used to advantage in systems that derive their energy from radiant sources, and in particular the sun.

A multifaceted program is in place to study optical interactions with the microstructure of materials. The three main elements of the program are: (1) the study of the direct absorption of concentrated sunlight by suspensions of small particles, (2) studies of microporous optical media, and (3) the investigation of the control and concentration of sunlight using diffractive optics based on holograms. All three elements share similar experimental and theoretical methodologies because of the central role played in each by the light scattering produced by the microstructure nature of the material. These program elements are described individually below.

## I. SOLAR ABSORPTION BY SMALL PARTICLES

The concept of using a suspension of ultrafine particles to absorb concentrated sunlight has been under investigation at LBL for several years.[1] The central activity in this project has been the development of a high temperature gas receiver to utilize the energy in concentrated sunlight to heat a gas.[2] The Small Particle Heat Exchange Receiver (SPHER) operates by injecting a very small mass of fine carbon particles

*This project was supported by the Solar Thermal Test Facilities Users Association; the Solar Thermal Research and Advanced Development Program managed by the San Francisco Operations Office, the Office of Energy Systems Research, and the Passive and Hybrid Solar Division, all under the Assistant Secretary for Conservation and Renewable Energy; and the Director's Discretionary Fund though the U.S. Department of Energy under Contract No. DE-AC03-76SF00098.

into a working gas before it enters a windowed solar receiver. The particles absorb focused solar radiation and quickly transfer the heat to the surrounding gas. The mixture heats to a maximum temperature that is determined by the oxidation of the particles. The gas may be heated to medium or high temperatures suitable for operating a gas turbine for electrical power production or for supplying industrial process heat.

Last year, the first direct-absorption gas receiver, designated the SPHER, Mark I, was designed[3] and its construction started.[4] The receiver was designed to utilize 30 kW of concentrated sunlight to heat ambient air to temperatures above 700°C. To prove the concept, the receiver was to absorb 90% of the incoming sunlight in the gas-particle suspension, reducing the flux density on the receiver walls to 10% of the value it would have if no particles were present. The absorbing particles for this test were produced by the pyrolysis of acetylene.

A particle generator based on pyrolysis that was capable of supplying the necessary flow of particles for the test was developed in the laboratory.[5] After the laboratory generator was developed, it was rebuilt into a form suitable for field use.

The Mark I receiver was designed to operate using the central receiver solar concentrator at the Department of Energy Advanced Component Test Facility (ACTF) at the Georgia Institute of Technology. To design the receiver, measured data on the flux distribution of the ACTF was used to predict radiant flux on the receiver walls for various absorption chamber shapes and particle densities, using algorithms developed at LBL.[6] The receiver size and shape were varied to optimize the absorption within the chamber. The low flux loadings on the walls allowed the receiver to be constructed of stainless steel rather than the high-temperature alloys usually employed for such temperatures.

## Accomplishments During FY 1982

This year, the SPHER program achieved a major goal with the completion and successful solar testing of the Mark I receiver. The design philosophy and construction of the receiver are discussed elsewhere.[7] Construction was completed in early January 1982, and the test was carried out at the ACTF during August and September. In the solar test of the Mark I, 550 one-meter-diameter mirrors concentrated sunlight by a factor of 2000 onto the 20-centimeter-diameter window of the receiver. The performance of the receiver was monitored by thermocouples, pressure transducers, and laser measurement devices to determine the absorption of the particle suspension.

Figure 1 is a schematic diagram of the experimental arrangement. The main components are the air supply system, particle generator, receiver chamber, sensors, and data acquisition system (not illustrated).

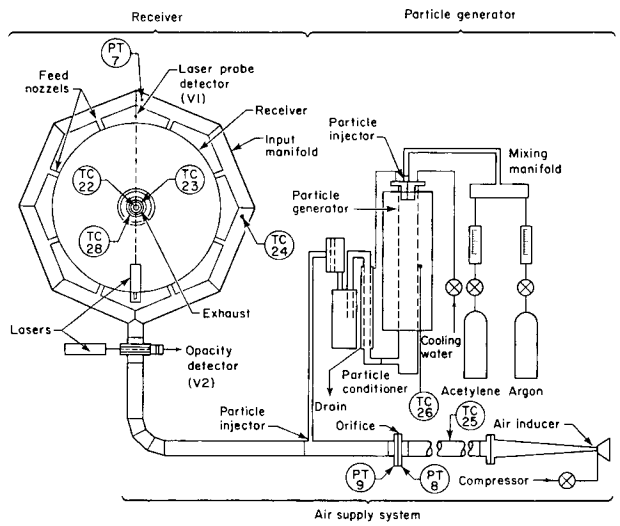


Figure 1. Schematic diagram of the experimental arrangement showing the three main components for the SPHER test. (XBL 8210-4782)

Ambient air to be heated is supplied by a Coanda-effect air inducer. This device produces a large flow of low-pressure air by using a small flow of higher-pressure air and provides an easily controllable and convenient source of air for the test. The mass flow rate of the air to the receiver was determined by measuring the pressure difference across a standard orifice plate. The particle generator produced a stream of carbon particles by the pyrolysis of acetylene in an argon carrier gas and injected them into the air supply system before it entered the receiver.

The temperature and pressure measurement points outside the receiver are also indicated in Figure 1. Temperatures inside the receiver were monitored by 26 thermocouples. A thermocouple with a four-component radiation shield determined the exhaust temperature. The receiver's power output was determined from the mass flow and the temperature rise. Solar input power was determined with a flux measuring system that was developed by the Engineering Experiment Station at the Georgia Institute of Technology. The system was designed to provide an

accurate determination of the input flux by utilizing an array of water-cooled calorimeters mounted in a paddle assembly that could be slid directly in front of the receiver window. Unfortunately, because of the intense solar radiation, the operation of the calorimeters became erratic and they began to fail within the first few hours of testing. Therefore, it was not possible to obtain an accurate value for the input flux. However, the approximate power could be determined from other flux measurements taken under conditions similar to those of the test.

*Test Results*

Solar testing was conducted on 13 days for a total testing time of 35 hours. All the major test objectives were met. The maximum output gas temperature was 750° C, and the output thermal power exceeded 30 kW. "Burn out," or oxidation of the particles, was achieved. The test established that concentrated sunlight can be absorbed directly within a working gas by small absorbing particles. The test also established that a window can be successfully used in a high-temperature environment and that carbon build-up on the window was not a problem.

Figure 2 illustrates the test results by showing the chamber temperatures for two different carbon particle loadings. The temperature of the output gas is

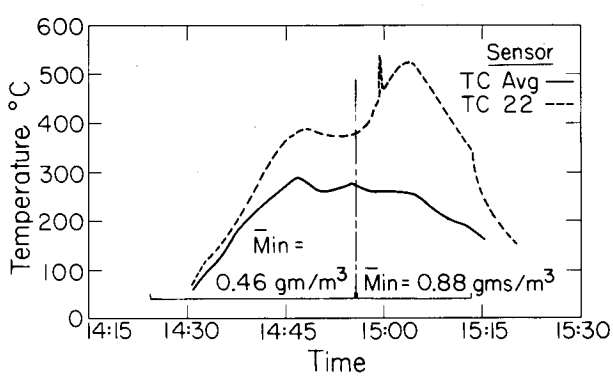


Figure 2. Exhaust gas temperature (TC 22) and average wall temperature (TC Avg) vs. time. The incoming particle density was increased from 0.46 to 0.88 gms/m$^3$ at 14:55. (XBL 8210-4783)

indicated by the dashed line, and the average interior-wall temperature by the solid line. It can be seen that the gas temperature exceeds the wall temperature over the entire run. In addition, the increase in density of the particle suspension (from 0.46 to 0.88 gms/m$^3$) at 14:55 was accompanied by a dramatic rise in the gas temperature with almost no increase in the wall temperature. The large difference in temperatures between the walls and the gas indicates that the gas particle suspension is being heated directly by sunlight and not by the walls.

## Planned Activities for FY 1983

As a result of the SPHER test program, several phenomena and potential applications in the area of direct radiant heating of two phase suspensions by solar thermal power were identified for further investigation. Analysis of the test data indicates that the majority of the heating can be localized in the absorbing gas-particle suspension. This phenomenon may be the key to achieving very high temperature direct-radiant processing. This localized heating could be used to isolate high-temperature chemical reactions from reactor walls, thereby reducing the demands on wall materials. If an ongoing chemical process can be separated from actively cooled walls without quenching the reaction, ultra-high-temperature solar-driven reactions may become feasible.

To investigate local heating effects, we plan a more detailed study of the coupling of concentrated radiation to absorbing suspensions. This is an interesting and complex problem because the large temperature variations cause density fluctuations in the gas that, in turn, change the optical absorption of the suspension. If time and resources permit, we plan to develop methods to predict and measure the density fluctuations in the suspension in the presence of a strong radiant flux density.

The second area we plan to investigate is the use of direct radiant heating of particle suspensions to produce chemical reactions.[8,9] We have identified several chemical processes of industrial importance that may be adapted for direct radiant solar heating. These include the detoxification of chemical wastes, the processing of phosphate rock to make elemental phosphorus, and cement processing. We plan to make a preliminary experimental investigation of direct radiant processing of suspensions of chemical feedstocks in FY 1983.

In a related but somewhat different area, we plan to investigate the capability of small particle suspensions to simultaneously capture sunlight and provide catalytic sites for gas-phase reactions. This effort will be an expansion of the direct radiant heating work.

## II. MICROPOROUS OPTICAL MATERIALS

Microporous optical material consists of a rigid matrix of nonabsorbing material with a pore size considerably less than a wavelength of light. Its density may be only a few percent of the density of the bulk material of which it is made. This material differs in a remarkable way from other porous materials in that it is highly transparent and has an effective index of refraction close to unity. The material is transparent because the pores are so small that they scatter very little visible light. It has a low index of refraction because propagating electromagnetic radiation responds to the *average* properties of the solid over dimensions comparable to the wavelength of light. The reflectivity of this material may also be very low because of its refractive index. Due to the low density and small pore size of this material, it is a very good thermal insulator.

The introduction of micropores into a solid opens new vistas in the materials science of the optical properties of solids. By varying the density, the index of refraction may be varied from the bulk value of the solid to nearly that of a vacuum. This offers a new degree of freedom for optical designers because it will be possible to specify the index of refraction of an optical element rather than being limited to existing materials. Graded index optical systems are possible by varying the local pore density of the material. Other approaches and processes in optics may benefit from the freedom of choice of the refractive index and low reflectivity.

For solar and conservation applications, the combination of transparency and low thermal conductivity makes the use of microporous materials for insulating windows and solar collector glazing very attractive. Microporous materials offer an alternative to conventional glazings in that they can replace double or triple pane glass with a package of similar thickness and transparency that possesses a higher R value.

The first transparent porous materials were made some time ago by using a process based on colloidal gels.[10] Materials prepared in this way are called aerogels. In this process, a colloid of the desired material is made sufficiently dense that the individual colloidal particles begin to link together. After cooling or aging, the material changes from a liquid state to that of a gel or jelly. The material is then a semisolid matrix of linked solids permeated by a liquid. Attempts to drive off the liquid by heating or drying inevitably lead to the collapse of the matrix, and the material shrinks to a fraction of its original size. This shrinkage occurs because, during drying, both liquid and gaseous states coexist in the matrix. Because of the very small size of the pores, surface tension effects between the gas and the liquid are very large, causing the structure to collapse during drying. The distinction between liquid and gas may be eliminated by raising the temperature and pressure of the liquid above its critical point. The resulting fluid may then be released from the gel without surface tension effects that would destroy the matrix. This process is referred to as supercritical drying.

Recently, interest in silica aerogels has resurged in Europe because of their application in Cherenkov detectors,[11] and a significant amount of material has been produced in Sweden.[12] Work started in this country[13] on using silica aerogels for windows, but it was discontinued. Several problems remain to be solved before these materials are ready for the commercial marketplace. While aerogels do not significantly interfere with directly transmitted light, they are slightly scattering, resulting in some haziness and color effects. Research in two main areas is required to improve the properties of aerogels before they may be used as glazing material. First, their physical and optical properties must be improved for them to gain widespread acceptance. Second, preparation techniques that are more suitable to mass production than the present laboratory technique need to be developed.

### Accomplishments During FY 1982

Work was initiated on porous optical materials in the spring of 1982 as part of the microstructure studies program. Samples of microporous material were obtained, and measurements of their scattering characteristics were performed. An angular nephelometer was borrowed for intensity and polarization measurements. Initial results indicated that the material did not have an angular scattering distribution characteristic of Rayleigh scattering. The polarization measurements were complicated by the discovery of rather striking birefringent effects. This phenomenon has not been previously reported in the literature. To explain these scattering properties, a tentative model was developed that is based on density fluctuations over distances larger than the pore size of the material.

A research effort was initiated late in FY 1982 with the support of the DOE Passive Solar Program to

develop techniques to produce transparent microporous materials and investigate their properties for insulating glazing applications.

### Planned Activities for FY 1983

In a joint effort with the Windows and Daylighting Group of the E & E Division, an experimental facility is being constructed to produce samples of porous silica for experiments. Production of small amounts of this material is expected to begin early in FY 1983. Facilities for producing the material are being set up, and equipment for detailed optical and scattering measurements will be assembled in FY 1983. A primary focus of the effort will be to determine the causes of the residual scattering in the aerogel and to reduce it. Alternative materials and methods for producing microporous optical material will also be explored.

## III. DIFFRACTIVE SOLAR COLLECTION SYSTEMS

This program element encompasses the use of diffractive optical devices to collect, redirect, and control sunlight.[14] Traditional solar collection systems rely on reflection or refraction of sunlight. The concept investigated here is based on using Holographic Optical Elements (HOE's) to intercept and diffract sunlight toward an energy conversion device, or on using HOE's as window or skylight coatings. Suitable energy conversion devices include photovoltaic cells or thermal receivers. Alternatively, a thin HOE coating may be placed on a window to diffract sunlight to an interior area that would not otherwise receive natural lighting.

A HOE is a simple type of hologram. The most familiar types of holograms act like 3-dimensional photographs and contain detailed information about the shape and lighting of the object. A HOE used for solar collection and control is more like a lens than a photograph. A simple HOE can be made by exposing a dye-sensitized emulsion to the interference between two beams of coherent light. Figure 3 illustrates two methods of making HOE's. Figure 3(a) illustrates the setup for making a transmission HOE that acts like a lens, and Figure 3(b) shows a method to make a reflection hologram that acts more like a mirror. The HOE characteristics are determined by the strengths and positions of the optical elements used to form the beams.

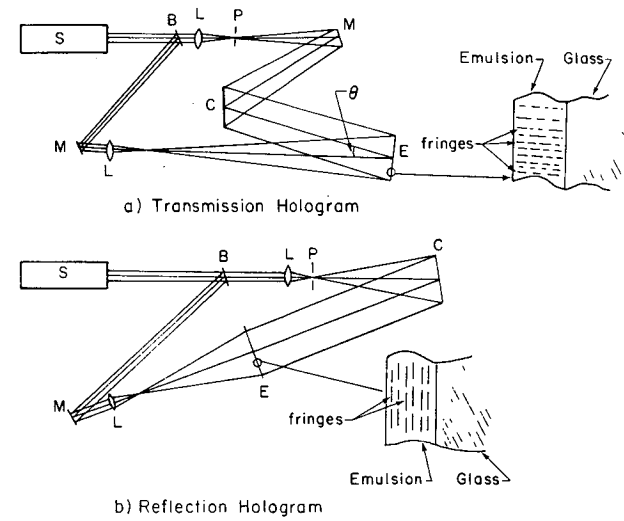


Figure 3. Typical holographic setup for (a) transmission hologram and (b) reflection hologram. Extreme enlargements of the emulsion cross sections are also shown. The components illustrated are the laser source S, beam splitter B, plane mirrors M, pinhole P, collimating mirror or lens C, emulsion E, and lenses L. (XBL 8211-7351)

### Accomplishments During FY 1982

Our investigation of the properties of HOE's for solar applications falls into three main areas: basic studies of the characteristics of diffractive devices for solar applications, including their wavelength and angular dependence; analytical calculations of the performance of specific concentrating HOE's; and experimental work to measure the efficiency of HOE's for solar energy applications.

During FY 1982, the study of HOE's for solar collection focused on the properties of volume (thick) holograms. Effects on the efficiency related to the Bragg condition were found to be important in applications where wide-angle response and high efficiency were required simultaneously. The application of HOE's for window coatings for daylighting purposes was explored in more detail. Figure 4 illustrates the use of HOE's placed on windows to redirect sunlight to the ceiling of a room, to substantially reject sunlight for some incident angles, or to redirect a rather narrow band of light deeply into a room independently of the solar angle.

### Planned Activities in FY 1983

The use of HOE's as window coatings will be pursued further as part of an assessment for the Office

of Energy Systems Research of the DOE Conservation Program. The project will investigate the possibilities, techniques, and effort required to develop holographic window coatings into practical systems for enhancing the use of daylight inside commercial and residential structures.

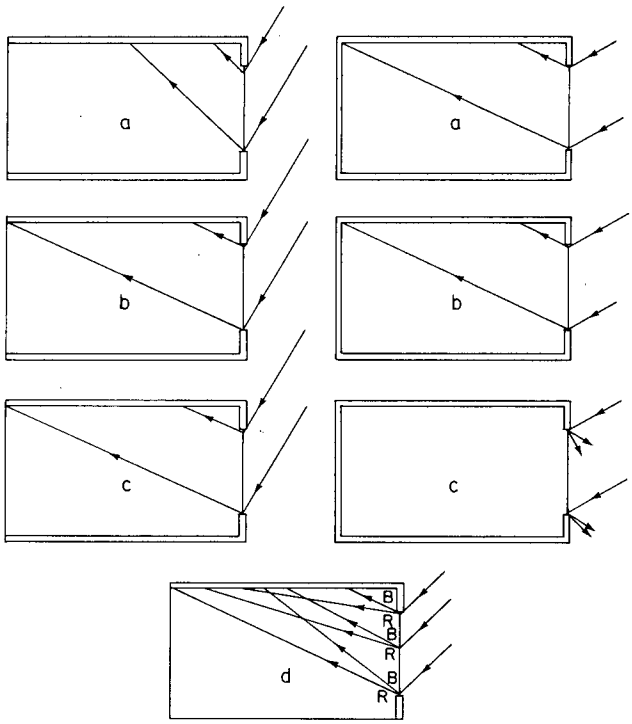


Figure 4. Holographic diffraction gratings for window coatings: (a) the action of a thin hologram with constant fringe spacing on light of one wavelength; (b) the use of a thick hologram to direct light to a portion of the room independent of the solar angle; (c) angular rejection of sunlight by a thick hologram; (d) spectral recombination with sunlight, using a thin hologram. (XBL 8211-7353)

## REFERENCES


1. Hunt, A.J. (1978), *Small Particle Heat Exchangers,* Lawrence Berkeley Laboratory Report LBL-7841.
2. Hunt, A.J. (1982), "Radiant Energy Collection and Conversion Apparatus," U.S. Patent No. 4,313,304, issued February 2, 1982.
3. Hunt, A.J., Hansen, L., and Evans, D.B. (1982), "Solar Heat Receiver and Process for Using Same," patent applied for.
4. Hunt, A.J., Deringer, M., Evans, D.B., Hansen, L., Hull, P.C., and Paydarfar, D. (1982), "Development of a 30-kW High Temperature Solar Receiver Using Small Particles as the Heat Exchangers," *Energy and Environment Division Annual Report FY 1981,* Lawrence Berkeley Laboratory Report LBL-13500, pp. 2-26 to 2-28.
5. Hunt, A.J. (1982), "Particle Generator," patent applied for.
6. Evans, D.B. and Hunt, A.J. (1981), "An Empirical Method for Determining Flux Distributions in Solar Thermal Receivers," *in Proceedings of the Workshop on Solar Flux Measurements,* Solar Thermal Test Facilities Users Association, Albuquerque, NM, 26-28 Oct. 1981, Lawrence Berkeley Report LBL-13523.
7. Hunt, A.J., and Evans, D. (1982), "The Design and Construction of a High Temperature Gas Receiver Utilizing Small Particles as the Heat Exchanger — (SPHER), Phase I Report," Lawrence Berkeley Laboratory Report LBL-13755, 1982.
8. Hunt, A.J. (1982), "Solar Radiant Heating of Small Particle Suspensions," in *Fundamentals of Solar Energy,* Vol. 3, published by AIChE, also Lawrence Berkeley Laboratory Report LBL-14077.
9. Hunt, A.J. (1982), "High Temperature Heat Exchangers Using Transparent Windows," invited paper at the Workshop on High Temperature Materials for Solar Thermal Applications, Cocoa Beach, FL, Jan. 21-22, 1982.
10. Kistler, S.S. (1931), *Nature 127,* 741.
11. Bourdinaud, M., et al. (1976), "Use of Silica Aerogels for Cherenkov Radiation Counter," *Nucl. Instrum. Meth. 136,* 99.
12. von Dardell, G., Professor, Lund University, Lund, Sweden, private communication.
13. Schmitt, W.J. (1981), "The Preparation of Acid Catalyzed Silica Aerogel," Presented at the Annual Meeting of the AIChE, New Orleans.
14. Evans, D.B. and Hunt, A.J. (1982), "Diffractive Solar Collection Systems," *Energy and Environment Division Annual Report 1981,* Lawrence Berkeley Laboratory Report LBL-13500, pp. 2-29 to 2-31.

# ENERGY EFFICIENT BUILDINGS PROGRAM

## INTRODUCTION

In 1982, the building sector accounted for 35% of United States resource energy consumption. In contrast, the energy burned as gasoline represented only 14% of our energy use. Since the crises in fuel scarcity and the attendant rise in fuel prices that occurred in the 1970s, industry has learned to make radical design changes in automobiles and buildings to enhance efficiency at the lowest possible cost and without compromising previous levels of service. In 1975, U.S.-built new cars averaged 14 miles per gallon; by 1985, new cars are expected to achieve about 28 mpg—a doubling of fuel efficiency. For existing buildings, research has shown that present resource energy use can be similarly reduced by 50% through careful retrofitting. New houses and commercial buildings are already being designed to use only half the energy of their pre-1975 counterparts, but our research findings suggest that, to minimize life-cycle cost, we should—and can—further reduce this figure to 20% of 1975 consumption—a factor-of-five increase in efficiency.

Although many of these gains would doubtless occur even without public-domain research programs such as ours, the natural time scale for commercialization is 5 to 10 years for cars and 10 to 20 years for buildings. (The energy efficiency of U.S. buildings is currently climbing at the rate of 3% per year.) Four examples of LBL research advancing the development of energy-saving products and techniques by 5 to 10 years will be given below. Each development—in ventilation, glazing, and lighting products—could save U.S. ratepayers at least $5 billion a year in utility bills, or $20 billion in all.

The Energy Efficient Buildings Program conducts theoretical and experimental research on various aspects of building technology that will permit such gains in energy efficiency without decreasing occupants' comfort or adversely affecting indoor air quality. To accomplish this goal, it has developed five major research groups whose findings and achievements are regularly reported in technical and scientific journals, presented at international conferences, and disseminated as Lawrence Berkeley Laboratory (LBL) reports.

A brief overview of the scope and objectives of each group follows.

### ENERGY PERFORMANCE OF BUILDINGS (EPB)

The EPB Group studies the flow of energy through all elements of a building. It thus tests air infiltration rates, thermal characteristics of structural elements, and the behavior of the interface between dissimilar materials. From an analysis of overall performance, the group can recommend cost-effective solutions for reducing infiltration and thermal losses, either by retrofitting existing buildings or by improving design features for new construction. This research is conducted in the laboratory and in the field; EPB also regularly conducts field measurements in single- and multi-family buildings, including a 350-unit apartment building in Oakland, a smaller Berkeley apartment house, and a high-rise dormitory at the University of California Berkeley campus.

EPB has also developed a public-domain microcomputer program, CIRA (Computerized Instrumented Residential Audit), which is designed to speed up and improve the accuracy of residential audits of energy consumption. It automatically provides the homeowner with a tailored list of retrofit options, ordered by return on investment, and a corresponding set of energy labels for the house.

A new activity has been the development of a prototype low-cost data acquisition system, the so-called Energy Signature Monitor. EPB is developing this 16-channel, all-solid-state recorder, complete with sensors and user-friendly installation and analysis software, for residential, and possibly commercial, applications. The ESM will allow cost-effective gathering of long-term data on energy use in large numbers of buildings, thus improving the poor statistics on which many analyses of building energy consumption have been based.

### BUILDING VENTILATION AND INDOOR AIR QUALITY (BVIAQ)

An obvious means of improving the energy efficiency of a building is to reduce air

infiltration/ventilation. Lowering the air-exchange rate, however, can trap indoor-generated pollutants within the building and enable them to build up to potentially harmful levels. The goals of this program are therefore to furnish a scientific basis for setting energy-efficient ventilation standards and to develop system designs that promote energy efficiency while maintaining the comfort, health, and safety of building occupants. Activities in support of these goals include: (1) development of new methodologies for measuring indoor air quality; (2) laboratory studies of emissions from building materials, soil, combustion appliances, and household products that may affect indoor air quality; and (3) field monitoring of indoor air quality in different types of buildings (schools, office buildings, residences) under a variety of ventilation conditions.

Closely related to this work is the investigation of strategies to prevent and control indoor air pollution without sacrificing energy efficiency. To this end, the BVIAQ group performs laboratory and field tests of various ventilation systems, including those that incorporate heat recuperation. Such recuperation can provide the necessary level of ventilation while recovering a substantial portion of the energy that would normally be lost in the exhaust air stream. This recuperated heat can be used to preheat either incoming air or domestic hot water.

Although the group was founded to study the hazards of reduced ventilation, it became evident that indoor air-quality problems occur even in "untightened" buildings and, indeed, that indoor air (which after all is only outdoor air with some additional pollutants) needs as much attention and monitoring as outdoor air. Specifically, it has found that, throughout the building stock, there are houses with unacceptably high levels of radioactive radon gas, formaldehyde, and combustion products. The problem in these cases is first to remove the sources of contamination and only then to reduce the ventilation.

If we can learn to reduce safely the infiltration rate of U.S. houses by 1/4 air change per hour, our annual resource energy savings would be about 0.8 $\times 10^{15}$ Btu, worth $6 billion.

## BUILDING ENERGY SIMULATION (BES)

The Building Energy Simulation Group develops techniques to simulate the energy performance of buildings. Starting in 1978, the group developed a family of computer programs, DOE-1 and DOE-2, that perform such simulations. These programs are now widely used by architects and engineers as a tool in the design of new buildings and the retrofit of existing ones; DOE-2 is also used extensively by researchers in building science. Each year, a new version of DOE-2 and its documentation is produced, incorporating the most recent research results of projects at LBL and elsewhere. During the past few years, DOE-2 has become the standard against which other calculation procedures or programs are compared. DOE-2 is used by many hundreds of groups around the United States and overseas.

The group is developing new techniques to calculate building loads and simulate heating, ventilating, and air-conditioning (HVAC) equipment. New techniques and algorithms have been developed to calculate the envelope element response to convective and radiative heat gains inside and outside of the building and to calculate the effect of using daylight. Calculation procedures for the analysis of passive solar designs, including direct gain, Trombe walls, and water walls, have been added, as have approaches to model more accurately the interactions between the thermal zones of multi-zone and multi-story buildings. Finally, new control and equipment models in the HVAC section of the program simulate nighttime ventilation, plenum heating systems, controls for variable flow systems, and controls for cogeneration equipment.

## WINDOWS AND DAYLIGHTING

The Windows and Daylighting Group focuses on developing the technical basis for understanding the energy-related performance of windows. If the flow of heat and light through windows and skylights can be properly filtered and controlled, these building elements not only can outperform any insulated wall or roof component, they can also provide net energy benefits to the building. The group's investigations are designed to develop the capability of accurately predicting fenestration performance. It develops analytical models and experimental procedures for determining the thermal and solar-optical properties of glazing materials; it also conducts materials-science studies to characterize a new generation of thin-film coatings and other advanced optical technologies that may someday enhance the performance of conventional glass and plastic glazings. The first generation of windows incorporating transparent heat mirrors (R-4.5 windows) is now reaching the market 6 years after their initial development in this program.

If they capture the market, as expected, they will save consumers $5 billion annually in heating bills.

The DOE-2 building-energy analysis model has been modified to enable daylighting effects to be calculated; it is also being used for extensive parametric studies to determine total building energy use and peak loads as functions of climate, orientation, and window properties. LBL daylighting studies now use a recently completed 24-foot-diameter sky simulator for testing scale models under carefully controlled conditions. Data from outdoor model tests and daylighting resource studies are still being collected and analyzed. Computational procedures will be validated with the Mobile Window Thermal Test (MoWiTT) facility, now nearing completion. This unique facility combines the accuracy and control of laboratory testing with the realism and complexity of dynamic climatic effects. It should, for the first time, enable controlled measurement of the interaction between fenestration systems and the building HVAC system.

## LIGHTING SYSTEMS RESEARCH

The research of the Lighting Group is divided into four major categories: technical engineering, building applications, visibility impacts, and health impacts.

The Technical Program is concerned primarily with developing new concepts for efficiently converting electrical energy into visible light. Areas of interest include mechanisms for reducing the ultra-violet self-absorption in gas-discharge lamps, and the excitation of the plasma gas at ultra-high frequency ranges (approximately $10^9$ hertz). These hold the promise of a more reliable and more efficient conversion of energy into light.

The Buildings Applications Program concentrates on the design of lighting systems, the effective use of lighting controls, and their interaction with a building's HVAC system.

The Visibility Impacts Program focuses primarily on basic information needed to establish lighting conditions that enhance productivity in a cost-effective manner. It also seeks to determine any undesirable visual effects, such as excessive fatigue, associated with the use of modern office equipment operating in an advanced lighting environment.

The Health Impacts Program extends electric lighting research to a wider class of human activities. Here, conditions can be varied, and nonsubjective responses to lighting can be measured by sensitive medical instruments.

Facilities for the Technical Program are located at LBL; the Visibility Impacts Program is located at the University of California School of Optometry at Berkeley; and the Health Impacts Program is located at the Medical Center on the San Francisco campus of the University of California.

The Lighting Group's successes include advancing the development of high-frequency solid-state ballasts for fluorescent lamps and several energy-efficient lamps to replace the familiar incandescent electric lamp. A two-year test of solid-state ballasts in a large office building showed an electricity savings of 40%; scaled to the entire country, this represents an annual savings of $5 billion. The energy-efficient lamps yield a factor-of-three improvement in efficacy, and this could provide further annual savings of perhaps $5 billion.

## BUILDINGS ENERGY DATA (BED)

The Buildings Energy Data Group compiles and evaluates data on end uses of energy, and on the costs and performance of energy-efficient technical measures, from both direct field measurements and secondary sources. Using these data, it prepares estimates of least-cost technical potentials for improving energy efficiency in new and existing homes and commercial buildings, often as a cooperative effort with utilities or state agencies. Individual conservation (or solar) measures can be catalogued in order of increasing unit-cost of conserved energy ($/MBtu or ¢/kWh), with careful attention paid to the interactions among conservation and solar measures that affect certain end uses (notably heating, cooling, and water heating). Using this technique, BED creates marginal cost curves (or supply curves) of conserved energy; these are comparable to the supply curves for other market commodities and show the expected levels of production as a function of unit price.

## RELATED RESEARCH IN OTHER PROGRAMS

Closely related research on energy-efficient buildings and appliances is carried on in other programs within the Energy and Environment Division and is reported in other chapters of this annual report. Specifically, the Energy Analysis chapter reviews building energy performance guidelines, appliance energy performance, rating systems for auditors and appraisers, and energy and peak-power modeling. The Solar Energy chapter summarizes the research of the Passive Solar Analysis and Design Group.

# ENERGY PERFORMANCE OF BUILDINGS (EPB)*

*R.C. Sonderegger, J.W. Adams, P.G. Cleary, R.C. Diamond, D.J. Dickerhoff, J.B. Dickinson, J.D. Dixon, J.Y. Garnier, D.T. Grimsrud, R.D. Lipschutz, M.P. Modera, M.H. Sherman, and B.V. Smith*

The Energy Performance of Buildings Group provides fundamental data on the energy performance of buildings. Our results form the basis of design and construction guidelines for new buildings and help the formulation of retrofit strategies for existing buildings. Two of our primary research areas are air infiltration and wall thermal performance. These studies involve work in the field, in the laboratory, and on computer models. A third research area concerns the development of an instrumented energy audit for residences; this audit was released for public use in FY 1982.

## AIR INFILTRATION

Because air infiltration can account for one-third to one-half of annual space-heating and space-cooling energy use, it has been the focus of the largest ongoing project in the Energy Performance of Buildings Group. Infiltration is any airflow that crosses the envelope of the building, and is caused by either natural or mechanical pressures. The resultant energy loss can be reduced substantially in new structures by changes in design and construction; in existing structures, a lesser reduction can be achieved by careful repair and maintenance. The characterization and prediction of infiltration are important for both comfort and indoor air quality as well as for energy conservation.

Our work in this area concerns measuring, modeling, and reducing air infiltration in buildings. Our objectives are to develop the theoretical and experimental expertise needed by researchers, architects, and engineers; to provide design guidelines; and to develop construction quality standards for optimal air leakage and infiltration. A major achievement of this program has been the development of a model that predicts infiltration from weather data and a single leakage parameter—"the effective leakage area." The magnitude of leakage area can serve as an important criterion for designers and builders and is a useful diagnostic aid for auditors or "house doctors."

### Accomplishments During FY 1982

Accomplishments included analysis and condensation of data collected in previous fiscal years as well as the measurement and reduction of new data. We completed the analysis of data from three field projects that had been carried out in FY 1981 in Rochester, New York, Midway, Washington, and Eugene, Oregon. We performed both leakage-area measurements in all these houses and measured tracer gas decays and indoor air quality in some of them.

Experience gained in making leakage measurements and retrofitting houses was used to produce a guide, called *The House Doctor's Manual*, for the Bonneville Power Administration following completion of the Midway house-tightening project. The guide is divided into two sections: the first provides a description and overview of the house-doctor procedure, including a discussion of heat losses and the tools available to diagnose and remedy them; the second section describes retrofit techniques performed during a typical house-doctor visit.

One of the most interesting experimental techniques we have developed is called AC pressurization. This is a method for determining the leakage of the envelope of a building at low pressures. It has several advantages over conventional (DC) fan pressurization, which uses a "blower door." AC pressurization has a much higher signal-to-noise ratio (i.e., it is more precise), is capable of working in the low pressures typical of natural infiltration (i.e., 1 to 10 pascals), and combines both pressurization and

*This work was supported by the Assistant Secretary for Conservation and Renewable Energy, Office of Building Energy Research and Development, Building Systems Division of the U.S. Department of Energy under Contract No. DE-AC03-76SF00098.

depressurization results simultaneously. The physical process of AC pressurization changes the effective volume of the test space periodically and monitors the resultant internal pressure change; knowing the size of the volume change and the pressure response as a function of time allows the direct (on-line) calculation of leakage.

The first version of AC pressurization was built to investigate the low pressure leakage behavior of a structure and to validate the technique. It was successful and led to the concept of effective leakage area. The second version was a stand-alone system that did not pierce the building envelope; it was designed to calculate the leakage area in real time. Measurements taken in FY 1982 included a study on a single structure at frequencies in the (sub-audible) range of 0.1-3.0 Hz; they showed that the apparatus could respond in real time to changes in the leakage area of the envelope at driving pressures on the order of 1 pascal. A sample output is shown in Fig. 1. The traces show, from bottom to top: the absolute pressure in the sealed back volume behind the piston; the changes in pressure in the test space caused by the changes in volume; the changes in volume in the test space (called the "volume drive," calculated in real time from the absolute pressure); and finally the leakage area, which is calculated in real time from the volume drive and the test-space pressure. The second version has laid the groundwork for a useful field instrument that could replace conventional fan pressurization; the final instrument may operate with acoustic techniques in the 10 Hz range.

The concept of effective leakage area combined with that of weather-induced pressures led to the development of the LBL infiltration model. It expresses natural ventilation as a function of total leakage area, wind speed, temperature, and building configuration and can be used to predict infiltration from weather and blower-door measurements for both short-term and long-term purposes. For short-term measurements, the model has an accuracy of approximately 20%; for longer-term averages, it can predict as well as 5%. The model is used in the computer programs Computerized Instrumented Residential Audit (CIRA), DOE-2.1, and BLAST and is included in the 1981 ASHRAE Handbook of Fundamentals. Other institutions have used the model, including the Naval Civil Engineering Laboratory, Retrospectors, and the Bonneville Power Administration.

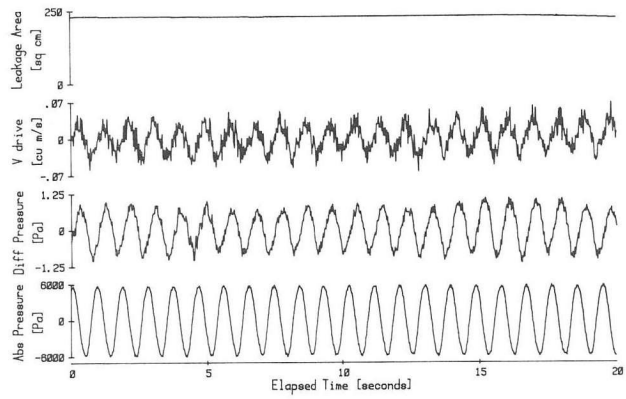


Figure 1. Output from the AC pressurization equipment, which measures effective leakage area in real time without penetrating the envelope of the building. For an explanation of the traces, see text. (XBL 826-10381)

This year we have made several sets of field measurements of infiltration and leakage. Our Mobile Infiltration Test Unit (MITU), a portable, full-size structure, makes simultaneous measurements of infiltration, pressure, wind, and temperature and records them for future analysis. Air infiltration is measured by the Continuous Infiltration Monitoring System (CIMS), which continuously injects a tracer gas. The mobile unit is shown in Fig. 2. Because of

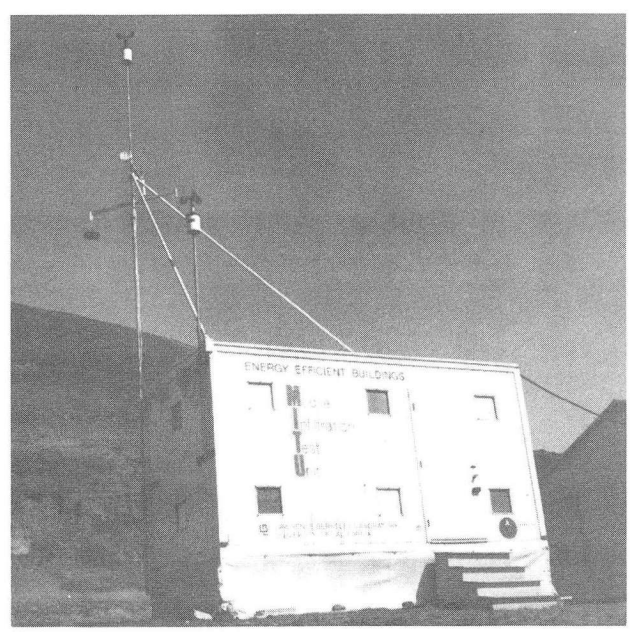


Figure 2. The Mobile Infiltration Test Unit at a site near Fort Cronkhite, CA. (XBB 810-9909)

the value of MITU for understanding and verifying infiltration models, we have continued to make field measurements with it; it was stationed this past winter and spring on the grounds of the Reno, Nevada, airport. Most of our work using MITU has been concentrated on the relationship between measured and predicted infiltration, but we have also used it to monitor independently the interior and exterior pressures on MITU. Figure 3 shows the dependence of the exterior pressure coefficient on angle for one of the faces of MITU. A pressure coefficient is a dimensionless factor giving the increase in pressure caused by the wind. It should be positive for windward orientations and negative for leeward ones.

This summer, we began a project to study the effect of wind on natural ventilation for its usefulness in mitigating cooling loads in hot, humid climates. Three different buildings at the Kaneohe Marine Corps Air Station (KMACS), Hawaii, were instrumented with surface pressure, temperature, humidity, and air velocity probes; on-site weather parameters (air temperature, humidity, wind speed, and wind direction) were also monitored. Field work elsewhere has included an investigation into component leakage in a small sample of houses, and several sets of long-term average infiltration measurements using our low-cost Average Infiltration Monitor (AIM).

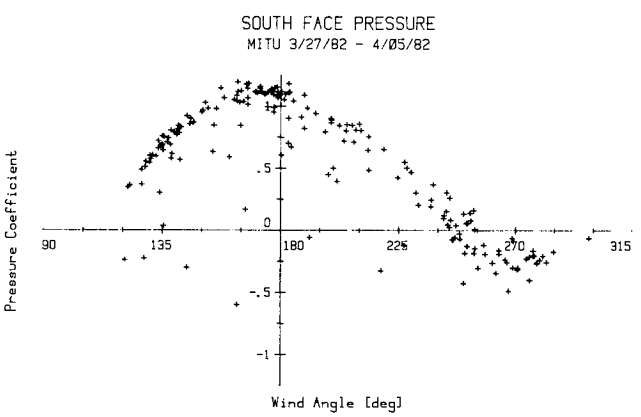


Figure 3. Instantaneous pressure coefficients measured by the Mobile Infiltration Test Unit (MITU) at Reno, NV.
(XBL 828-9591)

## Planned Activities for FY 1983

We will continue our research efforts into natural ventilation by analyzing full-scale measurements of wind-induced infiltration; the data from KMACS will continue to be analyzed. If the information is to be useful in hot, humid climates, it will be important to consider comfort levels as opposed to just air temperature in the analysis of the data. As the full-scale work progresses, we will begin to make scaled measurements in a wind tunnel. We plan to develop the AC pressurization equipment into a device that can easily be used to measure leakage area and that would replace the current fan-pressurization apparatus.

In the future, we will extend our investigations into new areas: multichamber infiltration, HVAC interactions with infiltration, and occupancy effects. We plan to instrument a multichamber facility with detailed temperature, pressure, infiltration, and air velocity measurement equipment to study air transport between zones. We plan to use MITU to make full-scale measurements on the interaction between HVAC systems and total ventilation, including flues and chimneys for combustion appliances and vents and stacks (powered or unpowered) for ventilation; we will also consider the effect of duct leakage and total ventilation. Since occupants can make such a large difference to the infiltration and total energy load on the building, we plan to make a large survey of measured infiltration rates in order to extract the occupant contribution to ventilation.

## THERMAL PERFORMANCE OF WALLS

Conduction of heat through a building's walls accounts for a large part of the energy load during the heating season. Although much information is available on the steady-state thermal performance of walls in a laboratory environment, there is very little information concerning actual performance of walls *in situ*. Existing field measurements do indicate, however, that steady-state wall resistances can show significant degradation when compared with standard calculations. The goal of our walls research is to develop a complete methodology for determining the dynamic performance of walls. The methodology contains two relatively independent constituents: (a) a measurement apparatus capable of both controlling and measuring instantaneous, dynamic heat flows and surface temperatures on both sides of an arbitrary wall and (b) a calculation procedure capable of interpreting heat flows and surface temperatures in terms of physical wall parameters. Once complete, this system can be used in the field to determine the behavior of a wide variety of wall constructions and placements and assess their impact on overall energy consumption.

## Accomplishments During FY 1982

Over the course of FY 1982, the major thrust of our walls research program has been to improve our measurement device, the Envelope Thermal Test Unit. Our first field test prototype, ETTU 1.2, built in FY 1981, was field tested early in FY 1982. The device consists of two insulation blankets fitted with computer-controlled heaters and temperature sensors. Tests on walls in the laboratory and in the field showed that lateral heat conduction within the wall and the insulating blanket caused unacceptable inaccuracies in the computation of the heat flux going through the wall.

During the middle part of FY 1982, major modifications of the ETTU 1.2 apparatus led to ETTU 1.3, illustrated in Fig. 4. These modifications were designed to eliminate the lateral heat conduction problem, increase measurement reliability in field tests, and incorporate our "Simplified Thermal Parameter" wall model into the algorithms which control the heat fluxes in the device. To eliminate lateral heat conduction, the surface of the primary heater was divided into a central and an edge region with independently controlled heat fluxes. The heat flux of the edge region is controlled to insure that the surface temperature of the wall near the edges is equal to that in the center section. Combining this control with that of the heaters on the exterior of the insulating blanket, ETTU 1.3 can be described as a hotplate guarded against both lateral and transverse heat losses. The control algorithms for the two "guard" heaters use the "Simplified Thermal Parameter" wall model to account for the dynamic nature of the heat transfer within both the device and the wall. From the mechanical viewpoint, the ETTU 1.3 modifications also reduce the differential thermal expansion that causes the structure to bow during operation.

## Planned Activities for FY 1983

The early part of FY 1983 will be spent preparing ETTU 1.3 for field testing. The hardware will be made more rugged to reduce costly breakdowns during field use. These modifications will also make setup in the field easier. Before the initial field tests, simulations of the apparatus and the wall will be performed using a dynamic three-dimensional finite-difference program. These simulations should allow for quicker field validation, since they provide an independent check on the measurement results.

The Envelope Thermal Test Unit will spend the latter part of FY 1983 at the National Bureau of Standards, serving as a field test device in its first application outside the Energy Performance of Buildings' wall research program.

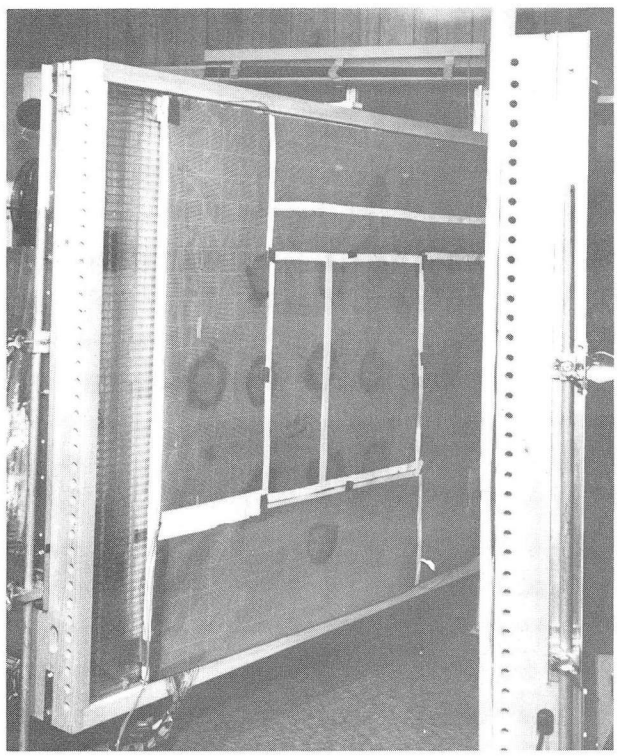

Figure 4. The Envelope Thermal Test Unit (ETTU 1.3). (CBB 832-1129)

# COMPUTERIZED, INSTRUMENTED RESIDENTIAL ANALYSIS (CIRA)

Building energy professionals such as government officials, architects, energy auditors, engineers, and contractors often need to know projected energy use in a given house; sometimes they may need to maximize energy savings within a fixed budget. Although several paper-and-pencil procedures exist to do these tasks, they always require lengthy calculations. Computerized procedures often require strict adherence to a particular input format, or knowledge of a special language. Two recent events promise to lessen the burden of calculations: the introduction of microcomputers and the development of user-friendly programs. Microcomputers have become cheap, and many different brands are available. User-friendly programs do not require the user to describe a building in some rigid format or special language. These

programs ask multiple-choice questions in plain English; the user selects the appropriate answer.

Computerized Instrumented Residential Analysis (CIRA), a user-friendly microcomputer program, couples the state of the art in interactive features with the latest developments in simplified computer models of building energy analysis. Its output is either such engineering parameters as month-by-month energy use ("design energy analysis"), or a list of the most economic retrofits to perform on a house. Output is available both on the screen and in printed form as shown in Fig. 5.

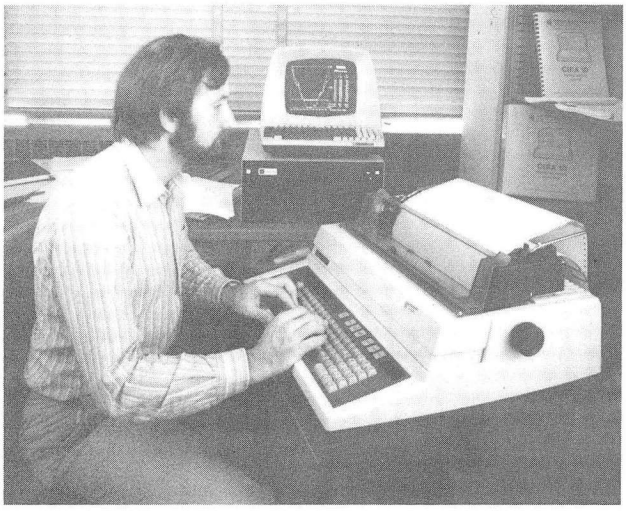

Figure 5. Viewing output from the Computerized Instrumented Residential Audit (CIRA) on a video terminal and a printer. (CBB 829-8281)

## Accomplishments During FY 1982

CIRA development has proceeded in two stages. The first, which occurred in FY 1981, was the development of building energy use algorithms suitable for microprocessor applications. This stage included original research into solar storage and thermostat setbacks, the evolution of variable-base degree-days, and the writing of a sophisticated, user-friendly, file-oriented data base language for data input and output. Space heating and cooling predictions using this method have been shown to approximate the results from the DOE-2.1 building simulation program within ±10%. Preliminary comparisons with measured energy consumption data from 42 houses have shown a comparable correspondence between measured and predicted yearly heating and appliance energy consumption, with higher discrepancies for month-by-month consumptions. The second stage was the evolution of algorithms to select the optimal package of retrofits for any given building. This work was carried out in FY 1982.

CIRA has a built-in library of retrofit measures from which it must chose the best package, subject to the conditions input by the user. These conditions include maximum investment, discount rate, time horizon, and energy costs and escalation rates. The catalog of possible retrofits approaches 100 items; it includes envelope performance retrofits (such as increased insulation and air leakage reduction), HVAC modifications (such as replacement burners and duct sealing), appliance improvements (such as water-heater blankets and efficient refrigerators) and other miscellaneous retrofits (such as clock thermostats). From the catalog, the program chooses those retrofits which are applicable to the building under consideration, and ranks them by decreasing savings-to-cost ratio. This ratio is defined for each retrofit as the incremental life-cycle savings (energy savings minus future maintenance and replacement costs) divided by the incremental first cost.

Optimizing a mix of retrofits on a building is a tedious process. It may be compared to the textbook case of ranking investments by return on investment. Each retrofit, then, is viewed as an investment in energy savings, and the monetary savings realized over the years to come constitute the return. However, the analogy is incomplete at best, as the returns on retrofit investments are a moving target. With each retrofit that the "investor" acquires, the rates of return on all remaining retrofits change, generally becoming lower.

In theory, a separate calculation of yearly energy consumption should be carried out for every retrofit to find the energy savings. To reduce the potentially large number of calculations to be carried out during optimization, a scheme has been developed to estimate energy savings by means of partial derivatives of yearly energy consumption. This method has been shown to yield reliable results. From the estimated energy savings, savings-to-cost ratios are calculated.

During optimization, retrofits are chosen in order of individual savings-to-cost ratio until the annual energy consumption has been reduced by an estimated 25%. At this stage, the chosen retrofits are "installed" in the house in the computer memory, the energy consumptions and derivatives are recalculated, and the estimated savings from the installed retrofits are adjusted so that the sum of the savings is correct.

This process of choosing, installing, and adjusting is repeated until either the dollar limit is reached or no more retrofits exist with savings-to-cost ratios greater than one, and the output is then printed.

The strategy used by CIRA to find the mix of retrofits with the largest net life-cycle savings is essentially that used by a blind person to find the highest point of a hill: follow the line of steepest ascent. That is, keep re-rating retrofits and implement those with the highest savings-to-cost ratio until the available budget is used up or the remaining retrofits point down. This pragmatic method is simple but effective. Figure 6, a graphical presentation of the CIRA output, shows how the lifetime savings for a sample house in Washington, D.C., vary with the amount of money invested in an optimal sequence of retrofits.

The yearly energy consumption of a building is neither a linear nor a simple function of the building parameters, let alone of the retrofits affecting these parameters. Furthermore, there is often little correlation between the cost of different manufacturers' wares and their thermal effectiveness. Therefore, unless radical assumptions are made about the cost structure of retrofits and unless the energy calculations are considerably simplified, the elegant analytical techniques of optimization under constraints are difficult to apply. It is partly because of these difficulties that the numerical, tedious approach to retrofit optimization was taken in CIRA. Rating retrofits by estimated savings and installing them in batches also enables the method to be efficient for microcomputer applications.

The economic optimization program was completed and tested, and in March, 1982, the complete CIRA program was released for public use. Response from the buildings community was favorable—several hundred requests for information are received each month—and by the end of FY 1982 approximately 60 copies of the program (which includes a 500-page user manual) had been distributed. Feedback from CIRA users has shown areas where the algorithms need to be improved, and has helped indicate directions where further research is required. It is hoped that the CIRA-users community will quickly become self-supporting.

Algorithm development continued after the program was released. Data from studies at Brookhaven National Laboratory (BNL) were used to produce a function describing the dependence of furnace efficiency on part load ratio, and work continues on the cooling system subprogram. A program was written to produce CIRA weather files from hour-by-hour weather tapes, and files were constructed for 180 U.S. cities. Information is being given to users in Canada, England, France, and Italy to enable them to construct their own files from local weather data. Development of a retrofit selection program was

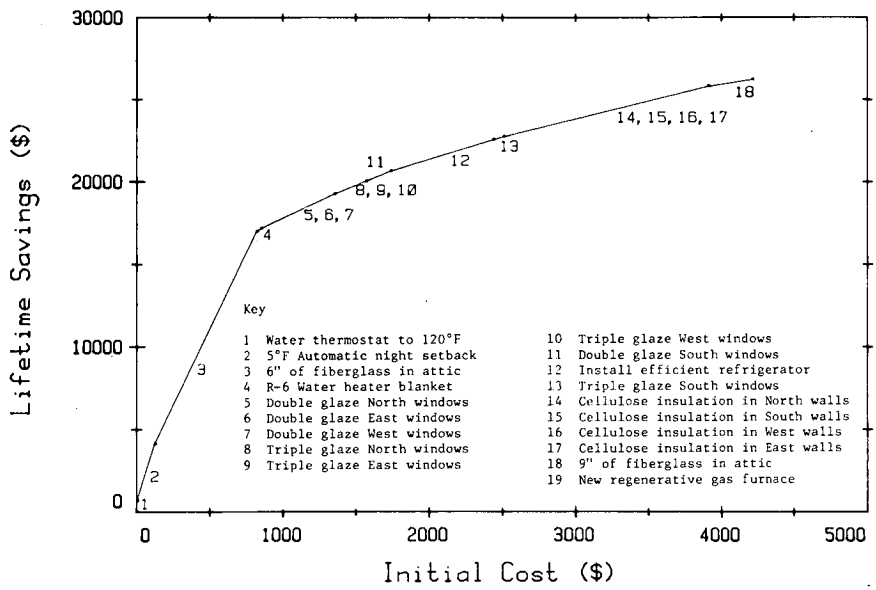


Figure 6. Lifetime savings from an optimized series of retrofits for a sample house in Washington, DC, weather. The data come from an output of the CIRA program. (XBL 8212-12434)

begun; this program will enable the user to choose which retrofits are to be installed at any cost, which are to be considered, and which are not to be considered. The program will also allow the user to change the cost of a retrofit.

### Planned Activities for FY 1983

In the year ahead, we plan to complete the retrofit selection program and to begin two other projects. The first is to adapt the program for small commercial buildings. This will require a re-orientation of the questions asked, and the development of new algorithms for the heating, ventilating, and air conditioning (HVAC) system subprogram. We plan to make use of survey data to ensure that this "commercial buildings" CIRA will find general applicability.

The second project is a longer-term effort: to split off the design energy section of CIRA from the retrofit optimization section. At present, both sections use the same energy calculation programs, CIRASTD and CIRAEGY. These programs are somewhat of a compromise between accuracy and speed. During retrofit optimization, CIRAEGY is used a number of times, once for each loop through the retrofit-sorting program, so it must be quick. An improved algorithm that required an added two seconds of computer time for each monthly calculation would therefore be unacceptable, because it would would increase total calculation time for a 10-loop retrofit optimization by 2 $\times$ 12 $\times$ 10 seconds, i.e. 4 minutes. However, this same improved algorithm would be acceptable for the design analysis, since the added computation time would be less than half a minute; design energy analysis requires one loop only. By splitting the two paths, a more sophisticated set of algorithms could be written for the design energy analysis and the original fast version could continue to be used for retrofit optimization. This project is expected to be completed in FY 1984.

## MULTI-UNIT ENERGY MONITORING

The aim of this project, which started in FY 1982, is twofold: firstly, to quantify design variables and occupancy effects that affect energy use in multi-unit housing, and secondly to work with the private sector in exploring energy utilization in multi-unit buildings. About half of the new dwelling units built in the U.S. are part of multi-family buildings. Although some results of work on single-family units are transferable to multi-unit buildings, there are problems unique to the larger buildings, e.g., metering and HVAC distribution systems, inter-unit air exchange, and heat stealing by adjacent units.

### Accomplishments During FY 1982

We identified a 15-story, 325-unit apartment building in Oakland, California, and secured permission from its board of directors to obtain the submetered billing records by guaranteeing anonymity of the occupants. Data analysis has been done to identify significant physical parameters accounting for the up to five-to-one variation in energy use among units with identical floor plans. Preliminary investigations as to the cause of such large variations have so far met with little success.

### Planned Activities for FY 1983

The second stage of the project is to conduct an extensive occupant survey to understand occupant behavior. Earlier work by other research groups has shown that much of the observed variation in energy for space heating in identical single-family dwelling units is due to occupant effects. On the basis of those results, we expect that occupant behavior will account for a large part of the variation in energy use at these apartments.

To resolve the remaining unexplained variation (if any remains of significant size), we will install Energy Signature Monitors (ESMs, described in the next section) in a selected sample of units. This information should be of great value to electric utilities, especially when correlated with occupant characteristics. In a subsequent funding year, we intend to install retrofits in selected units, matched with a suitable number of controls that have no retrofits installed. This focus on individual units is necessary since the building manager has already requested an energy audit, as a result of which he lowered the building hot water temperature and relamped the common areas.

In a separate project, we will work with a local architecture firm, Hirshen/Gammill/Trumbo, which designs multi-unit housing projects for low-income and elderly populations. During FY 1983, we will use CIRA to evaluate plans for a large multi-unit project having large heating and cooling requirements. Construction details will be reviewed for air tightness, using our past experience with energy-efficient tract housing construction in New York state. In a later year, we hope to install sensors during construction for detailed submetering of all fuel uses, and tem-

perature measurement; this will be done with the collaboration of the local utility. We also hope to evaluate construction quality using fan pressurization. A long-term goal is to structure the project so that builders, designers, and occupants are accustomed to measurement/feedback/learning patterns.

## ENERGY SIGNATURE MONITOR

Long-term measurements of energy utilization in buildings have traditionally used one of two approaches: either analysis of utility bills on a relatively large sample of units, or highly sophisticated instrumentation installed in a few test houses. The first approach may give statistically significant but relatively unspecific information on energy utilization in residences. The latter may be best suited to validate thermal calculation algorithms in computer simulation models; it is not a very cost-effective way to gain information that could be generalized to large classes of houses.

The Energy Signature Monitor (ESM), along with its attendant data analysis software, is designed to bridge the gap by trading some accuracy for much cost. The ESM installation procedure should take less than one man-day of technician time. To realize this goal, most sensor wires will be in an area close to electric service entry (typically a basement), and all sensors will be non-intrusive, that is, installed without interrupting electric or gas lines.

Preliminary data analysis is an integral part of ESM. The electronically stored data will always contain full information as to the sensors used and the house and site identity to avoid time-consuming cross-referencing with logbooks and installation reports. Transformation of raw readings to physical units will be done automatically by the data analysis software without further input by the user.

### Accomplishments During FY 1982

The ESM concept was developed, the prototype unit shown in Fig. 7 was built, and a number of sensors were designed and built. The software for data collection was written. At the end of the year, the unit was given a preliminary field test. ESM has a built-in microprocessor, 4K read-only memory (ROM), 4K random-access memory for intermediate storage, 24K physically removable erasable programmable read-only memory (EPROM), and up to 8 analog and 8 digital ("on-off") low-cost sensors with built-in signal conditioning. A typical installation may monitor the main electric power, heating and cooling systems, water heater, refrigerator, dryer, stove, indoor temperatures, outdoor temperature, solar flux, and humidity (the latter three channels may be "rotated" when several residences are monitored at the same site). EPROMs require no attendant reading or recording devices (ESM fills both of those functions); downloading a full month of data from an EPROM takes less than 30 seconds. Hourly values for each data channel are stored in EPROM, which can hold up to 5 weeks' worth of data. The EPROM is contained in a removable module for on-site replacement and mailing to a central data processing location. Data are retrieved from the EPROM by using an identical ESM unit connected to a microcomputer, a terminal, or a mainframe over a standard RS-232 interface. (In other words, ESM units can be used both to "write" and to "read" data.)

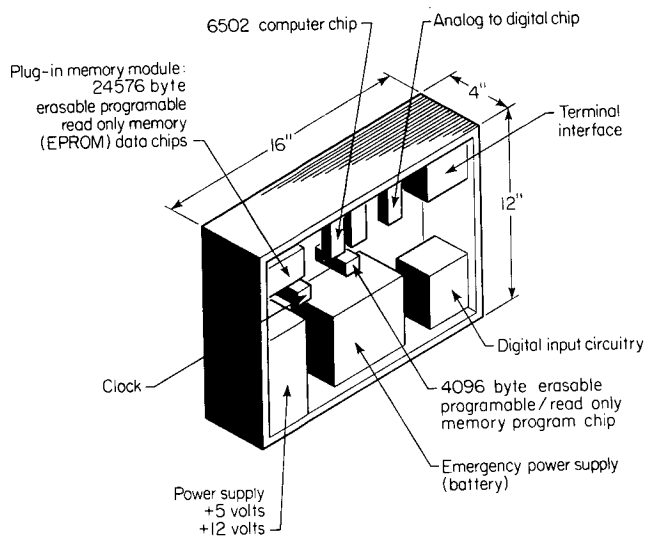


Figure 7. A schematic of the prototype Energy Signature Monitor (ESM). For details, see text. (XBL 831-1000)

### Planned Activities for FY 1983

The ESM with EPROM data storage will be completed. A small number of ESMs will be built, debugged, and field tested. Development of low-cost sensors will continue. Special attention is being paid to non-intrusive sensors for electric power and for gas appliances. A user-friendly software environment will be developed that will perform the functions of data splicing (for periods with missing data), data recovery (for erroneous data), and preliminary summarizing.

# BUILDING VENTILATION AND INDOOR AIR QUALITY*

*D.T. Grimsrud, A.V. Nero, Jr., J.R. Allen, M.G. Apte, K.M. Archer, A. Carruthers, J.F. Dillworth, S.M. Doyle, J. Eisenberg, P. Fischer, W.J. Fisk, K.L. Geisling, J.R. Girman, A.T. Hodgson, C.D. Hollowell, J.F. Koonce, Jr., V.M. Martin, B.A. Moed, W.W. Nazaroff, F.J. Offermann, Y. Otonari, B.S. Pedersen, B. Remijn, K.L. Revzan, A.W. Robb, B. Robison, R.G. Sextro, and G.W. Traynor*

Indoor air quality concerns are rapidly becoming a part of the public consciousness. The safety of kerosene heaters, adverse responses to formaldehyde emissions from building materials, the health effects of passive smoking, growing awareness of the "sick building" syndrome, and concern about exposure to radon are among the issues that provoke discussion and controversy. Much of this controversy is caused by a lack of information about pollutant concentrations, their sources, and their health effects.

Environmental questions about air pollution are not new; what is new is a concern about indoor air. Air quality standards exist for outdoor air (the National Ambient Air Quality Standards of the Environmental Protection Agency) and for the indoor work environment (the Occupational Air Quality Standards of the Occupational Safety and Health Administration). However, there are no federally accepted standards for air quality in buildings with general public access. Outdoor and indoor occupational standards are not applicable to general-purpose indoor spaces for several reasons: (1) the time spent indoors is considerably longer than time spent outdoors; (2) many pollutant sources that do not contribute to outdoor pollution are found inside buildings; and (3) occupational standards assume an 8-hour exposure to healthy adults—a description that does not apply to the general population exposed to indoor pollutants. These observations, coupled with the knowledge that ventilation rates are often being reduced to conserve energy, combine to focus concern on air quality within buildings.

*This work was supported by the Assistant Secretary for Conservation and Renewable Energy, Office of Building Energy Research and Development, Building Systems Division and by the Director, Office of Energy Research, Office of Health and Environmental Research, Human Health and Assessments Division and Pollutant Characterization and Safety Research Division of the U.S. Department of Energy under Contract No. DE-AC03-76SF00098.

The goals of the Building Ventilation and Indoor Air Quality (BVIAQ) Program are to characterize sources and concentrations of indoor air pollutants, to understand the interplay between building design and operation and indoor air quality, and to develop energy-efficient ventilation strategies that maintain the health and comfort of building occupants.

The BVIAQ program is organized into four project areas: (1) passive samplers and organic contaminants, (2) radon and radon progeny, (3) pollutant emissions from combustion appliances, and (4) indoor air quality control techniques. Major funding sources for the projects are the Department of Energy through its Office of Conservation and Renewable Energy and its Office of Health and Environmental Research. Other funding sources include the Bonneville Power Administration, the Environmental Protection Agency, the Consumer Product Safety Commission and the Office of Environmental Programs of the Department of Energy.

## PASSIVE SAMPLERS AND ORGANIC CONTAMINANTS

Field studies of indoor air quality and the effect of reduced ventilation have been limited because of the high cost of employing continuous monitors. Inexpensive passive samplers capable of measuring daily or weekly integrated contaminant concentrations without attention from trained technicians, external power, or accessories (e.g., pumps or chart recorders) offer a promising means of extending these studies. Large-scale audits could be conducted with these samplers to ensure that the implementation of energy conservation programs does not have adverse effects upon occupant health and safety. Passive samplers would also make possible large-scale surveys of the indoor air quality of existing buildings. Epidemiological studies, which have often relied upon exposures derived from distant, fixed monitors, could be improved by using passive samplers as personal monitors.

### Accomplishments During FY 1982

We have constructed an automatic calibration and exposure system to perform laboratory tests, evaluations, and calibrations of passive samplers. This system allows us to test the effects of temperature, humidity, and pressure as well as the effects of possible interfering gases. The system is controlled by a microprocessor, and the data are logged on magnetic

tape. A second facility for testing, evaluating, and calibrating formaldehyde passive samplers has been constructed and used extensively. Recent improvements to this system include the development of a stable source of airborne formaldehyde[1] and the addition of a mass-flow-controlled double dilution system using a high-flow clean-air generator to provide a wide range of formaldehyde concentrations.

*Formaldehyde Passive Samplers*

A diffusion sampler similar to the Palmes nitrogen dioxide sampler[2] was developed for formaldehyde using a glass filter impregnated with sodium bisulfite as the trapping agent and chromotropic acid as the analytical technique.[3] Most of the laboratory tests are complete for this sampler. Limited pre- and post-exposure stability tests demonstrate stability of at least 2 weeks. The quantification range for a 1-week sampling period was determined to be 0.018 ppm to over 1 ppm with good linearity, more than adequate for residential applications. Laboratory tests have also determined that the accuracy of the device is reduced when the average relative humidity exceeds 60% at 25°C. A recent field validation[4] of this sampler was completed in a variety of occupied residences (mobile homes, energy-efficient homes, passive solar homes, and homes with urea formaldehyde foam insulation). As illustrated by Fig. 1, the performance of the passive sampler compared favorably with a reference pump/bubbler sampler, demonstrating good linearity and precision over a wide range of formaldehyde concentrations. The results of the laboratory and field validation tests are summarized in Table 1.

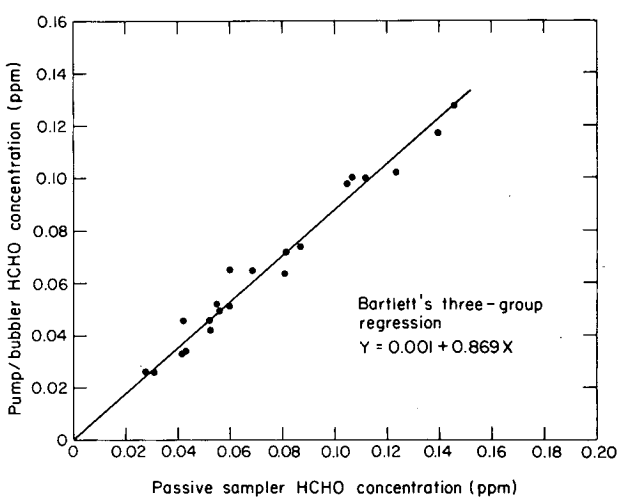


Figure 1. Passive-sampler formaldehyde (HCHO) concentrations versus pump/bubbler sampler concentrations for 21 field comparisons. (XBL 826-824)

Table 1. Description and specifications of the LBL formaldehyde passive sampler.

| CONTAMINANT: Formaldehyde (HCHO) | |
|---|---|
| SAMPLER: | Passive diffusion sampler; area, 3.98 $cm^2$; path length, 9.4 cm; collection medium, $NaHSO_3$ impregnated glass fiber filter |
| ANALYSIS: | Chromotropic acid spectrophotometric analysis, NIOSH P&CAM No. 125 |
| SAMPLING RATE: | 4.02 $cm^3$/min (0.296 $\mu$g/ppm-hr) at 1 atm and 20°C |
| SAMPLING PERIOD: | 1 week (168 hours) |
| SAMPLING RANGE: | 0.018 ppm to more than 1 ppm for 168 hours |
| ENVIRONMENTAL EFFECTS: | Independent of pressure, only slightly dependent on temperature<br>Accuracy reduced when average relative humidity exceeds 60% at 25°C |
| INTERFERENCES: | No identified significant interferences in residential environments |
| SHELF LIFE: | 2 weeks minimum |
| SAMPLE STABILITY: | 2 weeks minimum |
| OVERALL PRECISION: | Mean coefficient of variation = 6.7% |
| BIAS: | +13% based on field comparisons with reference method; true concentration = 0.87 × passive sampler concentration |
| OVERALL ACCURACY: | True concentration ± 95% confidence interval of 14% |

*Carbon Monoxide Passive Sampler*

We have identified a class of compounds reactive with carbon monoxide that could form the basis for a carbon monoxide sampler.[5] One analytical technique investigated uses the reflectance change that occurs in paper impregnated with one of these compounds upon exposure to carbon monoxide. We have developed a passive sampler based on this technique that has good sensitivity and linearity and have greatly stabilized its response to humidity.

*Nitrogen Dioxide Passive Sampler*

We have conducted extensive tests of the Palmes $NO_2$ samplers, including stability, temperature-dependence, humidity-dependence, and constant-exposure/variable-concentration tests as well as a large field comparison with an EPA reference method. These tests indicate a temperature dependence previously unreported despite extensive use of this sampler in field studies by many researchers.

## Planned Activities for FY 1983

The few remaining tests of the formaldehyde passive sampler will be completed. These tests include face velocity tests and extended pre- and post-storage stability tests. Development and laboratory testing of the carbon monoxide passive sampler will continue, addressing such concerns as stability, accuracy, and the effects of possible interferents. In the latter part of FY 1983, field testing of this sampler will begin, again with parallel sampling using a proven active sampler in a variety of environments. We will also begin development and testing of an inexpensive water vapor sampler based upon the weight gain of a molecular sieve in a diffusion sampler. Finally, we will intensify the literature search on techniques suitable for monitoring carbon dioxide and respirable suspended particles and begin preliminary tests on promising techniques.

# RADON AND RADON PROGENY

Radon (radon-222), a naturally occurring radioisotope and the heaviest of the noble gases, is produced by the decay of radium-226, a ubiquitous trace element in earth and earth-based materials. Concentrations of radon are often higher indoors than outside, commonly by an order of magnitude, because the house, acting as a leaky container, traps radon released from radium-bearing materials. The predominant source of indoor radon in the United States is the soil underneath a structure, but building materials and domestic water from underground wells can also contribute.

Radon decays to a series of four short-lived radioisotopes, known as radon progeny, which are chemically and physically active. An excess incidence of lung cancer among uranium and other hard-rock underground miners has been associated with their exposure to high levels of radon progeny. Based on studies of miners, exposure of the general population to the estimated mean indoor radon level of 1 picocurie per liter (pCi/l) could account for 2000 to 20,000 lung cancer deaths per year in the United States. Research by our group and others indicates that a small but significant fraction of U.S. houses have radon levels in excess of 10 pCi/l; occupants of these houses receive integrated exposures that are comparable to exposures received by miners in whom excess lung cancer incidence was observed.

Our research efforts are directed towards: (1) identifying housing where indoor radon levels are very high; (2) investigating possible measures to control high indoor radon levels; and (3) developing measures to avoid increases in the mean exposure that might result from, for example, residential weatherization programs. Currently, our work focuses on:

- Characterization of soil as a source of indoor radon, including the transport of radon across the soil-house interface.
- Laboratory and modeling studies of the properties of radon progeny relating to attachment to particulates, deposition on room surfaces, and filtration by mechanical devices.
- Development and evaluation of instrumentation for laboratory and field measurements of radon and radon progeny.

## Accomplishments During FY 1982

*Soil as a Source of Indoor Radon*

A single-family residence near Chicago, Illinois, known to have moderately high radon levels, was intensively monitored from February to July 1982 with assistance from Argonne National Laboratory. The AARDVARK instrumentation system[6] was used to measure air-exchange rates, radon concentrations indoors, airborne alpha activity from the soil near the house and above the sump cover in the basement, times of furnace operation, and weather. Air-exchange rates were commonly in the range of 0.1 to 0.4 air changes per hour; at corresponding times, the radon concentration varied from less than 0.5 to 16 pCi/l, indicating a substantial variability in the apparent rate of radon input. The sump and its connecting drain tile system were identified as a dominant pathway for radon entry. Figure 2 is a plot for a 1-week period of indoor radon concentration, radon source strength (calculated on a mass-balance basis from radon concentration and air-exchange rate measurements), and alpha activity rates for the soil

probe and sump monitor. Sump activity, radon concentration, and radon source strength show a high degree of both variability and correlation. The chief cause of the variability appears to be whether or not the pipe connecting the drain tile to the sump is occluded by water; when the line is open, a highly permeable pathway exists between the soil and the house, permitting the infiltration of soil gas bearing several hundred picocuries per liter of radon.

Two laboratory projects studying radon release and transport in soil were initiated: A soil column was established to study diffusion and pressure-driven transport of radon through soil; and a comparison of three techniques for measuring radon emanation from soil was conducted. In addition, we began investigating whether airborne radiometric measurements conducted by the National Uranium Resource Evaluation Program could identify regions in the United States where indoor radon is endemic.

*Radon Progeny Behavior*

Efforts in FY 1982 focused on continuing to establish measurement capabilities at the radon research house[7]; conducting experiments on air movement indoors with natural and forced convection; conducting preliminary experiments on the reduction of indoor radon progeny levels due to forced convection; and initiating development of a model of radon progeny behavior based on a physical air-movement model.

*Instrumentation*

We both expanded and improved our capabilities for measuring radon and radon progeny and associated parameters. The AARDVARK system was augmented by the addition of a radon soil probe and a passive-sampling radon monitor ("radon sniffer"). For the radon research house, the continuous radon monitors were rebuilt with 5-cm photomultiplier tubes and scintillation cells adapted from the design of Lucas[8] to achieve far greater stability of response than in the earlier version. The radon daughter carousel, an automated instrument for measuring indoor concentrations of individual radon progeny, is essentially complete; final performance tests are now under way. Work was initiated on a four-detector alpha-counting system with microcomputer-based timing control, intended for measurements of unattached radon progeny concentrations and analysis of progeny activity

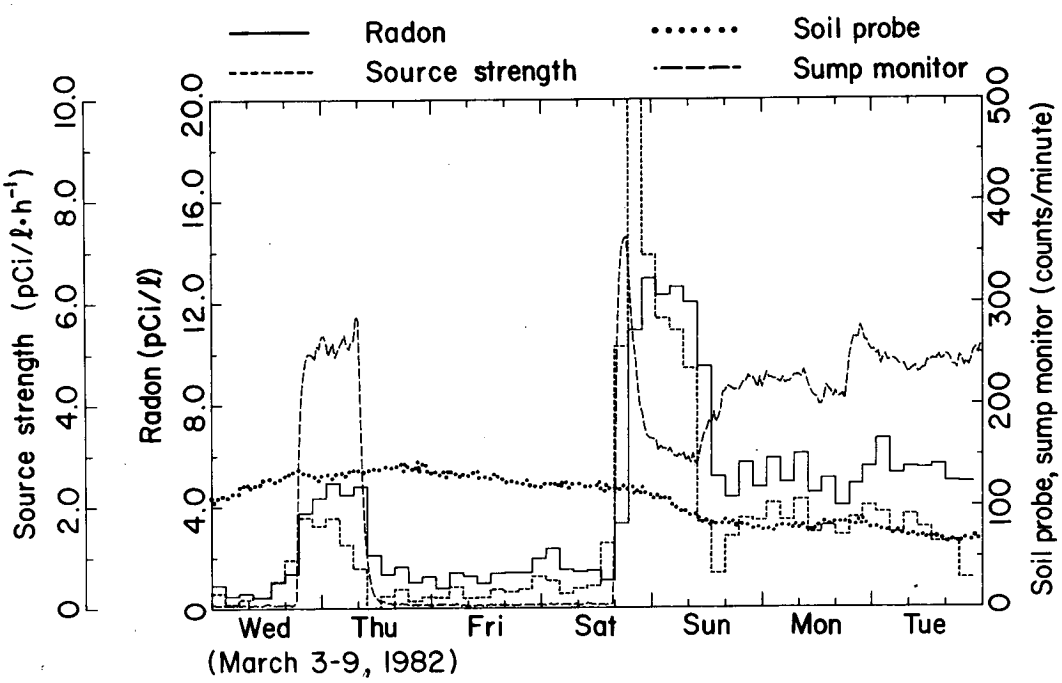


Figure 2. Radon concentration, radon source strength (calculated by mass balance from measured air-exchange rate and radon concentration), alpha activity in soil gas and in air above sump cover in basement of a single-family house near Chicago for the period March 3 through March 9, 1982. For the soil probe and the sump monitor, 100 counts per minute corresponds to roughly 200 pCi/l of radon; these devices also respond to thoron (radon-220) and its progeny and to other airborne alpha emitters so that some counts may not be due to radon. (XBL 8212-12300)

on airborne particulate samples collected with a cascade impactor. The sensitivity of a commonly used procedure for measurement of radon progeny was improved.[9] We began an effort to establish a state-of-the-art particulate monitoring capability for the research house.

Calibration of radon and radon progeny instrumentation continued to receive substantial attention. We continued to participate in the Interlaboratory Calibration of Radon and Radon Daughter Instrumentation.[10,11] We also improved our facilities for primary calibration of radon scintillation flasks, allowing more rapid and precise transfer of radon from the primary standard radium solution to a flask.

### Planned Activities for FY 1983

*Soil as a Source of Indoor Radon*

We plan to conduct two substantial projects in this area during the coming year. The first is a field study of the transport of radon from soil through a crawl space and into a house. The second is a regional assessment of the Pacific Northwest for radon potential based on aerial radiometric data. In addition to these efforts, we plan to complete work on the Chicago field project, and to initiate a study of moisture (and perhaps temperature) effects on radon emanation and transport through soil.

*Radon Progeny Behavior*

Considerable effort will be devoted to completing our particulate monitoring capability at the radon research house. The system is designed to make multi-point measurements of particle number concentrations and size distributions over a range of 0.01 to 5 microns with a cycle time of less than 5 minutes per sampling point. It will be used in conjunction with radon and radon progeny measurements to test the effectiveness of devices to control particulates and radon progeny. We also expect data from these tests to be useful in furthering our understanding of radon progeny attachment and deposition, and in the ongoing development of models of radon progeny behavior.

## POLLUTANT EMISSIONS FROM COMBUSTION APPLIANCES

Researchers in the Building Ventilation and Indoor Air Quality (BVIAQ) Program and elsewhere have demonstrated that operating unvented combustion appliances increases indoor pollutant concentrations. Specifically, increased indoor levels of carbon dioxide ($CO_2$), carbon monoxide (CO), nitrogen dioxide ($NO_2$), nitric oxide (NO), formaldehyde (HCHO), and respirable particles have all been observed. In FY 1982, the BVIAQ program conducted detailed laboratory and controlled field tests on unvented gas-fired space heaters and unvented portable kerosene-fired space heaters.[12-14]

Our research efforts are devoted to: (1) characterizing the emission rates and pollutant concentrations of the many types of combustion devices used within buildings, (2) assessing the health implications of exposures to combustion-related pollutants, and (3) exploring control techniques that will reduce pollutant concentrations while maintaining energy efficiency in buildings.

### Accomplishments During FY 1982

We conducted laboratory investigations of the two major types of portable kerosene-fired space heaters, convective and radiant, measuring their emissions of $CO_2$, CO, NO, $NO_2$, HCHO, and respirable particles, as well as their consumption of oxygen ($O_2$). Tests on portable kerosene-fired heaters were conducted in a 27-$m^3$ environmental chamber, approximately the size of a kitchen or small bedroom. The chamber was operated at a ventilation rate of 0.40 ± 0.03 air changes per hour (ach). The pollutant emission rates were quantified with a technique we had developed previously to determine pollutant emission rates from a gas range.[15] The monitoring equipment used for gaseous and particulate emissions has been described elsewhere.[13]

All four kerosene heaters tested were found to emit $CO_2$, CO, NO, $NO_2$, and HCHO; additionally, both radiant heaters and one convective heater emitted significant amounts of respirable particles. The concentrations of $CO_2$, CO, $NO_2$, and NO measured during and after operation of a convective heater are shown in Fig. 3. For both heater types, $CO_2$ levels from a one-hour burn reached twice the 8-hour U.S. occupational standard of 5,000 ppm.[16] Levels of $NO_2$ did not exceed the U.S. occupational standard of 5.0 ppm[16] with either heater but did exceed the California short-term (1-hour) standard of 0.25 ppm[17]—by a factor of seven for the convective heater and by a factor of two for the radiant model. Levels of CO from the radiant heaters exceeded the Environmental

Protection Agency's outdoor 8-hour standard of 9 ppm, but were below its 1-hour standard of 35 ppm.[18] The applicability of outdoor air quality standards to indoor environments has yet to be established, and the comparisons are included here only to provide reference values.

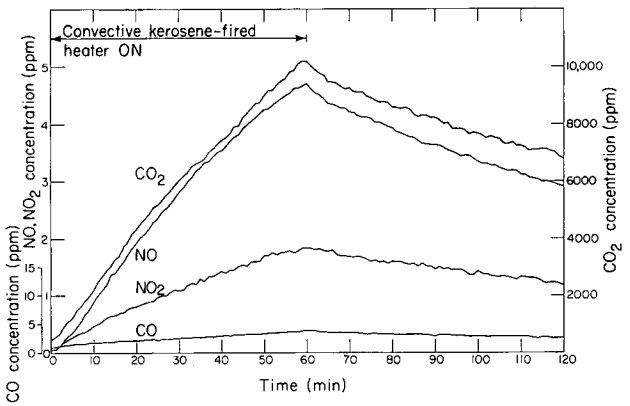


Figure 3. CO, $CO_2$, NO, and $NO_2$ concentrations measured during operation of a portable, convective-type, kerosene-fired space heater in a well-mixed 27 $m^3$ chamber. Fuel consumption was 7830 kJ/hr (7430 Btu/hr), and the air exchange rate was 0.39 ach. (XBL 822-4492)

Laboratory and controlled field investigations of pollutant emissions from unvented gas-fired space heaters (UVGSH) were also conducted. Laboratory investigations demonstrated that, as with kerosene-fired heaters, $CO_2$, CO, $NO_2$, NO, HCHO, and respirable particles were emitted by UVGSHs.[13] Additional tests showed that tuning (i.e., the air/fuel ratio) is extremely important for the emission of CO and HCHO by some heater models. We project that, even under well-tuned conditions, levels of $NO_2$ and $CO_2$ could be well above accepted air quality standards in residences where such space heaters are used and that levels of CO and HCHO could be high, relative to air quality standards, if the appliances are maltuned.

The controlled field investigations confirmed many of the laboratory-based predictions of indoor pollutant levels resulting from the use of UVGSHs.[14] Figure 4 shows the pollutant, temperature, dew-point, and wind-speed profiles during the operation of a well-tuned 31,600 kJ/hr (30,000 Btu/hr) heater in a 240 $m^3$ house at 0.49 ach. The indoor $CO_2$ levels were above the U.S. occupational standard[16] and the $NO_2$ levels exceeded the California short-term standard.[17]

## Planned Activities for FY 1983

We are planning research in three areas. First, we plan to conduct extensive tests of indoor pollutant levels resulting from kerosene heater use under actual field conditions. Various test parameters such as the size of the room heated and the duration of operation will, in part, be derived from a national survey of kerosene heater use patterns. Second, we plan to conduct field tests on pollutant emissions from wood-burning stoves. We plan to test several styles of stoves under controlled, actual conditions. Third, we will be conducting laboratory tests on a new generation of unvented, gas-fired space heaters that incorporate oxygen depletion sensors (ODS). Heaters with ODS devices are designed to minimize CO emission, and our tests will evaluate their effectiveness.

# INDOOR AIR QUALITY CONTROL TECHNIQUES

Techniques for controlling the indoor concentrations of air contaminants include: (1) source suppression or exclusion (i.e., reducing the rate of contaminant entry into the indoor air), (2) ventilation with outside air that has a lower concentration of contaminants, and (3) air cleaning (removing contaminants from the indoor air). Studies at LBL of indoor air quality control techniques include evaluations of the performance of residential mechanical ventilation systems with air-to-air heat exchangers (MVHX systems) and development and evaluation of air cleaning techniques. MVHX systems supply outdoor air with a low concentration of indoor-generated contaminants to the residence and exhaust an equal amount of indoor air with a higher concentration of these contaminants. A MVHX system includes an air-to-air heat exchanger in which heat is transferred between the incoming and exhaust airstreams (without mixing of the airstreams), thus saving energy by preheating the incoming ventilation air in the winter and pre-cooling the incoming air in the summer. Prior to FY 1982, we measured the energy and fan performance of residential MVHX systems in the laboratory,[19,20] assessed their impact on indoor air quality in a field study,[21] and performed a preliminary economic analysis[22] of their use. In FY 1982, we continued our investigation of MVHX systems and initiated studies of air-cleaning techniques, as described below.

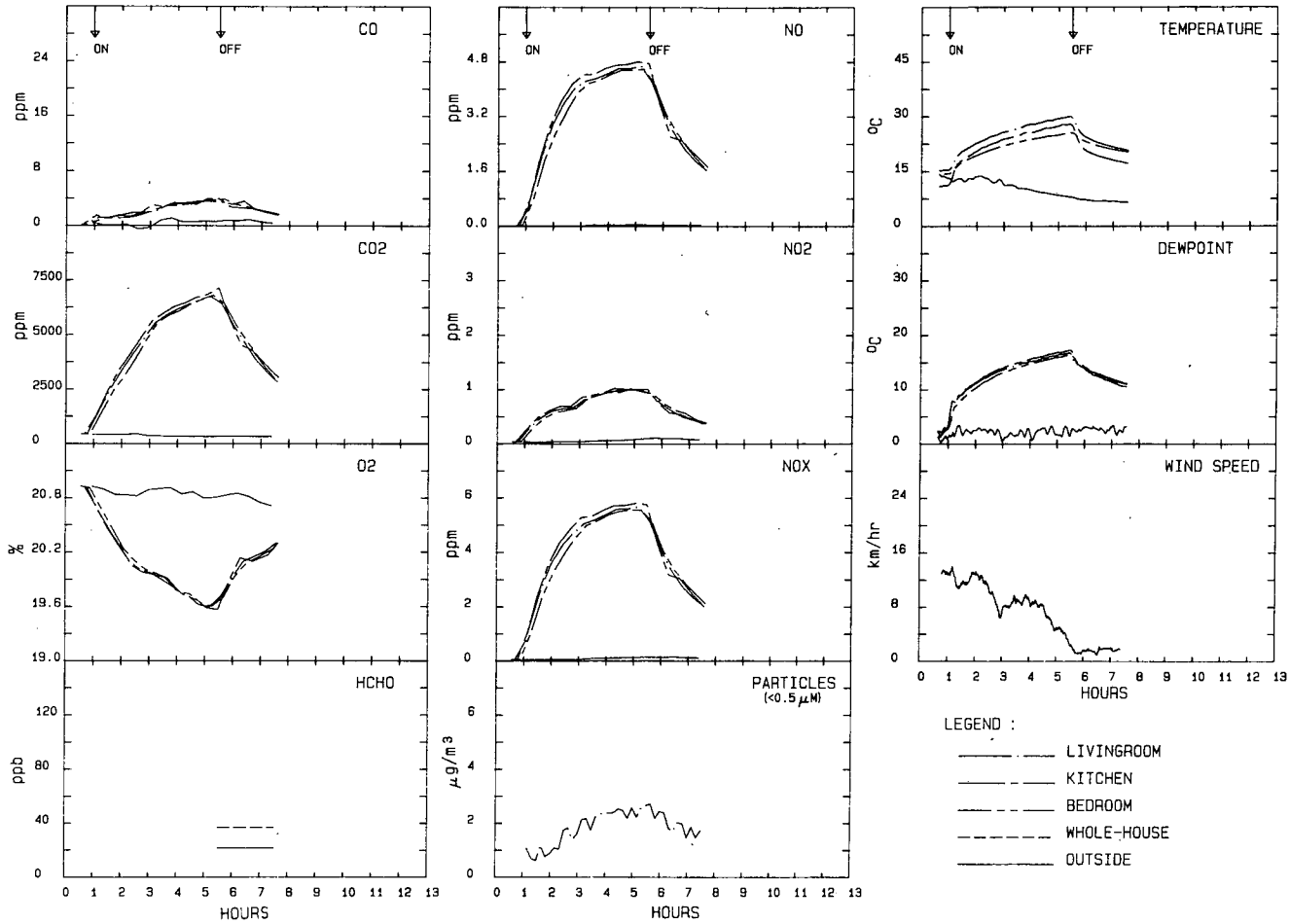


Figure 4. Profiles of pollutant concentration, temperature, dew point, and wind speed measured during the operation of a well-tuned 31,600 kJ/hr (30,000 Btu/hr) unvented gas-fired space heater in a 240 $m^3$ house. The air exchange rate was 0.49 ach. (XBL 8210-4790)

## Accomplishments During FY 1982

### *MVHX Systems*

Laboratory research in FY 1982 investigated the problem of freezing within MVHX systems and evaluated the ventilation efficiencies of MVHX systems that use no ductwork for air distribution. In addition, a computer model was developed to assess the economics of MVHX systems. These efforts are discussed below.

If a residential MVHX system is operating when the outdoor air is sufficiently cold, ice or frost can form within the core of the air-to-air heat exchanger and degrade the system's performance, reducing the amount of heat recovery and the flow of the exhausted airstream. In FY 1982, we initiated a study with the following objectives: (1) to determine the indoor and outdoor conditions for which freezing becomes a problem in various MVHX systems, (2) to determine the impact of freezing on system performance, and (3) to evaluate a simple freeze protection strategy that uses periodic defrost cycles. Measurements on one model indicated that, depending on the indoor humidity, freezing begins when outdoor temperatures range from −8 to −3°C. Typical curves of supply-stream effectiveness and exhaust-stream mass-flow rate versus time during freezing are shown for this model in Fig. 5. [Supply-stream effectiveness is defined here as the temperature rise of the incoming (cold) airstream divided by the difference between indoor and outdoor temperatures.] As the figure indicates, freezing causes a substantial degradation in performance.

Our studies included an evaluation of the ventilation efficiencies of two commercially available MVHX systems that are designed for installation through walls or windows.[23] This type of MVHX system is

used in the United States more often than systems that require ductwork. To assess their ventilation performance, multi-point measurements of tracer-gas concentration versus time (starting with an initially uniform concentration) were made with the MVHX systems operating in two multi-room structures. Tests were performed to determine the impact of installation location, electric baseboard heater operation, central furnace fan operation, and simultaneous operation of two units.

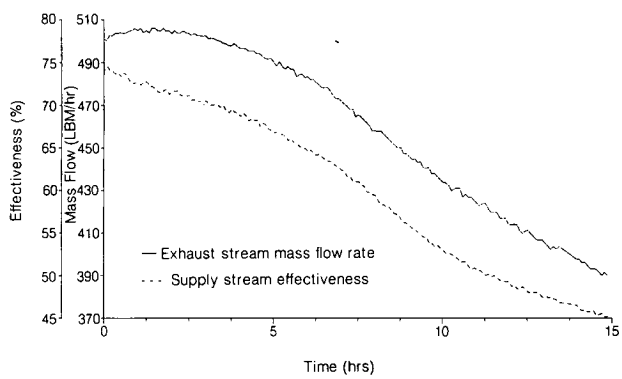


Figure 5. Typical curves of supply-stream effectiveness and exhaust-stream mass-flow rate versus time while freezing is occurring in the core of a cross-flow air-to-air heat exchanger. The temperature and relative humidity of the inlet exhaust stream were approximately 20°C and 30%, respectively. The temperature of the inlet supply airstream was approximately -11°C. (XBL 8211-7330)

Two measures of ventilation efficiency were calculated from the data. The nominal ventilation efficiency compares the measured average spatial increase in tracer-gas decay rate during operation to the increase that would occur for a reference case, assuming perfect mixing of the indoor air and no leakage between the two airstreams of the MVHX system. In 14 tests, nominal ventilation efficiency ranged from 0.44 to 0.66 and averaged 0.54, which indicates that these units provided on the average only 54% of the ventilation that would occur in the reference case.

The other measure is local ventilation efficiency. This was also calculated for the six indoor locations at which tracer concentrations were measured. Local ventilation efficiency compares the measured increase in the local air-exchange rate during system operation with the increase that would occur in the reference case. [A local air-exchange rate is the equivalent rate of air change with 100% outside (tracer-free) air that would cause the observed rate of change in tracer concentration.] A comparison of local ventilation efficiencies at different locations indicates how well the ventilation air supplied by the MVHX system is distributed. When the local ventilation efficiency of a room separated from the remainder of the structure by a closed door in four of the tests is excluded, the difference between the maximum and minimum local ventilation efficiencies ranged from 12% for one test to 63% for another test and averaged 33% for the 14 tests. The ventilation air was therefore not evenly distributed throughout the test spaces. As expected, the uniformity of air distribution was affected primarily by the location of MVHX system. The highest local ventilation efficiencies were at locations near the MVHX system and the lowest were in a room separated from the remainder of the structure by a closed door. This room received essentially no ventilation except when a central furnace fan was operating.

A third component of our study of MVHX systems was the development and use of a computer model to estimate energy savings and costs. The model was applied to MVHX systems with ductwork in new homes (with gas, oil, or electric heat) and to MVHX systems without ductwork installed as part of a weatherization program for electrically heated homes in the Pacific Northwest. For both analyses, we compared energy savings and energy costs in a typical house with those in a more airtight house having the same total ventilation rate but with some of the ventilation provided by an MVHX system. We also considered the winter heating season in four cities with different climates. Economic parameters calculated include net present benefit, benefit-to-cost ratio, discounted payback period, and cost of conserved energy.

The analysis of MVHX utilization in new homes[24] indicated an annual reduction in the load on the furnace system that ranged from 5.3 to 18.0 GJ. The MVHX's fan system required 2.2 to 3.6 GJ of electrical energy per year. The net present benefit and discounted payback period ranged from -$1350 to $2400 and from 5 to over 30 years, respectively. MVHX system performance, ventilation rate, climate, and heating fuel type had a large impact on the economic results. For the analysis of MVHX utilization in electrically heated, weatherized houses,[25] net annual energy savings were smaller, ranging from 1.7 to 2.7 GJ, discounted payback periods were greater than 30 years, and the cost of conserved energy ranged from 7.1 to 9.7 cents/kWh. MVHX systems did

not appear economical for this weatherization program largely because of the low electricity prices in the Pacific Northwest. However, the analysis indicated that these systems would be economical in regions with cold climates and high electricity prices.

*Other Accomplishments*

A literature survey of techniques for controlling indoor radon and formaldehyde concentrations was completed,[26] and studies of air cleaning techniques were initiated. A theoretical analysis was performed that indicated the feasibility of employing air washing to remove formaldehyde from indoor air. In preparation for laboratory studies of air washing and other techniques for formaldehyde control, a system that produces airstreams with a controlled temperature, humidity, flow rate, and formaldehyde concentration was designed and fabricated and is undergoing tests. In addition, we made preparations for a study of simultaneous particulate and radon daughter control by means of particulate control devices.

### Planned Activities for FY 1983

In FY 1983 the study of freezing within MVHX systems will be continued, laboratory measurements will assess the feasibility of air washing for control of indoor formaldehyde concentrations, and a study of simultaneous control of indoor particulate and radon daughter concentrations will be performed. In addition, further evaluations of the efficiencies of mechanical ventilation systems may be performed.

## COORDINATION AND SUPPORT OF INTERNATIONAL RESEARCH AND STANDARDS

Members of the BVIAQ program provide technical and administrative support for many indoor air quality issues in the worldwide research community. In FY 1982, this involvement included the following:

- Program members helped organize and coordinate the First International Symposium on Indoor Air Pollution, Health, and Energy Conservation held in Amherst, Massachusetts, in October 1982.
- Members of the BVIAQ Program were major contributors to the National Academy of Sciences publication, *Indoor Pollutants,* published in December 1981.[27]
- A.V. Nero (LBL) and W. Lowder (DOE) served as guest editors of a special issue of *Health Physics* devoted to indoor radon. This issue will contain 38 articles, reflecting the breadth of interest and involvement in this subject; eight of the papers were written by the staff of the radon project at LBL.
- Members of the program helped prepare the "Position Statement on Indoor Air Quality" of the American Society of Heating, Refrigeration, and Air-Conditioning Engineers (ASHRAE) published in July 1982.[28]
- The BVIAQ program continues to participate as a U.S. representative in Annex IX, "Minimum Ventilation Rates," of the International Energy Agency.
- The program contributes expertise to the American Physical Society "Panel on Public Affairs" on a regular basis.
- The staff participates in reviews of proposals for DOE and the Electric Power Research Institute (EPRI) and referees papers for *Environment International, Health Physics, ASHRAE Transactions*, and *Energy and Buildings.*
- The group is active in ASHRAE in both standards preparation and the work of technical committees. In particular, we have contributed to the preparation of Standard 62-1981, "Ventilation for Acceptable Indoor Air Quality"[29] and will be participating in its revision as members of the Special Project Committee that has been formed to revise Standard 62-1981.

We consider these support activities to be an essential part of our program and will maintain them in the future.

## REFERENCES


1. Geisling, K.L., Miksch, R.R., and Rappaport, S.M. (1982), "The Generation of Dry Formaldehyde at PPB to PPM levels by the Vapor-Phase Depolymerization of Trioxane," *Analytical Chemistry, 54*, p. 140.
2. Palmes, E.D. et al., (1976), "Personal Sampler for Nitrogen Dioxide," *American Industrial Hygiene Association Journal, 237*, p. 570.

3. Geisling, K.L. et al., (1981), *A Passive Sampling Device for Determining Formaldehyde in Indoor Air,* Lawrence Berkeley Laboratory Report LBL-12560 Revised.
4. Hodgson, A.T., Geisling, A.T., Remijn, B., and Girman, J.R. (1982), *Validation of a Passive Sampler for Determining Formaldehyde in Residential Indoor Air,* Lawrence Berkeley Laboratory Report LBL-14626.
5. Girman, J.R., Traynor, G.W., and Hollowell, C.D. (1982), *A Carbon Monoxide Passive Monitor: A Research Need,* Lawrence Berkeley Laboratory Report LBID-501.
6. Nazaroff, W.W., Offermann, F.J., and Robb, A.W. (1981), *Automated System for Measuring Air-Exchange Rate and Radon Concentration in Houses,* Lawrence Berkeley Laboratory Report LBL-12945, to be published in *Health Physics* special issue on indoor radon (1983).
7. Nazaroff, W.W., Revzan, K.L., and Robb, A.W. (1981), "Instrumentation for a Radon Research House," extended summary, presented at the International Symposium on Indoor Air Pollution, Health, and Energy Conservation, Amherst, MA, October 13-16, 1981; Lawrence Berkeley Laboratory Report LBL-12564.
8. Lucas, H.F. (1957), "Improved Low-Level Alpha-Scintillation Counter for Radon," *Rev. Sci. Instrum. 28,* 680-683.
9. Nazaroff, W.W. (1982), *Optimizing the Total-Alpha Three-Count Technique for Measuring Concentrations of Radon Progeny in Residences,* Lawrence Berkeley Laboratory Report LBL-14907, submitted to *Health Physics.*
10. Fisenne, I.M., George, A. and McGahan, M. (1983), "Radon Measurement Intercomparison," to be published in *Health Physics* special issue on indoor radon.
11. U.S. Bureau of Mines, Denver Research Center (1982), *Second Interlaboratory Comparison Test for Measuring Radon Daughters,* May 25-26.
12. Traynor, G.W. et al. (1982), *Pollutant Emissions from Portable Kerosene-Fired Space Heaters,* Lawrence Berkeley Laboratory Report LBL-14301.
13. Girman, J.R. et al. (1982), *Pollutant Emission Rates from Unvented Gas-Fired Space Heaters: A Laboratory Study,* Lawrence Berkeley Laboratory Report LBL-14502.
14. Traynor, G.W. et al. (1982), *Indoor Air Pollution Due to Unvented Gas-Fired Space Heaters: A Field Study.* Lawrence Berkeley Laboratory Report LBL-15130.
15. Traynor, G.W., Anthon, D.W., and Hollowell, C.D. (1982), "Technique for Determining Pollutant Emissions from a Gas-Fired Range," *Atmospheric Environment, 16,* pp. 2979-2988.
16. U.S. Government (1979) Code of Federal Regulations, Title 29, Section 1910.1000.
17. State of California (1977), California Administrative Code, Title 17, Subchapter 1.5, Section 70100.
18. U.S. Government (1975), Code of Federal Regulations, Title 40, Section 50.8.
19. Fisk, W.J., Roseme, G.D., and Hollowell, C.D. (1980), *Performance of Residential Air-to-Air Heat Exchangers: Test Methods and Results,* Lawrence Berkeley Laboratory Report LBL-11793.
20. Fisk, W.J. et al. (1981), "Performance Measurements for Residential Air-to-Air Heat Exchangers," presented at the International Symposium on Indoor Air Pollution, Health and Energy Conservation, Amherst, Massachusetts, Lawrence Berkeley Laboratory Report LBL-12559.
21. Offermann, F.J. et al. (1982), *Residential Air Leakage and Indoor Air Quality in Rochester, New York,* Lawrence Berkeley Laboratory Report LBL-13100.
22. Roseme, G.D., et al. (1979), "Residential Ventilation with Heat Recovery: Improving Indoor Air Quality and Saving Energy," in *Proceedings of the DOE/ASHRAE Conference on Thermal Performance of Exterior Envelopes of Buildings* (ASHRAE, New York), p. 609, Lawrence Berkeley Laboratory Report LBL-9749.
23. Offermann, F.J. et al. (1982), *Residential Air-to-Air Heat Exchangers: A Study of the Ventilation Efficiencies of Wall- or Window-Mounted Units,* Lawrence Berkeley Laboratory Report LBL-14358.
24. Fisk, W.J., and Turiel, I. (1982), *Residential Air-to-Air Heat Exchangers: Performance, Energy Savings, and Economics,* Lawrence Berkeley Laboratory Report LBL-13843, to be published in *Energy and Buildings.*
25. Turiel, I., Fisk, W.J., and Seedall, M. (1982), *Energy Savings and Cost-Effectiveness of Heat*

*Exchanger Use as an Indoor Air Quality Mitigation Measure in the BPA Weatherization Program,* Lawrence Berkeley Laboratory Report LBL-14784, to be published in *Energy, the International Journal.*

26. Alder, K., Hollowell, C.D., and Fisk, W.J. (1982), *Control of Formaldehyde and Radon in the Built Environment: A Survey of the Literature,* Lawrence Berkeley Laboratory Report LBID-625.
27. National Research Council (1981), *Indoor Pollutants,* National Academy Press, Washington, D.C.
28. American Society of Heating, Refrigeration, and Air-Conditioning Engineers, Inc. (1982), *Position Statement on Indoor Air Quality,* ASHRAE, Atlanta.
29. American Society of Heating, Refrigeration, and Air-Conditioning Engineers, Inc. (1982), Standard 62-1981, *Ventilation for Acceptable Indoor Air Quality,* ASHRAE, Atlanta.

## WINDOWS AND DAYLIGHTING*

*S.E. Selkowitz, S.U. Choi, D.L. DiBartolomeo, R.L. Johnson, J.D. Kessel, J.H. Klems, C.M. Lampert, M. Navvab, E. Ne'eman, M.D. Rubin, J. Ryan, and G.M. Wilde*

Approximately 20% of annual energy consumption in the United States is used for space conditioning of residential and commercial buildings. About 25% of this amount is required to offset heat loss and heat gain through windows. In other words, 5% of our national energy consumption—3.5 quads annually, or the equivalent of 1.7 million barrels of oil per day—is tied to the energy-related performance of windows.

The Windows and Daylighting Group aims to develop a sound technical base for predicting the net energy performance of windows and skylights, including both thermal and daylighting aspects. This capability will be used to generate guidelines for optimal design and retrofit strategies in residential and commercial buildings and to assist in exploratory development of new high-performance materials and designs.

One of our program's strengths is its breadth and depth: we examine energy-related aspects of windows from the perspective of electron microscopy at one extreme and perform field tests and *in-situ* experiments at the other. We have developed, validated, and now use a unique and powerful set of interrelated computational tools and experimental facilities that enable us to address the major research issues in our field.

It is also critically important that technical data developed by our program be effectively communicated to design professionals and to other public and private interest groups. We participate actively in all appropriate professional and scientific societies, national and international, to ensure that our research results are widely disseminated.

Our work is organized into four major areas:

- Analytical and physical models of fenestration performance
  —Thermal Analysis
  —Daylighting Analysis
- Materials science studies
- Fenestration optimization studies (thermal and daylighting)
- Field testing and *in-situ* performance characterization

## ANALYTICAL AND PHYSICAL MODELING—THERMAL ANALYSIS

### THERMAL MODELS

#### Accomplishments During FY 1982

Analytical models of thermal performance provide a technical basis for much of our research program. We have improved these general models of window heat transfer, as well as our optical and thermal models for windows having multilayer thin-film coatings, such as low-emittance heat-mirror coatings. In FY 1982, we initiated a study to determine thermal conductance, solar heat gain, and relative energy performance as a function of variation in solar optical properties for a variety of window configurations incorporating heat mirrors. Preliminary conclusions

*This work was supported by the Assistant Secretary for Conservation and Renewable Energy, Office of Building Energy Research and Development, Building Systems Division, and the Office of Solar Heat Technologies, Passive and Hybrid Solar Energy Division of the U.S. Department of Energy under Contract No. DE-AC03-76SF00098.

suggest that environmental conditions (such as wind conditions and temperature gradients) and the placement of the low-emittance film in the window can have a moderate effect on nominal performance values.

The fundamental optical properties of glazing materials must be known to calculate the thermal properties of the complete window system in which they are used. We derived a procedure for obtaining optical constants from photometric properties measured on sheet materials. We had previously completed a study to characterize the long-wave infrared emittance of thin plastic films of polyethylene terephthalate (PET). The emittance of glass should be well-known, but, surprisingly, we continue to find a wide range of contradictory values cited in technical literature. We are therefore completing a study to provide all the optical and emittance data necessary for thermal modeling of glass sheets.

The solar optical properties of windows change with the sun's angle of incidence. For geometrically complex shading systems (such as "egg crate" louvers), no adequate models exist to predict solar heat gain as a function of angle of solar incidence. In addition, solar gain from ground-reflected sunlight and diffuse light from the sky cannot readily be calculated for complex shading systems. We are developing a new technique for determining solar heat gain through complex fenestration systems based on a standard series of laboratory measurements of the fenestration system's optical properties. Transmittance will be measured using a large integrating sphere with the window system mounted in a port in the surface and illuminated with a sun simulator. For each sun position, total reflectance will be calculated by integrating measurements of bidirectional reflectance obtained from a scanning radiometer. The calculation of solar gain based on these optical measurements is computationally efficient and sensitive to sun position, making it useful in hour-by-hour energy analysis programs. Small prototypes of the integrating sphere were constructed and successfully tested in FY 1982.

### Planned Activities for FY 1983

We will make further refinements to our window heat-transfer models and complete additional validation studies. The study of the thermal properties of window systems incorporating heat mirrors will be expanded. Major new efforts will focus on developing the new solar heat-gain computational model and associated experimental apparatus. We will complete a full-size (7-foot-diameter) integrating sphere; a scanning radiometer for total reflectance measurements will also be fabricated and tested. The new solar heat-gain model to be incorporated into DOE-2.1 is shown schematically in Fig. 1.

## AIR INFILTRATION MODEL

During FY 1982, we extended the basic models developed by the Energy Performance of Buildings Group; our new models predict, as a function of window and building properties and of climate, the annual energy savings due to reductions in air leakage of windows in residences. We concluded that the annual energy consequences of window air leakage are often seriously overstated because of improper extrapolation from instantaneous test results to annual average performance.

## LABORATORY FACILITIES

### Accomplishments During FY 1982

In 1977, we established a Building Technology Laboratory in the College of Environmental Design at the University of California, Berkeley, to support our research and development activities and to provide independent testing and evaluation of fenestration materials and devices. This facility enables us to evaluate both experimental prototypes and new devices being introduced to the market. Testing facilities include a calibrated hotbox (Fig. 2), which is being used to test the thermal performance of windows and associated energy-conserving window accessories. A sample of devices now on the market was tested to establish a baseline against which to compare future improvements in window performance. Data from this test facility have also been used to validate our computer models. Air leakage tests on windows are made in this laboratory by measuring air flow for a range of positive and negative pressure differentials across a window. We have also developed capabilities for measuring a range of optical properties of glazing materials and coatings to fully characterize their performance.

During FY 1982, the facilities of the Building Technology Laboratory were used to prepare sensors and instrumentation for the Mobile Window Thermal Test facility and for heat-flow meter development, both described below.

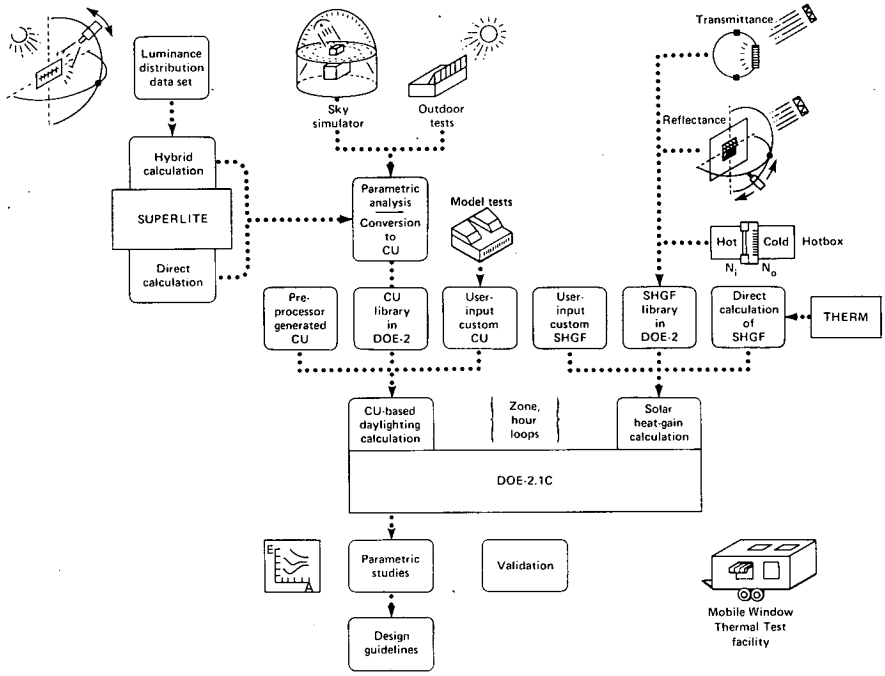


Figure 1. Schematic diagram of DOE-2.1 fenestration modeling capabilities under development. The new solar heat-gain model is shown on the right, the new illuminance model on the left. Both can be generated in a preprocessor, called from a library, or input by the user. (XBL 8212-4972)

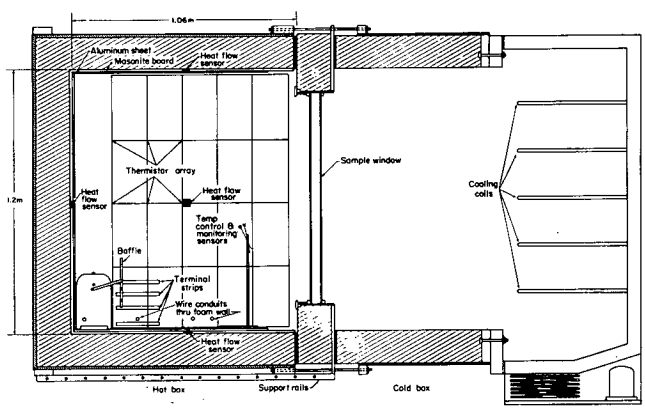


Figure 2. Cross section of calibrated hotbox showing hot and cold chambers and sample window. (XBL 799-2921A)

## ANALYTICAL AND PHYSICAL MODELING—DAYLIGHTING ANALYSIS

To predict the energy consequences of daylighting strategies, one must be able to predict the daylight illuminance distribution pattern in a building from any window or skylight under all types of sun and sky conditions. Since no single approach provides the best solution, we use a variety of techniques to assess different aspects of daylighting performance.

In previous years, we developed several simplified daylighting calculation methods (e.g., QUICKLITE) that are now widely used in the architectural and engineering professions. In 1982, we focused on further development and validation of advanced daylighting computational models.

### SUPERLITE, A DAYLIGHTING ILLUMINANCE MODEL

#### Accomplishments During FY 1982

This large, main-frame computer program was developed in cooperation with researchers at the University of Southern California. The program will calculate interior daylight illuminance under any sun and sky condition for a variety of nonstandard building configurations. Sample results are shown in Fig. 3. Calculated results for typical building cross sections compare well with data measured in scale models. Validation studies for more complex buildings are in progress. A version of the program, SUPERLITE 1.0, was readied for public release.

We modified the methods for inputting sky data so that the program can provide hourly results on a

daily, monthly, or seasonal basis. The program can now predict interior illuminance under four types of skies—uniform, overcast, clear sky without direct sun, and clear sky with direct sun. Several other reporting capabilities, such as calculation of average illuminance on the workplane and total light flux through windows, were added to the program.

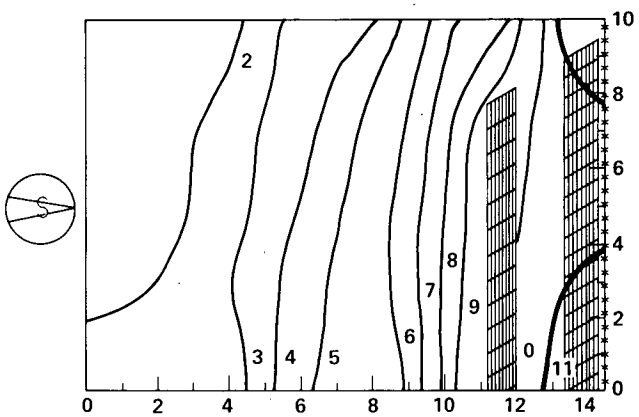


**Sky is clear**

**Sun position: 65° off zenith**

**30° off S to E**

**Horizontal illumination**

**Direct sun: 2407 fc**

**Sky: 1298 fc**

| Contour Number | Illum. Level (Ft-candles) |
|---|---|
| 1 | 20.0 |
| 2 | 40.0 |
| 3 | 60.0 |
| 4 | 80.0 |
| 5 | 100.0 |
| 6 | 150.0 |
| 7 | 200.0 |
| 8 | 250.0 |
| 9 | 300.0 |
| 10 | 400.0 |
| 11 | 500.0 |

**Windows marked by *******

**Sunny areas are hatched**

Figure 3. Isolux contours of daylight illuminance on the workplane in a 10 ft × 15 ft room that has a lower view window, a horizontal light shelf, and an upper clerestory window. Shaded portion shows where direct sunlight penetrates. (XBL 831-1155)

### Planned Activities for FY 1983

New algorithms are being added to SUPERLITE to allow the program to model illuminance from fenestration devices too complex for direct mathematical solutions. We measure an angle-dependent luminous transmittance function over a hemispherical field of view, which is entered into the program in functional form or as a data array. The program treats the device as a "black box" with specified luminous exitance properties. In 1983, we will build and calibrate an experimental facility to make the required optical measurements and test the new subroutines in SUPERLITE.

## DOE-2 DAYLIGHTING MODELS

### Accomplishments During FY 1982

As a result of collaborative efforts with the Building Energy Simulation Group, we completed development and testing of an operational daylighting model in DOE-2.1B. This model allows us to determine the direct effects of daylighting on lighting electrical consumption as well as on associated thermal loads. The model can simulate, on an hourly basis, the use of simple operable shading systems by altering the window solar optical properties in response to occupant requirements for thermal and visual comfort. New output reports not only indicate average hourly and monthly savings for each zone but also provide several types of statistical data summaries and frequency plots that enable us to examine the details of annual energy performance. The new daylighting model forms the technical basis for performance optimization studies now in progress.

### Planned Activities for FY 1983

The daylighting model will be expanded to simulate more complicated sun-shading devices and more sophisticated daylighting solutions such as light shelves. This improvement will be based on a new coefficient-of-utilization model derived from SUPERLITE calculations or model tests. The new model should enable the program to simulate, without additional revisions, the performance of building designs of arbitrary complexity. The planned procedure for calculating daylight illuminance and solar gains in the next version of DOE-2 is shown in Fig. 1.

## AVAILABILITY STUDIES

Studies of potential annual energy savings from use of daylight in buildings require data on daylight availability, including the frequency and intensity of daylight. No reliable source for such data currently exists for most of the United States. In 1977, the Pacific Gas and Electric Company (PG&E) building in San Francisco was instrumented to collect and record the amount of solar and visible radiation available at all building surfaces. An array of 9 pyranometers and photometers was installed to collect data at 15-minute intervals.

### Accomplishments for FY 1982

Analysis of the data from the PG&E building continued in 1982 in preparation for two papers to be presented at the International Daylighting Conference in early 1983. We coded and implemented algorithms for solar irradiance calculations and for correcting data for various experimental biases such as ground reflectance, daylight savings time, and shadow-band corrections. Analysis focused on the relationship of measured illuminance and irradiance to atmospheric parameters such as turbidity. Analysis was conducted to determine functional relationships between these parameters and luminous efficacy, zenith luminance, and illuminance values. Sample results are shown in Fig. 4.

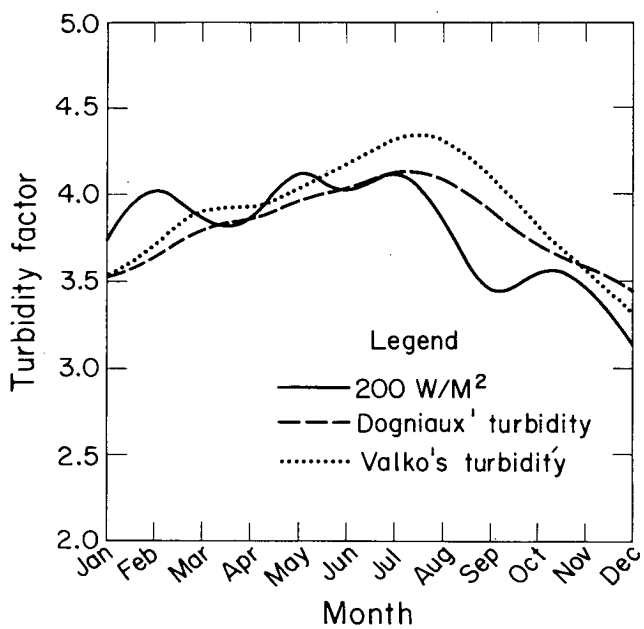


Figure 4. Comparison of measured turbidity factor (for direct solar radiation greater than 200 W/m$^2$) with predictions from two models using an annual average value for the Angstrom turbidity coefficient ($\beta$ = 0.0876) with monthly values of water vapor content. (XBL 833-1332)

### Planned Activities for FY 1983

We will complete analysis of the first several years of daylight-availability data and explore techniques for displaying results in a format useful to building designers. We will also use the results to upgrade the algorithms in our daylighting computational models and to work with other researchers to develop standard availability models for U.S. climates. We expect our results to suggest new areas for more detailed research, such as the time-dependent variability of daylight, spectral and polarization effects, and microclimate influences.

## DAYLIGHTING PHYSICAL MODELING—SKY SIMULATOR

A 24-foot-diameter hemispherical artificial sky [Fig. 5(a)], designed and built on the U.C. campus in 1979 to facilitate model studies for daylighting, became operational in 1980 with the simulation of luminance distributions for an overcast sky. In 1981, we designed and installed improved lighting controls in the dome in order to simulate complex luminance distributions for clear skies. Sky luminance distributions are reproduced on the underside of the hemisphere; light levels are then measured in a scale-model building under the artificial sky. From these measurements, we are able to predict daylighting illuminance patterns in real buildings.

### Accomplishments During FY 1982

The sky simulator was used to collect test data from scale models to validate the SUPERLITE and DOE-2 computer models and to help develop a new coefficient of utilization illuminance model. Toward the end of the year, the entire facility had to be moved 10 feet to accomodate the addition of a wind tunnel in the room. The move and other building renovations closed the facility for three months but provided the opportunity for several major additions.

We installed a new computerized data-acquisition system with 60 photometric sensors [Fig. 5(b)]. We designed a sun simulator that will travel from horizon to zenith and provide a 30-inch-diameter collimated beam. Design work was completed on a new lighting control system that will use dimmable electronic ballasts and permit precise control of the light output of every lamp in the system.

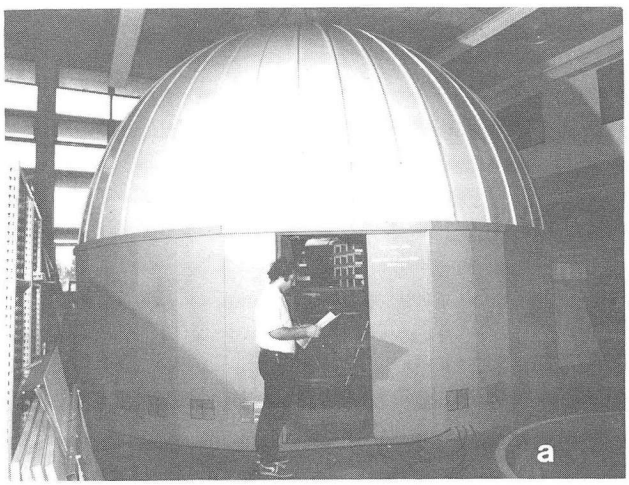


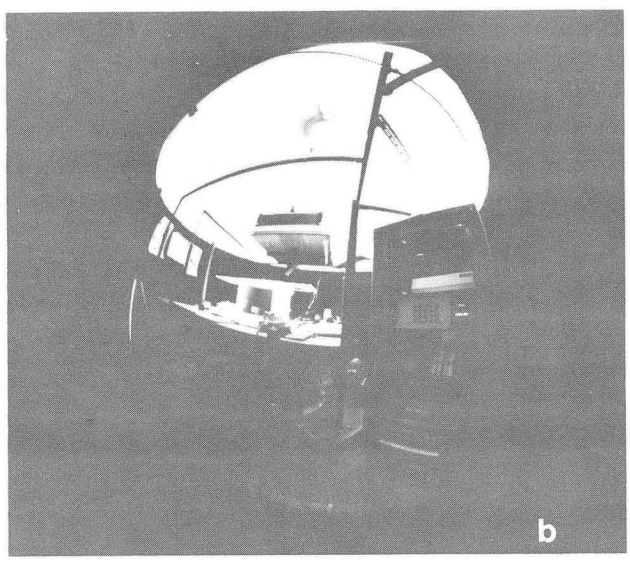


Figure 5. Hemispherical sky simulator: (a) exterior; (b) interior. [(a) CBB 823-2768C ; (b) CBB 833-2304]

### Planned Activities for 1983

The sun simulator will be completed, installed, and tested in the dome. A ground reflectance simulator has also been designed and will be installed in 1983. The facility will be completely rewired with a new dimmable fluorescent system, and appropriate operating software for the computer control system will be developed. By the end of the year, we hope to complete arrangements to make the facility available to design firms on a cost-recovery basis.

## MATERIALS SCIENCE STUDIES

Since the inception of our program in 1976, identification, characterization, and exploratory development of promising new fenestration materials have been major program activities. Research on new glazing materials and modifications to existing materials should lead to substantial reductions in building energy consumption. During the past 6 years, the Office of Building Energy Research and Development at DOE has supported research studies on heat-mirror films, electrochromic coatings, and graded-index materials as well as a number of smaller studies on other materials aspects of fenestration systems. In FY 1982, additional support for related exploratory studies was obtained from the LBL Director's Office and from the Office of Energy Systems Research, Division of Energy Conversion and Utilization Technologies in DOE. We also initiated a major new research program on advanced optical and thermal technologies for aperture control, with support from the Office of Solar Heat Technologies, Passive and Hybrid Solar Energy Division.

### HEAT-MIRROR FILMS

#### Accomplishments During FY 1982

The major high-performance optical technology studied in our program's first few years was low-emittance coatings (heat mirrors), which are important for developing low-conductance, high-transmittance windows. These coatings reduce the emittance of glass or plastic substrates from 0.8-0.9 to 0.1-0.2, thus reducing the large radiative component of window heat loss. These coatings, deposited on glass or plastic substrates, make it possible to have windows in the R4 to R10 insulation range while maintaining moderate to high solar transmittance. LBL studies were instrumental in the combined public and private efforts that finally led, in 1982, to market introduction of windows with heat-mirror films.

The first generation of commercially available heat mirrors is based on noble metals incorporated into metal-dielectric multilayer coatings; these coatings

must be enclosed in hermetically sealed insulating window units to ensure adequate lifetimes. Because sealed windows are not feasible in many applications, particularly in retrofitting older buildings, there is a need for more durable heat-mirror coatings.

An alternative to the multilayer coating is the use of a single-layer, highly doped semiconductor. The spectral relationship between an undoped semiconductor such as $SnO_2$ and a metal is shown in Fig. 6(a). To give the best heat-mirror properties, the metal's plasma edge must shift to longer wavelengths and the semiconductor to shorter wavelengths. For example, $SnO_2$:F has excellent properties and durability, but it can be used only with high-temperature substrates, and its visible reflectance losses are appreciable. In FY 1982, we initiated a study to see if grading the optical index of the film will reduce those losses.

Another possibility is to use the metallic transition-metal nitrides such as TiN, ZrN, and TaN, which are related to the highly doped transition-metal oxides. Very little is known about the optical properties of these materials. They are commonly used as hard-facing coatings because they provide extremely high durability under mechanical wear. Using LBL Director's funds, we initiated a study of these unusual optical materials in 1982. These nitride films are related to metals by their Drude-like conduction mechanism (free d-band electrons) in the infrared [Fig. 6(b)]. However, in the visible, TiN interband transitions predominate, producing its gold color. It is thought that we can enhance the visible transmittance by oxygen substitution or TiN-$TiO_x$ chemical grading in the film.

### Planned Activities for FY 1983

We will continue and expand our study of the possibilities of reducing the visible reflectance losses of $SnO_2$:F by grading the optical index of the film. We also expect to investigate other promising applications for graded-index films and coatings. The research on TiN-$TiO_x$ will continue and will include analysis of films made by reactive sputtering and plasma-enhanced deposition. We will continue to examine other materials and deposition processes that show promise as high-performance, durable heat-mirror films.

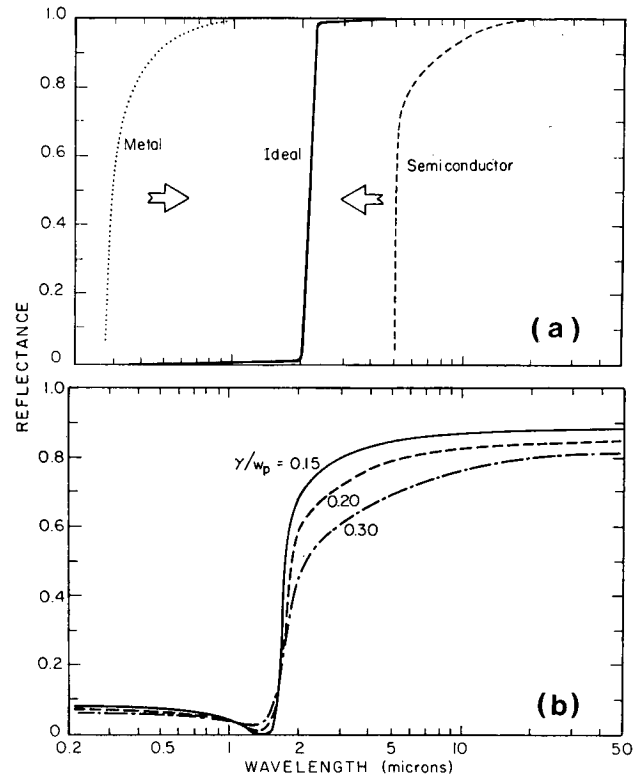


Figure 6. (a) Idealized spectral reflectance relationship of noble metals and oxide semiconductors. By shifting their respective plasma wavelengths, an ideal heat mirror can be produced. (b) Drude modeling of a hypothetical conductor like $SnO_2$ or TiN in the infrared region. The ratio of the relaxation frequency to plasma frequency $\gamma/w_p$ serves as a measure of wavelength selectivity.

[(a) XBL 793-5887A; (b) XBL 811-5131A]

## AEROGEL

### Accomplishments During FY 1982

We initiated research on a new class of transparent insulating materials called aerogels. These materials are formed by supercritically drying a colloidal gel, which leaves an open-cell silica network. Because the particle size is very small (~100 Å), there is little light scattering and the material can be made optically transparent. We completed initial studies of the light-transmittance and thermal properties of silica aerogel (Fig. 7). These studies indicate that window systems incorporating an aerogel layer could achieve an insulating value of R7 per inch with good optical clarity and high solar transmittance, a substantial improvement over current glazing technologies.

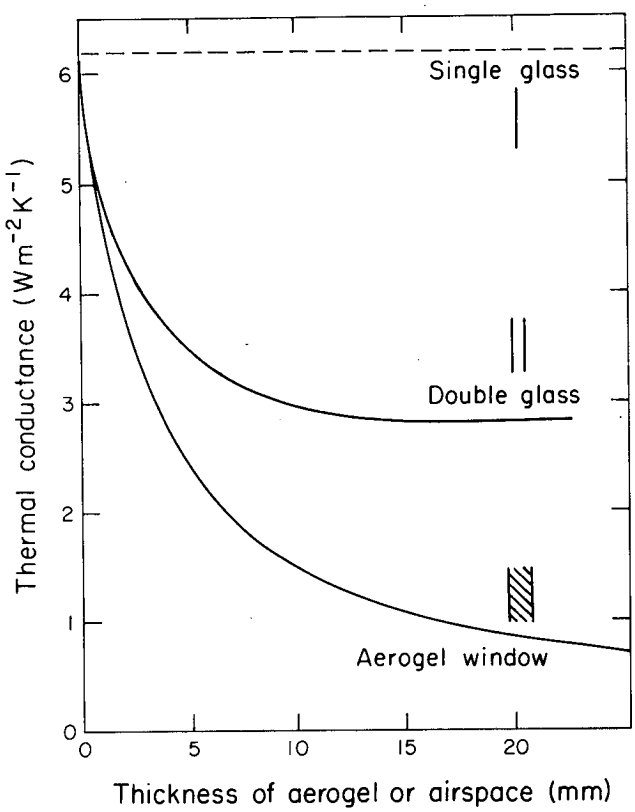


Figure 7. Calculated thermal conductance of aerogel window and of conventional single- and double-glass window vs. spacing between glass panes. (XBL 826-827)

## Planned Activities for FY 1983

Our studies of aerogel in collaboration with the Solar Group at LBL will be expanded to include measurements of angular scattering and mechanical properties. We will attempt to increase the thermal resistance of silica aerogel by using additives that absorb thermal radiation and by using low-conductance gas fills and low pressures to reduce convective and conductive heat transfer. Glazings with high solar transmittance and antireflection coatings will be used to make high-transmittance prototype aerogel windows. We will also investigate methods of sealing these windows against moisture intrusion or gas leakage. Aerogel samples will be produced in a new synthesizing facility now under construction.

Aerogels of other chemical types will be synthesized to determine which material offers the best balance between solar and mechanical properties. We will try to reduce the temperature/pressure requirements and the time required to produce aerogels by physical substitution of solvents having a lower critical point than ethanol.

# OPTICAL SWITCHING PROCESSES AND MATERIALS

Various optical switching materials or devices can be used to control solar heat gain and glare in buildings. An optical switch or shutter is transformed from highly transmitting to totally or partially reflecting (or absorbing) over the solar spectrum in response to changes in light intensity, spectral composition, heat, electrical field, or injected charge. Such a device would be used to control the flow of light and/or heat in and out of a building aperture, based on building energy management requirements. This device could also control illuminance and glare levels as well as transmitted thermal energy loads.

## Accomplishments During FY 1982

Several classes of devices can be considered candidate material systems. In 1982, we expanded earlier overview studies of the most promising systems based on chromogenic reactions such as electrochromism, photochromism, thermochromism, and electrodeposition; electrochromic systems showed the most promise.

While many of these materials have been explored for use in electronic display devices, there has been very little research on the use of electrochromic materials as optical switching devices for windows. An electrochromic material exhibits intense color change due to the formation of a colored compound in a reversible reaction. There are two major categories of electrochromic materials: transition-metal oxides and organic compounds. Organic electrochromics are based on several different materials systems and achieve coloration by an oxidation-reduction reaction, which may be coupled with a chemical reaction.

The inorganic materials that have attracted the most research interest due to their stability are $WO_3$, $MoO_3$, and $IrO_x$ films. A solid-state window device can be fabricated containing the layers shown in Fig. 8: transparent conductors (TC), an electrolyte or fast-ion conductor (FIC), counter electrode (CE), and electrochromic layer (EC). Our research is directed towards developing better electrochromic materials having good optical properties, high cyclical lifetimes, and short response times. This includes study of fast

ion conductors and solid electrolytes, essential components of electrochromic systems for window applications.

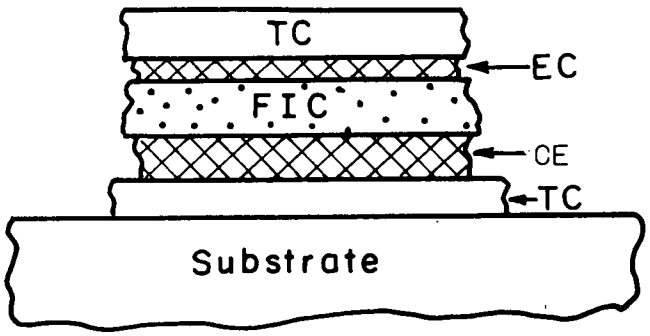


Figure 8. Schematic of a solid-state electrochromic device. (XBL 805-9713)

### Planned Activities for FY 1983

Although new technical studies in FY 1983 will focus on electrochromic coatings, we will complete an overview of the other switching-film mechanisms (e.g., thermochromics) to see if additional research is warranted. A detailed multi-year plan for switching-films research will be developed. Electrochromic studies at LBL will focus on characterizing the optical properties and microstructure of some of the promising but less well known materials systems.

## GRADED-INDEX COATINGS

### Accomplishments During FY 1982

Light reflection at the boundary between two media can be reduced through the use of single- or multiple-layer coatings. A layer having a continuously varying index of refraction can provide a very low reflectance over most of the solar spectrum. We have investigated the effect of adding a single-layer graded-index coating to polyethelene terephthalate (PET). The index of refraction for PET is about $n = 1.65$. With the addition of a graded coating with $n = 1.65 \rightarrow 1.0$, reflection losses can almost be eliminated. We have analyzed an existing steam-oxidized aluminum film on PET and identified the resulting dendritic films as aluminum hydroxide. A computer model was developed to predict the optical properties of dendritic films and other graded-index coatings.

### Planned Activities for FY 1983

Optical losses can be eliminated and system efficiency increased by using chemical or structural grading of a broad class of coatings. In 1983, we will extend these studies to validate our analytical models of graded-index coating performance against measured optical properties of the coatings.

## MATERIALS FOR IMPROVED DAYLIGHT UTILIZATION

The intensity and spatial distribution of daylight transmitted through windows and skylights must be controlled in order to reduce electric lighting requirements. Conventional solutions rely upon architectural elements and interior or exterior devices to control daylight admission and distribution. Greatly improved performance would result from materials or systems that could: (1) transmit maximum daylight with minimal cooling load impact (i.e., reject solar infrared radiation); (2) collect and distribute daylight beyond the perimeter zones in buildings; and (3) provide angular selectivity in the acceptance and redirection of incident light at the building envelope.

### Accomplishments During FY 1982

In earlier studies, we evaluated the performance of a variety of devices for daylight acceptance and control based upon reflective and refractive optics. In 1982, we turned our attention to innovative optical materials and devices that showed the potential for replacing more complex mechanical systems. We initiated a study of the feasibility of using approaches such as fiber-optic systems, hollow light guides, holographic coatings, selective-reflectance materials, and various scattering media. One promising approach for collecting and redirecting daylight is the subject of a patent disclosure.

### Planned Activities for FY 1983

We will complete an overview study to identify and characterize innovative optical materials technologies for daylighting. Several of the more promising approaches will be explored in greater depth.

# OPTIMIZATION STUDIES

Thermal and radiant energy flows through windows and skylights, unlike the flow through most other

building envelope components, can be managed so that these architectural elements provide net energy benefits to the building. While heat loss and cooling loads resulting from solar gain must be minimized, solar gains in winter and useful daylight throughout the year reduce conventional energy requirements. Optimization of window systems thus involves complex tradeoffs between competing requirements. The optimum solutions may be a sensitive function of building type, climate, orientation, and building operating parameters. These studies are designed to provide a better understanding of all aspects of optimizing fenestration performance and will lead to guidelines and analysis tools to assist the building design community. Our work originally focused on residential buildings but has shifted during the past 4 years to an emphasis on non-residential buildings, including daylighting and peak-load management issues. In the future, we expect to conduct studies of both building types.

## NON-RESIDENTIAL BUILDINGS

Most building optimization studies have focused on minimizing total energy consumption. Commercial and industrial customers, however, are generally billed for electricity use on the basis of both energy consumption and peak electrical demand. A complete study of the cost-effectiveness of fenestration systems, and particularly daylighting strategies, must thus include the impact on peak electrical loads as well as on energy savings. Although the energy impact of daylighting has been under study by our group and others, there have been no prior investigations of the impact of daylighting on peak loads.

### Accomplishments During FY 1982

The energy performance of a prototypical commercial office building was simulated with a modified version of DOE-2.1B for a wide range of glazing properties, window size, lighting load, orientation, and climate. The first phase of this study examined the impact of fenestration properties, including the effects of daylighting strategies, on office building performance. Lighting energy savings due to daylighting were examined for a range of fenestration properties and lighting control systems. Annual energy consumption of an office module was found to be sensitive to variations in the primary fenestration properties (U-value, shading coefficient, visible transmittance) as well as glazing area, orientation, climate, and operating strategy.

A significant result of these studies is a first attempt to quantify the impact of window management strategies for controlling thermal comfort and glare from windows. Although the specifics vary considerably from case to case (by as much ±50% of an average value of zone energy consumption over a range of typical fenestration parameters), we conclude that in almost all instances it is possible to find a fenestration system that outperforms a solid insulating wall, although the "solution" may not always be cost-effective. Sample results are shown in Figs. 9 and 10.

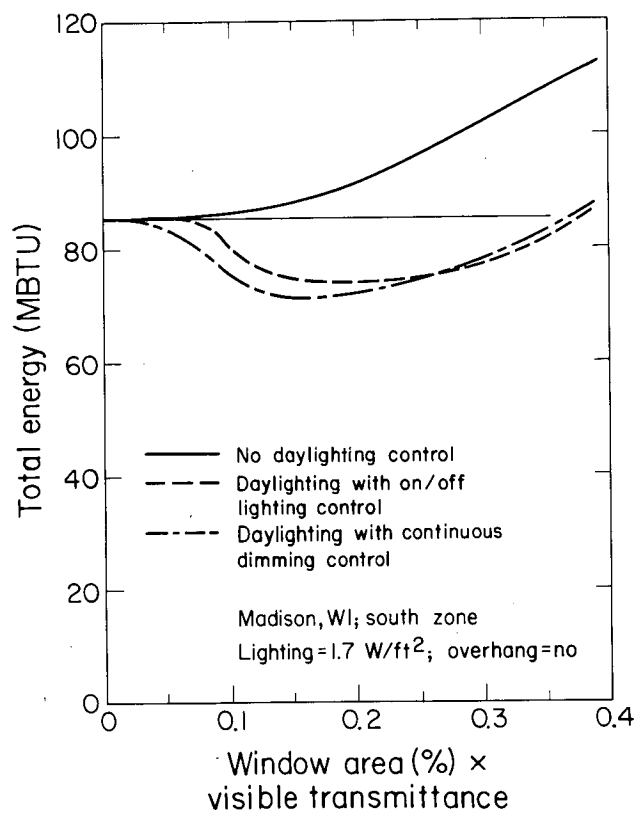


Figure 9. Energy consumption on the south zone of an office building in Madison, Wisconsin, showing the variation in annual energy consumption with window area and transmittance for an opaque exterior wall (thin horizontal line), a non-daylighted case, and daylighting with two types of lighting controls. (XBL 833-1318)

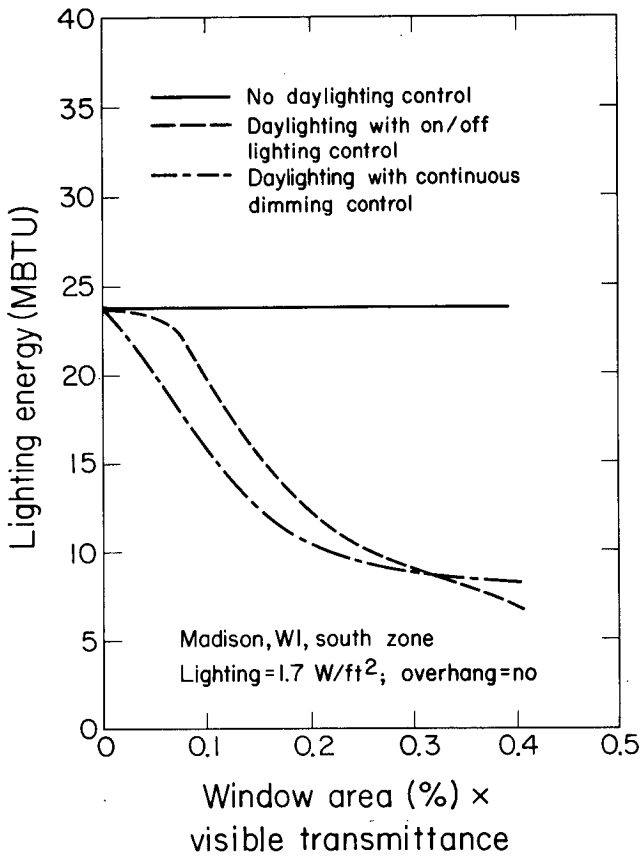


Figure 10. Energy consumption for electric lighting as a function of the product of window area and visible transmittance for a non-daylighted case, on-off lighting controls, and dimming lighting controls. (XBL 833-1317)

The second phase of this work concentrated on providing quantitative information on the peak-shaving potential of daylighting. Results show that daylighting can reduce a significant portion of the peak demand during summer months. Parametric studies indicate that peak demand is a nonlinear function of glazing properties and window size for the daylighting case, but the relationship is almost linear in the non-daylighting case. The critical tradeoffs—between electric lighting reductions due to daylighting, and cooling load increases due to increased window solar gain—help determine the combination of window properties that minimize building peak loads. The breakdown of the peak load component during annual peak conditions for a sample office building is shown for both the daylighted and nondaylighted cases in Fig. 11.

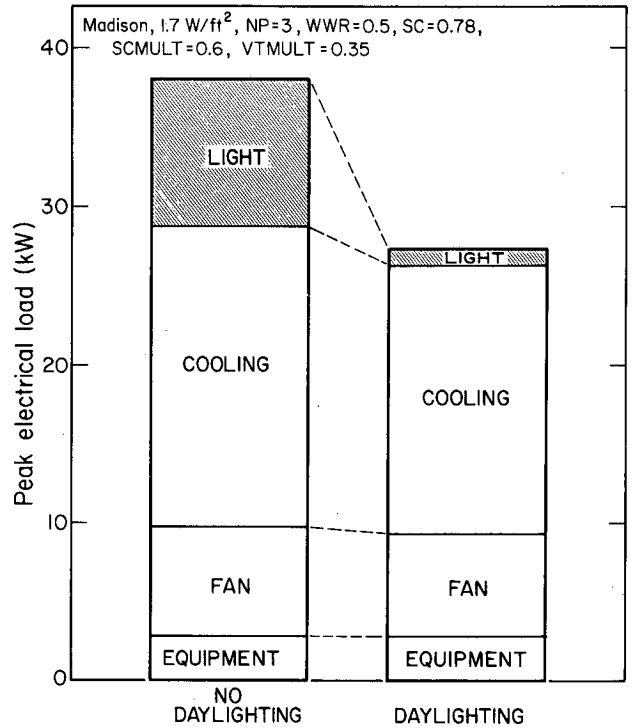


Figure 11. Peak-load breakdown for a five-zone office building in Madison, Wisconsin (1600 ft$^2$). The peak occurs at 4 pm on August 31. The windows are triple-glazed with a visible transmittance of 0.52 and cover 75% of the wall (floor to ceiling). Installed lighting power is 1.7 W/ft$^2$. (XBL 8212-7388)

## Planned Activities for FY 1983

Optimization studies will be extended to include additional fenestration materials and devices, new climates, skylighting systems, and other building types. The performance data resulting from some of these studies will be used by an ASHRAE technical committee as the technical basis for new voluntary building energy guidelines. This work will also lead to an examination of several alternative techniques for developing simplified energy models of fenestration performance. The detailed analysis of the impacts of daylighting on building peak loads will be continued and expanded. This includes analysis of electrical demand characteristics as a function of orientation, breakdown of peak demand into components, and investigation of impacts on cooling from reduced lighting load and fenestration. The benefits to the customer and the utility of reducing peak demand through daylighting will also be studied by adding a model for electric rate structures.

We also expect to resume work initiated in 1979 on

residential optimization. The first phase examined the performance of insulating shutter systems. The new phase will emphasize the performance of several high-performance window systems now emerging in the building sector and will also help set performance objectives for window systems under development.

## *In-Situ* TESTING—FIELD VALIDATION

Net energy performance under actual conditions of use in a building is the single piece of information most relevant to assessing the benefit to be the derived from a window or window improvement. This is a dynamic property, essential for predicting the performance of managed window systems (windows having thermal/optical properties that can be manually or automatically changed by building occupants). Most laboratory testing facilities, however, are designed primarily to conduct steady-state measurements of static materials and devices. No experimental methodology currently exists for measuring the net performance of windows *in situ.*

### MoWiTT

#### Accomplishments During FY 1982

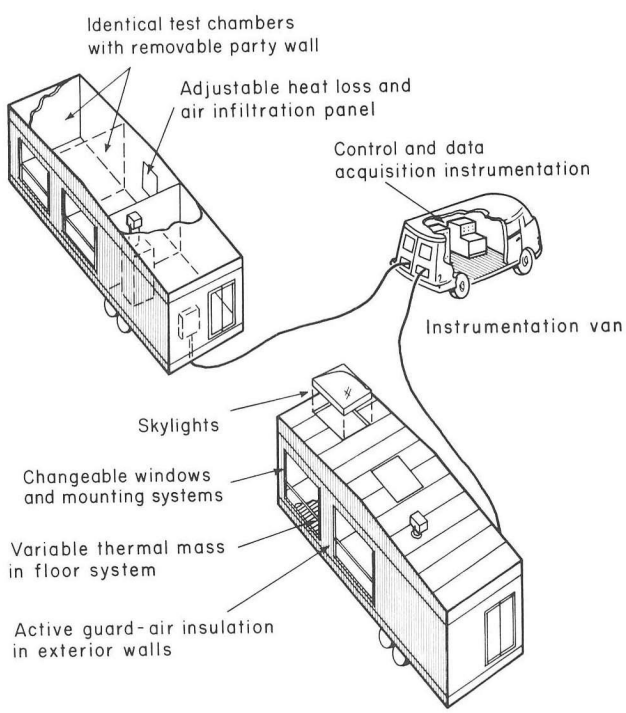


Figure 12. Schematic view of Mobile Window Thermal Test (MoWiTT) facility. (XBL 811-30)

During 1981, we began constructing a Mobile Window Thermal Test (MoWiTT) facility to fill this experimental gap (Fig. 12); the facility consists of one or more measurement modules with an instrumentation van. The measurement modules, which consist of twin guarded calorimeters, will enable dynamic studies of combined solar, infiltrative, conductive/ convective, and radiative heat transfers as a function of window type and orientation. During 1982, the first module was assembled (Fig. 13) and one calorimeter chamber completed. The module was moved to an outdoor test site and check-out begun.

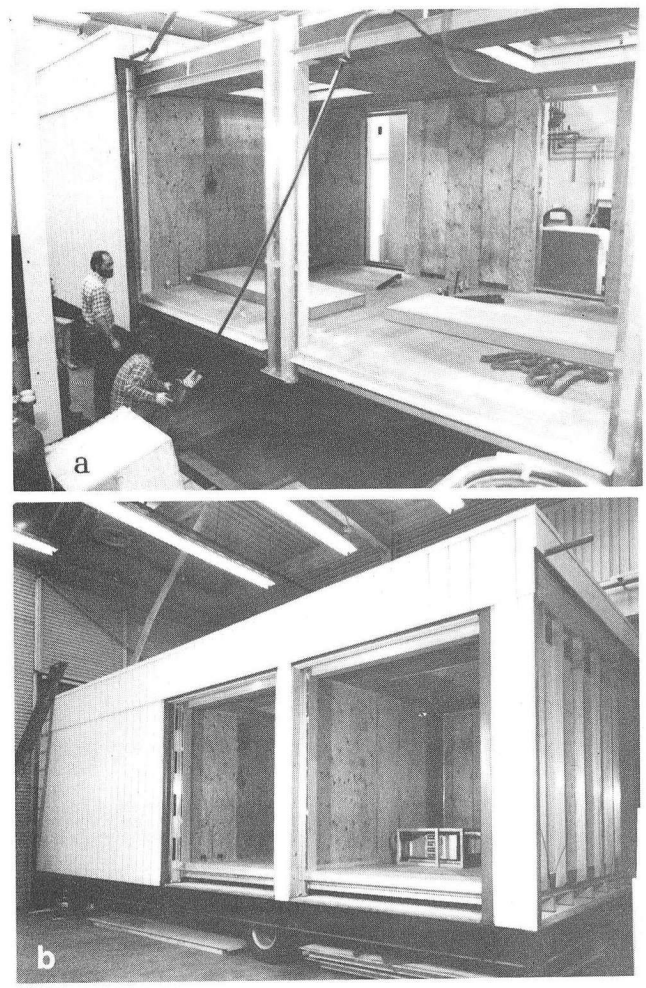


Figure 13. Progress of the MoWiTT facility. (a) Insertion of the calorimeter chambers. (b) The nearly-complete assembly. [(a) CBB 824-3063; (b) CBB 826-5379]

An outgrowth of work on the MoWiTT facility has been the development of a new heat-flow meter. Instead of measuring the temperature difference with a deposited thermopile across a known thermal resistance (the usual method), this heat-flow meter uses

AC resistance thermometry. Such heat-flow meters can be made economically in sizes large enough to cover entire walls, and we intend to incorporate them into the MoWiTT facility.

During 1981, a successful one-foot-square prototype heat-flow meter was built (Fig. 14 shows some test results). In 1982, a series of 1-ft$^2$ prototypes was built and tested in order to fix the design parameters for larger units, and approximately 400 ft$^2$ of full-sized units (up to 2 ft by 4 ft) were produced for installation in the MoWiTT (Fig. 15).

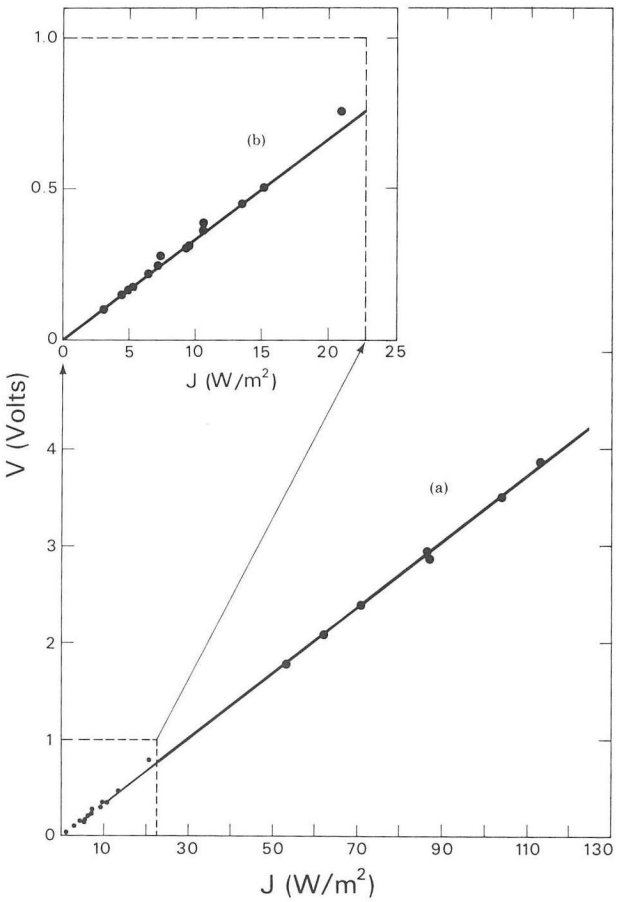


Figure 14. Calibration of a 1-ft$^2$ heat-flow meter prototype. (A) Complete calibration. (B) Expanded view of the small-signal region of the curve. Points are measurements made in the guarded hot plate and corrected to a 25 °C mean sensor temperature. The line is a least-squares fit to the data and has a slope of 37.6 mV(W/m$^2$)$^{-1}$. (XBL 8201-6)

Figure 15. Large-area heat-flow meters for use in MoWiTT. (CBB 828-7550)

## Planned Activities for FY 1983

We will complete the second calorimeter chamber in MoWiTT, calibrate the unit, and begin field testing at summer and winter test sites. The heat-flow meters will be calibrated in a large calibrated hot-plate, then installed in the completed MoWiTT chambers. A multi-year testing program will be developed with input from all sectors of the fenestration community.

## OCCUPANCY STUDY

Fenestration and lighting controls are essential to energy-efficient office buildings. Both daylighting and electric lighting control systems need to be designed to limit costly cooling loads and still provide thermal and visual comfort for building occupants. The availablity of control system components is rapidly increasing, along with advances in computers and hardware. Yet in many buildings where computerized controls have been implemented, occupants have not been satisfied with the quality of the work environment. The reasons are complex but, in general, automated systems do not involve building occupants.

The occupancy study will gather data for developing recommendations concerning fenestration and lighting control systems that will satisfy office occupants in their work areas.

## Accomplishments During FY 1982

We developed two tools to aid our evaluations of occupant response to building control systems: a questionnaire and physical measurements. The questionnaire allows occupants to rate their level of well-being and satisfaction with environmental conditions in their work areas. The related physical measurements include lighting and temperature levels in work areas. Architectural drawings and photography will also document work areas.

Analysis of the questionnaire data for each building will look for correlations between the light sources, their control systems, and work area locations and orientations, as well as differences among occupants such as age, sex, and tenure at their work areas.

## Planned Activities for FY 1983

We expect to locate a suitable office building for pilot and full-scale evaluations. Planned future studies will consider three general office building types: unmodified buildings, buildings with retrofitted shading and/or lighting controls, and energy-efficient buildings.

## REFERENCES

See Publications List, pp. 3-78 through 3-81.

# LIGHTING SYSTEMS RESEARCH*

*S.M. Berman, R.R. Verderber, R.D. Clear, O.C. Morse, F.M. Rubinstein, and R.K. Sun*

The Lawrence Berkeley Laboratory has managed the National Lighting Program for the Department of Energy since 1966. The primary goal of the past five years was to accelerate the introduction of energy-efficient lighting products and concepts to the marketplace—a strategy intended to accomplish the goal of a 50% reduction in U.S. energy consumption for lighting by the mid-1990s. This savings of energy, more than 200 billion kilowatt-hours, is equivalent to 381 million barrels of oil annually, or more than one million barrels of oil per day.

Projects initiated at LBL include development of the solid-state ballast for operating fluorescent lamps, lighting management systems, and energy-efficient light sources, as well as fundamental visibility-performance studies and investigations of the effects of artificial light on human health. As the lighting program grew, it was divided into three sections: the Technical Program—to study the fundamental properties of light sources in order to improve their efficacies; the Building Applications Program—to study advanced, energy-efficient lighting designs and their relationship to overall building energy performance; and the Impacts Program—to study the effects of energy-efficient lighting systems on visibility, and on the performance and health of those who work with them. This study will have some influence on the extent to which these energy-efficient systems will be used.

Our lighting program has been responsible not only for the appearance of solid-state ballasts in the marketplace, but also for a more widespread awareness of energy management systems and for light sources that are three to four times more efficient than the incandescent bulb. Our initial, fundamental work on visibility and performance, which reviewed the basis for establishing recommended light levels, suggested that further experiments were required. To execute these projects, three laboratory facilities were established: the Physical Lighting Laboratory, the Visibility Laboratory, and the Health and Environmental Laboratory. These laboratories are staffed with individuals specializing in various scientific disciplines: physicists, engineers, optometrists, psychiatrists, and physicians. Staff members interact closely on lighting and visibility problems selected for study. The LBL lighting laboratories are the only facilities diversified enough to resolve the critical technical problems surrounding the optimal performance of illumination.

The early and successful commercial applications of the technologies developed by the LBL program also introduced new issues—high-frequency operation and flicker—that must be addressed if the new technologies are to find widespread use. In addition, there is a need to expand research in preparation for the next, and more efficient, generation of electrical illumination systems.

To meet these needs, the 1982 Lighting Program included studies on the fundamental properties of plasmas (gas discharges) with regard to electric and magnetic fields; new, high-frequency ionizing materi-

*This work was supported by the Assistant Secretary for Conservation and Renewable Energy, Office of Building Energy Research and Development, Building Equipment Division of the U.S. Department of Energy under Contract No. DE-ACO3-76SF00098.

als; the effect of new light sources on visibility and performance; and the effect of these sources and systems on human health and existing electronic systems.

Described below are the highlights of the accomplishments realized in 1982 by our three major efforts—the technical, building applications, and impacts programs—and the activities planned for 1983.

## TECHNICAL PROGRAM

### SOLID-STATE BALLASTS

#### Accomplishments During FY 1982

Finalization of the circuit design of solid-state ballasts began with the delivery of high-pressure sodium (HPS) ballasts. Two contractors delivered their units,[1] and we life-tested them for 6 months. From experiments, we concluded that the efficacy of HPS lamps will not increase with high-frequency operation, but such operation still has some advantages, such as an increase in ballast efficiency of 5 to 10% and improved regulation and constant wattage output of the ballast. These factors contribute to an energy savings of 10 to 20% over the life of the lamps.

One serious problem, known as the acoustic resonance phenomenon, was noticed in the 200-watt HPS lamps. This phenomenon occurs when the frequency of the electrical drive is resonant with the mechanical modes of the discharge tube. The mechanical modes are a function of the physical dimensions of the arc tube. (Resonance was not observed in the 150-W or 400-W HPS lamps.) Several 200-W lamps from different manufacturers were tested, and we found that acoustic resonances occur at various frequencies between 20 and 40 kHz.

#### Planned Activities for FY 1983

The high-frequency operation of gas-discharge lamps will be tested by focusing on parameters such as filament power, crest factor, and critical frequency. The HPS solid-state ballasts and lamps will undergo life tests.

### ENERGY-EFFICIENT LIGHT BULBS (EELB)

#### Accomplishments During FY 1982

All subcontractors delivered prototypes for the energy-efficient light bulb project.[2-5] Each contractor met the goals of the program with regard to system efficacy. Table 1 lists the average performance of the EELBs tested by LBL. The three prototype lamps are shown in Fig. 1.

Table 1. Performance of energy-efficient lightbulbs compared with standard incandescent bulb.

| Type | Light (lumens) | Power (watts) | Life (hours) | Efficacies (l/W) |
|---|---|---|---|---|
| 100-W incandescent | 1750 | 100 | 750 | 17.50 |
| Coated filament | 1650 | 55 | 2500 | 30 |
| Compact fluorescent | 1700 | 34 | 7000 | 50 |
| Electrodeless fluorescent | 1700 | 31 | 10,000 | 55 |

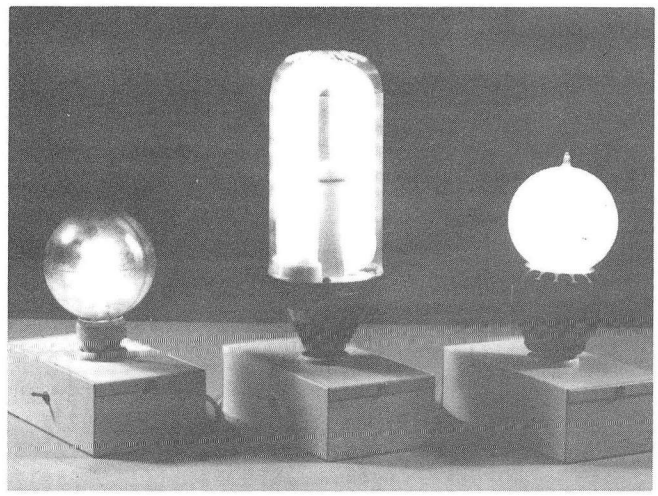

Figure 1. Three prototype energy-efficient light bulbs: (l-r) coated filament lamp, compact fluorescent lamp, and electrodeless fluorescent lamp. (CBB 828-7102)

These new light sources are more than three times as efficient as the incandescent lamp. Although the initial cost is higher, their longer lifetimes (2500 to 10,000 hours) and higher efficiency more than compensate for the higher first cost. With the use of solid-state ballasts in compact fluorescent lamps and further developments in electrodeless lamps, efficacies of 60 to 70 l/W are feasible in the near future.

### Planned Activities for FY 1983

The prototypes received will be life-tested to determine if they meet all performance criteria. In addition, other EELBs in development will be examined for performance.

## ELECTROMAGNETIC COMPATIBILITY

### Accomplishments During FY 1982

One barrier to the introduction of high-frequency lighting systems is the possible effect of the electromagnetic (EM) energy emitted by these systems. To address this issue, LBL conducted a two-day seminar—the Lighting/Electromagnetic Compatibility Conference, co-sponsored by the Institute for Electrical and Electronic Engineers, the Industrial Applications Society, the National Electrical Manufacturers Association, and the Naval Research and Development Laboratories—to identify potential problems and outline solutions. Nearly 100 people from all the major lamp manufacturers involved in high-frequency systems listened to invited speakers one day and exchanged ideas in smaller groups the second day. LBL compiled and published the proceedings.[6] The meeting identified several research needs, including a standard method for measuring electromagnetic interference (EMI), a simple instrument that could measure EMI in the field, some target specifications of the EMI limits that systems would have to meet to assure use in the commercial, industrial, and residential sectors, and coordination of efforts to exchange information, i.e., the establishment of a data base.

### Planned Activities for FY 1983

As recommended by the electromagnetic compatibility conference, we will measure the radiated and conducted EMI from new high-frequency lighting systems. Tests will be made in an open field, a screened room, and office spaces to relate measurements made in different environments. A simple field instrument will be developed for field measurements of EMI from lighting systems.

## FUNDAMENTAL PLASMA STUDIES

### Accomplishments During FY 1982

Building on earlier work, LBL began efforts to reduce the resonant entrapment from the $6P_1^3$ level to the ground state (2537 Å) to increase the efficacy of the low-pressure gas discharge in fluorescent lamps. This UV line excites the phosphor and is the most intense mercury (Hg) line at low Hg vapor pressures. The radiation is produced primarily by excitation of atomic Hg up to the $6P_1^3$ energy level. Natural Hg consists of several isotopes that absorb and re-radiate their own resonant radiation. However, as the Hg density increases (at higher lamp temperatures), the entrapment of the resonant radiation becomes predominant, resulting in a net decrease of the 2537 Å radiation exciting the phosphor. The entrapment process can be reduced by creating an optimum Hg isotope mix (about equal proportions of each isotope) through additions of Hg isotopes that are less abundant in natural Hg. For example, Hg isotope 196 makes up only 0.1% of natural Hg.

We calculated the optimum mix of Hg isotopes needed to produce the greatest net increase in resonant radiation and constructed a lamp in which predetermined Hg isotope mixes can be added. Before the crucial measurements are made, we must develop methods to add measured mixes of small amounts (5 mg) of Hg isotopes to the lamp. In conjunction with this study, we supported a commercial laboratory, General Telephone and Electronics (GTE), in devising a commercially viable method of separating the Hg isotopes. Chemical photo-ionization appears to be the most promising method, because it can produce the throughput of $10^5$ gm, the amount required annually to supply the lamp manufacturers.

Another means of reducing the entrapment is to split the $6P_1^3$ energy level into its components by applying a magnetic field (the Zeeman effect). This approach, too, can increase the generation of resonant radiation (2537 Å). Initial theoretical calculations indicate that using natural Hg can produce a two- to fivefold increase in the generation of resonant radiation. We completed most of the experimental setup needed to measure the changes in the intensity of the radiation as a function of magnetic field and gas temperature.

### Planned Activities for FY 1983

Measurements will be made of lamp performance in a magnetic field as a function of temperature and with various Hg isotope mixes. We will compare results with our theoretical calculations. The GTE contract will include the construction of a laboratory scale model of the Hg isotope separator.

Two new contracts are planned. One will explore the feasibility and problems associated with a gigahertz low-pressure discharge lamp. The other study will focus on the development of a high-intensity discharge lamp (HID) operating at high frequency (megahertz). This study should support manufacture of an electrodeless lamp while simultaneously exploring new types of ionizing materials.

## BUILDING APPLICATIONS

### Accomplishments During FY 1982

We completed two major lighting management demonstrations, one at the World Trade Center in New York and the other at the Pacific Gas and Electric (PG&E) building in San Francisco. Several papers were prepared to present some of the early results that show energy savings as high as 50%.[7-9] The data could not be used to validate the CONTROLITE computer program because this program, which predicts the energy performance of lighting systems, is still not complete. We used the QUICKLITE program for inputting daylighting, and this appears adequate.

Figure 2 shows data obtained from the World Trade Center and the reduction in energy from introducing several types of lighting control strategies. This effort identified several major issues in the use of daylighting. One is the method of placing the photocell, which senses and monitors the ambient illumination. Another is the lack of understanding of the interrelationship between the heat dissipated by the lighting system and the heating, ventilating, and air-conditioning systems of the building.

### Planned Activities for FY 1983

We plan to complete the analysis of the two lighting management systems and prepare a three-volume report on the results.

We also plan to study the design criteria for optimum placement of the photocell as a daylighting monitor. The experiments will require the construction of a scale model, which will be placed on the roof of an LBL building. The model will thus obtain daylighting data as well as information on how to maintain constant illumination on a task area.

The CONTROLITE program will be reviewed and errors corrected. In addition, the QUICKLITE program

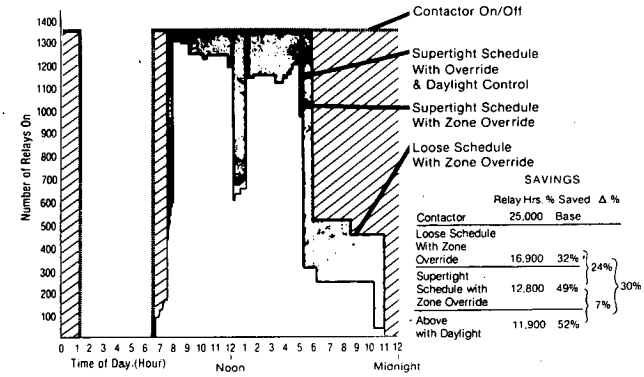


Figure 2. Experimental results showing the energy savings from different control strategies in an office in the World Trade Center. (XBL 823-8666)

will be integrated with the CONTROLITE program. A new advanced lighting design study will be initiated to develop futuristic layouts that use the most energy-efficient lighting systems. Some of these systems are still in development and will be introduced in the late 1980s. This study will provide a basis for future energy design targets for lighting systems.

## IMPACTS PROGRAM

### VISIBILITY AND PERFORMANCE

### Accomplishments During FY 1982

The connection between visibility and productivity continues to be of major interest. In 1981, the International Commission on Illumination (CIE) released its publication CIE 19/2, "An Analytic Model for Describing the Influence of Lighting Parameters upon Visual Performance."

A partial review by LBL of the original data used for the development of CIE 19/2 has revealed serious errors. In addition, data on the target size have been examined. Those data may be an important parameter for light levels. A report has been written on a cost-effective method of establishing light levels.[10]

### Planned Activities for FY 1983

Work will be continued with the aim of defining experiments that may be useful in scientifically establishing a set of recommended light levels related to performance.

## FATIGUE AND VIDEO DISPLAYS

### Accomplishments During FY 1982

The visibility laboratory—established in 1981 in conjunction with the University of California School of Optometry—was completed. This laboratory will assist in studies of fatigue in workers viewing video-display screens. The experimental facility is a test room where subjects are directed to perform a series of visual tasks that induce fatigue. As Fig. 3 shows, the test room has three screens and a ceiling lighting system. This lighting system can be controlled to vary the type of light source (incandescent or fluorescent), the intensity of the illumination, and the amount of flicker. Figure 4 shows the control room in which the experimenters manipulate the visual tasks and ambient lighting. All of the systems have been debugged.

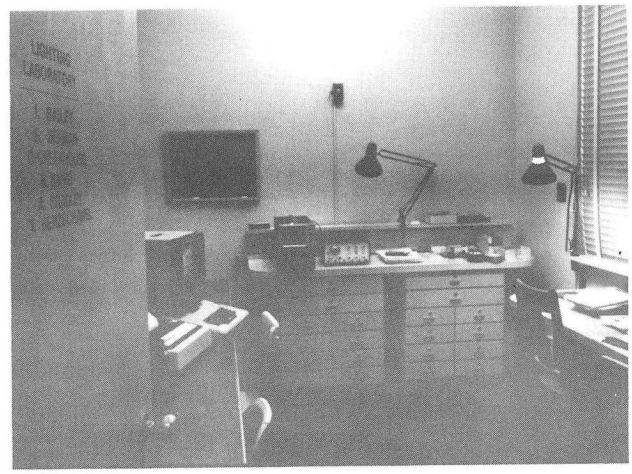

Figure 4. Control room for visibility laboratory at the University of California School of Optometry. (CBB 828-7208)

### Planned Activities for FY 1983

Subjects will be selected and tested in the visibility laboratory. In 1983 we expect to identify the primary factors in lighting systems that induce early fatigue. Parameters of particular interest are the interaction of the rate of flicker in lamps and the refreshment rate of the information displayed by the video screen.

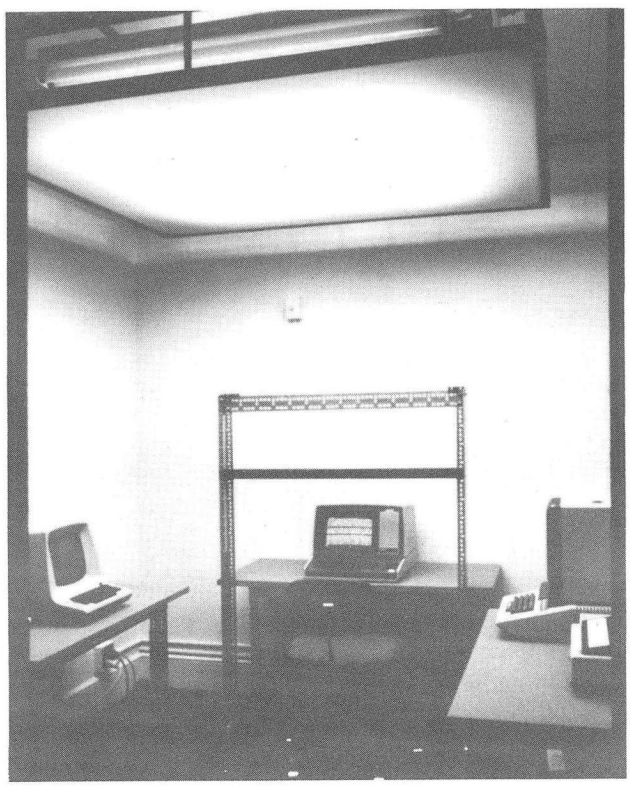

Figure 3. Testing laboratory at the University of California School of Optometry for measuring fatigue from viewing video displays. (CBB 828-7206)

## HEALTH AND ENVIRONMENT

### Accomplishments During FY 1982

The environmental laboratory, located in the University of California Medical School, San Francisco, was instrumented to measure the effects of illumination and lighting systems upon human subjects. The equipment consists of a large chamber in which a test subject is in a completely controlled environment, i.e., not subject to extraneous light, electromagnetic radiation, or noise. The subject will be exposed to various types of visual tasks; responses will be compiled on a computer. Illumination can be switched among different types (incandescent, fluorescent, or high-pressure sodium), and the intensity, amount of glare, and percent flicker can all be controlled. The object will be to induce stress that can be measured physiologically and objectively by changes in skin temperature, skin resistance, muscle strength, and blood pressure. This will be the first time that causal influences will be controlled and measured. Figure 5 shows a subject seated in the chamber, with an experimenter controlling the tasks and the lighting system. During an actual test, the

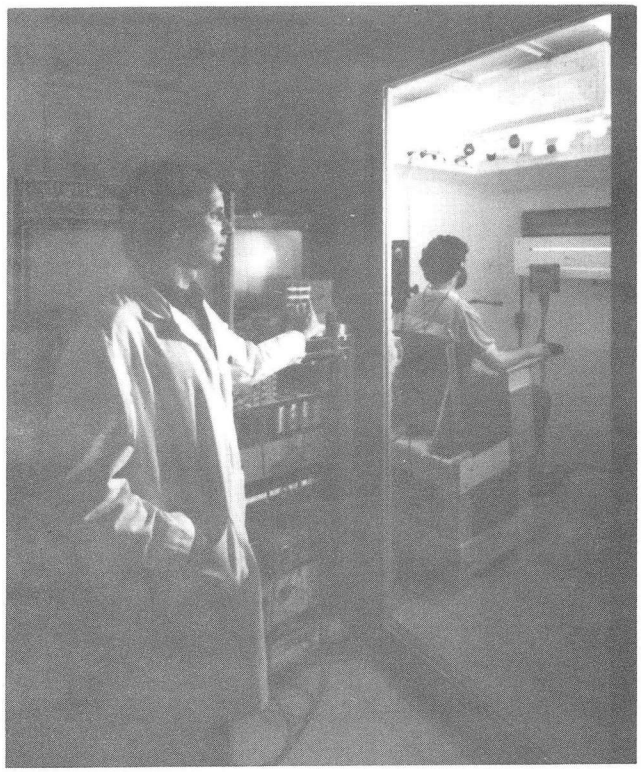

Figure 5. A view of the isolation chamber used to test the effects of lights upon human subjects. (CBB 828-7259)

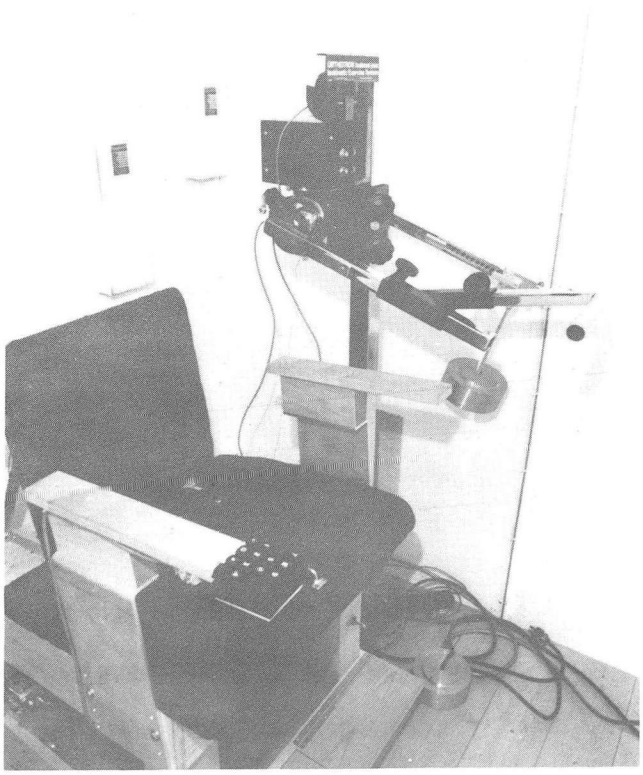

Figure 6. Close-up view of the test chair; apparatus to left of chair measures muscle strength. Subject uses keyboard in right armrest to perform visual tasks. (CBB 828-7370)

chamber door will be closed and there will be no visual communication between experimenter and subject. Figure 6 is a close-up photograph of the test chair. Behind the left armrest is the instrument for measuring muscle strength; on the right armrest is the keyboard that the subject operates.

Before initiating tests, an advisory committee was selected and convened to discuss all aspects of this program. The advisory committee is composed of internationally renowned physicians, psychiatrists, physicists, and optometrists involved in the health effects of lighting and radiation systems. The instrumentation and test procedures were critiqued and amended to comply with the recommendations of this committee.

## Planned Activities for FY 1983

Initial qualitative experiments will be carried out, using input from the advisory committee and LBL staff. We anticipate that the results of these experiments will determine the future and more quantitative experiments that are required. A government panel is being formed to coordinate these activities with similar studies being carried out in federal agencies. Communication with others in the field is necessary because many of the results of our studies will apply to many occupational situations where stress from lighting conditions could be catastrophic.

## REFERENCES


1. Felper, G. (1981), *High-Intensity Discharge 400-W Sodium Ballast: Phase II Final Report*, Lawrence Berkeley Laboratory Report LBL-13889.
2. Spellman High Voltage Electric Company (1981), *Energy Efficient Light Bulbs: The Magnetic Arc Spreading Fluorescent Lamp*, Lawrence Berkeley Laboratory Report LBID-525.
3. Duro-Test Corporation (1982), *Energy-Efficient Incandescent Lamp: Final Report*, Lawrence Berkeley Laboratory Report LBL-14546.
4. Litek International, Inc. (1981), *Electrodeless Fluorescent Lamp*, Lawrence Berkeley Laboratory Report LBL-13480.
5. Morton, E. W., Westinghouse Electric Corp. (1982), *Energy-Efficient Compact Screw-In Fluorescent Lamp: Final Report*, Lawrence Berkeley Laboratory Report LBL-15252.
6. Verderber, R. R., and Berman, S.M., eds. (1982), *Proceedings of the Lighting/*

*Electromagnetic Compatibility Conference,* Lawrence Berkeley Laboratory Report LBL-15199.

7. Rubinstein, F. (1981), *Energy-Saving Benefits of Automatic Lighting Controls,* Lawrence Berkeley Laboratory Report LBL-13299.
8. Peterson, D., and Rubinstein, F. (1982), *Energy Savings through Effective Lighting Controls,* Lawrence Berkeley Laboratory Report LBL-14201.
9. Rubinstein, F., and Karayel, M. (1982), *The Measured Savings from Two Lighting Controls Strategies,* Lawrence Berkeley Laboratory Report LBL-14657.
10. Clear, R., and Berman, S. (1982), *Relating Productivity to Visibility and Lighting,* Lawrence Berkeley Laboratory Report LBL-13931.

## BUILDINGS ENERGY DATA*

*J.P. Harris, B.L. Gardiner, C.A. Goldman, W. Luhrsen, V. Magnus, A.K. Meier, B.C. O'Regan, J.C. Ribot, A.H. Rosenfeld, A. Usibelli, B.S. Wagner, and L.W. Wall*

Millions of homes and commercial buildings have now been retrofitted or managed more carefully to save energy, and many new buildings are designed to be more efficient than conventional construction. But it is difficult to find good data on the energy savings that have actually occurred and the cost of achieving them. Most data have been collected for specific, short-term purposes, and the lack of consistency in definitions, data collection procedures, and reporting formats often makes it difficult to compare results. There is little long-term tracking of energy performance to determine the persistence of savings over several years, nor—until now—has there been any established mechanism to share or exchange energy performance data, or to independently review new data for technical accuracy.

All these constraints can be addressed through a series of regularly updated building energy performance data bases, designed to encourage collaboration and data sharing among public and private organizations. The model of a shared data base is well-established in the physical sciences, as evidenced by LBL's own compilations of international research on subatomic particles, properties of nuclear isotopes, environmental instrumentation, and indoor air quality. Applying this concept to buildings energy research is one sign of the field's growing maturity.

The Buildings Energy Data (BED) Group compiles, analyzes, updates, and publishes data bases on the measured performance, cost-effectiveness, and further potential of energy-saving technologies in new and retrofitted residential and non-residential buildings. A major goal of the BED group is to provide results that cut across traditional research and program boundaries. The data bases incorporate a full range of conservation and solar/renewable measures that reduce purchased energy, peak electrical demand, and costs. They provide a means for:

(1) monitoring changes in energy-related practices in building design, construction, and management;
(2) comparing current practice with estimated technical and economic potentials for saving energy;
(3) examining the range of energy savings and costs in order to identify technical, institutional, or other factors associated with successes and failures;
(4) comparing measured energy and electrical peak demand savings with predicted values and analyzing discrepancies; and
(5) encouraging the continuing exchange of documented conservation results among utilities, government agencies, private industry, and research establishments in the U.S. and abroad.

Updated results appear in the refereed literature and as LBL reports. Conference papers and journal articles help to reach an audience of practitioners as well as researchers.

Our intent is to make the energy performance data bases widely available to:

- designers, builders, and energy managers—to provide them with feedback on the accuracy of their energy analysis methods and the results of past design or retrofit recommendations;

*This work was supported by the Assistant Secretary for Conservation and Renewable Energy, Office of Building Energy Research and Development, Building Systems Division of the U.S. Department of Energy under Contract No. DE-AC03-76SF00098 and by the Bonneville Power Administration, Portland, Oregon, and the San Diego Gas and Electric Company.

- utility planners and managers—to help them improve demand forecasts, system planning decisions, and conservation programs;
- energy policy makers and program managers in federal, state, and local agencies—to help them establish a stronger empirical basis for allocating resources; and
- DOE and its national laboratories—to assist them in planning, setting priorities, and coordinating buildings energy research activities.

The BED Group has organized two main data bases and participates, in a limited way, in primary data collection. One data base, called Building Energy Use Compilation and Analysis (BECA), includes measured conservation results in new or retrofitted buildings. The BECA data are subdivided into several elements: low-energy new homes (BECA-A), existing "retrofitted" homes (BECA-B), new and retrofitted commercial buildings (BECA-C), and appliances and equipment (BECA-D). A fifth element includes comparison studies of measured building data versus computer model predictions (BECA-V).

The second data base deals with individual technical measures and provides estimates of the aggregate potential savings from applying today's best practices to the entire building stock. We collect data on the actual, *in situ* performance of today's energy-saving methods and track "advanced" technologies as they progress through research, development, field testing, and commercial production. We have used this data base, in collaboration with utilities and other outside organizations, to develop "supply" curves (marginal cost curves) for conserved energy (see below). Conservation supply curves provide a consistent accounting framework for evaluating the "technological frontier" of conservation in buildings.

The analysis of conservation potential complements our assessment of actual energy savings now being achieved. The BECA data, which reflect current conservation results, need to be compared not only to past inefficient practices but to the highest levels of efficiency that are technically and economically feasible. In turn, data from the BECA project keep our estimates of conservation potential realistic.

Finally, we participate, on a limited scale, in direct data-gathering activities and provide technical assistance to groups such as utilities, energy service firms, builders, and state or local governments, to help them improve the quality of their data; they, in turn make this information available for our own data bases. This role in the practical problems of data collection (equipment reliability, quality control, costs, etc.) also improves our ability to offer realistic advice to others and to properly interpret the data we receive.

The following sections highlight results from the past year and outline work planned for the future.

## BUILDINGS ENERGY USE COMPILATION AND ANALYSIS

### Accomplishments During FY 1982

We continued to refine and expand our data bases on new homes and on retrofitted residential and commercial buildings. We began to compile data on new commercial buildings, as well as results from studies that compare computer predictions with measured building performance (BECA-V). Major results in FY 1982 for each BECA subproject are summarized below.

*BECA-A: New Residences*

We have collected data on the heating performance and economics of new passive solar, active solar, and superinsulated homes throughout North America[1] and have evaluated submetered data for 276 of these homes (mostly single-family), of which 207 have adequate cost data to assess cost-effectiveness as well as performance.

In many of these houses, space heating energy use has been economically reduced to about one-fifth the level required in the average existing house, or about one-third the level estimated for typical new homes. Heating loads for the best superinsulated and passive solar homes in our sample were about 1.5 Btu/(ft$^2$-°F-day) [30 kJ/(m$^2$-°C-day)] per year. The average for 37 homes with the most complete data was 2.5 Btu/(ft$^2$-°F-day) [50], compared with the average of 8.9 [180] for the U.S. housing stock and about 5.0 [100] for all new single-family homes surveyed by the National Association of Home Builders (NAHB). In other words, it is not unusual to find low-energy homes, even in the coldest U.S. climates, where energy use for space heating is roughly the same as that required for heating water or operating domestic appliances.

Figure 1 plots energy performance vs. heating degree-days for a subsample of the best-documented homes in the data base. The low-energy homes are compared with heating usage under the proposed

federal energy performance guidelines (labeled "BEPG"), with current building practice, and with the existing stock (all normalized for floor area).

To make valid comparisons among low-energy homes, the metered space-heating energy data must be corrected for variations in inside thermostat settings and internal gains from appliances and occupants, as well as for local weather. Internal gains alone can account for half or more of the total space heating load. We made corrections for "standard" inside temperatures and internal gains for each house shown in Fig. 1.

Use of wood stoves, especially common in new solar and earth-sheltered homes, complicates performance analysis, since the wood represents a significant but unmetered energy flow into the house. Thus far, we have been forced to exclude from the data base all homes where wood stoves were used. In the future, we will urge our contributors to use a monitoring or analysis approach that realistically accounts for wood-stove heat contributions, or else to arrange for occupants to refrain from using the stove during periods of measurement.

New homes must be compared on the basis of cost-effectiveness as well as thermal performance. We obtained data on the incremental costs (materials and labor) of energy-saving features for about two-thirds of the BECA-A entries. The results are shown in Fig. 2, along with "reference lines" indicating the minimum level of gas or electric savings that would be cost-effective, for each added dollar invested in conservation. These reference lines were calculated using 30-year amortization periods and real interest rates of 3 and 6%. The gas and electric prices are current averages for U.S. residential customers. A home is cost-effective under these assumptions if the plotted point lies above the reference line for that fuel type.

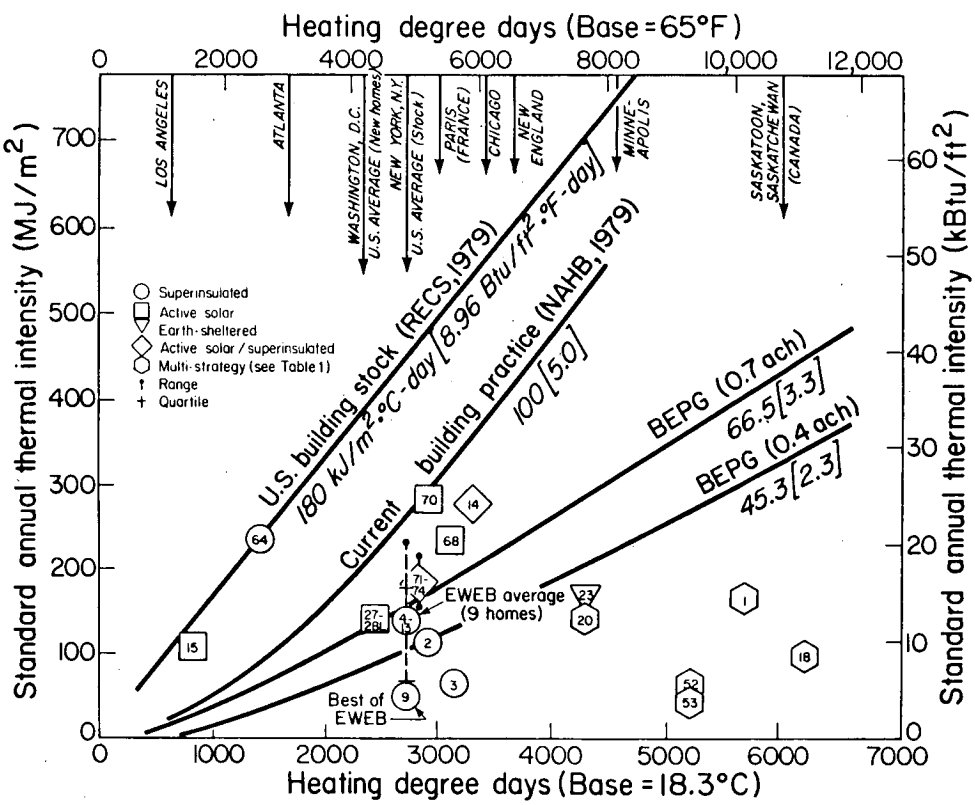


Figure 1. Scatter plot of 37 new homes in the BECA-A data base, "standardized" for thermal intensity (space heating load per ft$^2$) vs. climate. Shown for comparison are lines approximating the performance of all existing homes (RECS), typical new single-family homes (NAHB), and proposed federal guidelines for new construction (BEPG). The average space heating load per degree-day for the 37 homes is 2.5 Btu/(ft$^2$-°F-day) [=50 kJ/(m$^2$-°C-day)], one-half the energy required under current building practice.

(XBL 827-956)

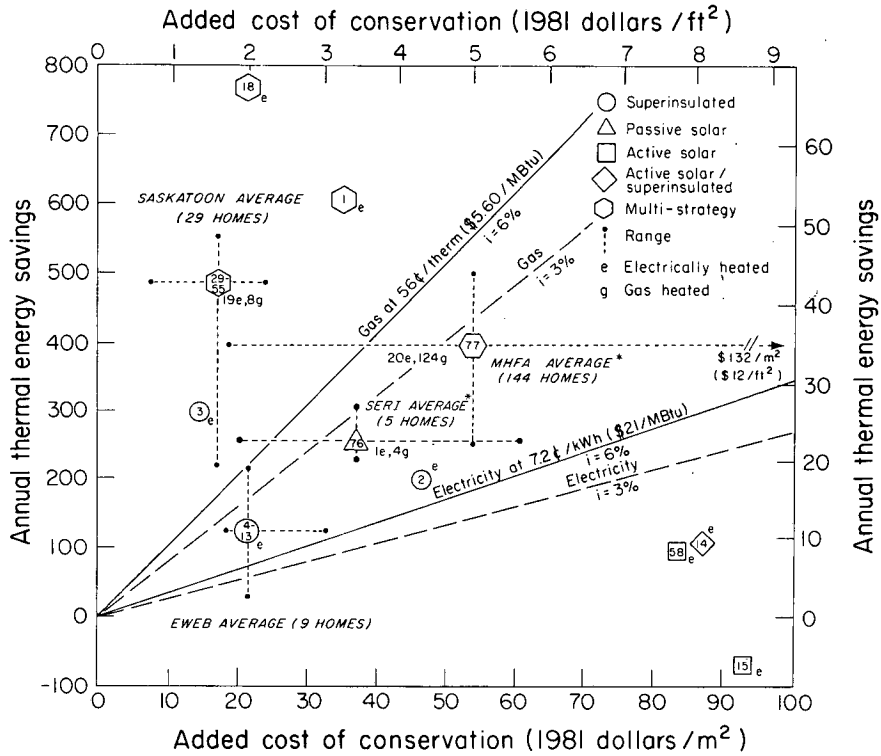


Figure 2. Scatter plot of annual space heating energy savings vs. added first-cost of conservation and solar measures for 237 new homes in BECA-A. Energy savings are calculated as the difference between each home's thermal intensity (space heating load per ft$^2$) and the thermal intensity value for that climate of the "current building practice" line in Fig. 1. Reference lines drawn from the origin represent the cost-effectiveness boundary, using mid-1982 U.S. average residential energy prices ($0.072/kWh and $0.56/therm of gas) and amortizing added first costs over 30 years at 3 and 6% (real) interest rates. A home's conservation features are cost-effective if they are plotted above the reference line(s) for that fuel type. (XBL 8211-7301)

Figure 2 suggests that the added cost of energy-saving features ranges from $2 to $6/ft$^2$ in most cases. The exceptions tend to be homes with active-solar heating or extensive south glazing areas, which cost more. Except for the three active solar homes, almost all the electrically heated homes in our sample were cost-effective, but (using our assumptions) only about half of the gas-heated homes saved energy at a cost lower than average gas prices. The homes that performed best, in both energy and cost-effectiveness, were either superinsulated or included passive-solar features with only moderate south glazing (i.e., not more than 10-12% of floorspace), as well as good insulation.

*BECA-B: Residential Retrofits*

The BECA-B data base addresses the technical performance and economics of energy-saving retrofits in existing homes.[2] The compilation includes more than 65 retrofit projects, with sample sizes ranging from 1 to 33,000 homes. Single-home data points are usually research or demonstration projects; the larger samples are from utility-sponsored programs. Most of the retrofits involve insulation or other shell improvements to reduce space-heating consumption, but results for space-heating equipment and water heating are starting to become available. Most of the data include the combined effects of several retrofit measures; it is still difficult to determine the relative contribution of individual measures. Good information on space-cooling performance is also difficult to obtain.

Figure 3 shows space heating energy savings (as a percent of pre-retrofit usage), plotted as a function of retrofit costs. For the overall sample, median space heating energy savings are 24% (28 MBtu/year), achieved at a median cost of about $1100 per home.

For the fuel-heated homes in our sample, the median cost of conserved energy was $3.86/MBtu (assuming a 15-year amortization and a 7% real interest rate). This is substantially less than average 1981 residential-sector prices for natural gas ($4.50/MBtu) and fuel oil ($8.70/MBtu). The 11 data points for electrically-heated homes had a median cost of conserved energy of 3.1 cents/kWh, compared to average residential electricity prices of 6.2 cents/kWh.

Although the data in Fig. 3 show a great deal of scatter, one conclusion may be that, with today's technology and energy prices, there is no evidence that investing more than $2000 in residential (envelope) retrofits yields significant returns. We are continuing to seek measured data on more extensive, but still cost-justified, retrofit projects.

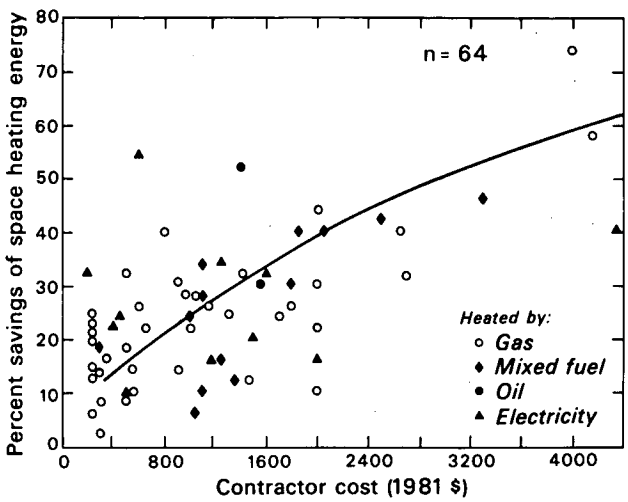


Figure 3. Scatter plot of percent savings in space heating energy vs. contractor cost for 64 residential retrofit projects in the BECA-B data base. There is no obvious correlation for the data points shown, but the "eyeball" relationship shown by the curved line suggests an average relationship that might be expected: about 25% savings from the first $1000 invested and about 40% from the first $2000. (XBL 822-161A)

*BECA-C: Commercial Buildings*

The BECA-C data base currently includes energy savings for 223 retrofitted commercial buildings, mainly schools and hospitals located in the eastern United States. Adequate data on both retrofit costs and energy savings are available for only one-fourth of the sample. In 1982, we began to extend the data base to new energy-efficient commercial buildings and will publish results in 1983.

The 223 sites in BECA-C were originally compiled and evaluated by Ross and Whalen[3] of DOE's Office of Building Energy Research and Development. Figure 4, which summarizes their results, shows a wide range of both absolute and percentage energy savings. Median fuel savings were 21% of pre-retrofit consumption, while electricity savings were 7%—a lower ratio of electricity to fuel savings than estimated in other studies of commercial-sector retrofits.[4] This might be explained by the relatively low pre-retrofit electricity usage in the sample, the small number of all-electric buildings, and the predominance of schools, which may have been originally designed to use daylight rather than intensive artificial lighting in classrooms.

One characteristic of the buildings in BECA-C was the emphasis on low-cost operation and maintenance measures, implemented in 95% of the buildings. This emphasis was reflected in the low level of retrofit investments (the median was about $0.56/ft$^2$, compared to typical annual energy costs of about $1.50/ft$^2$) and in short payback times (the median was less than 2 years).

From the building owner's perspective, this reluctance to invest more money in longer-payback measures may be explained not only in terms of capital cost and availability, but as a rational response to the perceived risks. In fact, about 9% of the buildings used more energy after retrofit than before. These negative results may have been due to poor operation and maintenance, or to product failure (in one case, for example, a window film failed to adhere). More data on "instructive failures" are needed to improve our understanding of such factors.

*BECA-V: Model Validation Data*

The BECA-V data base includes comparisons of predicted and measured building energy performance—ranging from the output of complex computer simulation models to simplified calculations used for energy audits or building efficiency "ratings." Eventually, we hope to collect and translate the most detailed and accurate data sets into standard formats that can be used to validate algorithms (or calibrate input assumptions) for a variety of building analysis models.

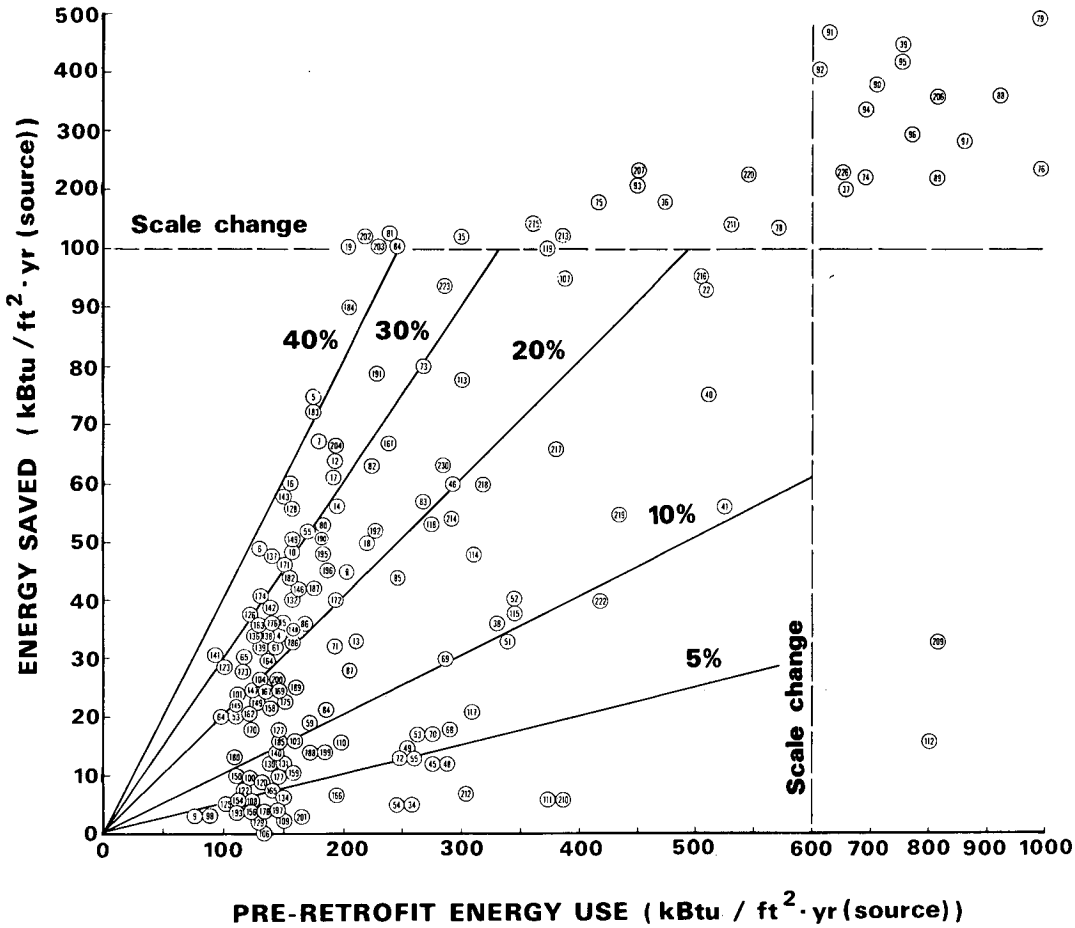


Figure 4. Energy savings vs. pre-retrofit energy use for 223 retrofitted commercial buildings in the BECA-C data base. While one might expect a general trend toward increased savings with larger pre-retrofit consumption, no simple correlations emerge from the current sample. We have plotted lines that bin the data points by percent of energy saved. Note the scale change on both axes, an indicator of wide variance among data points. The axes can be converted to SI units by using the factor 1 kBtu/ft$^2$/year = 11.36 MJ/m$^2$/year. (XBL 826-792)

The 12 validation studies examined to date include 63 data points, representing 202 buildings. Preliminary results are summarized in Wagner and Rosenfeld.[5] These studies compared computer model predictions with utility-metered or site-measured energy consumption, both for individual homes and commercial buildings, and for groups of up to 75 buildings. The sample does not include comparisons of measured data with energy savings predicted during an audit.[†]

On the whole, the complex computer models used (DOE-2, BLAST, NBSLD, REAP) were accurate to within 10%, both for total energy use and for space conditioning—provided that correct (i.e., measured or instrumented) input data were used. Simplified calculation procedures, or any program used to analyze a non-submetered building, were accurate to within ±15%. Figures 5 (a) and 5 (b) compare predicted and metered energy consumption (all end uses) for several residential and commercial buildings, or group averages, spanning a wide range of energy intensities. Most of the comparison studies we reviewed did not involve "blind" comparisons, i.e., the analyst had access to metered data while conducting the simulation.

The 12 studies reviewed so far are too limited a sample to justify more than tentative interpretations. However, we observe that space heating performance is easier to predict, with current techniques, than space cooling or other end uses. Predictive accuracy also improves with better input data, and with the training or experience of the model user (the author of a computer model is almost always able to make

[†] However, very limited subsamples of the BECA-B and BECA-C data bases (9 and 18 data points, respectively) contain both auditor predictions and actual measured savings. The data suggest that predictive accuracy is often poor for savings in individual buildings, but improves somewhat (to within ±20%) for larger groups of buildings. More comparisons are needed to confirm and quantify this tendency, and to identify possible causes.

the most accurate predictions). More data and more analyses are needed to establish the relative importance of these factors.

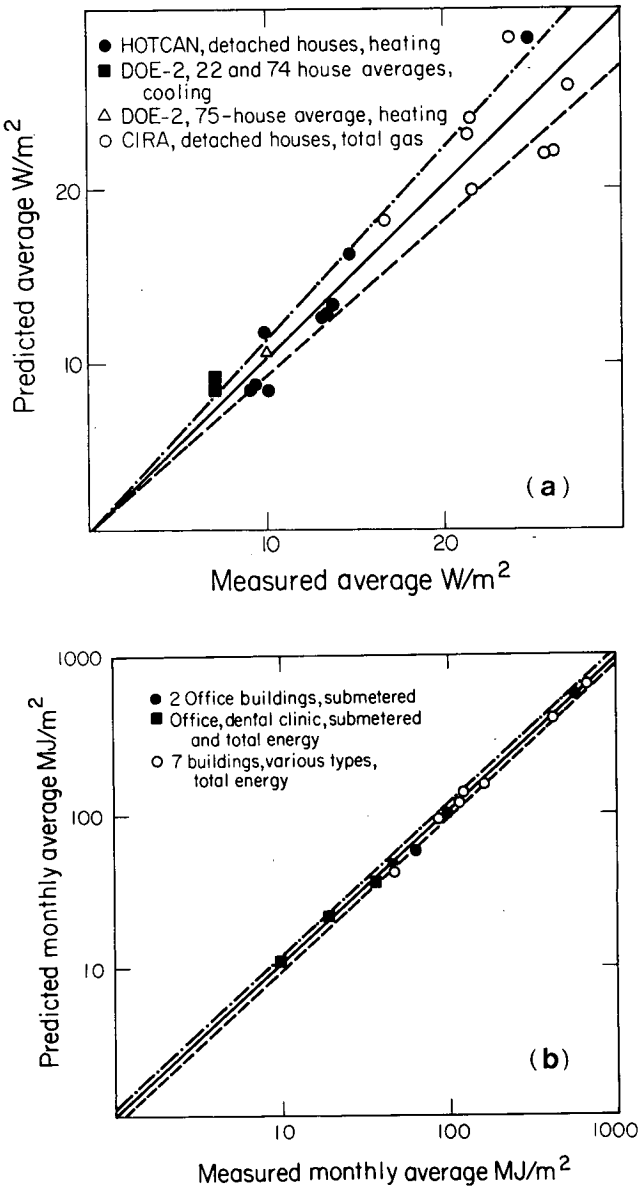


Figure 5. Predicted vs. measured energy consumption from the BECA-V data base: (a) individual residential buildings and group averages with no submetered or site-monitored data; (b) commercial buildings with relatively detailed submetered data (logarithmic scales).

[(a) XBL 832-65; (b) XBL 832-66]

## Planned Activities for FY 1983

In the coming year, we will expand the BECA data bases and begin to compile measured performance data for efficient appliances (BECA-D). New commercial buildings will also receive increased emphasis. Other priorities for the next one to two years include:

- Adding multi-year data for both new and retrofitted buildings, to track the persistence of energy savings and begin identifying the effects of physical degradation, lax operating practices, or shifts in occupant behavior.
- Obtaining more detailed, submetered data on individual buildings, to analyze component contributions to savings and cost-effectiveness and make better comparisons between predicted and actual performance.
- Establishing (for the existing stock and new construction) a more accurate definition of the "base case" against which efficient buildings are compared.
- Seeking measured conservation results for end uses other than space heating (cooling, water heating,‡ lighting and appliances), for buildings in mild climates, and for building types currently underrepresented in the data base (multi-family, mobile homes, several categories of commercial buildings).
- Adding data on more intensive commercial retrofits (including major renovations), and less extensive ("warm room") residential retrofits.
- Incorporating, especially for commercial buildings, the effects of design features or retrofits on peak electricity demand as well as energy use.
- Identifying improved techniques for monitoring or analytically accounting for the net contributions of wood heating systems in low-energy homes.
- Establishing a basis for climate-normalizing HVAC performance in commercial buildings that are shell-dominated or have high ventilation rates.

The BECA data bases will continue to serve as a repository for the quantitative results of DOE-funded buildings research. At the same time, we plan to use informal workshops, conference presentations, and other means to strengthen ties with utility, industry, and professional groups, both as prospective contributors of data and as clients and users of the data

‡ In the future, we will seek joint sponsorship by DOE's solar and buildings conservation programs to establish a new data base, BECA-W, on a full range of water-heating and hot-water-use technologies: heat pumps, solar collectors, heat recovery, demand heaters, high-efficiency storage water heaters, and reduced-flow appliances and plumbing.

bases. While DOE provides the core funding for maintaining and updating the BECA data bases, non-DOE sponsors may support specialized regional or subsector data compilations.

We plan to draw, as much as possible, upon past government-funded and industry-sponsored conservation programs as sources of BECA data. These include the Federal Energy Management Program (FEMP), the Institutional Conservation Program (ICP), HUD-sponsored public housing demonstration projects, and a joint effort with the California Department of General Services to analyze data on state-owned buildings. Among privately owned buildings, we will focus on national retail, restaurant, and motel chains that have already implemented energy management programs. Finally, we plan to collaborate with sponsors of major national energy design competitions (ASHRAE, Owens-Corning, AIA) to obtain follow-up data on the actual performance and cost of award-winning buildings.

## CONSERVATION TECHNOLOGIES DATA BASE AND POTENTIALS

### Accomplishments During FY 1982

For conservation measures already in commercial use, performance and cost data are compiled at the building level through the BECA project. The Conservation Technologies/Potentials project is concerned with new and prospective technologies. Laboratory and field data are obtained from R&D programs at LBL and other laboratories, and from innovative designers, manufacturers, builders, and utilities. The project has generated a detailed data base, by end use, for residential conservation technologies. Future work will extend this work to commercial buildings.

These data were used initially in preparing two major studies of the technical potential for improved residential energy efficiency: an analysis of conservation potential in California homes and appliances as of 1980,[6] and an assessment of the year 2000 conservation potential for all U.S. residential buildings.[4] During the past year, as part of a study sponsored by the Bonneville Power Administration (BPA), we undertook a major update of the data on residential electricity conservation measures, applied to the housing stock and climate of the Pacific Northwest.[7] Finally, we provided technical support to the San Diego Gas and Electric Company, as part of a project to estimate conservation opportunities in its service area.

For policy-making and utility planning, it is important to translate performance and cost data on individual technical measures into aggregate estimates of potential energy savings. To do this, we construct marginal cost curves (which we term "supply curves") for conserved energy. Such curves are fundamentally the same as those for any other commodity and provide a tool for comparing the cost and availability of saved energy with those of new energy supplies.[8]

The development of a supply curve for a given end use, region, and year (Fig. 6; Table 1) begins with the ranking of individual conservation measures in order of cost-effectiveness. This requires detailed information not only on the measure itself, but on the existing and projected characteristics of the building and equipment stock and their "baseline" energy consumption (the starting point for calculating savings). During the past year, we developed a subroutine, called WORK4, for our CPS 2.0 computer program. This subroutine performs the extensive accounting needed to calculate stock-average energy savings,

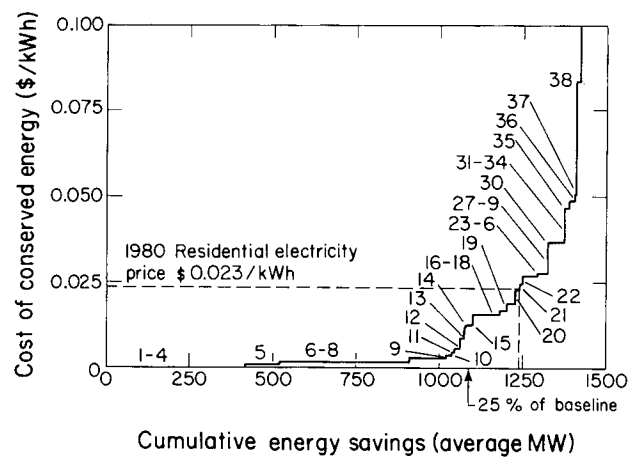


Figure 6. Conservation supply curve showing estimated technical potential for saving electricity in residential appliances, as of the year 2000, for the region served by the Bonneville Power Administration (BPA). Annual savings (horizontal axis) are plotted against cost per unit of energy saved (vertical axis). Each step represents regionwide application of one conservation measure listed in Table 1. Total annual savings potential for measures costing up to $.023/kWh (the 1980 average residential electricity price in the region) is 10.7 TWh (1226 average megawatts), or 28% of the baseline consumption projected for appliances in the year 2000. Savings are calculated (using the ORNL residential model) from a base case that assumes no change in average efficiencies of the 1980 appliance stock or in average additions to it. An "average megawatt" equals 8760 MW-hours. (XBL 832-1220)

Table 1. Residential electric appliance efficiency measures included in the conservation supply curve (Fig. 6) for the BPA region, as of the year 2000.

| Conservation Measure | Avg. Cost | Avg. Sav. | Life (Yrs.) | CCE ($/kWh) | Measure Sav. (GWh) | Cum. Sav. (TWh) | Cum. Sav. (Avg. MW) |
|---|---|---|---|---|---|---|---|
| 1 Television—b & w, solid-state improvement | 0. | 150. | 10 | 0. | 272.7 | 0.3 | 31.1 |
| 2 Television—color, solid-state improve. | 0. | 400. | 10 | 0. | 1883.1 | 2.2 | 246.1 |
| 3 Refrig.—side-by-side, buy eff. mkt. model | 10. | 1100. | 19 | 0.001 | 610.2 | 2.8 | 315.8 |
| 4 Freezer—chest manual, buy eff. mkt. model | 20. | 1000. | 21 | 0.001 | 880.6 | 3.6 | 416.3 |
| 5 Freezer—upright auto., buy eff. mdl./CPES | 40. | 1700. | 21 | 0.002 | 908.7 | 4.6 | 520.0 |
| 6 Refrig.—top/bottom-eff. mkt. model/CPES | 25. | 950. | 19 | 0.002 | 2507.0 | 7.1 | 806.2 |
| 7 Freezer—chest manual, CPES improvements | 5. | 160. | 21 | 0.002 | 123.5 | 7.2 | 820.3 |
| 8 Freezer—upright man., buy eff. mkt. model | 30. | 900. | 21 | 0.002 | 704.6 | 7.9 | 900.8 |
| 9 Refrig.—side-by-side, CPES improvements | 10. | 200. | 19 | 0.003 | 106.1 | 8.0 | 912.9 |
| 10 Refrig.—partial auto., eff. mkt. model/CPES | 35. | 665. | 19 | 0.004 | 954.5 | 9.0 | 1021.9 |
| 11 Freezer—upright man., CPES improvements | 15. | 200. | 21 | 0.005 | 137.3 | 9.1 | 1037.5 |
| 12 Waterbed, comforter cover | 20. | 400. | 10 | 0.006 | 80.4 | 9.2 | 1046.7 |
| 13 Refrig.—single-door, buy eff. mkt. model | 30. | 240. | 19 | 0.009 | 136.1 | 9.3 | 1062.2 |
| 14 Waterbed, insulate sides/bottom | 20. | 200. | 10 | 0.012 | 107.2 | 9.4 | 1074.5 |
| 15 Refrig.—single-door, CPES improvements | 10. | 55. | 19 | 0.013 | 29.7 | 9.4 | 1077.9 |
| 16 Lighting—sf, fluorescent in kitchen | 27. | 115. | 20 | 0.016 | 163.3 | 9.6 | 1096.5 |
| 17 Lighting—mh, fluorescent in kitchen | 27. | 115. | 20 | 0.016 | 23.4 | 9.6 | 1099.2 |
| 18 Lighting—mf, fluorescent in kitchen | 27. | 115. | 20 | 0.016 | 21.9 | 9.7 | 1101.7 |
| 19 Refrig.—top/bottom-1985 improvements | 75. | 300. | 19 | 0.017 | 688.3 | 10.3 | 1180.3 |
| 20 Refrig.—side-by-side, 1985 improvements | 100. | 370. | 19 | 0.019 | 177.7 | 10.5 | 1200.5 |
| 21 Refrig.—partial auto., 1985 improvements | 60. | 180. | 19 | 0.023 | 223.7 | 10.7 | 1226.1 |
| 22 Lighting—sf, fluorescent in bathroom | 30. | 80. | 20 | 0.025 | 113.6 | 10.9 | 1239.1 |
| 23 Refrig.—single-door, 1985 improvements | 50. | 130. | 19 | 0.027 | 63.0 | 10.9 | 1246.2 |
| 24 Lighting—mh, replace high use with SL | 20. | 50. | 20 | 0.027 | 25.4 | 10.9 | 1249.1 |
| 25 Lighting—mf, replace high use with SL | 20. | 50. | 20 | 0.027 | 23.8 | 11.0 | 1251.9 |
| 26 Lighting—sf, replace high use with SL | 40. | 100. | 20 | 0.027 | 355.0 | 11.3 | 1292.4 |
| 27 Lighting—mf, fluorescent outside | 25. | 60. | 20 | 0.028 | 5.7 | 11.3 | 1293.0 |
| 28 Lighting—sf, fluorescent outside | 25. | 60. | 20 | 0.028 | 63.9 | 11.4 | 1300.3 |
| 29 Lighting—mh, fluorescent outside | 25. | 60. | 20 | 0.028 | 9.1 | 11.4 | 1301.4 |
| 30 Cooking—elec. ranges/ovens, CPES improv. | 22. | 45. | 18 | 0.036 | 187.7 | 11.6 | 1322.8 |
| 31 Lighting—mf, fluorescent in bathroom | 30. | 55. | 20 | 0.037 | 10.5 | 11.6 | 1324.0 |
| 32 Lighting—mh, fluorescent in bathroom | 30. | 55. | 20 | 0.037 | 11.2 | 11.6 | 1325.3 |
| 33 Lighting—sf, replace med. use with SL | 80. | 115. | 20 | 0.047 | 408.3 | 12.0 | 1371.9 |
| 34 Television—b & w, 1985 improvement | 10. | 25. | 10 | 0.047 | 45.4 | 12.1 | 1377.1 |
| 35 Lighting—mf, replace med. use with SL | 60. | 85. | 20 | 0.047 | 40.4 | 12.1 | 1381.7 |
| 36 Lighting—mh, replace med. use with SL | 40. | 55. | 20 | 0.049 | 27.9 | 12.1 | 1384.9 |
| 37 Clothes dryer, moist./temp. sensor & insul. | 35. | 50. | 18 | 0.051 | 157.1 | 12.3 | 1402.8 |
| 38 Well pump, conservation measure | 100. | 100. | 15 | 0.084 | 37.2 | 12.3 | 1407.1 |
| 39 Clothes washer, improved efficiency | 50. | 30. | 10 | 0.195 | 104.5 | 12.4 | 1419.0 |
| 40 Dishwasher, motor efficiency | 150. | 50. | 10 | 0.352 | 111.3 | 12.5 | 1431.7 |

Note: mh = mobile home; mf = multi-family; sf = single-family.

over several years, from a given measure. The model accounts for additions and removals from the stock, and the measure's interaction with other energy-saving features in the same home.

To construct a supply curve, one must determine the stock-weighted average energy savings per unit, the average cost of saved energy, and the number of units to which the measure can be applied. The supply curve relates the unit cost of conserved energy (vertical axis in Fig. 6) to the cumulative annual energy savings (horizontal axis).

Figure 6 is a supply curve of conserved electricity in the BPA region for the year 2000 for one end use: home appliances. The data base used to generate this supply curve (Table 1) lists cost and performance characteristics for each measure, as well as the regionwide annual energy savings that could be achieved by implementing the measure in all technically feasible cases. (This assumption of 100% penetration allows us to quantify the opportunities addressed by energy conservation policies. Lower, "real-world" penetration rates can be modeled exogenously by the utility.)

A conservation measure, representing one "step" on the supply curve, is cost-effective if its cost of conserved energy is less than the cost of the energy it displaces. One can estimate the economical "reserves" of conserved energy by selecting a comparison price for the energy displaced. There are many ways of choosing this comparison price, depending on the policy or analytical perspective of the user.

In Fig. 6, we choose $0.023/kWh as a comparison price, representing the 1980 (base year) average residential electricity price in the region. An alternative comparison price might have been the projected long-run avoided cost (i.e., the savings per kWh from avoiding the need to build and operate new thermal generating capacity). This value is estimated by BPA at $0.15/kWh, which is off-scale in Fig. 6; the most expensive measure we considered (Table 1) costs $0.084/kWh saved.

For measures cost-effective at today's average electricity price, total potential savings in the year 2000 are over 1200 average MW (10.7 TWh), or 28% of the projected baseline consumption for appliances (the baseline assumes no change in current efficiencies). If we include additional measures with costs of conserved energy up to the long-run avoided cost, the potential year 2000 annual savings increase to 1400 average MW (12.3 TWh), or 32%. Similar end-use supply curves were constructed for residential electric space heating and water heating.

Note that the estimated annual energy savings represent only the *technical potential*, not the predicted level of conservation that will actually take place in response to assumed market conditions, government regulations, or utility-sponsored programs.

In our earlier studies, similar conservation supply curves were prepared for residential gas and electricity use in California and in the United States as a whole. The California study found that as much as 25% of the electricity and 34% of the natural gas used by the existing housing stock could be saved, at an average cost of conserved energy well below current average utility rates.

Our analysis of all U.S. homes included additional measures and a longer time horizon (20 years instead of 10). Even though the conservation measures included only those now on the market and economic at today's average energy prices, we identified technical opportunities to reduce residential energy use by the year 2000 to 30% below today's consumption—despite the projected addition of 40 million new homes. Compared to the year 2000 baseline forecast of the Energy Information Administration, these potential savings would be worth (at today's energy prices) about $75 billion per year.

## Planned Activities for FY 1983

We are continuing to update the technologies data base, replace engineering estimates with measurements, and to refine the techniques for evaluating conservation potential. We will begin extending the supply-curve analysis to non-residential buildings to include the potential for reducing electrical peak demand as well as energy use. The first subsector covered will probably be restaurants, because of the technical opportunities for improvements in refrigeration and heat recovery (see below, under Primary Data Collection).

As an outgrowth of our analysis of residential electricity conservation for BPA last year, we will compare our technology performance and cost data with the data used to generate technology-cost tradeoff curves for the Oak Ridge residential demand model[9] and determine the need for region-specific updates of these trade-off curves.

## PRIMARY DATA COLLECTION

### Accomplishments During FY 1982

*House-Doctor Demonstration Project*

Over the past 3 years, we conducted a cooperative project with Pacific Gas and Electric Company (PG&E) to determine the energy savings attributable to "house-doctoring."[10] House-doctoring is a term for an extended energy audit that includes installation of simple, cost-effective conservation measures and use of infiltration monitoring equipment to identify and seal major air leaks. We trained six PG&E weatherization specialists in house-doctoring techniques and chose Walnut Creek, California, as the site for a controlled experiment. Three groups of 10 randomly selected homes were included in the experiment. One group received a conventional PG&E (information-only) home energy audit. The second group received an audit plus house-doctor diagnosis and treatment. The third group received this treatment plus additional retrofits (principally wall and ceiling insulation) that were recommended in the course of the audit. (Analysis of post-retrofit data for this group has not been completed.) Results were compared with energy use for a control group of 10 homes and a comparison group consisting of all Walnut Creek homes.

Some results of the project are shown in Fig. 7. The two groups of house-doctored homes showed statistically significant savings of 11.4% in (weather-normalized) annual natural gas use. But these savings were not significantly different from the average for the audit-only group, which also saved 9.4% (see below). The small control group (6 homes) and the comparison group of all Walnut Creek homes both showed 7% savings over the same period.

There are several possible reasons for our failure to find, as expected, a statistically significant improvement in savings for the house-doctored homes. These include the limited sample size (due to budget limitations), the failure to monitor changes in thermostat setting or to submeter other energy uses (especially important in the mild Walnut Creek climate), and the significant variation within groups in pre-retrofit energy consumption. There were also considerable differences in the approach and quality of work by our newly trained house doctors.

But the most significant external influence was

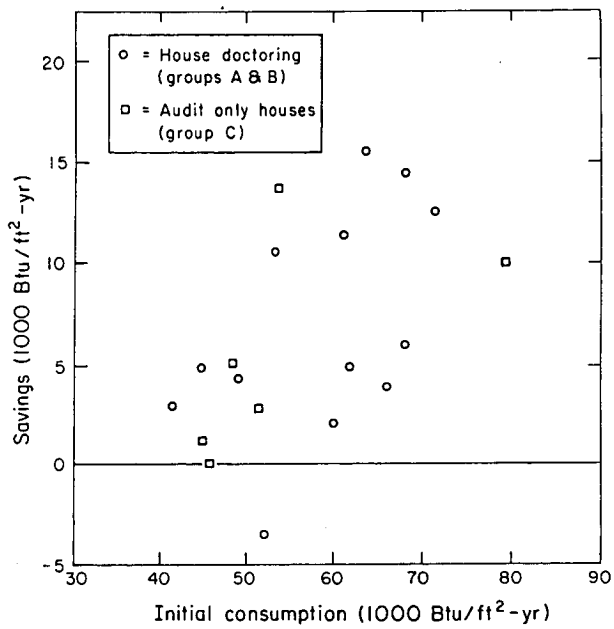


Figure 7. Scatter plot of natural gas savings vs. initial consumption, both normalized by square footage, for 19 homes (13 house-doctored and 6 audit-only) in the PG&E/LBL House Doctor Demonstration Project. Both groups achieved statistically significant savings, but there was no significant increase in savings for the house-doctored group. (XBL 829-1142)

a jump in residential gas prices of more than 50% (from $0.29 to $0.44/therm) between the pre-audit and post-audit periods. At the same time, electricity prices more than doubled (from $0.043 to $0.094/kWh). These energy price increases may have swamped any experimental effect of house-doctoring vs. conventional auditing, by affecting occupant behavior in both the experimental and control/ comparison groups. Price changes may also have stimulated "independent" retrofitting by the control group and by other Walnut Creek homeowners.

Although the experiment failed to show that house-doctoring can achieve significantly greater savings in total energy use (compared to conventional residential audits), we are reasonably confident of the estimated savings from one aspect of house-doctoring: reduced air infiltration. Reductions in seasonal infiltration were estimated from calibrated blower-door measurements before and after the house doctor visit.

Even before house-doctoring (contrary to our intent), the random sample of homes had considerably lower infiltration rates than the typical California

home (an average of 0.53 air changes/hour, compared to about 0.7 to 1.0 ach statewide). In Walnut Creek's mild climate, this meant that infiltration contributed only about 10% of the pre-retrofit annual energy use, so even a large percentage reduction in infiltration would have only a small effect on total energy use. After the house doctor visit, average infiltration was reduced to 0.40 ach, for an annual savings of about $18 (with gas at $0.44/therm) over the typical Walnut Creek heating season.

Although a number of factors—the mild climate, absence of submetering, small sample size, and concurrent sharp increases in utility rates—complicated the experiment and limited our ability to generalize results, a series of similar experiments were conducted by Princeton University in the colder climate of New York and New Jersey. These showed somewhat larger, cost-effective net savings from house-doctoring vs. control groups.[11]

In addition to some important lessons about the design of small-sample experiments in a mild heating climate, we conclude from this project that house doctors cannot approach all homes in the same way, even within the same community. For homes that are already reasonably airtight, further efforts to find and fix infiltration leaks will generally not pay. Some pre-screening, in the first hour of the visit—or even before the site visit, using billing data and phone interviews—might help identify the most cost-effective level of effort and mix of techniques for each home.

*Infiltration and Indoor Air Quality in New California Homes*

Since 1975, the State of California has required all new homes to meet minimum levels of energy efficiency and has revised and tightened these requirements twice (in 1978 and 1983). At present, there is little information on how well homes built to these standards really perform. There are also unanswered questions about the possible side effects of reduced infiltration on indoor air pollution levels in new California homes.

To begin addressing these questions, we collaborated with the University-wide Energy Research Group on a project sponsored by the California Energy Commission to measure air change rates and monitor indoor air quality in 16 new homes.[12] Limited resources forced us to focus on homes expected to have the poorest indoor air quality: newly built, low-infiltration homes with natural gas appliances. New construction materials and natural gas combustion are major sources of residential indoor air pollution, and tight houses tend to maintain higher concentrations of internally generated pollutants.

Pressurization tests showed that all 16 houses had average heating-season infiltration rates below 0.5 ach; the average was 0.34 ach. Prevailing state standards assumed infiltration rates of about 1.3 ach, while the proposed 1983 revisions require measures assumed to reduce infiltration to about 0.9 ach. We used "passive" monitors to measure concentrations of formaldehyde (typically released by outgassing from new building materials and furniture), nitrogen dioxide (a combustion product), and radon-222 (a decay product of naturally occurring radium in soil, groundwater, and some building materials).

Overall, the results indicated that new houses having low air-change rates do *not* necessarily experience poor indoor air quality, even without mechanical ventilation or other special measures. For example, Fig. 8 shows the weak correlation between infiltration rates and indoor nitrogen dioxide ($NO_2$) concentrations. Nitrogen dioxide levels ranged from 2.6 to 28 parts per billion, with an average of 10.4 ppb. All were well below the EPA limit (for outside air) of 50 ppb. Moreover, for many homes the indoor concentrations of $NO_2$ were lower than the outside concentration. Concentrations of $NO_2$ tended to increase with gas stove use.

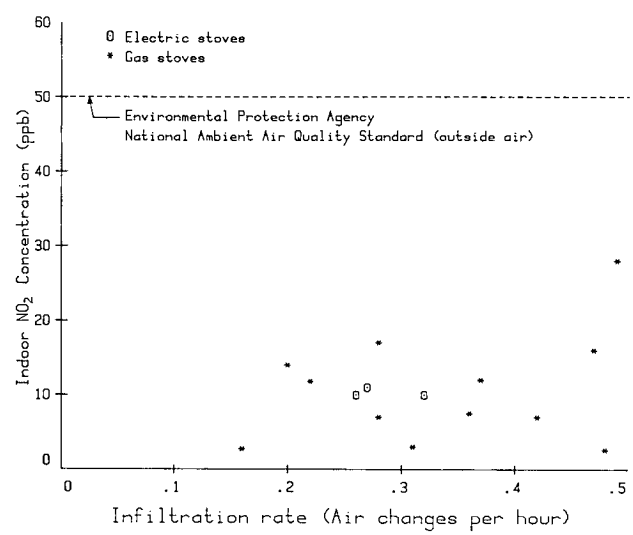


Figure 8. Average indoor concentrations of nitrogen dioxide ($NO_2$) vs. average infiltration rates in 15 new, low-infiltration California homes built to meet or exceed the 1978 state standards. These concentrations, measured over a one-week period, are all below the EPA standard for outside air. (XBL 833-8762)

Measured radon levels ranged from 0.32 to 2.24 picocuries/liter (pCi/l). The strictest indoor standards being considered in the United States or Sweden range from about 2 to 5 pCi/l; two homes were slightly above the low end of this range.

Measured indoor concentrations of formaldehyde (HCHO) varied from 78 to 163 ppb, a range overlapping the low end of the proposed standards. However, these measurements were made using prototypes of the HCHO passive monitors and may have been 15% high compared to conventional measurement procedures. All homes with concentrations over 100 ppb were less than 2 years old, so formaldehyde concentrations might be expected to decline as building materials and furnishings age. Conversely, other building types not tested (such as mobile homes) might have considerably higher HCHO concentrations, especially when new.

Because of the small sample size and the large number of factors affecting both pollutant source strength and indoor concentrations, these results do not necessarily mean that all new, tight homes have acceptable air quality. Localized "pockets" of radon in the soil, poorly vented gas appliances, or building materials and furnishings that release formaldehyde and other organics could create unhealthy air quality in some fraction of new houses. Our data suggest only that indoor air quality problems are not inevitable, even in fairly well sealed, energy-efficient houses.

We conclude that an effective strategy is needed, in California and elsewhere, for identifying and treating "problem" houses—whether or not there are building codes and retrofit programs aimed at reducing infiltration.

## Planned Activities for FY 1983

By establishing early contact with potential sources of data and offering informal suggestions, we hope to improve the quality of data eventually made available for the BECA compilations. In recent months, we have provided comments on experimental design and data collection techniques to:

- members of the DOE-funded Urban Consortium, on superinsulation retrofits and warm-room experiments
- the California Building Industry Association, on performance tests of unoccupied new homes, and
- the evaluation design team for the Hood River Residential Retrofit Demonstration Project, sponsored by the Bonneville Power Administration and Pacific Power and Light.

Beginning early in FY 1984, we will establish a loan pool of reliable, low-cost instrumentation (such as the "Energy Signature Monitor" being developed at LBL) to be made available to organizations with limited technical resources but good opportunities to generate the data needed to fill gaps in our compilations.

## Summer Study on Energy-Efficient Buildings

During 1982, we coordinated the planning for a major, week-long Summer Study held in August 1982 at the University of California campus in Santa Cruz. The Summer Study was organized by the American Council for an Energy-Efficient Economy (ACEEE). Besides LBL, co-sponsors included DOE, the Bonneville Power Administration, Texas Utilities, the Gas Research Institute, Electric Power Research Institute, and the University of California's Energy Research Institute. The Summer Study was judged highly successful by the 240 participants, who represented the building and utility industries, state and local governments, DOE, the national laboratories, and several other research organizations in the U.S. and Europe. Over 150 papers were presented, mainly in small-group sessions, over the course of the week.

This was the second Summer Study organized by ACEEE. At the first one, held in August 1980, participants from industry, government, and research organizations discussed the technical potential for conservation in buildings, as well as government policies and utility/industry practices needed to achieve that potential. BED staff played a major role in editing the proceedings and preparing them for publication.[13]

Whereas the 1980 meeting focused on potential, the 1982 meeting focused on what has been achieved. Its theme, "Documenting the Results of Energy Conservation in the Buildings Sector," was directly relevant to BED's data base effort, and we found a number of leads to new sources of data and possible opportunities for collaboration. Members of the group authored or co-authored eight papers presented at the Summer Study.

During 1983, BED will assist in compiling and editing the 1982 Summer Study proceedings, which will be published by the ACEEE and the American Solar Energy Society. These proceedings will represent a

major contribution to quantitative data on energy conservation in U.S. buildings.

## CONCLUSION

The past year has been a developmental period for all our data compilations. We have identified a number of major gaps in the data and will certainly uncover more in the future. Nevertheless, we can offer some tentative conclusions about the data compilation process, conservation results achieved to date, and the remaining potential.

First, some observations on the data compilation process:

- More and better quality data are beginning to become available, but most reported results still must be screened carefully to remove errors and assure comparability. Conservation programs that produce well-documented, empirical measurements of both energy savings and cost-effectiveness are still the exception rather than the rule.
- Data are still more plentiful for residences than for commercial buildings. In the commercial sector, serious measurement and analysis projects are just beginning to deal with complexities related to the diversity in physical characteristics and usage, criteria and methods for climate-normalizing space conditioning energy use in some buildings, and the interpretation of utility billing data where there are multiple buildings on a meter or multiple meters in a building.
- Data compilation is time-consuming. Even for promising "leads," there can be an attrition rate of 80 to 90% before data are finally obtained in a usable form. The lead time for new data can be 2 to 5 years, depending on the nature of the project and the sponsor's resources and commitment to providing high-quality data. This underscores the need for continuity over a multi-year period in maintaining and updating a conservation data base for buildings.
- For meaningful comparisons of energy performance, especially among energy-efficient buildings, new performance parameters for thermal comfort, visual performance, and other amenities must be defined and monitored. For example, when is it important to consider, not just average indoor temperature, but temperature fluctuations, radiant exchanges, and air movement as determinants of occupant comfort in a passive-solar or earth-sheltered home? When an attached sunspace is used intermittently, should it be included in the definition of "conditioned space" for comparison with other buildings? How can reductions in lighting energy use be compared for their effects on visual performance of various tasks, not simply in terms of illumination levels (footcandles)?

As for conservation results and potential, the data suggest that:

- Even after correcting for such obvious factors as building type, type of conservation measure, square footage, indoor temperatures, and climate, conservation projects still show a wide range of results in both performance (savings) and costs. But we still have little understanding of the reasons why some efforts succeed and others fail. It is clearly possible to save a large fraction of the energy used in "conventional" buildings, at very attractive costs of conserved energy—but it is not inevitable. There are both "failures" (higher energy consumption) and extremely sub-optimal projects (where the energy saved costs more per unit than purchased energy). It is especially hard to find data on well-documented failures.
- The most common investments by owners of both residences and commercial buildings are those involving relatively low initial cost, low perceived risk (because they are "familiar"), and short paybacks (1 to 5 years). These investments seldom approach the "societal" life-cycle cost optimum—nor are conservation investments yet treated the same as other public and private investments, including new energy supplies.
- We have no data on extensive, costly retrofit measures (or new design features) that are still attractive in terms of the cost of conserved energy. In some cases, the technology for more extensive, but still economic, retrofits needs further development, but in others it is more a question of making existing technology more widely available and assuring that its performance is adequately monitored and reported.

- Evidence on issues long debated by advocates of specific technologies (active vs. passive solar systems, solar gains vs. increased insulation) is preliminary and still inconclusive. The answers to these questions may never be clear-cut or universally applicable. For example, most of the best-performing low-energy homes monitored in recent Minnesota and Saskatchewan projects had relatively low solar apertures—but one set of large-aperture solar homes also performed well. The same rules of thumb for optimal glazing/insulation trade-offs in cold climates may not apply in milder climates (California), in cold, sunny ones (Colorado), or where effective night insulation has been installed and used conscientiously. In general, we may find that several technical approaches, applied sensibly, can produce roughly equivalent results.
- Major gaps in our data include: results from commercial buildings other than offices and schools, data on multi-family and manufactured housing, information on cooling performance in both dry and humid climates, multi-year savings and cost data for all types of new and retrofitted buildings, data on advanced conservation products and applications outside the United States (to be interpreted with caution, due to institutional and cultural differences), and well-documented, instructive *failures*—perhaps the hardest of all to add to a public data base. Our future efforts will address each of these areas.

## REFERENCES


1. Ribot, J., et al. (1982), "Monitored Low-Energy Houses in North America and Europe: A Compilation and Economic Analysis," presented at the ACEEE 1982 Summer Study on Energy-Efficient Buildings, Santa Cruz, California, August 22-28, 1982; Lawrence Berkeley Laboratory Report LBL-14788.
2. Wall, L., et al. (1982), "Building Energy Compilation and Analysis (BECA) Part B: Existing North American Residential Buildings," submitted to *Energy and Buildings;* Lawrence Berkeley Laboratory Report LBL-13385. Summary presented to the ACEEE 1982 Summer Study on Energy-Efficient Buildings, Santa Cruz, California, August 22-28, 1982 (LBL-14787).
3. Ross, H. and Whalen, S. (1982), "Building Energy Use Compilation and Analysis (BECA) Part C: Conservation Progress in Retrofitted Commercial Buildings," to be published in *Energy and Buildings,* 1983; Lawrence Berkeley Laboratory Report LBL-14827 (draft), May 1981; updated July 1982. Summary version by Wall and Flaherty presented at the ACEEE 1982 Summer Study on Energy-Efficient Buildings, Santa Cruz, California, August 22-28, 1982 (LBL-15375).
4. Rosenfeld, A.H., et al. (1981), Chapter 1: "Buildings," in *A New Prosperity: Building a Sustainable Energy Future,* Solar Energy Research Institute, Brick House Publishing Co., Andover, Mass.
5. Wagner, B.S. and Rosenfeld, A.H. (1982), "A Summary Report of Building Energy Compilation and Analysis (BECA) Part V: Validation of Energy Analysis Computer Programs," presented at the ACEEE 1982 Summer Study on Energy-Efficient Buildings, Santa Cruz, California, August 22-28, 1982; Lawrence Berkeley Laboratory Report LBL-14838.
6. Wright, J., et al. (1981), *Supplying Energy through Greater Efficiency: The Potential for Conservation in California's Residential Sector,* Lawrence Berkeley Laboratory Report LBL-10738, to be published by The University of California Press.
7. Usibelli, A., et al. (1983), *Technical Opportunities for Residential Electricity Conservation in the Pacific Northwest Region, 1980-2000* [working title], forthcoming as a Lawrence Berkeley Laboratory report in 1983.
8. Meier, A., et al. (1982), *Supply Curves of Conserved Energy,* Ph.D. Dissertation, Lawrence Berkeley Laboratory Report LBL-14686.
9. Hirst, E., et al. (1982), "The Oak Ridge National Laboratory's Residential Energy Use Model: Version 7.1," in *Electric Power Research Institute Workshop on End-Use Models and Conservation Analysis,* EPRI Report EA-2509. See also E. Hirst and J. Carney (1979), "The ORNL Residential End-Use Model," *Land Economics 55*(3).
10. O'Regan, B.C., et al. (1982), *Results of the Walnut Creek House Doctor Project,* Lawrence Berkeley Laboratory Report LBL-15083.

11. Dutt, G., et al. (1982), *The Modular Retrofit Experiment: Exploring the House Doctor Concept,* Princeton University, Center for Energy and Environmental Studies, PU/CEES Report No. 130.
12. Wagner, B.S. (1982), *Residential Indoor Air Quality/Air Infiltration Study,* Final Report under California Energy Commission Contract 700-80-042, Universitywide Energy Research Group, Berkeley, California, December, 1982.
13. Harris, J.P. and Hollander, J.M., editors (1982), *Improving Energy Efficiency in Buildings: Progress and Problems,* Proceedings of the 1980 Summer Study on Energy-Efficient Buildings, organized by the American Council for an Energy-Efficient Economy (ACEEE), University of California, Santa Cruz, California, August 10-22, 1980.

## BUILDING ENERGY SIMULATION GROUP*

*J.J. Hirsch, W.F. Buhl, R.B. Curtis, A.E. Erdem, K.H. Olson, and F.C. Winkelmann*

The purpose of this project has been to create, test, document, and maintain a user-oriented, public-domain computer program that will enable architects and engineers to perform design studies of whole-building energy use under actual weather conditions. The development of this program, which in its successive public generations has been known as Cal-ERDA, DOE-1.4, DOE-2.0, and, finally, DOE-2.1, has been guided by several objectives:

1. The description of the building by the user should be in quasi-English so that the input can easily be understood by non-computer scientists.
2. When possible, calculations should be based upon well-established or proven algorithms, i.e., the calculational procedures should be acceptable to the engineering and research communities.
3. The program should permit simulation of commonly available as well as innovative heating, ventilation, and air-conditioning (HVAC) equipment.
4. The computer costs of the program should be minimal.
5. The predicted energy use of a building should be acceptably close to measured values.

As can be seen in Fig. 1, DOE-2 is composed of two major segments: the Building Description Language (BDL) processor, which accepts quasi-English descriptions of building components, and the LOADS, SYSTEMS, PLANT, and ECONOMICS (LSPE) processor, which uses building descriptions to simulate building energy performance. Details of the development and structure of the DOE-2 program are available in past annual reports[1-3] and other published materials.[4-8]

### ACCOMPLISHMENTS DURING FY 1982

The DOE-2.1B version of the program was completed, and the writing of supplements to the program documentation[9-12] was begun. Additionally, the Engineers Manual[13] for DOE-2.1A was completed. This document describes all the algorithms used within the program to calculate building heat transfer and resultant energy use. LBL was assisted in this effort by the Q-11 Group at Los Alamos National Laboratory (LANL), which was responsible for producing the final DOE-2.1A Reference and Engineers Manuals from LBL-produced drafts. DOE-2.1A is currently available on DEC-10, DEC-VAX, CDC-Cybers, IBM, Data General MU8000, Honeywell level 6, and Cray-N machines.

The BES Group's ongoing research is divided into two parts. The first centers on modeling building-envelope components and systems. The second is the simulation of heating, ventilating, and air-conditioning (HVAC) equipment and their associated control systems. Major new features of DOE-2.1A and DOE-2.1B in these two areas are described below.

#### Building Envelope Heat-Transfer Modeling

The first step in the simulation of a building is modeling the heat transfer through the envelope components. During FY 1982, three major problems in envelope heat transfer were studied: (1) conductive gains through generalized layered walls and Trombe wall systems; (2) daylight transmission through win-

*This work was supported by the Assistant Secretary for Conservation and Renewable Energy, Office of Building Energy Research and Development, Building Systems Division of the U.S. Department of Energy under Contract No. DE-AC03-76SF00098.

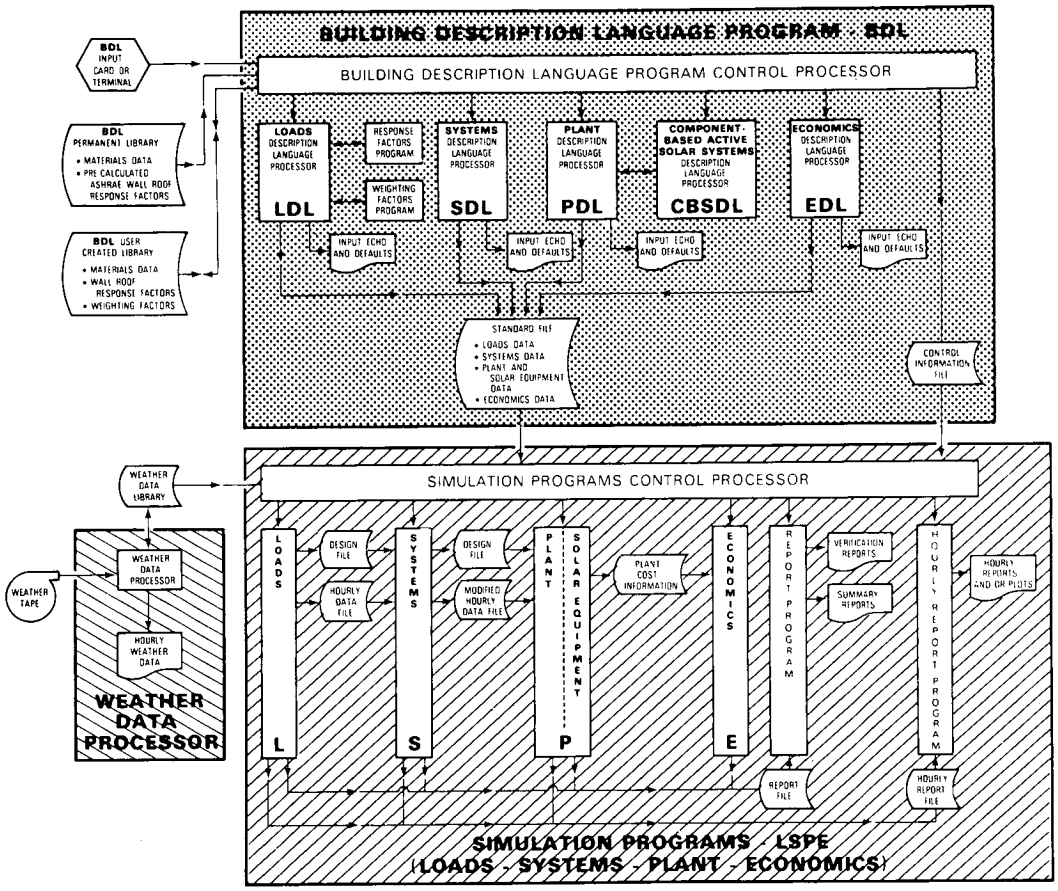


Figure 1. DOE-2.1A computer program configuration. (XBL 825-601)

dows and the thermal effects of alternative glazing systems; and (3) techniques for providing fast and accurate calculation of heating and cooling loads (or response) of whole spaces.

## Response Factors

Building energy-use analysis programs like DOE-2, which take into account transient heat flow, must simulate the delayed transmission of heat through layered walls. The most popular means of doing this are based on response factors developed by Mitalas and Stephenson.[14,15] Significant improvements in the computational speed of the algorithms generating the response factors were achieved through theoretical developments reported elsewhere.[3] These improvements were implemented into the DOE-2.1B version of the program, resulting in a reduction of up to a factor of 20 in the time required to compute response factors.

The gist of the improvements can be expressed as follows. In the usual computation of the thermal response of a multi-layered wall, each layer is summarized in a matrix. The thermal response of the composite wall is given by the product of the matrices for each layer. A method was found to evaluate the matrix elements of this product as a sum of terms with constant coefficients. This formulation avoids the necessity for making a matrix multiplication many times during the response-factor calculation.

## Trombe Walls

The available building-energy analysis programs, which have concentrated on energy transport by conduction and radiation, are incapable of simulating convective transport because it is so much more difficult to simulate than conduction and radiation. In many buildings, particularly those employing "passive" solar designs, convection can be an important and even a dominant effect.

The BES Group, in collaboration with LANL, has begun to integrate models of certain passive solar

elements into the DOE-2 building-energy analysis code.[16] A Trombe wall consists of a south-facing (in the Northern hemisphere) window (usually double- or triple-paned) separated from a massive masonry or concrete wall by an air gap (Fig. 2). The combination acts as a crude solar collector, with the heat capacity of the wall providing heat storage and preventing large temperature swings in the occupied space. Both vented and unvented Trombe walls are modeled. With unvented Trombe walls, heat enters the occupied space through conduction alone. The vented Trombe wall has vents at the bottom and top of the wall that enable warm air to flow directly into the living area by natural convection.

The unvented Trombe wall model, a straightforward extension of the capabilities of DOE-2, was implemented into an experimental version of DOE-2.1A in FY 1981, and in FY 1982, both the vented and unvented models were added to DOE-2.1B.

The vented case was the more difficult to simulate. A force-balance equation is written to obtain the airflow rate. The buoyancy force of the warm air is balanced by the opposing frictional forces caused by the air flowing through the vents and the air gap.

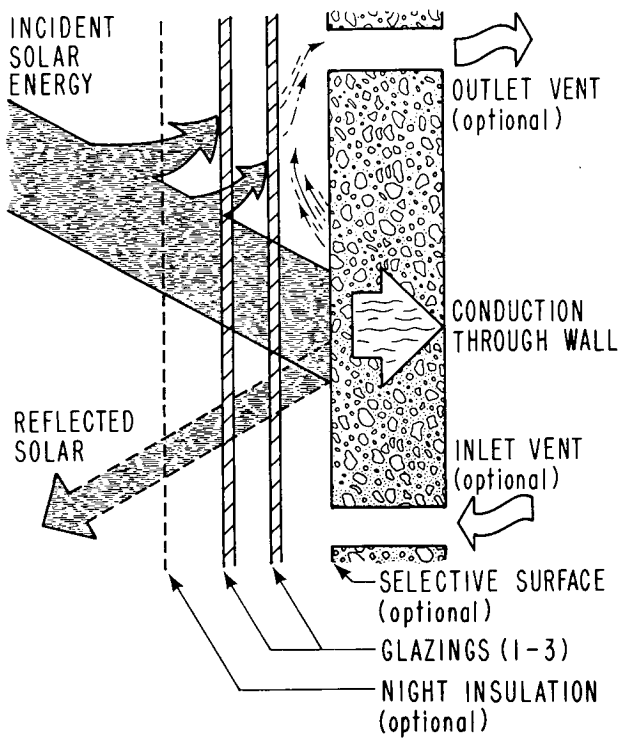


Figure 2. Diagram of heat flows in the DOE-2.1 thermal storage model.[16] (XBL 825-597)

Because the buoyancy of the air depends on its density, which is a strong function of the air temperature, the model must simultaneously do an energy balance on the wall and window surfaces to obtain surface and air temperatures. Because the operations are non-linear, they must be solved numerically, and the model must iterate between the two equations until a stable, simultaneous result is obtained for air flow, air temperature, and surface temperatures.

These problems are typical of the difficulties in modeling convective processes simultaneously with radiative and conductive heat transfer. The experience gained in modeling the Trombe wall will help in developing models for other situations in which convective heat transport is important.

## Daylighting

Lighting accounts for about 20% of total electrical energy consumption in the United States. Using natural lighting is a cost-effective way to reduce this consumption and, at the same time, enhance the quality of the indoor environment. For several years, architects and engineers have used scale models, hand calculator programs, and sophisticated mainframe computer programs (such as LUMEN-II) to determine levels of interior daylight for different building configurations. However, none of these tools determines the annual energy savings from daylighting, information which could have an important effect on design decisions.

For this reason, a daylighting simulation was added to DOE-2. Designers can now quickly and inexpensively determine the hourly, monthly, and yearly impact of daylighting on electrical energy consumption and peak electrical demand, as well as the impact on cooling and heating requirements and, perhaps most important, on annual energy cost.

Taken into account are such factors as window size, glass transmittance, inside surface reflectances of the space, sun-control devices such as blinds and overhangs, and the luminance distribution of the sky. Because this distribution depends on the position of the sun and the cloudiness of the sky, the calculation is made for standard clear- and overcast-sky conditions and for a series of 20 solar altitude and azimuth values covering the annual range of sun positions. The calculations are performed prior to the complete simulation, and the the resulting daylight factors are stored for later use. Analogous factors for glare are also calculated and stored.

For the hourly envelope simulation, the illuminance from each window is found by interpolating the stored daylight factors (using the current-hour sun-position and cloud cover), then multiplying by the current-hour exterior horizontal illuminance. If the glare-control option has been specified, the program will automatically close window blinds or drapes to decrease glare below a pre-defined comfort level. Adding the illuminance contributions from all the windows gives the total number of footcandles at each reference point.

An example of the daylighting calculation is shown in Figs. 3 and 4. The 400-ft$^2$ room in Fig. 3 has a 5-ft x 20-ft east-facing window with a glass transmittance of 80%. The window is covered on the inside by fixed drapery having a transmittance of 60%. A 4-ft-deep overhang runs the entire length of the window. Wall floor, and ceiling reflectance is 50%. The daylighting reference point is located mid-floor at desk height (30 in.). Overhead lighting of 2 W/ft$^2$ provides 50 fc of illuminance at full power between 8:00 a.m. and 6:00 p.m. The lights can be dimmed continuously to 10 fc at minimum (30%) power.

The results of a DOE-2 run of a partly cloudy June day in San Francisco are shown in Figs. 4a and 4b. Fig. 4a shows that the daylight illuminance varies from a minimum of 0.4 fc at 5:00 a.m. to a maximum of 64 fc at 9:00 a.m. Summing over the hours in Fig. 4b gives a net reduction in lighting energy use of 59%.

To verify that the DOE-2 daylighting calculation gives accurate results, program predictions are being checked against illuminance measurements obtained by the Windows and Daylighting Group, using scale models having various window configurations. An offshoot of this cross-check will be the development of a method for DOE-2 to directly use daylight factors from models (or calculated by programs such as LUMEN-II), thus making it possible to simulate virtually any daylighting configuration.

During FY 1982 the initial version of the daylighting model was completed and integrated into the DOE-2.1B version of the program.

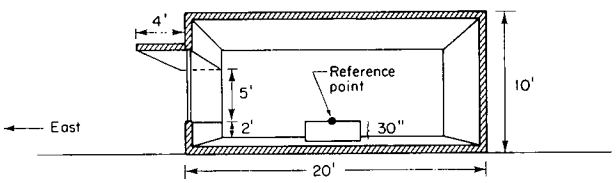


Figure 3. Test model for DOE-2.1 daylighting calculation. (XBL 825-596)

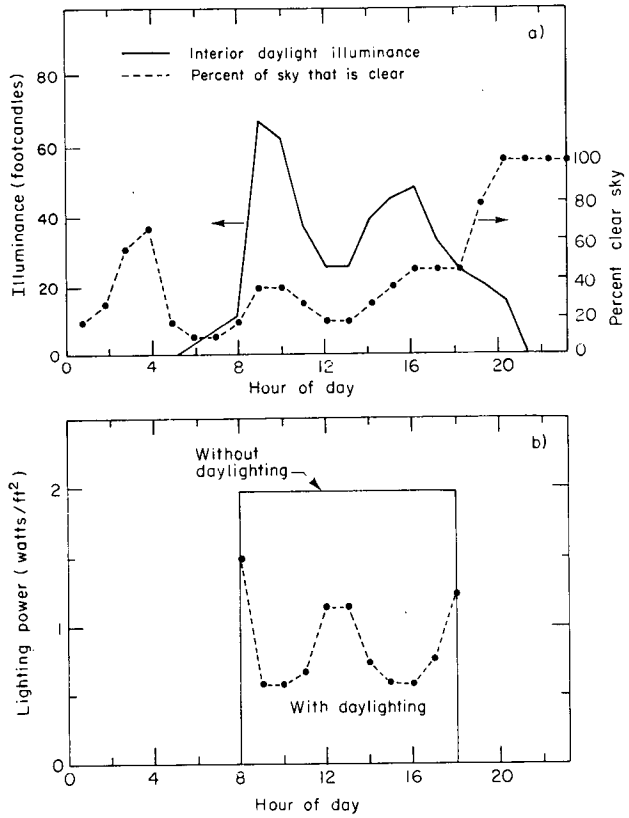


Figure 4. Results of DOE-2.1 daylighting calculation for a partly cloudy June day in San Francisco, for the test module shown in Fig. 3. (a) Daylight illuminance at the reference point and percent of sky that is clear. (b) Power consumption for electric lighting with and without daylighting. (XBL 825-598)

## Custom Weighting Factors and Thermal Balance Loads

Research continues on these two methods to substantially improve the calculation of heating and cooling loads in building spaces. In the "custom weighting factor" (CWF) method, a fast-executing transfer function is used. The second method, called "modified thermal balance," is more time-consuming but more accurate. Ultimately, the user will be able to choose the technique best suited to the application at hand.

The CWF approach calculates the heat gains from lights, solar radiation, people, equipment, and conduction through the envelope for each hour. Part of each gain will appear immediately as a load on the HVAC system; the remainder will be stored as heat in the walls, floor, furniture, and other mass in the building and will be released over time to the room air. The delays involved in this process are accounted for by the weighting factors.

In earlier versions of the program, "ASHRAE weighting factors" were used. These were calculated about 15 years ago by the National Research Council of Canada for buildings of very simple geometry and were adapted by the American Society of Heating, Refrigerating, and Air-Conditioning Engineers (ASHRAE).[13] LANL studies showed that the ASHRAE weighting factors lead to inaccurate results for buildings where direct gain is important.

A technique for calculating weighting factors specifically for the space configuration described by a user has been developed[13] and incorporated into DOE-2.1. In this technique, a detailed thermal-balance calculation is made initially to find the cooling-load profile produced by a unit impulse of heat gain from each of the sources listed above. By adding the CWF technique, it is possible to accurately account for the storage of heat in the thermal mass of the building; in particular, it enables direct-gain, passive solar buildings to be modeled with DOE-2.

In FY 1982, several important improvements were made to the weighting-factor calculations to more accurately represent multi-room and multi-story buildings, as well as to allow the modeling of a generalized lighting system. For multi-room and multi-story modeling, two major changes were made: first, several new types of interior zone surfaces with different heat-transfer properties (non-mass air exchange pathway, adiabatic mass walls, and mass partitions) were added; second, a new type of thermal zone MULTIPLIER was added to distinguish between vertically- and horizontally-duplicate thermal zones. In the lighting system model, the heat transfer is assumed to occur through three mechanisms: radiative transfer to surfaces in the zone with later heating of the air (radiation); direct heating of the air in the absence of forced air flow (natural convection); and direct heating of the air via forced flow over the lighting fixture (forced convection). The first two mechanisms have heat-load components from the lighting system into the lighted zone as well as into the plenum above the lighted zone. The third mechanism applies to systems that have the return air passing through the lighting fixture. These improved features were added to the DOE-2.1B version of the program and will be used by ASHRAE to update tables in the *ASHRAE Handbook of Fundamentals*.

The modified thermal balance (MTB) algorithm calculates space heating and cooling loads by considering the radiative coupling between the surfaces of the space. For each wall or window, the thermal-balance equations are written for the inside and outside surfaces. Thermal-balance equations include radiative, conductive, and convective heat transport. (The convective term is still in its simplest form and will be improved later.)

Coupling between the surfaces is achieved through a radiative interchange, in contrast to the CWF method, where the coupling between components of heating/cooling loads are calculated with a time series for each component. In the radiative interchange method, for each surface we lump all other surfaces into a single effective surface and assign a mean radiant temperature to it; then we do radiative interchange with the surface in question and the lumped surface. This calculation is repeated for each surface, and convergence is checked. Then we linearize the Boltzmann equation, which is fourth order, with respect to the surface temperature. Inside and outside surface temperatures are tracked. The heat storage and delayed transport through walls, floors, and furniture are handled with response factors. Solar gains on the outside surfaces are calculated in a similar manner, as in the weighting-factor LOADS program. Solar gain on an inside surface is calculated by computing the amount of solar radiation coming through the windows and hitting the surface.

Several primary approximations in modified thermal balance require further improvement:

- The view factors used in radiative interchange are proportional to the surface areas; more accurate view factors must be calculated.
- The room temperature used in the expressions is constant; this should be able to vary within a given range.
- The convective coupling between the surface and room air is a constant; it should vary with surface and air temperatures.

We believe that the MTB technique may be more accurate in certain situations than the weighting-factor approach. For example, it could model movable insulation being placed over windows at night. The CWF technique does not treat room transfer functions as functions of time, which is necessary when the conductance of the windows varies with time. MTB also computes the inside surface temperature as

a function of time. If these temperatures vary widely, the convective, and even the radiative, heat-transfer coefficients can vary enough to cause significant changes in building conditions. Human comfort depends strongly upon the inside surface temperatures, but the weighting-factor approach provides no information in this regard. Further studies will be made of the differences among the CWF, MTB, and full-thermal-balance techniques to determine when accuracy requires the more complex, and therefore more time-consuming, methods.

## HVAC Equipment and Controls

The SYSTEMS and PLANT sub-programs of DOE-2 were originally designed to estimate the energy consumption of the HVAC equipment of large buildings. Many modeling assumptions were based on the philosophy that the most important considerations should be those that have a significant impact upon the energy-consumption values integrated over time. The program made no attempt to simulate the actual performance of the equipment components on an hour-by-hour basis but, rather, predicted overall energy use. This approach was adequate because, in the past, HVAC equipment had been systematically oversized and tightly controlled. For modeling such systems, it was not necessary to consider performance parameters that depended on inside or outside environmental variables.

As DOE-2 gained popularity, the user community wanted to extend its use to small commercial and residential buildings. At the same time, the engineering community, in an effort to conserve energy, was moving away from recommending oversized systems and constant, year-round control points. These shifts prompted us to make substantial changes in the algorithms of both SYSTEMS and PLANT. The new algorithms are more concerned with modeling hourly performance of actual equipment.

In the SYSTEMS simulation, work during FY 1981 and 1982 concentrated in three areas: more accurate equipment sizing, more accurate control system interactions, and the implementation of new HVAC equipment configurations. In the PLANT simulation, work focused on: (1) the development of algorithms to simulate "free" cooling using cooling-tower water and (2) implementation of new electrical generation modes and peak shaving studies.

For equipment controlled by a zone thermostat, a linear relationship is assumed to describe the interaction of the thermostat, space temperature, and equipment output. As Fig. 5 shows, there are generally five regions of interest for thermostat-equipment interaction: upper and lower bound regions within which maximum cooling and heating, respectively, are supplied; heating- and cooling-action band regions within which proportional control of equipment output is effected; and a dead-band region within which the equipment action is constant and usually equal to that at the bottom of the cooling-action band. The space temperature and resultant thermostat reaction can change significantly during the basic one-hour time step used in DOE-2. Additionally, the heating- and cooling-action bands may each be composed of multiple regions within which different pieces of equipment function. Thus, the seemingly simple problem of modeling temperature-controlling equipment can become a complex set of interacting equations and boundary conditions. Improvements were made and incorporated into DOE-2.1A and DOE-2.1B to closely model these complex control strategies. Similar improvements were designed and implemented to model the control of space humidity.

During FY 1982, several additional capabilities were added to the HVAC SYSTEMS program. Among these are nighttime ventilation cooling (or alternative night fan controls), outside temperature activation of heating and cooling, warm-up cycle for variable flow systems, electric (or gas/oil) humidifiers, air-side false loading of chillers (by the closing of outside air dampers), and plenum heaters.

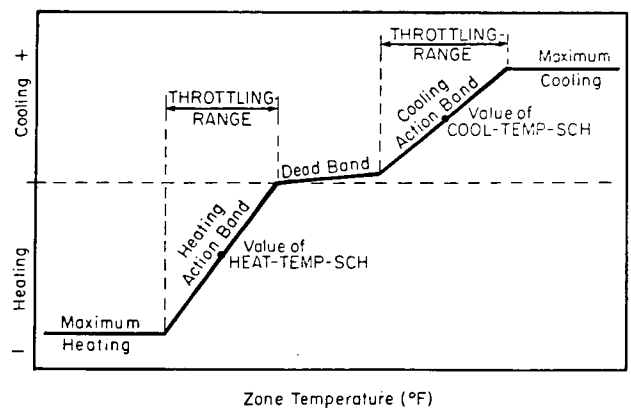


Figure 5. Five possible regions of thermostatic action. (XBL 825-600)

### New HVAC Configurations and Performance Curves

During FY 1982, work began on developing models for simulating new HVAC configurations, powered induction systems, and dual fan/dual duct systems. The powered induction system is an advancement on variable air volume systems that more effectively utilize waste heat from the building core and lighting system to condition the exterior thermal zones. This is done by introducing this warm air into the external zone with a small fan contained in the terminal box. This fan can be placed in series or parallel with the primary system airflow. The dual fan/dual duct system operates under the same principle, except that a central fan rather than individual zone fans introduces warm recirculated air into the exterior zones.

Another area of interest is collecting HVAC equipment performance data and producing empirical correlations for simulation models. This will be important in future work because of the lack of high-quality data. Results of this work are also valuable to other groups interested in HVAC equipment simulation.

### Direct Cooling

Two methods of providing "free" cooling from a central-plant cooling tower were researched and implemented in DOE-2.1A. The motivation is to find an inexpensive retrofit of existing chiller-cooling tower arrangements that will reduce cooling costs. The two "free" cooling concepts take advantage of periods during which the outdoor wet-bulb temperature is low enough (between 35°F and 50°F) to produce cooling-tower exit water that is cold enough to cool the building without using a chiller.

The first method, known as the strainer cycle, injects the cooling-tower water directly into the building chilled-water loop through a strainer that removes harmful impurities. Thus, the water-chiller equipment is entirely bypassed.

The second method, known as the thermocycle, uses the water-chiller equipment as a passive heat-exchanger. The cooling-tower water passes into the chiller-condenser section and cools the refrigerant. A small auxiliary pump, added during the retrofit, sprays the refrigerant onto the evaporator coils, thus cooling the water circulating in the chilled-water loop.

### Generation Strategies and Peak Shaving

Because of changes in the attitudes of utilities and state regulators toward small power producers, requirements that electrical generators in buildings only track the building's electrical demands have been loosened. A modification was incorporated into DOE-2.1B to model alternative strategies. This feature is currently limited to two strategies: generation to track building demands and generation at full capacity. Work was begun to upgrade the models of electrical generation equipment and to model the generation as driven by heating demands (a third strategy). Work was also begun on adding a generalized energy cost program to allow an integrated analysis of energy use, generation, and cost.

This follows earlier work over the past several years in which DOE-2 has been modified to model generalized equipment management based on time-of-day, season, and type as well as magnitude of load. These changes enable the study of strategies to reduce peak electrical demand by using on-site generation facilities. Our first study examined the use of emergency generators for this purpose in high-rise office buildings.[17]

### Advanced Control Simulation

Work began in FY 1982 on developing a major new feature for DOE-2. It will enable the simulation of innovative designs by allowing users to write specific algorithms that can be incorporated into the hourly simulation without modifying the program. These functions are written in a FORTRAN-like manner and entered into the BDL building description. They may include algebraic expressions and conditional decisions. With this capability, individual researchers will be able to entirely replace current DOE-2 algorithms or simply augment current algorithms with new features; researchers working on individual parts of the building simulation will be able to study their new components or controls without building an entire simulation program.

## PLANNED ACTIVITIES FOR FY 1983

Future plans for the program lead in two directions. On the one hand, the existing program will be maintained and supported, and its documentation will be clarified and supplemented as areas of confusion are uncovered. Several additions will also be made to the program to supplement its capabilities. These

include: (1) expanded output report capability, (2) an improved window and daylighting simulation in collaboration with the Windows and Daylighting Group, (3) an expanded user-library capability, (4) further research into the thermal balance LOADS program alternative, (5) completion of the functional values specification, and (6) the addition of new HVAC equipment and controls. We will also continue to carry out building energy performance studies.

The second direction for FY 1983 activity is exploratory. We will probe the development of a building energy-use analysis program that can be easily adapted to new developments in the building and conservation sciences.

## REFERENCES


1. *Energy & Environment Division Annual Report, FY 1979,* Lawrence Berkeley Laboratory Report LBL-11650.
2. *Energy & Environment Division Annual Report, FY 1980,* Lawrence Berkeley Laboratory Report LBL-11990.
3. *Energy & Environment Division Annual Report, FY 1981,* Lawrence Berkeley Laboratory Report LBL-13500.
4. Diamond, S.C., and Hunn, B.D. (1980), *The DOE-2 Verification Project: Phase I Results,* Los Alamos National Laboratory Publication LA-UR-80-357.
5. Schnurr, N.M., et al. (1979), *Applications of DOE-2 to Direct-Gain Passive Solar Systems: Implementation of a Weighting Factor Calculative Technique,* Los Alamos National Laboratory Publication LA-UR-79-2227.
6. Roschke, M.A., Hunn, B.D., and Diamond, S.C. (1978), *A Component Based Simulator for Solar Systems,* Los Alamos National Laboratory Publication LA-UR-78-1494.
7. Hirsch, J.J. (1982), *Simulation of HVAC Equipment in the DOE-2 Program,* Lawrence Berkeley Laboratory Report LBL-15214.
8. Curtis, R.B. (1981), *The Theoretical Basis of the DOE-2 Building Energy-Use Analysis Program,* Lawrence Berkeley Laboratory Report LBL-12300.
9. LBL Building Energy Analysis Group (1980), *DOE-2 Users Guide, Version 2.1,* Lawrence Berkeley Laboratory Report LBL-8689 Rev. 1.
10. LBL Building Energy Analysis Group (1980), *DOE-2 BDL Summary, Version 2.1,* Lawrence Berkeley Laboratory Report LBL-8688 Rev. 1.
11. LBL Building Energy Analysis Group (1980), *DOE-2 Sample Run Book, Version 2.1,* Lawrence Berkeley Laboratory Report LBL-8688 Rev. 1.
12. LANL Group Q-11, Solar Energy (1980), *DOE-2 Reference Manual (Part 1, Part 2), Version 2.1,* Lawrence Berkeley Laboratory Report LBL-8688, Rev. 1, and Los Alamos National Laboratory Publication LA-7689-M Version 2.1.
13. LBL Building Energy Analysis Group and LANL Group Q-11, Program Support (1980), *DOE-2 Engineers Manual, Version 2.1.,* Lawrence Berkeley Laboratory Report LBL-11353.
14. Stephenson, D.G., and Mitalas, G.P. (1967), "Cooling Load Calculations by Thermal Response Factor Method," *ASHRAE Transactions, 73,* Part 1.
15. Stephenson, D.G., and Mitalas, G.P. (1967), "Room Thermal Response Factors," *ASHRAE Transactions, 73,* Part 1.
16. Moore, J.E., et al. (1981), *Thermal Storage Wall Model Development in the DOE-2 Computer Program,* Los Alamos National Laboratory Publication LA-UR-81-981.
17. Choi, S., Hirsch, J., and Birdsall, B. (1982), *Use of a Diesel Engine-Driven Emergency Power Generating System for Peak Shaving in Buildings,* Lawrence Berkeley Laboratory Report LBL-12299.

# PUBLICATIONS LIST

The publications list through 1982 for the Energy Efficient Buildings Program is organized as follows:

*Energy Efficient Buildings* (EEB)—general reports not specific to any sub-group.
*Buildings Energy Data (BED)*—reports on the compilation and analysis of building energy performance data.
*Building Energy Simulation Group* (BES—including DOE-2)— reports concerning computer modelling and programming. (GR stands for Group Report, and represents an internal document).
*Building Energy Performance Standards* (BEPS)—reports specific to the proposed Federal Building Energy Performance Standards.
*Energy Conservation Inspection Service* (ECIS)—contains reports concerning the ECIS program.
*Energy Performance of Buildings*—reports specific to the energy performance of building envelopes.
*Hospitals*—reports related to the Hospitals Program.
*Schools*—reports specific to the Schools Program.
*Ventilation*—reports specific to building ventilation and indoor air quality.
*Windows and Daylighting*—reports specific to the energy-efficient design of windows and use of daylighting.
*Lighting Systems Research*—reports specific to the energy-efficient design of lighting systems, including daylighting.

Most reports have an LBL number and an EEB number, either of which may be used for ordering copies of the report. A longer version of this list including abstracts is also available.

## ENERGY EFFICIENT BUILDINGS (EEB)

### 1976

EEB 76-1, LBL-3274, *Projecting an Energy Efficient California.* D.B. Goldstein and A.H. Rosenfeld, 1976.

EEB 76-2, LBL-4438, *Conservation and Peak Power—Cost and Demand.* D.B. Goldstein and A.H. Rosenfeld, 1976.

### 1977

EEB 77-1, LBL-4411, *Efficient Use of Energy in Buildings.* A report of the 1975 Berkeley Summer Study, E. Dean and A.H. Rosenfeld, Editors, special issue of *Energy and Buildings,* 1977.

EEB 77-2, *Modeling Natural Energy Flow in Houses.* E. Dean and A.H. Rosenfeld, chapter 3 of above journal.

EEB 77-3, *Notes on Residential Fuel Use.* A.H. Rosenfeld, chapter 3a.

EEB 77-4, *Beam Daylighting.* A.H. Rosenfeld and S. Selkowitz, chapter 4.

EEB 77-5, *Energy Cost of Buildings.* R.A. Herendeen and A.H. Rosenfeld, chapter 8.

EEB 77-6, *Dual Solar-Control Venetian Blinds.* A.H. Rosenfeld, chapter 7a.

EEB 77-7, *Beam Daylighting: Direct Use of Solar Energy for Interior Lighting.* A.H. Rosenfeld and S.E. Selkowitz. Published in *Sharing the Sun, Solar Technology in the Seventies,* Proceedings of the ISES Conference, Winnipeg, Canada, 1976, vol. 7, pp. 375-391.

EEB 77-8, LBL-5236, *Energy Extension Services.* Proceedings of the 1976 Berkeley Workshop, P.P. Craig, A.H. Rosenfeld and C.M. York, Editors, 1977.

EEB 77-9, *Energy Extension for California: Context and Potential Impact.* P.P. Craig, et al., chapter of LBL-5236, available separately as UCID-3911.

EEB 77-10, *Electric Load Leveling by Chilled Water Storage.* A.H. Rosenfeld and F.S. Dubin.

EEB 77-11, LBL-5910, *Energy Conservation in Home Appliances through Comparison Shopping: Facts and Fact Sheets.* D.B. Goldstein and A.H. Rosenfeld, March 1978.

EEB 77-12, LBL-5271, *Conservation Options in Residential Energy Use: Studies Using the Computer Program Two-zone.* L.W. Wall, T. Day, A.J. Gadgil, A.B. Lilly, and A.H. Rosenfeld, August 1977.

EEB 77-13, LBL-5926, *Some Potential for Energy and Peak Power Conservation in California.* A.H. Rosenfeld. Published in the Proceedings of the International Conference on Energy Use Management, Tucson, AZ, October 24-28, 1977, pp. 987-1019.

**1978**

EEB-BEV 78-1, *Studies of Evaporative and Conventional Cooling of an Energy Conserving California House.* S.D. Gates, J. Baughn and A.H. Rosenfeld. Presented at the Second National Passive Solar Conference. Philadelphia, PA, March 1978, vol. II, p. 665.

EEB-BEV 78-2, UC95-C, LBL-6840, *Twozone Users Manual.* A.J. Gadgil, G. Gibson, and A.H. Rosenfeld, March 1978.

EEB-BEV 78-3, LBL-6865, *Saving Half of California's Energy and Peak Power in Buildings and Appliances via Long-Range Standards and Other Legislation.* A.H. Rosenfeld, D.B. Goldstein, A.J. Lichtenberg, and P.P. Craig. Submitted to the California Policy Seminar, May 1978.

EEB-BEV 78-4, *Marginal Cost Pricing with Refunds per Capita—MCP/RPC.* A.H. Rosenfeld and A.C. Fisher. Submitted to the July 1978 Hearings of the California Energy Commission on Load Management.

**1979**

EEB-BECA 79-1, LBL-8912, *Building Energy Use Compilation and Analysis (BECA): An International Comparison and Critical Review. Part A: Single Family Residences.* A.H. Rosenfeld, W.G. Colborne, C.D. Hollowell, L. Schipper, B. Adamson, M. Cadiergues, G. Olive, B. Hidemark, H. Ross, N. Milbank, and M. Uyttenbroeck, July 1979.

EEB 79-1, LBL-8913, *Storage of Heat and Coolth in Hollow-Core Concrete Slabs: Swedish Experience, and Application to Large, American Style Buildings.* L. Anderson, K. Bernander, E. Isfalt, and A. Rosenfeld, 1979. Presented at the Second International Conference on Energy Use Management, Los Angeles, CA, October 22-26, 1979.

EEB 79-2, LBL-9039, *Reducing Swimming Pool Heating Costs: Comparison of Pool Covers, Solar Collectors and Other Options.* H.W. Sigworth, Jr., J. Wei, and A.H. Rosenfeld, 1979.

LBL-9076, *The Broader Consequences of Improved Rural Transport: Three-Wheeled Vehicles in Crete.* A. Meier, May 1979. Presented at the World Future Society Meeting, Berlin, West Germany, May 8-10, 1979.

EEB 79-4, LBL-9816, *Evaluation of Residential Building Energy Performance Standards.* M. Levine, D. Goldstein, M. Lokmanhekim, and A.H. Rosenfeld, 1979. Presented at the Second International Conference on Energy Use Management, Los Angeles, CA, October 22-26, 1979.

UC-95a, LBL-7885, *Bibliography on Institutional Barriers to Energy Conservation.* C. York, C. Blumstein, B. Kreig, and L. Schipper, September 1979.

LBL-8299, *Overcoming Social and Institutional Barriers to Energy Conservation.* C. Blumstein, B. Kreig, L. Schipper, and C. York, April 1979. Submitted to *Energy, The International Journal.*

UC-95f, LBL-9139, *Inventory of Energy Conservation Potential in California: The Cement Industry.* P. Kuhn, L. Hudson, C. Blumstein, and C. York. April 1979.

LBL-9184, *Review of Data Analysis on the Domestic Crude Oil Entitlements System.* M. Horoitz, W. Klein, and C. York, July 1979.

LBL-9237, *Information Validation: A Working Paper.* M. Horoitz and C. York. June 1979.

**1980**

EEB 80-1, *Testimony Before the Subcommittee on Energy Development and Applications,* House Committee on Science and Technology, February 20, 1980. A.H. Rosenfeld.

EEB 80-2, LBL-10738, *Supplying Energy Through Greater Efficiency: The Potential for Energy Conservation in California's Residential Sector.* J. Wright, A. Meier, M. Maulhardt, H. Arin, and A.H. Rosenfeld, 1980.

EEB 80-3, *Saving Half of California's Energy and Peak Power in Building and Appliances.* A.H. Rosenfeld, D.B. Goldstein, A.J. Lichtenberg, and P.P. Craig. From *Energy Policy Modeling: United States and Canadian Experiences.*

EEB 80-4, *Testimony on BEPS, before the Subcommittee on Energy Regulation,* Senate Committee on Energy and Natural Resources. A.H. Rosenfeld, June 5, 1980.

EEB 80-5, LBL-11300, *Technical Potentials and Policy Recommendations for Conservation and Renewable Resources: A Least Cost Scenario, 1980-2000.* A.H. Rosenfeld, D. Goldstein, J. Harris, D. Claridge, and K. Gawell. July 1980.

EEB-BECA 80-1, LBL-8912 (Rev.), *Building Energy Use Compilation and Analysis (BECA) an International Comparison and Critical Review. Part A: New Residential Buildings.* A.H. Rosenfeld, W.G. Colborne, C.D. Hollowell, S.P. Meyers, L.J. Schipper, B. Adamson, B. Hidemark, H. Ross, N. Milbank, M.J. Uytten-

broeck, and G. Olive. November 1980.

EEB-BECA 80-1, LBL-13385, *North American Residential Retrofit,* L. Wall, 1981.

EEB 80-6, LBL-11332, *Utilizing the Thermal Mass of Structural Systems in Buildings for Energy Conservation and Peak Power Reduction.* C. Barnaby, E. Dean, F. Fuller, D. Nall, T. Shelley and T. Wexler. June 1980.

**1981**

EEB 81-1, *House Doctor Demonstration, Training, and Retrofit Monitoring Project,* A.H. Rosenfeld, June 1981.

EEB 81-2, LBL-12739, *Accelerating the Buildings Sector's Sluggish Response to Rising Energy Prices,* A.H. Rosenfeld and M.D. Levine, Testimony before the Interior Appropriations Committee, U.S. House of Representatives, April 8, 1981.

EEB 81-3, *Progress in Energy-Efficient Buildings - The Potential for Saving 8 Million Barrels a Day by 2000, at a Cost of $10 Per Conserved Barrel,* A.H. Rosenfeld, Testimony before the Subcommittee on Energy Conservation and Power of the Committee on Energy and Commerce, U.S. House of Representatives, May 20, 1981.

EEB 81-4, *Measurement and Control of Indoor Air Quality in Existing and New Homes,* A.H. Rosenfeld and C.D. Hollowell, Testimony before the Subcommittees on Energy Development and Applications and Natural Resources, Agriculture Research, and Environment of the Committee on Science and Technology, U.S. House of Representatives, May 28, 1981.

EEB 81-6, LBL 12889, *Technical Opportunities for Energy Efficient Buildings, A Least-Cost Scenario, 1980-2000,* A.H. Rosenfeld et al., September 1981.

EEB 81-7, *Energy Efficiency—The Impact of Conservation,* A.H. Rosenfeld, February 1981.

EEB 81-9, *A New Prosperity: Building A Sustainable Energy Future (the SERI Solar/Conservation Study:* Buildings Section), A.H. Rosenfeld, 1981.

EEB 81-10, LBL-6840 (Rev.), *TWOZONE Users Manual* (2nd ed., revised). A.J. Gadgil, G. Gibson, and A.H. Rosenfeld, October 1981.

EEB 81-11, LBL-13608, *Supply Curves of Conserved Energy for California's Residential Sector,* A.K. Meier, A.H. Rosenfeld, and J. Wright, December 1981.

EEB 81-12, *Energy Demand,* chapter from *AIP 50th Anniversary—Physics Vade Mecum,* A.H. Rosenfeld, and A.K. Meier, 1981.

EEB-81-13, *Impact of FY'82 and FY'83 Budget Cuts on Conservation Programs at LBL,* A.H. Rosenfeld, Testimony before Subcommittee on Energy Conservation and Power, Committee on Energy and Commerce, U.S. House of Representatives, December 3, 1981.

EEB 81-14, LBL-14146, *The Potential for Improved Energy Efficiency to Help Meet Future Energy Needs,* J.P. Harris, Testimony before the House Interior and Insular Affairs Committee, Subcommittee on Investigations and Oversight, October 9, 1981.

EEB 81-15, *Improving the Technical Quality and Effectiveness of Residential Conservation Retrofit in California: Issues and Recommendations,* J.P. Harris, Discussion Notes for the Subcommittee on Energy and Natural Resources, Interim Hearings, December 10, 1981.

EEB 81-16, LBL-14151, *Comments on Proposed Amendments to the Regulations for the DOE Residential Conservation Service,* J.P. Harris, DOE Public Hearings, December 11, 1981.

**1982**

EEB-82-2, LBL-15182, *Technology for Energy-Efficient Buildings.* A. H. Rosenfeld. To be published in proceedings of First U.S.-China Conference on Energy, Resources, and Environment, Beijing, China, November 7-12, 1982.

EEB 82-3, LBL-15183, *Energy Efficiency in Chinese Apartment Buildings: Parametric Runs with the DOE-2 Computer Program.* Y.J. Huang, M. Lokmanhekim, A.C. de Piedade, A.H. Rosenfeld, and D. Tseng. Presented at First U.S.-China Conference on Energy, Resources and Environment, Beijing, China, November 7-12, 1982.

## BUILDINGS ENERGY DATA

**1981**

EEB-BED 80-2, LBL-10738, *Supplying Energy Through Greater Efficiency: The Potential for Conservation in California's Residential Sector.* J. Wright, A. Meier, M. Maulhardt, and A.H. Rosenfeld, January 1981.

EEB-BED 81-11, LBL-13608, "Supply Curves of Conserved Energy for California's Residential Sector." A. Meier, A.H. Rosenfeld, and J. Wright, preprinted as an LBL Report December 1981. *Energy, 7,* pp. 347-358 (1982).

EEB-BED 81-14, LBL-14146, *The Potential for Improved Energy Efficiency to Help Meet Future Energy Needs.* J.P. Harris, October 9, 1981.

EEB-BED 81-15, *Improving the Technical Quality and Effectiveness of Residential Conservation Retrofit Programs in California: Issues and Recommendations.* J.P. Harris, December 11, 1981.

EEB-BED 81-17, "Conservation Will Always Be With Us." A. Meier, in *Energy, 6,* 1981.

**1982**

EEB-BED 82-01, LBL-14529, *Thermal and Economic Performance of Low-Income Housing.* R. Crenshaw, June 1982. Presented at PASSIVE '82, ASISES Conference, Knoxville TN, August 29-September 3, 1982.

EEB-BED 82-02, LBL-14576, *Monitored Superinsulated and Solar Houses in North America: A Compilation and Economic Analysis.* J.C. Ribot, J.G. Ingersoll, and A.H. Rosenfeld, June 1982. Presented at PASSIVE '82, ASISES Conference, Knoxville TN, August 29-September 3, 1982.

EEB-BED 82-03, LBL-14111, *Infiltration and Indoor Air Quality in a Sample of Passive Solar and Super Insulated Houses.* B.S. Wagner and A.H. Rosenfeld, June 1982. Presented at PASSIVE '82, ASISES Conference, Knoxville TN, August 29-September 3, 1982.

EEB-BED 82-04, LBL-14686, *Supply Curves of Conserved Energy.* A. Meier, Ph.D. Dissertation, May 1982.

EEB-BED 82-05, LBL-13385, "Building Energy Compilation and Analysis (BECA) Part B: Existing North American Residential Buildings." L. Wall, C.A. Goldman, A.H. Rosenfeld, and G.S. Dutt, July 1982. To be published in *Energy and Buildings.*

EEB-BED 82-07, LBL-14787, *A Summary Report of Building Energy Compilation and Analysis (BECA)—Part B: Existing North American Residential Buildings.* L.W. Wall, C.A. Goldman, and A.H. Rosenfeld, August 1982. To be published in the proceedings of the ACEEE 1982 Summer Study in Energy Efficient Buildings, Santa Cruz CA, August 22-28, 1982.

EEB-BED 82-08, LBL-14788, *Monitored Low-Energy Houses in North America and Europe: A Compilation and Economic Analysis.* J.C. Ribot and A.H. Rosenfeld, August 1982. To be published in the proceedings of the ACEEE 1982 Summer Study in Energy Efficient Buildings, Santa Cruz CA, August 22-28, 1982.

EEB-BED 82-09, LBL-14827, *Building Energy Use Compilation and Analysis (BECA) Part C: Conservation Progress in Retrofitted Commercial Buildings.* H. Ross and S. Whalen. To be published in the proceedings of the ACEEE 1982 Summer Study in Energy Efficient Buildings, Santa Cruz CA, August 22-28, 1982.

EEB-BED 82-10, LBL-14838, *A Summary Report of Building Energy Compilation and Analysis (BECA) Part V: Validation of Energy Analysis Computer Programs.* B.S. Wagner and A.H. Rosenfeld. To be published in the proceedings of the ACEEE 1982 Summer Study in Energy Efficient Buildings, Santa Cruz CA, August 22-28, 1982.

EEB-BED 82-11, LBL-14853, *Instrumented Audits.* R. Crenshaw. To be published in the proceedings of the ACEEE 1982 Summer Study in Energy Energy Efficient Buildings, Santa Cruz CA, August 22-28, 1982.

EEB-BED 82-12, LBL-14818, *New Utility Strategies for Saving Energy in the Commercial Sector.* S. Maves and J.P. Harris. To be published in the proceedings of the ACEEE 1982 Summer Study in Energy Efficient Buildings, Santa Cruz CA, August 22-28, 1982.

EEB-BED 82-13, LBL-14914, *Technical Issues for Building Energy Use Labels.* A.H. Rosenfeld and B.S. Wagner. To be published in the proceedings of the ACEEE 1982 Summer Study in Energy Efficient Buildings, Santa Cruz CA, August 22-28, 1982.

EEB-BED 82-14, LBL-14924, *Purchasing Patterns of Energy-Efficient Refrigerators and Implied Consumer Discount Rates.* A. Meier and J. Whittier. To be published in the proceedings of the ACEEE 1982 Summer Study in Energy Efficient Buildings, Santa Cruz CA, August 22-28, 1982.

EEB-BED 82-15, LBL-15083, *Results of the Walnut Creek House Doctor Project.* B.C. O'Regan, B.S. Wagner, and J.B. Dickinson, November 1982.

EEB-BED 82-16, LBL-15198, "The Cost of Conserved Energy as an Investment Statistic." A. Meier. *Harvard Business Review, 61* pp. 36-37 (January—February 1983).

EEB-BED 82-17, LBL-15375, *A Summary Review of Building Energy Use Compilation and Analysis (BECA) Part C: Conservation Progress in Retrofitted Commercial Buildings.* L.W. Wall and J. Flaherty. To be published in the proceedings of the ACEEE 1982 Summer Study in Energy Efficient Buildings, Santa Cruz CA, August 22-28, 1982.

EEB-BED 82-18, LBL-15374, *Progress in Energy Efficient Buildings.* L.W. Wall and A.H. Rosenfeld,

December 1982. Presented at the Association of Energy Engineers, 5th Energy Audit Symposium and Productivity Exposition, Los Angeles CA, February 17-18, 1983.

## BUILDING ENERGY SIMULATION

### 1978

EEB-DOE-1 78-1, LBL-7836, *DOE-1 (Formerly CAL ERDA), A New State-of-the-Art Computer Program for the Energy Utilization Analysis of Buildings.* M. Lokmanhekim, F.C. Winkelmann, A.H. Rosenfeld, Z. Cumali, G.S. Leighton, and H.D. Ross, May 1978. Presented at the Third International Symposium on the Use of Computers for Environmental Engineering Related to Buildings, Banff, Alberta, Canada, May 10-12, 1978.

EEB-DOE-1 78-2, UC-95d, LBL-6314, *Remote Operation of DOE-1 on the Lawrence Berkeley Laboratory CDC 7600, 6600 and 6400 Computers,* March 1978.

EEB-DOE-1 78-3, LBL-7826, *Energy Utilization Analysis of Buildings.* M. Lokmanhekim, June 1978. Invited lecture to the International Symposium—Workshop on Solar Energy, Cairo, Egypt, June 16-22, 1978.

EEB-DOE-1 78-4, LBL-8569. *DOE-1 Users Guide,* December 1978.

EEB-DOE-1 78-5, LBL-8568, *DOE-1 BDL Summary,* December 1978.

EEB-DOE-1 78-6, LBL-8481, *DOE-1 Sample Run Book,* December 1978.

EEB-DOE-1 78-7, ANL/ENG 78-01, *DOE-1 Reference Manual,* R.M. Graven, P.R. Hirsch, K.N. Patel, W.J. Taylor, G. Whittington, Argonne National Laboratory, December 1978.

EEB-DOE-1 78-8, ANL/ENG 78-02, *DOE-1 Program Manual,* S.C. Diamond, H.L. Horak, B.D. Hunn, J.L. Peterson, M.A. Roschke, E.F. Tucker, Los Alamos Scientific Laboratory, October 1978.

### 1978-79

GR-14, *Thermal Loads Analysis of the International Energy Agency Test Building IEA Using DOE-1, Phase I.* Palermo, Italy, June 1978.

GR-15, *Thermal Load Analysis of the International Energy Agency Test Building IEA Using DOE-1, Phase II* DOE-1 Group, Edinburgh, Scotland, November 1978.

GR-16, *Parametric Analysis of the International Energy Agency Test Building IEA-0 Using DOE-1,* DOE-1 Group, Edinburgh, Scotland, November 1978.

GR-17, *The DOE-2 Building Energy Analysis Computer Program.* B.D. Hunn, BEAG (LBL), March 8, 1979. Presented at the Conservation/Energy Management by Design Conference, El Paso, TX.

GR-18, EEB-DOE-2 79-6, LBL-8974, *DOE-2: A New State-of-the-Art Computer Program for the Energy Utilization Analysis of Buildings.* M. Lokmanhekim, F. Buhl, R. Curtis, S. Gates, J. Hirsch, S. Jaeger, A.H. Rosenfeld, F. Winkelmann, B. Hunn, M. Roschke, G. Leighton, and H. Ross. Presented at the Second International CIB Symposium on Energy Conservation in the Built Environment, Copenhagen, Denmark, May 27-June 1, 1979.

GR-19, *Thermal Load Analysis of the Avonbank Buildings Using DOE-2,* Building Energy Analysis Group, Copenhagen, Denmark, May 1979.

GR-29, UC-95d, LBL-8772, *Using DOE-2 at Lawrence Berkeley Laboratory.* Jewson Enterprises. September 1979.

GR-30, *Thermal Load Analysis of the Avonbank Building Using DOE-2.1 (Parametric Studies),* M. Lokmanhekim, F.C. Winkelmann, and W.F. Buhl, Zurich, Switzerland. December 1979.

EEB-DOE-2 79-1, LBL-8689, *DOE-2 Users Guide,* Building Energy Analysis Group, February 1979.

EEB-DOE-2 79-2, LBL-8688, *DOE-2 BDL Summary,* Building Energy Analysis Group, February 1979.

EEB-DOE-2 79-3, LBL-8679, *DOE-2 Sample Run Book,* Building Energy Analysis Group, February 1979.

EEB-DOE-2 79-4, LBL-8706, *DOE-2 Reference Manual,* Group WX-4, Los Alamos Scientific Laboratory, February 1979.

EEB-DOE-2 79-5, LBL-8705, *DOE-2 Program Manual,* Group WX-4 Los Alamos Scientific Laboratory, February 1979.

### 1980

EEB-BEAG 80-1, LBL-10690, *Manual for UNIX Users.* Plot: A UNIX Program for including Graphics in Documents, R. Curtis, April 1980.

EEB-DOE-2 80-1, LBL-8688 (Rev.), *DOE-2 BDL Summary,* Building Energy Analysis Group, May 1980.

EEB-DOE-2 80-2, LBL-8689 (Rev.), *DOE-2 Users Guide,* Building Energy Analysis Group, May 1980.

EEB-DOE-2 80-4, LBL-8706 (Rev.), *DOE-2 Reference Manual,* Building Energy Analysis Group, May 1980.

EEB-DOE-2 80-5, LBL-11526, *Application of DOE-2 to Residential Building Energy Performance Standards,*

M. Lokmanhekim, D.B. Goldstein, M.D. Levine, and A.H. Rosenfeld. May 1980.

EEB-DOE-2 80-6, LBL-11530, *Using DOE-2.1 at Lawrence Berkeley Laboratory,* Building Energy Analysis Group, September 1980.

EEB-DOE-2 80-7, LBL-11584, *Discussion on ASHRAE Weighting Factor Methods,* M. Lokmanhekim and F.C. Winkelmann. September 1980.

**1981**

EEB-DOE-2 81-1, LBL-12300, *The Theoretical Basis of the DOE-2 Building Energy-Use Analysis Program,* R.B. Curtis, April 1981.

EEB-DOE-2 81-2, LBL-12299, *Use of a Diesel Engine-Driven Emergency Power Generating System for Peak Shaving in Buildings,* S. Choi, J. Hirsch, and B. Birdsall, February 1981.

EEB-DOE-2 81-4, LBL-12298, *Life-Cycle Cost and Energy-Use Analysis of Sun-Control and Daylighting Options in a High-Rise Office Building,* F.C. Winkelmann and M. Lokmanhekim, May 1981.

EEB-DOE-2 81-5, LBL-8688 Rev. 2, *DOE-2 BDL Summary,* Building Energy Analysis Group, May 1981.

EEB-DOE-2 81-6, LBL-8689 Rev. 2, *DOE-2 Users Guide,* Building Energy Analysis Group, May 1981.

EEB-DOE-2 81-7, LBL-8706 Rev. 2, *DOE-2 Reference Manual,* Group WX-4, Los Alamos National Laboratory, May 1981.

EEB-DOE-2 81-8, LBL 12764, *Glazing Optimization for Energy Efficiency in Commercial Office Buildings,* R. Johnson, S. Selkowitz, F.C. Winkelmann, and M. Zentner, October 1981.

**1982**

EEB-DOE-2 82-1, LBL-11353, LA-8520-M, *DOE-2 Engineers Manual,* Building Energy Analysis Group and Group-11, Los Alamos National Laboratory, November 1982.

EEB-DOE-2 82-2, LBL-14026, *Simulation of HVAC Equipment in the DOE-2 Program,* J.J. Hirsch. Presented at the International Conference on Systems Simulation in Buildings, Liege, Belgium, December 1982.

## BUILDING ENERGY PERFORMANCE STANDARDS (BEPS)

**1979**

EEB-BEPS 79-1, *Economic Impacts of Building Energy Performance Standards.* Co-authored with PNL and ORNL, 1979.

EEB-BEPS 79-2, LBL-9816, *Evaluation of Residential Energy Performance Standards,* M.D. Levine, D.B. Goldstein, M. Lokmanhekim, and A.H. Rosenfeld, 1979. Presented at the DOE/ASHRAE Conference on the Thermal Performance of the Exterior Envelopes of Buildings, Orlando, FL, December 1979.

EEB-BEPS 79-3, LBL-9817, *Residential Energy Performance Standards: Comparison of HUD Minimum Property Standards and DOE's Proposed Standards.* M.D. Levine, D.B. Goldstein, and B. O'Neal, September 1979.

**1980**

EEB-BEPS 80-1, LBL-9731, *Uncertainty—an Argument for more Stringent Energy Conservation.* P.P. Craig, M.D. Levine, and J. Mass, to be published in *Energy: The International Journal, 1980.*

EEB-BEPS 80-2, *Testimony on BEPS,* before the California Energy Commission. M.D. Levine, January 1980.

EEB-BEPS 80-3, LBL-9110, *Residential Energy Performance Standards: Methodology and Assumptions.* D.B. Goldstein, M.D. Levine, and J. Mass, March 1980.

EEB-BEPS 80-4, *Data Base of DOE-2A Computer Simulations of Residential Building Energy Use,* used for DOE's Proposed Building Energy Performance Standards, May 1980.

EEB-BEPS 80-5, LBL-10440, *Energy Budgets and Masonry Houses: A Preliminary Analysis of the Comparative Energy Performance of Masonry and Wood-Frame Houses.* D.B. Goldstein, M.D. Levine, and J. Mass, May 1980.

EEB-BEPS 80-6, *Implementation of the 1978 California Building Energy Standards: A Case Study.* L. Danielson, June 1980.

EEB-BEPS 80-7, *Testimony on BEPS,* before the Senate Subcommittee on Energy Regulation. M.D. Levine, June 1980.

EEB-ECON 80-1, *Energy Conservation and Energy Decentralization: Issues and Prospects.* M.D. Levine and P.P. Craig, presented at AAAS Symposium, January 1980, and included in AAAS book.

EEB-ECON 80-2, *Energy Use and Appliance Acquisition Mechanisms.* F. Reid, February 1980.

EEB-AEPS 80-1, LBL-10797, *A Model for Water Heater Energy Consumption and Hot Water Use: Analysis of Survey and Test Data on Residential Hot Water Heating.* R.D. Clear and D.B. Goldstein, May 1980.

EEB-AEPS 80-2, *Economic Analysis Document: Consumer Products Energy Performance Standards.* Coauthor with SAI and other contractors, June 1980.

## ENERGY CONSERVATION INSPECTION SERVICE

### 1978

EEB-ECIS 78-1, UCID-4036, *Preliminary Report of the Energy Conservation Inspection Service.* S. Beckerman, R. Codina, B. Cornwall, and A.K. Meier, March 1978.

## ENERGY PERFORMANCE OF BUILDINGS

### 1978

EEB-ENV 78-1, LBL-6856, *Diagnostic Tests Determining the Thermal Response of a House.* R. Sonderegger, November 1977. *ASHRAE Trans., 84*(1), 1978.

EEB-ENV 78-2, LBL-7822, UC-92d, *Air Infiltration in Buildings: Literature Survey and Proposed Research Agenda.* H.D. Ross and D.T. Grimsrud, February 1978.

EEB-ENV 78-3, LBL-6849, *An Automated Controlled-Flow Air Infiltration Measurement System.* P.E. Condon, D.T. Grimsrud, M.H. Sherman, and R.C. Kammerud. To be published in *Proceedings of the Symposium on Air Infiltration and Air Change Measurements, ASTMM,* Washington, D.C., March 1978.

EEB-ENV 78-4, LBL-7830, *Case Studies in Air Infiltration.* D.T. Grimsrud. Published as a chapter in *Air Infiltration in Buildings,* International Energy Agency Draft Program Plan, May 1978.

EEB-ENV 78-5, LBL-7824, *Infiltration-Pressurization Correlations: Detailed Measurements on a California House.* D.T. Grimsrud, M.H. Sherman, R.C. Diamond, P.E. Condon, and A.H. Rosenfeld, August 1978. *ASHRAE Trans., 85*(1), 1979.

EEB-ENV 78-6, LBL-8394, *An Intercomparison of Tracer Gases Used for Air Infiltration Measurements.* D.T. Grimsrud, M.H. Sherman, J.E. Janssen, A.N. Pearman, and D. Harrje, November 1979.

### 1979

EEB-ENV 79-2, Pub. 266, *Stop the Draft.* R.C. Diamond. November 1978.

EEB-ENV 79-3, LBL-8822, *A New Measurement Strategy for In-Situ Testing of Wall Thermal Performance.* P.E. Condon, W.L. Carroll, and R.C. Sonderegger, September 1979. Presented at the DOE/ASHRAE Conference on the Thermal Performance of the Exterior Envelopes of Buildings, Orlando, FL, December 1979.

EEB-ENV 79-4, LBL-8785, *Infiltration-Pressurization Correlation: Surface Pressures and Terrain Effects.* M.H. Sherman, D.T. Grimsrud, and R.C. Diamond, March 1979. *ASHRAE Trans., 85*(2), 1979.

EEB-ENV 79-5, LBL-8925, *Thermal Performance of Buildings and Building Envelope Systems: An Annotated Bibliography.* W.L. Carroll, April 1979. Presented at the DOE/ASTM Thermal Insulation Conference, Tampa, FL, October 23-24, 1978.

EEB-ENV 79-6, LBL-8949, *Electric Co-Heating: A Method for Evaluating Seasonal Heating Efficiencies and Heat Loss Rates in Dwellings.* R.C. Sonderegger and M.P. Modera, March 1979. Published in *Proceedings of the Second Symposium on Energy Conservation in the Built Environment,* Copenhagen, Denmark, May 27-June 1, 1979.

EEB-ENV 79-7, LBL-8828, *Air Leakage, Surface Pressures and Infiltration Rates in Houses.* D.T. Grimsrud, M.H. Sherman, R.C. Diamond, and R.C. Sonderegger, March 1979. Published in *Proceedings* of the Second International CIB Symposium on Energy Conservation in the Built Environment, Copenhagen, Denmark, May 27-June 1, 1979.

EEB-ENV 79-8, LBL-9157, *Infiltration and Air Leakage Comparisons: Conventional and Energy Efficient House Designs.* D.T. Grimsrud, M.H. Sherman, A.K. Blomsterberg, and A.H. Rosenfeld, October 1979.

EEB-ENV 79-9, LBL-9625, *A Model Correlating Air Tightness and Air Infiltration in Houses.* A.K. Blomsterberg, M.H. Sherman, and D.T. Grimsrud, October 1979.

EEB-ENV 79-10, LBL-9162, *The Low Pressure Leakage Function of a Building.* M.H. Sherman, D.T. Grimsrud, and R.C. Sonderegger, November 1979.

**1980**

EEB-EPB 80-1 (EEB-ENV 79-23), LBL-10117, *In-situ Measurements of Residential Energy Performance Using Electric Co-heating.* R. Sonderegger, P.E. Condon, and M.P. Modera, January 1980.

EEB-EPB 80-2, LBL-10163, *Infiltration-Pressurization Correlation: Simplified Physical Modeling.* M.H. Sherman and D.T. Grimsrud, March 1980.

EEB-EPB 80-3, LBL-10705, *Air Infiltration Measurement Techniques.* M.H. Sherman, D.T. Grimsrud, P.E. Condon, and B.V. Smith, April 1980.

EEB-EPB 80-4, LBL-9821, *Measurement of In-situ Dynamic Thermal Performance of Building Envelopes Using Heat Flow Meter Arrays.* P.E. Condon and W.L. Carroll, July 1979. Presented at the DOE/ASHRAE Conference on the Thermal Performance of the Exterior Envelopes of Buildings, Orlando, FL, December 3-6, 1979.

EEB-EPB 80-6, LBL-10996, *Pressurization Test Results: BPA Energy Conservation Study.* D.L. Krinkel, D.J. Dickerhoff, J.J. Casey, and D.T. Grimsrud, December 1980.

EEB-EPB 80-7, Pub. 313, *What About Fireplaces?* R.C. Diamond, September 1980.

EEB-EPB 80-8, LBL-10701, UC-95d, *Determination of In-Situ Performance of Fireplaces.* M.P. Modera, and R. Sonderegger, August 1980.

EEB-EPB 80-9, LBL-Pub. 313, *What About the Fireplaces?* R.C. Diamond, September 1980.

EEB-EPB 80-10, LBL-10996, *Pressurization Test Results: BPA Energy Conservation Study,* D.L. Krinkel, D.J. Dickerhoff, J.J. Casey, and D.T. Grimsrud, December 1980.

EEB-EPB 80-11, LBL-10852, *The Measurement of Infiltration Using Fan Pressurization and Weather Data,* M.H. Sherman and D.T. Grimsrud, October 1980.

**1981**

EEB-EPB 81-1, LBL-Pub. 384, *Find and Fix the Leaks,* R.C. Diamond, January 1981.

EEB-EPB 81-2, LBL-12259, *The Mobile Infiltration Test Unit—Its Design and Capabilities: Preliminary Experimental Results,* A.K. Blomsterberg, M.P. Modera, and D.T. Grimsrud, January 1981.

EEB-EPB 81-3, LBL-11674, *Infiltration and Air Conditioning: A Case Study,* D.J. Dickerhoff, D.T. Grimsrud, and B.B. Shohl, February 1981.

EEB-EPB 81-5, LBL-12924, *Infiltration and Indoor Air Quality in Energy Efficient Houses in Eugene, Oregon, R.D. Lipschutz, J.R. Girman, J.B. Dickinson, J.R. Allen, and G.W. Traynor, August 1981.*

EEB-EPB 81-10, LBL-12221, *Infiltration Measurements in Audit and Retrofit Programs,* D.T. Grimsrud, R.C. Sonderegger, and M.H. Sherman, April 1981.

EEB-EPB 81-13, LBL-13520, *A Predictive Air Infiltration Model—Field Validation and Sensitivity Analysis,* M.H. Sherman, M.P. Modera, and D.T. Grimsrud, October 1981.

EEB-EPB 81-14, LBL-13436, *The Envelope Thermal Test Unit (ETTU): Field Measurement of Wall Performance,* R.C. Sonderegger, M.H. Sherman, and J.W. Adams, October 1981.

EEB-EPB 81-15, LBL-13505, *Guidelines for Infiltration Reduction in Light-Frame Buildings,* R.C. Diamond and D.T. Grimsrud, September 1981.

EEB-EPB 81-16, LBL-13504, *Long-Term Infiltration Measurements in a Full-Scale Test Structure,* M.P. Modera, M.H. Sherman, and D.T. Grimsrud, September 1981.

EEB-EPB 81-17, LBL-13503, *Dynamic Measurement of Wall Thermal Performance in the Field,* M.H. Sherman, J.W. Adams, and R.C. Sonderegger, December 1981.

EEB-EPB 81-18, LBL-13508, *A Simplified Method for Calculating Heating and Cooling Energy in Residential Buildings,* R.C. Sonderegger and J.Y. Garnier, October 1981.

EEB-EPB 81-19, LBL-13509, *A Predictive Air Infiltration Model—Long-Term Field Test Validation,* M.P. Modera, M.H. Sherman, and D.T. Grimsrud, November 1981.

EEB-EPB 81-20, LBL-13510, *The Determination of the Dynamic Performance of Walls,* M.H. Sherman, R.C. Sonderegger, and J.W. Adams, November 1981.

EEB-EPB 81-21, LBL-Pub. 425R, *Computerized, Instrumented, Residential Analysis (CIRA),* R.C Sonderegger, J.Y. Garnier, and J.D. Dixon, November 1981.

**1982**

EEB-EPB, LBL-PUB-442, *CIRA Reference Manual.* Energy Performance of Buildings Group, May 1982.

EEB-EPB, LBL-PUB-448, *CIRA Source Listings and Source Disks.* Energy Performance of Buildings Group, July 1982.

EEB-EPB 82-4, LBL-12742, *Results of the Bonneville Power Administration Weatherization and Tightening Projects at the Midway Substation Residential Community.* J.B. Dickinson, D.T. Grimsrud, D.L. Krinkel, and R.D. Lipschutz, February 1982.

EEB-EPB 82-5, LBL-13949, *Wind and Infiltration Interaction for Small Buildings.* M.H. Sherman and D.T. Grimsrud. Presented at ASCE Annual Meeting, New Orleans LA, October 23-29, 1982.

EEB-EPB 82-6, LBL-13678, *A Comparison of Alternate Ventilation Strategies.* M.H. Sherman and D.T. Grimsrud. Presented at the Third AIC Conference, London, UK, September 1982.

EEB-EPB 82-7, LBL-14733, *Infiltration and Leakage Measurements in New Houses Incorporating Energy Efficient Features.* R.D. Lipschutz, J.B. Dickinson, and R.C. Diamond. To be published in the proceedings of the ACEEE 1982 Summer Study in Energy Efficient Buildings, Santa Cruz CA, August 22-28, 1982.

EEB-EPB 82-8, LBL-14734, *Results of Recent Weatherization Retrofit Projects.* J.B. Dickinson, R.D. Lipschutz, B. O'Regan, and B.S. Wagner. To be published in the proceedings of the ACEEE 1982 Summer Study in Energy Efficient Buildings, Santa Cruz CA, August 22-28, 1982.

EEB-EPB 82-9, LBL-14735, *Component Leakage Testing in Residential Buildings,* D.J. Dickerhoff, D.T. Grimsrud, and R.D. Lipschutz. To be published in the proceedings of the ACEEE 1982 Summer Study in Energy Efficient Buildings, Santa Cruz CA, August 22-28, 1982.

## HOSPITALS

**1978**

EEB-Hosp 78-1, UC-95d, LBL-8257, *Hospital Ventilation Standards and Energy Conservation: Proceedings of the 1978 International Working Conference,* October 1978.

EEB-Hosp 78-2, UCID-8060, *Hospital Ventilation Standards and Energy Conservation: Bibliographic Keywords.* R. DeRoos, R. Banks, and D. Rainer, September 1978.

EEB-Hosp 78-3, UC-95d, LBL-8316, *Hospital Ventilation Standards and Energy Conservation: A Summary of the Literature with Conclusions and Recommendations, FY 78 Final Report.* R. DeRoos, R. Banks, D. Rainer, J. Anderson, and G. Michaelsen, August 1979.

**1979**

EEB-Hosp 79-1, UCID-8108, *Energy Study of the Naval Regional Medical Center.* Consultants Computation Bureau, January 1979.

EEB-Hosp 79-2, LBID-082, *Energy Efficient Water Use in Hospitals: Final Summary Report.* T. Alereza, A. Benjamin, and B. Gilmer, July 1979.

EEB-Hosp 79-3, LBL-9356, *Hospital Energy Audits: A Bibliography.* R.I. Pollack, J. Boe, G.D. Roseme, M. Chatigny, and D.D. Devincenzi, November 1979.

EEB-Hosp 79-4, LBID-111, *Energy Conservation in Hospitals: Actions to Improve the Impact of the National Energy Act.* R.I. Pollack, December 1979.

EEB-Hosp 79-5, LBL-9987, *Hospital Laundry Standards and Energy Conservation: A Program Plan.* D.R. Battles, D. Vesley, and R.S. Banks, January 1980.

EEB-Hosp 79-6, LBL-10475, *Chemical Contamination of Hospital Air.* D. Rainer, and G.S. Michaelsen, March 1980.

EEB-Hosp 79-7, LBL-10628, *Hospital Ventilation Standards and Energy Conservation: A Review of Governmental and Private Agency Energy Conservation Initiatives.* R.S. Banks and D. Rainer, March 1980.

## SCHOOLS

**1978-79**

EEB-Schools 78-1, LBL-7861, *Instrumentation Design for Energy Analysis in Three Elementary Schools.* A.J. Heitz, A.H. Rosenfeld, T. Fujita and H.W. Sigworth, Jr., October 1978.

EEB-Schools 78-2, UCID-8063, *Status Report: Energy Monitoring Results,* Eastridge Elementary School, Lincoln, Nebraska. H.W. Sigworth, Jr. and A.H. Rosenfeld, August 1978.

EEB-Schools 78-3, UCID-8064, *Energy Savings Due to Night Thermostat Setback at an Elementary School.*

H.W. Sigworth, Jr. and A.H. Rosenfeld, October 1978.

EEB-Schools 78-4, LBL-9449, *DOE-1 Simulations of Ten Elementary Schools: Base Case Reports.* H.W. Sigworth, Jr., R.B. Curtis, M.T. Bee, and A.H. Rosenfeld, November 1978.

EEB-SCH-Colleges 78-1, LBL-7862, *A Final Report on a Pilot Study of Energy Conservation Strategies on Community College Campuses.* P.C. Rowe and C.M. York, August 1978.

EEB-SCH-Colleges 78-2, UC-95d, LBL-7813, *Energy Management: A Program of Energy Conservation for the Community College Facility.* P. Rowe and H. Miller, October 1978.

EEB-Schools 79-1, *Status Report: Modification Costs for 10 Schools· "Saving Schoolhouse Energy" Program.* A.J. Heitz and A.H. Rosenfeld, January 1979.

EEB-Schools 79-2, LBL-8449, *DOE-1 Simulations of Nine Elementary Schools: Retrofit Reports.* H.W. Sigworth, Jr., M.T. Bee, R.B. Curtis, and A.H. Rosenfeld, January 1979.

EEB-79-3, UC-95d, LBL-9106, *Saving Schoolhouse Energy: Final Report.* J. Rudy, H.W. Sigworth, and A.H. Rosenfeld, June 1979.

## VENTILATION

### 1978

EEB-Vent 78-1, *Energy Efficient Buildings Mobile Laboratory,* Current Status—January 15, 1978. J.V. Berk, C.D. Hollowell, C. Lin and J.H. Pepper; January 1978.

EEB-Vent 78-2, UC-11, LBL-7817 Rev., *Design of a Mobile Laboratory for Ventilation Studies and Indoor Air Pollution Monitoring.* J.V. Berk, C.D. Hollowell, C.I. Lin, and J.H. Pepper, April 1978.

EEB-Vent 78-3, LBL-7831, *Indoor Air Quality Measurements in Energy Efficient Buildings.* C.D. Hollowell, J.V. Berk, and G.W. Traynor. Presented at the 71st Air Pollution Control Association Meeting, Houston, TX, June 25-19, 1978.

EEB-Vent 78-4, *Energy Efficient Buildings Mobile Laboratory, Current Status—June 15, 1978.* J.V. Berk, C.D. Hollowell, C.I. Lin, and J.H. Pepper, June 1978.

EEB-Vent 78-5, UC-11, LBL-7809, *Human Disease from Radon Exposures: The Impact of Energy Conservation in Buildings.* R.J. Budnitz, J.V. Berk, C.D. Hollowell, W.W. Nazaroff, A.V. Nero, and A.H. Rosenfeld, August 1978.

EEB-Vent 78-6, LBL-8470, *Impact of Reduced Infiltration and Ventilation on Indoor Air Quality in Residential Buildings.* C.D. Hollowell, J.V. Berk, and G.W. Traynor, November 1978. Presented at the ASHRAE Symposium on Air Infiltration, Philadelphia, PA, January 1979.

LBL-7832, *Combustion-Generated Indoor Air Pollution.* C.D. Hollowell, and G.W. Traynor, April 1978.

### 1979

EEB-Vent 79-1, LBID-045, *Studies of Effects of Energy Conservation Measures on Air Hygiene in Public Buildings.* R.L. Dimmick and H. Wolochow, April 1979.

EEB-Vent 79-2, LBL-8892, *Indoor Air Quality in Energy-Efficient Buildings.* C.D. Hollowell, J.V. Berk, C. Lin, and I. Turiel, March 1979. Presented at the Second International CIB Symposium on Energy Conservation in the Built Environment, Copenhagen, Denmark, May 27-June 1, 1979.

EEB-Vent 79-3, LBL-8893, *Automatic Variable Ventilation Control Systems Based on Air Quality Detection.* I. Turiel, C.D. Hollowell, and B.E. Thurston, March 1979. Presented at the Second International CIB Symposium on Energy Conservation in the Built Environment, Copenhagen, Denmark, May 27-June 1, 1979.

EEB-Vent 79-4, LBL-8894, *Indoor Air Quality Measurements in Energy-Efficient Houses.* J.V. Berk, C.D. Hollowell, C. Lin, July 1979. Presented at the Air Pollution Control Association 72nd Annual Meeting, Cincinnati, OH, June 25-29, 1979.

EEB-Vent 79-5, UC-95d, LBL-9174, *The Effects of Energy Efficient Ventilation Rates on Indoor Air Quality at a California High School.* J.V. Berk, C.D. Hollowell, C. Lin, and I. Turiel, July 1979.

EEB-Vent 79-6, LBL-9284, *Building Ventilation and Indoor Air Quality Program.* Chapter from Energy and Environment Division Annual Report, July 1979.

EEB-Vent 79-7, LBL-9397, *Indoor/Outdoor Measurements of Formaldehyde and Total Aldehydes.* C. Lin, R. Anaclerio, D. Anthon, L. Fanning, and C.D. Hollowell, July 1979. Presented at the 178th National Meeting of the American Chemical Society, Division of Environmental Chemistry, Washington, D.C., September 9-14, 1979.

EEB-Vent 79-8, LBL-9402, *Radon-222 in Energy-Efficient Buildings.* C.D. Hollowell, M.L. Boegel, J.G. Ingersoll, and W.W. Nazaroff, June 1979. Presented at the American Nuclear Society Meeting, San Francisco, CA, November 11-16, 1979.

EEB-Vent 79-9, LBL-9379, *Impact of Energy Conservation in Buildings on Health.* C.D. Hollowell, J.V. Berk, C. Lin, W.W. Nazaroff, and G. Traynor, June 1979. Presented at the International Conference on Energy Use Management, Los Angeles, CA, October 22-26, 1979.

EEB-Vent 79-10, LBL-9380, *Variable Ventilation Control Systems: Saving Energy and Maintaining Indoor Air Quality.* I. Turiel, C.D. Hollowell, and B.E. Thurston, June 1979. Presented at the International Conference on Energy Use Management, Los Angeles, CA, October 22-26, 1979.

EEB-Vent 79-11, LBL-9381, *Air-to-Air Heat Exchangers: Saving Energy and Improving Indoor Air Quality.* G. Roseme, C.D. Hollowell, A. Meier, A.H. Rosenfeld, and I. Turiel, June 1979. Presented at the International Conference on Energy Use Management, Los Angeles, CA, October 22-26, 1979.

EEB-Vent 79-12, LBL-9382, *The Effect of Reduced Ventilation on Indoor Air Quality and Energy Use in Schools.* J.V. Berk, C.D. Hollowell, C. Lin, and I. Turiel, June 1979. Presented at the International Conference on Energy Use Management, Los Angeles, CA, October 22-26, 1979.

EEB-Vent 79-13, LBL-9403, *A Flow Control System for Accurate Sampling of Air.* D.W. Anthon, L.Z. Fanning, C.D. Hollowell, and C. Lin, December 1979. Submitted to *Analytical Chemistry.*

EEB-Vent 79-14, LBL-10246, *Instructions for Operating LBL Passive Environmental Radon Monitor (PERM).* M.L. Boegel, W.W. Nazaroff, and J.G. Ingersoll, August 1979.

EEB-Vent 79-15, LBL-9986, *An Improved Technique for Measuring Radon Daughter Working Levels in Residences.* W.W. Nazaroff, December 1979.

EEB-Vent 79-16, LBL-9560, *Radon in Energy Efficient Residences. C.D. Hollowell, J.V. Berk, M.L. Boegel, J.G. Ingersoll,* D.L. Krinkel and W.W. Nazaroff, February 1980.

EEB-Vent 79-17, LBID-084, *Formaldehyde in Office Trailers.* L.Z. Fanning, October 1979.

EEB-Vent 79-18, LBID-085, *Contaminant Control in the Built Environment: State-of-the-Art Summary.* R.G. Langenborg, July 1979.

EEB-Vent 79-19, LBL-9578, *Ventilation and Odor Control: Prospects for Energy Efficiency.* W.S. Cain, L.G. Berglund, R.A. Duffee and A. Turk, November 1979.

**1980**

EEB-Vent 80-1, LBL-10390, *Building Ventilation and Indoor Air Quality, 1979 Annual Report.* C.D. Hollowell, January 1980.

EEB-Vent 80-2, LBL-10553, *Effects of Energy Conservation Measures on Air Hygiene in Public Buildings: Final Report.* R.L. Dimmick and H. Wolochow, February 1980.

EEB-Vent 80-3, LBL-10391, *Building Ventilation and Indoor Air Quality.* C.D. Hollowell, J.V. Berk, M.L. Boegel, R.R. Miksch, W.W. Nazaroff, G.W. Traynor, January 1980.

EEB-Vent 80-4, LBL-10525, *Indoor Radiation Exposures from Radon and its Daughters: A View of the Issues.* A.V. Nero, March 1980.

EEB-Vent 80-5, LBL-10527, *The Impact of Reduced Ventilation on Indoor Air Quality in Residential Buildings.* J.V. Berk, C.D. Hollowell, J.H. Pepper, and R.A. Young, March 1980.

EEB-Vent 80-6, LBL-10222, *The Control of Radon and Radon Daughter Concentrations in a Low Infiltration House Using Mechanical Ventilation with Heat Recovery.* W.W. Nazaroff, M.L. Boegel, C.D. Hollowell and G.D. Roseme, March 1980.

EEB-Vent 80-7, LBL-11378, *Trace Organics in Offices.* H.E. Schmidt, C.D. Hollowell, R.R. Miksch, and A.S. Newton, April 1980.

EEB-Vent 80-8, LBL-8894 Rev, *Indoor Air Quality Measurements in Energy-Efficient Buildings.* J.V. Berk, C.D. Hollowell, J.H. Pepper, and R. Young, May 1980.

EEB-Vent 80-9, LBL-10223, *The Effects of Energy-Efficient Ventilation Rates on Indoor Air Quality at an Ohio Elementary School.* J.V. Berk, R. Young, C.D. Hollowell, I. Turiel, and J. Pepper, April 1980.

EEB-Vent 80-10, LBL-9749, *Residential Ventilation with Heat Recovery: Improving Indoor Air Quality and Saving Energy.* G.D. Roseme, J.V. Berk, M.L. Boegel, C.D. Hollowell, A.H. Rosenfeld, G.W. Traynor, and I. Turiel, April 1980.

EEB-Vent 80-11, LBL-9785, *A Modified Pararosaniline Method for Determination of Formaldehyde in Air.* R.R. Miksch, D.W. Anthon, L.Z. Fanning, K. Revzan, J. Glanville, and C.D. Hollowell, April 1980.

EEB-Vent 80-12, LBL-10629, *Instructions for Operating the LBL Formaldehyde Sampler.* L.Z. Fanning and R.R. Miksch, April 1980.

EEB-Vent 80-13, LBL-11097, *Operating Instructions for LBL Radon Measurement Facilities.* J.G. Ingersoll, June 1980.

EEB-Vent 80-15, LBL-10496, *Occupant-Generated $CO_2$ as an Indicator of Ventilation Rate.* I. Turiel and J. Rudy, April 1980.

EEB-Vent 80-16, LBL-11771, *A Survey of Radionuclide Contents and Radon Emanation on Rates in Building Materials Used in the U.S.* J.G. Ingersoll, B.D. Stitt, and G.H. Zapalac.

EEB-Vent 80-17, LBL-11052, *Radon Daughter Exposures in Energy Efficient Buildings.* A.V. Nero.

EEB-Vent 80-18, LBL-11793, *Performance of Residential Air-to-Air Heat Exchangers: Test Results and Methods.* W.J. Fisk, and G.D. Roseme, and C.D. Hollowell.

EEB-Vent 80-19, LBL-10479, *The Effect of Reduced Ventilation on Indoor Air Quality in An Office Building.* I. Turiel, C.D. Hollowell, R.R. Miksch, J.V. Rudy, and R.A. Young.

EEB-Vent 80-21, LBL-10769, *Alpha Spectroscopic Techniques for Field Measurements of Radon Daughters.* W.W. Nazaroff, A.V. Nero, and K. Revzan.

EEB-Vent 80-23, LBL-11828, *Indoor Air Quality Under Energy Efficient Ventilation Rates at a New York City Elementary School.* R.A. Young, J.V. Berk, C.D. Hollowell, J.H. Pepper and I. Turiel.

**1981**

EEB-Vent 81-1, *Building Ventilation and Indoor Air Quality, 1980 Annual Report,* C.D. Hollowell et al., January 1981.

EEB-Vent 81-2, LBL-12189, *Impact of Energy-Conserving Retrofits on Indoor Air Quality in Residential Housing,* J.V. Berk, R.A. Young, S.R. Brown, and C.D. Hollowell, January 1981.

EEB-Vent 81-3, LBID-330, *VIAQ Data Base Tutorial,* S. Lepman, January 1981.

EEB-Vent 81-4, LBL-12199, *Organic Contaminants: A Bibliography,* S.R. Lepman, R.R. Miksch, and C.D. Hollowell, January 1981.

EEB-Vent 81-5, LBL-12200, *Radon: A Bibliography,* S.R. Lepman, M.L. Boegel, and C.D. Hollowell, January 1981.

EEB-Vent 81-6, LBL-12280, *Test Results and Methods—Residential Air-to-Air Heat Exchangers for Maintaining Indoor Air Quality and Saving Energy,* W.J. Fisk and G.D. Roseme, February 1981.

EEB-Vent 81-7, LBL-12387, *Indoor Air Quality: Potential Audit Strategies,* G.W. Traynor, March 1981.

EEB-Vent 81-8, LBL-12484, *Measuring Radon Source Magnitude in Residential Buildings,* W.W. Nazaroff, M.L. Boegel, and A.V. Nero, August 1981.

EEB-Vent 81-9, LBL-12589, *Ventilation Requirements for Control of Occupancy Odor and Tobacco Smoke Odor: Laboratory Studies,* W.S. Cain, B. Isseroff, B.P. Leaderer, E.D. Lipsitt, R.J. Huey, D. Perlman, L.G. Bergdund, and J.D. Dunn, April 1981.

EEB-Vent 81-10, LBL-12632, *Ventilation/Odor Study Field Study (Vol. II Appendices contained in LBID-390),* R.A. Duffee and P.E. Jann, April 1981.

EEB-Vent 81-11, LBL-12847, *Energy-Conserving Retrofits and Indoor Air Quality in Residential Housing,* R.A. Young, J.V. Berk, S.R. Brown, and C.D. Hollowell, September 1981.

EEB-Vent 81-12, LBL-12590, *Radon and Aldehyde Concentrations in the Indoor Environment,* D.J. Moschandreas and H.E. Rector, April 1981.

EEB-Vent 81-13, LBL-12740, *The Generation of Dry Formaldehyde at PPB to PPM Levels by the Vapor-Phase Depolymerization of Trioxane,* K.L. Geisling, R.R. Miksch, and S.R. Rappaport, May 1981.

EEB-Vent 81-14, LBL-12526, *A Fast and Accurate Method for Measuring Radon Exhalation Rates from Building Materials,* J.G. Ingersoll, B.D. Stitt, and G.H. Zapalac, April 1981.

EEB-Vent 81-15, LBL-12777, *Midway House-Tightening Project: A Study of Indoor Air Quality,* F.J. Offermann, J.R. Girman, and C.D. Hollowell, May 1981.

EEB-Vent 81-16, LBL-12886, *Indoor Air Pollution from Domestic Combustion Appliances,* G.W. Traynor, M.G. Apte, J.R. Girman, and C.D. Hollowell, June 1981.

EEB-Vent 81-17, LBL-12887, *Indoor Air Quality,* C.D. Hollowell, June 1981.

EEB-Vent 81-18, LBL-11870, *A Time-Dependent Method for Characterizing the Diffusion of Radon-222 in Concrete,* G.H. Zapalac, July 1981.

EEB-Vent 81-19, LBL-12924, *Infiltration and Indoor Air Quality in Energy Efficient Buildings in Eugene, Oregon,* R.D. Lipschutz, J.R. Girman, J.B. Dickinson, J.R. Allen, and G.W. Traynor, August 1981.

EEB-Vent 81-20, LBL-11854, *A Rapid Spectroscopic Technique for Determining the Potential Alpha Energy Concentration of Radon Decay Products,* K.L. Revzan and W.W. Nazaroff, July 1981.

EEB-Vent 81-21, LBL-12945, *Automated System for Measuring Air-Exchange Rate and Radon Concentration in Houses,* W.W. Nazaroff, F.J. Offermann, and A.W. Robb, September 1981.

EEB-Vent 81-22, LBL-13589, *Indoor Air Quality Health Risk Analysis,* A.V. Nero, April 1981.

EEB-Vent 81-23, LBL-12932, *Indoor Radon Sources, Concentrations, and Standards,* A.V. Nero, July 1981.

EEB-Vent 81-24, LBL-12559, *Performance Measurements for Residential Air-to-Air Heat Exchangers,* W.J. Fisk, K.M. Archer, P. Boonchanta, and C.D. Hollowell, November 1981.

EEB-Vent 81-25, LBL-12560, *A New Passive Monitor for Determining Formaldehyde in Indoor Air,* K. Geisling, M.K. Tashima, J.R. Girman, and R.R. Miksch, November 1981.

EEB-Vent 81-26, LBL-12561, *Trace Organic Contaminants in Office Spaces,* R.R. Miksch, C.D. Hollowell, and H. Schmidt, November 1981.

EEB-Vent 81-27, LBL-12562, *Pollutant Emission Rates from Indoor Combustion Appliances and Sidestream Cigarette Smoke,* J.R. Girman, M.G. Apte, G.W. Traynor, and C.D. Hollowell, November 1981.

EEB-Vent 81-28, LBL-12563, *The Effects of Ventilation on Residential Air Pollution Due to Emissions from a Gas-Fired Range,* G.W. Traynor, M.G. Apte, J.F. Dillworth, C.D. Hollowell, and E.M. Sterling, November 1981.

EEB-Vent 81-29, LBL-12564, *Instrumentation for a Radon Research House,* W.W. Nazaroff, K.L. Revzan, and A.W. Robb, July 1981.

EEB-Vent 81-30, LBL-12565, *Distribution of Indoor Radon Concentrations and Source Magnitudes: Measurements and Policy Implications,* A.V. Nero and W.W. Nazaroff, December 1981.

EEB-Vent 81-31, LBL-12566, *Indoor Air Quality in New Energy-Efficient Houses and Retrofitted Houses,* C.D. Hollowell, J.V. Berk, S.R. Brown, J. Dillworth, J.F. Koonce, and R.A. Young, December 1981.

EEB-Vent 81-32, LBL-12567, *Low Infiltration Housing in Rochester, New York: A Study of Air-Exchange Rates and Indoor Air Quality,* F.J. Offermann, C.D. Hollowell, G.D. Roseme, and J.E. Rizzuto, November 1981.

EEB-Vent 81-33, LBL-13194, *A Recommendation for Combining the Standard Analytical Methods for the Determinations of Formaldehyde and Total Aldehydes in Air,* R.R. Miksch and D.W. Anthon, August 1981.

EEB-Vent 81-34, LBL-13195, *Sources and Concentrations of Organic Compounds in Indoor Environments,* C.D. Hollowell and R.R. Miksch, July 1981.

EEB-Vent 81-35, LBL-12948, *Airborne Radionuclides and Radiation in Buildings: A Review,* A.V. Nero, August 1981.

EEB-Vent 81-36, LBL-13306, *Analytical Methods for the Determination of Aldehydes,* R.R. Miksch, D.W. Anthon, L.Z. Zebre, and C.D. Hollowell, September 1981.

EEB-Vent 81-37, LBL-9522, *Technique for Determining Pollutant Emissions from a Gas-Fired Range,* G.W. Traynor, D.W. Anthon, and C.D. Hollowell, December 1981.

EEB-Vent 81-38, LBL-13415, *Radon Concentrations and Infiltration Rates Measured in Conventional and Energy-Efficient Houses,* A.V. Nero, M.L. Boegel, C.D. Hollowell, J.G. Ingersoll, and W.W. Nazaroff, September 1981.

LBL-12927, *Impregnated Filters for the Determination of Formaldehyde In Indoor Environments,* K.L. Geisling (M.S. Thesis), July 1981.

Pub. #384, *Find and Fix the Leaks: A Guide to Air Infiltration Reduction and Indoor Air Quality Control,* January 1981.

LBID-390, *Ventilation/Odor Study Field Studies Final Report,* R.A. Duffee and P.R. Jann, June 1980.

LBID-389, *Automatic Variable Ventilation Control System,* Honeywell, Inc., April 1981.

LBID-427, *Feasibility Study for Using Mechanical Ventilation Systems with Air-to-Air Heat Exchangers to Maintain Satisfactory Air Quality Without Losing the Energy Efficiency of a Tightly Constructed House,* J. Lieble, D. Talbott, and R. Johnson, September 1981.

LBID-448, *IDEPP, An Interactive Data Editing and Plotting Program,* S. Brown, September 1981.

LBID-449, *A Survey Study of Residential Radon Levels,* D.J. Moschandreas, H.E. Rector, and P.O. Tierney, January 1981.

**1982**

EEB-Vent 80-14, LBL-10631, *A Method for Estimating the Exhalation of Radon from Building Materials.* J.G. Ingersoll, B.D. Stitt, and G.H. Zapalac, February 1982.

EEB-Vent 80-16, LBL-11771, "A Survey of Radionuclide Content and Radon Emanation Rates in Building Materials in the United States," J.G. Ingersoll. To be published in *Health Physics.*

EEB-Vent 80-22, LBL-10775, "Radon and Its Daughters in Energy Efficient Buildings." A.V. Nero, M.L. Boegel, C.D. Hollowell, J.C. Ingersoll, W.W. Nazaroff, and K. Revzan in *National Radiation Environment,* K.G. Vohrae et al., eds. Wiley Easter, Ltd., New Delhi, India (1982).

EEB-Vent 82-2, LBL-13843, "Residential Air-to-Air Heat Exchangers: Performance, Energy Savings, and

Economics. W.J. Fisk and I. Turiel, March 1982. Submitted to *Energy and Buildings.*

EEB-Vent 82-3, LBL-14027, *Indoor Air Pollution from Portable Kerosene-fired Space Heaters, Wood-burning Stoves, and Wood-burning Furnaces.* G.W. Traynor, J.R. Allen, M.G. Apte, J.F. Dillworth, J.R. Girman, C.D. Hollowell, and J.F. Koonce, March 1982. Presented at APCA Speciality Meeting: Residential Wood and Coal Combustion, Louisville KY, March 1-2, 1982, proceedings forthcoming.

EEB-Vent 82-4, LBID-501, *A Carbon Monoxide Passive Monitor: A Research Need.* J.R. Girman, G.W. Traynor, and C.D. Hollowell, March 1982.

EEB-Vent 82-5, LBL-14031, "Pollutant Emissions from Portable Kerosene-fired Space Heaters." G.W. Traynor, J.R. Allen, M.G. Apte, J.R. Girman, and C.D. Hollowell, April 1982. To be published in *Environmental Science and Technology.*

EEB-Vent 82-6, LBL-14448, *Experimental and Predicted Overall Heat Transfer Coefficients for Four Residential Air-to-Air Heat Exchangers,* R.A. Seban, A. Rostami, and M. Zarringhalam, May 1982.

EEB-Vent 82-7, LBL-14467, *Exclusion List Methodology for Weatherization Program in the Pacific Northwest,* A.V. Nero, I. Turiel, W.J. Fisk, J.R. Girman, and G.W. Traynor, August 1982.

EEB-Vent 82-9, LBL-13100, *Residential Air-Leakage and Indoor Air Quality in Rochester, New York.* F.J. Offermann, J.B. Dickinson, W.J. Fisk, D.T. Grimsrud, C.D. Hollowell, D.L. Krinkel, and G.D. Roseme, June 1982.

EEB-Vent 82-10, LBL-14616, *Validation of a Passive Sampler for Determining Formaldehyde in Residential Air.* A.T. Hodgson, K.L. Geisling, B. Remijn, and J.R. Girman, June 1982.

EEB-Vent 82-11, LBL-14784, "Energy Savings and Cost-Effectiveness of Heat Exchanger Use as an Indoor Air Quality Mitigation Measure in the BPA Weatherization Program." I. Turiel, W.J. Fisk, and M. Seedall, July 1982. To be published in the proceedings of the ACEEE Summer Study in Energy Efficient Buildings, Santa Cruz CA, August 22-28, 1982, and in *Energy.*

EEB-Vent 82-13, LBL-14907, "Optimizing the Total-Alpha Three-Count Technique for Measuring Concentrations of Radon Progeny in Residences." W.W. Nazaroff, September 1982. Submitted to *Health Physics.*

EEB-Vent 82-14, LBL-14358, *Residential Air-to-Air Heat Exchangers: A Study of Ventilation Efficiencies.* F.J. Offermann, W.J. Fisk, B. Pedersen, and K.L. Revzan, September 1982.

EEB-Vent 80-20, LBID-625, *Contaminant Control in the Built Environment: Formaldehyde and Radon.* K. Alder and C.D. Hollowell, September 1982.

## IAQ-RELATED BOOKS AND PROCEEDINGS

BVIAQ staff contributed significantly to the following publications, which may be obtained from the sources referenced.

National Academy of Sciences, Indoor Pollutants, Washington, 1981 (report of the Committee on Indoor Pollutants, whose membership included Craig Hollowell, with contributions from other LBL staff).

G.F. Clemente, A.V. Nero, F. Steinhäusler, and M.E. Wrenn (editors), *The Assessment of Radon and Daughter Exposure and Related Biological Effects,* proceedings of specialist meeting held in Rome, Italy, March 3-8, 1980, RD Press, Salt Lake City, 1982.

J. Spengler, C.D. Hollowell, D. Moschandreas, and O. Fanger (guest editors), *Indoor Air Pollution,* special issue of *Environment International* (based on the International Symposium on Indoor Air Pollution, Health and Energy Conservation, Amherst, Mass., Oct. 13-16, 1981), Vol. 8, pp. 1-534, 1982.

R.J. Budnitz, A.V. Nero, D.J. Murphy, and R. Graven (principal authors), *Instrumentation for Environmental Monitoring, Vol. 1: Radiation* (Lawrence Berkeley Laboratory Environmental Instrumentation Survey), Wiley-Interscience, New York, in press (for April 1983).

A.V. Nero and W.M. Lowder (guest editors), *Indoor Radon,* special issue of *Health Physics,* in press (for July 1983).

## WINDOWS AND DAYLIGHTING

### 1978-79

EEB-W 78-01, UC-95f, LBL-7812, *A Discussion of Heat Mirror Film: Performance, Production Process, and Cost Estimates.* B.P. Levin and P.E. Schumacher, October 1977.

EEB-W 78-02, UC-95d, LBL-7825, *High Performance Solar Control Office Windows.* W.J. King, December 1977.

EEB-W 78-03, LBL-7829, *Transparent Heat Mirrors for Passive Solar Heating Applications.* S. Selkowitz, March 1978.

EEB-W 78-04, LBL-7840, *Energy Efficient Windows Program Activities.* S. Selkowitz and S. Berman, 1978.

EEB-W 79-01, LBL-7833, *Transparent Heat Mirrors for Passive Solar Heating Applications.* S. Selkowitz, March 1978. Published in the Proceedings of the Third National Passive Solar Conference of the IES, San Jose, CA, January 11-13, 1979.

EEB-W 79-03, *Effective Daylighting in Buildings: Part 1.* S. Selkowitz, February 1979.

EEB-W 79-05, LBL-8583, *Modeling Passive Solar Buildings with Hand Calculations.* D.B. Goldstein, January 1979.

EEB-W 79-06, LBL-8825, *Daylighting and Passive Solar Buildings.* S.E. Selkowitz, 1979.

EEB-W 79-07, LBL-8835, *Thermal Performance of Insulating Window Systems.* S.E. Selkowitz, December 1978. Presented at the ASHRAE Symposium, "Window Management as it Affects Energy Conservation in Buildings," Detroit, June 24-28, 1979. Published in *ASHRAE Trans. 85*(2), Paper DE-79-5 #5.

EEB-W 79-08, LBL-9048, *A Simplified Procedure for Calculating the Effects of Daylight from Clear Skies.* H.J. Bryan, September 1979. Presented at the Annual Illuminating Engineering Society Technical Conference, Atlantic City, NJ, September 16-20, 1979.

EEB-W 79-09, LBL-9371, *Design Calculations for Passive Solar Buildings by a Programmable Hand Calculator.* D.B. Goldstein, M. Lokmanhekim, and R. Clear, August 1979. Presented at the Izmir International Symposium—II on Solar Energy Fundamentals and Applications, Izmir, Turkey, August 6-8, 1979.

EEB-W 79-10, UC-95d, LBL-9307, *An Energy Efficient Window System: Final Report.* Suntek Research Associates, August 1979.

EEB-W 79-12, LBL-9598, *Energy Efficient Windows Program.* S. Berman, J. Klems, M. Rubin, S. Selkowitz, and R. Verderber. Excerpt from the *1978 Energy and Environment Division Annual Report* (LBL-8619), July 1979.

EEB-W 79-13, UC-95d, LBL-9608, *Aerospace Technology Review for LBL Window/Passive Solar Program: Final Report.* R. Viswanathan, June 1979.

EEB-W 79-14, LBL-9653 Rev., *The Mobile Window Thermal Test Facility (MoWTT).* J.H. Klems and S. Selkowitz. Presented at the ASHRAE/DOE Conference on the Thermal Performance of the Exterior Envelopes of Buildings, Orlando, FL, December 3-5, 1979.

EEB-W 79-15, LBL-9654, *Average Transmittance Factors for Multiple Glazed Window Systems.* S. Selkowitz, M. Rubin, and R. Cresewick. Presented at the AS/IEA Fourth Annual Passive Solar Conference, Kansas City, MO, October 2-5, 1979.

EEB-W 79-17, LBL-9653, Rev., *The Mobile Window Thermal Test Facility (MoWTT).* J.H. Klems and S.E. Selkowitz, October 1979.

EEB-W 79-18, LBL-9803, *A Calibrated Hotbox for Testing Window Systems—Construction, Calibration and Measurements on Prototype High-Performance Windows.* J.H. Klems, October 1979. Presented at the ASHRAE/DOE Conference on the Thermal Performance of the Exterior Envelopes of Buildings, Orlando, FL, December 3-5, 1979.

EEB-W 79-19, LBL-9787, *A Simple Method for Computing the Dynamic Response of Passive Solar Buildings to Design Weather Conditions.* D.B. Goldstein and M. Lokmanhekim. September 1979. Presented at the Second Miami International Conference on Alternative Energy Sources, Miami, FL, December 10-13, 1979.

EEB-W 79-20, LBL-9588, *Optimum Lumped Parameters for Modeling the Thermal Performance of Buildings.* R. Richardson and S. Berman, August 1979.

EEB-W 79-21, LBL-9933, *Thermal Performance of Managed Window Systems.* S.E. Selkowitz and V. Bazjanac. Presented at the DOE/ASHRAE Conference on the Thermal Performance of the Exterior Envelopes of Buildings, Orlando, FL, December 3-5, 1979.

EEB-W 79-22, LBL-9934, *Solar Optical Properties of Windows: Calculation Procedures.* M. Rubin, October 1979. Submitted to the *Journal of Applied Optics.*

EEB-W 79-23, LBL-9937, *Field Air Leakage of Newly Installed Residential Windows.* J. Weidt, J.L. Weidt and S. Selkowitz, October 1979. Presented at the DOE/ASHRAE Conference on the Thermal Performance of the Exterior Envelopes of Buildings, Orlando, FL, December 3-5, 1979.

EEB-W 79-25, *LBL/DOE Energy-Efficient Windows Research Program.* S. Berman and S. Selkowitz, February 1979.

**1980**

EEB-W 80-09, LBID-166, *Multiple Glazing Systems with Between Panes Ventilation.* R. Johnson,

November 1979.

EEB-W 80-10, LBL-10862, *Thin Film Electrochromic Materials for Energy Efficient Windows.* C.M. Lampert.

EEB-W 80-11, LBL-11186, *A Procedure for Calculating Interior Daylight Illumination with a Programmable Hand Calculator.* H.J. Bryan and R.D. Clear, October 1980.

EEB-W 80-12, LBL-11111, *Air Leakage of Newly Installed Residential Windows.* J.L. Weidt and J. Weidt, June 1980.

EEB-W 80-13, LBL-11408, *Transparent Heat Mirrors for Windows: Thermal Performance.* M. Rubin, R. Creswick and S. Selkowitz, August 1980.

EEB-W 80-14, LBL-11446, *Heat Mirror Coatings for Energy Conserving Windows.* C. Lampert, September 1980.

EEB-W 80-15, LBL-8803, *Coatings for Enhanced Photothermal Energy Collection II: Non-Selective and Energy Control Films.* C.M. Lampert, April 1979.

EEB-W 80-16, LBL-11687, *Calculating Interior Daylight Illumination with a Programmable Hand Calculator.* H.J. Bryan and R.D. Clear, August 1980.

EEB-W 80-19, LBL-11796, *The Daylighting Solution.* S. Selkowitz and R. Johnson, August 1980.

EEB-W 80-21, LBL-7811, *Some Analytical Models of Passive Solar Building Performance,* M. Goldstein, November 1978.

**1981**

EEB-W 81-01, LBL-12248, *Quicklite 1, A Daylighting Program for the TI-59 Calculator,* H. Bryan, R. Clear, J. Rosen, and S. Selkowitz, April 1981.

EEB-W 81-02, LBL-12119, *High-Performance Solar-Control Windows: Final Report,* W.J. King, Kinetic Coatings, April 1980.

EEB-W 81-03, LBL-12286, *A Hemispherical Sky Simulator for Daylighting Studies: Design, Construction, and Operation,* S. Selkowitz, D. MacGowan, B. McSwain, and M. Navvab, September 1981.

EEB-W 81-05, LBL-12599, *Daylighting Calculations for Non-Rectangular Interior Spaces with Shading Devices,* M. Modest, June 1981.

EEB-W 81-06, LBL-12486, *Calculating Heat Transfer through Windows,* M. Rubin, May 1981.

EEB-W 81-10, LBL-12891, *Methods of Estimating Air Infiltration through Windows,* J. Klems, September 1981.

EEB-W 81-11, LBL-12967, *A Hemispherical Sky Simulator for Daylighting Model Studies,* S. Selkowitz, July 1981.

EEB-W 81-12, LBL-12288, *Thermal Performance of Windows Having High Solar Transmittance,* M. Rubin and S. Selkowitz, July 1981.

EEB-W 81-13, LBL-11901, *Calculating Optical Constants of Glazing Materials,* M. Rubin, August 1981.

EEB-W 81-14, LBL-13171, *Daylighting as a Design and Energy Strategy: Overview of Opportunities and Conflicts,* S. Selkowitz, June 1981.

EEB-W 81-15, LBL-13172, *Daylighting Research Activities in the Energy Efficient Buildings Program at Lawrence Berkeley Laboratory,* S. Selkowitz, August 1981.

EEB-W 81-17, LBL-12285, *Daylighting Design Overlays for Equidistant Sun-Path Projections,* S. Selkowitz, August 1981.

EEB-W 81-19, LBL-13305, *The Use of Physical Scale Models for Daylighting Analysis,* H. Bryan, A. Lohr, R.C. Mathis, and J. Rosen, September 1981.

EEB-W 81-20, LBL-12765, *A Mobile Facility for Measuring Net Energy Performance of Windows and Skylights,* J. Klems, S. Selkowitz, and S. Horowitz, October 1981.

EEB-W 81-21, LBL-13374, *Infrared Properties of Polyethylene Terephthalate Films,* M. Rubin, October 1981.

EEB-W 81-23, LBL-13399, *Efficient Daylighting in Thermally Controlled Environments,* E. Ne'eman and S. Selkowitz, October 1981.

EEB-W 81-24, LBL-12764, *Glazing Optimization Study for Energy Efficiency in Commercial Office Buildings,* R. Johnson, S. Selkowitz, F. Winkelmann, and M. Zentner, October 1981.

EEB-W 81-25, LBL-13502, *Materials Chemistry and Optical Properties of Transparent Thin Films for Solar Energy Utilization,* C. Lampert, November 1981.

EEB-W 81-27, LBL-13400, *Development and Use of a Hemispherical Sky Simulator,* M. Navvab, (M.A. Thesis) October 1981.

**1982**

EEB-W 82-01, LBL-13753, "Durable Solar Optical Materials—The International Challenge." C.M. Lampert, January 1982. *Proceedings of SPIE*, the International Society for Optical Engineering, *324* (3), 1982.

EEB-W 82-02, LBL-13756, "A Large-Area, High-Sensitivity Heat-Flow Sensor." J.H. Klems and D. DiBartolomeo, February 1982. *Review of Scientific Instruments, 53* (10), 1609-1612, October 1982.

EEB-W 82-03, LBL-14250, "Advanced Heat-Mirror

Films for Energy-Efficient Windows." C.M. Lampert, March 1982. *The Renewable Challenge*, Proceedings of the 1982 Annual Meeting of the American Section of the International Solar Energy Society (ASISES), Houston TX, June 1-5, 1982.

EEB-W 82-04, LBL-14369, *Energy Conservation through Interior Shading of Windows: An Analysis, Test and Evaluation of Reflective Venetian Blinds.* R.L. Van Dyck and T.P. Konen, Stevens Institute of Technology, March 1982.

EEB-W 82-05, LBL-14462, "Transparent Silica Aerogels for Window Insulation." M. Rubin and C.M. Lampert, June 1982. *Solar Energy Materials*, 7(4), 1983.

EEB-W 82-06, LBL-14569, "The DOE-2 and SUPER-LITE Daylighting Programs." S. Selkowitz, J. Kim, M. Navvab, and F. Winkelmann, June 1982. To be published in the *PASSIVE '82,* the Proceedings of the Seventh National Passive Solar Conference, Knoxville TN, August 29-September 3, 1982.

EEB-W 82-07, LBL-14590, "Advanced Optical Materials for Energy Efficiency and Solar Conversion." C.M. Lampert, June 1982. To be published in *Advanced Solar Materials* (Plenum, New York) in 1983.

EEB-W 82-08, LBID-560, *Evaluation of Air-Flow Windows: Final Report.* K. Brandle, R.F. Boehm, University of Utah, May 1981.

EEB-W 82-09, LBL-14694, "Solar Optical Materials for Innovative Window Design." C.M. Lampert, August 1982. To be published in *International Journal of Energy Research.*

EEB-W 82-10, LBL-14863, "Design Tools for Daylighting Illumination and Energy Analysis." S. Selkowitz, July 1982. To be published in the *Proceedings of the Workshop on Designing and Managing Energy-Conscious Commercial Buildings,* Denver CO, July 19-20, 1982.

EEB-W 82-11, LBL-15131, "Advanced Optical and Thermal Technologies for Aperture Control." S. Selkowitz, C.M. Lampert, and M. Rubin, September 1982. To be published in the *Proceedings of the Passive and Hybrid Solar Energy Update,* Washington, D.C., September 15-17, 1982.

EEB-W 82-12, LBL-15258, *Transparent Heat-Mirror Materials and Deposition Technology.* Compiled by C.M. Lampert and S. Selkowitz, July 1982. Papers selected from the Proceedings of the International Society for Optical Engineering (SPIE) Conference on Optical Coatings for Energy Efficiency and Solar Applications and the Conference on Optical Thin Films, Los Angeles CA, January 25-29, 1982.

## LIGHTING SYSTEMS RESEARCH

### 1978-79

EEB-L 78-1, LBL-7810, *The History and Technical Evolution of High Frequency Fluorescent Lighting. J.H. Campbell, December 1977.*

LBL-7811, *Some Analytic Models of Passive Solar Building Performance: A Theoretical Approach to the Design of Energy-Conserving Buildings.* D.B. Goldstein, 1978.

EEB-L 78-3, UC-95d, LBL-7871, *Phase II Report on Energy Efficient Electronic Ballast for a Two-40 Watt Fluorescent Lamp System.* IOTA Engineering, Inc., July 1978.

EEB-L 78-4, UC-95a, LBL-7852, *Phase I Final Report Subcontract No. 2019702 "Energy Efficient Fluorescent Ballasts."* Stevens Luminoptics Corporation, June 1978.

EEB-L 78-05, LBL-7828, *Energy Efficiency and Performance of Solid State Ballasts.* R. Verderber, S. Selkowitz, and S. Berman, June 1978.

EEB-L 79-01, LBL-8315, *Testing of Energy Conservation of Electronic Ballasts for Fluorescent Lighting—Review of Recent Results and Recommendations for Design Goals.* R. Verderber, D. Cooper, and D. Ross, October 1978. Presented at the IEEE-IAS 1978 Annual Meeting, Toronto, Canada, October 3, 1978.

EEB-L 79-02, LBID-063, *Lighting Energy Conservation in Federal Office Buildings: Implementation Procedures and Obstacles.* P. Benenson and J. Nides, June 1979.

EEB-L 79-03, LBL-9483, *High Frequency Lighting Systems.* J. Campbell, June 1979.

EEB-L 79-04, LBL-9599, *Energy Efficient Lighting Program.* S. Berman, R. Clear, J. Klems, S. Selkowitz, and R. Verderber, 1978.

EEB-L 79-05, LBL-8671, *Can Polarized Lighting Panels Reduce Energy Consumption and Improve Visibility in Building Interiors?* S. Berman and R. Clear, November 1979.

EEB-L 79-06, LBL-9492, *Equivalent Sphere Illumination and Visibility Levels.* R. Richardson and S. Berman, August 1979.

EEB-L 79-07, L-27, LBL-9960, *Energy Efficiency and Performance of Solid State Ballasts.* J. Jewell, S. Selkowitz, and R. Verderber, September 1979. Presented at the Commission International de l'Eclairage, Kyoto, Japan, 1979.

**1980**

EEB-L 80-01, LBL-10707, *The "Real" Energy Savings with Electronic Ballasts.* R.R. Verderber, March 1980.

EEB-L 80-02, LBL-10514, *Cost Effectiveness of Visibility-Based Design Procedures for General Office Lighting.* R. Clear and S. Berman, August, 1980.

EEB-L 80-03, LBL-10789, *Cost Effectiveness of Long Life Incandescent Lamps and Energy Buttons. R. Verderber and O. Morse, April 1980.*

EEB-L 80-05, LBL-11254, *High Intensity Discharge 400-Watt Sodium Ballast Phase I Final Report.* G. Felper, June 1980.

EEB-L 80-06, LBL-11255, *Electronic Screw-In Ballast and Improved Circline Lamp Phase I Final Report.* T.P. Kohler, September 1980.

EEB-L 80-07, LBL-11619, *On-Site Demonstration Procedure for Solid-State Fluorescent Ballast.* R. Verderber and O. Morse, September 1980.

EEB-L 80-09, *High Intensity Discharge Solid-State Ballast Program,* W.R. Alling, Luminoptics, September 1980.

EEB-L 80-10, LBL-11863, *Cost-effective Visibility-Based Design Procedures for General Office Lighting.* R. Clear and S. Berman, August 1980.

**1981**

EEB-L 81-01, LBL-12176, *Optical Interference Coatings for Improved Luminaire Performance: Final Report.* Rubins, Optical Coating Laboratory, Inc., January 1981.

EEB-L 81-03, LBL-12595, *Energy Savings with Solid-State Ballasted High-Pressure Sodium Lamps,* R. Verderber and O. Morse, April 1981.

EEB-L 81-04, LBID-391, *Energy Efficient H.I.D. Solid-State Ballast,* Jefferson Electric, November 1980.

EEB-L 81-05, LBL-12659, *Energy-Efficient Management of Lighting in a Veterans Administration Medical Center,* R. Verderber, A. Arthur, O. Morse, and F. Rubinstein, March 1981.

EEB-L 81-06, LBL-12461, *Energy Savings with Solid-State Ballasts in a V.A. Hospital,* R. Verderber, O. Morse, A. Arthur, F. Rubinstein, May 1981.

EEB-L 81-07, LBL-12462, *Electromagnetic Interference (EMI) Measurement of Fluorescent Lamps Operated with Solid-State Ballasts,* A. Arthur, R. Verderber, F. Rubinstein, and O. Morse, May 1981.

EEB-L 81-08, LBL-12496, *A New Look at Models of Visual Performance,* R. Clear and S. Berman, June 1981.

EEB-L 81-09, LBL-13206, *Gas-Discharge Lamps Having Solid-State Ballasts,* R. Verderber, August 1981.

EEB-L 81-10, LBL-13290, *High-Frequency Starting of Fluorescent Lamps,* O. Morse, September 1981.

EEB-L 81-11, LBL-13299, *Energy-Saving Benefits of Automatic Lighting Controls,* F. Rubinstein, September 1981.

EEB-L 81-13, LBL-13480, *Electrodeless Fluorescent Lamp: Final Report,* Litek International, October 1981.

EEB-L 81-14, PUB. 427, *The Lawrence Berkeley Laboratory/University of California Lighting Program Overview,* S. Berman, December 1981.

**1982**

EEB-L 82-01, LBL-13889, *High-Intensity Discharge 400W Sodium Ballast: Phase II Final Report.* G. Felper, October 1981.

EEB-L 82-02, LBL-13894, *A Computer Program for Analyzing the Energy Consumption of Automatically Controlled Lighting Systems: Final Report.* The Lighting Group, Smith, Hinchman and Grylls Associates, Inc., January 1982.

EEB-L 82-03, LBL-13931, *Relating Productivity to Visibility and Lighting.* R. Clear and S. Berman, January 1982. Presented at the Public Works Canada Symposium "The Integration of Visual Performance Criteria into the Illumination Design Process," Ottawa, Ontario, January 25-27, 1982.

EEB-L 82-04, LBL-14201, *Energy Saving Through Effective Lighting Control.* D. Peterson and F. Rubinstein. Presented at the 9th Energy Technology Conference and Exposition, Washington, D.C., February 16-18, 1982.

EEB-L 82-05, LBID-525, *Energy Efficient Light Bulbs: The Magnetic Arc Spreading Fluorescent Lamp.* Spellman High Voltage Electric Company, November 1981.

EEB-L 82-06, LBL-14546, *Energy-Efficient Incandescent Lamp: Final Report.* Duro-Test Corporation, April 1982.

EEB-L 82-07, LBL-14596, "Measurement of UV Radiation in a Low-Pressure Vapor-Discharge Tube with Mercury Isotopes." R.K. Sun, August 1982. Submitted to *Review of Scientific Instruments.*

EEB-L 82-08, LBL-14561, *The Measured Energy Savings from Two Lighting Control Strategies.* F. Rubinstein and M. Karayel, June 1982. Presented at the IEEE Industry Applications Society 1982 Annual Meeting, San Francisco CA, October 4-8, 1982.

EEB-L 82-09, LBL-15199, *Proceedings of the Lighting-Electromagnetic Compatibility Conference.* Ed. R. Verderber and S. Berman, September 1982.

EEB-L 82-10, LBL-15251, *Integrated Circuit Control for Two-Lamp Electronic Ballast: Final Report.* T. Kohler, November 1982.

EEB-L 82-11, LBL-15252, *Energy-Efficient Compact Screw-in Fluorescent Lamp: Final Report.* E.W. Morton, Westinghouse Electric Corporation, November 1982.

# ENVIRONMENTAL RESEARCH PROGRAM

## INTRODUCTION

The primary concern of the Environmental Research Program is the understanding of pollutant formation, transport, and transformation and the impacts of pollutants on the environment. These impacts include global, regional, and local effects on the atmosphere and hydrosphere, and on certain aspects of human health. This multidisciplinary research program includes fundamental and applied research in physics, chemistry, and biology, as well as research on the development of advanced methods of measurement and analysis. During FY 1982, research was concentrated on atmospheric physics and chemistry, applied physics and laser spectroscopy, combustion research, environmental effects of oil shale processing, fresh-water ecology and acid precipitation, trace element analysis for the investigation of present and historical environmental impacts, and a continuing survey of instrumentation for environmental monitoring.

Each of these areas is covered by a different research group or program. Atmospheric physics and chemistry, for example, is the province of the Atmospheric Aerosol Research Group, which has focused its studies on aerosol characterization, formation, and transformation and on the effects of aerosols on precipitation, visibility, and climate. At present, the main research interests of the group involve chemical processes, including those that occur in clouds and fogs, atmospheric aerosol nitrogen chemistry, and the role of particulate carbon in global climate modification. To accomplish these research objectives, the group has developed novel analytical methods, such as a laser transmission method for optical characterization of particles and thermal evolved gas analysis for the characterization of carbonaceous and nitrogenous aerosol species. Members of the group were also the first to apply photoelectron and Raman spectroscopy to aerosol characterization.

The Applied Physics and Laser Spectroscopy Research Group applies advanced laser spectroscopy and condensed-matter physics to energy and environmental problems. Emphasis is on the development of physical methods, as opposed to conventional chemical analysis techniques. The ultrahigh sensitivity, narrow line width, and tunability of lasers and the minimal sample preparation required make it possible for team members to apply such techniques to energy production and to test novel methods for energy conversion, such as photovoltaic solar cells and superionic electrical energy storage devices. The experience of the group accumulated during the past six years will be employed in attacking such significant problems as the increase in global carbon dioxide. Emphasis will be placed on remote sensing.

The LBL Oil Shale Program studies the environmental and waste-treatment problems that would arise from the tremendously large quantities of solid and liquid wastes a commercial-scale shale oil industry would generate. Surface and in-situ oil shale processing will probably create environmental problems through wastewater and solid waste production, emission of atmospheric pollutants during shale disposal, and leaching of organic and inorganic residuals from disposed shale. Developers propose to use process wastewaters to cool the hot processed (spent) shale, moisten it for dust control, and facilitate its compaction, a process called "codisposal." A major task of the oil shale program currently is to delineate the potential problems of such waste codisposal, in particular the estimation of the types and quantitites of uncontrollable air emissions that may result from such use of wastewaters (raw or treated). Its second major task is the development of economical approaches to the treatment of process wastewaters. Because of their turbidity and high concentrations of organic and inorganic solutes, they present tremendous difficulties to any water management scheme that entails reuse or discharge. This research effort is conducted in cooperation with the Sanitary Engineering and Environmental Health Research Laboratory of the University of California.

The Scrubber Chemistry Group has been investigating the chemical character of pollutants generated by the combustion of fossil fuels to develop new, efficient strategies for pollutant

emission control. Current research has been directed toward understanding the kinetics and mechanisms of homogeneous and heterogeneous catalysis of the interactions of sulfur dioxide and nitrogen oxides, both among themselves and with other compounds. When this fundamental chemistry is understood, it will be applied to the development of an efficient, cost-effective scrubber for simultaneous desulfurization and denitrification of flue gases. The same knowledge can also be applied to improving the performance of lime/limestone desulfurization scrubbing systems, currently the most widely used type of scrubber in the utility industry.

Approximately 90% of energy consumption in the United States is attributable to combustion processes. The Combustion Research Group has worked to achieve control over complex combustion processes by acquiring a fundamental understanding of the complex chemical and physical processes that determine combustion efficiency, emissions, and safety. Development of suitable analytical techniques for measuring intermediate and product species formed during the oxidation of fossil fuels and for characterizing turbulence has been a major effort. The characterization and understanding of turbulence and high-temperature chemistry are of high priority in this program. Areas of application which dominate these studies are engine research, pollutant abatement in utilities, control of unwanted fires, and ignition phenomena.

Ecotoxicology is the science that seeks to determine the pathways, fate, and effects of toxic substances in the natural environment. The projects of the Lake Ecotoxicology Research Group focus on one particular type of natural environment, freshwater lakes. Research has proceeded in two converging directions: the development of laboratory microcosms for lake ecotoxicology and the study of acid precipitation in the western United States. The group has demonstrated that lake microcosms can be designed and operated to provide realistic toxic-substance test systems and has applied microcosms to analyze effects of acid precipitation. Field studies on acid precipitation and its effects in the Sierra Nevada and the Colorado Rockies have been another major focus of the group. A combination of microcosm technology and field work is being designed with the goal of predicting the chronology of acidification in the western United States.

Two major projects have occupied members of the Trace Element Analysis Group. The first is the continuation of the survey of instrumentation for environmental monitoring. Commercial publication of that part of the survey dealing with radiation monitoring was completed in 1983. Wiley Interscience is handling the distribution of this 1130-page work. It is expected that material devoted to water monitoring will be updated and published in 1984. The second project is the study of the relationship between massive repetitive life extinctions on the earth and asteroid (or other extraterrestrial) impacts. Studies of this relationship have concentrated on searches for unusually high iridium abundances in geochemical samples from rock layers which are known or expected to mark life-extinction horizons. Geochemical and other tests are made to determine if the iridium-rich rocks are of extraterrestrial origin and hence related to impacts. The nature of the sedimentation of the rocks, the worldwide extent of the extinction horizons and the extent to which the extinctions (as indicated from fossil studies by collaborating paleontologists) are related to impacts are also studied.

During FY 1982, the research groups of the Environmental Research Program conducted the studies described in the short reports that follow. In many cases, more detailed reports have been or will be published.

# EVIDENCE FOR PRIMARY OXIDANTS OF $SO_2$*

*W.H. Benner, P.M. McKinney, and T. Novakov*

A number of pathways by which $SO_2$ is oxidized in aqueous atmospheric droplets have recently been compared.[1,2] Oxidation occurs either by reaction with gas-phase oxidants like $O_3$ and $H_2O_2$ after they have been absorbed into the droplets, or catalytically with trace metals or soot particles. The gas-phase oxidants have been assumed to originate solely from secondary photochemical reactions in the atmosphere. However, we have recently found evidence for combustion-generated (i.e., primary) oxidants of $SO_2$. In this article, we describe our preliminary observations.

## ACCOMPLISHMENTS DURING FY 1982

A schematic sketch of the experimental system is shown in Fig. 1. An axially positioned torch in the cylindrical chimney burns gaseous fuels, such as propane, natural gas, CO, and $H_2$, in selectable fuel-to-air or fuel-to-$O_2$ ratios. The flame is electrically ignited and can burn continuously or intermittently (e.g., 5 sec on, 5 sec off). A Fluoropore filter prevents the combustion-generated soot particles from reaching the $SO_2$ detector (TECO, pulsed fluorescence) or the bubblers. $SO_2$ can be introduced into the chimney or after the filter.

When $SO_2$ is introduced into the air flow in the chimney at a rate that maintains its concentration at ~1 ppm, an instantaneous decrease in this concentration is observed when a fuel such as propane (50 ml/min) is burned in the torch. For a diffusion flame, the $SO_2$ concentration decreases approximately 80%. Combustion of natural gas or tobacco, or pyrolysis of oils, produces similar $SO_2$ decreases.

*This work was supported by the Director, Office of Energy Research, Office of Health and Environmental Research, Physical and Technological Research Division of the U.S. Department of Energy under Contract No. DE-AC03-76SF00098, and by the National Science Foundation under Contract No. ATM 82-10343.

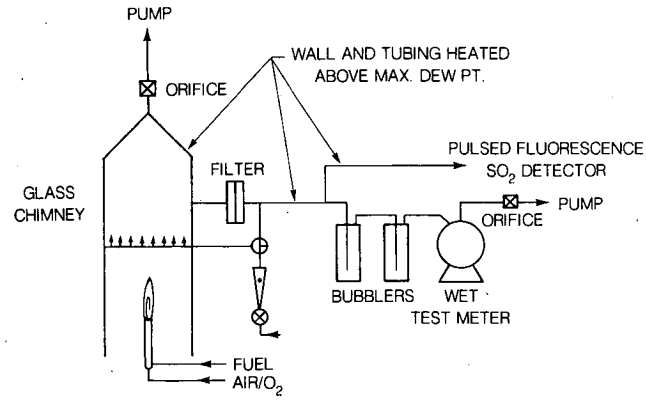


Figure 1. Apparatus for sampling primary oxidants. (XBL 834-173)

This observation is essentially similar to one we have described in the past[3] and can be explained by one or more of the following processes: (1) $SO_2$ is scavenged by the condensed combustion-generated water; (2) $SO_2$ is converted to sulfate by oxidation or adsorption on combustion-generated particles; (3) the $SO_2$ detector is subject to a negative interference by some of the combustion effluents; or (4) $SO_2$ reacts in the gas phase with combustion products to produce gaseous sulfur species not detected by the $SO_2$ detector.

The first possibility was eliminated or at least minimized by maintaining the entire system at a temperature above the maximum measured dew point; furthermore, when $H_2$ was burned at a flow rate designed to produce the same concentration of $H_2O$ vapor as that produced by the propane flame, only a small (5%) reduction in [$SO_2$] was noted. The second possibility was eliminated when filter samples collected while a flame was burning showed that particulate sulfur could not account for the observed decrease in [$SO_2$]. The possibility that the observed $SO_2$ decrease was caused by species interfering with the $SO_2$ detector is unlikely. Consultation with the manufacturer of the $SO_2$ detector (TECO) indicated that no known interfering species cause a decrease in the apparent $SO_2$ signal: all known interferents, such as fluorescent hydrocarbons, are positive interferents.

This leaves the fourth possibility, a gas-phase reaction between $SO_2$ and combustion gases, a suggestion that was supported by additional experiments. A

steady (2-min) diffusion flame produced a smaller reduction in $[SO_2]$ than did an intermittent flame (5 sec on, 5 sec off for 4 min) that burned the same total amount of fuel. When propane was premixed with air before combustion, the reduction in $[SO_2]$ was less; and premixing with $O_2$ caused essentially no reduction in $[SO_2]$. Results similar to those described thus far were also obtained when $SO_2$ was added after the filter (Fig. 1).

Further insights were gained by using water bubblers to collect $SO_2$, the combustion gases, and any $SO_2$ reaction products (Fig. 1). Ion chromatography was used to analyze the anions in the bubbler solution. When $SO_2$ alone was drawn through the bubbler, 100% of the expected $SO_2$ was recovered—95% as S(IV) and 5% as $SO_4^=$. When filtered combustion gases and $SO_2$ were sampled through the bubbler, 90% of the gas-phase sulfur was recovered, but only 10% of the aqueous S was detected as S(IV); the remaining 90% was $SO_4^=$. (The use of 1% $H_2O_2$ in the bubbler increased the recovery to 100%, and thus the presence of an undissociated S species in the water bubbler was indicated.) The combustion gases caused a large fraction of the $SO_2$ to be oxidized to $SO_4^=$.

In addition, filtered combustion gases without added $SO_2$ were sampled through the bubbler. S(IV) was then added to the bubbler solution so that the diluted final concentration was several ppm. This S(IV), upon immediate analysis, was found to have been oxidized to $SO_4^=$. The fraction of S(IV) that was oxidized in the bubbler can be related to flame conditions and fuel type. For comparable amounts of fuel burned, S(IV) oxidation increases in this order: intermittent flame > steady flame > air-premixed flame > $O_2$-premixed flame $\approx$ CO $\approx$ $H_2$. The combustion gases contain $NO_2$, but ion chromatographic analysis of the bubbler solution indicated that $NO_2^-$ was not involved in S(IV) oxidation.

Filtered combustion gases that did not contain added $SO_2$ were sampled into a bubbler, and $10^{-5}$ to $10^{-4}$ molar levels of peroxides were detected via a nonspecific total peroxide technique.[4] A technique[5] that is specific for $H_2O_2$ showed that a sizable fraction of the total peroxide was $H_2O_2$.

These bubbler results indicate that (1) combustion is a source of one or more oxidants or of organic species that react with water to produce oxidants for $SO_2$ and/or S(IV); and (2) there appears to be a reaction intermediate or another sulfur-containing reaction product that is not dissociated and thus not detectable by ion chromatographic analysis.

We have also conducted some preliminary experiments to determine if automobiles are sources of primary oxidants. Filtered exhaust from several automobiles was sampled through a water bubbler, and analysis showed that

$$S_{SO_4^=}/S_{S(IV)} + S_{SO_4^=} \approx 0.25 \quad .$$

This indicated that one-fourth of the $SO_2$ released from automobiles was oxidized to $SO_4^=$. ($SO_3$ would form $SO_4^=$ upon contact with water, but $SO_3$ is only a few percent of the $SO_2$ concentration.) When S(IV) was added to the bubbler solution, immediate analysis showed that the added S(IV) could be oxidized to $SO_4^=$. It is not yet known if the $SO_4^=$ collected in the bubbler results only from aqueous reactions or if preceding gas-phase reactions are important. However, the sulfate formation that occurs when S(IV) is added to the sampled exhaust indicates that aqueous reactions are important.

Finally, by using the results of these two steps—the amount of $SO_4^=$ found in a bubbler when filtered automobile exhaust is sampled, plus the amount of $SO_4^=$ that forms when S(IV) is added to the bubbler—we have estimated that the concentration of oxidants in the exhaust is about 1 ppm. Automobiles thus could be a significant source of primary oxidants.

## PLANNED ACTIVITIES FOR FY 1983

We are attempting to speciate the various oxidants that can be released by combustion sources. Once this is done, a kinetic study of the $SO_2$ + oxidant reaction will be started. The ultimate goal is to develop a reaction rate expression.

## REFERENCES


1. Middleton, P., Kiang, C.S., and Mohnen, V.A. (1980), "Theoretical Estimates of the Relative Importance of Various Urban Sulfate Aerosol Production Mechanisms," *Atmos. Environ. 14*, p. 463.
2. Chang, S.-G., Toossi, R., and Novakov, T. (1981), "The Importance of Soot Particles and Nitrous Acid in Oxidizing $SO_2$ in Atmospheric Aqueous Droplets," *Atmos. Environ. 15*, p. 1287.

3. Novakov, T., Chang, S.-G., and Harker, A.B. (1974), "Sulfates as Pollution Particulates: Catalytic Formation on Carbon (Soot) Particles," *Science 186*, p. 259.
4. Wolfe, W.C. (1962), "Spectrophotometric Determination of Hydroperoxide in Diethyl Ether," *Anal. Chem. 34*, p. 1328.
5. Zika, R.G., and Saltzman, E.S. (1982), "Interactions of Ozone and Hydrogen Peroxide in Water: Implications for Analysis of $H_2O_2$ in Air," *Geophys. Res. Lett. 9*, p. 231.

## S(IV) OXIDATION BY AMBIENT PARTICULATE MATTER*

*W.H. Benner and T. Novakov*

Our investigation of $SO_2$ oxidation in the atmosphere has focused on heterogeneous oxidation pathways.[1-3] We have found that aqueous suspensions of activated carbons (used as model systems to simulate droplets with particulate carbon) and aqueous suspensions of traffic-generated combustion particles collected in a highway tunnel oxidize S(IV) to sulfate. These results suggest that ambient soot particles, and perhaps other ambient particles, can oxidize $SO_2$ to sulfate. This article describes our current efforts to determine the role of particulate matter in oxidizing $SO_2$ to sulfate.

## ACCOMPLISHMENTS DURING FY 1982

### Oxidation of S(IV) by Ambient Particulate Matter

Samples of particulate material, amounting to several grams, were collected continuously over one week from City of Hope, California (Los Angeles air basin) in an electrostatic precipitator. Portions of some samples were multiply extracted in 0.1 *M* NaOH to remove organic material, along with the large amounts of sulfate that were present. With the sulfate removed, S(IV) could be properly separated and detected conductimetrically by ion chromatography (IC).

*This work was supported by the Director, Office of Energy Research, Office of Health and Environmental Research, Physical and Technological Research Division of the U.S. Department of Energy under Contract No. DE-AC03-76SF00098, and by the National Science Foundation under Contract No. ATM 82-10343.

To determine if these particles can oxidize S(IV), aqueous suspensions of the particulate matter were prepared. S(IV), as a dilute solution of $Na_2S_2O_5$, was added to suspensions of extracted particles, and the [S(IV)] was determined periodically by IC analysis of filtered aliquots. For details of these experiments, see Ref. 1.

The results of the studies with ambient particulate matter are presented in Fig. 1, which shows the rate of S(IV) disappearance in moles S(IV)/gram C·sec, plotted as a function of the [S(IV)]. The rate expression is normalized to the concentration of suspended particulate carbon because we assumed that the catalytic activity is due to particulate carbon (surface-activated graphitic component). In the caption to Fig. 1, the percentage of carbon in each sample is indicated; knowing this percentage, one can calculate the rate based on total weight of suspended particles by multiplying the rate by fraction carbon. Figure 1 also includes a plot for extracted tunnel soot from Brodzinsky et al.[1]

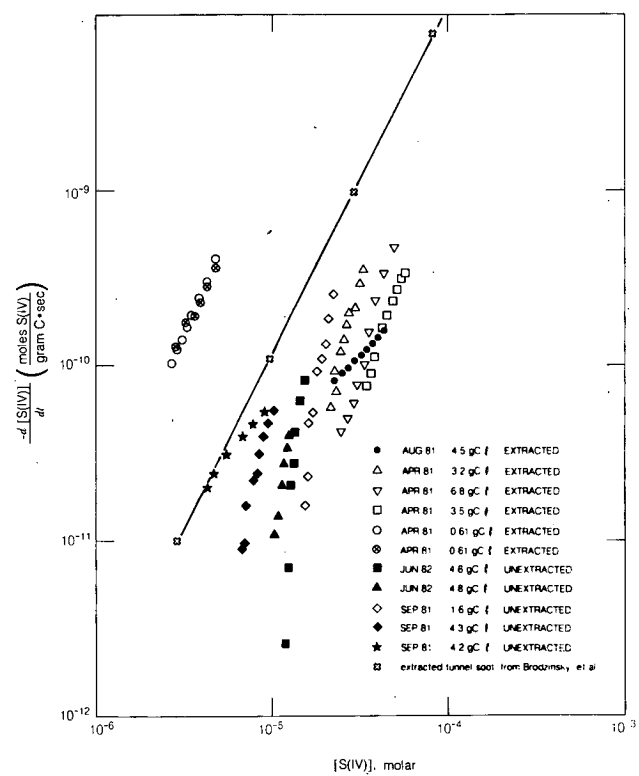


Figure 1. Oxidation of S(IV) by ambient particulate matter. Carbon comprised the following percentages by weight of the particulate matter: August 1981 (extracted), 7.2%; April 1981 (extracted), 9.8%; June 1982 (unextracted), 9.5%; and September 1981 (unextracted), 8.5%.

(XBL 834-176)

The plots in Fig. 1 show that all suspensions of ambient particulate matter oxidize S(IV) to sulfate. The rate of oxidation is variable from batch to batch; and, for some individual samples, the rate was variable from experiment to experiment. The importance of these findings depends on the interpretation one applies to the APR 81 (April 1981) sample. For this sample, relatively large concentrations (3–6 g C/l) of particulate carbon showed a reaction rate slower than that of extracted tunnel soot, while relatively low concentrations (0.61 g C/l) showed a much higher rate of S(IV) oxidation. If the plot of rate vs. [S(IV)] for the low concentration of APR 81 particulate matter was extended and found to have the same general shape as the extracted tunnel soot curve, then the oxidation of $SO_2$ by ambient particles would be an important reaction pathway for the formation of particulate sulfate; but if this extrapolation fell below the extracted tunnel soot curve, as suggested by the high concentration experiments, then such oxidation would be only a minor pathway. This apparent paradox cannot be solved at present, but it led us to re-examine some earlier data and to perform more experiments with tunnel soot suspensions. The results reported in the following section shed some light on the problem.

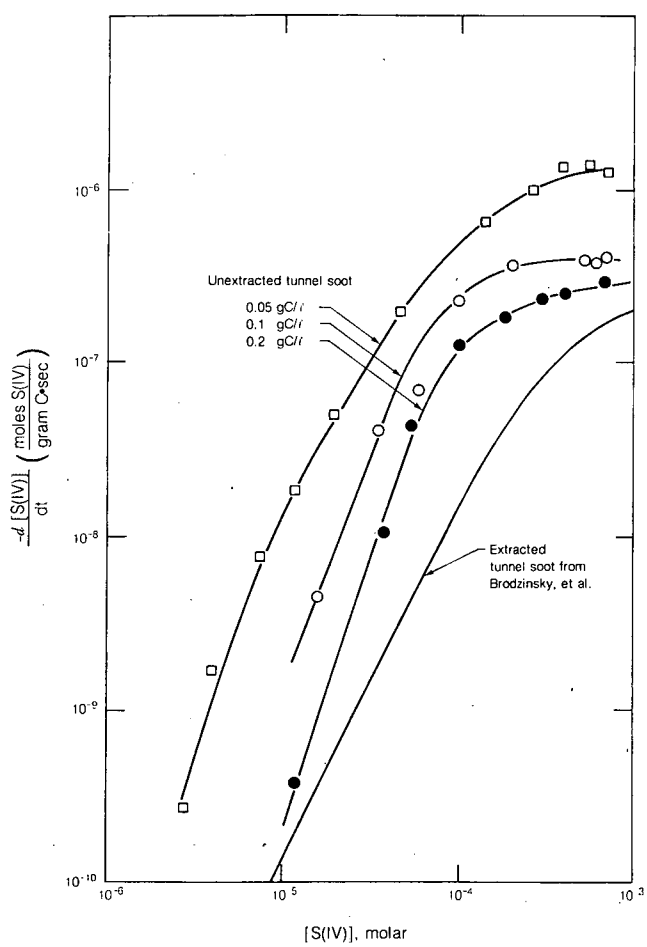


Figure 2. Oxidation of S(IV) by highway tunnel soot particles. (XBL 834-174)

## Oxidation of S(IV) by Unextracted Tunnel Soot

The earlier work done with extracted tunnel soot[1] (reproduced for comparison in Figs. 1 and 2) was conducted with suspensions having drastically different concentrations of particulate carbon (e.g., an order of magnitude between runs). The apparent paradox observed for APR 81 particles (Fig. 1) was not seen in the extracted tunnel soot runs. In fact, normalization of the reaction rate to the particulate carbon concentration in the extracted tunnel soot experiments unified all experimental data into the curve reproduced in Figs. 1 and 2.

S(IV) experiments were conducted with three concentrations of *unextracted* tunnel soot particles to see if normalization to the particulate carbon concentration would again unify the data. The results (Fig. 2) show that the reaction rate was higher than the previous reported rate curve for extracted tunnel soot and that the curve is shifted to higher rates as the particulate carbon concentration is lowered. These results indicate that normalizing the rate of S(IV) disappearance to the particulate carbon concentration may not be entirely appropriate, which supports our findings for the APR 81 particle suspensions.

At least two possibilities are suggested by these results:

1) At high concentrations of particulate carbon, a minor component of the particulate matter desorbs and poisons the catalyst, while at low concentrations of particulate carbon, the concentration of this minor component is too small to cause an effect.
2) There are consecutive and parallel reactions so that one pathway becomes important as the concentration of the catalyst decreases.

## Conclusions

These studies show that suspensions of ambient particulate matter can oxidize S(IV) to sulfate. The importance of this reaction pathway in the troposphere is not yet clear. Suspensions of unextracted tunnel soot oxidize S(IV) relatively rapidly, and com-

parison of these reaction rates to the values used in modeling studies[2] indicates that the soot-catalyzed rate may be important due to this unrecognized concentration effect.

## PLANNED ACTIVITIES FOR FY 1983

We plan to continue this study and hope to determine the importance of $SO_2$ oxidation by ambient particulate matter. A problem that has to be overcome is the difficulty of obtaining gram quantities of ambient particulate matter. Electrostatic precipitation of the particles was used in the past, but less artifact-prone samples are needed.

## REFERENCES


1. Brodzinsky, R., Chang, S.G., Markowitz, S.S., and Novakov, T. (1980), "Kinetics and Mechanism for the Catalytic Oxidation of Sulfur Dioxide on Carbon in Aqueous Suspension," *J. Phys. Chem. 84*, p. 3354.
2. Chang, S.G., Toossi, R., and Novakov, T. (1981), "The Importance of Soot Particles and Nitrous Acid in Oxidizing $SO_2$ in Atmospheric Aqueous Droplets," *Atmos. Environ. 15*, p. 1287.
3. Benner, W.H., Brodzinsky, R., and Novakov, T. (1982), "Oxidation of $SO_2$ in Droplets Which Contain Soot Particles," *Atmos. Environ. 16*, p. 1333.


# REAL-TIME MEASUREMENT OF THE ABSORPTION COEFFICIENT OF AEROSOL PARTICLES*†


*A.D.A. Hansen, H.J. Rosen, and T. Novakov*


Recent studies have shown that large concentrations of graphitic carbon particles are found in the atmosphere in both urban and remote locations.[1,2] These particles are produced in combustion and have a large optical absorption cross section, on the order of 10 $m^2/g$. Their presence affects radiation transfer through the atmosphere, causing visibility degradation[3] and possible changes in the regional or global radiation balance.[4] The size of these effects depends critically on both the concentration of the particles and their single-scattering albedo,[5] which is determined by the relative magnitude of the scattering and absorption coefficients. The scattering coefficient is easily measured by the nephelometer.[6,7]

However, measurements of the absorption coefficient of an ambient aerosol are difficult, mainly because of the small magnitude of this coefficient: typically, $b_{abs}$ is $\sim 10^{-3}$ to $10^{-6}$ $m^{-1}$. Measurement systems based on mirror-folded paths[8] and photoacoustic techniques[9] have been developed, but they require sophisticated apparatus that are inconvenient for routine use. In this article, we outline the development of an instrument that measures the attenuation of a light beam transmitted through particles that are being continuously collected on a suitable filter.[10] We have named this instrument the aethalometer, derived from the Greek word αιθαλουν ("to blacken with soot").

## ACCOMPLISHMENTS DURING FY 1982

The principle of operation of the aethalometer is illustrated in Fig. 1. The method is based on the laser transmission technique.[11] As predicted theoretically[12] for a deposit of absorbing particles on a diffusely reflecting substrate, the laser transmission technique is sensitive only to absorption, a result confirmed by photoacoustic measurements.[13]

A cellulose fiber filter (e.g., Millipore) is partially covered with a transparent mask so that air is drawn through only a small part of the filter on which the particles are collected. The noncollecting portion of the filter covered by the mask is used as a reference. Light from a stabilized incandescent lamp passes through a 530-nm bandpass filter and is then directed by a quartz light guide to uniformly illuminate the collecting and reference areas of the cellulose filter. The light transmitted through these two portions of the filter is picked up by optical fibers set into the filter support, giving signal and reference beam intensities of $I$ and $I_0$. The fibers conduct these beams to silicon detectors coupled to a logarithmic ratiometer.[14] The voltage output from this unit is proportional to the optical attenuation, which is defined as $A = -\ln(I/I_0)$ and is due to the collected absorbing particles.


*This work was supported by the Director, Office of Energy Research, Office of Health and Environmental Research, Physical and Technological Research Division, and the $CO_2$ Research Division of the U.S. Department of Energy under Contract No. DE-AC03-76SF00098.


†Abridged from an article published in *Applied Optics 21*, p. 3060 (1982).

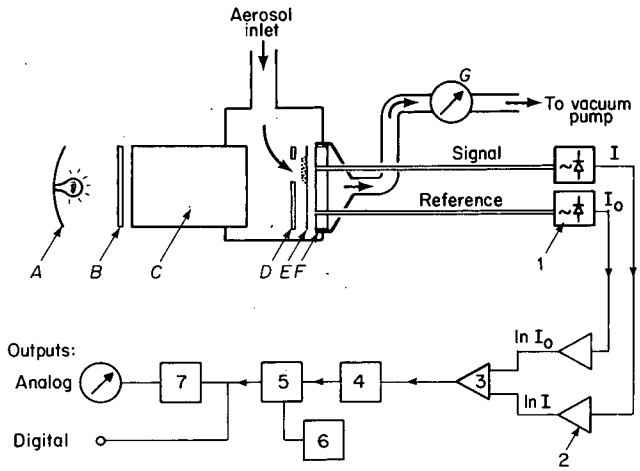


Figure 1. Block diagram of LBL aethalometer. Optical and aerosol collection components: *A*, light source; *B*, 530-nm bandpass filter; *C*, quartz light guide; *D*, transparent mask; *E*, filter with particles collected on portion underneath hole in mask; *F*, filter support with optical fibers set in; *G*, flowmeter. Electronic system components: 1, silicon photodetectors; 2, logarithmic amplifiers; 3, difference amplifier giving output proportional to $\ln(I/I_0)$; 4, A/D converter; 5, storage and subtraction; 6, variable time base; 7, D/A converter. (XBL 826-722)

If the instantaneous absorption coefficient of the aerosol in the air column being drawn through the filter is $b_a(x,t)$ and $v$ is the airstream velocity at the filter face, the attenuation at time $T$ from the deposit on the filter will be

$$A(T) \propto \int_0^T b_a(x,t) \cdot v dt \quad .$$

Differentiation of the voltage proportional to $A(T)$ will then yield a measure of $b_a(x,t)$. Since the rate of increase of $A(T)$ is rather slow (typically 0.1%/min), we use digital methods to perform the differentiation. At selected time intervals, the signal is digitized and stored. Each result is subtracted from the previous measurement, giving a difference proportional to the average of the absorption coefficient during the averaging time interval. The output is available in digital form for further processing and is also converted back to an analog signal for display on a chart recorder.

The instrument was calibrated by operating it in parallel with a sampler collecting aerosol particles on prefired quartz-fiber filters. It has been shown that the dominant absorbing species in urban aerosols is graphitic carbon,[15] which may be measured on quartz-fiber filters by a combined solvent-extraction and thermal-analysis technique.[16,17] Comparison of the two results enabled us to calibrate the aethalometer output in terms of a concentration of graphitic carbon in micrograms per cubic meter. To calculate the absorption coefficient of this material in suspended form, we used an absorption cross section of 10 $m^2/g$, which is compatible with reported theoretical[18] and experimental results.[19,20] We then employed the convenient relationship:

$$[\text{absorption coefficient (units } 10^{-6}\ m^{-1})]$$
$$= [\text{concentration (units } \mu g/m^3)]$$
$$\times [\text{cross section (units } m^2/g)].$$

In the present configuration, the estimated minimum detectable increment in attenuation corresponds to an incremental loading of 10 $ng/cm^2$ of graphitic carbon in the filter. With an airstream velocity of 2.5 m/sec at the filter face, the sensitivity may be represented by a value of the product [(minimum detectable absorption coefficient) $\times$ (averaging time)] of $4 \times 10^{-4}$ sec/m. Using an averaging time of 5 minutes, we can detect a graphitic carbon concentration of 0.13 $\mu g/m^3$, which corresponds to an absorption coefficient of $1.3 \times 10^{-6}\ m^{-1}$.

Figure 2 shows an example of the aethalometer output taken when sampling ambient air in Berkeley. It is clear that there is a strong diurnal variation of the absorption coefficient that may be linked to the movement of air masses as well as variations in emissions. In addition, we can see events that may be

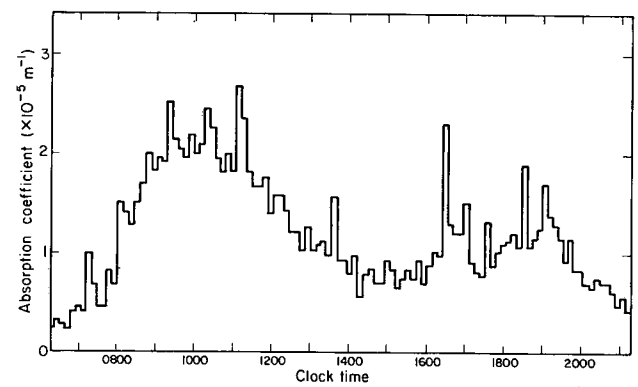


Figure 2. Absorption coefficient vs. clock time at Lawrence Berkeley Laboratory, 1 September 1981. Individual events (e.g., at 1630) may be due to the occasional passage of heavy vehicles on a nearby service road. (XBL 826-721)

attributable to the passage of individual heavy diesel vehicles on a lightly traveled road some 90 m (100 yards) from the sampling location.

The instrument was also used in the field during an Environmental Protection Agency visibility study in Houston, Texas, in September 1980.[21] Figure 3 shows a result from that study, where the output has been smoothed with a time constant of ~20 min. The figure also shows the simultaneous nephelometer measurement of the scattering coefficient and the calculated single-scattering albedo. It is clear in this case that the magnitudes of the scattering and absorption coefficients are not in constant proportion to one another and that a real-time instrument such as the aethalometer is necessary to determine this variation.

## PLANNED ACTIVITIES FOR FY 1983

Work is in progress to improve the stability of the electronic and optical systems and thereby increase the resolution. We are also working on a new filter head that may allow the airstream velocity $v$ to be increased by a factor of 50, which will similarly increase the sensitivity. As there is considerable interest in deploying the aethalometer on an aircraft to determine the vertical profile of aerosol absorption, the instrument is also being strengthened to minimize the effects of vibration.

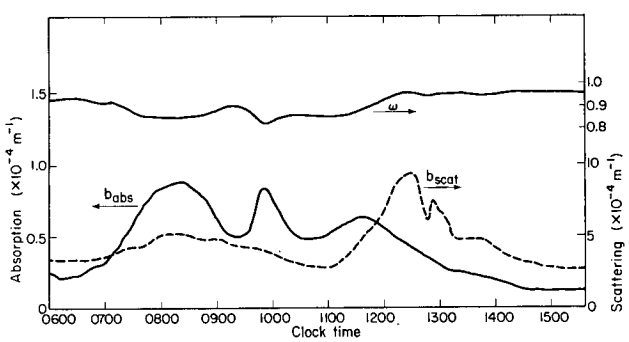


Figure 3. Smoothed data from Houston, Texas, 13 September 1980. Lower curves show absorption coefficient $b_{abs}$ measured by the LBL aethalometer and scattering coefficient $b_{scat}$ measured by a conventional integrating nephelometer vs. clock time. Upper curve shows the variation in single-scattering albedo $\omega = b_{scat}/(b_{scat} + b_{abs})$. Note that absorption and scattering vary most strongly at different times of the day. The absorption peaks, which occur earlier, may correspond to local and regional vehicular emission patterns, while the scattering peak occurs later. Variations in the albedo are significant, although somewhat reduced by the unusually large magnitude of the scattering coefficient. (XBL 826-720)

## REFERENCES


1. Novakov, T. (1982) "Soot in the Atmosphere," in *Particulate Carbon: Atmospheric Life Cycle*, G.T. Wolff and R.L. Klimisch, Eds., Plenum, New York, p. 19.
2. Rosen, H., et al. (1982), "Graphitic Carbon in Urban Environments and the Arctic," in *Particulate Carbon: Atmospheric Life Cycle*, G.T. Wolff and R.L. Klimisch, Eds., Plenum, New York, p. 273.
3. Wolff, G.T., Groblicki, P.J., Cadle, S.H., and Countess, R.J. (1982), "Particulate Carbon at Various Locations in the United States," in *Particulate Carbon: Atmospheric Life,* G.T. Wolff and R.L. Klimisch, Eds., Plenum, New York, p. 297.
4. Paltridge, G.W., and Platt, C.M.R. (1976), in *Radiative Processes in Meteorology and Climatology*, Elsevier, Oxford.
5. Chylek, P., and Coakley, J.A. (1974), "Aerosols and Climate," *Science 183*, p. 75.
6. Buettel, R.G., and Brewer, A.W. (1949), "Instruments for the Measurement of Visual Range," *J. Sci. Instrum. 26*, p. 357.
7. Charlson, R.J., Ahlquist, N.C., Selvidge, H., and MacCready, P.B. (1969), "Monitoring of Atmospheric Aerosol Parameters with the Integrating Nephelometer," *J. Air Poll. Cont. Assoc. 19*, p. 943.
8. Rosen, H., Hansen, A.D.A., and Novakov, T. (1980), "An Instrument for the Quasi-Real-Time Measurement of the Optical Absorption Coefficient of Ambient Aerosols," Lawrence Berkeley Laboratory Report LBID-256.
9. Gerber, H.E. (1979), "Portable Cell for Simultaneously Measuring the Coefficients of Light Scattering and Extinction for Ambient Aerosols," *Appl. Opt. 18*, p. 1009.
10. Terhune, R.W., and Anderson, J.E. (1977), "Spectrophone Measurements of the Absorption of Visible Light by Aerosols in the Atmosphere," *Opt. Lett. 1*, p. 70.
11. Rosen, H., and Novakov, T. (1982), "Lawrence Berkeley Laboratory Laser Transmission Method," in *Light Absorption by Aerosol Particles*, H. Gerber, Ed., Spectrum, Hampton, Virginia, p. 321.
12. Rosen, H., and Novakov, T. (1978), "Optical Attenuation: A Measurement of the Absorbing Properties of Aerosol Particles," in *Atmospheric*

*Aerosol Research Annual Report, 1977–78*, Lawrence Berkeley Laboratory Report LBL-8696, p. 54.
13. Yasa, Z., Amer, N.A., Rosen, H., Hansen, A.D.A., and Novakov, T. (1979), "A Photoacoustic Investigation of Urban Aerosol Particles," *Appl. Opt. 18*, p. 2528.
14. Optical multimeter, Model 22XL, Photodyne, Inc., Westlake Village, California.
15. Rosen, H., Hansen, A.D.A., Gundel, L., and Novakov, T. (1978), "Identification of the Optically Absorbing Component in Urban Aerosols," *Appl. Opt. 17*, p. 3859.
16. Novakov, T. (1981), "Microchemical Characterization of Aerosols," in *Nature, Aim, and Methods of Microchemistry*, H. Malissa, M. Grasserbauer, and R. Belcher, Eds., Springer-Verlag, Vienna, p. 141.
17. Gundel, L., Dod, R., and Novakov, T. (1981), "Determination of Black Carbon by Thermal Analysis," in *Energy and Environment Division Annual Report 1980*, Lawrence Berkeley Laboratory Report LBL-11990, p. 5-26.
18. Medalia, A.I., and Richards, L.W. (1972), "Tinting Strength of Carbon Black," *J. Colloid Interface Sci. 40*, p. 223.
19. Truex, T.J., and Anderson, J.E. (1979), "Mass Monitoring of Carbonaceous Aerosols with a Spectrophone," *Atmos. Environ. 13*, p. 507.
20. Szkarlat, A.C., and Japar, S.M. (1981), "Light Absorption by Airborne Aerosols: Comparison of Integrating Plate and Spectrophone Techniques," *Appl. Opt. 20*, p. 1151.
21. Dzubay, T.G., et al. (1982), "Visibility and Aerosol Composition in Houston, Texas," *Environ. Sci. Technol. 16*, p. 514.

## THE RELATIONSHIP BETWEEN OPTICAL ATTENUATION AND BLACK CARBON CONCENTRATION FOR CARBONACEOUS PARTICLES*

*L.A. Gundel, R.L. Dod,*
*H.J. Rosen, and T. Novakov*

Aerosol particulate material from ambient air and combustion sources usually appears black when collected on filters because of the presence of light-absorbing black carbon.[1] In the atmosphere, this light absorption can degrade visibility[2] and perturb the tropospheric energy balance.[3,4]

Light absorption provides the basis for a fast and nondestructive method for determining concentrations of black carbon on filter samples—the LBL laser transmission technique.[1] This measures the attenuation (ATN) of visible light as it passes through the filter. ATN is defined as 100 ln $I_0/I$, where $I_0$ and $I$ are the intensities of light transmitted through blank and loaded filters, respectively. When the relationship between ATN and black carbon concentration ([BC]) is known, a good estimate of [BC] can be derived from the simple ATN measurements. For example, if ATN has a linear dependence on [BC], then [BC] = ATN/$\sigma$, where $\sigma$ is the specific attenuation for black carbon. This application relies on the assumption of similar optical properties for both source and ambient particles.

In this study, we measured [BC] and ATN simultaneously for a large group of source and ambient filter samples. The results were used to calibrate the LBL laser transmission technique and to provide a value for the specific attenuation.

### ACCOMPLISHMENTS DURING FY 1982

Samples of ambient aerosol particulate material were collected on prefired quartz-fiber filters in Berkeley and Anaheim, California; Denver, Colorado; Warren, Michigan; and Vienna, Austria. Combustion-source samples were from a natural-gas-fired boiler, a propane burner, and a diesel bus. Samples representing an average motor vehicle population were collected in a highway tunnel and in a parking garage. Before analysis, the samples were sequentially extracted by benzene and a methanol-chloroform mixture (1:2, v:v).[5,6]

Combustion thermal analysis (EGA†) with continuous light-absorption[7] monitoring was used to identify and quantitate black carbon (carbon combusted as

*This work was supported by the Director, Office of Energy Research, Office of Health and Environmental Research, Physical and Technological Research Division of the U.S. Department of Energy under Contract No. DE-AC03-76SF00098, and by the National Science Foundation under contract No. ATM 82-10343.

†Evolved gas analysis—see the article "Qualitative and Quantitative Aspects of Evolved Gas Analysis" for a discussion of this technique.

the light transmission increases), as shown in the shaded areas of Fig. 1. Solvent extraction of the samples does not remove the black carbon (as shown by lack of change in ATN) but does remove nonabsorbing organic materials that can interfere with quantitative determination of the black carbon component.

This method of determining of black carbon was validated by an extensive 11-laboratory round-robin intercomparison.[8] Attenuation measured during thermal analysis, ATN (TA), was validated by comparison to ATN(LBL), measured for the same filters using the LBL laser transmission technique.[1] For 61 extracted filters,

$$ATN(TA) = -2.8 \pm 3.9 + (0.97 \pm 0.02) \times ATN(LBL) .$$

This is excellent agreement. Estimates of measurement variability and quantitation limits are given below. The limits of detection (LOD) and limits of quantitation (LOQ) are defined as[9] $3s$ and $10s$, where $s$ is the standard deviation for measurements of blanks.

Black carbon:
LOD = 0.6 $\mu$g cm$^{-2}$ LOQ = 2.0 $\mu$g cm$^{-2}$

ATN (both methods):
LOD = 6 LOQ = 20

Ambient black carbon concentrations are given in Table 1. In Berkeley, [BC] ranged from 0.8 to 4.6 $\mu$g m$^{-3}$, with a mean black carbon fraction of 0.20 ± 0.04 for eleven 24-hour filters. These direct measurements of [BC] are consistent with earlier estimates that used ATN(LBL) for the same locations.[10]

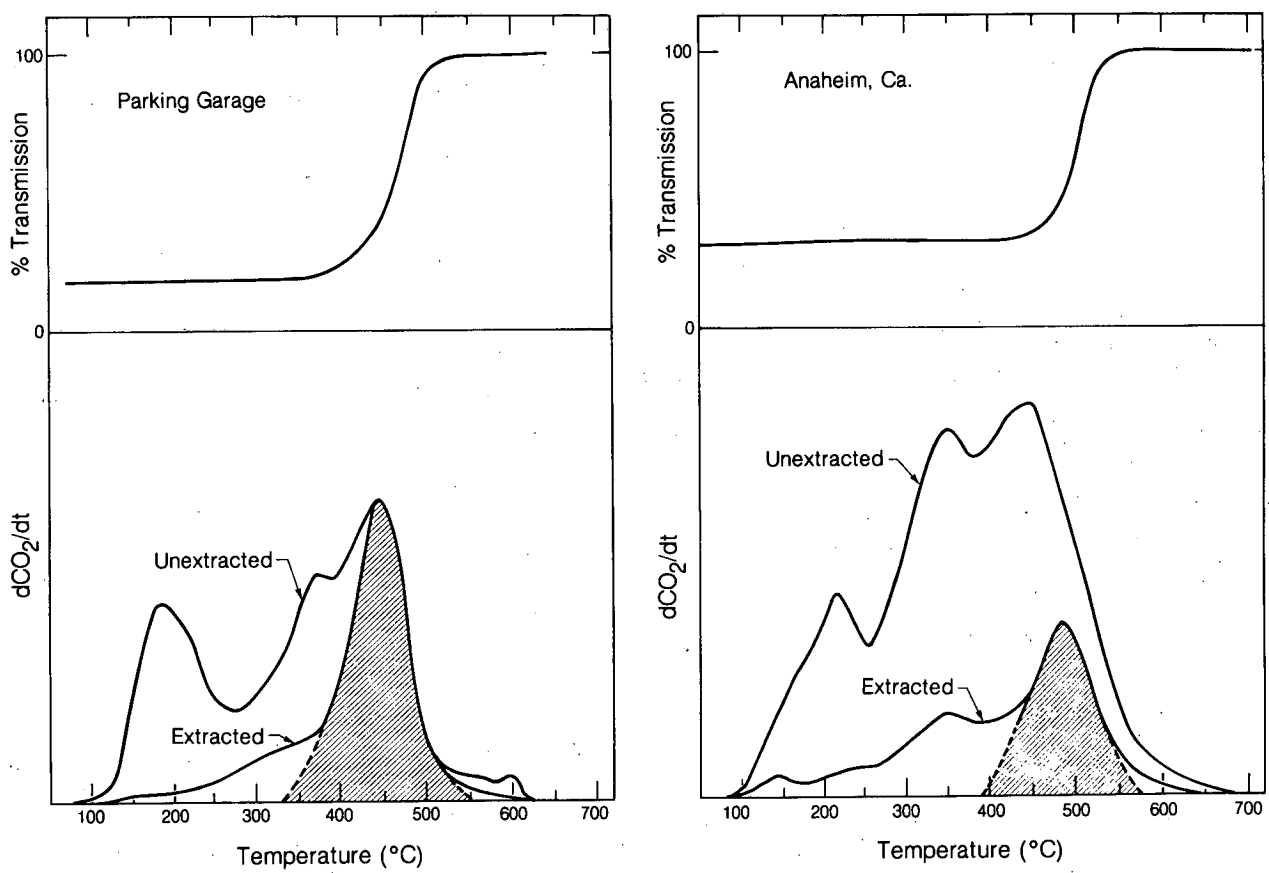


Figure 1. Thermograms of particulate carbon collected in a Berkeley parking garage and in Anaheim, California. Black carbon is represented by the shaded areas. The upper traces show light transmission through the filter samples. (XBL 835-918A)

Table 1. Ambient particulate carbon concentrations.[a]

| Site | Date | Range [BC] $\mu g\ m^{-3}$ | Range $[C_{tot}]$ $\mu g\ m^{-3}$ | Mean $[BC]/[C_{tot}]$ | No. of Samples |
|---|---|---|---|---|---|
| Berkeley, CA (LBL) | Sept 79–Oct 81 | 0.8–4.6 | 4.4–22.8 | 0.20±0.04 | 11 |
| Berkeley, CA (freeway) | Sept–Nov 79 | 3.1–10.5 | 10.5–34.0 | 0.33±0.7 | 5 |
| Anaheim, CA | Sept–Nov 79 | 3.9–5.7 | 20.3–5.2 | 0.22±0.06 | 3 |
| Riverside, CA | June 81 | 1.0-4.7 | 6.5–24.7 | 0.17±0.02 | 4 |
| Denver, CO | Nov 78–May 79 | 1.3–2.9 | 7.0–16.6 | 0.19±0.01 | 5 |
| Warren, MI[b] | Winter 80–81 | 2.8–14.5 | 11.1–42.0 | 0.30±0.05 | 3 |
| Vienna, Austria | Sept–Oct 81 | 6.8–10.6 | 18.2–35.9 | 0.32±0.04 | 6 |

[a]Black carbon concentrations have been adjusted for losses during extraction. Average BC loss is 7%, as determined from the ratio of ATN values before and after extraction.

[b]These samples were analyzed as part of the General Motors-sponsored intercomparison study of methods for the determination of black carbon.[8]

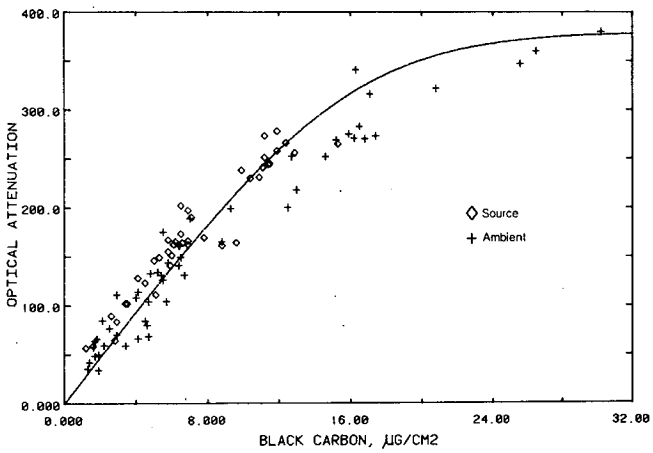


Figure 2. The relationship between optical attenuation and black carbon concentration for source and ambient particles collected on quartz-fiber filters. The line represents Eq. (1) in the text, where $\alpha = 0.02$ and $\sigma = 24.4 \pm 1.5$ $cm^2\ \mu g^{-1}$. (XBL 834-178)

The relationship between ATN and [BC] is shown in Fig. 2. For source particles where ATN is below 200 and [BC] is below 8 $\mu g\ cm^{-2}$:

$$ATN = (10.6 \pm 16.6) + (24.1 \pm 2.8)[BC]$$

with the correlation coefficient $r = 0.859$. For ambient particles:

$$ATN = (-0.8 \pm 9.8) + (24.1 \pm 2.3)[BC]$$

with $r = 0.893$. There is no significant difference between source and ambient particles in this relationship.

For all data with ATN $< 200$ and [BC] $< 8\ \mu g\ cm^{-2}$:

$$ATN = (-1.6 \pm 8.7) + (25.4 \pm 1.7)[BC]$$

with $r = 0.883$. Since the intercept is not significantly different from zero, the slope of the line is the specific attenuation. Here $\sigma = 25.4 \pm 1.7$.

All data, regardless of sample loading, can be fit to the equation

$$ATN = -100 \ln [(1 - \alpha)\ e^{-\sigma[BC]} - \alpha] \qquad (1)$$

which reflects the observation that a small fraction, $\alpha$ (~0.02), of the incident light is conducted along the quartz fibers of the filter without interaction with the particle deposit. Using this equation, we find that specific attenuation is $24.4 \pm 1.5\ cm^2\ \mu g^{-1}$ for all data.

## PLANNED ACTIVITIES FOR FY 1983

We plan to investigate the influence of particle size and composition on the specific attenuation and to increase our data set with samples collected from other sources and ambient locations.

## REFERENCES


1. Rosen, H., Hansen, A.D.A., Gundel, L., and Novakov, T. (1978), "Identification of the Optically Absorbing Component in Urban Aerosols," *Appl. Opt. 17*, p. 3859.
2. Weiss, R.E., et al. (1979), "Studies of the Optical, Physical, and Chemical Properties of Light Absorbing Aerosols," in *Proceedings, Conference on Carbonaceous Particles in the Atmosphere*, Lawrence Berkeley Laboratory Report LBL-9037, p. 257.

3. Porch, W.M., and MacCracken, M.C. (1982), "Parametric Study of the Effects of Arctic Soot on Solar Radiation," *Atmos. Environ. 16*, p. 1365.
4. Cess, R.D. (1982), "Arctic Aerosols: Model Estimates of Interactive Influences upon the Surface-Troposphere Radiation Budget," *Atmos. Environ.* (submitted).
5. Appel, B.R., et al. (1979), "Analysis of Carbonaceous Material in Southern California Atmospheric Aerosols," *Environ. Sci. Technol. 13*, p. 98.
6. Gundel, L.A., and Novakov, T. (1982), "Application of Selective Solvent Extraction to Carbonaceous Aerosols," in *Energy and Environment Annual Report, FY 1981*, Lawrence Berkeley Laboratory Report LBL-13500, p. 4-16.
7. Dod, R.L., Rosen, H., and Novakov, T. (1979), "Optico-Thermal Analysis of the Carbonaceous Fraction of Aerosol Particles," *Atmospheric Aerosol Research Annual Report, 1977–78*, Lawrence Berkeley Laboratory Report LBL-8696, p. 2.
8. Groblicki, P.J., Cadle, S.H., Ang, C.C., and Mullawa, P.A. (1982), *Interlaboratory Comparison of Methods for the Determination of Organic and Elemental Carbon in Atmospheric Particulate Matter*, Report GMR 4054, General Motors Research Laboratory, Warren, Michigan.
9. ACS Committee on Environmental Improvement (1980), "Guidelines for Data Acquisition and Data Quality Evaluation in Environmental Chemistry," *Anal. Chem. 52*, p. 2242.
10. Hansen, A.D.A., et al. (1980), "The Use of an Optical Attenuation Technique to Estimate the Carbonaceous Component of Urban Aerosols," *Atmospheric Aerosol Research, FY 1979*, Lawrence Berkeley Laboratory Report LBL-10735, p. 16.

## GRAPHITIC-CARBON-TO-LEAD RATIO AS A TRACER FOR SOURCES OF THE ARCTIC AEROSOL*†

*H.J. Rosen, A.D.A. Hansen, and T. Novakov*

Recent studies at Barrow, Alaska, indicate the presence of large aerosol concentrations that appear to be characteristic of the Arctic region as a whole.[1–4] If the obvious natural aerosol components (e.g., sea salt and soil) are excluded, the predominant components of the Arctic aerosol are carbon- and sulfur-containing particles. These particles occur at concentrations comparable to those found in urban areas in the continental United States.[1,2]

There is considerable indirect evidence that a major part of the Arctic aerosol is produced from combustion processes. However, the strongest and most direct substantiation of this inference has been provided by the identification of large concentrations of graphitic carbon in the Arctic atmosphere.[1] These graphitic species, which have a structure similar to carbon black, can be produced only by combustion processes. The concentration of these particles at Barrow during the winter and spring approaches those found in urban areas (the concentrations are only a factor of 4 less than the average values found in Berkeley, California, and Gaithersburg, Maryland, and a factor of 10 less than those found in New York City).

Associated with these graphitic species are large optical absorption coefficients ($\sim 10\ m^2\ g^{-1}$), which could produce a significant perturbation of the heat balance over the Arctic. Preliminary model calculations indicate that present springtime concentrations of graphitic particles could increase the atmospheric heating rate by an amount comparable to that expected from a doubling of the $CO_2$ concentration.[5,6]

The sources of the Arctic aerosol are unknown at present. Part of the aerosol may come from local Alaskan sources, but there is considerable evidence that a major fraction is due to long-range transport from other industrialized regions,[7,8] with Eurasia suggested as a major source area.[2] Use of the ratio of graphitic carbon to lead as a tracer for the sources of the Arctic aerosol is described here.

*This work was supported by the Director, Office of Energy Research, $CO_2$ Research Division of the U.S. Department of Energy under Contract No. DE-AC03-76SF00098 and by the National Oceanic and Atmospheric Administration.

†Published in *Geophysical Monitoring for Climatic Change No. 10* (1982), B.A. Bodhaine and J.M. Harris, Eds., National Oceanic and Atmospheric Administration, Washington, D.C., p. 134.

## ACCOMPLISHMENTS DURING FY 1982

An aerosol sampler has been operating at Barrow since October 1979, collecting parallel filter samples on 47-mm quartz-fiber and Millipore substrates at a flow rate of approximately 1.5 $ft^3$ $min^{-1}$. Measurements of graphitic carbon and particulate lead concentrations over eight months—from October 1979 through May 1980—are reported here. The graphitic carbon concentrations were obtained using the LBL laser transmission technique[9] with an empirical calibration curve developed for urban particulates in the United States.[10] Independent measurements of the graphitic carbon concentration by an opticothermal analysis technique are under way. Lead concentrations were determined through x-ray fluorescence analyses, performed by Robert Giauque.

Natural concentrations of particulate lead are very low, and it is usually assumed that in polluted environments the major source is from the burning of leaded gasoline by automobiles. Typical ground-level lead concentrations in urban atmospheres in the United States are ~2 $\mu g$ $m^{-3}$. In the Arctic the concentrations are much smaller, as shown in Fig. 1(a), but are probably also combustion-generated since the enrichment factors relative to the earth's average crustal abundance are large. For comparison, the graphitic carbon concentration as a function of the time of year is shown in Fig. 1(b).

Although both aerosol components show their largest concentrations during the winter and spring, their seasonal variations are quite distinct. Whereas the graphitic carbon concentrations are roughly constant from December through April, the lead concentrations show a rather sharp peak in November and December and relatively low values for the rest of the year. As a result of these differences in behavior, the relative concentrations of graphitic carbon and lead change substantially throughout the year, as shown in Fig. 2. These variations could represent the contributions of different source regions during different times of the year or a seasonal variation in the fuel mix of source regions. It should be emphasized that the results reported here are only for 1 year, and interannual variation due to variability in the air trajectories that arrive at Barrow from year to year could be considerable.

Interpretations of these results are based on several crucial assumptions: (1) the graphitic-carbon-to-lead ratio does not change significantly during transport because of different deposition rates for

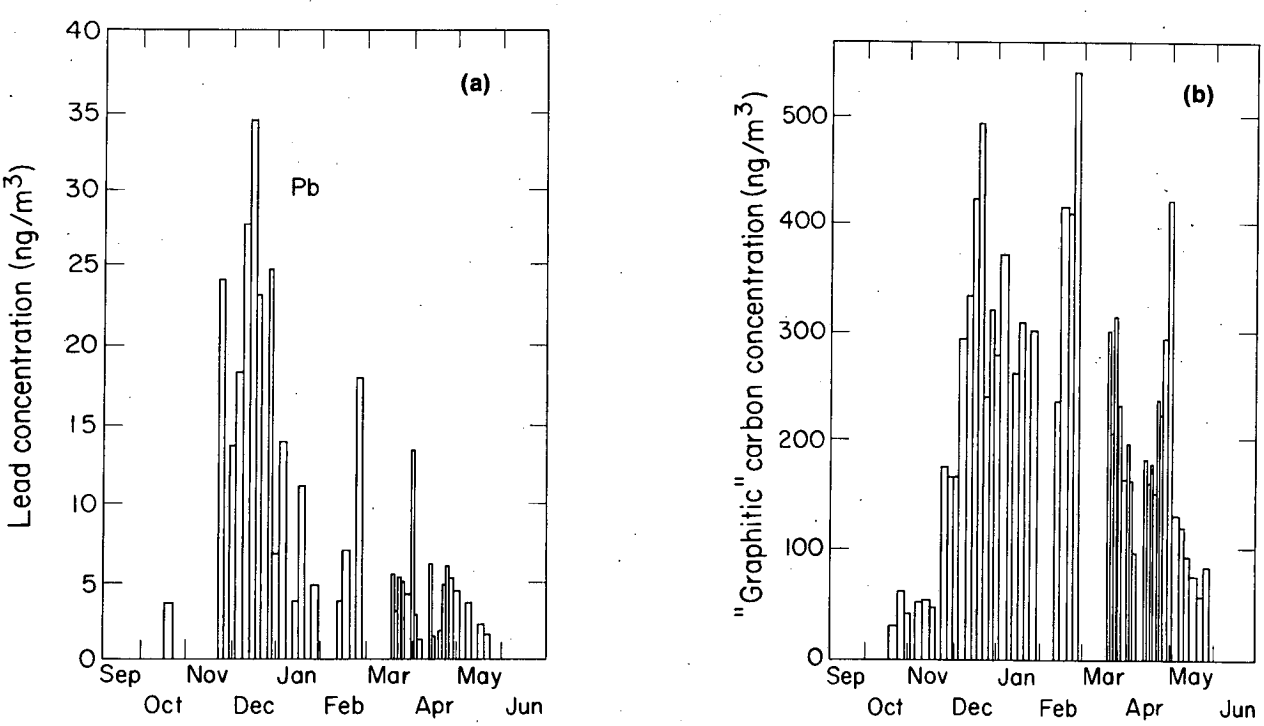


Figure 1. (a) Particulate lead concentration and (b) graphitic carbon concentration, each as a function of the time of year for 1979–1980. [(a) XBL 827-7185; (b) XBL 827-7186]

particulate lead and graphitic carbon, and (2) source regions may be characterized by ground-level graphitic-carbon-to-lead ratios (i.e., these ratios do not change appreciably with altitude). These assumptions need further investigation.

Finally, we compare the graphitic-carbon-to-lead ratios in the Arctic with typical values in the western and eastern United States. As shown in Fig. 2, the values in the Arctic are considerably larger than those found in the United States, especially during March and April, when the average value is 10 times that found in the eastern U. S. and 30 times that found in the western U. S. If the graphitic-carbon-to-lead ratio in the western U. S. is used to represent a source region dominated by automotive emissions, then these results could imply that source regions of the Barrow aerosol during March and April do not have a large automotive component relative to other soot-generating combustion sources. Such a region could have a large diesel, wood-burning, or stationary-source component relative to automobiles. Furthermore, these results could imply that the United States or other regions with similar fuel mixtures do not contribute significantly to the Arctic haze during these periods of high graphitic-carbon-to-lead ratios.

## PLANNED ACTIVITIES FOR FY 1983

The use of the graphitic-carbon-to-lead ratio represents a first attempt to identify the sources of the Arctic haze. Future work will extend the technique to other parts of the Arctic and develop new methods of analysis to identify combustion source contributions.

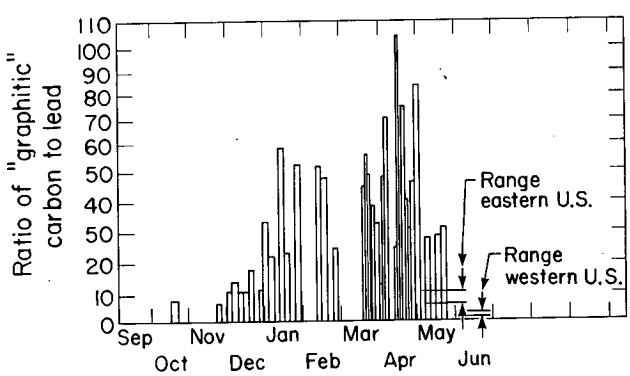


Figure 2. Ratio of concentrations of graphitic carbon to particulate lead as a function of the time of year for 1979–1980. Also shown is the range of values for the western United States (Anaheim, Berkeley, and Fremont, California) and the eastern United States (New York City; Argonne, Illinois; and Gaithersburg, Maryland). The range of values is defined as those values within one standard deviation of the average. (XBL 827-7100)


## ACKNOWLEDGMENT

We would like to acknowledge Robert Giauque for careful XRF analyses of samples.


## REFERENCES


1. Rosen, H., Novakov, T., and Bodhaine, B.A. (1981), "Soot in the Arctic," *Atmos. Environ. 15*, p. 1371.
2. Rahn, K.A., and McCaffrey, R.J. (1980), "On the Origin and Transport of Winter Arctic Aerosol," *Ann. N.Y. Acad. Sci. 338*, p. 486.
3. Shaw, G.E. (1981), "Eddy Diffusion Transport of Arctic Pollution from the Mid Latitudes: A Preliminary Model," *Atmos. Environ. 15*, p. 1483.
4. Bodhaine, B.A., Harris, J.M., and Herbert, G.A. (1981), "Aerosol Light Scattering and Condensation Nuclei Measurements at Barrow, Alaska," *Atmos. Environ. 15*, p. 1375.
5. Porch, W.M., and MacCracken, M.C. (1982), "Parametric Study of the Effects of Arctic Soot on Solar Radiation," *Atmos. Environ. 16*, p. 1365.
6. Cess, R.D. (1982), "Arctic Aerosols: Model Estimates of Interactive Influences upon the Surface-Troposphere Radiation Budget," *Atmos. Environ.* (submitted).
7. Peterson, J.T., Hanson, K.J., Bodhaine, B.A., and Oltmans, S.J. (1980), "Dependence of $CO_2$, Aerosol, and Ozone Concentrations on Wind Direction at Barrow, Alaska, During Winter," *Geophys. Res. Lett. 7*, p. 349.
8. Barrie, L.W., Hoff, R.M., and Daggupaty, S.M. (1981), "The Influence of Mid-Latitudinal Pollution Sources on Haze in the Canadian Arctic," *Atmos. Environ. 15*, p. 1407.
9. Rosen, H., Hansen, A.D.A., Gundel, L., and Novakov, T. (1978), "Identification of the Optically Absorbing Component in Urban Aerosols," *Appl. Opt. 17*, p. 3859.
10. Gundel, L., Dod, R., and Novakov, T. (1981), "Determination of Black Carbon by Thermal Analysis," *Environmental Pollutant Studies*, Lawrence Berkeley Laboratory Report LBL-11986, p. 5.

# THE OXYGEN CONTENT OF AMBIENT PARTICULATE MATTER*

*W.H. Benner, C. Chuang, A.D.A. Hansen, and T. Novakov*

The light-scattering, haze-forming particles of the troposphere can come from primary sources like combustion engines and wind-blown dust or from secondary sources, i.e., chemical reactions that transform gases into particles. Oxygen in the particles can be grouped into several fractions: organic oxygen, carbonates, nitrates, sulfates, silicates, and metal oxides. In general, primary particulate matter contains carbonates, silicates, and metal oxides (from resuspended soil and fly ash) and is likely to contain organic oxygen from incompletely burned fuels. Secondary particulate matter contains sulfates, nitrates, and presumably organic oxygen from photochemically initiated reactions. We are attempting to determine the relative importance of the primary and secondary origins of oxygenated-organic particulate matter; this article describes our initial efforts.

## ACCOMPLISHMENTS DURING FY 1982

To determine oxygen in particulate matter, several analytical techniques were combined.[1-5] Figure 1 shows the analytical system. Gas samples were injected into the pyrolysis tube via a septum. A multiport valve changed the direction of flow through the pyrolysis tube. Solid samples and filter samples were loaded into a small platinum boat (formed from 5-mil Pt foil) and placed into the cool zone of the pyrolysis tube during backflushing with $N_2$ so that room air did not contact the hot carbon. After a sample was loaded, the pyrolysis tube was resealed (at the O-ring seal); any air entrained in the tube was backflushed from the system (~4 min), and the multiport valve was switched. Finally, after the CO detector stabilized, the sample boat was slid into the hot zone with a magnetically moved plunger.

*This work was supported by the Director, Office of Energy Research, Office of Health and Environmental Research, Physical and Technological Research Division of the U.S. Department of Energy under Contract No. DE-AC03-76SF00098, and by the National Science Foundation under Contract No. ATM 82-10343.

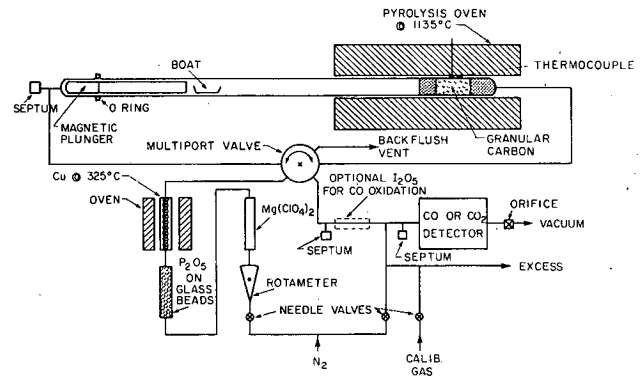


Figure 1. Schematic diagram of oxygen analysis system. (XBL 833-127)

This method thermally decomposes the sample, and the oxygen-containing decomposition products react with the hot carbon (1130°C) to produce CO. Oxygen can be determined in all materials that decompose at $T < 1130°C$. In ambient particulate matter, oxygenated organics, nitrates, sulfates, $H_2O$, adsorbed oxygen-containing gases, and carbonates will decompose; but silica and alumina ($Al_2O_3$) will not decompose at this temperature. However, silica contains OH functional groups, and these presumably decompose. All samples were dessicated over $P_2O_5$ to remove $H_2O$.

A variety of standard compounds, injections of $CO_2$, and samples of filtered ambient particulate matter were analyzed. Direct injections of $CO_2$ showed good recovery (100.0%) with a standard deviation ($\sigma$) of 0.4%. A number of oxygenated compounds, including ammonium nitrate, ammonium sulfate, 2,4-dihydroxy-benzaldehyde, benzoic acid, m-hydroxybenzoic acid, glutaric acid, myristic acid, phthalic acid, and potassium phthlate (KHP), were analyzed. The recovery for all standards was 101.8 ± 4.5% ($n$ = 65). The analytical limit of detection (LOD) and limit of quantitation (LOQ) for recovery of standards from pieces of quartz-fiber filters are:

$$\text{LOD} = blank + 3\sigma_{blank} = 6.9 + 1.2 = 8.1\ \mu\text{g O}$$

$$\text{LOQ} = blank + 10\sigma_{blank} = 6.9 + 4.0 = 10.9\ \mu\text{g O}$$

Figures 2(a) and 2(b) show the linearity and the scatter that can be expected for the analysis of standards prepared by the evaporation of solutions onto 1-$cm^2$ quartz-fiber discs. Each datum point is the determination of oxygen on a 1-$cm^2$ disc.

Replicate analyses of two ambient air filter samples are presented in Table 1 to show the applicability of

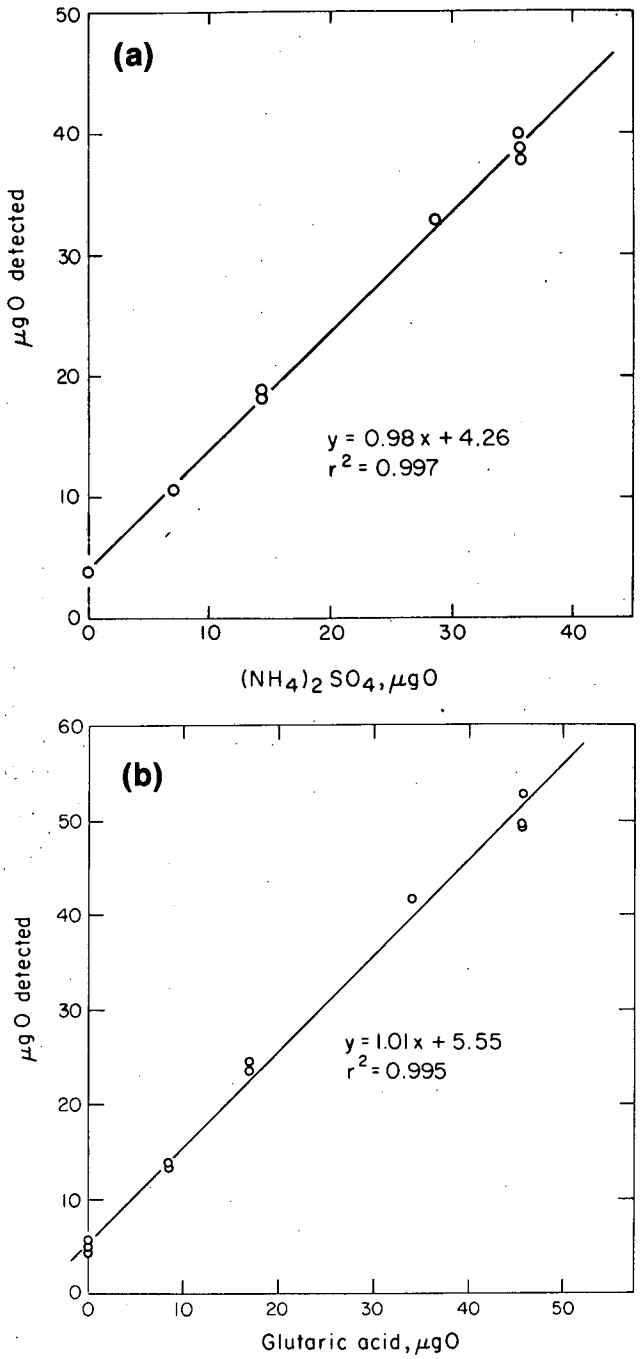


Figure 2. (a) Recovery of oxygen from $(NH_4)_2SO_4$ standards. (b) Recovery of oxygen from glutaric acid standards. [(a) XBL 833-129; (b) XBL 833-128]

this technique. A high-volume filter sampler (~1100 liters per minute of ambient air was drawn through 400-$cm^2$ prefired quartz-fiber filters for several hours) was used to collect samples in Berkeley, California. Multiple 1-$cm^2$ discs of these filters were dessicated for 12 hours over $P_2O_5$ and then analyzed for oxygen. Analysis for particulate carbon used a separate technique.[6] The results indicate that the volumetric flow rates frequently used to sample ambient particulate matter will collect enough oxygenated particulate matter so that 1 $cm^2$ of filter will give a signal above the LOQ in the nondispersive infrared analysis scheme. Comparison of the carbon loadings in Table 1 of this article and those in Table 2 of Novakov[7] indicates that these loadings are typical for many United States sampling sites.

Table 1. Analysis of filtered ambient particulate matter.

| Sample[a] | μg O/cm² [b] | μg O/m³ | μg C/cm² | μg C/m³ |
|---|---|---|---|---|
| *Daytime* | | | | |
| 1000–1715 hrs, 11 Mar 81 | 20.5, 20.3, 20.2, 20.2 | 16.3 | 13.7 | 11.0 |
| *Nighttime* | | | | |
| 1800–0600 hrs, 11–12 Mar 81 | 21.0, 20.5 | 10.1 | 12.9 | 6.3 |

[a]Both samples were collected in Berkeley, California.
[b]Blank corrected replicates.

## PLANNED ACTIVITIES FOR FY 1983

The technique described here is being applied to the determination of oxygen in filter samples of ambient particulate matter. Samples from a variety of rural and urban locations have been collected and will be analyzed to determine the parameters (e.g., origin, exposure to photochemical reactive species, exposure to fog, and age) that influence the oxygen content of particles.

## REFERENCES

1. Schütze, M. (1939), (*Z. Anal. Chem. 118*, p. 241, 1939), reprinted in *Standard Methods of Chemical Analysis*, Vol. 1 (6th ed.), N.H. Furman, Ed., Van Nostrand, Princeton, p. 780 (1962).
2. Unterzeucher, J. (1940), (*Ber. 73B*, p. 391, 1940), reprinted in *Standard Methods of Chemical Analysis*, Vol. 1 (6th ed.), N.H. Furman, Ed., Van Nostrand, Princeton, p. 780 (1962).

3. Oita, I.J. and Conway, H.S. (1954), "Direct Determination of Oxygen in Organic Substances—Modified Schütze Method," *Anal. Chem. 26*, p. 600.
4. Campanile, V.A., et al. (1951), "Improved Method for Determination of Oxygen," *Anal. Chem. 23*, p. 1421.
5. Uhedová, J. and Rezl, V. (1981), "Determination of Oxygen in Organic Substances by Reaction–Frontal Gas Chromatography," *Anal. Chem. 53*, p. 164.
6. Huffman, Jr., E. (1977), "Performance of a New Automatic Carbon Dioxide Coulometer," *Microchem. J. 22*, p. 567.
7. Novakov, T. (1981), "Microchemical Characterization of Aerosols," in *Nature, Aim and Methods of Microchemistry*, H. Malissa, M. Grasserbauer, and R. Belcher, Eds., Springer-Verlag, Vienna, p. 141.

## QUALITATIVE AND QUANTITATIVE ASPECTS OF EVOLVED GAS ANALYSIS*

*L.A. Gundel, R.L. Dod, and T. Novakov*

Thermal analytical methods, such as thermogravimetric analysis (TGA) and differential scanning calorimetry (DSC), have long been used to provide information about the thermal stability and chemical composition of a variety of materials. Until recently, a method closely related to TGA—evolved gas analysis (EGA)—received relatively little attention. TGA detects the mass loss of a sample as a function of temperature when the sample is heated in an oxidizing or inert atmosphere. EGA, in contrast, determines the rate of evolution of gaseous species from the sample. In EGA, a sample is gradually heated in a stream of oxygen or nitrogen, and the evolved gases are measured by one or more gas-specific detectors as a function of the sample temperature. For characterizing carbon- and nitrogen-containing materials, it is convenient to use oxygen as the carrier gas with simultaneous detection of $CO_2$ and $NO_x$. (A catalyst, such as CuO, is used to convert all carbon- and nitrogen-containing gases to $CO_2$ and $NO_x$.)

A plot of concentration of $CO_2$ and $NO_x$ vs. time or temperature constitutes the EGA thermogram. Thermograms consist of peaks or groups of peaks resulting from the volatilization, decomposition, and combustion of the sample material, thus providing information about the chemical bonding of C and N in the sample. The area under the thermograms is proportional to the concentrations of these elements.

EGA requires no special sample preparation or preseparation and is therefore applicable to both soluble and insoluble sample components. This feature, combined with the high sensitivity of the method, was found to be especially useful in analysis of environmental samples, where some of the most interesting applications have been made. Malissa et al.[1] used conductometric $CO_2$ and $SO_2$ detectors to perform simultaneous carbon and sulfur analysis of dust samples. Puxbaum[2] used a TGA system followed by $CO_2$ and $SO_2$ detection to analyze aerosol particles and demonstrated the close correspondence between TGA and EGA results for such samples. Malissa et al.[3] used EGA with flame ionization detection to determine volatile aerosol organic materials. Bauer and Natusch[4] used EGA with $CO_2$ detection to identify carbonate compounds in coal fly ash.

The EGA method was further improved in our laboratory by incorporating continuous monitoring of the light attenuation of the aerosol sample.[5] An examination of the $CO_2$ and optical thermograms enables the assignment of the $CO_2$ thermogram peaks that correspond to the optically absorbing black carbon. Because these peaks result from the combustion of black carbon, they are accompanied by a sudden decrease in the sample absorptivity. This apparatus was used to quantitate the black and organic carbon content in aerosol samples[6] and to assess the primary and secondary organic aerosol material.[7]

Recently, we redesigned our EGA system to simultaneously analyze both carbon and nitrogen. This was accomplished by using a chemiluminescent $NO_x$ detector (ThermoElectron Model 14D/E) in series with a nondispersive infrared $CO_2$ analyzer (MSA Model 202S).[5]

*This work was supported by the Director, Office of Energy Research, Office of Health and Environmental Research, Physical and Technological Research Division of the U.S. Department of Energy under Contract No. DE-AC03-76SF00098, and by the National Science Foundation under Contract No. ATM 82-10343.

## ACCOMPLISHMENTS DURING FY 1982

For individual compounds, EGA, like TGA, may result in single- or multiple-peak thermograms, depending on whether the thermal decomposition occurs in single or multiple stages. With the latter, EGA will give information about both the initial compound and intermediate compounds produced during the heating process. The following examples, obtained with several inorganic nitrogen compounds, illustrate these features of EGA.

$NO_x$ thermograms of $NH_4NO_3$, $NH_4HSO_4$, $(NH_4)_2SO_4$, and $NaNO_3$ are shown in Fig. 1. $NH_4NO_3$, $NH_4HSO_4$, and $NaNO_3$ result in single-peak thermograms characteristic of single-stage thermal decomposition processes. In contrast, $(NH_4)_2SO_4$ shows a doublet with peaks at 225 and 290°C. The second peak coincides with the $NH_4HSO_4$ peak. This observation is consistent with a two-stage decomposition process, where one ammonia molecule is released first, leaving a residue of $NH_4HSO_4$, which decomposes at 290°C. The samples of these compounds, and all others reported here, were prepared for EGA by deposition of aliquots of standard solution onto clean, fired quartz-fiber filters, followed by drying at temperatures between 30 and 50°C before analysis.

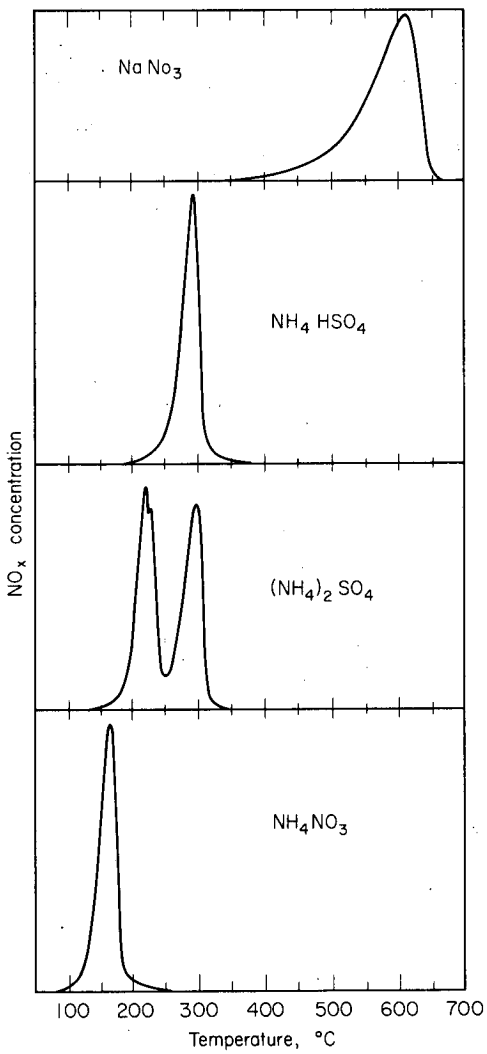


Figure 1. $NO_x$ thermograms of some inorganic compounds. (XBL 8111-1624)

A number of organic compounds were also studied. Some examples showing simple, essentially single-peak thermograms are shown in Fig. 2. This figure shows that the peak temperatures are characteristic of the compounds, as are the more detailed features, such as the peak shapes and widths. Examples of organic compounds showing complex thermogram features are shown in Fig. 3. With the exception of brucine, $NO_x$ and $CO_2$ thermograms show similar features.

It is obvious from these examples that EGA thermograms can be used for qualitatively analyzing different compounds and, with proper standards, for determining specific compounds in a mixture. EGA can also be used for quantitative analysis, provided that the compound does not decompose or sublime at temperatures corresponding to the start of the run. For our samples, this temperature is about 50°C because of the heating of the sample by the catalyst furnace, which is closely coupled to the sample furnace. An example of the quantitative aspect of EGA is shown in Table 1, where carbon and nitrogen recovery as a fraction of the known amounts of C and N are shown. The data show that the carbon recovery is essentially 100%, while the nitrogen recovery depends in some samples on the chemical composition of the sample material.

To illustrate the correspondence between EGA and TGA in Fig. 4, we show the EGA ($CO_2$) thermogram of potassium hydrogen phthalate (KHP), $KHC_8H_4O_4$. This compound was studied extensively by TGA, and a TGA curve of it (taken from the literature) is shown in the figure for comparison. The following decomposition sequence has been proposed.[8] At lower temperatures (<300°C), water and phthalic anhydride volatilize to form a residue of dipotassium phthalate. This compound then decomposes to form potassium carbonate and elemental carbon. The decomposition of the intermediate species takes place between

*(Text continues on page 4–23)*

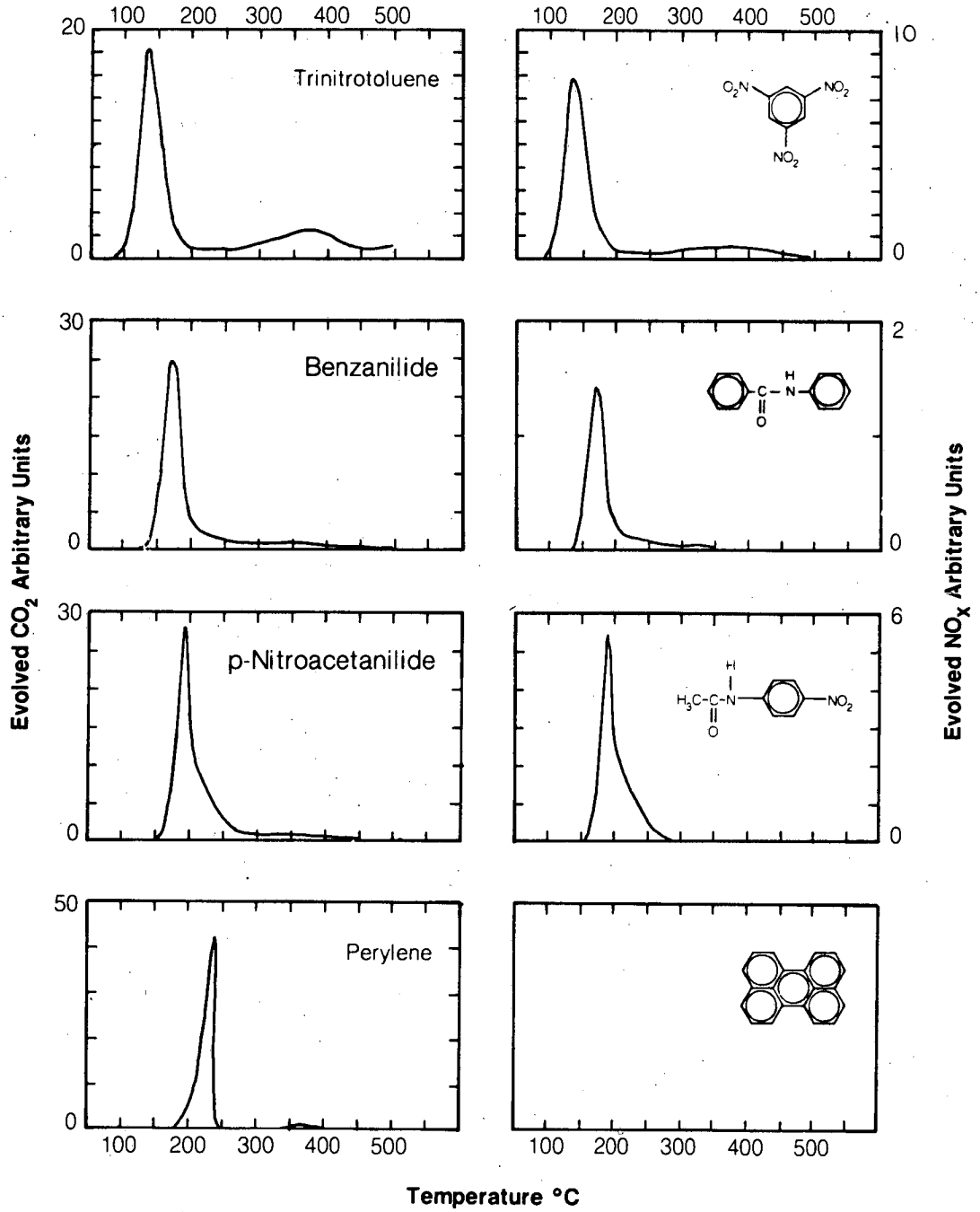


Figure 2. Single-peak thermograms for some organic compounds. (XBL 834-9403)

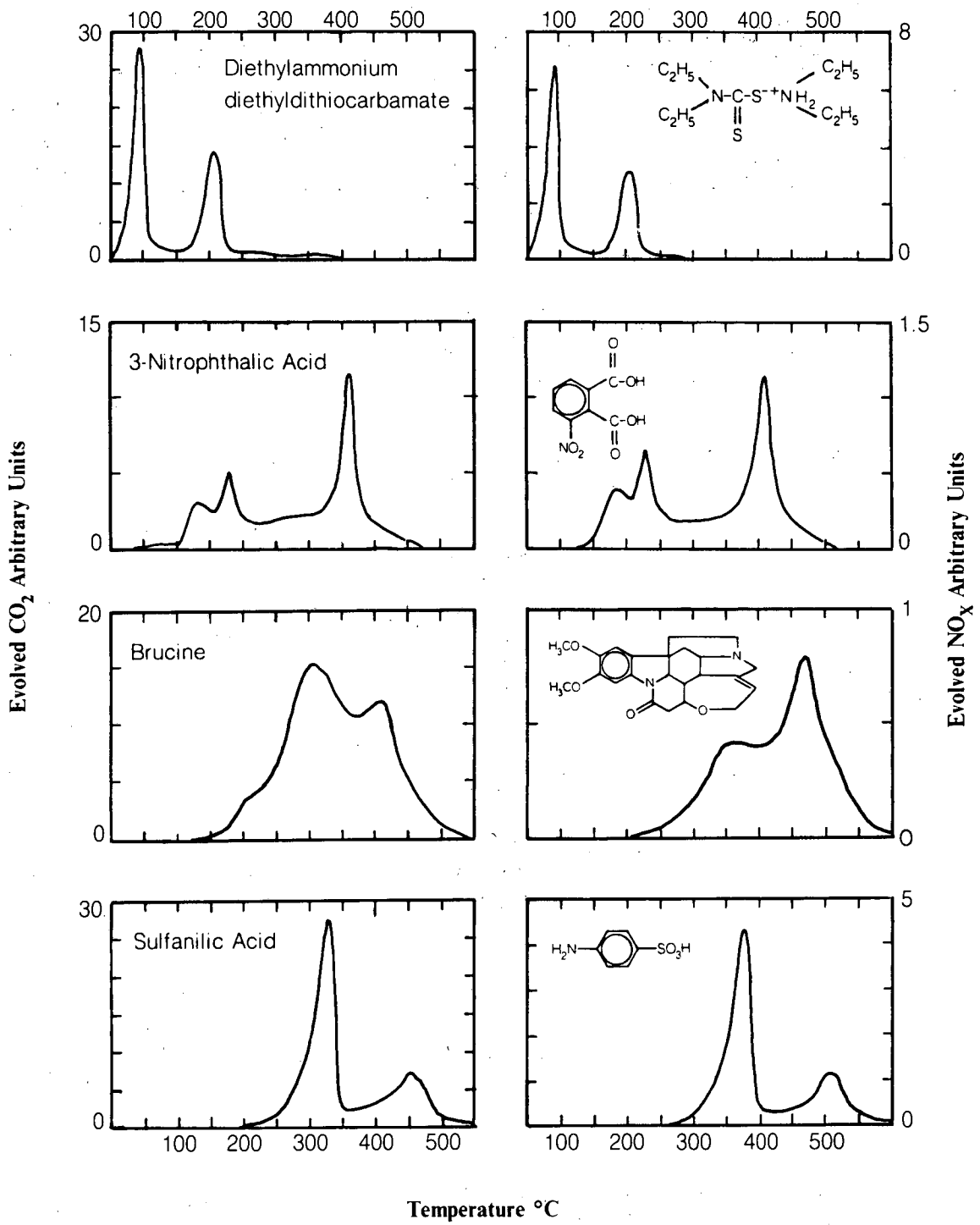


Figure 3. Complex thermograms for some organic compounds. (XBL 834-9404)

Table 1. Carbon and nitrogen recovery for organic compounds.

| Compound | Structure | Carbon Recovery Fraction | Nitrogen Recovery Fraction |
|---|---|---|---|
| Trinitrotoluene | 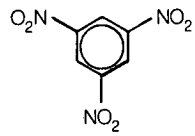 | 0.989 | 0.903 |
| p-Nitroacetanilide | 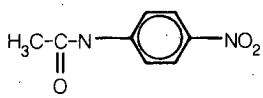 | 1.076 | 0.753 |
| Perylene | 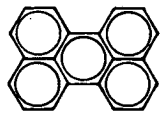 | 0.977 | — |
| 3-Nitrophthalic Acid | 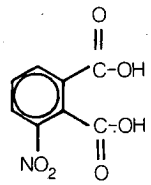 | 0.944 | 0.889 |
| Brucine | 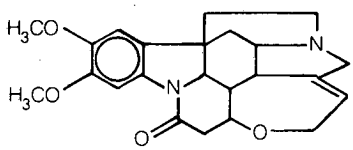 | 0.924 | 0.515 |
| Sulfanilic Acid | 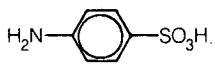 | 0.960 | 0.844 |
| Ascorbic Acid | 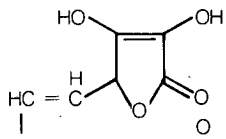 | 0.955 | — |
| Potassium Hydrogen Phthalate | 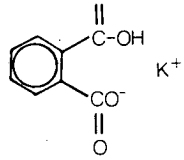 | 1.022 | |
| | **Averages** | **0.981 ± 0.049** | **0.781 ± 0.160** |

~325 and 650°C. The combustion of elemental carbon is responsible for the sharp EGA peak at ~475°C, while the $KCO_3$ decomposes at ~600°C. There is a good correspondence between EGA and TGA for this compound in terms of specific thermogram features and their temperatures. The TGA curve was obtained with a 0.1-g sample in air with a heating rate of 5°C/minute. The carbon content of the EGA sample was 29.6 μg, and the heating rate in oxygen was 10°C/min.

## PLANNED ACTIVITIES FOR FY 1983

The second generation of the EGA apparatus will be constructed. The new version will provide hydrogen detection, improved sample handling and throughput, and variable heating rates. A data acquisition and handling system will also be designed.

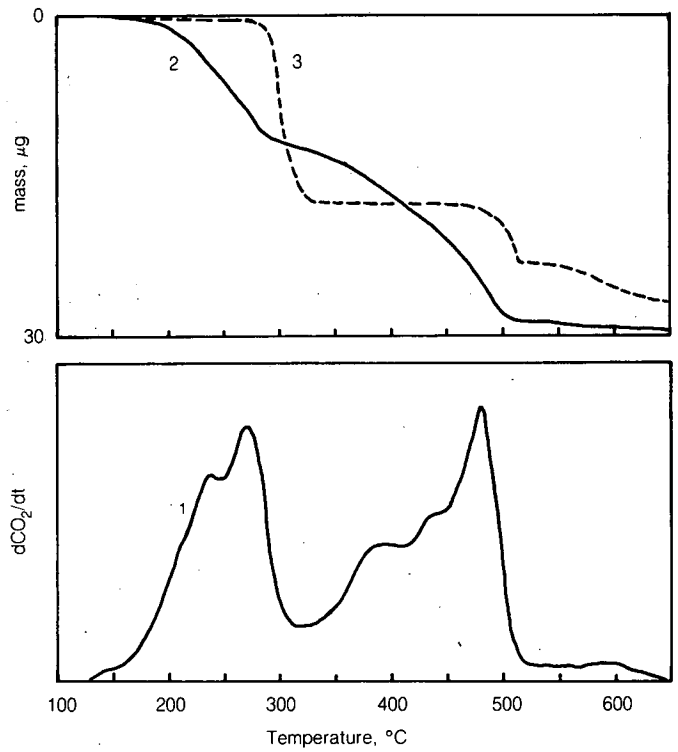


Figure 4. Thermograms of potassium acid phthalate by EGA and TGA methods. Curves are as follows: (1) $CO_2$ EGA (heating rate: 10°C/min). (2) Integral of curve 1: 29.6 μg carbon. (3) TGA of 0.1-g sample, scaled to fit curve 2 (heating rate: 5°C/min), from Ref. 9.

(XBL 834-9401)

## REFERENCES


1. Malissa, H., Puxbaum, H., and Pell, E. (1976), "Zur simultanen relativkonduktometrischen Kohlenstoff- und Schwefelbestimmung in Stäuben," *Z. Anal. Chem. 282*, p. 109.
2. Puxbaum, H. (1979), "Charakterisierung von Kohlenstoff-, Schwefel- und Stickstoffverbindungen in luftgetragenen Stäuben durch kombinierte thermische und gasanalytische Methoden," *Z. Anal. Chem. 299*, p. 33.
3. Malissa, H., Puxbaum, H., and Zojer, K. (1981), "Bestimmung flütchtiger organischer Verbindungen in atmosphärischen Aerosolproben durch thermische Desorption und FIG-Detektion," *Mikrochemica Acta [Wien] I*, p. 1.
4. Bauer, C.F., and Natusch, D.F.S. (1981), "Identification and Quantitation of Carbonate Compounds in Coal Fly Ash," *Environ. Sci. Technol. 15*, p. 783.
5. Dod, R.L., Rosen, H., and Novakov, T. (1979), "Optico-Thermal Analysis of the Carbonaceous Fraction of Aerosol Particles," *Atmospheric Aerosol Research Annual Report 1977–78*, Lawrence Berkeley Laboratory Report LBL-8696, p. 2.
6. Gundel, L.A., Dod, R.L., Rosen, H.J., and Novakov, T. (1983), "The Relationship Between Optical Attenuation and Black Carbon Concentration for Carbonaceous Particles," this annual report.
7. Novakov, T. (1982), "Soot in the Atmosphere," in *Particulate Carbon: Atmospheric Life Cycle,* G.T. Wolff and R.L. Klimisch, Eds., Plenum, New York, p. 19.
8. Wendlandt, W.W. (1974), *Thermal Methods of Analysis,* Wiley, New York, p. 116.
9. Dupuis, T., and Duval, C. (1958), *Mikrochim. Acta. 186.*

# DETERMINATION OF NON-AMMONIUM, NON-NITRATE NITROGEN IN ATMOSPHERIC AEROSOL PARTICLES*

*R.L. Dod, L.A. Gundel, and T. Novakov*

It is commonly assumed that $NO_3^-$ and $NH_4^+$, present as $NH_4NO_3$, $NH_4HSO_4$, and $(NH_4)_2SO_4$, are the only nitrogenous species in atmospheric particulate matter. This view was challenged about 10 years ago by the results obtained with a technique, then new, of photoelectron spectroscopy, or ESCA. According to these results,[1] a significant fraction (~50%) of the total reduced nitrogen is present not as ammonium but in a previously unrecognized form, which for simplicity we shall call $N_x$. It was later postulated that these species consist of particulate amines, amides, and heterocyclic nitrogen compounds.[2]

Until now, there was no direct confirmation of $N_x$ by another analytical method. Commonly used wet chemical determinations are designed for detecting specific ions such as $NH_4^+$ and are therefore not convenient for detecting an unknown species or group of species. Also, there is evidence that some $N_x$ species can easily be hydrolyzed and detected as ammonium ions.[3] The preferred method for this purpose would be one that is a bulk analytical method (unlike ESCA, which is a surface method) and that does not require any chemical sample preparation or separation. Thermal evolved gas analysis (EGA) is such a method.[4] Its application to filter-collected samples has confirmed the existence of $N_x$ species and could enable their quantitative determination.

## ACCOMPLISHMENTS DURING FY 1982

It is obvious from the examples shown in the preceding article[4] that EGA should be able to distinguish common species such as $NH_4NO_3$ and $(NH_4)_2SO_4$ from those that constitute $N_x$. To explore this possibility, an ambient sample (collected in Ljubljana, Yugoslavia) was chosen because its ESCA spectrum clearly indicated the presence of both $NH_4^+$ and $N_x$ with the ratio of $NH_4^+$ to $N_x$ nitrogen ≈ 1.4. The nitrogen ESCA spectrum of the sample is shown in Fig. 1. The $NO_x$ EGA thermogram of that sample is shown in Fig. 2, together with the thermogram of the $(NH_4)_2SO_4$ standard. It is obvious that the pronounced doublet in the ambient sample corresponds to $(NH_4)_2SO_4$, and the small peak at ~150°C to $NH_4NO_3$. However, in addition to these peaks, a substantial amount of nitrogen is seen in a region from 300 to 500°C, indicated by the crosshatched area in Fig. 2. This nitrogen corresponds to $N_x$. EGA gives a $N_{NH_4}/N_x$ ratio of ~1.7, which is in reasonable agreement with the ratio derived from ESCA.

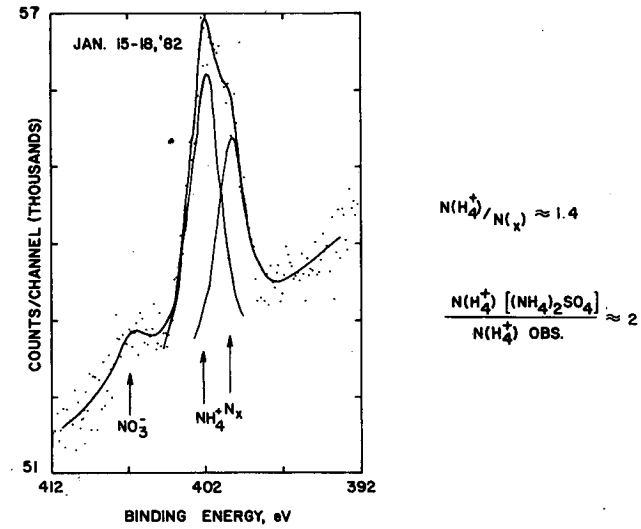


Figure 1. ESCA spectrum (N 1s region) of ambient particulate aerosol sample 111 from Ljubljana, Yugoslavia.
(XBL 834-9174)

A further insight into the nature of $N_x$ is obtained by EGA analysis of an ambient Berkeley sample (Fig. 3). Here the dominant feature of the $NO_x$ thermogram is nitrate. In addition to nitrate, ammonium sulfate or $N_x$ is also seen. $N_x$ here is a relatively small part of the total nitrogen. The $N_x$ peak corresponds closely to the $CO_2$ peak appearing just before the black carbon peak. Figure 4 shows the thermogram of this sample after sequential extraction with benzene and a methanol/chloroform mixture. It is clear that the extraction has removed most of the $N_x$, along with the rest of the organic material. This indicates that the $N_x$ species are organic nitrogen compounds associated with relatively high molecular weight organic material.

*This work was supported by the Director, Office of Energy Research, Office of Health and Environmental Research, Physical and Technological Research Division of the U.S. Department of Energy under Contract No. DE-AC03-76SF00098, and by the National Science Foundation under Contract No. ATM 82-10343.

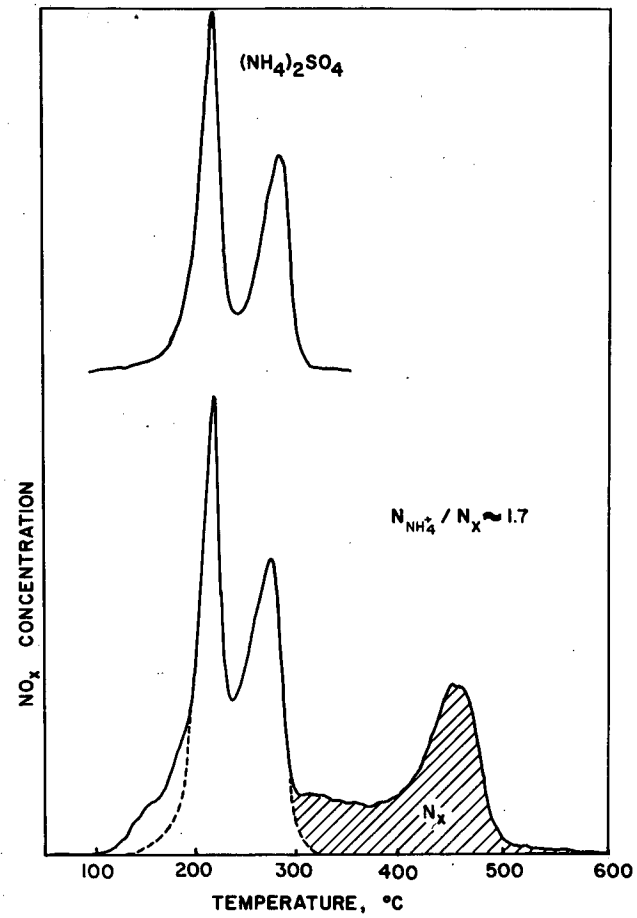


Figure 2. $NO_x$ EGA thermogram of sample 111 from Ljubljana, Yugoslavia. (XBL 834-9175)

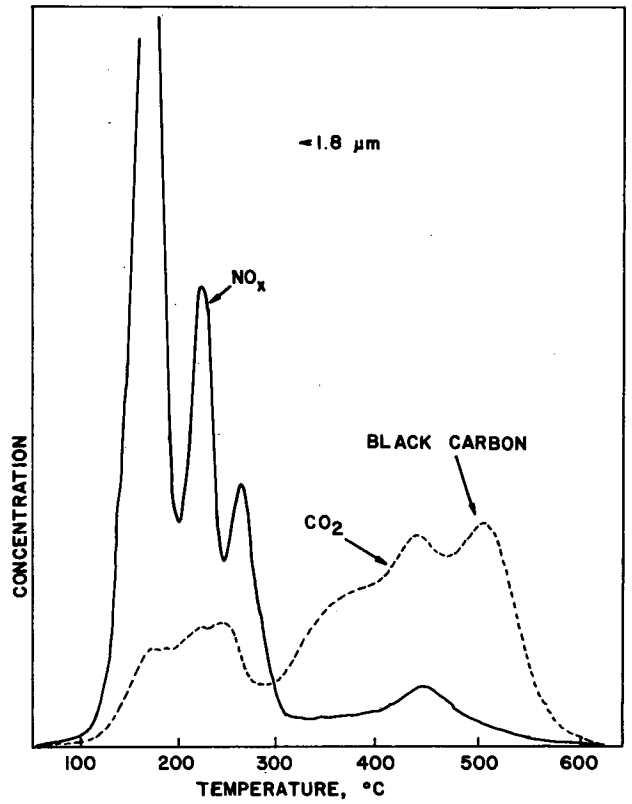


Figure 3. $NO_x$ and $CO_2$ EGA thermograms of ambient particulate aerosol sample taken 22 October 1981 in Berkeley, California. (XBL 834-9171)

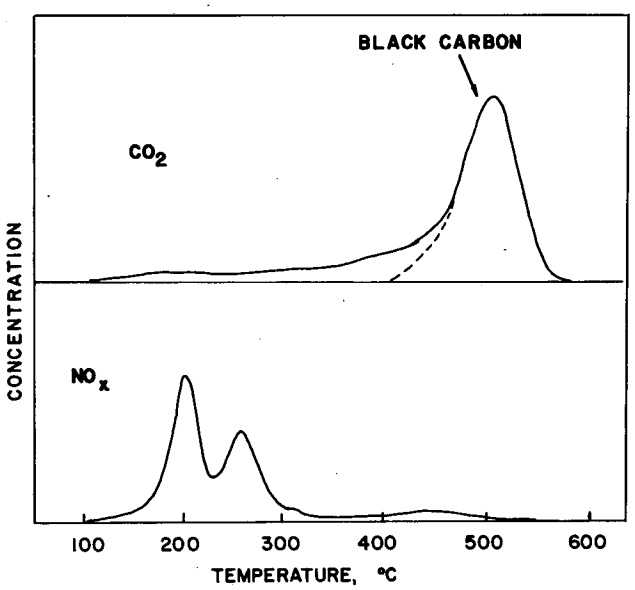


Figure 4. $NO_x$ and $CO_2$ EGA thermograms of Fig. 3 sample after sequential solvent extraction. (XBL 834-9172)

## PLANNED ACTIVITIES FOR FY 1983

Systematic studies involving ESCA, EGA, and ion chromatography will be initiated to quantitatively determine the concentration and structure of $N_x$ species.

## REFERENCES


1. Novakov, T., Mueller, P.K., Alcocer, A.E., and Otvos, J.W. (1972), "Chemical Composition of Pasadena Aerosol by Particle Size and Time of Day: Chemical States of Nitrogen and Sulfur by Photoelectron Spectroscopy," *J. Coll. Interface Sci. 39*, p. 225.
2. Chang, S.-G., and Novakov, T. (1975), "Formation of Pollution Particulate Nitrogen Compounds by NO-Soot and $NH_3$-Soot Gas-Particle Surface Reactions," *Atmos. Environ. 9*, p. 495.

3. Gundel, L.A., et al. (1979), "Characterization of Particulate Amines," in *Nitrogenous Air Pollutants,* D. Grosjean, Ed., Ann Arbor Science, Ann Arbor, Michigan, p. 211.
4. Gundel, L.A., and Dod, R.L., and Novakov, T. (1983), "Qualitative and Quantitative Aspects of Evolved Gas Analysis," this annual report.

## INVESTIGATION OF THE RELATIONSHIP OF PARTICULATE NITROGEN AND SULFATE*

*R.L. Dod, W.H. Benner, and T. Novakov*

While it is generally known that water extraction of ambient aerosol particulate material usually produces a solution containing ammonium, sulfate, and nitrate ions, what compounds existed in the particles before extraction remains uncertain. We have postulated that, in addition to the simple compounds of these ions, nitrogenous functional groups on the organic and/or elemental carbon present in the particles may act as cationic sites to which sulfate and nitrate are "bonded."

To study this postulated relationship among sulfur, nitrogen, and carbon, we are using a variety of techniques with complementary strengths that help to overcome the limitations of each one alone. X-ray photoelectron spectroscopy (ESCA) can provide relative quantitative information regarding elemental composition as well as oxidation states and can be used without sample preparation.[1] However, ESCA analyzes only the sample surface, and the sample must be in high vacuum and exposed to x radiation for the time (typically tens of minutes) necessary to complete the analysis. ESCA results therefore may not be representative of the bulk composition. Some volatile species could be lost because of the vacuum, and in principle the x-ray bombardment could cause chemical changes in some species.

Combustion thermal analysis (EGA)[2] requires no sample preparation, and the sample is analyzed in an environment very similar to ambient. The information obtained from EGA regarding quantitation and chemical states of nitrogen often requires supplementary analytical results to be fully explained.

Ion chromatography (IC) is a very sensitive and specific method for determining ionic concentrations in aqueous solution. However, it has the limitations of other wet chemical techniques: some compounds in a solid sample may not be soluble, and others may transform during dissolution. Thus the results of IC analysis may not be totally representative of the original sample.

### ACCOMPLISHMENTS DURING FY 1982

A set of 23 ambient-particle filter samples from Anaheim, California; Argonne, Illinois; Gaithersburg, Maryland; New York City, and Ljubljana, Yugoslavia, representing a wide range of total carbon and sulfur concentrations, was assembled for the initial investigation. Fractions of each sample were analyzed by ESCA, EGA, and IC for their sulfur and nitrogen content.

Although these samples were widely disparate in concentration, nearly all exhibited a doublet in their $NO_x$ thermograms similar to that of $(NH_4)_2SO_4$ (Fig. 1).[3] This was usually the dominant feature in the $NO_x$ thermogram, indicating that much of the particulate nitrogen is present either as ammonium sulfate or as a compound in which organic nitrogenous functional groups are bonded to sulfate.[4]

In some samples, nitrate nitrogen is detected by ESCA, but it is lost during exposure of the sample to vacuum for several hours. Accompanying this loss is the simultaneous loss of an equivalent amount of ammonium nitrogen, which is taken as evidence that nitrate is present as the compound $NH_4NO_3$. For all samples, more nitrate is found by IC than by ESCA, an observation consistent with such volatility. We therefore assume that most, if not all, nitrate is present in these samples as ammonium nitrate.

When the measured ammonium concentration is reduced by the amount necessary to provide counterions for nitrate, the remainder is available to associate with sulfate. This association is indicated by the $NO_x$ EGA results. IC analysis indicates that the average ratio of available ammonium to sulfate for these samples is ~1.5. From ESCA, for the same sample set, the average ratio is ~1.0. If all reduced nitrogen ($NH_4^+ + N_x$) determined by ESCA is taken as ammonium, the average ratio of available ammonium

*This work was supported by the Director, Office of Energy Research, Office of Health and Environmental Research, Physical and Technological Research Division of the U.S. Department of Energy under Contract No. DE-AC03-76SF00098, and by the National Science Foundation under Contract No. ATM 82-10343.

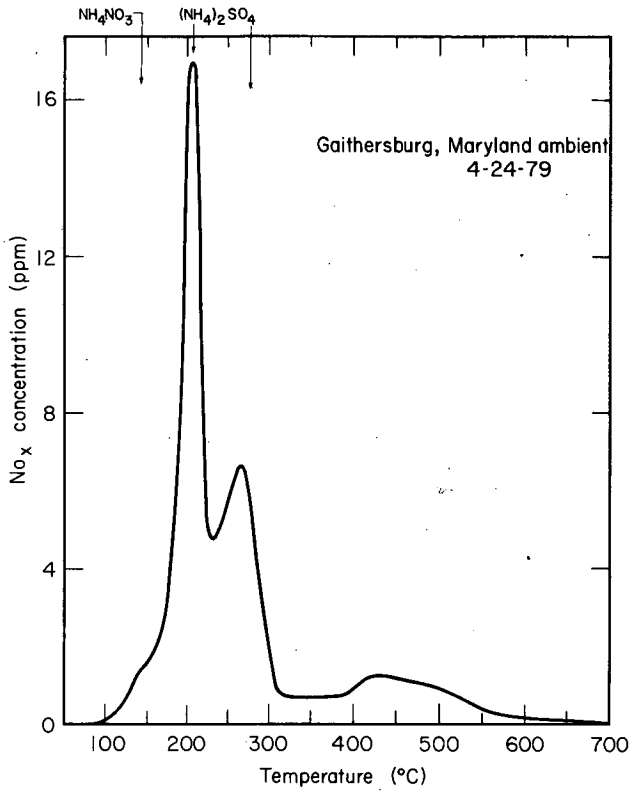


Figure 1. $NO_x$ EGA thermogram showing peak doublet similar to $(NH_4)_2SO_4$. (XBL 8111-1622)

to sulfate becomes ~1.6, somewhat larger than—but much closer to—the ratio determined by IC. This implies that much of the $N_x$ is extractable as ammonium, a conclusion consistent with past results.[5]

The observed similarity to ammonium sulfate in the $NO_x$ thermograms of these samples, when considered with the similarity between the concentration of $NH_4^+$ determined by IC and the concentration of total reduced nitrogen determined by ESCA, provides substantial evidence for the formation of ionic compounds between sulfate and organic nitrogenous functional groups.

## PLANNED ACTIVITIES FOR FY 1983

We intend to expand our sample set, including standard compounds; to study the effect of heating in ESCA on the samples; and to observe with EGA and IC the effect on the samples of vacuum exposure.

## REFERENCES


1. Siegbahn, K., et al. (1967), "ESCA: Atomic, Molecular and Solid State Structure Studied by Means of Electron Spectroscopy," *Nova Acta Regiae Soc. Sci. Ups. Ser IV. 20,* p. 5.
2. Dod, R.L., et al. (1980), "Application of Thermal Analysis to the Characterization of Nitrogenous Aerosol Species," in *Energy & Environment Division Annual Report, 1979,* Lawrence Berkeley Laboratory Report LBL-11650, p. 8-25.
3. Dod, R.L., Gundel, L.A., and Novakov, T. (1983), "Determination of Non-Ammonium, Non-Nitrate Nitrogen in Atmospheric Aerosol Particles," Fig. 2, this annual report.
4. Dod, R.L., and Novakov, T. (1982), "Application of Thermal Analysis and Photoelectron Spectroscopy of the Characterization of Particulate Matter," in *Industrial Applications of Surface Analysis,* L.A. Casper and C.J. Powell, Eds., ACS Symposium Series 199, American Chemical Society, Washington, D.C., p. 397.
5. Gundel, L.A. (1979), "Characterization of Particulate Amines," in *Nitrogenous Air Pollutants,* D. Grosjean, Ed., Ann Arbor Science, Ann Arbor, Michigan, p. 211.


# A COMPUTER-BASED CONTROL AND DATA ACQUISITION SYSTEM FOR EVOLVED GAS ANALYSIS*


*A.D.A. Hansen, W.H. Benner, and T. Novakov*


Ambient aerosol particles are a complex mixture of organic and inorganic chemical compounds, speciation of which can yield information on the origins and atmospheric transformations of the aerosol. The major species of anthropogenic origin are compounds of carbon, hydrogen, oxygen, nitrogen, and sulfur. A powerful analytical tool that is related to other "thermal" methods of physical-chemical analysis and that was first applied to the analysis of aerosol particles by Malissa[1] is the evolved gas analysis (EGA) technique. This technique can identify certain individual compounds and classify broad groups according to the temperatures at which they decompose in either


*This work was supported by the Director, Office of Energy Research, Office of Health and Environmental Research, Physical and Technological Research Division of the U.S. Department of Energy under Contract No. DE-AC03-76SF00098, and by the National Science Foundation under Contract No. ATM 82-10343.

reactive or inert atmospheres. Considerable development of the method has taken place at LBL and elsewhere, and it has been applied to the analysis of carbon,[2] nitrogen,[3] sulfur,[4] and oxygen[5] compounds. The apparatus must include (1) a temperature-programmed furnace region, in which the sample is heated from room temperature to ~1000°C at a rate of 10 to 30°C per minute, and (2) a data acquisition and reduction system. Early in FY 1982, we decided to automate these otherwise time-consuming functions. Here we outline hardware and software developments that have led to a system fulfilling these requirements.

## ACCOMPLISHMENTS DURING FY 1982

### Software Development

We decided to develop a system that would control the temperature ramp and would acquire and display the data in a configuration that would be rapidly interchangeable between our different EGA analyzers. The furnaces of these analyzers are totally dissimilar, both in the electrical and thermal characteristics of the heating elements and in the thermal coupling of the furnace to the sample and to the temperature-measuring thermocouple. The temperature-control software must therefore be able to learn the characteristics of each furnace and be self-correcting during each run. The data acquisition and processing requirements are modest: at 10-second intervals as the run progresses, the signal is plotted against temperature on an X–Y recorder while the computer's screen shows temperature control data and provides for operator interaction. At the end of the run, while the oven is cooling down, the data may be processed (e.g., baseline subtraction, calibration factor rescaling, peak integration), replotted in different ways, or recorded on tape. The furnace power is digitally controlled directly and is proportional to a "control number" $K$ calculated by the program. During each run, continuous adjustment of the power control is effected by feedback of a temperature error signal. The power supplied to the furnace in the $n^{th}$ interval at time $t$ is proportional to:

$$K_n = K_n^0 + f \cdot [T_{ramp(t)} - T_{actual\,(t)}] \quad ,$$

where $f$ is the error feedback strength and the sequence of numbers $K_n^0$ is the previously learned power control profile. However, due to the imperfect thermal coupling between the furnace heating elements and the sample (usually in a boat in a quartz or ceramic tube), the temperature response of the sample lags relative to the power supplied to the furnace. Thus, at the end of the run, the sequence of control numbers is recomputed retrospectively so that an error in the $n^{th}$ interval is anticipated by adjusting the $K_m$ for $m < n$ . These relearned values then form the basis set $K_n^0$ for the next run. The program can run unattended in a purely "learning" mode so that it can be applied to a furnace-thermocouple combination of unknown electrical and thermal characteristics; after a few cycles, it will have learned the power control profile necessary to achieve the desired temperature ramp to within an acceptable accuracy.

### Hardware Development†

The equipment used is a commercial microcomputer using the BASIC language, with a multichannel A/D input converter, a semi-intelligent X–Y plotter, a printer, and a serial input/output port. This port transmits the 8-bit control number $K$ (i.e., $0 \leq K \leq 255$) to the digital power-control interface (DPCI). The isolation provided by this link reduces the coupling of electrical transients and could allow the DPCI to be remotely located.

Development of the DPCI as the means whereby a computer program can rapidly and flexibly control kilowatts of electrical power was essential to this project, since such a unit is not available commercially. The DPCI is therefore able to control AC power from a true zero to full load, limited only by the triac rating.

### System Performance

This system has been an integral part of oxygen-EGA development and has demonstrated reliability of temperature control and convenience of use. The adaptive nature of the learning program results in runs from room temperature to 1100°C whose root-mean-square temperature error rarely exceeds 2 degrees, despite changes in experimental conditions and ambient temperatures. The data handling and display routines produce both high-quality graphics and all pertinent numerical information, eliminating the need for further processing.

## PLANNED ACTIVITIES FOR FY 1983

Among future software developments is the inclusion of a library of thermograms of standard compounds for quantitative comparison with each sample analysis. Planned hardware developments include the automation of other experimental parameters, such as carrier gas switching, backflushing, sample handling, etc. The field of thermal analysis is expanding rapidly and adds considerably to our understanding of aerosol particles. Automation of the analytical apparatus allows the necessarily large number of samples to be run with minimal manpower demand.

## REFERENCES


1. Malissa, H., Puxbaum, H., and Pell, E. (1976), "Zur simultanen relativkonduktometrischen Kohlenstoff und Schwefelbestimmung in Stäuben," *Z. Anal. Chem. 282,* p. 109.
2. Dod, R.L., Rosen, H., and Novakov, T. (1978), "Optico-Thermal Analysis of the Carbonaceous Fraction of Aerosol Particles," *Atmospheric Aerosol Research Annual Report, 1977-78,* Lawrence Berkeley Laboratory Report LBL-8696, p. 2.
3. Dod, R.L., et al. (1980), "Application of Thermal Analysis to the Characterization of Nitrogenous Aerosol Species," *Atmospheric Aerosol Research Report FY 1979,* Lawrence Berkeley Laboratory Report LBL-10735, p. 35.
4. Dod, R.L., and Gundel, L.A., private communication.
5. Benner, W.H. (1983), "The Oxygen Content of Ambient Particulate Matter," this annual report; also Benner, W.H., private communication concerning adaptation of the technique described therein to temperature-programmed EGA.


†Details of the hardware invention have been reported to the DOE Office of Patent Counsel.

# APPLIED PHYSICS AND LASER SPECTROSCOPY RESEARCH

*N.M. Amer,* M.S. Cooper, R.W. Gerlach, A. Hitachi, W. Imler, M.A. Olmstead, A. Skumanich, D.R. Wake, D. Wei,*

The research philosophy of our group is to apply advanced laser spectroscopy and condensed-matter physics to energy and environmental problems. Because of the narrow line width and tunability of lasers, unsurpassed sensitivity and specificity can be achieved in detecting trace contaminants of the environment, for example. The advanced state of condensed-matter physics also makes it possible to apply this knowledge to energy production and to test novel methods of energy conversion such as photovoltaic solar cells, superionic electrical energy storage devices, and the recovery and extraction of oil from abandoned wells and oil shale with lyotropic liquid-crystal emulsifiers.

## ACCOMPLISHMENTS DURING FY 1982

### LASER PHOTOTHERMAL MEASUREMENTS AND CHARACTERIZATION†

Laser photothermal spectroscopies provide powerful tools for detecting trace contaminants in air and water, as well as for investigating the fundamental properties of gaseous, liquid, and solid phases of matter. One goal of this project is to develop ultrasensitive, multiparameter elemental and molecular detectors for characterizing trace constituents, with emphasis on remote sensing. Another is to maintain a state-of-the-art capability in photothermal detection by fully understanding the physics of these techniques. We are also developing, as needed, new or modified laser systems in support of these efforts.

#### Photothermal Displacement Spectroscopy‡

The optical properties of electronic surface states are important for both fundamental and technological reasons, and a variety of optical spectroscopic techniques have been used to investigate them.[1] Most prominent among these techniques are reflectance and ellipsometric methods. To determine the contribution of surface states, however, the difference between the spectra of clean and intentionally contaminated surfaces must be measured.

We have recently developed a sensitive new technique, photothermal displacement spectroscopy,[2] for directly measuring the optical and thermal properties of surfaces and thin films. The technique, which is relatively easy to implement, is particularly suited for studies requiring wide ranges of pressures and temperatures.

The physical principle underlying photothermal displacement spectroscopy is that when a modulated beam of electromagnetic radiation (a pump beam) is absorbed, heating of the absorbing medium will occur. As the illuminated surface expands with heating, it buckles and is displaced. The magnitude of the displacement is related quantitatively to the optical absorption coefficient.[2]

The surface displacement $h$ is given by

$$h = \alpha_{th}\beta P/(2A\, f\rho C) \qquad (1)$$

where

$\alpha_{th}$ = the thermal expansion coefficient of the material,
$\beta$ = the fraction of absorbed light,
$P$ = the incident power,
$f$ = the modulation frequency,
$A$ = the optically heated area,
$\rho$ = the mass density, and
$C$ = the heat capacity.

An important parameter in photothermal spectroscopy is the thermal diffusion length, $L_{th}$, which defines the depth within the sample from which the photothermal signal is generated; it is given by

$$L_{th} = (K_{th}/\pi\, f\rho c)^{1/2} \qquad (2)$$

where $K_{th}$ is the thermal conductivity of the material. The frequency dependence of the thermal diffusion length is what we exploit to differentiate between sur-

*Group Leader.

†This work was supported by the Director, Office of Energy Research, Physical and Technological Research Division of the U.S. Department of Energy under Contract No. DE-AC03-76SF00098; and by the Defense Advanced Research Projects Agency under DARPA Contract No. 3343.

‡Complete versions to appear in *J. Vac. Sci. Techn. B* (July 1983) and in *Appl. Phys. A.*

face and bulk contributions to the photothermal signal. It can readily be seen from Eq. (2) that, by increasing the modulation frequency of the pump beam, one can enhance the ratio of surface to bulk contributions.

Figure 1 shows two possible configurations for performing photothermal displacement spectroscopy: a beam deflection scheme that measures the slope of the photoinduced displacement, and an interferometric scheme that measures the displacement itself.

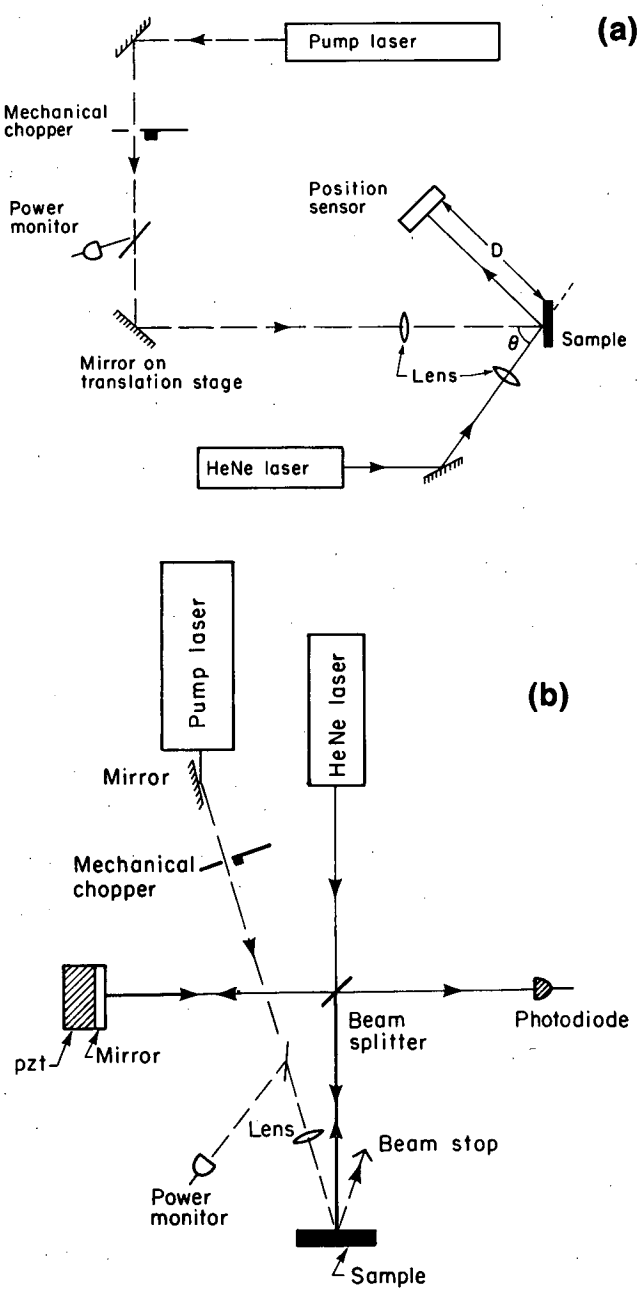


Figure 1. Two experimental configurations for photothermal displacement spectroscopy: (a) beam deflection scheme; (b) interferometric scheme.
[(a) XBL 831-22; (b) XBL 832-7779]

Figure 1(a) shows the details of the beam deflection scheme. The time-dependent change in the slope of the photoinduced surface buckling is measured as a time-dependent change in the deflection angle of a weak probe beam (typically a He-Ne laser), as detected by a position sensor.

The interferometric scheme is shown in Fig. 1(b). The sample of interest serves as one arm of a Michelson interferometer. The position of the mirror in the other arm is modulated to overcome thermally induced drifts and the effect of mechanical vibration on the interferometer.

Both schemes have comparable sensitivities ($\alpha \ell \approx 10^{-6}$), but the beam deflection approach is easier.

To demonstrate the spectroscopic feasibility of this technique, we measured the absorption spectrum of didymium glass in the 700–800 nm range (Fig. 2). Spectra were obtained at atmospheric pressure and at 20 m Torr. To establish that photothermal displacement spectroscopy indeed measures the optical absorption, we also derived the absorption spectrum in this wavelength region by conventional transmission methods.

The ability of the technique to differentiate between surface and bulk absorptions is demonstrated in Fig. 3(a). A 50-Å gold film was evaporated on 2-mm-thick didymium glass. The absorption spectra of gold only and of didymium only are given in Fig. 3(b). In the wavelength region of 700–800 nm, approximately 25% of the incident light is absorbed by the gold film, with didymium having a strong

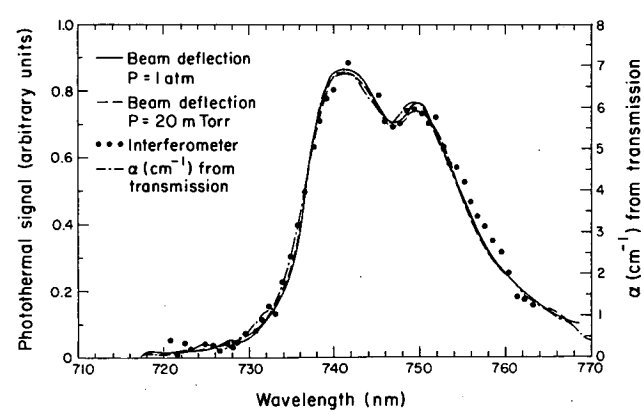


Figure 2. Absorption spectra of didymium. (XBL 831-20)

absorption peak of ~6.5 $cm^{-5}$ around 740 nm. As shown in Fig. 3(a), at a modulation frequency of 5 Hz, the photothermal signal of the gold-coated didymium is the sum of the featureless gold absorption plus the peaks of the didymium absorption band. As the modulation frequency is increased to 127 Hz, the gold signal decreases by a factor of 2, while the didymium peaks decrease by an additional factor of 2 or 3. Clearly, higher modulation frequencies would still further reduce the substrate (bulk) contribution to the photothermal signal.

In conclusion, this sensitive new photothermal technique[3] directly measures the optical absorption of surfaces and obviates the need for spectra subtraction that is necessary in conventional optical absorption spectroscopy. It is readily suited for ultra-high vacuum studies, requires no mechanical or electrical contacts, and is linear over a wide range of absorption coefficients.

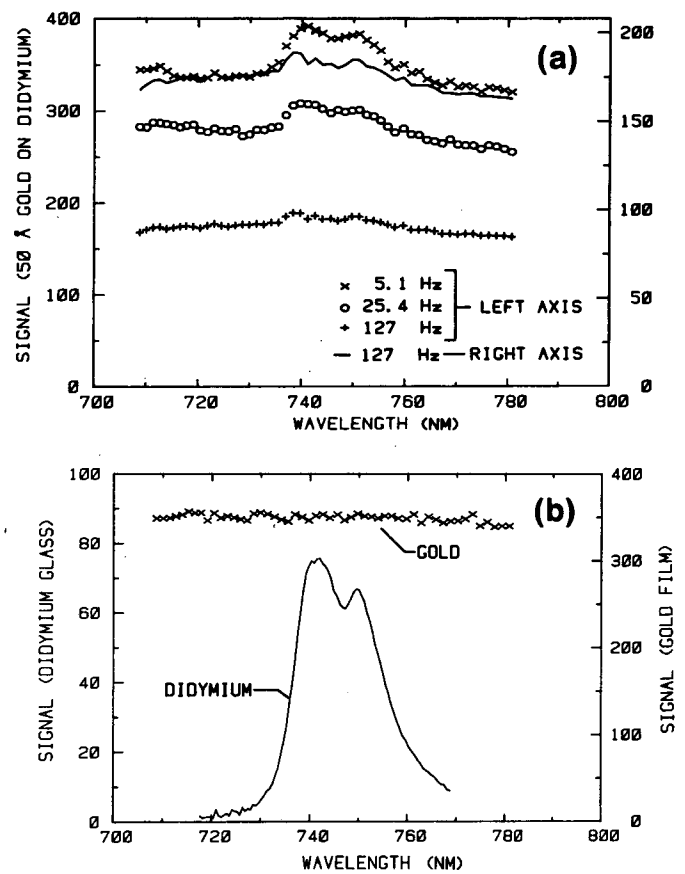


Figure 3. (a) A demonstration of the ability of PDS to differentiate between surface (gold) and bulk (didymium) absorptions; the central peaks represent the didymium contributions, which decrease as the modulation frequency increases. (b) Spectra of 50-Å gold film (top) and of didymium (bottom). [(a) XBL 832-7825; (b) XBL 832-7824]

## AMORPHOUS PHOTOVOLTAIC SEMICONDUCTORS*

Amorphous photovoltaic semiconductors, such as hydrogenated amorphous silicon, hold promise for meeting DOE cost and efficiency guidelines for thin-film solar cells before 1990. To achieve the higher conversion efficiencies required, it is necessary to better characterize the unique optical and transport properties of these materials. Photoacoustic and photothermal spectroscopies can provide such elucidation. Of particular interest is the investigation of the optical properties near the so-called bandgap. By combining luminescence studies, photoconductivity, and optical absorption, a full and accurate characterization of the deexcitation of these photoexcited amorphous semiconductors can be achieved.

Experiments investigating the optical properties of amorphous semiconductors are currently under way. These experiments are designed to yield new information on the details of their optical absorption, the nature of the bandgap, and their electronic and transport properties.

### Role of Dangling Bond Defects in Early Recombination in Amorphous Silicon†:

Dangling bond (DB) defects are the focus of many investigations dealing with tetrahedrally bonded amorphous semiconductors.[4] A DB defect can be pictured as an unsatisfied tetrahedral bond with an unpaired electron, a situation that is disruptive both structurally and electronically. The presence of DB defects correlates strongly with luminescence quenching,[5] short free-carrier lifetime,[6] increased subgap absorption,[7] and the shape of the absorption edge.[8,9] DB defects can be passivated in amorphous silicon (*a*-Si) by alloying with hydrogen (*a*-Si:H). The defect density, which is observable by electron spin resonance (ESR), is controlled by material deposition conditions; it is increased with hydrogen evolution and is partially diminished by rehydrogenation.

Strong circumstantial evidence from several experiments indicates that DB defects play an active role in electron hole recombination in amorphous silicon[4]

*This work was supported by the Assistant Secretary for Conservation and Solar Energy, Office of Solar Energy, Photovoltaic Energy Systems Division, U.S. Department of Energy under Contract No. DE-AC03-76SF00098.

†Appeared in *Phys. Rev. B 27*, 2598 (1983).

analogous to that of defects in crystalline materials.[10] In particular, at low temperatures fast recombination by direct tunneling of carriers to DB defects is assumed to be the main mechanism that limits carrier lifetime and quenches luminescence.[5] We have presented evidence that DB defects are not fast recombination centers; instead, the dispersive influence of the exponential distribution of localized states extending into the gap (the band tail) dominates the recombination process in the multiple trapping model (MTM)[11].

Photoexciting carriers across the gap in *a*-Si:H allows the absorption of infrared radiation (IR) by the nonequilibrium population of electrons and holes, as these carriers make transitions to the extended states deeper in the bands. Similar photoinduced absorption (PA) data have been reported for *a*-Si:H for times from 0.5 $\mu$sec and have been interpreted in terms of multiple trapping.[12,13] Our data span the period from 4 to 500 nsec, when very few carriers have actually recombined, although trapping processes and luminescence quenching have begun and carrier thermalization is important.

We used a 10-Hz Nd:Yag pumped dye laser with 4 nsec (FWHM) pulses of 2.2 eV photons to photoexcite a carrier density of $\sim 10^{18}$ cm$^{-3}$ in *a*-Si:H. A cw IR beam (0.9 to 1.45 eV) from a filtered tungsten lamp was passed through this carrier population, and changes in the IR transparency were detected by a fast Ge photodiode with a rise time of 1.5 nsec. Changing the spectral width of the IR with a crystalline Si filter had no effect on the PA response. At low temperatures, luminescence is unavoidably emitted into the photodiode optics, but it was separately recorded and subtracted. Data were taken for undoped samples of various defect densities over a temperature range of 10 to 300 K.

Figure 4 shows the PA data for representative *a*-Si:H samples. The defect density, $N_S$, is measured by ESR at $g = 2.0055$. A simple power law describes the PA decay of these samples over this time period very well with an exponent of "$\alpha$". The rate of decay systematically decreases with increasing defect density. This trend is opposite to that expected if DB defects were controlling recombination.

We can, however, successfully interpret these results in terms of a multiple trapping model[11] with a distribution of localized trapping states, $N_t(E)$, whose density declines exponentially into the gap; $N_t(E) = N_o \exp(-E/E_o)$, where $E$ is the depth of the trap level

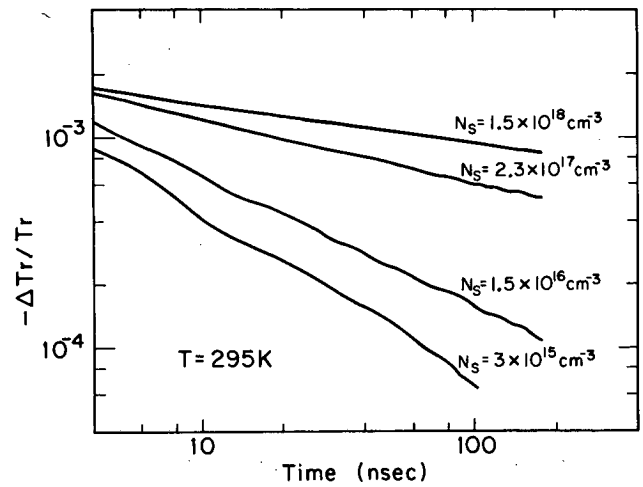


Figure 4. Relative change in transmission (photoinduced absorption) vs. time delay for samples of various defect densities, showing a power-law decay $t^{-\alpha}$.

(XBL 828-4057)

from the band edge and $E_o$ is the width of this band tail. There is evidence that this is the case not only for *a*-Si:H but also for a large number of amorphous and disordered crystalline systems. The model implicity assumes that direct transitions either within the band tail or to deep centers are negligible when compared to thermally stimulated transitions to the band edge followed by retrapping. Upon photoexcitation, the carriers are quickly trapped into the band tails,[6] acquiring an exponential energy distribution that parallels the density of trap states. The top of the trapped distribution thermalizes; the level at which thermalization begins, $E_d$, descends through the distribution as $E_d = k_B T \ln \nu t$, where $\nu$ is an attempt-to-escape frequency on the order of $10^{13}$ sec$^{-1}$. Below $E_d$, the probability of thermal release at time $t$ is negligible. The consequence is an exponentially spiked distribution of charge localized (energetically) near $E_d$. Capture by carriers of opposite charge or deeper levels that are not part of the band tail competes with retrapping; when the probability of capture there exceeds the probability of retrapment at states below $E_d$, the population in the band tail diminishes as $t^{-\alpha}$, where $\alpha = T/T_o$, and $T_o = E_o/k_B$. This time dependence is observed from our earliest time of 4 nsec.

The shape of the trap distribution, then, determines the exit rate of the carriers from the band tail. Other experiments have shown that increasing the DB defect density leads to widening of the band edge,

increasing $E_0$.[8,9] Since $E_d$ descends through the band tail at a rate independent of trap or defect density, a larger fraction of carriers is localized below $E_d$ in a highly defect-dense material than in a low-defect-dense material at comparable times. The high-defect-density material holds carriers in the band tail longer.

A test of this interpretation is to decrease the temperature. In Fig. 5 we plot "$\alpha$," obtained from the power-law fit to PA at 200 nsec, as a function of temperature for a sample of defect density of $1.5 \times 10^{16}$ $cm^{-3}$. As predicted by the MTM, $\alpha$ varies linearly with temperature between 50 and 250 K. A similar temperature dependence has already been observed at longer times.[12] Figure 5 shows that $E_0 = 46$ meV or $T_0 = 534$ K.

We have also measured $E_0$ directly from optical absorption; Figure 6 compares $k_B T/E_0$ with the "$\alpha$" from PA. Since the optical absorption data represents a joint density of states involving both the valence and conduction bands, the convolution of a narrow feature of one band with a broad feature of the other band will map out the broad feature in the absorption spectrum. The broader of the two band tails will dominate the optical absorption edge; in *a*-Si:H, this is the valence band edge.[14] Thus the excellent agreement in Fig. 6 for all but the lowest-defect density samples ($<10^{16}$ $cm^{-3}$) indicates that the shape of the valence band tail determines the rate of PA decay. O'Connor and Tauc[15] concluded that they

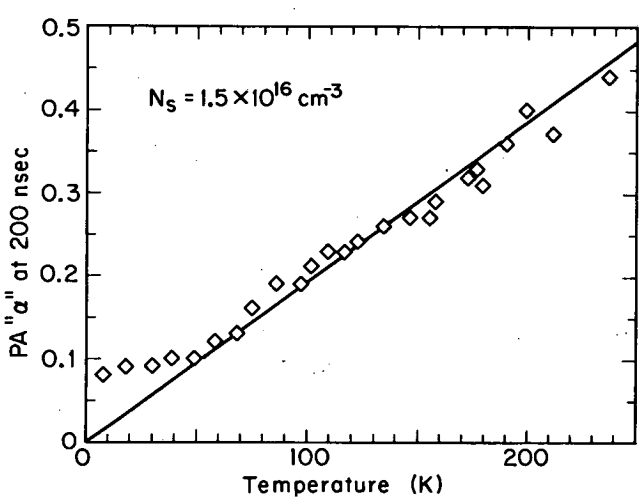


Figure 5. Temperature dependence of $\alpha$. The weakening of the temperature dependence at low temperature is most likely due to a competing local-to-local recombination process. (XBL 828-4058)

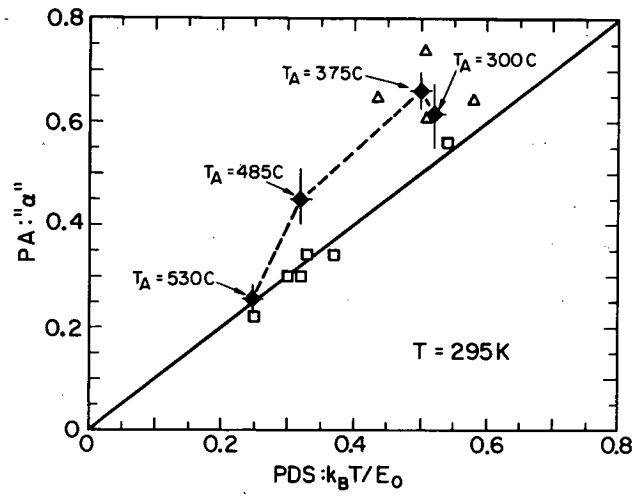


Figure 6. $\alpha$ from a transient photoinduced absorption compared with $k_B T/E_0$ from optical absorption at 295 K. Open symbols represent samples deposited under a range of conditions that vary $N_s$ (ESR), triangles being the "optimal," low-defect-density samples. Solid symbols show the effect of evolving H from a single sample. (XBL 828-4059)

were not observing electrons in their PA experiments on *a*-Si:H, and we interpret our similar results as strong and direct evidence that the PA decay is due to hole activity. In the lowest-defect density samples, the PA decays faster than the rate predicted by optical absorption, indicating that hole movement is not the limiting rate that it is in the samples with more defects. This suggests that electron transport assists band-to-band recombination in the samples with lowest defect density and that the faster decay may yield information on the conduction band instead of the valence band.

Figure 4 shows that, at 295 K, the low-defect-density sample relaxes much more quickly than the high-defect-density sample. Below 50 K, both samples relax at about the same rate, $\alpha \approx 0.07$ (very slowly), and the PA signal is approximately equal for all samples near 10 nsec.[16] This is in sharp contrast to luminescence experiments which show that the low-defect-density material has a luminescence quantum efficiency near unity for the 1.4 eV emission while the high-defect-density material has a weaker band at 0.9 eV.[17] One interpretation of this has been that the carriers are rapidly tunneling to the DB defects, which act as nonradiative recombination centers. The PA results indicate that this is not happening. At low $T$, the highest defect density sample's IR absorption is reduced only 50% at 2 $\mu$secs; yet the luminescence is weak and decays

rapidly. The rate of PA decay correlates better with band-tail widths than with spin density. We conclude that the DB defect is not a rapid recombination center in undoped amorphous silicon, but instead influences the recombination process indirectly by its effect on the width of the band tail.

For the luminescence results, we can only suggest alternative quenching mechanisms such as charged-defect electric field quenching,[18] DB-induced strains, or tightly localized carriers in the higher-defect-density material. We do not completely rule out the possibility that the electrons are rapidly captured by DB defects followed by a slower capture of holes. But serious difficulties exist with all of these suggestions and will be discussed in a future paper.

In order to separate the role of defects from the effects of various deposition conditions used in the samples in Fig. 6, we stepwise-evolved hydrogen from an initially low-defect-density sample by annealing it to temperatures of 300 to 530°C. We directly monitored the optical absorption edge with photothermal deflection spectroscopy[19] and found that the edge widened ($E_0$ increased) as the DB defect density increased, in agreement with Cody et al.[8] The dashed line of Fig. 6 follows the comparison between the PA "$\alpha$" and $k_BT/E_0$ as the sample is annealed to higher temperatures. The comparison is complicated by the faster decay noted for the lower-defect-density material, but the trend to slower PA decay with increasing $E_0$ is confirmed.

We find it unlikely that PA and luminescence do not arise from the same population of electrons and holes because of the following considerations. (1) Assuming oscillator strengths of unity for the IR cross sections over the bandwidth used, we find a minimum estimate for the population observed when PA is at its highest (earliest) level. We obtain a value from an integrated absorption estimate[20] that is ~80% of that expected from the photoexcited carrier density. Coupled with an estimated luminescence efficiency of 50-100% in low-defect-density material, this argues against separate populations. (2) PA and luminescence have very similar temperature quenching dependences. (3) Similar PA maximum amplitudes near 10 nsec for all the samples support the argument that nearly all of the photoexcited population is being observed. (4) Luminescence recombination kinetics have been observed[21] to change from monomolecular to bimolecular at a photoexcited carrier density $N_p$ of 1–2 $\times$ $10^{18}$ $cm^{-3}$. We have discovered[22] a similar change in recombination kinetics at the same density of 1 $\times$ $10^{18}$ $cm^{-3}$, where the PA amplitude shifts from $N_p^{0.9}$ to $N_p^{0.5}$ with increasing excitation density. A more extensive study of this transition is in progress.

There may be another deep gap state more important in recombination than the DB since even at $N_s >$ $10^{18}$ $cm^{-3}$ the recombination is slow. Evidence for other states exists in the light-induced Staebler-Wronski states,[23] the hole trap state deduced from photoconductivity,[24] and the hole trap states observed in *a*-Si:H:P.[25] The luminescence line due to oxygen is occasionally reported, but other impurities may exist at significant densities in a typical sample. Surface states may also play a role. Clearly, more work is needed.

In conclusion, our PA data show that the band tail of *a*-Si:H plays a more important role in the early recombination process than does the DB defect density and that DB defects are not fast recombination centers. We suggest another, more important recombination channel may exist, despite the difficulty of reconciling this with non-PA experiments that seem to imply otherwise. Luminescence does not detect carriers that do not radiatively recombine, and photoconductivity does not detect carriers immobilized in deep traps. PA is a complementary probe for studying the time evolution of the carrier population. If the DB defects are not important recombination centers, then other roles proposed for this state[26] must be more fully considered.

## The Contribution of the Staebler-Wronski Effect to Gap-State Absorption in Hydrogenated Amorphous Silicon*

Reversible photoinduced changes in hydrogenated amorphous silicon (*a*-Si:H) have recently attracted attention.[23,27–34] The exact mechanism responsible remains to be fully elucidated. However, it is generally accepted that illumination creates metastable defects, which are annealed away by heating. An interesting question is how these photoinduced changes affect the optical absorption spectrum of the gap states in this material. The answer provides information on the number of states affected and, more important, gives the energy level at which these states reside in the gap. We have employed photothermal deflection spectroscopy[19] to investigate the contribution of these photoinduced defects to gap-state absorption.

*Complete version appeared in *Physica 117B*, 897 (1983).

The photothermal deflection spectroscopy technique has been described elsewhere.[19] Our samples were undoped, singly doped, and compensated films deposited by glow discharge. The illumination-annealing cycle consisted of exposing the *a*-Si:H films to 0.5 W/cm$^2$ of unfiltered light from a quartz tungsten-halogen lamp. Exposure time was typically 1.5 hours. Annealing was achieved by heating the films at 175°C for 1.5 hours in vacuum and in total darkness.

Figure 7 shows the effect of illumination upon the optical absorption of the undoped material. It can be readily seen that exposure to light enchances gap-state absorption. Furthermore, annealing at 175°C restores the magnitude of this absorption to its original value. Little or no change is seen in the Urbach tail absorption.

We showed earlier that the magnitude of gap-state absorption in *a*-Si:H correlate directly to the number of spins as determined by ESR and that these states are due to silicon dangling bonds.[7] Since illumination yields a qualitatively similar absorption spectrum, with the only difference being the increase in the absorption of gap-states, one can employ the procedure described in Ref. 7 to calculate the number of photoinduced spins, $\Delta N_s$, in the various samples we investigated. In Fig. 8 we plot the optically-deduced $\Delta N_s$ for singly doped and compensated materials as a function of dopant concentration. As can be seen, for singly doped material, the photoinduced spins increase in density with increasing dopant concentration. The compensated material exhibited a light-induced enhancement comparable to that measured in the undoped films.

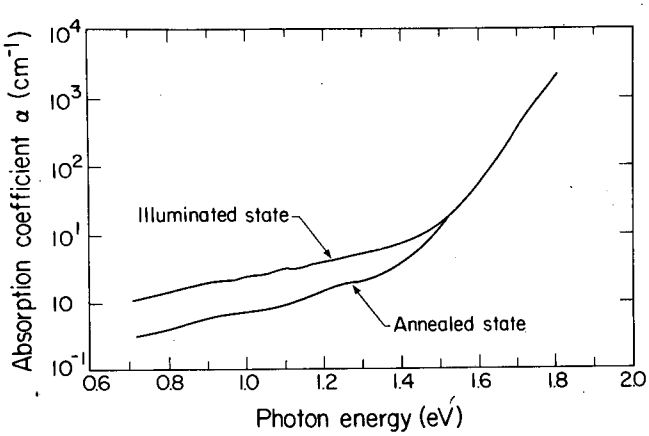


Figure 7. The effect of illumination on the absorption spectrum of undoped *a*-Si:H. (XBL 836-10266)

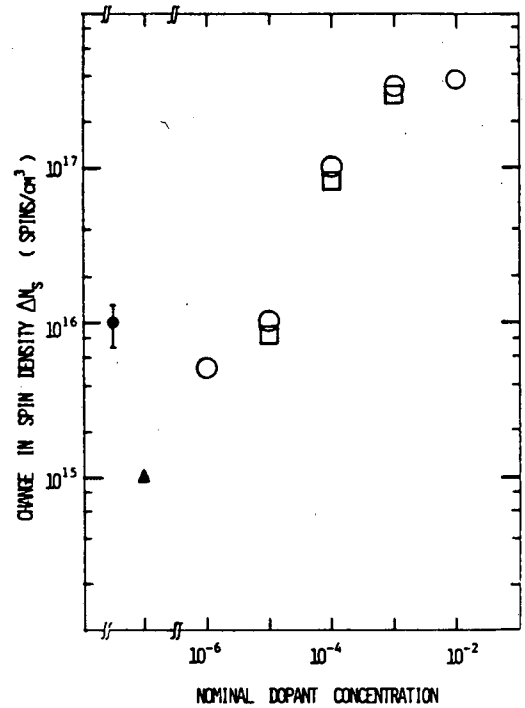


Figure 8. Photoinduced change in spin density as a function of doping: open squares, boron; open circles, phosphorus; triangle, compensated ($10^{-3}$ P, $10^{-3}$ B in vapor phase); filled circle, undoped. (XBL 837-10556)

From our results, we deduce that illumination appears to increase the density of those states residing ~1.2–1.3 eV below the conduction band. This conclusion holds for all of our samples, implying that the photoinduced metastable defect is probably the same for the doped and the undoped materials.

Given our earlier finding that the maximum in the density of state 1.2–1.3 eV below the conduction band is due to Si dangling bonds, we tentatively conclude that the observed photoinduced enhancement in gap-state absorption is caused by an increase in the number of these Si dangling bonds. This conclusion is further supported by ESR and field-effect data.[29,33] Illumination apparently break the "weak" Si-Si bonds, which is followed by the relaxation of the surrounding network.

We would like to point out, however, that the photoinduced increase in the density of states near midgap does not uniquely imply the creation of additional dangling bond defects. A shift in the Fermi level, without any increase in the number of gap states, will also result in apparent increase in the number of these states. Clearly, more work is needed in order to understand the origin of the photoinduced metastable gap state.

## NOVEL LASER SYSTEMS*

Our research activities sometimes require the development of new laser systems to meet a specific need. Of current interest to us is the generation of subpicosecond tunable laser pulses for probing elementary excitation in amorphous photovoltaic semiconductors. We also have a long-standing interest in laser waveguides that would provide high power, compactness, and ruggedness.

### Highly Efficient, Widely Tunable Double Mode-Locked Dye Laser†

With the advent of synchronously pumped dye lasers,[35–38] picosecond spectroscopy is becoming widely investigated. Despite the difficulty of achieving subpicosecond operation, these dye lasers have the favorable characteristics of high average output power (~100 mW) and wide tuning range (~600 Å) in the picosecond regime. Conventional passively mode-locked dye lasers,[39–42] on the other hand, while generating shorter pulses, yield low output power (~10 mW) and have a relatively restricted tuning range (~200 Å).

We have developed a passively double mode-locked dye laser that produces subpicosecond pulses (0.5 psec) with high output power (~150 mW) and high conversion efficiency (5–10%) over a wide tuning range (~600 Å). In addition, through double mode-locking,[43,44] a highly synchronous secondary picosecond beam, tunable over a similar range, is generated at longer wavelengths.

Furthermore, we point out that, in the subpicosecond regime, passively mode-locked dye lasers are ultimately more efficient than their synchronously pumped counterparts, as demonstrated below.

A cw $Ar^+$ laser (5145 Å) pumped rhodamine 6G (R6G) laser is double mode-locked by a mixture of rhodamine 101 (R101) and cresyl violet (CV) in an independently tunable cavity configuration (Fig. 9). The following factors optimize the operation of this laser:

(1) Output coupler $M_3$ has a transmission value $T$ of 3% to 10%, thus yielding high output coupling efficiency.

(2) The double mode-locking mixture R101/CV has an absorption spectrum that closely matches the gain spectrum of R6G, thus enabling easy tunability over a wide wavelength range.

(3) Cavity length $L$ is kept at about 75 cm to avoid multiple pulse operation.

(4) The R6G jet is placed near the center of the cavity to maximize the gain for single-pulse operation.[45]

(5) The ratio of the radii of curvature $R_4/R_1$ of mirror $M_4$ and $M_1$, respectively, is kept high, resulting in a wide wavelength range of stable mode-locking.

(6) Folding angles are kept to the minimum possible to obtain good astigmatic compensation. Mode structure of the R6G beam is maintained as a good Gaussian.

(7) The angle between the two beams in the R101/CV jet is minimized to obtain maximum overlap.

(8) The thickness of the birefringent tuning filter (LF1) is sufficiently thin (0.375 mm) to suppress a red lasing tendency in the R6G cavity. This also results in less dispersion.

With these conditions satisfied and the cavity lengths matched, this double mode-locked dye laser provides 0.5 psec pulses (yellow) with a wide tuning range (570–630 nm), and high average power (~150 mW for 2-W pump power). Typical efficiencies of 5–10% for pump laser powers of 1–2.5 W are readily obtained, with a weak dependence on pulse width. To our knowledge, this is the highest output power and efficiency for a cw mode-locked subpicosecond dye laser ever reported. Excellent pulse stability and compact autocorrelation tracers are maintained over many hours of operation. Multiple and satellite pulsing problems are readily eliminated. Subpicosecond pulses are obtained near and also significantly above threshold. Finally, picosecond operation remains stable with no need to adjust the pump power or the cavity alignment while the birefringent tuning filter is continuously rotated over nearly the entire tuning range.

Assuming a $\text{sech}^2$ pulse shape, we measure a pulsewidth $\Delta t$ of 500 femtoseconds. Pulsewidth-bandwidth products $\Delta\nu\Delta t$ are typically in the range of 0.5–1.0. Peak powers correspond to ~1.5 kW for a repetition rate of 200 MHz.

Through the double mode-locking process,[43] independently tunable picosecond pulses are synchronously[46,47] generated at a longer wavelength (red), tunable over 630–660 nm. With the output

*This work was supported by the Office of Energy Research Pollutant Characterization and Safety Research Division of the U.S. Department of Energy under Contract No. DE-AC03-76SF00098.

†Appeared in *Opt. Commun. 42*, p. 281 (1982).

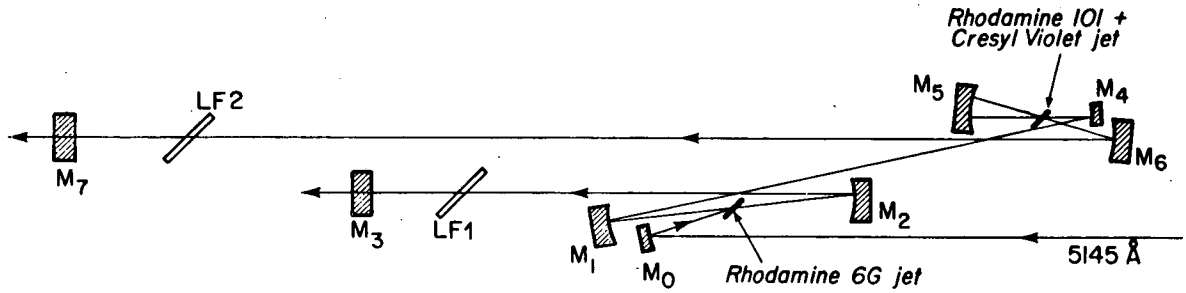


Figure 9. Cavity configuration of the independently tunable double mode-locked dye laser. $M_1$, $M_2$ and $M_4$ are R6G high reflectors (560–650 nm) with radii of curvature $R_1 = R_2 = 10$ cm and $R_4 = 3.5$ cm (or 5 cm). $M_5$ is a broadband high reflector with $R_5 = 2.5$ cm. $M_6$ is a red high-reflecting mirror (600–700 nm) with $R_6 = 5$ cm. $M_3$ and $M_7$ are output couplers: $M_3$ has $T = 3\%$ or 10% and $M_7$ has $T = 1\%$. LF1 and LF2 are single-plate birefringent filters. (XBL 823-296)

coupler of $T = 1\%$, typical average power for these red pulses was a few mW. The long wavelength limit was set by the coating characteristics on M5. In principle, the tuning range of the red beam should encompass most of the lasing spectrum of the R 101/CV mixture (620 nm–700 nm). In the present work, optimizing the red pulses was not attempted. We observed that as the shorter wavelength (yellow) was tuned towards 630 nm, the mode-locker ceases to lase, with the yellow beam remaining conventionally passively mode-locked.

Double mode-locked operation of this laser depends on the close matching of the lengths of the two cavities. For subpicosecond pulses, cavity lengths needed to be matched to within a few $\mu$m. At present, thickness fluctuations of the R6G jet is likely to be the main pulsewidth limiting factor. This independently tunable separate-cavity configuration provides for the correction of the inherent cavity mismatch (due to different group delays of the pulses in various optical elements) present in the collinear cavity configuration previously described.[44] Similar results of pulsewidth (yellow), output power, and tuning range were also obtained in the collinear configuration, indicating a dynamic compensation of the mismatch. The average power in the red beam was higher (~20 mW) in the collinear configuration, as contributed by the R6G gain. However, independent tunability is difficult to obtain. The present configuration also improves on the prism-tuned configuration[48] in that the thickness of the tuning elements can be kept smaller (less dispersion), while the cavity length is kept shorter to avoid multiple pulsing.

The absorption spectrum of the double mode-locking mixture is given in Fig. 10. The peak absorptance corresponds to a single-pass, small-signal absorption of 8% (0.15-mm-thick jet) and a threshold pump power of ≈2 W for $T = 3\%$. The corresponding dye concentrations are $1.4 \times 10^{-5}$ molar for R101 and $1.3 \times 10^{-5}$ molar for CV. Also shown in Fig. 10 is the emission spectrum of R6G. The excellent matching of the two spectra is important for the demonstrated wide tunability.

In Fig. 11 we plot the output pulse energy and ultimate pulsewidth for an ideal (stable pump pulses, no cavity length perturbation, no dispersion) conventional synchronously pumped dye laser ($T = 50\%$, pump pulsewidth = 100 psec) as a function of cavity

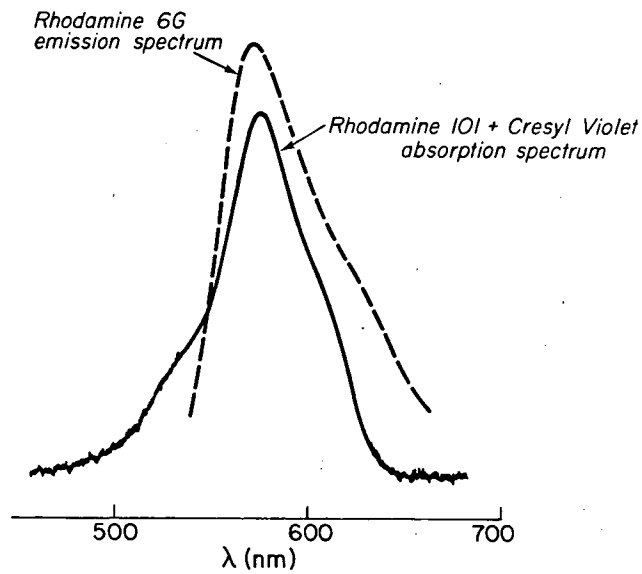


Figure 10. Absorption spectrum of the mode-locking mixture of R101/CV and the emission spectrum of R6G. Peak absorptance of R101/CV is ≈ 0.4 for a 1-mm path length. (XBL 823-295)

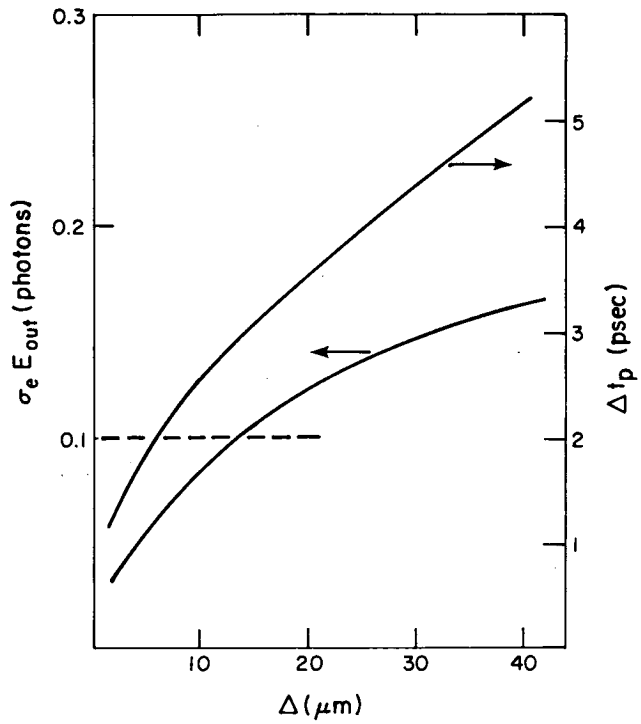


Figure 11. Pulsewidth and energy/pulse for synchronously pumped dye lasers ($T$ = 50%, pump pulsewidth = 100 ps) vs. cavity mismatch. Also shown is a typical output energy value (0.1 photons) for a subpicosecond passively mode-locked dye laser pulse. (XBL 823-286)

mismatch.[49] The pulsewidth and energy of the conventional passively mode-locked lasers depend upon parameters such as $S = F\sigma_a/\sigma_e$ (where $F$ is the ratio of the focal spot areas in the two dye jets, $\sigma_a$ is the absorption cross section of the mode-locking dye, and $\sigma_e$ is the emission cross section of the laser dye), cavity length, threshold pump power, and the output coupler transmission. A typical energy/pulse for $T$ = 3% under ideal conditions (no triplet losses, etc.) is $\sigma_e E_{out} \approx 0.1$ photons.[45] The corresponding pulsewidth depends on the cavity dispersion but can be in the subpicosecond range. This value is plotted in Fig. 11 as a straight line. It can readily be seen that the pulse energy of synchronously pumped dye lasers decreases significantly as the pulsewidth decreases, to below the pulse energy value for passively mode-locked lasers in the subpicosecond regime.

Hence, Fig. 11 depicts the generally unrecognized fact that, despite its apparent higher losses, the passively mode-locked dye laser has pulse-compression dynamics in its cavity such that *subpicosecond pulses of higher energy can be stably sustained,* as compared to a conventional synchronously pumped dye laser. In the latter case, only a small fraction of the available gain is usable for sustaining a subpicosecond pulse,[49] the remainder being lost to fluorescence or to the generation of spurious satellite pulses. Pulses of higher energy become stable in a synchronously pumped dye laser cavity only at the expense of a broadened pulsewidth.

The extent of the role of the double mode-locking process (lasing of the mode-locking dye) in the demonstrated high efficiency of our system remains to be fully understood. However, there is a strong indication that this phenomenon enables stable subpicosecond operation at high values of $S$, which also correspond to higher pulse energies.[46] On the other hand, for conventional passively mode-locked dye lasers, there exists theoretical[45] and experimental evidence that $S$ must not reach very high values, particularly for long cavity lengths; this may result in lower pulse energies. The wide tuning range of our double mode-locked laser provides further evidence in support of this argument.

In summary, a highly efficient cw double mode-locked dye laser has been developed. In addition to generating widely tunable, compact subpicosecond pulses with high power, a highly synchronous and independently tunable pulse is simultaneously generated at a longer wavelength. This two-color cw ultra-short pulsed laser source should prove to be a versatile tool for excite-and-probe experiments in picosecond spectroscopy.

## Waveguide Laser Physics

Waveguide gas lasers, in which the beam propagates as a guided wave in a hollow dielectric tube, are of increasing technological and commercial importance. Practical waveguide lasers fall into two categories: (1) internal-mirror lasers, in which the mirrors forming the optical resonator are inside the vacuum enclosure, where they can be placed very close to the ends of the waveguide; and (2) external-mirror lasers, in which the vacuum enclosure terminates in Brewster-angle windows.

The mirrors in internal-mirror lasers can be flat because the beam spreads out very little in propagating the short distances from the ends of the waveguide to the mirrors and back, keeping the diffraction losses very low. However, in external-mirror lasers, short-radius concave mirrors must be used to refocus the diverging beam into the ends of

the waveguide. For $CO_2$ waveguide lasers, typical mirror radii of curvature are in the 10–40 cm range; these must generally be custom-made and can be quite expensive.

We have investigated, theoretically and experimentally, how low cavity losses might be obtained using ordinary flat mirrors placed significant distances from the ends of the waveguide, as in external-mirror lasers. Our theoretical treatment involves finding the eigenvalues of a matrix describing the effects on the beam of propagating one round trip through the cavity. This matrix is a product of a number of other matrices representing various portions of the round trip, such as one describing the phase shifts and attenuations of the waveguide modes in propagating through the tube, another for transforming the waveguide modes to a set of free-space modes to describe propagation to the mirror and back, and so forth. In a major improvement over previous theoretical analyses of waveguide laser resonators, we have replaced most of the numerical integrations used by previous authors with analytical transformations, greatly reducing the amount of computer time required.

For a wavelength laser cavity formed by flat mirrors at equal distances $d$ from the ends of a hollow circular dielectric waveguide of length $L$ and radius $a$, operating at wavelength $\lambda$ and having propagation constant $k = 2\pi/\lambda$, we find that low loss cavity configurations occur along the curves in Fig. 12(a). These curves are labeled with a parameter Re $\nu_n/ka$, which is a measure of the waveguide losses;

$$\nu_n = \frac{\nu^2 + 1}{2(\nu^2 - 1)^{1/2}}$$

where $\nu$ is the complex refractive index of the waveguide material. Within the waveguide, the beam propagates mainly as a combination of the $HE_{11}$ and $HE_{12}$ modes. When the beam emerges into the free-space region, these modes couple strongly to the $TEM_{00}$ and $TEM_{10}$ Laguerre-Gaussian modes, respectively, for a particular optimal choice of the spot size $w_0$. These latter two free-space modes both diverge as they propagate from the waveguide to the mirror and back again, but if they have the proper relative phase when launched, the relative phase shift they undergo in propagating through the free-space region will result in a destructive interference in the outer part of the beam and a constructive interference near the center when the beam reenters the waveguide, so that most of the power is concentrated within a small radius and couples back into the waveguide. The curves along which cavity losses are minimized are approximately those for which the sum of the $HE_{12}$–$HE_{11}$ phase shift in the waveguide plus the $TEM_{10}$–$TEM_{00}$ phase shifts in the free-space regions is $2\pi$ (or a multiple thereof). Some experimental points on the optimum $d$ vs. $L$ curve are also included in Fig. 12(a), and it is seen that they agree reasonably well with theory, although they are displaced upward slightly. The parameter $\nu_n$ is not known for our laser.

If we calculate the minimum loss along the curves in Fig. 12(a) as a function of the mirror distance $d$, we obtain the curves in Fig. 12(b). We see that as long as $d/ka^2 \lesssim 0.1$, cavity losses generally remain low, not greatly exceeding the (unavoidable) losses due to the waveguide alone. For a $CO_2$ waveguide

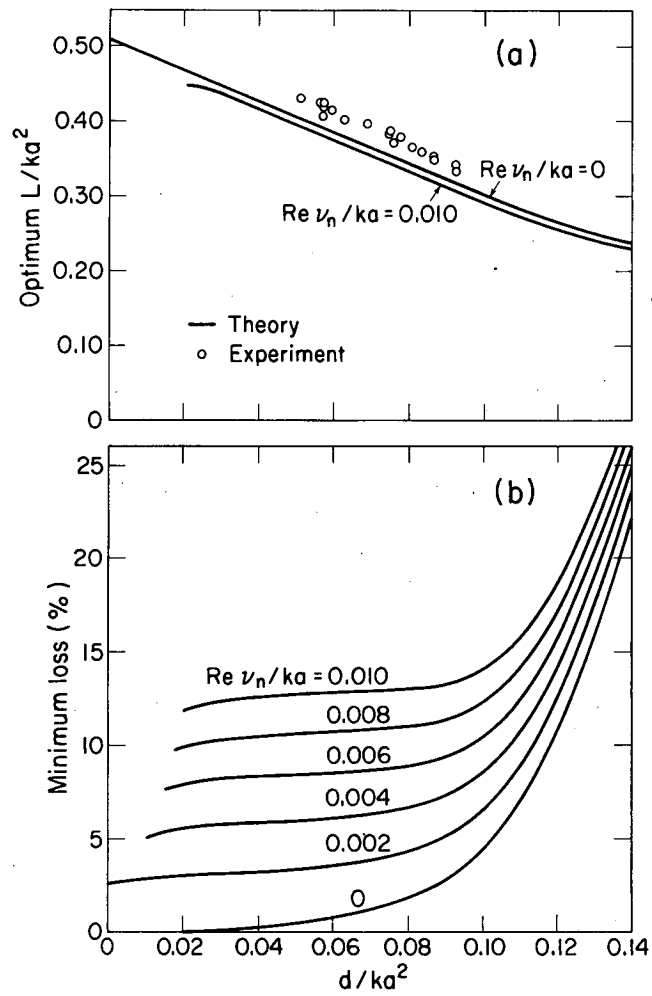


Figure 12. (a) Optimum cavity configuration as a function of $d/ka^2$; curves from theoretical calculations show good agreement with experimental results. (b) Theoretical minimum diffraction loss along the curves in (a) as a function of mirror distance $d$. (XBL 836-1868)

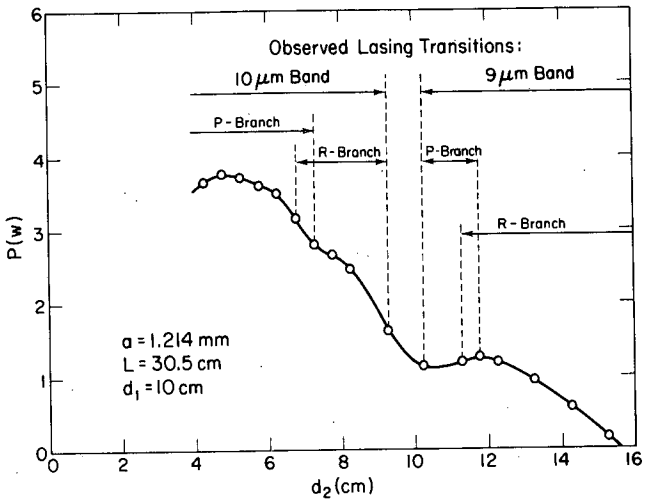


Figure 13. Experimental data showing wavelength selectivity obtained by varying mirror position in an asymmetric cavity. (XBL 836-1869)

laser operating at 10.5 $\mu$m and having a typical bore diameter of 2 mm, this corresponds to $d \lesssim 6$ cm, which is a very practical mirror distance for an external-mirror waveguide laser.

We have also analyzed asymmetric laser cavities, for which the mirror distances $d_1$ and $d_2$ are unequal. For a given waveguide length $L$, we find that low losses occur approximately along a straight line: i.e., $d_1 + d_2 =$ constant; we have confirmed this experimentally. We have also found that by varying the position of one of the mirrors, we can exert a coarse wavelength tuning on the cavity, sufficiently selective to determine which of the four possible band-branches in the 9–11 $\mu$m region the laser operates on. Some experimental data demonstrating the wavelength selectivity appear in Fig. 13. As we varied one mirror distance $d_2$ while holding the other distance $d_1$ fixed, we observed a variation in output power and also a switching by the laser from one branch to another, consistent with the predictions of our theory.

A paper presenting the details of these results will be published shortly. We are also working on extending our theoretical analysis to resonators using curved mirrors, since the greater efficiency of replacing numerical methods with analytical ones will be useful there as well as for flat-mirror resonators.

## PLANNED ACTIVITIES FOR FY 1983

In the area of laser photothermal spectroscopy and detection, emphasis will continue to be placed on unambiguous remote sensing of atmospheric constituents. Methods to overcome atmospheric turbulence and speckle will be investigated. Pulsed photothermal displacement spectroscopy will be studied, and extensions of this technique for the study of liquids will be devised. Nonlinear photoacoustic spectroscopy of gases will be initiated.

Research on amorphous semiconductors will focus on the physics of defects in hydrogenated amorphous silicon and germanium. The elucidation of the nature of the metastable photoinduced defects in amorphous silicon will continue to be of interest to us.

A new activity will be the investigation of surface and interface states of semiconductors., In addition, processes at the liquid-semiconductor and gas-semiconductor interfaces will be studied.

Finally, we will continue our research on laser physics and technology with the goal being the production of widely tunable, high-average-power pulses a few femtoseconds wide.

## REFERENCES


1. See, for example, H. Lüth (1975), *Appl. Phys. 8,* p. 1.
2. Olmstead, M.A., Amer, N.M., Kohn, S., Fournier, D., and Boccara, A.C., submitted to *Appl. Phys. A.*
3. Other photothermal techniques include photoacoustic spectroscopy—see, for example, *Optoacoustic Spectroscopy and Detection,* Y.-H. Pao, Ed., Academic Press, New York, 1977; W.B. Jackson and N.M. Amer, *J. Appl. Phys. 51,* p. 3343 (1980)—and photothermal deflection spectroscopy (see Ref. 19, below). However, these techniques are not suited for experiments which require UHV or a wide range of temperatures.
4. See, for example, Fritzsche, H. (1980), *Solar Energy Mater. 3,* p. 447, Street, R.A. (1981), *Adv. Phys. 30,* p. 593, and references within.

5. Tsang, C., and Street, R.A. (1979), *Phys. Rev. B 19,* p. 3027; Street, R.A., Knights, J.C., and Biegelsen, D.K. (1978), *Phys. Rev. B 18,* p. 1880.
6. Johnson, A.M., et al. (1981), *Phys. Rev. B 23,* p. 6816.
7. Jackson, W.B., and Amer, N.M. (1982), *Phys. Rev. B 25,* p. 5559.
8. Cody, G., et al. (1981), *Phys. Rev. Lett. 47,* p. 1480.
9. Jackson, W.B. and Amer, N.M. (1982), *J. Phys.* (Paris) *42,* p. C4-293.
10. Schockley, W., and Read, T. (1952), *Phys. Rev. 87,* p. 835.
11. Orenstein, J., and Kastner, M.A. (1981), *Phys. Rev. Lett. 46,* p. 1421, and *Solid State. Comm. 40,* p. 85; Tiedje, T., and Rose, A. (1980), *Solid State. Comm. 37,* p. 49.
12. Ray, S., et al. (1981), in *Tetrahedrally Bonded Amorphous Semiconductors—1981,* R.A. Street, D.K. Biegelsen, and J.C. Knights, Eds., AIP Conference Proceedings No. 73, American Institute of Physics, New York, p. 253.
13. Ray, S., Vardeny, Z., and Tauc, J. (1981), *J. Phys.* (Paris) *41,* p. C4-555.
14. Tiedje, T., Cebulka, J.M., Morel, D.L., and Abeles, B. (1981), *Phys. Rev. Lett. 46,* p. 1425.
15. O'Connor, P. and Tauc, J. (1980), *Solid State Comm. 36,* p. 947.
16. Wake, D.R., and Amer, N.M., to be published.
17. We have not spectrally resolved the luminescence but have confirmed that the luminescence is quenched in our high-defect-density samples and that the temperature dependence of the high-defect-density luminescence is substantially weaker, as expected.
18. Pankove, J.I., and Carlson, D.E. (1976), *Appl. Phys. Lett. 29,* p. 610, and Engeman, D.E. and Fischer, R. (1977), *Phys. Status Solidi(b) 79,* p. 195; however, R.A. Street has pointed out that charged defects are unlikely to provide sufficiently strong homogeneous fields (private communication).
19. Jackson, W.B., Amer, N.M., Boccara, A.C., and Fournier, D. (1981), *Appl. Optics 20,* p. 1333.
20. Following the procedure of Ref. 9.
21. Rehm, W., and Fischer, R. (1979), *Phys. Status Solidi(b) 94,* p. 595 (1979); Shah, J., Bagley, B.G., and Alexander, F.B., Jr. (1980), *Solid State Comm. 36,* p. 199.
22. Wake, D.R., and Amer, N.M., to be published.
23. Staebler, D.L. and Wronski, C.R. (1980), *J. Appl. Phys. 51,* p. 3262.
24. Persans, P.D., (1980), *Solid State Comm. 36,* p. 851; P.E. Vanier and Griffith, R.W. (1982), *J. Appl. Phys. 53,* p. 3098.
25. Vardeny, Z., Strait, J., Pfost, D., and Tauc, J. (1982), *Phys. Rev. Lett. 48,* p. 1132.
26. Depinna, S.P., Cavenett, B.C., Austin, I.G., and Searle, T.M. (1982), *Solid State Comm. 41,* p. 263.
27. Staebler, D.L., and Wronski, C.R. (1977), *Appl. Phys. Lett. 31,* p. 292.
28. Jousse, D., Basset, R., Deliouibus, S., and Bourdon, B. (1980), *Appl. Phys. Lett. 37,* p. 208.
29. Dersch, H., Stuke, J., and Beichler, J. (1981), *Appl. Phys. Lett. 38,* p. 456.
30. Pankove, J.I. and Berkeyheiser, J.E. (1980), *Appl. Phys. Lett. 37,* p. 705.
31. Lang, D.V., Cohen, J.D., Harbison, J.P., and Sargent, A.M. (1982), *Appl. Phys. Lett. 40,* p. 474.
32. Solomon, I., Dietl, T., and Kaplan, D. (1978), *J. Physique 39,* p. 1241.
33. Goodman, N.B. (1982), *Phil. Mag. B45,* p. 407; Tanielian, M.H., Goodman, N.B., and Fritzsche, H. (1981), *J. Phys.* (Paris) *42,* p. C4-293.
34. Morigaki, K., et al. (1980), *Solid State Commun. 33,* p. 851.
35. Heritage, J.P., and Jain, R.K. (1978), *Appl. Phys. Lett. 32,* p. 727.
36. Ferguson, A.I., Eckstein, J.N., and Hansch, T.W. (1978), *J. Appl. Phys. 49,* p. 5389.
37. Kuhl, J., Klingenberg, H., and von der Linde, D. (1979), *Appl. Phys. 18,* p. 279.
38. Ryan, J.P., Goldberg, L.S., and Bradley, D.J. (1978), *Opt. Commun. 27,* p. 127.
39. Ippen, E.P., Shank, C-V., and Dienes, A. (1972), *Appl. Phys. Lett. 21,* p. 348.
40. Ruddock, I.S., and Bradley, D.J. (1976), *Appl. Phys. Lett. 29,* p. 296.
41. Diels, J.C., Van Stryland, E., and Benedict, G. (1978), *Opt. Commun. 25,* p. 93.
42. Rosen, D., et al. (1981), *J. Quantum Electron. QE-17,* p. 2264.
43. Yasa, Z.A., and Teschke, D. (1975), *Appl. Phys. Lett. 27,* p. 446, and Yasa, Z.A. (1975), *J. Appl. Phys. 46,* p. 4895.
44. Yasa, Z.A., Dienes, A., and Whinnery, J.R. (1977), *Appl. Phys. Lett. 30,* p. 24.

45. Yasa, Z.A. (1976), Ph.D. Thesis, University of California, Berkeley.
46. Bourkoff, E., Dienes, A., and Whinnery, J.R. (1979), *Appl. Phys. Lett. 34,* p. 455.
47. Arjavalingam, G., Dienes, A., and Whinnery, J.R. (1982), *Opt. Lett. 7,* p. 193.
48. Bourkoff, E. and Whinnery, J.R. (1979), *Opt. Lett. 4,* p. 179.
49. Yasa, Z.A. and Amer, N.M., to be published.

# OIL SHALE WASTEWATER TREATMENT: EFFECT OF OZONATION AND UV IRRADIATION ON BIOREFRACTORY ORGANIC SOLUTES*

*B.M. Jones, G.W. Langlois, R.H. Sakaji, J.F. Thomas, and C.G. Daughton*†

Wastewaters from the pilot-scale retorting of oil shale have been tremendously variable in their chemical characteristics, but in general retort water is characterized by a complex spectrum of polar and nonpolar organic solutes in extremely high concentrations. The major classes of organic compounds include alkanes, carboxylic acids, polyhydric phenols, and nitrogenous and oxygenated heterocycles. The extreme levels of contaminative organic solutes, the presence of surfactants, suspended oil, tars, and particulates, the possibility of toxicity to microorganisms, the high level of dissolved inorganic salts and gases, and the undersirable color and odor of these wastes—all frustrate both the application of established pollution control technologies and the determination of treatment performance by standard analytical methodologies. To minimize intrasample variation and to allow for interlaboratory comparison of experimental results, our research has concentrated on composited samples of modified in-situ (MIS) retort water and gas condensate from Occidental Oil Shale Company's retort burn No. 6 (Oxy-6).[1]

Biological treatment is the conventional method of removing organic contaminants from a wastewater stream. An acclimated microbial community can convert dissolved organic solutes into cellular biomass, heat, and gases. This scheme can fail, however, if

(a) the resultant cells are not separable from the liquid,
(b) nutrients essential for growth are not available in the solution,
(c) components of the medium are toxic to the microorganisms,
(d) the microorganisms are enzymatically incapable of mineralizing the organic material, or
(e) many of the compounds are inherently resistant to microbial alteration.

Biological treatment of Oxy-6 retort water is initially limited by inorganic orthophosphate.[1,2] Paradoxically, the nutrient that subsequently limits microbial growth is carbon, even though repeated studies have shown that about half of the dissolved organic carbon (DOC) remains after exhaustive biological treatment[2]; adding trace elements does not elicit further growth or DOC removal. Secondary growth is observed, however, when these same cultures are supplemented with an exogenous source of easily degraded carbon such as aliphatic carboxylic acids.[2] Nitrogen and oxygen heterocycles and aromatic amines have been implicated[3] as the major chemical classes accounting for the extraordinary recalcitrance of organic carbon in the extracellular fluid (i.e., spent retort water) that remains after exhaustive biooxidation. This hypothesis has been strengthened by several reports on the chemical characterization of Oxy-6 retort water extracts[4] indicating the presence of numerous aromatic amines and unsaturated, oxygenated nitrogen heterocycles, each at low part-per-million concentrations.

Successful treatment of oil shale wastewater undoubtedly will require using more than one technology. A particular method may be extremely effective in removing a specific class of organic compounds, but, in a heterogeneous mixture such as retort water, this class may represent only a fraction of the contaminative solutes. Effective treatment will require a combination of methods that yield complementary or enhanced performance when used simultaneously or in sequence. The integration of these processes should be evaluated carefully because the final degree of treatment could be additive (the sum of the individual processes), synergistic (greater than the sum of the processes), antagonistic (lower than any of the processes), or a combination thereof.

Ozonation and ultraviolet (UV) irradiation were investigated as pretreatment methods to augment or

*This work was supported by the Assistant Secretary for Fossil Energy, Office of Oil Shale, Division of Oil, Gas, and Shale Technology of the U.S. Department of Energy under Contract No. DE-AC03-76SF00098.

†Sanitary Engineering and Environmental Health Research Laboratory, University of California (Berkeley), Richmond, California 94804.

enhance the biological treatment of oil shale wastewaters by mineralizing or oxidatively altering organic solutes that are biorecalcitrant or bactericidal. It was also possible that these processes could, instead, hinder biooxidation by producing toxicants, polymerizing solutes that would ordinarily be biodegradable, or creating a multitude of new solutes, each present at a low concentration; the latter possibility would amplify an already existing problem. The effects of ozonation and UV irradiation could, in any case, be used as a predictor of the maximum capacity of aerobic biooxidation achievable through oxygenases.[5] The extent of oxidation from UV irradiation can also give an indication of the photochemical alterations to be expected during storage of these waters in ponds at the high elevations typical of western oil shale deposits.

## BACKGROUND

### UV Irradiation

The degradation of organic solutes by exposure to UV radiation occurs by three mechanisms: (1) sufficient radiant energy is absorbed to cleave intramolecular bonds, producing lower-molecular-weight fragments; (2) reactive organic free radicals are generated; and (3) interaction of these free radicals with molecular oxygen produces peroxy and hydroperoxy radicals, which are capable of structural alteration or complete mineralization of the lower-molecular-weight fragments by oxygenation, hydrogen abstraction, or the initiation of chain reactions.[6-8] Furthermore, the photolysis of endogenous organic compounds in natural surface waters has been shown to generate hydroxyl radicals (OH·) and singlet oxygen, both capable of subsequently transforming synthetic organic solutes.[9]

A more efficient use of UV radiation than direct mineralization may be as an aid to biooxidation; thus oxygenated or fragmented, otherwise biorefractory molecules may become amenable to biodegradation. UV radiation has been implicated in the degradation of pesticides in the environment[6] and in aiding the biodegradation of certain synthetic polymers.[10]

Photooxidation characteristically produces a variety of products from a given reactant and each of these products may vary in its susceptibility to microbial metabolism.[11] This plethora of products is especially significant with respect to the photooxidation of oil shale wastewaters. Two factors[12] that exacerbate the refractory nature of the substituted heterocyclic compounds in spent retort water are (1) the presence of numerous heterocycle homologs and variants, each of which can require a specialized catabolic enzyme system, and (2) the low individual heterocycle concentrations,[4] which, being below the affinity or threshold values, render the enzymes ineffective. Although photooxidation may generate more degradable solutes, it may also exacerbate the purported problems of enzyme specificity and threshold-concentration effects.

### Ozonation

Ozone is a very selective and highly versatile oxidizing agent; it is used not only in organic chemistry, but as a disinfectant for potable water and as a wastewater treatment aid. In an aqueous solution, the oxidative capacity of ozone appears to depend on pH and the organic and inorganic solute concentrations. For acidic and slightly alkaline solutions (pH less than 9.0), ozone reacts predominantly as the parent ozone molecule; these reactions are relatively slow and highly specific, depending on the class and bonding structure of the organic reactant. Furthermore, oxidation by ozone is reportedly almost entirely ineffective in highly acidic aqueous solutions (pH below 2.0).[13] In contrast, ozone is catalytically decomposed by hydroxide ion (pH greater than 10.0) to a variety of products, including OH· and superoxide ion.

The hydroxyl radical is the most potent and effective oxidant known to occur in aqueous solutions,[14] having an oxidation potential of 2.8 V ($H^+$ = 1.0 *M*) compared with 2.07 V for ozone in acidic solutions and 1.36 V for chlorine gas.[15] At a pH of 10.5, approximately one-half mole of OH· is formed per mole of $O_3$ decomposed.[14]

Hydroxyl radicals are extremely reactive and easily oxidize organic material; they react with inorganic solutes with little substrate specificity. They are quickly consumed (within microseconds), but their intense reactivity makes them critically important to aqueous ozone chemistry.[16] Hydroxyl radicals are vigorously scavenged by carbonate ion and, to a lesser extent, by bicarbonate species; scavenging accelerates the disproportionation of ozone to its reactive decomposition products,[17] but decreases the oxidative capacity by quenching chain reactions. Free ammonia can be oxidized to nitrate by ozone and OH·, but this reaction will be significant only

when ammonia concentrations are equal to those of carbonate species and organic solutes.[18]

Retort water often contains high ammonia and dissolved inorganic carbon (DIC) concentrations, both of which scavenge or react with ozone or ozone-disproportionation products. Furthermore, substituted nitrogen heterocycles, a major biorefractory organic chemical class is spent retort water, are not particularly susceptible to attack by ozone, unlike most non-nitrogen heterocycles. Pyridine reacts extremely slowly, and ozone preferentially attacks the carbocyclic ring of quinoline.[19]

A preliminary examination of the effect of ozone on Oxy-6 oil-shale retort water showed that high alkalinity interferes with the oxidation of organic compounds; pretreatment with powdered activated carbon (PAC), however, reduces the alkalinity and appears to increase the effectiveness of ozonation.[20] A second study used ozonation and ammonia stripping as preliminary steps before PAC-aided biooxidation of Oxy-6 retort water.[21] The results of these experiments revealed that low dosages of ozone (70 mg/l) appear to slightly increase the biodegradability of Oxy-6 retort water. Ozonation also removes much of the color, indicating that some of the nitrogen heterocycles may have been oxidized. Following extensive integrated treatment, the major portion of the base/neutral organic compounds was not altered or mineralized. The predominant refractory chemical groups were unsaturated, oxygenated nitrogen heterocyles, especially pyrrolidinones, piperidinones, cyclohexanopyrrolidinones, and cyclopentanopiperidinones.

Partial oxidation or cleavage of ozonation of complex high-molecular-weight organic compounds (which are commonly biorefractory) into polar, oxygenated, lower-molecular-weight fragments can substantially affect biodegradability.[22] The benefit of partial oxidation has been shown for nonbiodegradable water-soluble polymers.[23] Ozonation of polyethylene glycol, polyvinyl alcohol, polyvinylpyrrolidone, and sodium polyacrylate reduces the molecular weights and improves biooxidation.

Chemical oxidation by ozone or by ozone-decomposition radicals can also be used to predict the extent of oxidation of biorefractory organic solutes in retort water by acclimated bacteria with competent oxygenase enzyme systems. Ozonation can therefore be viewed as a facile means for predicting the maximum theoretical degree of oxidation that could be effected by aerobic biological treatment.

## Combined UV Irradiation/Ozonation

UV radiation catalyzes the disproportionation of ozone into OH·,[19] and superoxide ion, and promotes the production of organic free radicals. In contrast to hydroxide-ion mitigated ozone decomposition, ozone disproportionation by UV radiation is not restricted to the alkaline pH range. The existence of ozone decomposition products at acidic and neutral pH ranges precludes carbonate scavenging and ammonia oxidation due to shifts in the ion equilibria; this is a major advantage of the combined UV/ozone approach. In addition, chemical reactions mediated by UV/ozonation are significantly faster in the acidic than in the basic pH range.[24] Combined UV/ozonation has been reported as superior to either treatment alone for the elimination of biorefractory organic solutes from water and for the treatment of industrial wastewaters.[17,19,25] Mineralization of refractory organic species by simultaneous UV/ozonation has been extensively reviewed.[26]

Combined ultraviolet irradiation and ozonation as a pretreatment to biooxidation may be more economical than complete chemical mineralization of refractory compounds. Structural alterations of solutes effected by a brief exposure to UV/ozone may be sufficient to allow acclimated microorganisms to mineralize a significant portion of the formerly recalcitrant solutes. Preliminary experiments show that some pesticides and industrial wastes can be sufficiently altered by UV/ozone treatment to make them degradable by acclimated soil microbiota.[27] Perhaps the major drawback to this approach with respect to oil shale wastewaters is that, in a manner analogous to UV photolysis, both combined UV irradiation/ozonation, and ozonation alone create multiple products from each oxidizable compound, complicating subsequent treatment.[17,28]

In addition to its role as a pretreatment to biooxidation, the chemical alterations effected by UV/ozonation may also model the degradative potential of microbial systems. If OH· produced by combined UV irradiation/ozonation is unable to completely mineralize refractory organic solutes in a waste stream, then it is unlikely that microbial oxygenases would be effective.

## ACCOMPLISHMENTS DURING FY 1982

As part of the Oil Shale Project's waste treatment research, ozonation and UV irradiation were evaluated both for their ability to directly oxidize organic solutes and for their indirect influence on biodegradability through minor structural alterations of refractory compounds in Oxy-6 retort water. Possible mechanisms of organic solute alterations were investigated by determining organic carbon[29] in reverse-phase fractions[30] of time-course samples.

### UV Irradiation

Short exposure to intense UV radiation was insufficient to mineralize or alter the recalcitrant compounds in raw or spent retort water. The results of extensive UV irradiation of spent Oxy-6 retort water followed by biological treatment are presented in Fig. 1. The lower graph is the cumulative UV energy supplied to the photoreactor. Each pair of bars represents a sample withdrawn from the photoreactor at hourly intervals. For each pair, the first bar is the DOC concentration remaining after UV irradiation, and the second bar is the DOC concentration after subsequent biological treatment. The solid portion of each bar is the DOC concentration of the polar organic solutes (hydrophilic fraction, HpF), and the remaining portion is the concentration of the less-polar solutes (lipophilic fraction, LpF).[30] Five hours of intensive irradiation did not mineralize a significant amount of DOC (<2%), remove the chromophoric substances that give retort water its characteristic color, or change the relative polarities of the organic constituents. Furthermore, UV irradiation did not appear to structurally alter the biorefractory organic compounds; biooxidation after photochemical pretreatment did not mineralize additional carbon compared with nonirradiated reinoculated control cultures (i.e., the difference in DOC for each pair of bars was equivalent to the control).

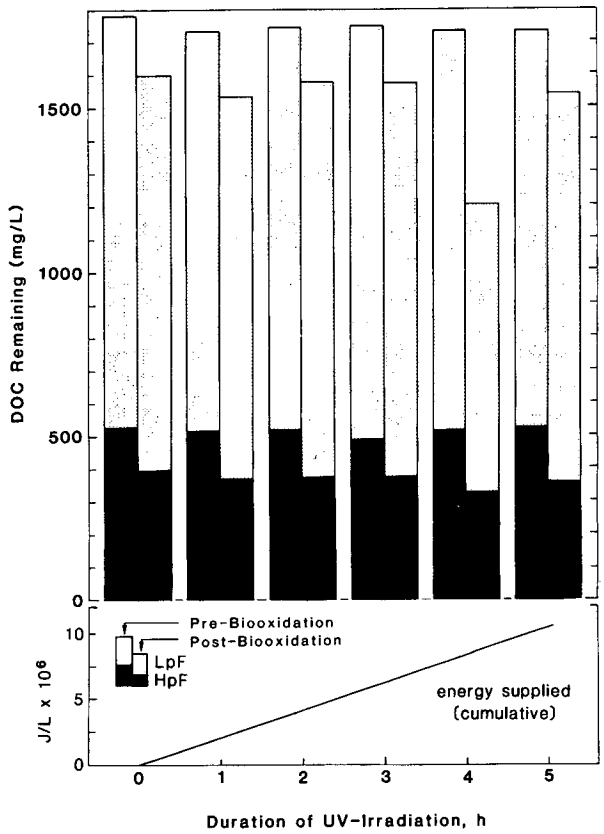


Figure 1. Biooxidation of UV-pretreated spent Oxy-6 retort water. Left bar of each pair shows dissolved organic carbon after UV irradiation; right bar, after subsequent biological treatment. Lower chart shows UV energy supplied. HpF = hydrophilic fraction (polar organic solutes); LpF = lipophilic fraction (nonpolar organic solutes).

(XBL 832-8321)

Ultraviolet irradiation of retort water may have been ineffective because of the presence of photooxidation inhibitors.[31] Particulate and colloidal carbonates can protect organic solutes from the effects of UV irradiation,[7] and the high concentrations of these species in this retort water may have prevented photoalterations. In addition, the chromophoric solutes of the water may have absorbed a significant amount of the UV radiant energy, preventing effective penetration into the water.

### Ozonation

When low dosages of ozone gas were sparged through raw or spent retort water for short periods, the DOC concentration was not substantially reduced, nor were the structures of the biorefractory organic solutes altered. The effects of extensive ozonation of spent retort water are presented in Fig. 2; the lower graph represents the cumulative amount of ozone consumed. Although 5 hours of ozonation (7.1 mg/l-min) resulted in total ozone consumption and solubilization of more than 1.6 g/l, only a small portion of the DOC was mineralized (4%). This portion, however, was primarily responsible for the color of spent retort water.

In contrast to the low dosages of ozone used in preliminary experiments, extensive ozonation of spent retort water altered a significant portion of the residual organic solutes; 14% of the DOC that was previ-

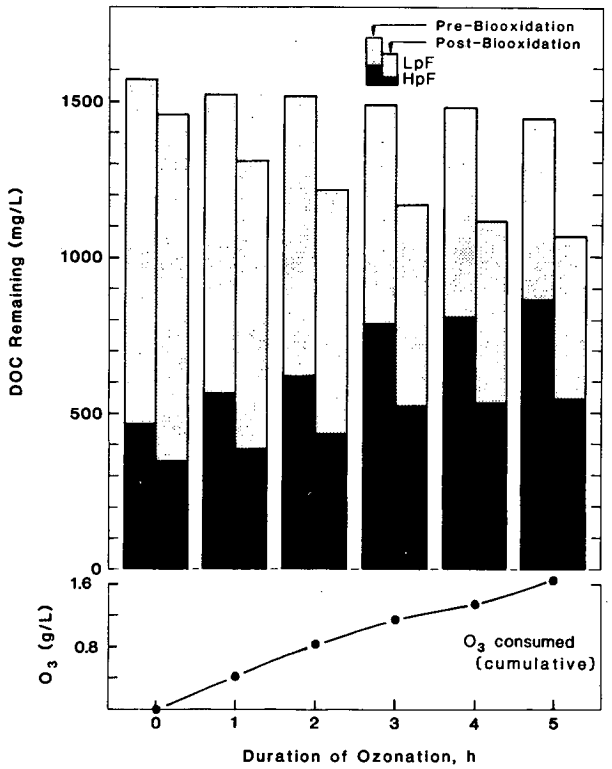


Figure 2. Biooxidation of ozone-pretreated spent Oxy-6 retort water. Bars as in Fig. 1. Lower chart shows ozone consumed. (XBL 832-8322)

ously recalcitrant became amenable to microbial mineralization. Of the DOC converted into biologically oxidizable structures (380 mg/l), approximately 320 mg/l, or 84%, was at the expense of carbon in the HpF. Despite this result, the DOC concentration in the HpF after biological oxidation of the 5-hour, ozone-treated sample was higher than in the time-zero, nonozonated, biologically treated sample (spent retort water); some of the more highly oxidized ozonation products became even less degradable.

Although prolific foaming is a major drawback to ozonation of raw retort water, foaming was not evident, when spent retort water was ozonated. This change probably resulted from the microbial mineralization of aliphatic carboxylic acids, which can act as surfactants. The possibility of excessive consumption of ozone or free radicals by unprotonated ammonia or carbonate ions had been minimized by stripping ammonia from raw retort water by vigorous aeration during primary biooxidation (the ammonia concentration after 100 hours of incubation was reduced from 86 m*M* to less than 2 m*M*) and by conducting the experiments at the unaltered pH of retort water, which is below 9.0.

The alteration of the refractory organic compounds and the elimination of the chromophoric substances most likely resulted from direct oxidation by the parent ozone molecule; the solution pH probably precluded the decomposition of ozone by $OH^-$ into its highly reactive radicals. The susceptible solutes were gradually modified until the solution was devoid of these compounds, at which point ozone was no longer an effective oxidant.

## Combined UV Irradiation/Ozonation

The organic solutes in raw and spent retort water were resistant to mineralization by short exposures to low dosages of ozone in conjunction with UV radiation, and subsequent biooxidation was not improved. In contrast, 6 hours of simultaneous ozonation and UV irradiation of spent retort water mineralized 20% of the organic carbon and appeared to significantly alter the remaining biorefractory compounds. These latter results are presented in Fig. 3; the lower graph shows the cumulative amount of both ozone consumed and UV energy supplied.

Extensive UV/ozone treatment initially either mineralized the LpF organic solutes or transformed them into HpF solutes; oxidation of compounds would

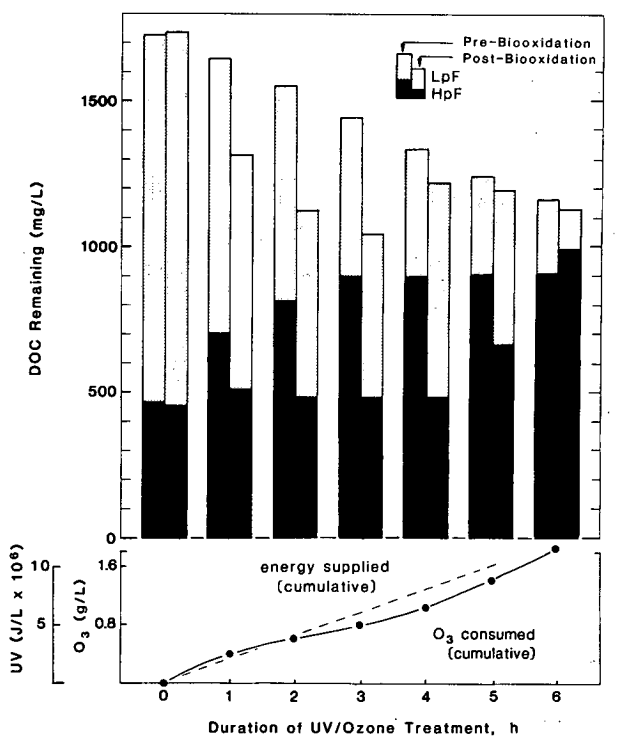


Figure 3. Biooxidation of UV/ozone-pretreated spent Oxy-6 retort water. Lower chart shows cumulative UV energy supplied and ozone consumed. (XBL 832-8323)

be expected to increase their polarities. After 3 hours of treatment, the LpF carbon continued to be mineralized, but further conversion to HpF carbon was not observed. The intense color of the spent retort water was almost entirely eliminated, and the usually persistent odor of the water became almost undetectable.

Three hours of intensive ozonation coupled with UV irradiation also effected considerable structural alterations of the organic solutes in spent retort water so that an acclimated microbial seed was able to use approximately 400 mg/l of DOC that was normally unavailable. This auxiliary biooxidation was entirely at the expense of newly created HpF organic compounds; biodegradability of retort waters seems to correlate with increasing content of HpF organic carbon.[30] The composition of the water following the serial application of biooxidation, three hours of UV/ozonation, and exhaustive secondary biological treatment was similar to that of spent water after 5 hours of ozonation followed by biotreatment.

Simultaneous UV/ozone treatment of spent water beyond 3 hours resulted in a reversal of the trend of increasing biodegradability. Further biodegradable HpF carbon was not generated, and the HpF that remained appeared to become biorefractory. After 6 hours of combined UV/ozonation of spent retort water, only 1% of the DOC was susceptible to microbial attack, although most of the remaining solutes comprised HpF carbon. For the 6-hour sample, the HpF carbon actually increased as a result of secondary biotreatment; the bacteria were growing at the expense of the LpF carbon and apparently altering a portion of this carbon to refractory HpF compounds. Microbial catabolic incompetence may not have been the only factor limiting the degradation of the remaining solutes; increased toxicity, threshold-concentration effects, or the lack of a specific nutrient or enzyme cofactor may have limited further mineralization of the DOC.

The LpF carbon from raw, spent, and UV/ozonated spent retort water was analyzed by gas/liquid chromatography for volatile nitrogenous organic compounds. Six hours of UV/ozonation eliminated most of the lower- and higher-molecular weight volatile nitrogen-containing compounds from the LpF (Fig. 4). In addition, the concentration of the intermediate-molecular-weight nitrogenous compounds in the LpF was greatly reduced. These compounds were either mineralized or transformed into HpF nitrogen-bearing compounds.

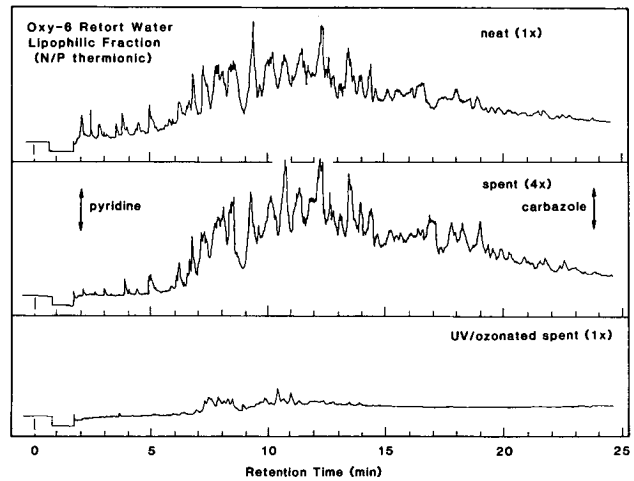


Figure 4. Gas chromatograms of raw, spent, and UV/ozone-treated spent Oxy-6 retort water (nitrogen-selective detection); the UV/ozone treatment has clearly eliminated most of the nitrogen-containing compounds from the lipophilic fraction. (XBL 832-8324)

Extensive UV irradiation combined with ozonation mineralized much of the DOC after 6 hours, but further biological treatment was unsuccessful. Although color and odor were nearly eliminated, 41% of the DOC of raw retort water remained after exhaustive serial treatment by primary biooxidation, UV/ozonation, and secondary biooxidation. The organic solutes that remained appeared to be refractory to both chemical and microbial oxidative alteration or mineralization. Other physicochemical methods that effect complementary treatment may be required to upgrade oil shale wastewaters for reuse or codisposal.

## PLANNED ACTIVITIES FOR FY 1983

The nonspecific application of UV irradiation and ozonation may exacerbate the problems of bacterial enzyme specificity and solute threshold-concentration effects by producing a multitude of oxidation products, each varying in its susceptibility to microbial attack. UV irradiation and ozonation should be judged for their combined abilities to mineralize organic material, but their effect on the subsequent biotreatability of residual solutes should not be neglected.

Research will continue on the inability of microorganisms to degrade the organic solutes that remain in spent retort waters. Emphasis will be placed on inducing the enzyme systems required for the catabolism of nitrogen heterocycles. Data from the

exhaustive biotreatment of waters from a range of retorting processes may give an indication of the possible success or reasons for failure of this treatment method.

Fixed-film bioreactors or trickling filters have been used successfully to treat industrial wastes, and they hold promise for upgrading oil shale process waters for reuse. The use of spent or raw shale as a support for a fixed microbial film will be assessed.

Five analytical methods have been validated for oil shale process waters, and detailed operator protocols and background theories have been compiled in a recently completed manual.[32] A prerequisite of continued research on these process waters is the development of valid analytical methods for the determination of specific chemical classes, such as nitrogen heterocycles, and for the determination of solute molecular weight distributions. Such new methods will be reported in a subsequent edition of the manual.

## REFERENCES


1. Jones, B.M., Sakaji, R.H., and Daughton, C.G., (1981), "Treatment of Wastewater from Modified In-Situ Oil Shale Retorting," in *Energy and Environment Division Annual Report 1980*, Lawrence Berkeley Laboratory Report LBL-11989.
2. Jones, B.M., Sakaji, R.H., Thomas, J.F., and Daughton, C.G., (1982), "Microbial Aspects of Oil Shale Wastewater Treatment," in *Energy and Environment Division Annual Report 1981*, Lawrence Berkeley Laboratory Report LBL-13500.
3. Daughton, C.G., Sakaji, R.H., and Jones, B.M., (1982), unpublished data, LBL-SEEHRL Oil Shale Waste Treatment Program.
4. Raphaelian, L.A., and Harrison, W., (1981), *Organic Constituents in Process Water from the In-Situ Retorting of Oil from Oil-Shale Kerogen*, Argonne National Laboratory Report ANL/PAG-5.
5. Jones, B.M., Langlois, G.W., Sakaji, R.H., and Daughton, C.G., (1982), "Ozonation and UV Irradiation: Effect on Oil Shale Wastewater Biorefractory Organic Solutes," LBL-SEEHRL Oil Shale Waste Treatment Program, Lawrence Berkeley Laboratory Report, LBID-549.
6. Crosby, D.G., (1972), "Environmental Photooxidation of Pesticides," in *Proceedings of the Conference on the Degradation of Synthetic Molecules in the Biosphere: Natural, Pesticidal, and Various Other Man-Made Compounds*, National Academy of Sciences, Washington, D.C., p. 260.
7. Manny, B.A., Miller, M.C., and Wetzel, R.G., (1971), "Ultraviolet Combustion of Dissolved Organic Nitrogen Compounds in Lake Waters," *Limnol. Oceanog., 16*, p. 71.
8. Plimmer, J.R., (1972), "Principles of Photodecomposition of Pesticides," in *Proceedings of the Conference on the Degradation of Synthetic Molecules in the Biosphere, p. 279.*
9. Mill, T., Hendry, D.G., and Richardson, H., (1980), "Free-Radical Oxidants in Natural Waters," *Science 207*, p. 886.
10. Jones, P.H., et al., (1974), "Biodegradability of Photodegraded Polymers: I. Development of Experimental Procedures," *Environ. Sci. Technol. 8*, p. 919.
11. Bull, A.T., (1980), "Biodegradation: Some Attitudes and Strategies of Microorganisms and Microbiologists," in *Contemporary Microbial Ecology*, D.C. Ellwood, et al., Eds., Academic Press, New York, p. 107.
12. Daughton, C.G., (1981), "Biodegradation of Heterocycles in Synfuel Wastes," Department of Energy Invention Case No. IB-417.
13. Suzuki, J., (1976), "Study on Ozone Treatment of Water-Soluble Polymers: I. Ozone Degradation of Polyethylene Glycol in Water," *J. Appl. Polym. Sci. 20*, p. 93.
14. Hoigné, J. and Bader, H., (1978), "Ozone and Hydroxyl Radical-Initiated Oxidations of Organic and Organometallic Trace Impurities in Water," *ACS Symp. Ser. 82*, p. 292.
15. Peleg, M., (1976), "Review Paper: The Chemistry of Ozone in the Treatment of Water," *Water Res. 10*, p. 361.
16. Hoigné, J. and Bader, H., (1979), "Ozonation of Water: Selectivity and Rate of Oxidation of Solutes," in *Ozone: Science and Engineering*, Vol. 1, Pergamon Press, New York and London, p. 73.
17. Hoigné, J. and Bader, H., (1976), "The Role of Hydroxyl Radical Reactions in Ozonation Processes in Aqueous Solutions," *Water Res. 10*, p. 377.
18. Hoigné, J. and Bader, H., (1978), "Ozonation of Water: Kinetics of Oxidation of Ammonia by

Ozone and Hydroxyl Radicals," *Environ. Sci. Technol. 12*, p. 79.

19. Bailey, P.S., (1982), *Ozonation in Organic Chemistry: Nonolefinic Compounds*, Vol. 2, Academic Press, New York.
20. Sierka, R.A., (1982), "A Preliminary Evaluation of Oil Shale Wastewater Treatment by Ozone and Activated Carbon," in *Fifteenth Oil Shale Symposium Proceedings*, Colorado School of Mines, Golden, Colorado, p. 479.
21. Torpy, M.F., Luthy, R.G., and Raphaelian, L.A., (1982), "Activated-Sludge Treatment and Organic Characterization of Oil Shale Retort Water," in *Fifteenth Oil Shale Symposium Proceedings*, p. 487.
22. Rice, R.G. and Browning, M.E., (1980), *Ozone for Industrial Water and Wastewater Treatment: A Literature Survey*, Environmental Protection Agency Report EPA-600/2-80-060, Washington, D.C.
23. Suzuki, J., Hukushima, K., and Suzuki, S., (1978), "Effect of Ozone Treatment upon Biodegradability of Water-Soluble Polymers," *Environ. Sci. Technol. 12*, p. 1180.
24. Peyton, G.R., Huang, F.Y., Burleson, J.L., and Glaze, W.H., (1982), "Destruction of Pollutants in Water with Ozone in Combination with Ultraviolet Radiation. 1. General Principles and Oxidation of Tetrachloroethylene," *Environ. Sci. Technol. 16*, p. 448.
25. Kuo, P.P.K., Chian, E.S.K., and Chang, B.J., (1977), "Identification of End Products Resulting from Ozonation and Chlorination of Organic Compounds Commonly Found in Water," *Environ. Sci. Technol. 11*, p. 1177.
26. Glaze, W.H., et al., (1980), *Oxidation of Water Supply Refractory Species by Ozone with Ultraviolet Radiation*, Environmental Protection Agency Report EPA-600/2-80-110, Washington, D.C.
27. Kearney, P.C., Plimmer, J.R., and Li, Z.-M., (1982), "UV-Ozonation and Land Disposal of Aqueous Pesticide Wastes," *Fifth International Congress of Pesticide Chemistry Proceedings*, Pergamon Press, London, (in press).
28. Kolonko, K.J., Shapiro, R.H., Barkley, R.M., and Sievers, R.E., (1979), "Ozonation of Caffeine in Aqueous Solution," *J. Org. Chem., 44*, p. 3769.
29. Langlois, G.W., Jones, B.M., Sakaji, R.H., and Daughton, C.G., (1982), "Coulometric Quantitation of Carbon in Oil Shale Process Wastewaters via UV-Peroxydisulfate or High-Temperature Oxidation, in *Quantitation of Oil Shale Wastewater Quality: A Manual of Analytical Methods*, C.G. Daughton, Ed., University of California Sanitary Engineering and Environmental Health Research Laboratory, Richmond, CA, UCB/SEEHRL Report No. 82-6.
30. Daughton, C.G., Jones, B.M., and Sakaji, R.H., (1982), "Rapid Fractionation of Oil Shale Wastewater by Reverse-Phase Separation," in *Quantitation of Oil Shale Wastewater Quality*, UCB/SEEHRL Report No. 82-6.
31. Larson, R.A., (1978), "Environmental Chemistry of Reactive Oxygen Species," *CRC Crit. Rev. Environ. Cont. 8*, p. 197.
32. Daughton, C.G., Ed., (1982), *Quantitation of Oil Shale Wastewater Quality*, UCB/SEEHRL Report 82-6.

# THEORETICAL AND EXPERIMENTAL STUDIES OF REACTIONS IMPORTANT IN COMBUSTION*

*N.J. Brown, J.A. Miller,† and O.M. Rashed*

Combustion chemistry consists of complex, multistep chain mechanisms involving reactive radicals which are present in small concentrations. The complexity of the mechanisms, the inherent difficulties of working in high-temperature environments, and the large number of species involved with the oxidation of a fuel—all make the study of combustion chemistry quite difficult.

Our current research is concerned with the application of theoretical chemical kinetics to study unimolecular and bimolecular reactions important in combustion processes. We also use modeling techniques to extract mechanistic information for catalytic combustion and to acquire a better understanding of combustion inhibition. The theoretical studies are investigated using classical trajectories with realistic potential energy surfaces. Special emphasis is placed upon elucidating the role of molecular angular momentum on intramolecular and intermolecular energy transfer and reactivity. Recently, we have investigated intermolecular energy transfer important in low-pressure-limit unimolecular kinetics and reactivity in a four-center bimolecular system.

## ACCOMPLISHMENTS DURING FY 1982

With Dr. James A. Miller of Sandia National Laboratory, we have investigated the low-pressure-limit unimolecular dissociation of $HO_2$ resulting from collisions with He. A potential energy surface which accounts for the rare-gas/$HO_2$ interaction has been constructed. The surface with the He atom at infinity is the *ab initio* surface of Melius and Blint[1] that we used in our high-pressure-limit studies.[2] The rare-gas interaction with the three atoms is added to the Melius-Blint surface and is derived from experimental studies of rare-gas scattering. The collisions have been investigated as a function of translational temperature, total molecular internal energy, and total molecular angular momentum. Threshold energy for $HO_2$ is approximately 47 kcal/mol, and our calculations were performed at molecular internal energies between 30 and 46 kcal/mol. At the termination of each trajectory, the energy transferred into each degree of freedom and the angular momentum transferred are calculated. Averages of these quantities are computed for a given set of trajectories characterized by a common translational temperature, internal molecular energy, and distribution of molecular angular momentum. The energy transfer is also separated into up and down portions, which are also averaged for comparison with commonly used theories. Histograms describing the energy transfer distributions and two-dimensional histograms which provide insight into the energy coupling in the molecule were determined for the various sets. Correlation coefficients were also calculated to provide information on the coupling among the three types of energy.

The most remarkable and somewhat disheartening feature of the energy transfer distributions is that they have very long tails. With the loss-and-gain energy transfer mechanisms, these tails account for the slow convergence of the averages in a particular ensemble. A meaningful average for the kinetic, rotational, and vibrational energy transferred requires on the order of 5000 trajectories. A two-dimensional histogram showing the distribution of the rotational and vibrational energy transferred for an ensemble is shown in Fig. 1. Note that the long tails on the distributions are in conflict with the commonly used exponential-gap model of energy transfer.

The effect of increasing the initial kinetic energy on the energy transfer characteristics is to increase the width of the energy distributions. On the average, kinetic energy is gained in sets of collisions characterized by small values of initial molecular angular momentum (less than $10\hbar$). The average vibrational energy transferred in a collision increases with initial molecular angular momentum for a fixed

*This work was supported by the Director, Office of Basic Energy Sciences, Chemical Sciences Division of the U.S. Department of Energy under Contract No. DE-AC03-76SF00098.

†Combustion Research Facility, Sandia National Laboratories, Livermore, California.

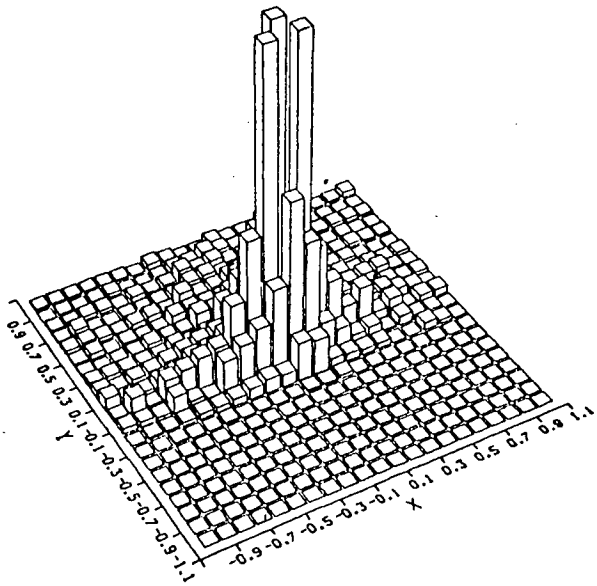


Figure 1. A two-dimensional histogram showing the distribution of energy transferred to the rotational degrees of freedom of $HO_2$ from collisions with He in an ensemble characterized by a temperature of 800 K, 46 kcal/mol initial molecular energy, and initial angular momentum less than $10\hbar$. The Y-axis indicates change in rotational energy while the X-axis indicates the change in the vibrational energy. The ordinate represents the fractional population of the ensemble. (XBL 837-10550)

total energy. Energy transfer mechanisms involve energy transfer among kinetic, rotational, and vibrational degrees of freedom. Average angular momentum changes in the molecule were usually less than three angular momentum units.

We began work on a microcanonical transition theory that includes molecular rotation and tunneling corrections. Reliable saddle-point characteristics are needed to use this theory. We are attempting to explore the limitations of this approach and to elucidate its positive attributes. We will use this formalism to compute rate coefficients for molecules of interest in combustion.

We have made progress with our classical dynamics study of the reaction $H_2 + OH \rightarrow H_2O + H$. This work has as its primary objective the determination of the effect of initial rotational energy on reactivity. The potential energy surface used is the analytical form of Schatz and Elgersma[3] of the *ab initio* Walsh and Dunning[4] surface. In the determination of the integration conditions, we began observing some anomalous trajectories in which a rather long-range orbiting type of behavior was noted as the $H_2$ and OH were moving apart. Further investigation led to the conclusion that there were some long-range wells in the surface that were artifacts of the analytical fit. This was verified by evaluating the potential energy for several geometries when the reactant molecules were at intermediate distances as well as quite far apart. Subsequent work was concerned with evaluating the effect of anomalous potential surface characteristics on the reactive attributes of the system. At high initial kinetic energies, the potential is suitable for use in dynamics studies. The question of lower initial kinetic energies can only be answered by removing these unusual surface properties and thereby generating a surface with the proper asymptotic behavior while retaining the favorable description at close distances. We are currently exploring this approach. We are also investigating methods for computing the product energy distribution.

Papers describing modeling studies of flame inhibition and catalytic combustion have been completed.[5,6] In the flame inhibition study, the combustion environment was treated as a well-stirred reactor. The inhibitors considered were HCl and HBr, and the combustion mixtures were of hydrogen/oxygen/argon in varying equivalence ratios. Inhibition was investigated as a function of pressure, equivalence ratio, and inhibitor concentration. Inhibitor effectiveness was determined by the competition between the radical-scavenging ability of an inhibitor and the exothermicity of the scavenging reactions. For all cases considered, HBr was more effective in scavenging active radicals than HCl. At 0.01 atmospheres, HCl was a more effective inhibitor in lean and stoichiometric mixtures while HBr was more effective for rich mixtures at 0.01 atmospheres and for all atmospheric pressure mixtures. The effectiveness of HBr over HCl is illustrated in Fig. 2, where blowout residence time is plotted as a function of inhibitor concentration.

The high-temperature oxidation of $H_2$ on a platinum catalyst in the presence of excess air has been studied over a range of surface temperatures from 450 to 1070 K and equivalence ratios from 0.05 to 0.20. The experimental system considered was the laminar boundary layer of a heated catalytic plate. Under all conditions considered, the surface reaction rapidly became diffusion-limited downstream of the plate-leading edge. A finite-difference scheme was used to model numerically the flow field above the plate surface. This enabled surface reaction rate data to be obtained under conditions in which surface reaction

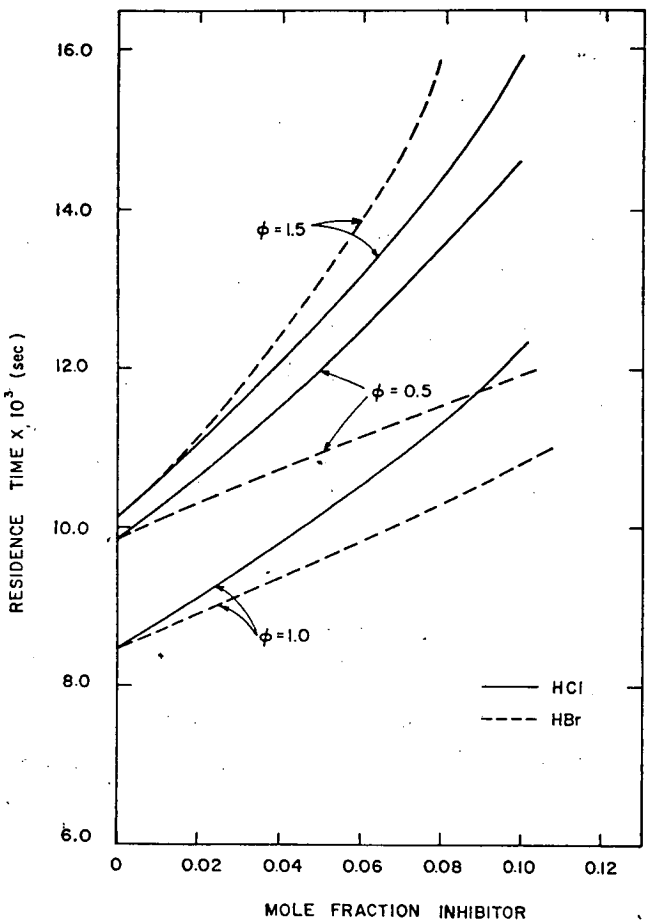


Figure 2. Residence time at blowout (sec) as a function of inhibitor concentration in mole fraction for mixtures at 1.0 atmosphere. Solid lines indicate HCl and dashed lines indicate HBr. (XBL 837-10549)

rates were significantly influenced by transport effects. On the basis of a one-step model for $H_2$ oxidation, the data were found to correlate well with a reaction rate expression of the form

$$R_s = 1.4 \times 10^3 [H_2]_s \exp(-3850/RT) (\mathrm{mol/cm^2 sec})$$

where $R_s$ is the surface reaction rate and $[H_2]_s$ is the $H_2$ concentration at the surface. The surface reaction rate coefficient is plotted as a function of inverse temperature in Fig. 3. The effects of the heat and mass transfer on the kinetics were also investigated.

## PLANNED ACTIVITIES FOR FY 1983

The analysis of the energy transfer of the $He/HO_2$ system will be completed. Derived expressions for energy transfer will be compared with models used to describe low-pressure-limit unimolecular kinetics. The analytical representation of the potential surface

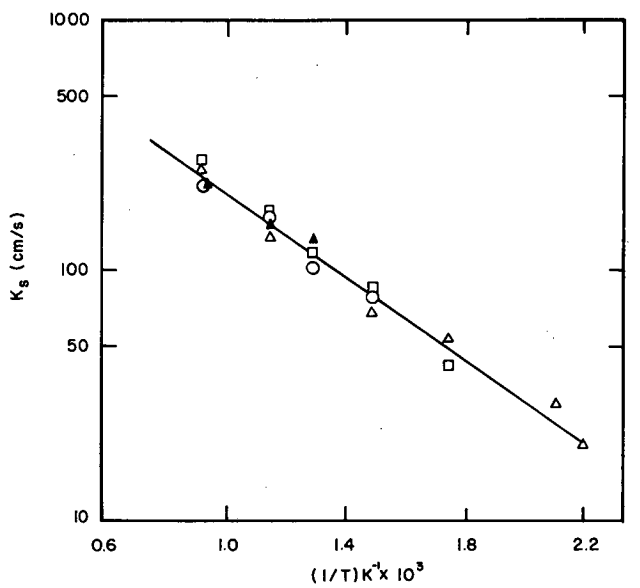


Figure 3. Surface reaction rate coefficient as a function of inverse temperature for $H_2$ combustion on a platinum-coated plate for mixtures of various equivalence ratios. (XBL 832-8284)

for the $H_2/OH$ system will be refitted to give reasonable asymptotic limits, and studies of the bimolecular reaction will continue. Work will begin on the unimolecular kinetics of a four-atom polyatomic molecule. Research will also continue on statistical theories of reactions important in combustion science.

## REFERENCES


1. Melius, C.F. and Blint, R.J. (1979), *Chem. Phys. Lett. 264*, p. 183.
2. Miller, J.A. and Brown, N.J. (1982), "The Dynamics of Unimolecular Dissociation of $HO_2$: Phase Space Sampling, Microcanonical Rate Coefficients and Rotational Effects," *J. Phys. Chem. 86*, p. 772.
3. Schatz, G.C. and Elgersma, H. (1981), *Chem. Phys. Lett. 73*, p. 21.
4. Walsh, S.P. and Dunning, T.H. (1980), *J. Chem. Phys. 72*, p. 1303.
5. Schefer, R.W. and Brown, N.J. (1982), "A Comparative Study of HCl and HBr Combustion Inhibition," *Combustion Sci. Tech., 29*, p. 113.
6. Brown, N.J., Schefer, R.W., and Robben, F. (1983), "High Temperature Oxidation of $H_2$ on a Platinum Catalyst," accepted for publication in *Combustion and Flame*; Lawrence Berkeley Laboratory Report LBL-13744.

# NUMERICAL MODELING OF TURBULENT COMBUSTION*

*A.F. Ghoniem, A.J. Chorin, and A.K. Oppenheim*

Our approach uses the random vortex method to treat turbulent flow fields associated with combustion. Flame fronts are considered as interfaces between reactants and products propagating with the flow and at the same time advancing in the direction normal to themselves at a specified burning speed. Burning speed is associated with the generation of specific volume (the flame front acting, in effect, as the locus of volumetric sources) to account for the expansion of the flow field from the exothermicity of the combustion process. The model was applied to the flow in a channel equipped with a rearward-facing step. The results we obtained revealed the mechanism of formation of large-scale turbulent structures in the wake of the step, as well as the stabilization of the flame on the outer edges of these eddies.[1]

## ACCOMPLISHMENTS DURING FY 1982

We concentrated upon three topics:

(1) Fundamental aspects of the modeling technique.
(2) Application of the model to the formation of a turbulent jet.
(3) Development of an aerodynamic approach to the properties of turbulent flames.

### Fundamental Aspects of Modeling

Three problems have been successfully pursued. The first was to develop the random-element method,[2] an application of the random-walk technique to model diffusion of energy. Instead of vortex sheets and vortex blobs, the method uses heat-transfer sheets, or temperature-jump elements, and blobs of internal energy that carry thermal gradients from heat-conducting walls to the interior of the field, redistributing them by diffusion. The fundamental idea behind random-walk modeling of diffusion is the identity between the Green's function representing the solution of the diffusion equation and the probability density function of a Gaussian random variable with zero mean (see Table 2 in Ref. 3). Preliminary results obtained by this method were presented last year (Fig. 5 in Ref. 3).

The extension of this technique to handle two-dimensional diffusion is presented in Table 1. A one-dimensional approximation close to the walls is employed to implement isothermal boundary conditions, while energy elements are used in the interior to diffuse its energy. Figure 1 compares the temperature profiles along the diagonal of a corner and a square with the corresponding analytical solutions.

The second fundamental problem we solved was the generation of vorticity by the interaction between the pressure field and density gradients—a mechanism important to both flames and buoyancy effects. The motion of the temperature-jump elements, governed by the algorithm of the random-element method, generates elements of vorticity in the interior of the field, while additional elements are generated by the no-slip condition at the walls. Table 2 describes how the random-walk method is used in conjunction with the principle of time splitting to solve the system of equations that describes a natural convection field over a vertical infinite isothermal wall. Figure 2 shows our solution (thick lines) in comparsion to one obtained by a finite-difference technique for two values of the Prandtl number.[4]

The third problem was flame propagation. Our original computations[1] considered the flame as, essentially, a jump in density. Its front was treated, therefore, as an interface propagating as a consequence of advection and self-advancement at a specified normal burning speed. In order to treat flame propagation as the propagation of a reacting surface governed by a chemical reaction proceeding at a finite rate, the problem was recast in terms of a reaction-diffusion equation in temperature. The algorithm of the random-element method was then applied to solve this problem by adjusting the strength of the temperature-jump elements as they move according to the rate of reaction (Table 3). The random-element algorithm was tested by comparing its solution with those of the finite-difference and finite-element methods, demonstrating its capability to calculate flame propagation with proper accuracy. Figure 3 shows the results of numerical computations evaluated for $f(T) = T(1-T)$, when the integration of the reaction part of the equation is done using a first-order Euler scheme in the first case [Fig. 3(a)] and an exact integral in the second case [Fig. 3(b)], both in comparison to the analytical solution.

*This work was supported by NASA on Grant NAS 3-131 and by the Office of Basic Energy Sciences, Division of Engineering Research of the U.S. Department of Energy under Contract No. DE-AC03-76SF00098.

Table 1. A hybrid scheme for representing two-dimensional diffusion in combustion.

| Domain | Boundary ($y < \delta_S$) | Interior ($y > \delta_s$) |
|---|---|---|
| Differential | $\frac{\partial T}{\partial t} = \alpha \frac{\partial^2 T}{\partial y^2}$ | $\frac{\partial T}{\partial t} = \alpha \nabla^2 T$ |
| Boundary condition | $T = 1$ | $T = \delta(y-\delta_S)$ |
| Diffusing element | $\delta T_i$ | $\delta e_i$ |
| Coupling | $\delta e_i = \delta T_i * (y_i - \delta_s)$ | $\partial T_i = \pm \delta e_i / \delta_s$ |
| Stochastic solution | $\mathbf{r}_i(t+\Delta t) = \mathbf{r}_i(t) + \eta_i$ | $\mathbf{r}_i(t+\Delta t) = \mathbf{r}_i(t) + \eta_i$ |
| Sampling | $T = \frac{\Sigma\, \delta e_i}{\delta_s \cdot dx} + \Sigma\, \delta T_i H(y-y_i)$ | $T = \frac{1}{\delta A_i} \Sigma\, \delta e_i\, \delta(\mathbf{r}-\mathbf{r}_i)$ |

Note: $\partial_2 = 2\sigma$, the thickness of the one-dimensional diffusion layer; $\partial A_i$ = area element.

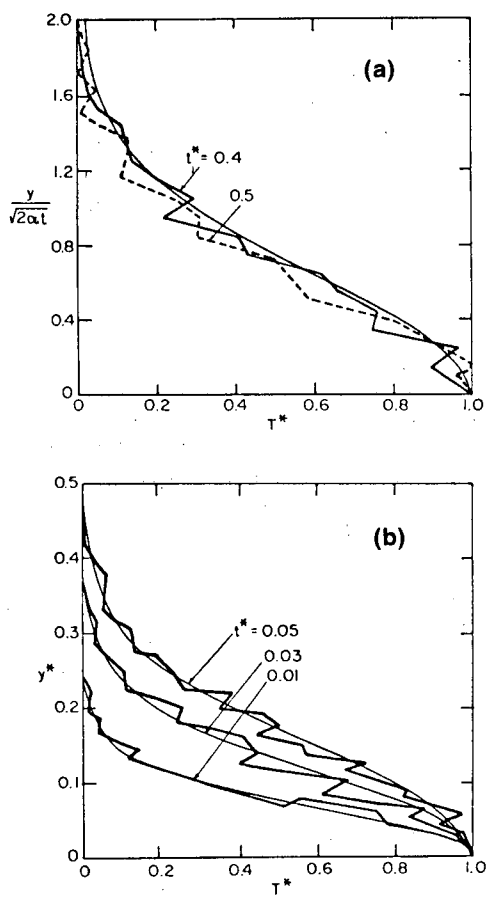


Figure 1. Temperature distribution along the diagonal with two isothermal walls at $T = 1$: (a) for a corner; (b) for a square. (XBL 832-8042)

Table 2. Pressure-density interaction: Random-walk method.

| | |
|---|---|
| Differential equations | $\frac{\partial T}{\partial t} = \alpha \frac{\partial^2 T}{\partial x^2}$ |
| | $\frac{\partial u}{\partial t} = \nu \frac{\partial^2 u}{\partial x^2} + g\beta\,(T - T_\infty)$ |
| Initial conditions | $T = 0;\quad u = 0$ |
| Boundary conditions | $x = 0;\quad T = 1;\quad u = 0$ |
| | $x = \infty;\quad T = 0;\quad u = 0$ |
| Fractional steps | $\frac{\partial T}{\partial t} = \alpha \frac{\partial^2 T}{\partial x^2};\quad \frac{\partial \xi}{\partial t} = \nu \frac{\partial^2 \xi}{\partial x^2}$ |
| | $\frac{\partial \xi}{\partial t} = g\beta \frac{\partial T}{\partial x}$ |
| Vorticity production | $\delta\gamma = g\beta\, \delta T$ |
| | $T = \sum_n \delta T\, H(x-x_i)$ |
| | $\gamma = \sum_N \delta\gamma\, H(x-x_i)$ |
| | $N(t+\Delta t) = N(t) + 2n$ |

Note: $n$ = number of temperature jump elements; $N$ = number of vortex elements.

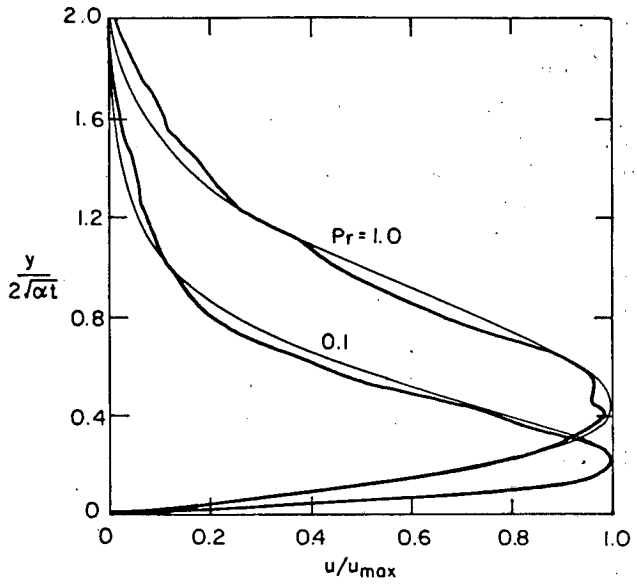


Figure 2. Velocity profiles parallel to a vertical plane set at $T = 1$ in a fluid initially at $T = 0$. (The motion is induced by natural convection.) Thick lines represent our solution (random-element method); thin lines, those of a finite-difference technique. Solutions are for two values of the Prandtl number. (XBL 832-8043)

Table 3. Reaction-diffusion equation.

| | |
|---|---|
| Differential equation | $\frac{\partial T}{\partial t} = \frac{\partial^2 T}{\partial x^2} + f(T)$ |
| Initial condition | $T(x,0) = T_o(x)$ |
| Boundary conditions | $T(+\infty,0) = 0; \quad T(-\infty,0) = 1$ |
| Solution: | |
| Fractional steps | $T(n\Delta t) = [R(\Delta t)\, D(\Delta t)]^n\, T_o$ |
| Reaction | $\frac{dT}{dt} = f(T)$ |
| Diffusion | $\frac{\partial T}{\partial t} = \frac{\partial_2 T}{\partial x^2}$ |
| Deterministic result | $\delta T_i(t + \Delta t) = \delta T_i(t) + f(T_i)\Delta t$ |
| Stochastic result | $T = \Sigma\, \delta T_i\, H(x - x_i)$ |
| | $x_i(t + \Delta t) = x_i(t) + \eta_i$ |
| | $E[\eta] = 0; \quad E[\eta^2] = 2\Delta t$ |

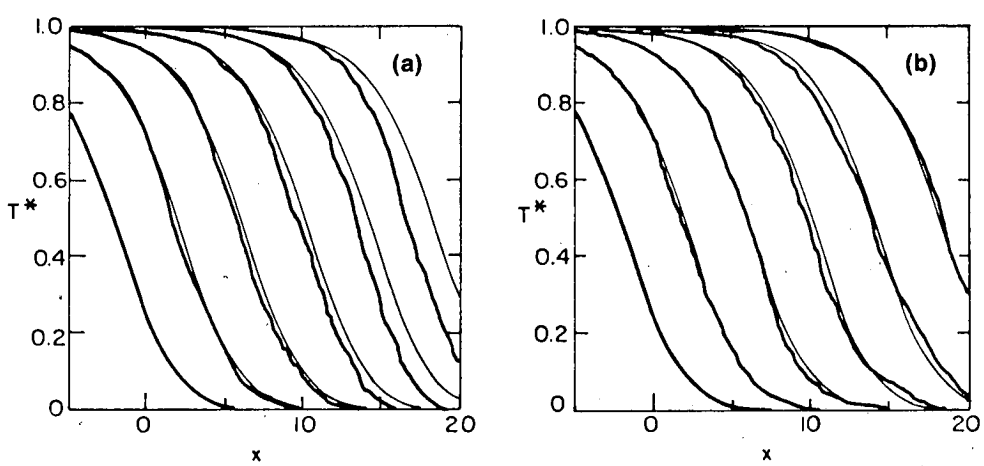


Figure 3. Temperature profiles in a flame described by a single reaction-diffusion equation: (a) integration of the reaction equation performed by the use of a first-order Euler scheme; (b) numerical solution obtained using exact solution of the reaction equation. Thin curves represent the analytical solution. (XBL 832-8044)

## Application to Turbulent-Jet Formation

The random-vortex method was applied to the problem of the formation of a planar, two-dimensional turbulent jet at high Reynolds numbers. Figure 3 in Ref. 5 describes the elementary processes of the random vortex method and their implementation to solve the convection-diffusion equation. The results, expressed in terms of the development of the vorticity field, are presented in Fig. 4. They reveal the formation of large-scale turbulent eddy structures on both sides of the jet with a potential core inside. A few jet widths downstream, the two layers start to interact, and the flow becomes dominated by the pairing of eddies on both sides. The turbulent eddies grow by entraining the nonturbulent fluid, while, as a result of the interaction between positive and negative vorticity, their trajectories become more and more convoluted. These pictures display a remarkable resemblence to experimental photographs obtained by Dimotakis et al.[6] across the plane of symmetry of an axisymmetric jet.

## Aerodynamic Theory

Our numerical modeling studies, supported by experimental observations of turbulent flames, lead to our third topic, the development of an aerodynamic theory of turbulent flame propagation. The theory is based on the concept that the flow field is dominated by a large-scale eddy structure, while the flame front is established at the outer contours of the eddies and acts as a semi-permeable membrane around the burnt gas. We are now studying[7] the aerodynamic patterns produced by the interaction between these eddies and the expansion due to the exothermic effects of the combustion process.

# PLANNED ACTIVITIES FOR FY 1983

The next phase of our work will be concerned primarily with applications of the random-walk methods we developed to a variety of problems in turbulent flow and combustion. This effort will be enhanced

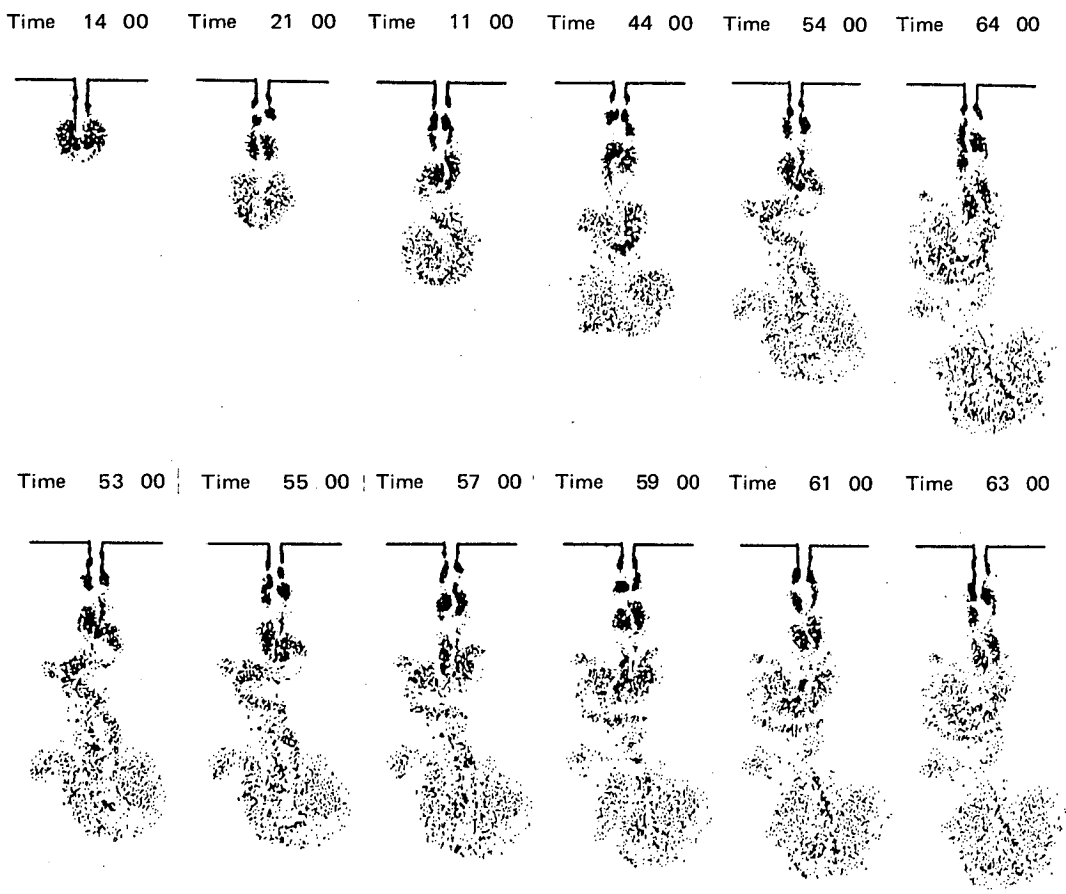


Figure 4. Sequential series of computer plots of vortex fields in a turbulent jet at a Reynolds number Re = $10^4$.
(XBL 832-8045)

significantly by arrangements to use the Cray computer at the NASA-Ames Research Center.

Of the particular problems we plan to treat, the most prominent are the following:

(1) Inflammation (i.e., the spreading of the flame front in a flow field) of a turbulent jet.
(2) Inflammation of turbulent flow in a channel.
(3) Response of the turbulent combustion system in a channel behind rear-facing steps of various aspect ratios (ratios of step height to channel width) to an increase in the exothermicity of the combustible mixture (corresponding to an increase in the fuel/air ratio); the results should provide specific information on the mechanism of flashback.
(4) Behavior of flames governed by a given reaction-rate law in a two-dimensional flow system.

Concomitantly to numerical modeling, we intend to pursue analytic studies of the rudimentary aerodynamic components of turbulent flames along the lines specified at the end of the last section, i.e., the interaction between eddies and exothermic expansion.

## REFERENCES


1. Ghoniem, A.F., Chorin, A.J., and Oppenheim, A.K. (1982), "Numerical Modeling of Turbulent Flow in a Combustion Tunnel," *Phil. Trans. Roy. Soc. Lond. A304*, p. 303.
2. Ghoniem, A.F., and Oppenheim, A.K. (1982), "Random Element Method for Numerical Modeling of Diffusional Processes," in *Eighth International Conference on Numerical Methods in Fluid Dynamics*, Aachen, W. Germany, June 1982, p. 224.
3. Chorin, A.J., Ghoniem, A.F., and Oppenheim, A.K. (1982), "Numerical Modeling of Turbulent Combustion," *Energy and Environment Division Annual Report FY 1981*, p. 4-93.
4. Ghoniem, A.F., and Sherman, F. (1983), "Random Walk Simulation of Diffusion Processes," *J. Comp. Phys.* (in press).
5. Ghoniem, A.F., and Oppenheim, A.K. (1983), "Solution of the Problem of Flame Propagation by the Use of the Random Element Method," presented at the American Institute of Aeronautics and Astronautics 21st Aerospace Sciences Meeting, AIAA Paper No. 83-0600, Reno, Nevada, January 1983.
6. Dimotakis, P.E., Miake-Lye, R.C., and Papantonic, D.A. (1982), "Structure and Dynamics of Round Turbulent Jets," California Institute of Technology Graduate Aeronautical Laboratories, Pasadena, California GALCIT Report FM82-01.
7. Oppenheim, A.K., and Ghoniem, A.F. (1983), "Aerodynamic Features of Turbulent Flames," presented at the American Institute of Aeronautics and Astronautics 21st Aerospace Sciences Meeting, AIAA Paper No. 83-0470, Reno, Nevada, January 1983.


## CONTROLLED COMBUSTION*


*N.J. Brown, C.D. Carter, K. Hom, F.C. Hurlbut, D. Lucas, A.K. Oppenheim, R.B. Peterson, R.F. Sawyer, and H.E. Stewart*


The principal objective of this project is to acquire fundamental knowledge for the development of controlled combustion systems. For power plant and internal combustion engine technologies, such systems offer the prospect of simultaneously maximizing thermal energy conversion efficiency, minimizing pollutant emissions, and optimizing the tolerance to a wide variety of fuels. Of key significance in this respect is the establishment of as homogeneous a combustion process as possible in a lean, gaseous air-fuel mixture—a process that is associated with a distributed, multipoint initiation. A thorough understanding of ignition—the initiation of the self-sustained exothermic process of combustion—is thus essential, and the primary emphasis is therefore placed on an experimental study of the fundamental features of ignition. Using as the test media an assortment of lean gaseous mixtures, ranging from noble gas-diluted hydrogen-oxygen to relatively heavy hydrocarbon vapor-air, all contained in a closed vessel, we employ a variety of ignition methods, including flash photolysis, electric spark discharge, plasma jets, and jets of incomplete combustion products.


*This work was supported by Assistant Secretary for Conservation and Renewable Energy, Office of Transportation Programs, Division of Transportation Energy of the U.S. Department of Energy under Contract No. DE-AC03-76SF00098.

The major objective of the experimental program is to determine the particular role played in ignition by active radicals. Consequently, the most important measurement is concerned with their concentration histories. This measurement is accomplished with a high-frequency-response molecular-beam mass spectrometer that has been designed and built especially for this purpose. The results will be interpreted by a thermochemical analysis that follows the theoretical concepts of Semenov[1] and Frank-Kamenetskii[2] for the rationalization of the transient process of ignition in a closed system. This is supplemented by numerical modeling of flame propagation in turbulent flow, carried out by the use of the random-walk methods we have developed in collaboration with their originator, Professor A. Chorin of the University of California, who is actively participating with us in this endeavor.

The operating characteristics of the molecular-beam mass spectrometer have proven most satisfactory after its relocation from the UC Berkeley campus to LBL, and the experimental testing program is in progress, with flash photolysis of $NO_2$ used to ignite a helium-diluted hydrogen-oxygen mixture. In the concomitant analytical studies, we have been able to deduce the classical ignition limits by appropriate scaling of the thermal relaxation time. The technique we developed for numerical modeling of combustion in a turbulent flow system has recently been published in *Philosophical Transactions of the Royal Society*.

## ACCOMPLISHMENTS DURING FY 1982

Our work last year consisted of the development of the theoretical as well as experimental methods of approach. The first was concerned with the fundamental aspects of the thermochemistry of ignition; the second, with a molecular-beam mass spectroscopy of sufficiently high resolution and frequency response to record the variation of active radicals that appear in extremely low concentrations over a submillisecond of time. Progress made in both endeavors is reported here in turn.

### Thermochemistry

To formulate the analytical features of ignition, it is sufficient to consider a thermodynamically closed, homogeneous chemical system surrounded by a compressible medium that may absorb the work of expansion and act as a heat sink. The basic theory of this process has been formulated by Semenov[1] and Frank-Kamenetskii,[2] and some of its analytical features have been included in the recently published textbook of Zeldovich et al.[3] Its essential properties with respect to the case of photoignition have been exposed by Gray and Yang,[4] while the more general case of a thermochemical process has been treated by Guirguis et al.[5] The salient features of this approach have been described in the 1980 Annual Report.[6] A brief rendition is as follows.

The dynamic behavior of the system in the course of ignition can be described by reaction rate expressions, which specify the speed with which molecular species are transformed by chemical reaction, and by the energy conservation equation, including the effect of losses to surroundings.

The solution is expressed in terms of integral curves on a multidimensional phase-space whose coordinates are the temperature and concentrations of all the chemical species participating in the reaction. The results provide a sharp definition for "ignition temperature"—a threshold between ignition and extinction which, for a given chemical system, is a function of the thermal relaxation time (the time constant of temperature decay due to heat transfer losses).

The results we obtained on this basis for the hydrogen-oxygen system are in remarkably good agreement with the classical auto-ignition limits (usually referred to in the literature by the misnomer "explosion limits").

This is in drastic contrast to the views expressed so far in the literature, where each segment has been credited to different effects: the so-called "first explosion limit" at low pressures was believed to be due to quenching by wall effects; the "second explosion limit" at intermediate pressure to the direct effects of chain branching; and the "third explosion limit" to the effects of heat conduction.[7] Thus, getting all three as a consequence of one comprehensive theory is indeed quite an accomplishment.

We are provided, moreover, with a satisfactory demonstration of the physical validity of our relatively simple method of approach and a proof that the *a priori* artificial assumption of a constant relaxation time is in fact quite realistic. Encouraged with these results, we are now ready to tackle the more practical case of heavier hydrocarbon-air mixtures for which there is as yet just a modicum of chemical kinetic-rate data available.

## Molecular Beam Mass Spectrometer

This apparatus has been relocated from the UC Berkeley campus to Building 70 of LBL. The move was associated with a number of modifications, as a consequence of which the performance of the system has been significantly improved. Most prominent among them are the following (see Fig. 1):

(1) The beam path was shortened to ~30 cm by the installation of a completely redesigned skimmer support and cone.

(2) A new source nozzle permitting sustained operation at high temperatures and elevated pressures was designed and fabricated.

(3) Pumping capacity was increased by the installation of a 10-inch diffusion pump in the first stage and a 6-inch closed-cycle cryopump in the third stage. The first pump makes it possible to have a source nozzle as large as 0.018 cm in diameter while maintaining a pressure of $\sim 4 \times 10^{-4}$ Torr in the first stage with an atmospheric pressure in the test space. The second greatly reduces the background noise.

(4) A new chopper/trigger pulse system was built to eliminate fluctuations we encountered earlier; these were due to speed variation and mechanical imperfections in the original setup.

(5) The signal train of the quadrupole was ameliorated by a suitable modification of the electronic circuit.

(6) Test cells for photolysis-induced ignition experiments using high-power flash tubes were designed and constructed—one for molecular-beam sampling, and another for a separate operation using standard measuring techniques and optical diagnostics, such as high-speed schlieren cinematography.

The remodeled apparatus was then subjected to the following performance tests:

(1) Examination of the properties of the molecular beam under the influence of the distance between the source and the nozzle and the alignment of the source cone. A Mach number of ~10 was routinely achieved for air beams at atmospheric pressure and room temperature.

(2) Observation of major effects of ignition in a mixture of $H_2/O_2/NO_2/Ar$ initiated by flash photolysis, particularly the variation of pressure and the time-of-flight signal due to the change of state of inert diluent. This is illustrated by Fig. 2, presenting the pressure transducer and the argon quadrupole signals recorded by our high-speed multichannel analog/digital converter in a 3/61/20 mixture of the constituents specified above at an initial pressure of 0.4 atm.

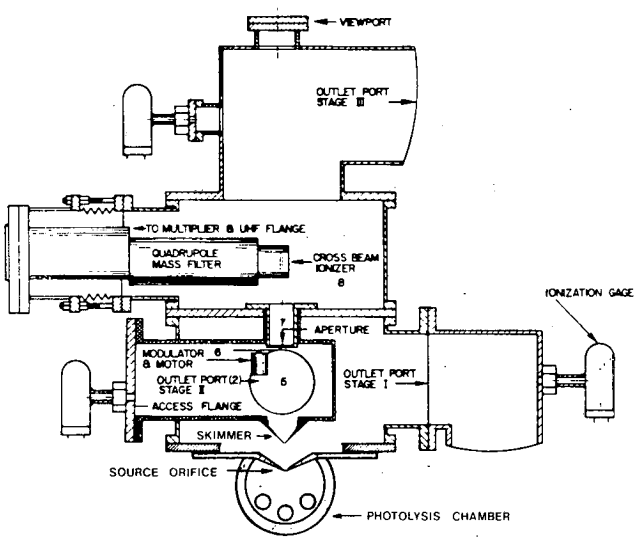


Figure 1. Molecular-beam mass spectrometer system.
(XBL 831-7596)

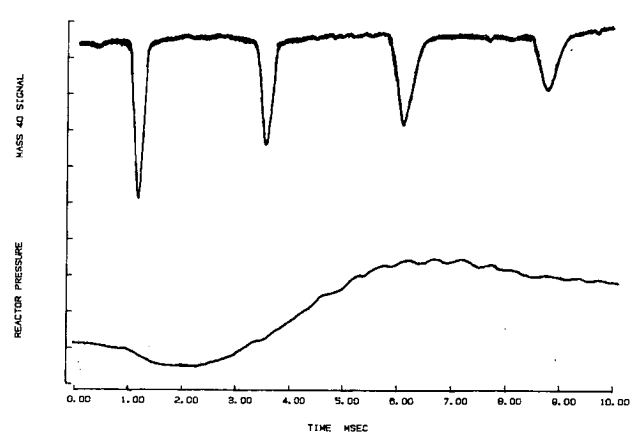


Figure 2. Argon signal (mass 40) and pressure transducer record in the course of flash photolysis of $Ar/H_2/O_2/NO_2$ mixture at 0.4 atm pressure and room temperature.
(XBL 831-7597)

(3) Investigation of the effects of rapidly varying pressure and temperature on the quadrupole signal—a necessary prerequisite for the measurement of composition changes using the mass spectrometer, so that such effects could be eliminated. Whereas the influence of pressure has been studied previously,[9] the effects of temperature have so far been unexplored. The pressure effects we observed are in good agreement with previous studies.[10] Some of the results we obtained with different source temperatures are displayed in Fig. 3. The record presents signals of an Ar beam at two source temperatures, 300 K and 900 K, with atmospheric pressure maintained in both cases. The higher temperature beam arrives at the detector sooner and has a different width. The signals were normalized by their amplitudes, hence their peak values are the same.

To facilitate the interpretation of data provided by the time-of-flight signals, a computer program was developed to calculate the expected beam performance. Its results are used to fit arrival times and Mach numbers to those measured experimentally. Preliminary tests indicate that sampling from a homogeneous mixture is not ideal, as evidenced by alterations in arrival times due to admixing of cooler gas coming from the boundary layer at the wall of the nozzle. This effect evidently has to be taken into account in concentration measurements.

In analyzing the effects of beam chopping during a transient event, we have found that it should be possible to attain a time resolution of ~100 microseconds in the course of combustion, when the gas temperature is in excess of 1700 K. This directly contradicts recently published estimates[11] that suggested time resolution might be drastically reduced at typical hydrocarbon-air flame temperatures.

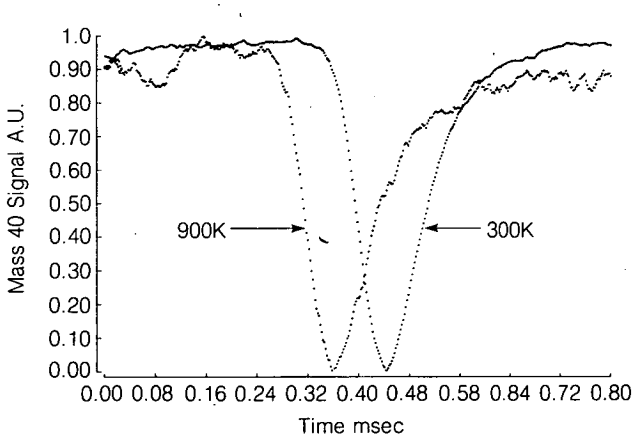


Figure 3. Time-of-flight signal of argon beam at 300 and 900 K. (XBL 831-7598)

## PLANNED ACTIVITIES FOR FY 1983

Our objectives for the next phase of these studies will be to:

(1) Apply our theory of ignition to hydrocarbon-air mixtures.

(2) Measure concentration history of chemical species participating in the photolytic ignition of $H_2/O_2/NO_2/Ar$ mixtures, and the concomitant physical properties of the reacting medium contained in the test cell.

## REFERENCES


1. Semenov, N.N. (1943), "On Types of Kinetic Curves in Chain Reactions. I. Laws of the Autocatalytic Type," *Comptes Rendus (Doklady) de l'Academie des Sciences de l'URSS 43*(8), p. 342; (1944), "On Types of Kinetic Curves in Chain Reactions. II. Consideration of the Interaction of Active Particles," *Comptes Rendus 44*(2), p. 62; "On types of Kinetic Curves in Chain Reactions. Allowance for Chain Rupture on Walls of Reaction Vessel in the Case of Oxidation of Hydrogen," *Comptes Rendus 44*(6), p. 241; (1958, 1959), *Some Problems in Chemical Kinetics and Reactivity*, M. Boudart, translator, Princeton University Press, Princeton (2 vols.).
2. Frank-Kamenetskii, D.A. (1947, transl. 1955), *Diffusion and Heat Exchange in Chemical Kinetics*, N. Thon, translator, Princeton University Press, Princeton, New Jersey.
3. Zeldovich, Ya.B., Barenblatt, G.I., Librovich, V.B., and Machviladze, G.M. (1980), *Mathematical Theory of Combustion and Explosion*, Izdvatelstvo "Nauka," Moscow.
4. Gray, B.F., and Yang, C.H. (1965), "On the Unification of the Thermal and Chain Theories of Explosion Limits," *J. Phys. Chem. 69*(8), p. 2747; Yang, C.H., and Gray, B.F. (1967), "The Determination of Explosion Limits from a Unified Thermal and Chain Theory," in *Eleventh Sympo-*

*sium (International) on Combustion,* p. 1099, The Combustion Institute, Pittsburgh, Pennsylvania.

5. Guirguis, R.H., Oppenheim, A.K., Karasalo, I., and Creighton, J.R., (1981), "Thermochemistry of Methane Ignition," *Prog. Astronaut. and Aeronaut. 76*, p. 134.
6. Oppenheim, A.K., Hurlbut, F.C., and Robben, F. (1980), "Ignition Studies," *Energy and Environment Division Annual Report 1979,* p. 6-5, Lawrence Berkeley Laboratory Report LBL-11650.
7. Gear, C.W. (1971), *Numerical Initial Value Problems in Ordinary Differential Equations,* Prentice-Hall, Inc., Englewood Cliffs, New Jersey.
8. Lewis, B. and von Elbe, G. (1961), *Combustion, Flames and Explosions of Gases*, p. 22–70, Academic Press, Inc., New York and London.
9. Young, W.S., Rodgers, W.E., Cullian, C.A., and Knuth, E.L. (1971), "Supersonic Molecular Beams with Cycling-Pressure Sources," *AIAA Journal 9*, p. 2.
10. Bossel, U. (1968), *Investigation of Skimmer Interaction Influences on the Production of Aerodynamically Intensified Molecular Beams*, Ph.D. Thesis, University of California, Berkeley.
11. Sloane, T.M., and Ratcliffe, J.W. (1982), *Time Resolved Mass Spectrometry of a Propagating Methane-Oxygen-Argon Flame,* Western States Section/The Combustion Institute, Paper No. 82-48.

## HEAT AND MASS TRANSFER WITH COMBUSTION*

*R. Greif, J. Woodard, S. Vosen, and C. Yen*

A major goal of this research has been the experimental and theoretical determination of the variation over time in the heat and mass fluxes during compression and combustion. This is not only of considerable practical importance, but also of fundamental interest since it is anticipated that these results will elucidate basic aspects of combustion phenomena.

Previously, measurements were carried out in a single-pulse, compression-expansion apparatus built to study reciprocating engine processes under well-controlled laboratory conditions simulating the operation of a spark-ignition engine.[1] Completed studies in the apparatus have included the experimental and theoretical determination of the unsteady wall heat transfer in nonreacting gases during piston compression.[2,3]

That work has been extended to include reacting gases. In view of the complex nature of piston compression processes, it was decided to first carry out measurements during combustion in a shock tube in the end-wall region behind the reflected shock wave.[4,5] This is desirable because, during the pre-ignition period, the free-stream temperature and pressure are constant, and the phenomena during this period are well understood. When ignition occurs, the effects of combustion are clearly displayed, providing a useful basis for appraisal.[4,5]

Here we report on heat and mass transfer studies of reacting gases. This work was conducted in conjunction with flame-propagation studies in two constant-volume cells. The experiments were performed in a new facility constructed for this purpose.

### ACCOMPLISHMENTS DURING FY 1982

Pressures, wall temperatures, and schlieren films were obtained simultaneously for a series of combustion processes in which premixed methane and air reacted in a constant-volume chamber.[6] From these data, the temporal variation of the flame speed and the wall heat flux were determined. This portion of the research was carried out in collaboration with Professor R. F. Sawyer and D. Hirvo.[7,8] Data were obtained for equivalence ratios varying from 1.1 to 0.6. The experiments were carried out in a single-pulse compression-expansion apparatus which permitted full optical access to the phenomena.[1] In these experiments, the piston was fully withdrawn so that the test section served as a constant-volume system. The results indicate that side-wall interactions affect flame speed. The wall heat-flux data show that heat transfer varied with distance from the flame; they also show a strong sensitivity to the equivalence ratio. Specifically, for an equivalence ratio of 0.6, the upper wall (at locations far from ignition) reaches a maximum heat flux at significantly later times than the

*This work was supported by the Assistant Secretary for Conservation and Renewable Energy, Office of Transportation Programs, Division of Transportation Energy Conservation of the U.S. Department of Energy under Contract No. DE-AC03-76SF00098.

bottom wall. This is due to the more horizontal orientation of the flame at this equivalence ratio, which is attributed to the effect of buoyancy.[8]

Tests have also been carried out in a new test cell designed and constructed under the supervision of Professor A. K. Oppenheim. The test cell has the approximate shape of two bisecting 9 inch cylinders, 3-1/2 inches in diameter. Optical measurements may be made through 1-1/4 inch quartz windows that lie along the axis of one of the cylinders. Other instrumentation may be mounted through end ports at the ends of the second axis. Four additional ports provide access for a pressure transducer, and a spark plug, an inlet for the combustible gas mixture, and an outlet for the burnt gases. Some tests have been carried out for a methane-air flame encountering a cold, impermeable end wall. Pressures, wall temperatures, and schlieren films have been obtained for these runs. The wall heat flux has also been determined for several conditions.

Preliminary predictions of the unsteady wall heat fluxes have been made by C. Westbrook of the Lawrence Livermore National Laboratory, using the computer program HCT.[9] These calculations show trends very similar to the data. Further work is needed to extend the calculations to conditions corresponding to the test cases.

## PLANNED ACTIVITIES FOR FY 1983

Additional experiments will be carried out in the new test cell over a range of pressures and equivalence ratios. Predictions of the wall heat fluxes and the species distributions will also be made, using extended versions of the HCT code. In addition, results will also be obtained on the basis of integral, quasi-steady, and numerical methods. The planned comparison of the theoretical predictions with the data should elucidate fundamental aspects of combustion phenomena. It is also planned to carry out measurements and calculations for reacting gases during piston compression.

## REFERENCES


1. Oppenheim, A.K., et al. (1976), "A Cinematographic Study of Combustion in an Enclosure Fitted with a Reciprocating Piston," in *Stratified Charge Engines*, Institute of Mechanical Engineers Conference Publication 1976-11, p. 127.
2. Nikanjam, M., and Greif, R., (1978), "Heat Transfer During Piston Compression," *J. Heat Transfer*, 100, p. 527.
3. Greif, R., Namba, T., and Nikanjam, M. (1979), "Heat Transfer During Piston Compression Including Side Wall and Convection Effects," *Int. J. Heat Mass Transfer, 22*, p. 901.
4. Heperkan, H.A. (1980), "An Experimental and Theoretical Study of Heat Transfer with Combustion," Ph.D. Dissertation, University of California, Berkeley; Lawrence Berkeley Laboratory Report LBL-10868.
5. Heperkan, H., and Greif, R. (1982), "Heat Transfer During the Shock-Induced Ignition of an Explosive Gas," *Int. J. Heat Mass Transfer 25*, p. 267.
6. Woodard, J. B. (1982), "An Experimental and Theoretical Study of Heat Transfer in Constant Volume and Compression-Expansion Systems Including the Effects of Flame Propagation," Ph.D. Dissertation, University of California, Berkeley; Lawrence Berkeley Laboratory Report LBL-14097.
7. Woodard, J.B, Hirvo, D.H., Greif, R., and Sawyer, R.F. (1981), "Wall Heat Transfer and Flame Propagation in a Constant Volume Duct," presented at the Western States Section/The Combustion Institute Fall Meeting, October 19–20, 1981, Tempe, Arizona; Lawrence Berkeley Laboratory Report LBL–13021.
8. Woodard, J.B., Hirvo, D.H., Greif, R., and Sawyer, R.F. (1982), *Flame Propagation, Wall Heat Transfer, and Their Interaction in Lean Premixed Gases*, Lawrence Berkeley Laboratory Report LBL-13950.
9. Westbrook, C.K. Lawrence Livermore National Laboratory, personal communication.
10. Vosen, S. (1983), *Unsteady Heat Transfer During the Interaction of a Laminar Flame with a Cold Wall*, Ph.D. Dissertation, University of California, Berkeley.

## FLAME PROPAGATION*

*D. Dunn-Rankin and R.F. Sawyer*

Operation of internal combustion engines under lean conditions offers the possibility of improved efficiency and reduced emissions. The difficulties associated with lean combustion include reduced flame-propagation speed and flame quenching. This fundamental study of flame propagation under internal combustion conditions is directed at understanding and solving these difficulties.

### ACCOMPLISHMENTS DURING FY 1982

A study of approximately two-dimensional flame propagation in a constant-volume enclosure was conducted. The chamber had a square cross section (38 × 38 mm) and variable length. A line ignition source was used to produce a nearly two-dimensional flame. Simultaneous records of pressure versus time and flame position versus time allowed calculation of both flame speed and rate of reactant consumption. Flame shape and flame location were determined from high-speed schlieren cinematographic records.

Two fuels were used in the study. First, the effect of equivalence ratio on ethylene/air flame propagation was explored. This extended the previous work of Woodard et al.[1] to a new fuel. Second, the effect of chamber length on methane/air flames of unity equivalence ratio was investigated.

Ethylene/air flames demonstrated similar shape development to methane/air flames despite their differing flame speeds (Fig. 1). Duct length greatly influenced flame shape development (Fig. 2). Lean-mixture flame speeds were considerably lower than stoichiometric-mixture flame speeds (Fig. 3). The rate of reactant consumption provided a more reliable measure of flame behavior than did the flame speed when wall effects were significant.

### PLANNED ACTIVITIES FOR FY 1983

The flame propagation study will be extended to a compression-expansion environment. The focus will be on lean flame behavior. Provision will be made for laser sheet access through the igniter port. This will allow flow visualization of the unburned gas and definitive location of the flame front.

*This work was supported by the Assistant Secretary for Conservation and Renewable Energy, Office of Transportation Programs, Division of Transportation Energy of the U.S. Department of Energy under Contract No. DE-AC03-76SF00098.

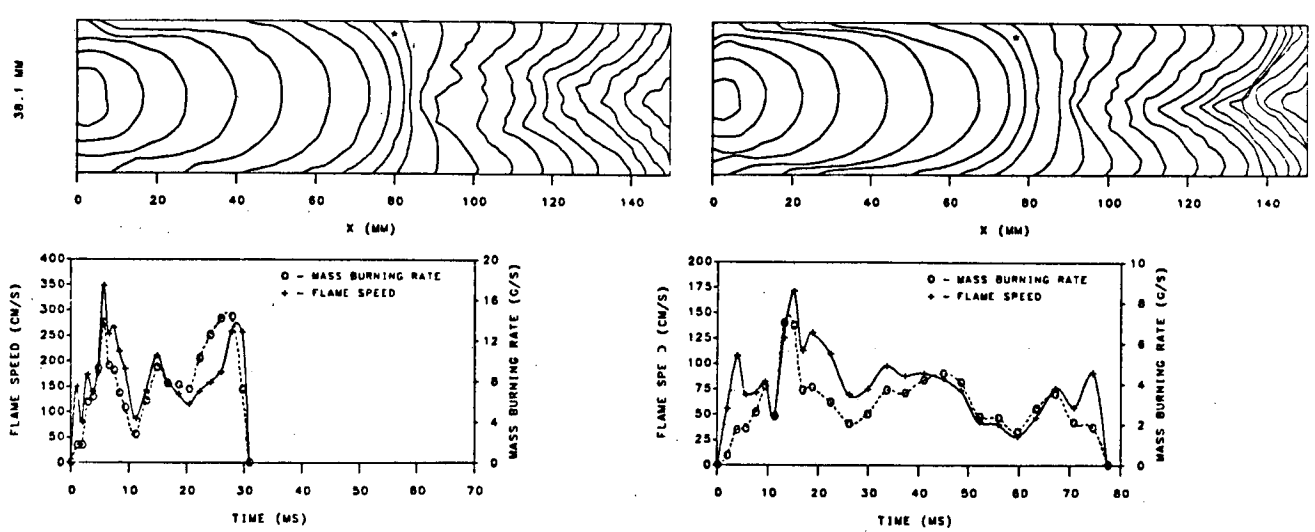


Figure 1. Comparison between ethylene/air (left) and methane/air (right) flame propagation in a constant-volume duct. Upper portions show flame shapes. (XBL 837-10551)

REFERENCE

1. Woodard, J.B., Hirvo, D.H., Greif, R., and Sawyer, R.F. (1981), "Wall Heat Transfer and Flame Propagation in a Constant Volume Duct," Western States Section/The Combustion Institute Paper No. 81-51 and Lawrence Berkeley Laboratory Report LBL-13021.


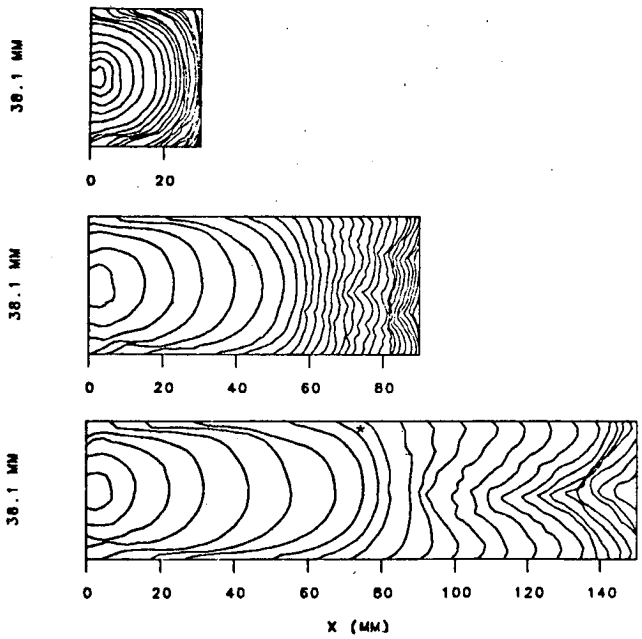


Figure 2. Flame shape in ducts of different length, for a methane/air flame; equivalence ratio is 1.0.
(XBL 837-10552)

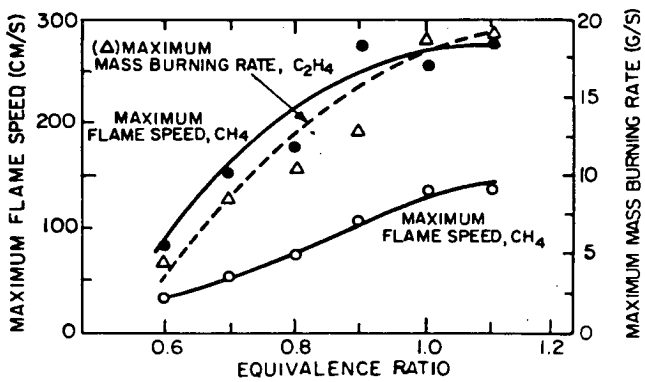


Figure 3. Effect of equivalence ratio on maximum flame speed.
(XBL 837-10553)

# MEASUREMENT OF COMBUSTION-GENERATED POLLUTANT SPECIES*


*N.J. Brown, E. Cuellar, and D. Lucas*


Developing analytical techniques and demonstrating their suitability for characterizing combustion emissions is a crucial step in the sequence leading to source emission inventories and assessments of their health effects. Reliable measurement techniques are also needed to understand the mechanisms of pollutant formation and destruction.

Measuring such emissions and understanding their chemistry present particularly difficult analytical problems because of the high temperatures and ambient pressures of combustion processes. Many species are present, and the chemistry of pollutant formation and destruction mechanisms is multistep and frequently dominated by radical species which occur in low concentrations.

Our research is directed toward the development and characterization of techniques to quantify pollutant emissions from combustion systems utilizing synfuels. Emphasis is placed upon the measurement of nitrogen- and sulfur-containing species as well as gas-phase hydrocarbon species which are precursors to soot formation. Measurements of pollutant species are made in premixed laminar flames and in a turbulent-flow reactor in which the well-characterized combustion of prototype synthetic fuels occurs.

We are interested in the development and application of a novel optical absorption technique called tunable atomic line molecular spectroscopy (TALMS) for the measurement of pollutant species in combustion systems. This technique was pioneered at the Lawrence Berkeley Laboratory by Dr. Tetsuo Hadeishi and his co-workers and has been used in the analytical determination of atomic species and small molecules exhibiting sharp rotational electronic structure. The technique is based upon the Zeeman effect and is highly sensitive and selective. A detailed description of TALMS was presented in our earlier work,[4,5] and a summary will be presented below. We have completed a comparative study of nitric oxide measurement in the post-combustion environment of atmospheric pressure, premixed


*This research was supported by the Director, Office of Energy Research, Office of Health and Environmental Research of the U.S. Department of Energy under Contract No. DE-AC03-76SF00098.

methane-air stoichiometric flames. One of the analytical techniques used is sample extraction with uncooled quartz microprobes, followed by chemiluminescent analysis in a specially constructed analyzer; the other technique is TALMS.

## ACCOMPLISHMENTS DURING FY 1982

A schematic diagram of the experimental system is shown in Fig. 1. Methane-air flames were stabilized at atmospheric pressure on a water-cooled, porous-plug, flat-flame burner. The burner was mounted below the optical path of the TALM spectrometer through an opening in the optical bench. A micrometer-driven X–Y–Z translation stage permitted the burner to be moved with respect to the fixed optical beam. Stable methane-air flames were obtained over a wide range of equivalence ratios and total gas flows. We operated the burner at a total flow of 30,000 sccm, corresponding to a linear velocity of 17.7 cm/sec. Stable flames, at this flow, could be obtained at equivalence ratios ranging from 0.75 to 1.5. Radial and axial temperature profiles were measured in the flame with Pt/Pt–13% Rh thermocouples; radial profiles indicated the one-dimensional nature of the flame, and axial profiles indicated the location of the post-combustion zone.

Gas samples were withdrawn from the flame through a 10-cm long, 1-mm i.d. uncooled quartz probe with an orifice diameter of 314 microns. The probe was mounted on the adjustable stage. A heated Teflon line connected the probe to a valve at the rear of a laboratory-built chemiluminescent gas analyzer (CLA) which measured nitrogen oxides (NO and $NO_x$). This analyzer is similar to commercially available instruments but incorporates several features that significantly reduce the corrections needed for viscosity and third-body quenching effects. The response of the CLA was measured and found to be linear in NO concentrations to at least 6000 ppm NO.

Koizumi et al[6] have employed TALMS to determine low concentrations of NO in a room-temperature absorption cell with high selectivity and sensitivity, using the accidental near-coincidence between the Cd-ion line at 124.438 nm and a discrete rotational-vibrational line in the $A^2\Sigma^+ - X^2\pi$, $\gamma$ bands of NO. The basis for detection of molecules by tunable atomic line molecular spectroscopy is the splitting and polarization of atomic emission lines by an external magnetic field. By varying the strength of the

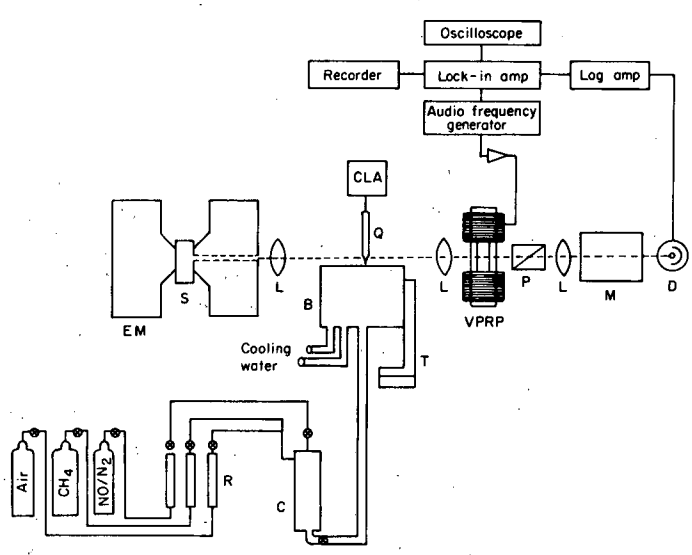


Figure 1. Schematic diagram of the experimental apparatus: *EM*, electromagnet; *S*, atomic light source; *L*, quartz lens; *B*, porous plug burner; *T*, X–Y–Z translation stage; *Q*, uncooled quartz probe; CLA, chemiluminescent gas analyzer; *VPRP*, variable phase retardation plate; *M*, monochromator; *D*, photomultiplier tube; *C*, mixing chamber; *R*, rotameters. (XBL 822-4489)

magnetic field, one of the Zeeman components of the Cd emission lines is tuned into exact coincidence with a discrete rotational-vibrational line of NO. The matching Zeeman component indicates the extent of absorption by NO, while the unmatched component indicates background absorption only. A differential measurement of the matched and unmatched Zeeman components of the Cd emission line provides a quantitative measurement of the NO in the optical path.

The TALM spectrometer is shown schematically in Fig. 1. The lamp consists of a sealed-off quartz U-tube containing a small amount of cadmium metal (natural-abundance Cd) and an inert buffer gas. Nichrome wire heaters wrapped around the U-tube heat the lamp to a few hundred degrees Celsius and provide a small amount of vaporized Cd (~1 torr), which is excited by an electric discharge through the gas. The lamp is housed between the poles of a Varian electromagnet, and the light, emitted parallel to the magnetic field, is focused with a quartz lens to a 2-mm-diameter spot above the burner surface. The variable phase retardation plate in combination with the linear polarizer allows for the alternate transmission of the matched and unmatched Zeeman components through the monochromator to the detector. The output of the photomultiplier tube is processed electronically and displayed on a strip-chart recorder.

To determine the conditions of maximum sensitivity, the differential absorption between Zeeman components was measured as a function of magnetic field strength, as shown in Fig. 2. Maximum sensitivity was obtained at 11 kilogauss, and all measurements were then taken at this field strength. The response of the TALM spectrometer to increasing NO concentration is shown in Fig. 3. In these experiments, the $CH_4$ and air were introduced into the gas-mixing chamber, varying amounts of 4.41% $NO/N_2$ gas were added, and the total mixture was then passed through a 7.5-cm-long flow cell placed in the optical path of the spectrometer. The observed signal was linear in NO concentration to about 1200 ppm NO. At 2000 ppm NO, the transmission through the absorption cell was about 28%, and the observed signal was 10% low with respect to the extrapolated linear response.

Vertical and horizontal profiles of NO concentration were measured, using the uncooled quartz probe and the CLA. Thermal NO is produced by oxidation of atmospheric $N_2$ via the Zeldovich mechanism, and the

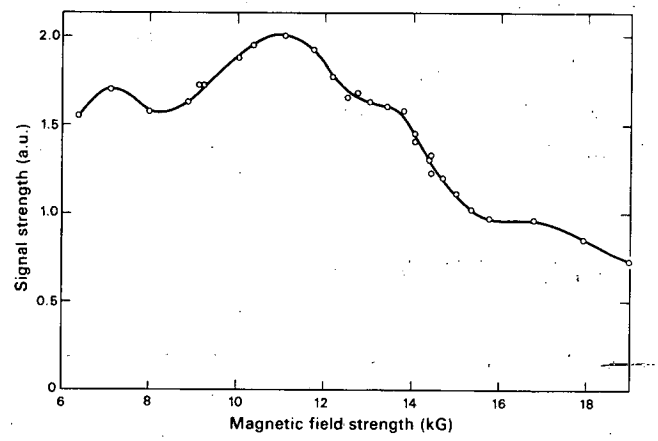


Figure 2. Differential absorption signal from NO as a function of magnetic field strength. Maximum sensitivity was observed at 11 kG. The Cd light source contained natural-abundance cadmium. (XBL 825-9789)

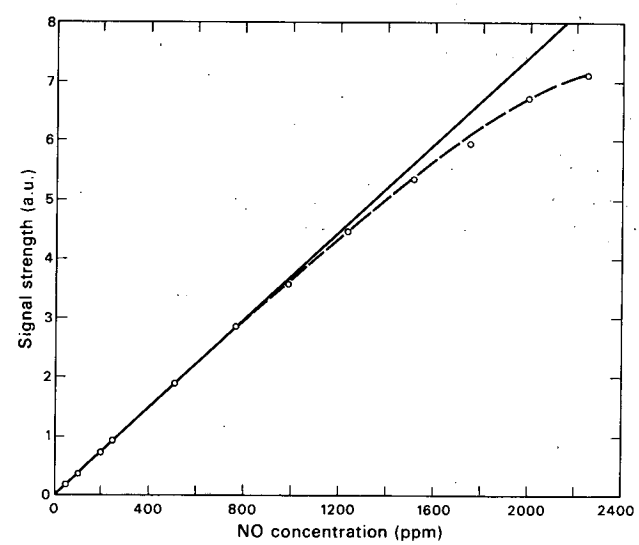


Figure 3. TALMS signal as a function of increasing concentration of NO. Solid line represents the linear response. At 1000 ppm NO, the measured signal is 2.8% below the extrapolated linear response. This deviation from linearity increases to 5.1% at 1500 ppm NO and to 10.4% at 2000 ppm NO. (XBL 825-9794)

measured values of thermal NO are less than 10 ppm. The results of adding known amounts of NO to the burner and sampling with the probe are shown in Fig. 4. The probe position was kept constant at a height of 5.0 mm above the center of the burner surface. The dashed line represents 100% survival of NO. The survival of NO, defined as the ratio NO measured/NO added, is approximately 80%. The TALMS measure-

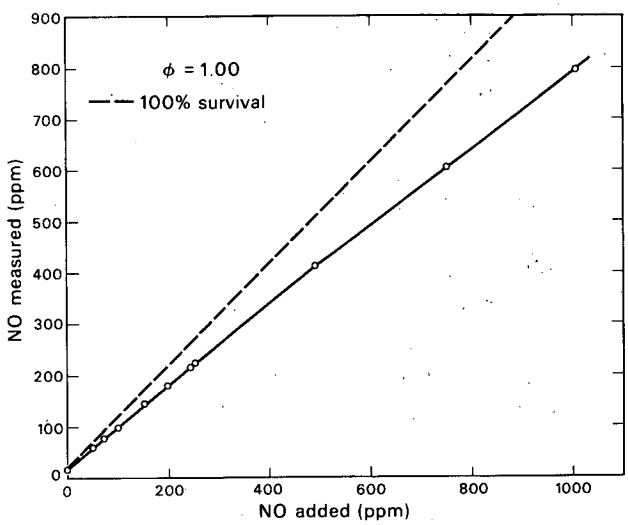


Figure 4. Nitric oxide measured vs. NO added as determined with an uncooled quartz probe and the chemiluminescent gas analyzer. The probe is fixed 5.0 mm above the center of the burner. Significant deviation from the dashed line representing 100% NO survival is observed. The thermal NO concentration is 16 ppm. (XBL 825-9793)

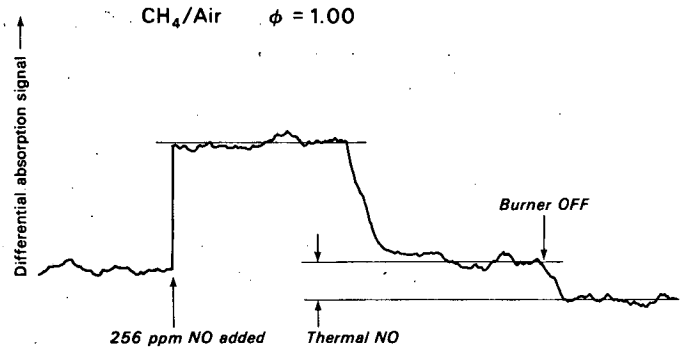


Figure 5. Strip-chart recorder trace showing the differential absorption signal obtained by TALMS. The recorder was stopped when NO was added, and restarted when the signal stabilized (~1 minute later). The maximum differential absorption signal corresponds to 256 ppm added NO plus thermal NO. The decay of this signal corresponds to halting the added NO; turning the burner off results in the loss of thermal NO. (XBL 825-9797)

ments of NO were obtained by doping the burner gases with known amounts of NO. A typical recorder trace of the differential absorption signal observed by thermal NO and added NO is shown in Fig. 5. A range of NO concentrations from 50 to 1000 ppm was added to the burner, and a plot of the observed signal strength as a function of NO added is shown in Fig. 6. Extrapolation to zero doping of NO results in an estimate of the thermal NO.

Table 1 summarizes the data shown graphically in Figs. 4 and 6. In both cases, the experimental points were fitted by a least-squares analysis, and the regression constants obtained were used to calculate the measured $NO_{CLA}$ and $NO_{TALMS}$ for given added NO. The $NO_{TALMS}$ were determined assuming no nitric oxide losses in the flame. At NO concentrations comparable to those used by other experimenters, the ratio $NO_{TALMS}/NO_{probe}$ assumes values similar to those reported in the literature for comparisons between optical and probe measurements. These tabulated ratios would be somewhat smaller, however, if a loss mechanism were assumed for the $NO_{TALMS}$ values. The TALMS technique offers greater sensitivity than previous *in situ* optical measurements of NO. At these lower NO concentrations, the discrepancy between *in situ* and probe measurements is significantly greater.

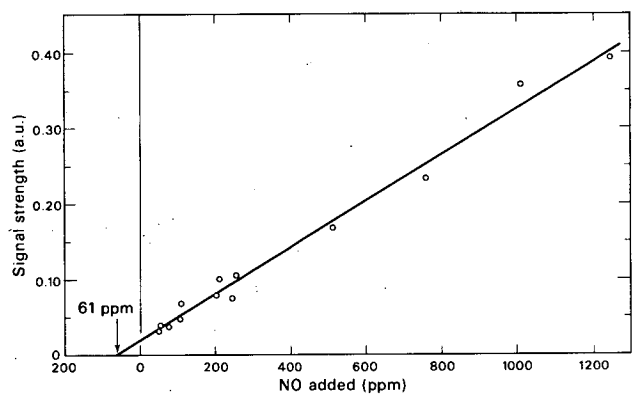


Figure 6. Signal strength measured by TALMS vs. NO added, for a stoichiometric $CH_4$-air flame ($\Phi$ = 1.00). A least-squares fit of the data points results in the equation $S = 3.07 \times 10^{-4}\,[NO]_{added} + 1.87 \times 10^{-2}$, where $S$ is the signal strength in arbitrary units, and the coefficient of correlation is 0.987. (XBL 825-9796)

In a series of separate experiments, measurements of ammonia emissions in the exhaust gases of a lean-burning laboratory combustion tunnel were made with a variety of analytical techniques; a common sampling method allowed for meaningful intercomparisons. Combustion parameters were varied from cold flow conditions to a range of equivalence ratios, sampling techniques, and dopant concentrations. We have reviewed the advantages and disadvantages of these and other techniques in detail in a recent publication.[7]

Table 1. Measured concentrations of NO in the postcombustion environment.

| $NO_{added}$ (ppm) | $NO_{CLA}$ (ppm) | $NO_{TALMS}$ (ppm) | $\frac{NO_{optical}}{NO_{probe}}$ |
|---|---|---|---|
| 50 | 61 | 110 | 1.80 |
| 75 | 81 | 136 | 1.68 |
| 100 | 100 | 160 | 1.60 |
| 150 | 139 | 210 | 1.51 |
| 200 | 178 | 260 | 1.46 |
| 250 | 217 | 310 | 1.43 |
| 500 | 411 | 560 | 1.36 |
| 750 | 605 | 810 | 1.34 |
| 1000 | 799 | 1060 | 1.33 |
| 1250 | 993 | 1310 | 1.32 |
| 1500 | 1187 | 1560 | 1.31 |

## PLANNED ACTIVITIES FOR FY 1983

Emphasis will be placed upon performing a comparative study of $SO_2$ sulfur dioxide measurements in the postcombustion environment. Sulfur dioxide will be measured with probe sampling and and a continuous gas analyzer that detects the emission from $SO_2$ fluorescence. Quenching measurements for the chaperone gases present in combustion mixtures will be performed. TALMS will also be used to detect $SO_2$. Construction of a molecular-beam sampling system interfaced with a quadrupole mass spectrometer will be initiated. This system will monitor gas-phase hydrocarbon species which are precursors to soot formation in the combustion of alternate fuels.

## REFERENCES


1. Hadeishi, T. and McLaughlin, R.D. (1971), "Hyperfine Zeeman Effect: Atomic Absorption Spectrometer for Mercury," *Science 174*, p. 404; Hadeishi, T. (1972), "Isotope Shift Zeeman Effect for Trace-Element Detection: An Application of Atomic Physics to Environmental Problems," *Appl. Phys. Lett. 21*, p. 438.
2. Koizumi, H., Hadeishi, T., and McLaughlin, R.D. (1979), "Detection of Small Molecules by Magnetically Tuned Frequency Modulated Atomic Line Sources," *Appl. Phys. Lett. 34*, p. 382.
3. Koizumi, H., Hadeishi, T. and McLaughlin, R.D. (1979), "A New Technique for the Determination of Isotopic Species Using Zeeman Scanning of an Atomic Line," *Appl. Phys. Lett. 34*, p. 277.
4. Cuellar, E. and Brown, N.J. (1981), "Combustion Diagnostics by Tunable Atomic Line Molecular Spectroscopy," *First Specialists Meeting (International) of the Combustion Institute 2*, p. 545.
5. Cuellar, E. and Brown, N.J. (1982), "Detection of $S_2$ by Magnetic Tuning of a Chromium Atomic Emission Line," *J. Phys. Chem. 86*, p. 1966.
6. Koizumi, H., Hadeishi, T., and McLaughlin, R.D. (1980), "Nitric Oxide Determination by a Zeeman Tuned Frequency Modulated Atomic Line Source," *Anal. Chem. 52*, p. 500.
7. Lucas, D. and Brown, N.J. (1983), "The Measurement of Ammonia in Lean Combustion Exhaust Gases," *Combustion and Flame. 49*, p. 283.


# COMBUSTION IN A TURBULENT BOUNDARY LAYER*


*R.K. Cheng, F. Robben, and L. Talbot*


Combustion in premixed gases sustained in a turbulent boundary layer over a strongly heated surface is a problem with many engineering and fire safety applications. It is also a unique flow configuration for the study of the mutual interaction between combustion and fluid dynamic turbulence. Turbulence structures and their development in isothermal turbulent boundaries have been studied quite extensively in many experimental and theoretical investigations. Since the turbulent boundary layer is well-characterized, the effect of combustion heat release can be readily identified. Also, by adjusting the flow and wall temperatures, a wider range of fuel-to-air ratios can be investigated than is possible with conventional flame configurations.

In FY 1981, we reported density and velocity statistical measurements in isothermal, heated, and


*This work was supported by the Director, Office of Energy Research, Office of Basic Energy Sciences, Chemical Sciences Division of the U.S. Department of Energy under Contract No. DE-AC03-76SF00098.

reacting turbulent boundary layers. Some of the conclusions we have drawn are as follows. The large-scale turbulent structures in the layers are found to dominate the development of both the thermal and flame structures within the boundary layer. In the case of the nonreacting layer, strong wall heating is found not to influence the intensity of the root-mean-square (rms) velocity fluctuations throughout the layer, or the Reynolds stress distributions, as compared to the isothermal layer. However, when combustion is present, the Reynolds stress in the wall region is significantly reduced compared with the isothermal layer at the same free-stream Reynolds number.

## ACCOMPLISHMENTS DURING FY 1982

Velocity fluctuations and correlations in isothermal, heated, and reacting turbulent boundary layers have been studied in more detail with a two-component laser Doppler velocimetry (LDV) system that allowed simultaneous measurement of two local velocity components. The data were reduced to obtain conditional statistics of the Reynolds stress, which provided further insight into the cause of Reynolds stress reduction by combustion in the wall region.

The experimental conditions of free-stream velocity, $U_\infty$, of 19 m/s, wall temperature, $T_w$, of 1000 K, and ethylene/air equivalence ratio of 0.35 are similar to those of our previous studies.[1-4] Quantities deduced from the data included two mean velocities, $U$ and $V$, two rms velocity fluctuation intensities $u'$ and $v'$, the Reynolds stress $-\overline{uv}$, and the third moments $\overline{u}^3$, $\overline{vu}^2$, $\overline{uv}^2$, and $\overline{v}^3$. These results compare well with those we obtained using a single-component LDV system. Since the two-color LDV provides a direct measurement of the velocity correlations, this comparison demonstrates that both techniques are reliable for measurements of velocity correlations, although the indirect method is more time-consuming.

Conditional analysis is a powerful technique for studying the Reynolds stress contribution associated with the movement of the large-scale turbulent structures. By sorting the Reynolds stress contribution into four velocity correlation quadrants according to sign, it has been shown that in the isothermal turbulent boundary layer, the major contributions are due to in-rushing of high-momentum fluid from the free stream towards the wall (inrush) and bursting of low-momentum fluid from the wall region into the outer region (bursting). Our first concern was to validate the technique by comparing the isothermal layer results with hot-wire measurements reported in the literature, since the two-color LDV technique has not been used extensively for deducing conditioned Reynolds stress statistics. The data were reduced to show the fraction of contributions from each of the four quadrants and analyzed to examine the large contributions of $-\overline{uv}$ in each quadrant (the so-called "hole" analysis). As shown in Fig. 1, our results compared extremely well with typical hot-wire results.

Similar data analyses were made for the heated and the reacting boundary layers. Typical results are shown in Fig. 2. In the heated layer, no significant change in the contributions was observed, except for a slight decrease in the contribution from the burst event at positions close to the end of the heated section. In the reacting layers, contributions in three quadrants remained unchanged, compared to the isothermal and heated layers. At positions near the heated wall, significant reduction was found in the quadrant associated with the burst event. Since the bursting cycle in the reacting layer consisted essentially of inrushing of cold reactants and bursting of hot products, the reduction in the burst quadrant indicated that combustion heat release caused the turbulence fluctuations in the products to be less correlated.

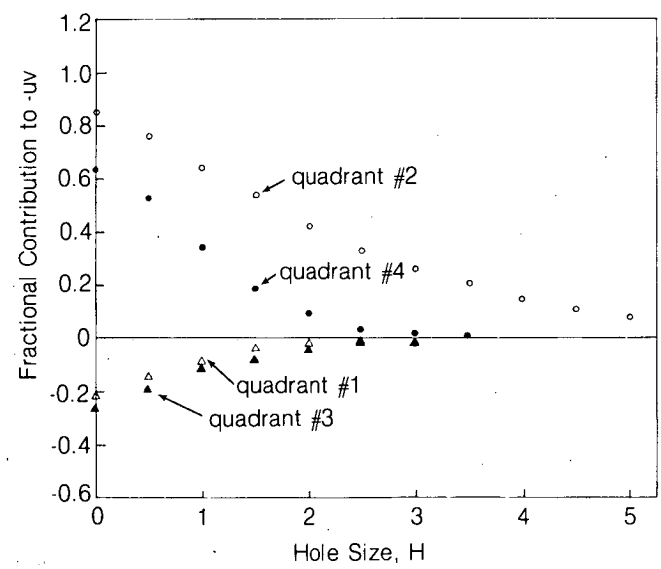


Figure 1. Quadrant analysis of the Reynolds stress in an isothermal turbulent boundary layer at $y/\delta u = 0.7$.

(XBL 834-9425)

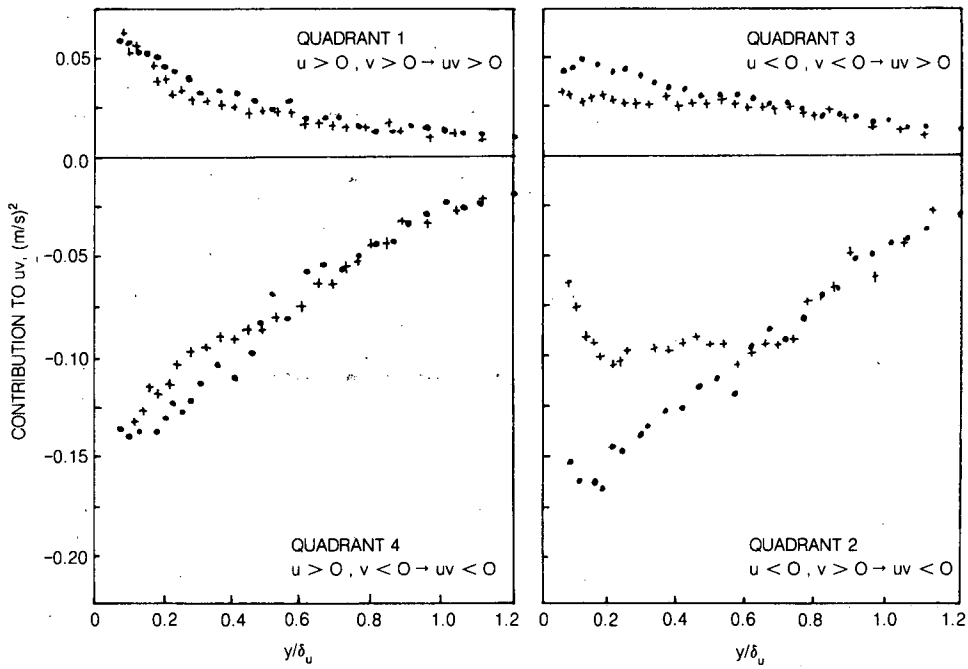


Figure 2. Comparison of the contributions of conditional velocity correlations in heated (•) and reacting (+) turbulent boundary layers. (XBL 834-9424)

## PLANNED ACTIVITIES FOR FY 1983

In FY 1983, we expect to determine the statistical spatial character of the thermal and flame structures seen in the schlieren movies by using the two-point Reyleigh scattering technique. This technique simultaneously measures the density fluctuations at two points separated by an adjustable distance. These data will be used to obtain spatial and temporal scales of the density fluctuation, their joint probability density functions (jpdf), and higher-order moments. The overall features and development of the thermal and flame structures revealed by schlieren observation can be validated by this quantitative local measurement.

The two-point density correlation is expected to yield a more complete description of the physical processes during ignition and transport of packets of reacting fluid in the heated wall region. This information should provide further insight into the observed reduction of Reynolds stress associated with the bursting event. It will also be of particular interest to determine how strongly the combustion-heat-release-induced local flow acceleration is related to the observed change in turbulence intensities. In a reacting layer, nonreacting heated fluid and reacting fluid co-exist. Schlieren observations and single-point density statistics cannot differentiate the change in density associated with the two different types of fluid. Analysis of the two-point density correlations should be useful to identify some characteristic features of the reacting fluids and to map the regions where chemical reactions occur; these regions can then be compared with the regions where changes in turbulence intensities take place.

Other useful quantities that can be deduced are the periodicity of the passage of the structures and their overall geometry, such as their inclination with respect to the wall. These results can then be compared with the large-scale turbulent structures reported in many investigations. Such comparisons should show whether or not the thermal and flame structures scale with the same free-stream variables as the large turbulence structures.

## REFERENCES

1. Ng, T.T. (1981), *Experimental Study of a Chemically Reacting Turbulent Boundary Layer*, Ph.D. Thesis, Department of Mechanical Engineering,

University of California, Berkeley, Lawrence Berkeley Laboratory Report LBL-13325.

2. Ng, T.T., Cheng, R.K., Robben, F., and Talbot, L. (1982), "Combustion-Turbulence Interaction in the Turbulent Boundary Layer Over a Hot Surface," in *Nineteenth Symposium (International) on Combustion*, The Combustion Institute, p. 359.
3. Ng, T.T. (1981), "Measurements of Velocity Fluctuation Correlations using a Single-Component Laser Doppler Velocimetry System," submitted to *AIAA Journal*; Lawrence Berkeley Laboratory Report LBL-13702.
4. Ng, T.T., Talbot, L., Cheng, R.K., and Robben, F. (1982), "The Turbulent Boundary Layer over a Flat Plate with Strong Stepwise Heating," in *International Symposium on Application of Laser Doppler Anemometry to Fluid Mechanics*, in press.
5. Cheng, R.K., and Ng, T.T. (1983), "The Influence of Combustion on Reynolds Stress in a Strongly Heated Turbulent Boundary Layer," in preparation.

## TURBULENT BURNING VELOCITY IN PREMIXED TURBULENT FLAMES*

*R.K. Cheng, T.T. Ng, F. Robben, and L. Talbot*

The study of turbulent burning velocity is part of our continuing experimental program in premixed turbulent combustion. The overall objective is to investigate the interaction between fluid dynamic turbulence and combustion; together these constitute the majority of combustion phenomena. The flame configuration we have chosen to study is unconfined, rod-stabilized, V-shaped flames propagating in a turbulent flow generated by a grid or perforated plate. This configuration is similar to those found in many practical burners but is more idealized because it is free of geometry and flow constraints. In FY 1981, we reported velocity statistical data obtained by the use of laser Doppler velocimetry (LDV).[1] Reported here are the turbulent burning velocities deduced from the statistical data.

Turbulent burning velocity, $S_t$, is a measure of the most significant aspect of turbulent combustion—the increase in flame propagation speed above the laminar burning speed, $S_u$, due to fluid dynamics turbulence. It is therefore useful both for the design of more efficient combustion systems and for comparison with theoretical predictions. Determination of turbulent burning velocity has been the subject of many experimental investigations, and data obtained in many stabilized and unstabilized flame configurations have been reported. In general, these data show an increase in $S_t$ with increasing turbulence intensity, and many empirical parameters have been used to correlate these data. However, a universally applicable formula has yet to be determined.

### ACCOMPLISHMENTS IN FY 1982

The conventional method for deducing the turbulent burning velocity in a V-shaped flame is to measure the velocity and direction of the flow entering the flame region and establish a flame surface representing the overall geometry of the flame brush. This method is not highly accurate because the flame brush is much thicker than the laminar flame thickness and the value of the turbulent burning velocity depends on where the mean flame surface is defined. For example, as demonstrated in Fig. 1, which shows the velocity vectors measured in the flow field of a flame we studied, the $S_t$ determined with respect to the cold boundary would be much larger than the $S_t$ determined with respect to the mean flame surface. Different investigators have used one surface or the other to define the turbulent burning velocity, and as a result, the data in the literature are not very consistent. Shown in Fig. 2 are the turbulent burning velocities determined for our V-shaped flame using the mean flame surface. These data are compared with the correlation obtained by Abdel-Gayed and Bradley.[2] As can be seen, our data are lower than the correlation. Furthermore, some of our results are even lower than the laminar burning velocity.

To improve the accuracy and consistency of these measurements, a method based on an effective flame orientation is proposed. In our turbulent flame with relatively low incident turbulence, the flame sheet is thin and convoluted. This type of turbulent flame is generally classified as wrinkled laminar flame. The

*This work was supported by the Director, Office of Energy Research, Office of Basic Energy Sciences, Chemical Sciences Division of the U.S. Department of Energy under Contract No. DE-AC03-76SF00098.

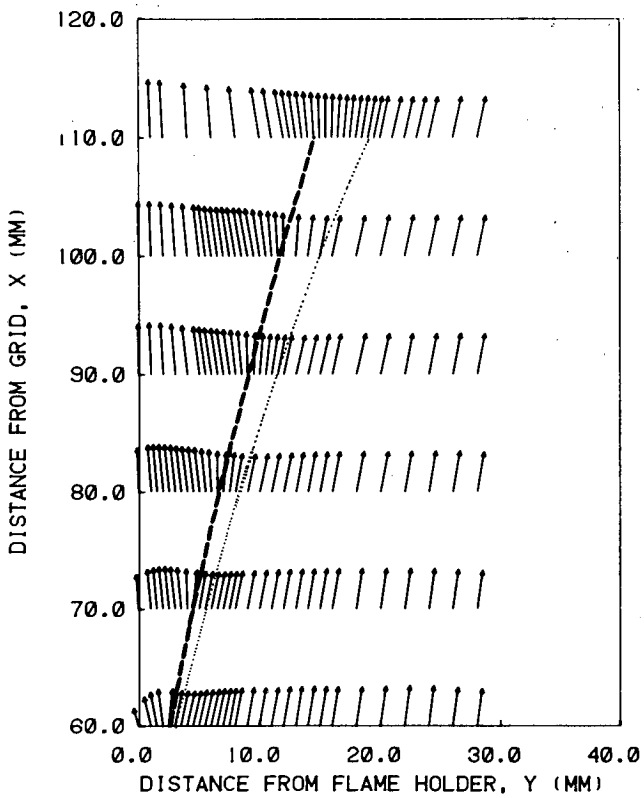


Figure 1. Two-dimensional velocity vectors in the flow field of a V-shaped flame in grid-generated turbulence. Dashed curve represents the time-mean flame surface, dotted curve the cold boundary. (XBL 834-9423)

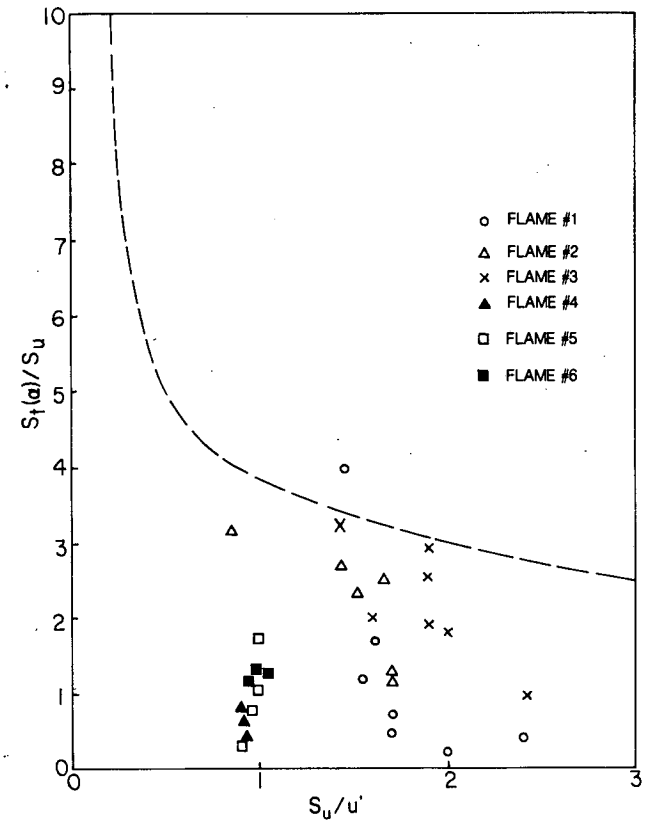


Figure 2. Comparison of turbulent burning velocity, defined with respect to mean flame surface, with correlation of Abdel-Gayed and Bradley[2] (dashed curve). (XBL 834-9422)

interaction of the thin fluctuating flame sheet with the turbulent flow causes overall flow deflection, as shown in Fig. 1. We have used this fluctuating thin flame phenomenon to explain both the increase in turbulence intensities and Reynolds stress in the flame region.[1]

By applying a conserved tangential velocity criterion to the flow through the flame region, an effective flame orientation for the fluctuating thin flame can be deduced. The turbulent burning velocities defined with respect to this effective flame orientation are shown in Fig. 3. These results compare with Ref. 2 much better than do those shown in Fig. 2. Our analysis demonstrates that for the determination of turbulent burning velocity to be of physical significance, the flame surface criterion is of crucial importance.

## PLANNED ACTIVITIES FOR FY 1983

The apparent increase in turbulent intensities in the flame region and the true makeup of the Reynolds stress will be investigated further. A two-color LDV system will be used to measure two velocity components simultaneously. Analysis of the data will enable us to determine the contribution to the turbulent intensities caused by the intermittent measurement of the velocities in the burnt and unburnt states as the thin flame sheet fluctuates past the stationary laser probe. Conditional statistics of the Reynolds stress will be useful to clarify the physical phenomenon causing the increase in Reynolds stress.

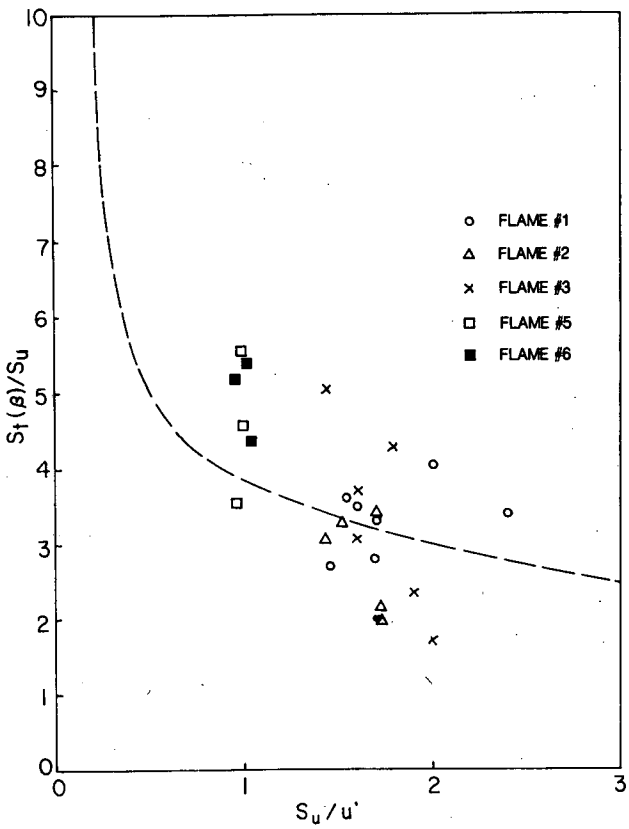


Figure 3. Comparison of turbulent burning velocity, defined with respect to the effect of flame orientation, with the correlation of Abdel-Gayed and Bradley[2] (dashed curve). (XBL 834-9421)

## REFERENCES


1. Cheng, R.K., and Ng, T.T. (1983), "Velocity Statistics in Premixed Turbulent Flames," *Combustion and Flame*, in press.
2. Abdel-Gayed, R.G., and Bradley, D. (1977), "Turbulent Flame Propagation in Premixed Gases: Theory and Experiment," in *Sixteenth Symposium (International) on Combustion*, The Combustion Institute, p. 1752.


# PLASMA IGNITION STUDIES*


*A.K. Oppenheim, J. Cavolowsky, C. Edwards, K. Hom, and H.E. Stewart*


## ACCOMPLISHMENTS DURING FY 1982

Following our earlier investigations of the operating characteristics of jet igniters,[1-4] we have studied the performance of an array of plasma ignition systems in a CFR engine. Included among the igniters were a conventional spark plug, a surface discharge plug, and several types of plasma jet. Information was obtained to determine the specific emissions, mean effective pressure, ignition delay, and duration of the exothermic combustion process. Statistical analysis was performed on the pressure-derived data (mean effective pressure, ignition delay, and combustion duration) in order to quantify the cycle-to-cycle variation in the engine and thus the stability of operation.

The results demonstrate the advantages of enhanced ignition systems over a conventional spark discharge. Figure 1 displays the ignition delay and combustion duration for a typical plasma jet and a standard spark system. It is apparent that the plasma allows for an extension of the lean operating limit of the engine from 0.68 to 0.53 in equivalence ratio. In addition, the plasma jet significantly reduces the ignition delay throughout the lean range of equivalence ratios. Combustion duration remains comparable for the two systems down to an


*This work was supported by the Assistant Secretary for Conservation and Renewable Energy, Office of Transportation Programs, Division of Transportation Energy of the U.S. Department of Energy under Contract No. DE-AC03-76SF00098.

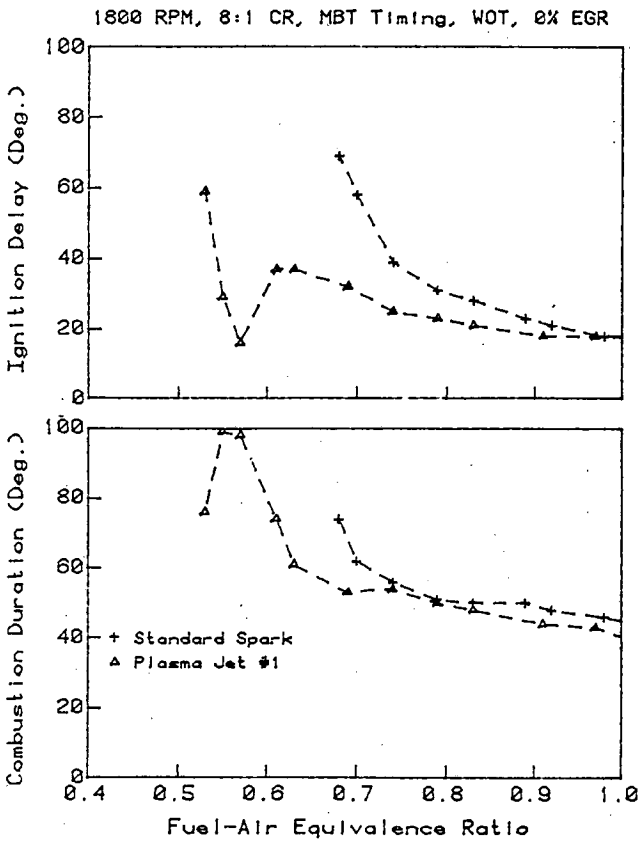


Figure 1. Ensemble-averaged values of ignition delay and combustion duration for the standard-spark and plasma-jet ignitors. (XBL 837-10554)

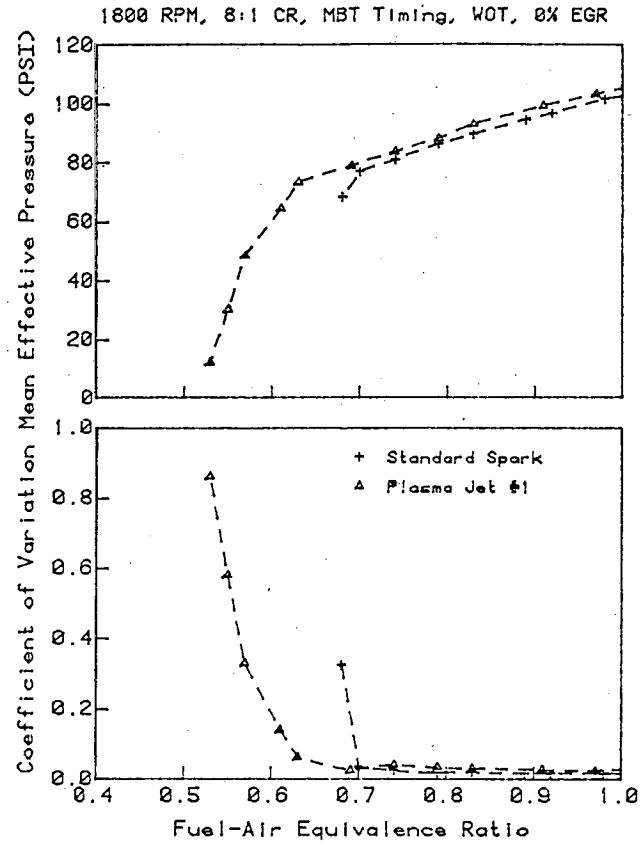


Figure 2. Ensemble-averaged values of, and cyclic variation in, indicated mean effective pressure for the standard spark and plasma-jet ignitors. (XBL 837-10555)

equivalence ratio of 0.72, after which the plasma jet provides for an extension of ~0.08 in equivalence ratio before exhibiting an increase similar to that of the standard spark.

Figure 2 shows the work output of the two systems expressed in terms of mean effective pressure. Data obtained with plasma jet and standard spark exhibit similar characteristics down to an equivalence ratio of 0.7. At leaner mixtures, the engine run with a standard spark manifests the effects of misfire and soon becomes completely inoperable, as evidenced by the sharp discontinuity in the coefficient of variation. When it is run with a plasma jet, however, misfire does not occur; instead, as the mixture is leaned, the work output decays to zero while the cyclic variation grows to infinity.

Emission characteristics for the two systems remain virtually the same, NO, HC, and CO being primarily a function of equivalence ratio rather than of the particular method of ignition.

## PLANNED ACTIVITIES FOR FY 1983

Two phases of investigation are envisaged:

(1) Study of performance of characteristics of plasma jet ignition systems in a CFR engine along the same lines as reported here, but with the addition of exhaust-gas recirculation.

(2) Laser cinematographic study of plasma jet ignition, using a high-pressure combustion cell (bomb) and a single-pulse machine (Mark II).

## REFERENCES

1. Weinberg, F.J., Hom, K., Oppenheim, A.K. and Teichman, K. (1978), "Ignition by Plasma Jet," *Nature 272*, p. 341.
2. Oppenheim, A.K., Teichman, K., Hom, K., and Stewart, H.E. (1978), "Jet Ignition of an Ultra-

Lean Mixture," *SAE Transactions (Sect. 3) 87*, p. 2416.

3. Cetegen, B., Teichman, K.Y., Weinberg, F.J., and Oppenheim, A.K. (1980), "Performance of a Plasma Jet Igniter," Paper No. 800042, presented at the Society of Automotive Engineers Congress and Exposition, Detroit, Michigan, 1980.
4. Dale, J.D. and Oppenheim, A.K. (1981), "Enhanced Ignition for I.C. Engines with Premixed Gases," SAE Technical Paper No. 810146, presented at the Society of Automotive Engineers International Congress and Exposition, Detroit, Michigan, 1981.

# STRUCTURE OF A V-SHAPED TURBULENT FLAME*

*M. Namazian, J. Hertzberg, L. Talbot and F. Robben*

In the quest for more efficient combustors, the interaction between turbulence and combustion must be understood at a fundamental level. To accomplish this, the structure of a V-shaped premixed turbulent flame is being studied. Two experimental methods are employed. The first is a two-point Rayleigh scattering technique that gives the density of the gas at two points in space.[1] The second is a visualization of the flame front by light scattering from oil particles fed into the flow.

## ACCOMPLISHMENTS DURING FY 1982

### Two-Point Rayleigh Scattering

Gas density was measured simultaneously at two separate points in a V-shaped turbulent flame. The measurements were performed by the Rayleigh scattering method. Figure 1 shows a schematic diagram of the premixed combustor and collection optics. We used two independent sets of scattered-light collection optics plus a method of splitting the laser beam and varying the separation of the two sampled points. As indicated in Fig. 1, the two-point measurements were performed in three directions: *x*, along the jet; *y*, normal to the jet and the flame holder; and *z*, normal to the jet and parallel to the flame holder. In this article, we refer to the two measurement points as points 1 and 2. The two-point density measurements were performed in ethylene-air, at an equivalence ratio of 0.60. The jet velocity was 7 m/sec.

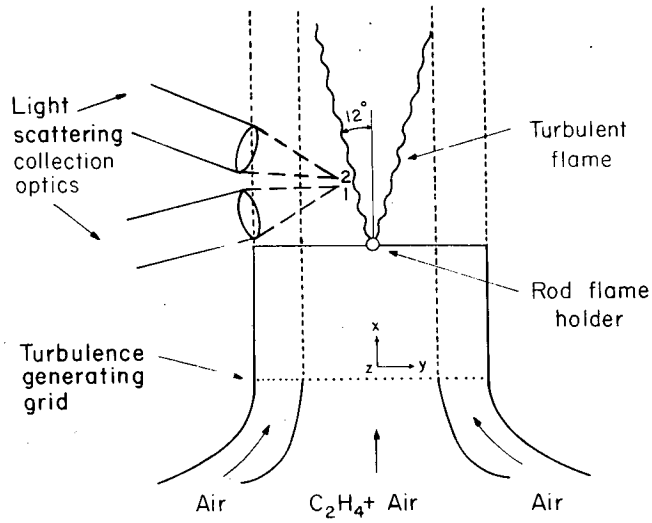


Figure 1. Schematic of experimental apparatus for two-point Rayleigh scattering measurements.. (XBL 823-8761)

Important information on the structure of the flame can be obtained by analyzing the joint probability density function (jpdf) of the two-point Rayleigh scattering density measurements. Figure 2 shows the jpdf of densities measured at two points separated by 1.2 mm in the *y* direction; the inset shows the relative position of the sampled points with respect to the flame brush. Note that point 2 lies further into the flame zone than point 1. Also note that the density axes are normalized by the unburned gas density.

Since the laminar flame thickness (about I mm) is smaller than the turbulent flame zone (about 5 mm), the jpdf of the densities principally shows the probabilities of finding either burned or unburned gas at the point of measurement. In Fig. 2, the jpdf has three peaks, indicating that the probability of simultaneously finding burned gas at point 1 and unburned gas at point 2 is zero. This result is found to be true for all positions of the two points across the flame.

For the low-intensity-turbulence regime of the

*This work was supported by the Air Force Office of Scientific Research under Contract No. F-44620-76-C-0083 through the Office of Research Services, College of Engineering, University of California, Berkeley. Additional equipment and facility support were provided by the Office of Energy Research, Basic Energy Sciences, Chemical Science Division of the U.S. Department of Energy under Contract No. DE-AC03-76SF00098.

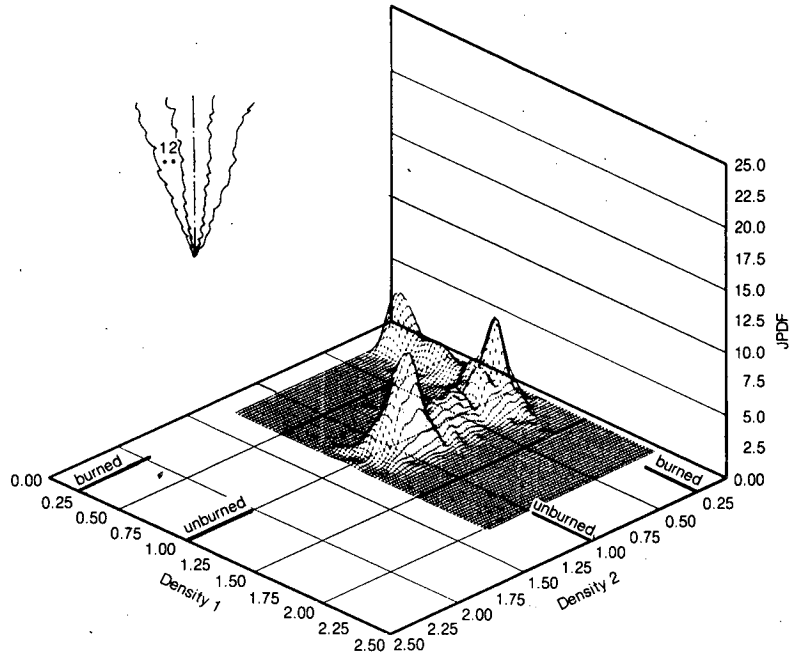


Figure 2. Joint probability density function of the two-point Rayleigh scattering density measurements. The points 1 and 2 are separated by 1.2 mm across the flame, as shown in the inset. (XBL 825-9994)

present experiments, it is generally agreed that the physical structure of the turbulent flame zone consists of a wrinkled laminar flame that fluctuates in position and shape. Under these conditions, the wrinkled laminar flame is continuous, with no ruptures or pockets of flame. On the other hand, higher turbulence intensity of sufficient length would cause progressive disintegration of this wrinkled flame, giving rise to discontinuities in the structure and to isolated flamelets. Such flamelets are shown schematically in Fig. 3(a). If the present flame contained flamelets, there should be some cases where burned gas occurs at point 1 and unburned gas at point 2. Since such cases have not been found (the missing peak in Fig. 2), we conclude that there are no flamelets. The same reasoning shows that the present flame cannot be as highly convoluted as sketched in Fig. 3(b). However, the flame orientations sketched in Figs. 3(c), (d), and (e) are possible, and each causes one of the peaks in the jpdf shown in Fig. 2.

For cases where the axis of the points lies either in the flow direction, $x$, or in the plane of the flame, $z$, the jpdf's show four peaks, indicating the presence of all possibilities of burned and unburned gas at the sampled points.

We will present below the result of flame-front visualization. This result also supports our conclusion

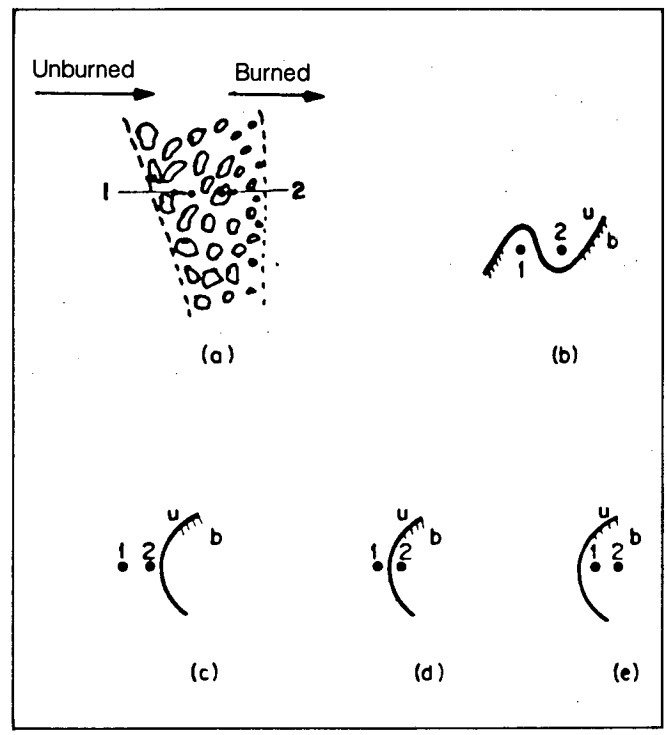


Figure 3. Examples of possible flame structure and orientation with respect to the two measurement points. Flamelets (a) and convolutions (b) are unlikely in the present flame. The orientations shown in (c), (d), and (e) each contribute to one peak in Figure 2. (XBL 834-9441)

that the thick flame brush (about 5 mm) consists of a thinner reaction front (about 1 mm) that fluctuates in shape and position. Here, we will present some information on the fluctuation of the reaction front across the flame brush.

Further analysis of the two-point measurements allows the derivation of the probability density function (pdf) for the flame-front position. By measuring the fraction of time that the front was found between the two measurement points and repeating this measurement across the width of the brush, we derived the bell-shaped curve in Fig. 4. The *S*-shaped curve shows the corresponding mean density profile. The measurements were made 80 mm above the flameholder, and the separation between the two points was 1.2 mm, slightly greater than the laminar flame thickness of I mm.

The pdf of the flame-front position is almost a normal distribution, with the mean at the center of the flame brush. This is also true for experiments at different heights above the flame-holding rod.

## Flame-Front Visualization Method

A time-resolved qualitative method of delineating a two-dimensional flame sheet has been developed. As shown in Fig. 5, premixed ethylene and air is seeded with a translucent cloud of oil droplets. The droplets are formed from liquid silicone oil in a sprayer and average 1 micron in diameter. Because of their small size, they are easily convected with the flow. As the cloud passes through the rod-stabilized flame, the droplets evaporate and burn; the burned gases are now transparent. The entire system is illuminated with a sheet of laser light, created with a simple cylindrical lens. The oil cloud scatters the laser light and essentially "lights up" while the unseeded and the burned regions remain dark. The flame thus appears as the interface between the bright and dark areas.

Because of the intensity of the laser sheet, the result can be photographed and filmed at high speed, providing time resolution. One such photograph is shown in Fig. 6; the equivalence was 0.6 and the jet velocity was 2 m/sec. The flow is turbulent, resulting

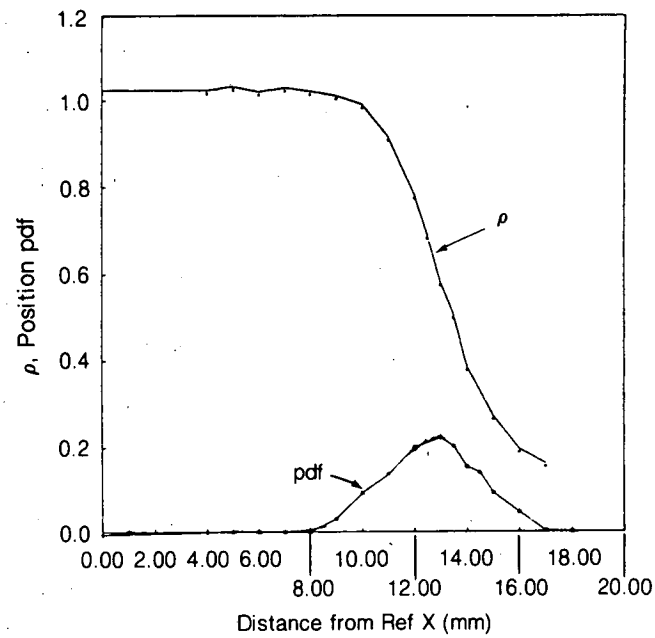


Figure 4. Measured mean density $\rho$ and the pdf of the reaction front position across the flame. (XBL 834-9442)

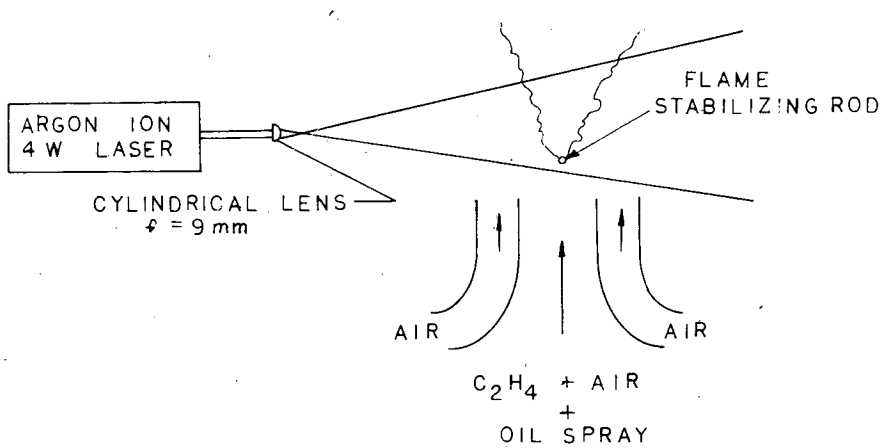


Figure 5. Schematic of the set-up for flame-front visualization. (XBL 834-9443)

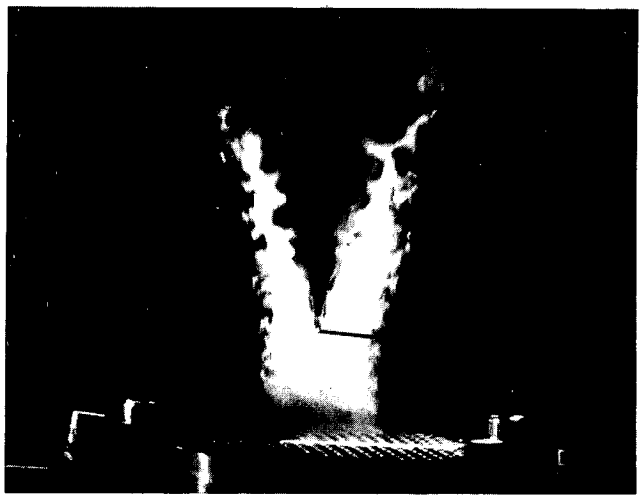

Figure 6. A V-shaped turbulent flame front that has become visible due to the evaporation of oil particulates on the hot side. Unburned areas outside the front are illuminated by particulate scattering of laser light; dark areas within the V are burned. (XBB 8210-9615)

in the irregular appearance of the flame, which is seen as the edges of the V shape. The reaction front appears to be continuous, supporting the results of our two-point density measurements.

## PLANNED ACTIVITIES FOR FY 1983

- The structure of a flame with higher incoming turbulence intensity will be studied.
- Further two-point Rayleigh scattering data, which have already been taken, will be reduced.
- A new program to investigate flame stabilization behind bluff bodies will be started. The basic features of the flame stabilization region will be mapped by first measuring the density and then the velocity of this region. The measurements will also be done near the blow-off velocity.

## REFERENCE


1. Namazian, M., Talbot, L., Robben, F. and Cheng, R. K. (1982), "Two-Point Rayleigh Scattering Measurements in a V-shaped Turbulent Flame," in *Nineteenth Symposium (International) on Combustion*, p. 487.


# TESTS AND CRITERIA FOR FIRE PROTECTION OF CABLE PENETRATIONS AND ELECTRICAL CABINETS*


*R.B. Williamson, F. L. Fisher, and F.W. Mowrer*


The spread of fire in nuclear reactors depends critically on the barrier qualities of the cable penetrations in fire-resistant walls and floor/ceiling assemblies. A new ASTM standard, E-814,[1] is now available for the evaluation of "penetration fire stops." This new fire test is similiar to the earlier ASTM E-119, except that it is written specifically to cover assemblies, such as cable and pipe penetration devices, in fire-rated construction. The new standard calls for the pressure differential in the test furnace to be measured and specifies how it should be determined.

The ASTM E-119 Fire Endurance Test Method has been used for seventy years to qualify unpenetrated wall and floor/ceiling assemblies. However, it became evident that there was a need for special attention when such assemblies contained cable penetrations, and the new standard, ASTM E-814, was developed for this purpose. The validation of E-814 and the concept of requiring positive pressure in the test furnace have been the focus of this project for the last four years; recently, a new aspect was added, namely the fire safety of electrical cabinets.

One way the potential spread of fire in nuclear reactors can be controlled is by fire-resistant wall and floor/ceiling assemblies that define "fire areas" or zones. An overriding consideration in the safe operation of nuclear reactors is that all systems and associated circuits used for safe shutdown be free from fire damage. This objective is achieved in part by identifying "redundant" systems necessary for safe shutdown and then assuring that the systems will not be subject to damage from the same fire. This can be accomplished by locating the redundant systems in fire areas separated by fire-rated barriers or, in some instances, by using "substantial physical separation."[2] It has, however, been recognized that:

> Unpierced fire barriers offer the best protection of separating redundant trains of


*This work was supported by the U.S. Nuclear Regulatory Commission through Sandia Laboratories, Albuquerque, New Mexico under Contract No. 46-6967 and No. 50-9723 and through the U.S. Department of Energy under Contract No. DE-AC03-76SF00098.

safety-related or safe shutdown equipment. However, these barriers must be pierced for both control and power cables. These penetrations must be sealed to achieve a degree of fire resistance equivalent to that required of the barrier that is unpierced.

(Ref. 2, p. 76608.1)

The fire conditions represented by the E-119 test method are termed "post-flashover" conditions in which fire fully involves a compartment, although the test itself is conducted in a furnace that is not closely controlled by the standard. Under actual conditions, as opposed to laboratory test furnaces, post-flashover fires are characterized by a positive pressure differential between the upper half of the fire compartment and the unexposed face of the wall and floor/ceiling assemblies making up its boundaries. The beginning of this post-flashover period also is characterized by excess amounts of pyrolyzed fuel. Since flames commonly emerge from the doors and windows of both actual and laboratory post-flashover building fires, there is no doubt that these phenomena—postive pressure and excess pyrolyzates—occur.

## ACCOMPLISHMENTS DURING FY 1982

A new concept for evaluating penetrations through walls or floor/ceiling assemblies in a true post-flashover compartment fire exposure was discovered during 1981. This concept may have far-reaching consequences for the evaluation of all penetrations of fire-resistive barriers. Many problems with E-119 test furnaces can be attributed to the fact that they are furnaces and not compartments. Thus, by returning to an actual compartment geometry and creating a true post-flashover compartment fire, the pressure differentials, excess pyrolyzates, and other characteristic features of post-flashover fires will be automatically accomplished.

During 1982, we finished instrumenting a pre-flashover room test facility at the University of California's Richmond Field Station for post-flashover experiments. Special attention was paid to developing realistic fire conditions while at the same time retaining control of the fire itself. One objective was to create a controlled amount of excess pyrolyzates in the area of penetration and simultaneously control the temperature of the compartment so as to follow either the standard or a special time-temperature curve. In addition, a positive pressure differential needed to be created in the upper part of the compartment to duplicate actual fire situations.

To characterize fire conditions within the compartment, an aspirated thermocouple "tree" was constructed and calibrated. This allows for the assessment of the effects of radiation on thermocouples distributed within the compartment. Since radiation is very important in post-flashover fires, aspirated thermocouples may be necessary to characterize them.

A set of pressure probes was installed in the compartment at eight locations from 0.5 m to 2.34 m above the floor level. The associated instrumentation was installed and calibrated to give as accurate a measurement as possible of the differential pressure between the interior of the fire compartment and the external space. Special effort is being made to quantify the accuracy of this measurement. The importance of pressure measurements is well-recognized and is one of the principal reasons for the change from a furnace to a compartment geometry.

An array of 16 thermocouples was placed in the exhaust plenum above the collection hood outside the fire compartment. The measurement of the temperatures within the plenum allows an assessment of the enthalpy flow in the exhaust system; since the energy release in the fire compartment is known, a heat balance can be performed for the experiments. This should be particularly important when correlating these experiments with theoretical models.

The gas-sampling equipment and instrumentation were placed in a protective housing adjacent to the stack above the test compartment. This allows measurement of both the products of combustion and the rate of heat release by the oxygen consumption method.

A set of four experiments (conducted partially under separate sponsorship) were performed in which the special instrumentation described above was monitored to ensure the accuracy and validity of the measurements. A report is being prepared on the results.

A second set of experiments explored methods of producing a controlled post-flashover fire condition on the end wall and ceiling of the test compartment. This entailed placing a "line" burner against the wall and trying to produce a flame zone adjacent to the wall. These experiments proved very discouraging because the flame was not stable and would wander

from side to side. At the beginning of FY 1983, however, a flame holder was installed inside the line burner, and this stabilized the flame.

Another accomplishment was the development of simple microcomputer methods to calculate the expected temperature, pressure, and excess pyrolyzate histories for sample compartments with different fuel loads, using post-flashover fire models. Previous work had led to a post-flashover computer model, COMPF,[3,4] which required a mainframe computer, and we originally intended to download the program to the NOVA-2 minicomputer used in our laboratory for data acquisition and reduction. However, the experimental work took precedence, and the COMPF program was not fully implemented to run under the Data General FORTRAN compiler. As we looked at the problem, it became clear that a much simpler approach would be more effective. This was to use a microcomputer to solve the "closed-form" approximation of Babrauska,[5] which has been shown to be within 3% of the gas temperatures calculated by the numerical methods of COMPF.

By the end of this reporting period, the closed-form calculations had been set up on "Supercalc," the popular microcomputer "spread-sheet" program. The use of the spread sheet to calculate post-flashover fire conditions is very exciting, because it gives the fire protection engineer the benefits of a computer fire model that can be run on a microcomputer.

This is to be the last year for the study of cable penetrations, and a report is being prepared that summarizes our research on this subject. This report will give a detailed analysis on how fire resistance of cable penetrations should be evaluated using the new fire test standard, ASTM E-814, and how this standard relates to other standards, such as IEEE 635.

Another accomplishment was the further development of the probabilistic network approach to modeling fire spread. A Ph.D. thesis entitled *Application of Probabilistic Networks to Fire Protection* was completed in August 1982 by Wai-Ching Teresa Ling. A principal feature of this approach is that fire-resistive elements can be tested under different conditions to provide for a quantitative interpretation of their expected performance under potential fire conditions.

A new topic of research, the assessment of the susceptibility of components within electrical cabinets to damage from a fire either within or outside of the cabinet was started. As of the end of FY 1982, there were no major findings to be reported. This research is being continued in FY 1983.

## PLANNED ACTIVITIES FOR FY 1983

The principal research task for this year will be to conduct fire test experiments on electrical cabinets exposed to both interior and exterior fires.

## REFERENCES


1. *Annual Book of ASTM Standards*, 1981 ed., American Society for Testing and Materials, Philadelphia, Pennsylvania.
2. "Fire Protection Program for Operating Nuclear Power Plants," 10CFR Part 50, *Federal Register 45*, No. 225, p. 76602-76616, Nov. 19, 1980.
3. Babrauskas, V., and Williamson, R.B. (1978), "Post-Flashover Compartment Fires: Basis of a Theoretical Model," *Fire and Materials 2* (2), p. 39.
4. Babrauskas, V., and Williamson, R.B. (1979), "Post-Flashover Compartment Fires—Application of a Theoretical Model," *Fire and Materials 3* (1), p. 1.
5. Babrauskas, V. (1981), "A Closed-Form Approximation for Post-Flashover Compartment Fire Temperatures," *Fire Safety J. 4*, p. 63.

# THE EFFECTS OF METAL CHELATES ON WET FLUE GAS SCRUBBING CHEMISTRY*

*S.G. Chang, D. Littlejohn, and S. Lynn*

Power-plant flue gas frequently contains several hundred ppm $NO_x$ and up to several thousand ppm $SO_2$. Most of the $NO_x$ is in the form of relatively insoluble NO. Several simultaneous desulfurization and denitrification processes,[1-3] still in the development stage, are based on the addition of metal chelates such as $Fe^{2+}$ (EDTA) to the aqueous scrubbing liquor to promote absorption of NO. These metal chelates can bind NO to form nitrosyl metal chelates, which can in turn react with absorbed $SO_2$ to produce reduced nitrogen species such as $N_2O$, $N_2$, and sulfate while metal chelates are regenerated. Identification of an optimum metal chelate for greater efficiency in removing NO and $SO_2$ in a wet scrubber requires knowledge of the thermodynamics and kinetics of the coordination of NO to various metal chelates. Knowledge of the kinetics and mechanisms of the reactions between nitrosyl metal chelates and absorbed $SO_2$ is also needed to calculate the regeneration rate of metal chelates and to control the products of reaction by adjusting the operating conditions.

## ACCOMPLISHMENTS DURING FY 82

We have investigated some of the important factors that should be considered in identifying an optimum metal chelate catalyst and in developing an efficient scrubber for the simultaneous desulfurization and denitrification of a power-plant stack gas.

### Thermodynamic Equilibrium and Kinetics of NO Absorption

*Thermodynamics*

Nitric oxide is nonreactive in water (in the absence of oxygen), and the solubility of NO in aqueous solutions is very small. The absorption of NO is enhanced by some water-soluble metal chelate compounds that form complexes with NO.[4] Many studies have been published on the structure of these chelates, but only a few on their thermodynamic properties and reaction rates. Hishinuma et al.[5] and Lin et al.[6] have recently determined the equilibrium constants, enthalpy, and entropy for the coordination of NO to $Fe^{2+}$ (EDTA) and $Fe^{2+}$ (NTA) respectively.

The binding of NO to $Fe^{2+}(L)$ can be expressed by the following reaction:

$$n\mathrm{NO} + \mathrm{Fe}^{2+}(\mathrm{L}) \underset{k_{-1}}{\overset{k_1}{\leftrightarrows}} \mathrm{Fe}^{2+}(\mathrm{L})(\mathrm{NO})_n \qquad (1)$$

where L is a ligand. The equilibrium constant of this reaction can be written as:

$$K = \frac{k_1}{k_{-1}} = \frac{[\mathrm{Fe}^{2+}(\mathrm{L})(\mathrm{NO})_n]}{[\mathrm{NO}]^n[\mathrm{Fe}^{2+}(\mathrm{L})]} \qquad (2)$$

$$= \frac{[\mathrm{Fe}^{2+}(\mathrm{L})(\mathrm{NO})_n]}{[\mathrm{NO}]^n[\mathrm{Fe}^{2+}(\mathrm{L})]_0 - [\mathrm{Fe}^{2+}(\mathrm{L})(\mathrm{NO})_n]}$$

Equation (2) can be rearranged to become

$$\frac{[\mathrm{Fe}^{2+}(\mathrm{L})]_0}{[\mathrm{Fe}^{2+}(\mathrm{L})(\mathrm{NO})_n]} - 1 = \frac{1}{KH^n p_{\mathrm{NO}}^n} \qquad (3)$$

where $[Fe^{2+}(L)]_0$ is the initial concentration of $Fe^{2+}(L)$, $[Fe^{2+}(L)(NO)_n]$ is the concentration of the NO adduct obtained by graphically integrating the outlet NO concentration, $p_{NO}$ is the partial pressure of NO in the gas, and $H$ is the constant for solubility of NO in the water. The experiments were performed at several $p_{NO}$ to calculate $n$ and $K$, and at several temperatures to evaluate enthalpy and entropy of the reaction (Table 1).

Littlejohn and Chang[4] have recently determined the equilibrium constant for the coordination of NO to $Fe^{2+}(H_2O)_6$, $Fe^{2+}$(citrate), and $Fe^{2+}(acac)_2$, using a temperature-jump approach (Table 1) similar to that described by Czerlinski and Eigen.[7]

The reciprocal of the relaxation time obtained from the temperature-jump system equals the forward rate constant times the sum of the final equilibrium concentrations of $Fe^{2+}(L)$ and NO plus the backward rate constant.[7] When the reciprocal of the relaxation

*This work was supported by the Morgantown Energy Technology Center under Contract No. 81MC14002 through the Assistant Secretary of Fossil Energy of the U.S. Department of Energy under Contract No. DE-AC03-76SF00098.

Table 1. Kinetic and thermodynamic data for reversible NO coordination to ferrous chelates.

| Ferrous chelates | $k_1$ (moles/lit-sec) | $k_{-1}$ ($sec^{-1}$) | $K$ (liter/mole at 298°K) | $H$ (kcal/mole) | S (e.u) |
|---|---|---|---|---|---|
| $Fe^{2+}(H_2O)_5(NO)$ | $(7.1 \pm 1.0) \times 10^5$ | $(1.5 \pm 0.6) \times 10^3$ | $(4.7 \pm 2.0) \times 10^2$ | | |
| $Fe^{2+}$(citrate)(NO) | $(4.4 \pm 0.8) \times 10^5$ | $(6.6 \pm 2.4) \times 10^2$ | $(6.7 \pm 2.0) \times 10^2$ | | |
| $Fe^{2+}(acac)_2(NO)$ | $(4.0 \pm 3.0) \times 10^2$ | $24 \pm 2$ | $17 \pm 14$ | | |
| $Fe^{2+}$(NTA)(NO) | $\geq 7 \times 10^7$ | $\geq 35$ | $2.14 \times 10^6$ | -11.94 | -11.0 |
| $Fe^{2+}$(EDTA)(NO) | $\geq 6 \times 10^7$ | $\geq 60$ | $1.15 \times 10^7$ | -15.8 | -20.7 |

time is plotted against the final concentrations of $Fe^{2+}(L)$ + NO, the slope of the curve gives the forward rate constant ($k_1$) and the point of interception gives the backward rate constant ($k_{-1}$).

A comparison of the equilibrium constants of the reactions listed in Table 1 makes it obvious that $Fe^{2+}$(EDTA) and $Fe^{2+}$(NTA) have much larger absorption capacities for NO than do $Fe^{2+}(H_2O)_5$, $Fe^{2+}$(citrate), or $Fe^{2+}(acac)_2$. For an aqueous scrubbing solution initially containing 0.1 mole/liter $Fe^{2+}$(NTA) at 50°C, $\mu$ = 0.1 mole/liter, the fraction of the iron chelate that is converted to $Fe^{2+}$(NTA)(NO) is about 36% when the solution is in equilibrium with a gas containing 1000 ppm NO at one atmosphere. For a gas containing 100 ppm NO, the conversion is about 5%. Thus, the presence of the iron chelate increases the capacity of the scrubbing solution for NO by a factor of 30,000 or more.

*Kinetics*

With the temperature-jump technique, Littlejohn and Chang,[4] directly measured the formation and dissociation rate constants of $Fe^{2+}(H_2O)_5NO$, $Fe^{2+}$(citrate)NO, $Fe^{2+}(acac)_2NO$, $Fe^{2+}$(EDTA)NO, and $Fe^{2+}$(NTA)NO (Table 1). The forward and reverse rate constants for the formation of $Fe^{2+}$(citrate)NO are somewhat smaller than the values for the $Fe^{2+}(H_2O)_5NO$ complex, while the equilibrium constant is larger. The kinetics for the formation and dissociation of the $Fe^{2+}(acac)_2NO$ complex are much slower than for any other complex studied.

For both $Fe^{2+}$(EDTA)NO and $Fe^{2+}$(NTA)NO, the relaxation times due to the temperature jump were too short to be measured. However, an upper limit of 10 microseconds was established for the relaxation times for both complexes. By using this value with the equilibrium constants determined for $Fe^{2+}$(EDTA)NO by Hishinuma et al.[5] and for $Fe^{2+}$(NTA)NO by Lin et al.,[6] the lower limits of forward and reverse rate constants were calculated (Table 1).

## Thermodynamic Equilibrium and Kinetics of $SO_2$ Absorption

*Thermodynamics*

Sulfur dioxide is moderately soluble in water; four major $S^{4+}$ species are produced after dissolution of $SO_2$ in aqueous solutions: $SO_2(aq)$, $HSO_3^-$, $SO_3^{2-}$, and $S_2O_5^{2-}$. The equilibrium concentrations of these $S^{4+}$ species depend on both the partial pressure of $SO_2$ and the pH of the solution. The solubility coefficient of $SO_2$ is 1.24 mole/liter-atm at 25°C. Hydrated $SO_2$ can ionize to form bisulfite ion, $HSO_3^-$, which in turn can undergo further ionization to produce sulfite ion, $SO_3^{2-}$:

$$SO_2(g) + H_2O \rightleftarrows SO_2(aq) \quad (4)$$

$$SO_2(aq) \rightleftarrows H^+ + HSO_3^- \quad (5)$$

($K = 1.27 \times 10^{-2}$ mole/liter at 25°C)

$$HSO_3^- \rightleftarrows H^+ + SO_3^{2-} \quad (6)$$

($K = 6.24 \times 10^{-8}$ mole/liter at 25°C)

Bisulfite ion is also in equilibrium with the disulfite ion, $S_2O_5^{2-}$:

$$2HSO_3^- \rightleftarrows S_2O_5^{2-} + H_2O \quad (7)$$

($K = 7 \times 10^{-2}$ liter/mole at 25°C)

*Kinetics*

Dissolution of $SO_2$ can be expressed by Reactions (4)–(7). Reaction (5) proceeds very fast, as can be seen from the rate constant ($k_3$) and reverse rate constant ($k_{-3}$) measured by Eigen et al.[8] using a relaxation technique: $k_3 = 3.4 \times 10^6$ sec$^{-1}$ and $k_{-3} = 2.0 \times 10^8$ mole/liter-second at 20°C.

## Regeneration Rate of Metal Chelate Catalysts

We have started to investigate the reaction kinetics between $Fe^{2+}$(NTA)NO and sodium sulfite/bisulfite as a model for the reactions of $SO_2$-NO-metal chelates in aqueous solutions. The reaction can be expressed as follows:

$$a\ NO + Fe^{2+}(NTA) \rightleftarrows Fe^{2+}(NTA)(NO)_a \quad (8)$$

$$Fe^{2+}(NTA)(NO)_a + b\ SO_3^{2-} \quad (9)$$

$$\rightleftarrows Fe^{2+}(NTA) + c\ N_2O + d\ N_2$$

$$+ e\ \text{N–S complexes} + f\ SO_4^{2-}$$

The experiments were performed under $O_2$-free conditions to avoid oxidation of $Fe^{2+}$, NO, and $S^{4+}$. The concentration of $Fe^{2+}$(NTA)NO was monitored by visible-absorption spectrometry during the course of the reaction. A spectrum of the $Fe^{2+}$(NTA)NO complex is shown in Fig. 1 and has been found to obey Beer's law over the concentration range ($10^{-4}$ mole/liter to $10^{-3}$ mole/liter) employed in the experiments. The rate of disappearance of $Fe^{2+}$(NTA)NO in the presence of $SO_3^{2-}$ or $HSO_3^-$ has been found to have a second-order dependence on the concentration of $Fe^{2+}$(NTA)NO and a first-order dependence on the concentration of $SO_3^{2-}$ or $HSO_3^-$. The rates can be expressed as follows:

$$\frac{-d[Fe^{2+}(NTA)NO]}{dt} = (k_7[SO_3^{2-}] + k_7'[HSO_3^-])\,[Fe^{2+}(NTA)NO]^2 \quad (10)$$

Tentative values for $k_7$ and $k_7'$ have been obtained. At pH 8.0, $k_7 = 3.16 \times 10^3$ (liter/mole)$^2$/sec; and at pH 3.5, $k_7' = 4.3 \times 10^2$ (liter/mole)$^2$/sec. These values were obtained at 20°C. The dependence of the reaction rate on ionic strength at conditions near neutral pH was found to be negligible.

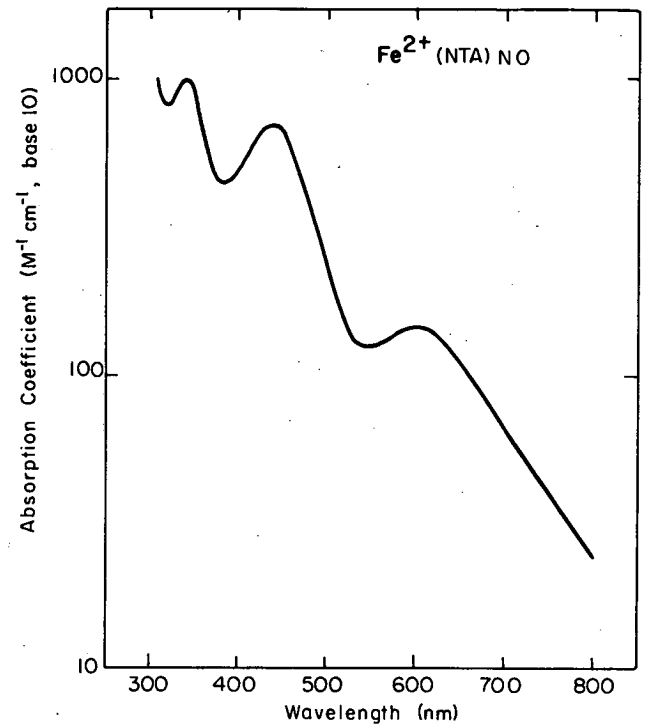


Figure 1. An absorption spectrum of $Fe^{2+}$(NTA)NO from 800 to 300 nm. (XBL 816-5927)

## Identification of Reaction Products

The intermediate and final products that can be formed from the reaction of $SO_2$, NO, and ferrous chelates in aqueous solutions have not yet been well characterized, although a few compounds such as $SO_4^{2-}$, $N_2O$, and some N–S complexes (sulfamate[9] and amine disulfonate[1,2]) have been found. It is necessary to identify such intermediate and final products so that reaction kinetics and mechanisms can be characterized and, from this knowledge, an optimum stack gas scrubber developed. To this end, we have begun to develop analytical techniques so that species can be directly, rapidly, and quantitatively determined and the mass balances of the reactions between nitrosyl metal chelates and $SO_2$ in aqueous solutions performed. Laser Raman spectroscopy appears to have the potential to identify the species present in mixtures of $SO_2$, NO, and metal chelates efficiently and unambiguously.

The first step in the identification process is to acquire Raman spectra[10] of potential reaction products so that the relative scattering efficiencies and

Raman shifts will be known. The species studied to date, along with their Raman shifts and scattering efficiencies relative to sulfate ion, are shown in Table 2.

Laser Raman spectroscopy has been used to detect the products of the reactions of $Fe^{2+}(NTA)NO$ with sulfite ion and $Fe^{2+}(H_2O)_5NO$ with bisulfite ion. Figures 2(a) and 2(b) are Raman spectra of amine disulfonate (ADS) and sulfamate (SFA) respectively. Sulfate ion was added to the solutions as a reference so that the relative scattering efficiencies could be obtained. The ADS peak is at 1084 $cm^{-1}$, the SFA peak is at 1049 $cm^{-1}$, and the $SO_4^{2-}$ peak is at 981 $cm^{-1}$.

Figure 2(c) is a spectrum of a solution with initial concentrations of 0.037 mole/liter $Fe^{2+}(H_2O)_5NO$ and 0.19 mole/liter bisulfite ion at pH ~4. The 985 $cm^{-1}$ sulfate peak is from the ferrous sulfate used to prepare the solution and the sulfate created as a reaction product. The peak due to ADS is apparent at 1087 $cm^{-1}$. The peak at 1052 $cm^{-1}$ could be from both SFA and disulfite ions. The species responsible for some of the other peaks present, such as the 1245 and 1280 $cm^{-1}$ peaks, have not yet been identified. The solution is colorless after the completion of the reaction. The 488 nm $Ar^+$ laser line was used to obtain the spectra.

Figure 2(d) is a spectrum of $Fe^{2+}(NTA)NO$ and sulfite ion at pH 8.3, with initial concentrations of

Table 2. Raman shifts and scattering efficiencies of some species relative to sulfate ion.

| Compound | Raman shift ($cm^{-1}$) | Relative scattering efficiency ($SO_4^{2-}$ = 1.00) |
|---|---|---|
| $SO_4^{2-}$ | 985 | 1.00 |
| $SO_3^{2-}$ | ~970 | 0.067 |
| $NO_2^-$ | 818/1332 | 0.0235/0.055 |
| $NO_3^-$ | 1050 | 0.42 |
| $N_2O$ | 1285 | 0.08 |
| $HN(SO_3)_2^{2-}$(ADS) | 1087 | 0.025 |
| $H_2NSO_3^-$(SFA) | 1052 | 0.18 |

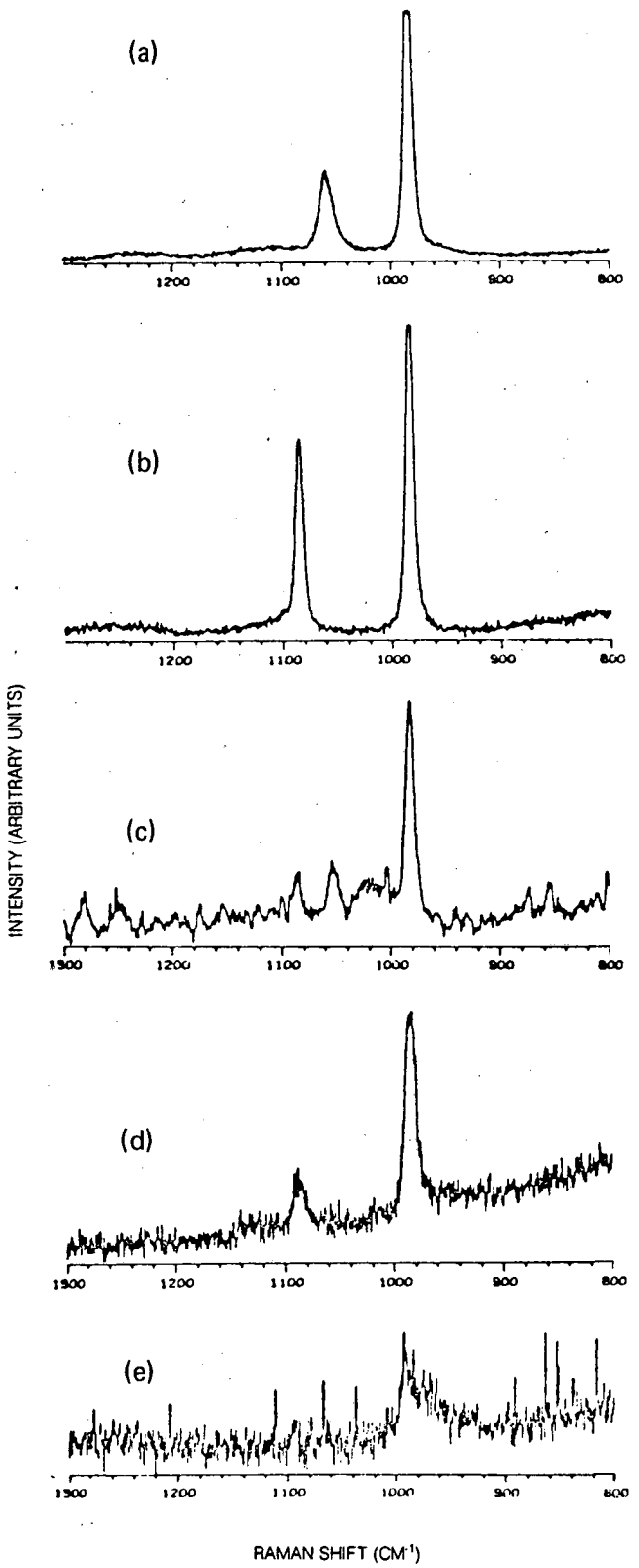


Figure 2. Raman spectra of (a) sulfamates(SFA), (b) aminedisulfonates (ADS), and reaction mixtures of (c) $Fe^{2+}(H_2O)_5NO$ with $HSO_3^-$, and (d) and (e) $Fe^{2+}(NTA)NO$ with $HSO_3^-$ and $SO_3^{2-}$, respectively. (XBL 835-9685)

0.043 mole/liter and 0.100 mole/liter, respectively. Additional sulfate ion was added to the solution at the time of mixing, making a total of 0.091 mole/liter sulfate added to the solution. The peak due to ADS is prominent at 1087 $cm^{-1}$. Since the solution is basic, ADS will not be rapidly hydrolyzed to form SFA. The reacted solution absorbs strongly in the blue region of the spectrum, so the 647 nm $Kr^+$ laser line was used for this spectrum.

Figure 2(e) is a spectrum of an initial concentration of 0.012 mole/liter $Fe^{2+}$(NTA)NO and 0.100 mole/liter sulfite ion at pH ~7. The 985 $cm^{-1}$ sulfate peak overlaps with the broader sulfite peak centered at 970 $cm^{-1}$. The peaks ascribed to ADS and SFA are weak but visible at 1087 and 1052 $cm^{-1}$. While the reacted solution does absorb in the blue region of the spectrum, the absorption is sufficiently weak to allow the 488 nm $Ar^+$ laser line to be used. The sharp spikes in the spectrum are due to noise in the laser output.

## Implications for Scrubber Design

The results of these studies show the technical feasibility of designing and operating a scrubber capable of removing both $NO_x$ and $SO_x$ well enough to meet national air quality standards.

*NO Removal*

The data given in Table 1 show that $Fe^{2+}$ chelated by either NTA or EDTA reacts rapidly with NO under scrubber conditions. A large fraction of the iron chelate is converted to the nitrosyl complex when equilibrated with NO at concentrations commonly found in stack gases. The rate constant for forming NO complexes is so large that for either chelating agent the reaction is effectively instantaneous. Since NTA costs less per pound than EDTA and has a lower molecular weight, it appears to be the agent of choice at this time.

*$SO_2$ Removal*

The reaction between the NO complexes and $HSO_3^-$ is too slow to affect the rate of absorption of $SO_2$. One must, instead, depend upon the buffering capacity of the solution for absorbing $SO_2$, and upon subsequent reaction for removing it from the solution. As shown in Table 3, the pH of the solution in the scrubber is thus advantageously kept in the range of 5 to 7. However, examination of the acid constants of NTA[11] ($pK_{a_1}$ = 1.97; $pK_{a_2}$ = 2.57; and $pK_{a_3}$ = 9.81) shows that the NTA cannot provide buffering in this pH range. The buffering must, therefore, be provided by adding some other soluble base to the scrubbing solution. Ammonia, sodium carbonate, sodium citrate and sodium phosphate are examples of bases that may be useful.

*Solution Regeneration*

To be economically attractive, a scrubbing solution must be regenerable with little or no loss of active ingredients. For a scrubbing solution containing $Fe^{2+}$(NTA) together with an appropriate buffer, regeneration will be a complex process. Neumann and Lynn[12] have shown that $Fe^{2+}$(NTA) reacts rapidly with oxygen to form $Fe^{3+}$(NTA). The fraction of $Fe^{2+}$ oxidized will depend on the $O_2$ content of the flue gas. Besides removing the absorbed NO and $SO_2$, the regeneration must then reduce the $Fe^{3+}$ back to $Fe^{2+}$. Lynn and Dubs[13] found that $H_2S$ reacts stoichiometrically with $Fe^{3+}$(NTA) to form $Fe^{2+}$(NTA) and elemental sulfur in the pH range 3.5 to 4.5. When the pH of the solution is above 7.0, some thiosulfate and polythionates may be formed. Neumann and Lynn[12] showed that the rate of the absorp-

Table 3. Equilibrium concentration of sulfites (mole/liter) at $P_{SO_2}$ = 100 ppm at 25°C.

| Sulfites | pH 7 | pH 6 | pH 5 | pH 4 | pH 3 |
|---|---|---|---|---|---|
| $SO_2 \cdot H_2O$ | $1.24 \times 10^{-3}$ | $1.24 \times 10^{-3}$ | $1.24 \times 10^{-3}$ | $1.24 \times 10^{-3}$ | $1.24 \times 10^{-3}$ |
| $HSO_3^-$ | $1.58 \times 10^{+2}$ | $1.58 \times 10^{+1}$ | 1.58 | $1.58 \times 10^{-1}$ | $1.58 \times 10^{-2}$ |
| $SO_3^-$ | $9.82 \times 10^{+1}$ | $9.82 \times 10^{-1}$ | $9.82 \times 10^{-3}$ | $9.82 \times 10^{-5}$ | $9.82 \times 10^{-7}$ |
| $S_2O_5^=$ | $1.75 \times 10^{+3}$ | $1.75 \times 10^{+1}$ | $1.75 \times 10^{-1}$ | $1.75 \times 10^{-3}$ | $1.75 \times 10^{-5}$ |

tion of $H_2S$ by $Fe^{3+}$(NTA) solution indicated the rate of reaction to be effectively instantaneous in the pH range 3.5 to 4.5. Absorption rates and reaction products in the pH range 5 to 7 must still be determined.

Several methods are available for removing the absorbed $SO_2$ from the scrubber liquid during regeneration. One approach is to add lime and precipitate a mixture of $CaSO_3$ and $CaSO_4$. This would require technology similar to that used in the various double-alkali processes for $SO_2$ scrubbing. Thorough washing of the precipitate to avoid excessive loss of scrubber-liquid chemicals would be required. A second approach is to react dissolved $SO_2$ with $H_2S$ to form elemental sulfur. The technology for this approach has been demonstrated in the citrate process of the U.S. Bureau of Mines and Stauffer Chemical's AquaClaus process. With this approach, a salable form of sulfur is produced, and costs may be reduced as a result. The reaction of $H_2S$ and $HSO_3^-$ in the presence of chelated iron compounds has not yet been studied.

## PLANNED ACTIVITIES FOR FY 1983

We plan to determine quantitatively the amounts of the observed products that are produced by the reactions of ferrous nitrosyl complexes with sulfite and bisulfite ions. We also plan to study the interaction of $H_2S$ with this system.

## REFERENCES


1. Yaverbaum, L.H. (1979), *Nitrogen Oxides Control and Removal, Recent Developments,* Noyes Data Corporation, Park Ridge, New Jersey.
2. Martin, A.E., Ed. (1981), *Emission Control Technology for Industrial Boilers,* Noyes Data Corporation, Park Ridge, New Jersey.
3. Chang, S.G., Littlejohn, D., and Lin, N.H. (1982), "Kinetics of Reactions in a Wet Flue Gas Simultaneous Desulfurization and Denitrification System," in *Flue Gas Desulfurization,* ACS Symposium Series 188, American Chemical Society, Washington, D.C.
4. Littlejohn, D., and Chang, S.G. (1982), "Kinetic Study of Ferrous Nitrosyl Chelates," *J. Phys. Chem. 86,* p. 537.
5. Hishinuma, Y., et al. (1979), "Reversible Binding of NO to Fe(II)EDTA," *Bull. Chem. Soc. Japan 52,* p. 2863.
6. Lin, N.H., Littlejohn, D., and Chang, S.G. (1982), "The Thermodynamics and Kinetics of the Coordination of $NO^{\prime}$ to $Fe^{+2}$(NTA) in Aqueous Solutions," *I&EC Process Res. Dev. 21,* p. 725.
7. Czerlinski, G., and Eigen, M. (1959), "Eine Temperatursprungmethode zur Untersuchung Chemischer Relaxation," *Z. Elektrochem. 63,* p. 652.
8. Eigen, M. (1961), "Investigation on Rapid Reactions by Means of Relaxation Spectrometry," *Suomen Kemistilekti 34A,* p. 25.
9. Sawai, K. and Gorai, T. (1976), "Simultaneous Removal of Sulfur Dioxide and Nitrogen Oxides from Flue Gases by the CEC Method," *Kyusan to Kogyo,* p. 187.
10. Littlejohn, D., and Chang, S.G., (1982), "Identification of Species in a Wet Flue Gas Desulfurization and Denitrification System by Laser Raman Spectroscopy," submitted for publication in *Environ. Sci. Tech.*, Lawrence Berkeley Laboratory Report LBL-14756.
11. Pietrezyk, D.J., and Frank, C.W. (1974), *Analytical Chemistry,* Academic Press, New York, p. 453.
12. Neumann, D.W., and Lynn, S. (1981), "Oxidative Absorption of $H_2S$ and $O_2$ by Iron Chelate Solutions," presented at the AIChE Annual Meeting, New Orleans, and submitted for publication to *AIChE Journal.*
13. Lynn, S., and Dubs, B.J.-L., U.S. Patent No. 4,278,646, July 1981.


# THE REACTION OF FERROUS NITROSYL COMPLEXES WITH SULFITE AND BISULFITE IONS*


*D. Littlejohn, E. Griffiths, and S.G. Chang*


Untreated flue gases from coal-fired power plants contain substantial amounts of sulfur dioxide ($SO_2$) and nitrogen oxides ($NO_x$). A number of control strategies are being developed to reduce the concentrations of these pollutants to acceptable levels.[1] Since $SO_2$ is fairly soluble in water, it can be effectively removed by scrubbing the flue gases with aqueous


*This work was supported by the Morgantown Energy Technology Center under Contract No. 81MC14002 through the Assistant Secretary of Fossil Energy of the U.S. Department of Energy under Contract No. DE-AC03-76SF00098.

solutions. Nitric oxide (NO) is the major constituent of nitrogen oxides; the rest of the $NO_x$ consists mainly of nitrogen dioxide ($NO_2$). While $NO_2$ is readily dissolved in aqueous solutions, NO is relatively insoluble. One promising technique for enhancing the solubility of NO is to use ferrous chelates to form ferrous nitrosyl complexes in aqueous solutions.

A scrubbing process based on this procedure must be able to regenerate the ferrous chelate so that it may absorb more NO. One method of regeneration is to react the ferrous nitrosyl compound with the dissolved $SO_2$, which exists as bisulfite ($HSO_3^-$) and sulfite ($SO_3^=$) ions, depending on the pH of the solution.[2] These ions will be referred to collectively as S(IV). The behavior of this reaction needs to be known so that a scrubber based on this method can be properly designed.

## ACCOMPLISHMENTS DURING FY 1982

We have begun a systematic study of the reaction of ferrous nitrosyl complexes with S(IV) and have obtained a preliminary rate expression. We have also identified the major products of the reaction.

### Kinetic Studies

The ferrous nitrosyl complexes were prepared under oxygen-free conditions.[3] Concentrations of the complexes were determined spectrophotometrically. Solutions of the ferrous nitrosyl complexes were mixed with degassed solutions of S(IV) ions. After mixing, the concentration of the complexes was monitored over time, using its visible absorption band. Solutions were prepared such that the concentration of S(IV) was much greater than that of the ferrous nitrosyl complex. Most of the work has involved the two complexes that bind NO most efficiently: Fe(II)(NTA)NO[4] and Fe(II)(EDTA)NO.[5] Kinetic studies have been done at 25°C for Fe(II)(NTA)NO, and at 25°C and 55°C for Fe(II)(EDTA)NO. Analysis of the kinetic data was done using values of the change with time in [Fe(II)(L)NO] (L representing the chelate in use), $dc/dt$, obtained from the initial decay of the ferrous nitrosyl complex.

### Determination of Reaction Products

Gaseous products of the reaction were analyzed by gas chromatographic and mass spectrometric techniques. The solutions containing the reaction mixture were kept in a sealed container under an argon atmosphere. Gas samples were withdrawn after allowing the reaction to go to completion and permitting the solution to equilibrate with the gas above it.

Other products remaining in solution were measured either spectrophotometrically or by laser Raman spectroscopy (LRS). Not all of the product compounds can be easily determined by spectrophotometric methods. The major limitations of LRS are its relatively low sensitivity and the difficulty of working with strongly colored solutions. Practically all product compounds can be determined by LRS, however, if their concentrations are sufficiently high.[6]

## Results and Discussion

### *Kinetic Results*

Values of *dc/dt* obtained from experiments were used to obtain rate information on the reaction. Figure 1 illustrates the dependence of the reaction rate on the pH of the solution containing Fe(II)(NTA)NO + S(IV). The data were obtained from experiments using [Fe(II)(NTA)NO] at $2.5 \times 10^{-4}$ *M* and [S(IV)] at $\sim 4 \times 10^{-2}$ *M*. The decrease in rate at pH below 3 is attributed to two factors: the decreasing fraction of S(IV) in the form of $HSO_3^-$, and the decreasing ability of Fe(II)(NTA) to bind with NO.[4] The increase in rate around pH 6 is due to the increasing fraction of S(IV) as $SO_3^=$. The cause of the decrease in rate above pH 7 is currently not well understood, but may be due to $OH^-$ complexing with Fe(II)(NTA)NO and inhibiting the reaction.

Plots of log ($dc/dt$) vs. log (S(IV)) have been used to determine the rate dependence on S(IV). Within the accuracy of our results, we find first order dependence on S(IV) throughout the pH range of 4 to 8.

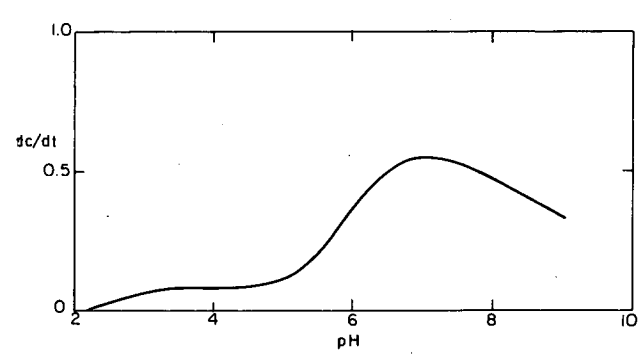


Figure 1. Dependence of reaction rate ($dc/dt$) on pH for [Fe(II)(NTA)NO] $\approx 2.5 \times 10^{-4}$ *M* and [S(IV)] $\approx 4 \times 10^{-2}$ *M*.

(XBL 832-5298)

This is true for both ferrous nitrosyl complexes. This appears to be valid over a S(IV) range of 0.01 to 0.1 *M* when [S(IV)] > [Fe(II)(L)NO].

Plots of log $(dc/dt)$ vs. log (Fe(II)(L)NO) were used to determine the dependence of the reaction rate on the ferrous nitrosyl complex concentration. A representative plot is shown in Fig. 2. At high pH conditions where $SO_3^{=}$ is the only S(IV) species, there is a first order dependence on Fe(II)(L)NO over a concentration range of $10^{-3}$ *M* to $10^{-4}$ *M*. Above $10^{-2}$ *M* in Fe(II)(L)NO concentration, the dependence appears to approach zero order. At low pH conditions, where $HSO_3^-$ is the only S(IV) species, there appears to be zero order dependence on Fe(II)(L)NO at all concentrations studied ($10^{-4}$ *M* to $10^{-2}$ *M*).

A study done on ionic strength dependence at pH 7, where both $HSO_3^-$ and $SO_3^{=}$ are present, found no dependence on ionic strength over the range of $\mu$ = 0.01 to $\mu$ = 1.0.

From our results, we have obtained the following rate expressions:

Fe(II)(NTA)NO at 25°C:

$$\{d[\text{Fe(II)(NTA)NO}]\}/dt = 1.2 \times 10^{-5}\ \text{sec}^{-1}[HSO_3^-] + 0.13 M^{-1}\text{sec}^{-1}[\text{Fe(II)(NTA)NO}][SO_3^-]$$

(valid for pH ≈ 3 to 8, [Fe(II)(NTA)NO] ≈ $10^{-4}$ to $10^{-3}$ *M*, [S(IV)] ≈ 0.01 to 0.1 *M*).

Fe(II)(EDTA)NO:

$$\{-d[\text{Fe(II)(EDTA)NO}]\}/dt = k_1[HSO_3^-] + k_2[\text{Fe(II)(EDTA)NO}][SO_3^{=}]$$

where $k_1$ at 25°C = $5.62 \times 10^{-5}$ sec$^{-1}$, and $k_2$ at 25°C = 0.175 $M^{-1}$ sec$^{-1}$; $k_1$ at 55°C = $9.00 \times 10^{-5}$ sec$^{-1}$, and $k_2$ at 55°C = 0.60 $M^{-1}$ sec$^{-1}$. (pH range ≈ 4 to 8.5, [Fe(II)(EDTA)NO] = $10^{-4}$ to $10^{-3}$ *M*, [S(IV)] $10^{-3}$ to $10^{-1}$ *M*.)

*Reaction Products*

Nitrous oxide ($N_2O$) and nitrogen gas ($N_2$) were found to be among the major nitrogen-containing products of the reaction of ferrous nitrosyl complexes with S(IV). Nitrous oxide was analyzed by both gas chromatographic and mass spectrometric techniques, and $N_2$ was analyzed by mass spectrometry alone.

The fraction of nitrogen that is NO converted to $N_2O$ is affected by pH and the concentration of the ferrous nitrosyl complex. Figure 3 shows the pH dependence for $N_2O$ production for [Fe(II)(NTA)NO] < $5 \times 10^{-3}$ *M* when reacted with excess S(IV). The fraction of $N_2O$ produced decreases as the

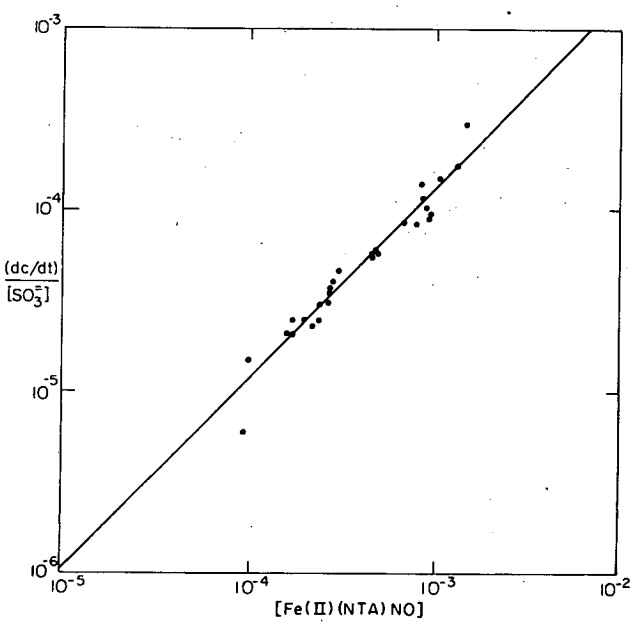


Figure 2. Reaction rate dependence on Fe(II)(NTA)NO: log $\{(dc/dt)/[SO_3^{=}]\}$ vs. log {[Fe(II)(NTA)NO]} at pH ≥ 8. Slope = 1.06 ± 0.05.

(XBL 832-5297)

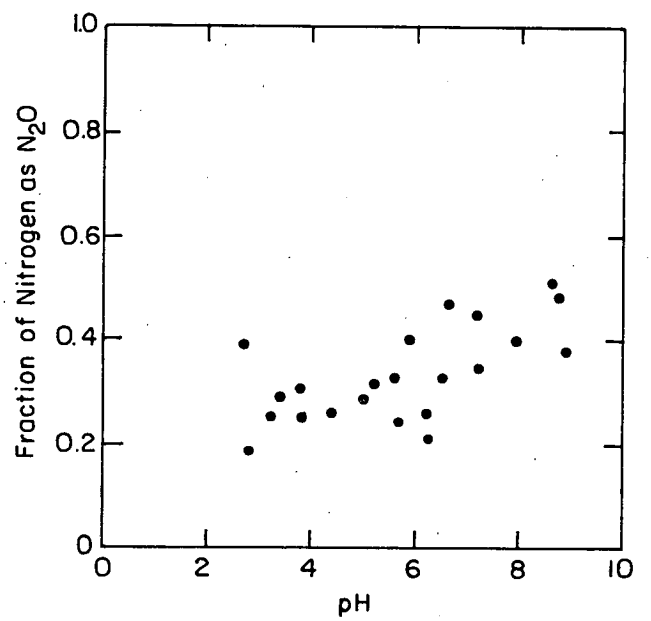


Figure 3. pH dependence on $N_2O$ production for reaction of Fe(II)(NTA)NO + S(IV). [Fe(II)(NTA)NO] < $5 \times 10^{-3}$ *M*.

(XBL 823-5380)

Fe(II)(NTA)NO concentration is raised above this level. Similar behavior is observed for Fe(II)(EDTA)NO.

Nitrogen gas appears to be an important nitrogen-containing product, although the effects of pH and concentration on its production have not yet been determined. Its concentrations have been found to be much higher than those of $N_2O$ at the Fe(II)(NTA)NO concentrations estimated to occur in this type of scrubber.

Hydroxylamine disulfonate (HADS) was found to be another reaction product. HADS can react with S(IV) and can hydrolyze to form other compounds.[2] HADS determinations were made by LRS and by oxidation of HADS to nitrosodisulfonate (NDS), which can be measured by its optical absorption.[7] A limited number of measurements on HADS indicate that it and the compounds it forms in the reaction mixture also contain a substantial fraction of the nitrogen originally in the form of NO.

Sulfate ion ($SO_4^{=}$) appears to be the major product into which S(IV) is converted. It has been observed by LRS and by wet analytical methods.

Spectra taken several days after mixing Fe(II)(L)NO with S(IV) under alkaline conditions show the appearance of the characteristic spectra of Fe(III)(NTA)$OH^-$ and Fe(III)(EDTA)$OH^-$.[8] This indicates that Fe(II) is slowly being oxidized to Fe(III). The reaction continues to occur long after the primary reaction has gone to completion. The oxidizing agent has not yet been identified.

From studies of reactions of similar compounds[9,10] and knowledge of the reaction products, a tentative reaction scheme can be proposed:

$$\text{Fe(II)(L)NO} + \text{S(IV)} \rightarrow \text{ONSO}_3^{=} + \text{Fe(II)(L)}$$

$$\text{Fe(II)(L)NO} \rightleftarrows \text{Fe(II)(L)} + \text{NO}$$

$$\text{NO} + \text{S(IV)} \rightarrow \text{ONSO}_3^{=}$$

$$\text{NO} + \text{ONSO}_3^{=} \rightarrow {}^{-}\text{ON(NO)SO}_3^{-}$$

$$\text{S(IV)} + \text{ONSO}_3^{=} \rightarrow \text{HADS}$$

$$\text{ONSO}_3^{=} + \text{H}_2\text{O} \xrightarrow{\text{H}^+} \text{NOH} + \text{HSO}_4^{-} \quad \text{(see Ref. 11)}$$

$$\text{NOH} + \text{NOH} \rightarrow \text{H}_2\text{N}_2\text{O}_2 \quad \text{(see Ref. 11)}$$

$${}^{-}\text{ON(NO)SO}_3^{-} \xrightarrow{\text{H}^+} \text{N}_2\text{O} + \text{SO}_4^{=}$$

$$\text{H}_2\text{N}_2\text{O}_2 \xrightarrow{\text{H}^+} \text{N}_2\text{O} + \text{H}_2\text{O}$$

$$\text{H}_2\text{N}_2\text{O}_2 \rightarrow \text{N}_2 + 2\text{OH} \quad \text{(see Ref. 10)}$$

Not included in this scheme are reactions in which HADS is converted into other nitrogen-sulfur compounds. These are discussed in detail elsewhere.[2]

## PLANNED ACTIVITIES FOR FY 1983

We plan to extend the range of concentrations of S(IV) and Fe(II)(L)NO under study to develop a more complete rate expression. A mass balance for the nitrogen-containing products will be made, and the factors influencing the relative amounts of these compounds will be determined. With this knowledge, it will be possible to develop an efficient system for simultaneous desulfurization and denitrification of power-plant flue gases.

## REFERENCES


1. Yaverbaum, L.H. (1979), "Nitrogen Oxides Control and Removal, Recent Developments," Noyes Data Corp., Park Ridge, New Jersey.
2. Chang, S.G., Littlejohn, D., and Lin, N.H. (1982), "Kinetics of Reactions in a Wet Flue Gas Simultaneous Desulfurization and Denitrification System," in *Flue Gas Desulfurization,* ACS Symposium Series 188, American Chemical Society, Washington, D.C.
3. Littlejohn, D. and Chang, S.G., (1982), "Kinetic Study of Ferrous Nitrosyl Complexes," *J. Phys. Chem. 86,* p. 537.
4. Lin, N.H., Littlejohn, D., and Chang, S.G. (1982), "Thermodynamics and Kinetics of the Coordination of NO to Fe(II)NTA in Aqueous Solutions," *I & EC Proc. Design Dev. 21,* p. 725.
5. Hishinuma, Y., et al. (1979), "Reversible Binding of NO to Fe(II)EDTA," *Bull. Chem. Soc. Japan 52,* p. 2863.
6. Littlejohn, D., and Chang, S.G. (1983), "Identification of Species in a Wet Flue Gas Desulfurization and Denitrification System by Laser Raman Spectroscopy," submitted to *Environ. Sci. Tech.*
7. Oblath, S.B. (1981), *Kinetics of the Reduction of Nitrite Ion by Sulfur Dioxide in Aqueous Solution,* Ph.D. Thesis, Chemistry Department, University of California, Berkeley.
8. Jones, S.S., and Long, F.A. (1952), "Complex

Ions From Iron and Ethylenediaminetetraacetate: General Properties and Radioactive Exchange," *J. Phys. Chem. 56,* p. 25.
9. Nunes, T.L., and Powell, R.E. (1970), "Kinetics of the Reaction of Nitric Oxide with Sulfite," *Inorg. Chem. 9,* p. 1916.
10. Buchholz, J.R., and Powell, R.E., (1963), "The Decomposition of Hyponitrous Acid. I. The Non-Chain Reaction," *J. Amer. Chem. Soc. 85,* p. 509.
11. Oblath, S.B., Markowitz, S.S., Novakov, T., and Chang, S.G. (1982), "Kinetics of the Initial Reaction of Nitrite Ion in Bisulfite Solutions," *J. Phys. Chem. 86,* p. 4853.

## IDENTIFICATION OF SPECIES IN A WET FLUE GAS DESULFURIZATION AND DENITRIFICATION SYSTEM BY LASER RAMAN SPECTROSCOPY*

*D. Littlejohn and S.G. Chang*

Several wet processes[1,2] for simultaneous removal of $SO_2$ and $NO_x$ from power-plant flue gases are based on injecting a gaseous oxidant such as $O_3$ into the flue gas to selectively oxidize the relatively insoluble NO to the more soluble $NO_2$. The flue gas is subsequently passed to a $NO_2/SO_2$ absorber. The major fraction of the absorbed $NO_x$ in these processes has been found to be in the form of nitrogen-sulfur complexes,[1-8] which are the compounds produced in the reaction between nitrite and bisulfite ions.

Some of the reactions that can occur in this system are illustrated in Fig. 1. The intermediate species nitrosulfonic acid ($HO_3SNO$) has never been identified, but its existence has been inferred from the behavior of the nitrite ion–bisulfite ion reaction. Some of the compounds identified in the figure are abbreviated as follows: HADS for hydroxylamine disulfonate (disulfonic acid at low pH), HAMS for hydroxylamine monosulfonate, HA for hydroxylamine, ATS for amine trisulfonate (trisulfonic acid at low pH), ADS for amine disulfonate, and SA for sulfamic acid.

In studying these processes to determine an optimum design and operating condition for scrubbers, one problem is to detect quantitatively all the species present under a wide range of solution conditions. Our work is intended to overcome this difficulty.

*This work was supported by the Morgantown Energy Technology Center under Contract No. 81MC14002 through the Assistant Secretary of Fossil Energy of the U.S. Department of Energy under Contract No. DE-AC03-76SF00098.

### ACCOMPLISHMENTS DURING FY 1982

Using laser Raman specrsocopy, we have investigated the reaction system of nitrite ions and bisulfite ions in aqueous solutions. The reaction products have been identified, and the effect of reactant concentrations and solution pH has been studied.

The Raman system has been described in detail elsewhere.[9] Spectra were obtained using the 488.0 nm argon ion laser line as the exciting light. Raman spectra were obtained for the reactants and potential reaction products. For most species, the relative molar intensity (RMI) was determined as follows:

$$\mathrm{RMI} = \frac{H_i/C_i}{(981\ \mathrm{cm}^{-1}\ H_{\mathrm{sulfate}})/(C_{\mathrm{sulfate}})}$$

where $H_i$ is the ion peak height, $C_i$ is the ion molarity, $H_{\mathrm{sulfate}}$ is the sulfate ion peak height, and $C_{\mathrm{sulfate}}$ is the sulfate ion molarity. The Raman shifts and relative molar intensities are given in Table 1.

The solutions containing the reaction mixtures of nitrite ions and bisulfite or sulfite ions were prepared in a vacuum line to prevent oxidation of the sulfur (IV) species to sulfate ion. The solutions were transferred to 8-mm-diameter Pyrex tubes under an argon atmosphere and sealed, after which Raman spectra were obtained. To investigate the nitrite ion–bisulfite ion reaction, four solutions with varying nitrite ion–bisulfite ion ratios were prepared. The initial pH of the solutions was about pH 4, and the initial concentrations were:

(A) 0.10 $M\ NO_2^-$ + 0.50 $M\ HSO_3^-$

(B) 0.26 $M\ NO_2^-$ + 0.50 $M\ HSO_3^-$

(C) 0.51 $M\ NO_2^-$ + 0.50 $M\ HSO_3^-$

(D) 1.02 $M\ NO_2^-$ + 0.50 $M\ HSO_3^-$

A solution containing 1.02 $M\ NO_2^-$ and 0.50 $M\ SO_3^=$ was also prepared at pH 10 for an investigation of the reaction at high pH conditions.

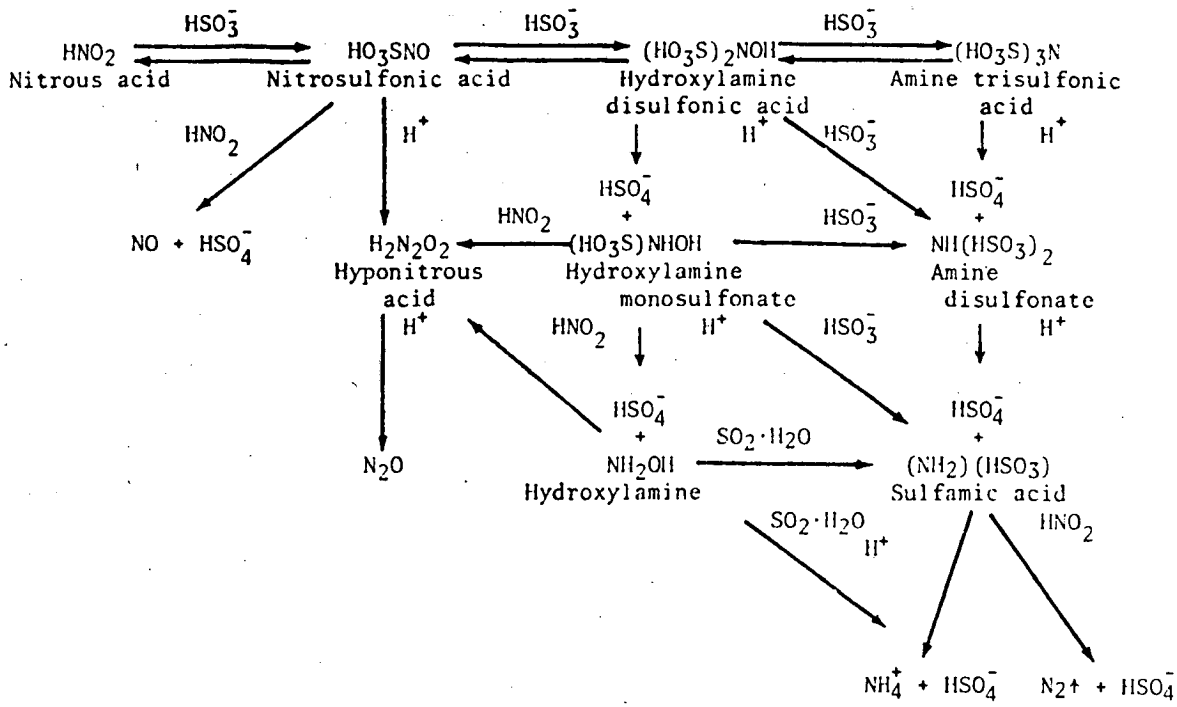


Figure 1. Reactions that occur in the nitrogen oxyacid–sulfur oxyacid system. (XBL 8112-13061)

## Results and Discussion

Raman spectra of the four nitrite ion–bisulfite ion solutions taken 24 hours after mixing are shown in Fig. 2. The spectrum of mixture A in Fig. 2(a) shows the presence of sulfite ion ($SO_3^=$) at 970 $cm^{-1}$ (the shoulder on the 980 $cm^{-1}$ peak), sulfate ion ($SO_4^=$) at 980 $cm^{-1}$, bisulfite ion ($HSO_3^-$) at 1025 $cm^{-1}$, disulfite ion ($S_2O_5^=$) at 1050 $cm^{-1}$, HADS at 1085 $cm^{-1}$, and ATS at 1100 $cm^{-1}$. Since bisulfite ion and disulfite ion exist in equilibrium in solution, the 1050 $cm^{-1}$ peak is attributed to disulfite ion, and not to nitrate ion. The spectrum of mixture B, shown in Fig. 2(b), is less complicated, with sulfite ion at 970 $cm^{-1}$, HADS at 1085 $cm^{-1}$, and ATS at 1100 $cm^{-1}$. Sulfate ion is much less prominent in the spectrum of mixture B. The spectra of mixtures C and D are similar to that of mixture B, except for increasingly strong nitrite bands at 820 $cm^{-1}$ and 1240 $cm^{-1}$ and an increasingly weak ATS band. The 1240 $cm^{-1}$ band of nitrite ion is broad and overlaps with the 1330 $cm^{-1}$ nitrite band.

Figure 2(a) shows that some of the bisulfite ion has been converted to sulfite ion. In Figs. 2(b), (c), and (d), all the bisulfite ion has been converted into sulfite ion. This is due to the reaction producing HADS:

$$NO_2^- + 2HSO_3^- \rightarrow (^-O_3S)_2NOH + OH^- \quad .$$

The occurrence of the hydrolysis reactions will cause a decrease in pH. For example, the hydrolysis of HADS and ATS produce $H^+$:

$$(^-O_3S)_2NOH + H_2O \rightarrow (^-O_3S)NHOH + SO_4^= + H^+ \quad ;$$

$$(^-O_3S)_3N + H_2O \rightarrow (^-O_3S)_2NH + SO_4^= + H^+ \quad .$$

The hydrolysis reactions in this reaction scheme are all hydrogen-ion catalyzed and are slower than the initial reaction between nitrite ion and bisulfite ion.

In mixture A, the nitrite ion–bisulfite ion ratio is much less than 1:2, the stoichiometry of the initial reaction to produce HADS. Under these conditions, the kinetics of the system will be considerably different than in mixtures B, C, and D. In this situation, the amount of HADS produced should be limited by the amount of nitrite ion present. Since bisulfite ion should remain after the nitrite ion has been consumed, it can react with HADS to produce ATS. There should be less hydroxyl ion produced than in the other mixtures, so that the hydrogen ion–catalyzed hydrolysis reactions should occur more rapidly. The relative amount of ATS in Fig. 3(a) is much larger than in the other spectra. Sulfate ion is

Table 1. Raman shifts and relative molar intensities of species studied in this investigation.

| Species | Raman shift ($cm^{-1}$) | Relative molar intensity[a] |
|---|---|---|
| $NO_2^-$ | 818 | 0.053 |
| | 1240 | ~0.025 |
| | 1331 | 0.125 |
| $NO_3^-$ | 1050 | 0.95 |
| $NO_2O_2^=$ | 692[b] | weak[b] |
| | 1115[b] | weak[b] |
| | 1383[b] | strong[b] |
| $N_2O$ | 1285 | ~0.18 |
| $SO_3^=$ | 967 | 0.12 |
| $HSO_3^-$ | 1023 | 0.10 |
| $SO_4^=$ | ~455 | ~0.07 |
| | 981 | 1.00 |
| $S_2O_5^=$ | 1055 | ~0.9 |
| $HSO_4^-$ | 1050 | 0.05 |
| HADS | ~700 | ~0.20 |
| | 1084 | 1.43 |
| HAMS | ~420 | ~0.13 |
| | ~760 | ~0.08 |
| | 1058 | 0.48 |
| HA (pH $\leq$ 7) | 1004 | 0.21 |
| HA (pH $\geq$ 9) | 918 | 0.09 |
| ATS | 1097 | 0.10 |
| ADS | 1084 | 0.056 |
| SA (pH $\leq$ 1) | 1063 | c |
| SA (pH $\geq$ 3) | 1049 | 0.41 |

[a]$SO_4^=$ $cm^{-1}$ line = 1.000.
[b]From Ref. 10.
[c]No value obtained.

produced only by the hydrolysis reactions, according to the reaction scheme in Fig. 1. The sulfate ion peak at 980 $cm^{-1}$ is much more prominent in Fig. 3(a) than in the other figures, indicating that more hydrolysis has occurred. Since no HAMS is apparent at 1060 $cm^{-1}$, the sulfate ion must be due to the hydrolysis of ATS to ADS. The 1085 $cm^{-1}$ peak is, therefore, due to both ADS and HADS.

The spectra of mixtures B, C, and D did not display much change with time since the hydrolysis reactions are fairly slow. The spectra of mixture A did change considerably; the change with time is shown in Fig. 3, over the range of 900 to 1300 $cm^{-1}$. The times after mixing and the number of scans for the spectra are: Fig. 3(a)—20 min. and 1 scan; Fig. 3(b)—2 hours and 1 scan; Fig. 3(c)—24 hours and 4 scans, Fig. 3(d)—105 days and 4 scans. In the first spectrum in Fig. 3(a), HADS is prominent at 1085 $cm^{-1}$. The presence of ATS is indicated by the peak at 1100 $cm^{-1}$, and $HSO_3^-$ and $S_2O_5^=$ are visible at 1025 and 1050 $cm^{-1}$. There is weak evidence for $SO_3^=$ and $SO_4^=$ at 960 and 980 $cm^{-1}$. In Fig. 3(b), the ATS and sulfate ion peaks have become more prominent. In Fig. 3(c), the ATS

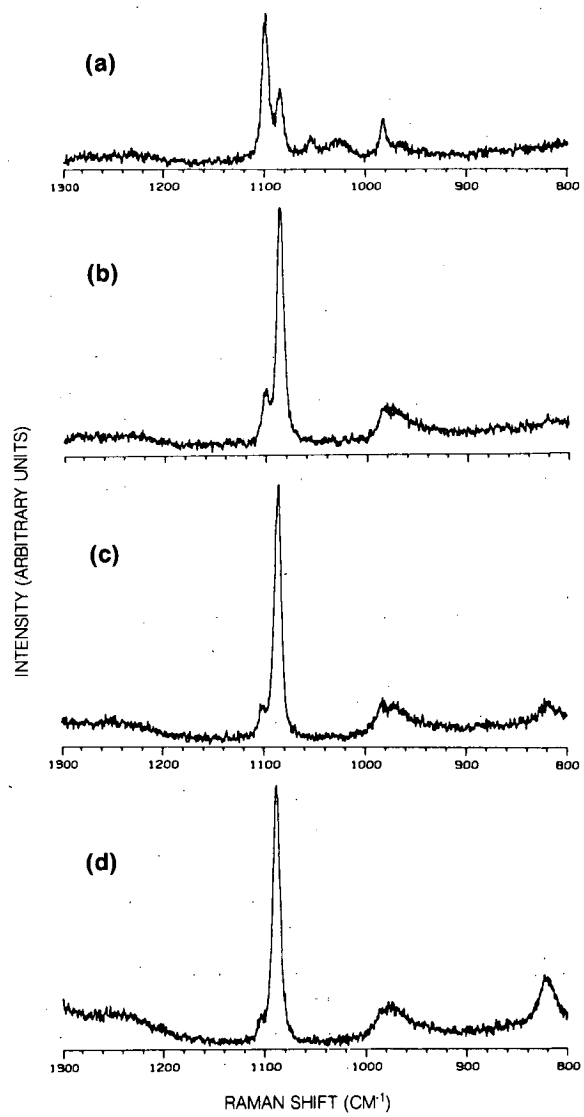


Figure 2. Raman spectra of nitrite ion–bisulfite ion mixtures taken 24 hours after mixing: (a) 0.10 $M$ $NO_2^-$ + 0.50 $M$ $HSO_3^-$; (b) 0.26 $M$ $NO_2^-$ + 0.50 $M$ $HSO_3^-$; (c) 0.51 $M$ $NO_2^-$ + 0.50 $M$ $HSO_3^-$; (d) 1.02 $M$ $NO_2^-$ + 0.50 $M$ $HSO_3^-$.
(XBL 828-10805)

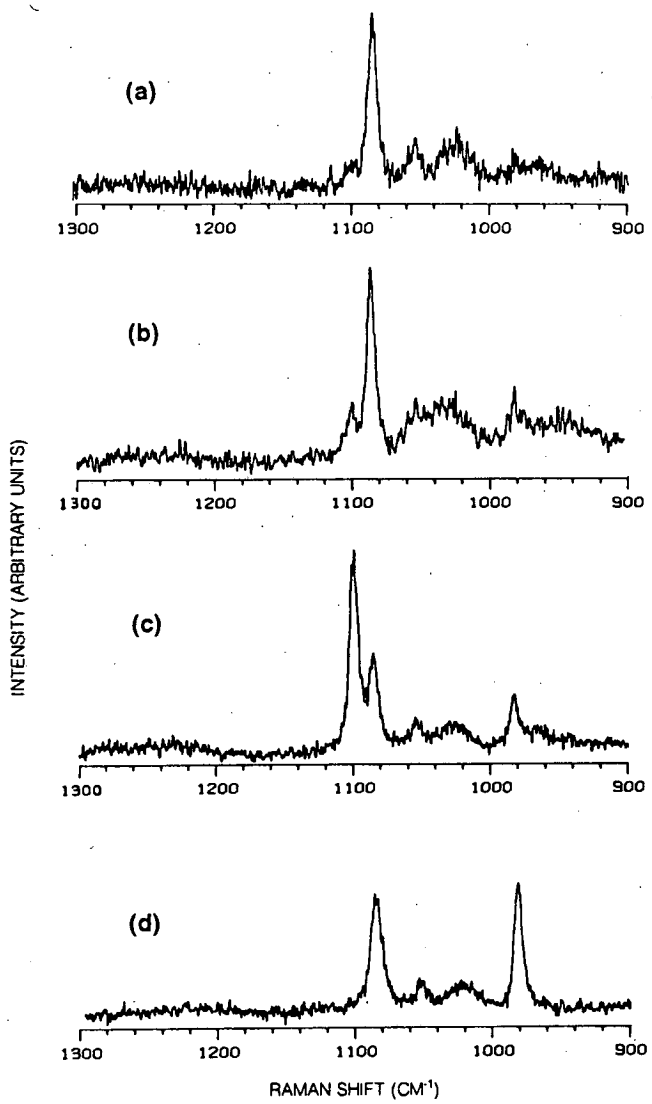


Figure 3. Raman spectra of 0.10 *M* nitrite ion–0.50 *M* bisulfite ion mixture: (a) 20 minutes after mixing; (b) 2 hours after mixing; (c) 24 hours after mixing; (d) 105 days after mixing. (XBL 828-10831)

peak is very prominent, the HADS/ADS peak is smaller, sulfate ion is larger, and sulfite ion is still present. In Fig. 3(d), the peak due to ATS is absent, the 1085-$cm^{-1}$ peak is due solely to ADS (because of the absence of the 700-$cm^{-1}$ HADS peak), and the 970-$cm^{-1}$ $SO_3^=$ peak is absent.

The chemistry occurring in mixture A is consistent with the reaction scheme shown in Fig. 1. The reaction producing HADS is fairly rapid and was essentially completed by the time the first spectrum was taken. The conversion of HADS to ATS has started as well. The second spectrum shows further conversion of HADS to ATS. Hydrolysis is also occurring as evidenced by the growth of the sulfate ion peak at 980 $cm^{-1}$. The size of the sulfite ion peak relative to the bisulfite ion peak has increased from Fig. 3(a), indicating that the solution has become more basic from the production of HADS. In Fig. 3(c), much of nitrogen from the nitrite ion is in the form of ATS, with the rest as ADS and a little HADS. Considerable hydrolysis of ATS has occurred, shown by the growth of the sulfate ion peak. The solution is at a higher pH than it was originally, as indicated by the presence of sulfite ion as well as bisulfite ion. In the last spectrum, all the ATS has been hydrolyzed to ADS, and hydrolysis of ADS to SA is beginning. The hydrolysis rate of ADS is much slower than that of ATS, so evidence of its occurrence will be much slower in appearing.

Mixtures B, C, and D all show the presence of sulfite ion and nitrite ion in solution 24 hours after mixing, indicating that the reaction between them and the reaction between HADS and sulfite ion is fairly slow. This was confirmed by preparing a solution of 1.02 *M* nitrite ion and 0.50 *M* sulfite ion at pH 10. A Raman spectrum obtained shortly after mixing showed no evidence of any reaction products, and a spectrum taken one week later (Fig. 4) showed no change. From this, we conclude that the reaction between sulfite ion and nitrite ion occurs very slowly, if at all. This is consistent with the reaction mechanism proposed by Oblath et al.[5] and by Seel et al.[11] for bisulfite ion in HADS and ATS production.

We have confirmed the accuracy of the reaction scheme shown in Fig. 1. These results are of great value in developing and improving wet flue gas scrubber systems. Our work indicates that, for optimum scrubber operation, the $SO_2/NO_x$ ratio in the flue gases should be large enough that the ratio of bisulfite ion to nitrite ion in solution is greater than 2. The results also show that the pH of the scrubbing solution should be mildly acidic, so that bisulfite ion is the dominant form of sulfur oxyanion in solution. These scrubber conditions will permit optimum conversion of $SO_2$ and $NO_x$ into other compounds.

## PLANNED ACTIVITIES FOR FY 1983

Laser Raman spectroscopy holds promise for studying other reactions occurring in aqueous solutions. Among the reactions of interest are the reactions of ferrous nitrosyl complexes with sulfite and bisulfite ions and the oxidation of sulfite and bisulfite ions by

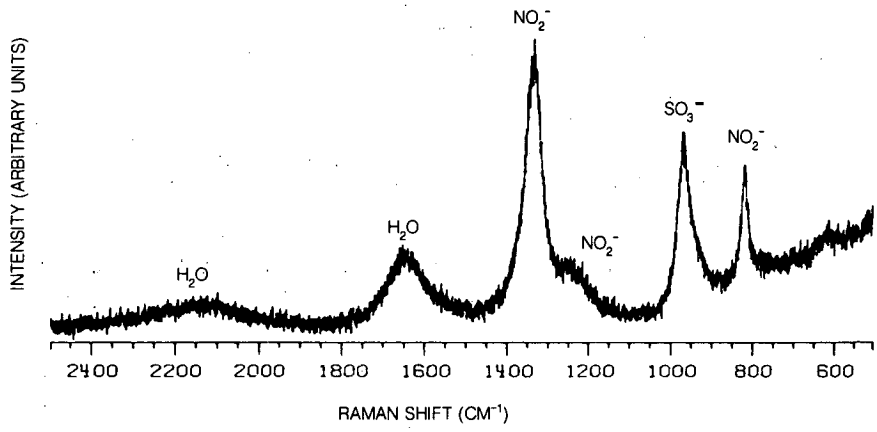


Figure 4. Raman spectrum of a 1.02 *M* nitrite ion–0.50 *M* sulfite ion mixture taken one week after mixing. (XBL 828-10803)

dissolved oxygen in aqueous solutions. Iron and manganese ions appear to catalytically affect the latter reactions, and their influence is especially worthy of study.

## REFERENCES


1. Chang, S.G., et al. (1982), *Flue Gas Desulfurization,* ACS Symposium Series 188, American Chemical Society, Washington, D.C.
2. Martin, A.E. (1981), *Emission Control Technology for Industrial Boilers,* Park Ridge, New Jersey, Noyes Data Corp.
3. Yaverbaum, L.H. (1979), *Nitrogen Oxide Control and Removal, Recent Developments,* Park Ridge, New Jersey, Noyes Data Corp.
4. Chang, S.G., et al. (1981), "The Importance of Soot Particles and Nitrous Acid in Oxidizing $SO_2$ in Atmospheric Aqueous Droplets," *Atmos. Environ. 15,* p. 1287.
5. Oblath, S.B., et al. (1981), "Kinetics of the Formation of Hydroxylamine Disulfonate by Reaction of Nitrite with Sulfites," *J. Phys. Chem. 85,* p. 1017.
6. Gomiscek, S. et al. (1981), "Kinetics of the Reaction Between Hydroxylamine and Sodium Bisulfite," *J. Phys. Chem. 85,* p. 2567.
7. Oblath, S.B. et al. (1983), "Reaction of Nitrite Ion with Hydroxylamine-N-Sulfonate in Aqueous Solution," *Inorg. Chem. 22,* p. 579.
8. Oblath, S.B. (1981), *Kinetics of the Reduction of Nitrite Ion by Sulfur Dioxide in Aqueous Solution,* Ph.D. Thesis, Chemistry Department, University of California, Berkeley, Lawrence Berkeley Laboratory Report LBL-13026.
9. Littlejohn, D., and Chang, S.G. (1983), "Identification of Species in a Wet Flue Gas Desulfurization and Denitrification System by Laser Raman Spectroscopy," submitted to *Environ. Sci. & Tech.*
10. Rauch, J.E., and Decius, J.C. (1966), *Spectrochim. Acta 22,* p. 1963.
11. Seel, V.F. et al. (1956), "Kinetik und Chemismus der Raschigschen Hydroxylamin-Synthese," *Z. Anorg. Allg. Chem. 284,* p. 101.

# REALISM AND REPLICABILITY OF LENTIC MICROCOSMS AS A FUNCTION OF WATER AGITATION

*J. Harte, D.J. Levy, G.P. Lockett, J.M. Oldfather, J.T. Rees, E.I. Saegebarth, and R.A. Schneider*

Microcosms can be defined as experimental units containing inorganic and biological materials from, and exhibiting important processes occurring in, a whole ecosystem. Traditionally, microcosms have been used in chemical uptake studies, enrichment studies, and primary productivity measurements. Such applications are typically of short duration (4 to 48 hours) and are carried out in small samples, of a few liters volume or less, from a natural system. More recently, larger microcosms have been proposed for longer-term studies to determine the effects of pollutants on ecosystem functions and species composition.[1–3] A potential obstacle to such applications is that over longer time periods (weeks or months), microcosms may replicate poorly and their chemical and biotic behavior may diverge from the natural system from which they were derived. The results reported here contribute to our understanding of the potential for such divergence.

In a series of experiments, we have been analyzing how the design of lentic (freshwater) microcosms and the conditions under which they are operated affect their replicability and realism.[4,5] A partial list of the factors that can affect lentic microcosm replicability and realism includes: container size and shape, light and temperature levels, rate of water agitation, rate of hydraulic flow-through, presence or absence of macroflora and macrofauna, and presence or absence of algal wall growth.[4–6] It has been demonstrated that the degree of water agitation in estuarine microcosms effects significantly the degree to which these systems simulate the estuary from which they were derived.[6] In the present experiments,[7] the ability of lentic freshwater microcosms to replicate well and to simulate accurately the pelagic epilimnion of a stratified reservoir is explored as a function of the degree of water agitation. Lessons learned from earlier studies concerning tank size, water temperature control, and the need to prevent algal wall growth are incorporated into the experimental design.

## ACCOMPLISHMENTS DURING FY 1982

In 1981, two experiments, lasting 7 and 5 weeks respectively, were carried out. The water source and field-comparison system was Briones Reservoir in Contra Costa County, California. Experiment I (June 6–July 20) used water taken in equal amounts from depths of 5 and 8 m. The epilimnion depth of the reservoir was 8 to 10 m, and the depth-integrated temperature increased from 18.5°C to ~20.5°C over the course of the experiment. Experiment II (October 21–November 23) used water taken in equal amounts from 0, 5, and 10 m. The epilimnion depth was 15-20 m, and the depth-integrated temperature decreased from 17.6°C to 15°. In both experiments, water was obtained approximately 100 m from the nearest shore, using a 12-liter Van Dorn bottle.

The water was placed in a large mixing tank in the laboratory, then siphoned into cylindrical Nalgene tanks (diameter = 33.0 cm; height = 70.5 cm), which were filled with 58 liters of water. (Experiment I had 6 tanks, Experiment II had 12.) Previous work had demonstrated that microcosms 50 liters or larger best simulate relatively isolated pelagic surface water.[5]

In Experiment I, two levels of agitation—A and D—were examined, while in experiment II, four levels of agitation—A, B, C, and D—were examined. Three replicate tanks were used to study each level of agitation. In Experiment I, systems A were not agitated while systems D were agitated by Pyrex stirring propellers (4 blades; $r$ = 2.5 cm) inserted to a depth of 15 cm and rotated at ~600 rpm by standard stirring motors. Motors were on during light periods and off during dark periods. In Experiment II, systems A were not agitated. Systems B were agitated by air bubbling out of a capillary tube at a rate of 1 liter/min.; the tube extended 15 cm below the water surface. Systems C were agitated by slowly rotating (75 rpm) flat Lucite paddles (20 cm × 7.5 cm × 0.5 cm)

*This work was supported by the Environment and Energy Analysis Division of the Electric Power Research Institute and the Office of Toxic Substances of the Environmental Protection Agency through the U.S. Department of Energy under Contract No. DE-AC03-76SF00098.

inserted to a depth of 23 cm. Systems D were agitated by rapidly rotating (600 rpm) Teflon stirring propellers (3 blades, $r = 2.2$ cm) inserted to a depth of 23 cm. The stirring motors in systems C and D were on continuously.

Sampling was done weekly in both the reservoir and the microcosms, and always within a day of each other. In the reservoir, sampling was done from a small aluminum boat at approximately the same position from which the microcosm water was drawn. The variables measured included phytoplankton and zooplankton (number density by genus), ammonia, dissolved silica, pH, total organic carbon, dissolved organic carbon, temperature, light levels, and water agitation rate (the last by measuring the rate of dissolution of small gypsum blocks suspended in the reservoir and in the microcosms).

In both experiments, the dissolution rate in the most vigorously agitated microcosms, systems D, most nearly matched that measured in the reservoir epilimnion. The dissolution rate in the least agitated microcosms, systems A, was on the order of one-tenth that measured in the most agitated microcosms.

Nearly all chemical measurements showed good replication within a set of microcosms ($\chi^2 \leq 6.00$ and/or coefficient of variation $\leq 0.10$). In the microcosms, the chemical variables in both experiments did not depend strongly on the level of agitation, whereas the taxonomic variables in the microcosms did exhibit definite trends as a function of agitation. The taxonomic variables in sets of microcosms with no agitation (systems A) and agitation accomplished by bubbling (systems B) exhibited slightly better replication than did the mechanically agitated microcosms (systems C and D).

Time-averaged values of the taxonomic variables were used to compare quantitatively each set of microcosms with the reservoir. A variable in a set of microcosms was considered to exhibit good tracking if it replicated well with the set ($\chi^2 \leq 6.00$), and if its mean value (averaged over the set of microcosms) was close ($|t| \leq 2.92$, d.f. $= 2$) to the depth-averaged value observed in the reservoir epilimnion. By these criteria, the taxonomic variables in Experiment I tracked poorly with only 17% of the taxonomic data entries satisfying them in the mechanically agitated systems. Nonetheless, for 5 weeks the major population changes exhibited by the dominant phytoplankton and zooplankton in the reservoir were well followed by these variables in the microcosms. In Experiment II, the unagitated and bubbled systems tracked the reservoir quite well, while the mechanically agitated systems did not (the above tracking criteria were satisfied by 79%, 69%, 21%, and 14% of the taxonomic data entries in systems A, B, C, and D respectively). A further indication that important relationships in the reservoir during Experiment I were also present in the microcosms is the fact that the identical functional and numerical relationship between $SiO_2$ concentrations and total diatom volume observed in the reservoir was observed in the microcosms.

This work can be compared to another set of experiments, similar in design to ours, which investigated the effects of mechanical agitation on microcosms derived from one point in Narragansett Bay.[6] This study concluded that the level of mechanical agitation in estuarine microcosms should be set to match the dissolution rate in the field system being investigated. This conclusion was based on the assumption that the matching of physical parameters, in particular the gypsum dissolution rate, is more important than achieving maximum realism of biological population densities.

The matching of lake or estuarine turbulence levels in microcosms is a desirable goal, but we urge that some caution be exercised in interpreting gypsum dissolution rates too literally. In particular, water movement in the reservoir can be characterized by scales of motion ranging from the small (e.g., small-scale turbulence) to the large (e.g., wind-driven currents). The dissolution rates of the tethered gypsum blocks measured in the reservoir may reflect increased dissolution due to large-scale motion not present in the microcosms. Thus, by matching gypsum dissolution rates, it is possible that microturbulence in the microcosms is set well above the value in the natural system.

We conclude that freshwater microcosms designed to mimic the pelagic epilimnion of a lentic body can be run for periods of 3 to 6 weeks with statistically acceptable replicability and realism. In most cases, gentle, nonmechanical agitation is the most successful technique for insuring good tracking and replicability. Gypsum dissolution rates very likely do not provide a realistic measure of biologically-relevant turbulence.

## PLANNED ACTIVITIES FOR FY 1983

Further studies to determine how microcosm design and operating conditions affect replicability and realism of performance are planned. In particular, studies on appropriate procedures for including benthic sediments in microcosms will be continued and the results analyzed according to the statistical criteria developed for the water agitation research.

An application of lentic microcosms to determine effects of prolonged darkness on aquatic food chains is planned. In addition, an application of microcosms to determine the effects of trace metals on phosphatase activity will be carried out. A successful model for describing mineralization processes in lakewaters,[8] previously developed from microcosm studies[9] of nitrogen cycling will be extended to describe the phosphorous cycle. Finally, the development of soil microcosms for use in acid deposition research is also planned.

## REFERENCES


1. Pilson, M.E.Q., Oviatt, C.A., and Nixon, S.W. (1980), "Annual Nutrient Cycles in a Marine Microcosm," in *Microcosms in Ecological Research,* J.P. Giesy, Jr., Ed., Technical Information Center, U.S. Department of Energy, Oak Ridge, Tennessee, CONF-781101, p. 753.
2. Giesy, J.P., Jr., Ed. (1980), *Microcosms in Ecological Research,* Technical Information Center, U.S. Department of Energy, Oak Ridge, Tennessee, CONF-781101.
3. National Academy of Sciences (1981), *Testing for Effects of Chemicals on Ecosystems. A Report by the Committee to Review Methods for Ecotoxicology,* National Academy Press, Washington D.C., pp. 62–77.
4. Harte, J., Levy, D., and Rees, J. (1983), "Pelagic Diatom Populations in Lentic Freshwater Microcosms," *Int. Rev. der Gesamten Hydrobiol.,* in press.
5. Harte, J., Levy, D., Rees, J., and Saegebarth, E. (1981), "Assessment of Optimum Aquatic Microcosm Design for Pollution Impact Studies," Electric Power Research Institute Report EA-1989, Palo Alto, California.
6. Perez, K.T., et al. (1977), "The Importance of Physical and Biotic Scaling to the Experimental Simulation of a Coastal Marine System," *Helgolander wiss. Meeresunters 30,* p. 144.
7. Harte, J., et al. (1983), "Realism and Replicability of Freshwater Lentic Microcosms as a Function of Water Agitation," submitted to *Freshwater Biology,* Lawrence Berkeley Laboratory Report LBL-16133.


# ACID PRECIPITATION AND SURFACE-WATER VULNERABILITY ON THE WESTERN SLOPE OF THE HIGH COLORADO ROCKIES*†


*J. Harte, G.P. Lockett, R.A. Schneider, H. Michaels, and C. Blanchard*


Acid precipitation has been a subject of intense research for more than a decade, since it was discovered and documented in Scandinavia and in the northeastern United States. Defined as a precipitation with a pH substantially below 5.65 (the normal equilibrium value) and composed primarily of dilute sulfuric and nitric acids (which come from the burning of fossil fuels), acid precipitation has also been reported in several locations in the western states, most notably in central and southern California[1,2] and on the eastern slope of the Colorado Rockies.[3] We report here on the site-specific incidence and potential effects of acid precipitation on the western slope of the Rockies.

Increased fossil fuel consumption in California, the Great Basin, or in the upper or lower Colorado River drainage regions could subject the western slope of the Rockies to acidic precipitation. For that reason, this investigation was designed to obtain reliable baseline data on precipitation and surface water chemistry on the western slope. Such data provide a means of assessing the present sensitivity of watersheds in the region to acidification and will


*This work was supported by the Nature Conservancy, the Environment and Energy Analysis Division of the Electric Power Research Institute, and the Office of Toxic Substances of the Environmental Protection Agency through the U.S. Department of Energy under Contract No. DE-AC03-76SF00098.


†A paper with this title (LBL-14542) has been submitted to *Environmental Science and Technology* by the authors.

allow future determination of a possible worsening trend in precipitation quality.

Our study site (Fig. 1) is a remote and relatively pristine high-elevation watershed located in the Elk Mountains of west-central Colorado and includes the entire upstream drainage. It is largely on land owned by The Nature Conservancy and is called the Galena Mountain/Mexican Cut Preserve. The study to date includes 21 non-consecutive months of observations over a 26-month period.

The two major results reported here are evidence for numerous storm events with pH considerably below 5.6 and evidence of very poorly buffered surface waters, as measured by titratable alkalinity. In addition, biological species likely to be sensitive to acidification have been located at the site, and preliminary censuses of these populations have been carried out.

## ACCOMPLISHMENTS DURING FY 1982

Table 1 shows time averages of precipitation pH. In Figs. 2 and 3, the pH values of the individual storm samples are plotted against the amount of precipitation and the time between an event and its predecessor. Figure 2 shows that both the very high and the very low pH measurements correspond to samples with a relatively small amount of precipitation. Figure 3 suggests a weak inverse relationship between pH and sample interval. A considerable amount of scatter is evident in these plots. Measurement of anion correlations indicates that the most acidic winter events show a slight tendency toward higher nitrate-to-sulfate ratios.

For several rain events, we measured the pH immediately afterwards and then one to three days later in samples sealed in glass flasks after initial measurement. In all cases, the pH rose from one-half to one pH unit during that interval, presumably because of the presence of buffering agents in the samples. Rain splash on the dusty ground near the collector was one likely source for such agents. We note, in addition, that the generally alkaline soils at lower elevations in the western United States could

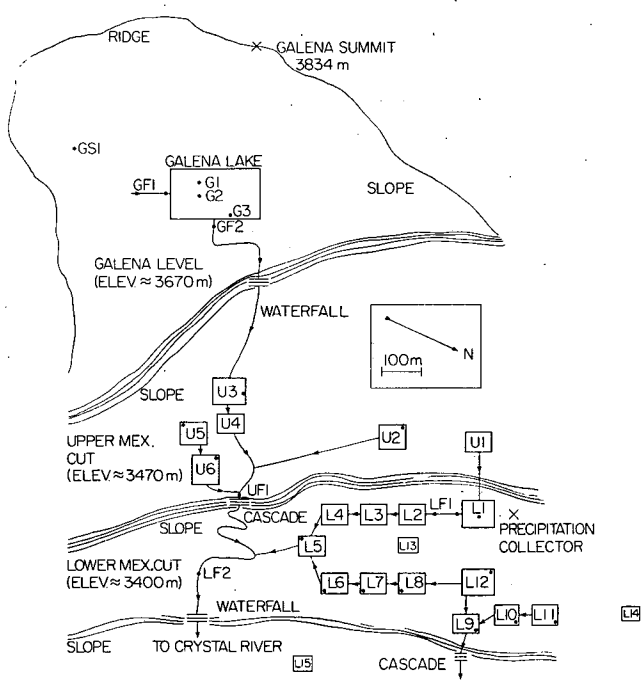


Figure 1. A schematic map of the Galena Mountain/Mexican Cut watershed. Sampling sites are indicated by dots, the lake, tarn, and ponds by boxes, and connecting streams by lines with arrows in the direction of flow.

(XBL 825-674)

Table 1. Precipitation acidity averages, with and without a precipitation-amount weighting factor (centimeters of precipitation).

| Period | $N^a$ | Average[b] precipitation pH with $P_i$ weighting factor | Average[c] precipitation pH without $P_i$ weighting factor |
|---|---|---|---|
| Summer 1980 | 4 | | 4.35 |
| Winter 1980-81 | 35 | 4.28 | 4.17 |
| Summer 1981 | 14 | 4.68 | 4.64 |
| Winter 1981-82 | 24 | 5.12 | 5.09 |
| | | 4.55 | 4.40 |
| Total $N$ | | 73 | 77 |

[a]Number of samples

[b]Average precipitation pH is expressed by the formula

$$-\log \left\{ \sum_{i=1}^{N} [H_i^+]\, P_i \Big/ \sum_{i=1}^{N} P_i \right\}$$

where $P_i$ is the precipitation amount.

[c]Average pH without rainfall amount factor is expressed by the formula

$$-\log \sum_{i=1}^{N} \frac{[H_i^+]}{N}$$

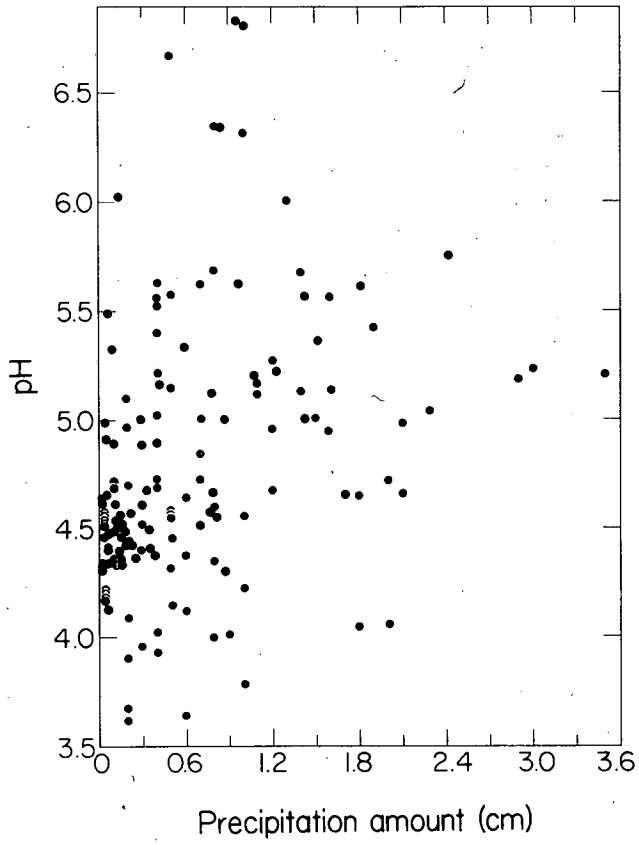


Figure 2. Precipitation pH vs. precipitation amount. (XBL 825-669)

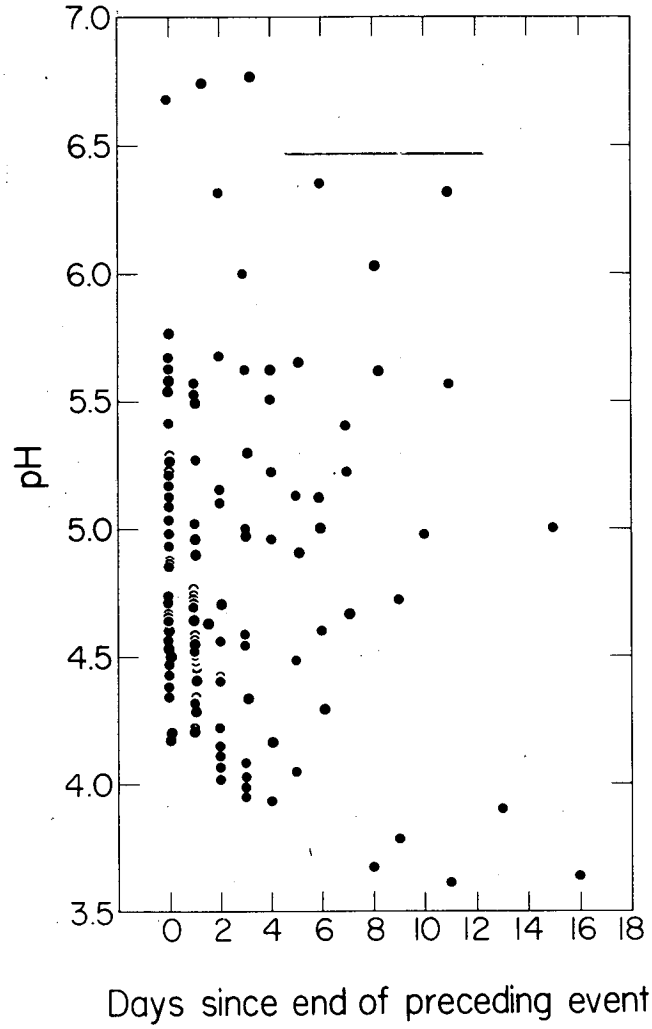


Figure 3. Precipitation pH vs. time between sampled events, rounded off to the nearest day. Sample collection always occurred either in the midst of a storm or immediately after precipitation ceased. (XBL 825-673)

be the source of buffering agents in precipitation even at higher elevations. Calcium plus magnesium concentrations measured in the summer 1981 precipitation samples (for which rain splash was eliminated) ranged from 9.0 to 18.2 microequivalents per liter, supporting this speculation and suggesting that the precipitation pH could have been lower than measured had partial neutralization not occurred. The presence of buffering materials in the precipitation may account for the spread in Fig. 3; long intervals between storms can allow acidic materials to build up in the atmosphere under some circumstances, alkaline agents under others.[4]

Surface waters were also measured for pH, alkalinity, and calcium and magnesium concentrations. In Fig. 4, the plot of pH vs. alkalinity for the surface-water samples shows that all of the data lie below the theoretical curve. The formula for this curve is $[H^+] + [\text{alkalinity}] = 10^{-11.5}/[H^+]$. It is derived under the assumption that all the alkalinity is due to the bicarbonate system, and is based on the standard equilibrium relations for atmospheric $CO_2$ (at 3500 m) and aqueous $OH^-$, $CO_3^{2-}$, $HCO_3^{2-}$, $CO_2$, and $H^+$. The figure suggests that other sources of alkalinity besides bicarbonate are present. For those samples for which calcium and magnesium concentrations were measured, a linear regression of alkalinity against the sum of the calcium and magnesium concentrations (expressed as microequivalents/liter) yields:

$$\text{alkalinity} = 10.6 + 0.65\,([Ca] + [Mg]) \quad ,$$

with $r = 0.97$, $n = 30$. This suggests that a portion of the bicarbonate alkalinity associated with the calcium and magnesium is gone, but that other sources of buffering, perhaps of organic origin, are present.

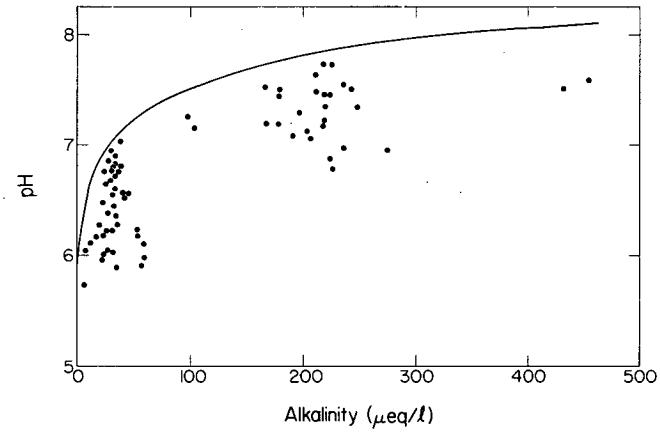


Figure 4. Plot of pH vs. alkalinity for all surface-water samples. The curve expresses a theoretical relationship between pH and carbonate-bicarbonate alkalinity.

(XBL 825-672)

A species of salamander, *Ambystoma tigrinum,* inhabits many of the ponds in the Mexican Cut. Censusing has been carried out over two summers in pond L1 (see Fig. 1) and for all ponds in 1981. Because this species belongs to the same genus as the acid-sensitive spotted salamander (*Ambystoma maculatum*) of the Adirondacks[5] it may serve as a valuable biological indicator of a decreasing trend in surface water pH during snow melt, when routine measurements are extremely difficult to carry out. Other populations at the site that may serve as useful indicators are cutthroat trout (*Salmo clarki*), lichens, and several species of *Daphnia*, including *D. pulex,* which may be sensitive to declining pond-water pH.[6]

Our results provide evidence of acidic precipitation in the west Elk Mountains of Colorado. The period of study was too short to allow estimation of a temporal trend in the total acidity or the ionic composition of the samples, but our sampling and chemical analysis of precipitation at the site are continuing, and we expect to be able to characterize such trends after several more years of investigation.

In several respects, the precipitation data presented here differ qualitatively from those in the northeastern United States. Comparing winter snow with summer rain events, we find the variation in pH from storm to storm considerably greater in winter than in summer at our site. The 15 precipitation samples with lowest pH all occurred in winter, as did the 19 events with highest pH. Elsewhere, the most acidic events and the widest range of pH values appear to occur in summer.[7]

The considerable amount of scatter when pH is regressed against the logarithm of precipitation amount ($r = 0.25$, $n = 71$) or against the interval between samples ($r = 0.3$, $n = 65$) is also in contrast to observations in the northeastern U.S., where pH tends to be more positively correlated with precipitation amount and negatively with storm interval.[7-9]

Precipitation data from the eastern states indicate typical annually averaged nitrate-to-sulfate (equivalents) ratios of 0.4,[8,10] in contrast to our measured value of 0.9. In this respect, our results are more typical of the western U.S.[1-3]

In the eastern U.S., precipitation events in the colder months tend to have a significantly higher nitrate-to-sulfate ratio than those in the warmer months. Our data show no significant trend of that sort; during the summer of 1981, the average nitrate-to-sulfate ratio differed from the summer-plus-winter average by less than 3%.

Our data differ also from measurements for the northeastern U.S. in the large ammonium concentrations we observed. In this respect, our data are similar to those taken in the southwestern U.S.[4] For those samples in which sulfate, nitrate, and ammonium were measured (summer 1981), $[NH_4^+]$ averages 15.0 μeq/l, $[SO_4^{2-}]$ averages 20.9 μeq/l, $[NO_3^-]$ averages 17.3 μeq/l, and $[H^+]$ averages 23.1 μeq/l. The ammonium-to-sulfate ratio of 0.72 is considerably higher than in the northeastern U.S., where the ratio of ammonium-to-sulfate in precipitation averages about 0.2.[7,9,10] Our results are suggestive of aerosol composition characterized by roughly equal parts of $(NH_4)_2SO_4$ and $NH_4HSO_4$. However, we are not suggesting that the precipitation resembles aerosol in other respects. In particular, for our summer 1981 samples, the ratio of $[H^+]$ to $[SO_4^{2-}]$ is 1.1 and the ratio of $[NO_3^+]$ to $NH_4^-]$ is 1.2. Both ratios are considerably higher than for aerosols in the northeastern U.S., where 0.2 and 0.04, respectively, are typical values.[11]

The variations in $[NH_4^+]$ and $[H^+]$ measurements from event to event in summer 1981 can be about equally well explained by variation in the nitrate and sulfate concentrations separately. In particular, linear regression yields:

$$[NH^+] = 0.79\,[SO_4^{2-}] - 1.20\,,\ r = 0.80\,,\ n = 13\,;$$

$$[NH^+] = 0.94\,[NO_3^-] - 1.00\,,\ r = 0.87\,,\ n = 13\,;$$

$$[H^+] = 0.63\,[SO_4^{2-}] + 10.7\,,\ r = 0.73\,,\ n = 14\,;$$

and

$$[H^+] = 0.74\,[NO_3^-] + 10.9\,,\ r = 0.79\,,\ n = 14\,,$$

where all concentrations are expressed as microequivalents per liter.

This discussion is based on comparisons of concentrations. Volume-weighted comparisons would yield the same qualitative results. A safe generalization is that the precipitation chemistry at our site on the western slope of the Colorado Rockies bears a closer resemblance to the precipitation chemistry in California and the southwestern United States than it does to the precipitation chemistry in the northeastern U.S. and Scandinavia.

The surface-water and soil analyses indicate that some of the water bodies in this high-elevation watershed are quite vulnerable to acidification. In particular, the alkalinities of Galena Lake and of ponds L6, L8, L9, L10, L11, and L12 average below 60 μeq/liter. Other ponds have considerably higher alkalinity. In some of the ponds below timberline with alkalinity above 60 μeq/l, relatively high biological productivity could be a contributing factor. However, the two ponds with the highest alkalinity in the watershed—ponds U5 and U6, with alkalinities of 462 and 902 μeq/l, respectively—are above timberline in the upper Cut and had considerably less visible accumulations of water-column organic materials by midsummer than did the ponds below timberline, such as pond L1. Organic acids from conifers surrounding the ponds in the lower Cut are a minor cause of the lower pH and alkalinity found there, whereas ground water in contact with subterranean limestone is the major cause of the high alkalinity seen in ponds U5 and U6.

A watershed is at risk from acid precipitation when three criteria are met: acid precipitation is falling in the watershed, buffering agents are present only in low concentrations, and sensitive biological species inhabit the site. All three criteria are satisfied in the Galena Mountain/Mexican Cut Preserve; if precipitation in the region continues to be acidic in the future, chemical and biological transformations can be anticipated.

## PLANNED ACTIVITIES FOR FY 1983

A continuation of the collection and analysis of baseline data is planned. A careful statistical treatment of surface water alkalinity changes over time will be carried out to determine whether acidic precipitation has resulted in the decline of watershed buffering capacity. A mathematical model will be constructed for predicting the chronology of watershed acidification (i.e., the period over which alkalinity will gradually decline to zero, when surface-water pH will plummet).

Research on snow melt dynamics and its relation to the spring "acid pulse" is also planned for the Sierra Nevada, where our earlier work[12] indicated high vulnerability of surface waters to acid deposition. Finally, a policy-oriented paper will be prepared on acid precipitation risks in the developing nations; this will be based in part on results of our field research in China.[13]

## REFERENCES


1. Liljestrand, H.M., and Morgan, J.J. (1978), *Environ. Sci. Technol. 12,* p. 1271.
2. McColl, J.G. (1980), "A Survey of Acid Precipitation in Northern California," California Air Resources Board, Sacramento, California, Final Report for Contract A7-149-30.
3. Lewis, W.M., and Grant, M.C. (1979), *Ecology, 60,* p. 1093.
4. Dawson, G.A. (1978), *Atmos. Environ. 12,* p. 1991.
5. Pough, F.M. (1974), *Science 192,* p. 68.
6. Davis, P. and Ozborn, G.W. (1969), *Canad. J. of Zoology 47,* p. 1173.
7. Johannes, A.M., Altwicker, E.R., and Clesceri, N.L. (1981), *Characterization of Acidic Precipitation in the Adirondack Region,* Electric Power Research Institute Report EA-1826, Palo Alto, California.
8. Baker, M., Caniparoli, D., and Harrison, H. (1981), *Atmos. Environ. 15,* p. 43.
9. Raynor, G.S., and Hayes, J.V. (1981), *Water, Air, Soil Pollut. 15,* p. 229.
10. McNaughton, D.J. (1981), *Atmos. Environ. 15,* p. 1075.
11. Johnson, S.A., et al. (1981), *The Map's Aerosol Acidity Network: A Progress Report and Data Summary,* Argonne National Laboratory Report ANL-81-63.

12. Tonnessen K. and Harte, J. (1982), "Acid Rain and Ecological Damage: Implications of Sierra Nevada Lake Studies," *Publ. Aff. Rep. 23*, p. 1.

13. Harte, J. (1983), *Atmos. Envir. 17*, p. 403.

# SURVEY OF INSTRUMENTATION FOR ENVIRONMENTAL MONITORING*

*M. Quinby-Hunt, R. McLaughlin, A. Quintanilha, G. Morton, and C. Case*

The environmental impact of pollutants resulting from current and future technological development is of continuing concern to responsible societies. Governments are increasingly aware that an accurate analysis of such effects is required if efficient and effective measures are to be taken to correct or prevent the potentially dangerous consequences of trace contaminants and other hazards of new processes and materials. Fortunately, instruments and techniques are continuously being developed that allow the rapid characterization and quantification of most pollutants associated with established and developing technologies.

Over the past 12 years, the Environmental Instrumentation Survey has collected information on instrumentation for environmental monitoring. The Survey reviews three major areas: (1) environmental information about the constituents to be monitored; (2) analytical techniques; and (3) commercial instrumentation. The first area gives an overview of the sources, characteristics, and effects of a wide variety of environmental constituents and pollutants; it also provides information on regulatory means of control. The second area describes and evaluates those analytical techniques currently used, including "standard," "reference," and developing methods for the identification and quantification of pollutants. The third area gives a detailed description of commercially available analytical instrumentation; these "instrument notes" cover modes of operation, ranges, performance, features, options available, and cost.

The inclusion of these three distinct areas into a single source has proven to be extremely valuable to many workers because it facilitates and expedites the choice of appropriate instrumentation by the laboratories concerned (state, federal, industrial, and those of other institutions).

The work has been subdivided into four major fields: Radiation, Water, Air, and Biomedical Monitoring. Wiley Interscience has published the Radiation volume[1] and has contracted to publish the second, Water.

## ACCOMPLISHMENTS DURING FY 1982

### Radiation

The Radiation volume was completely rewritten and will be commercially published by Wiley Interscience in April 1983 as a volume of 1130 + xix pages; all 20 chapters were updated and carefully edited prior to publication. The instrument notes were completely revised so that the latest information (up to January 1983) could be included for each manufacturer.

### Water

We have completed new sections on bacteria, residues (solids), halogens, and cyanide, and an update on asbestos. These sections contain descriptions of instrumental techniques, including ion chromatography, ion-selective electrodes, and electron-microscope methods for monitoring asbestos. Three sections on organics in water (phenolics, pesticides, and petrochemicals) have been updated.

### Air (Particulates)

Sections on neutron activation techniques for measurement of trace metals in airborne particulate

*This work was supported by the Assistant Secretary for Environment, Office of Health and Environmental Research, Pollutant Characterization and Safety Research Division, U.S. Department of Energy under Contract No. DE-AC03-76SF00098.

matter and x-ray spectrometry and diffractometry have been reviewed, and a new section on the composition of atmospheric particulate matter is currently being reviewed.

## PLANNED ACTIVITIES FOR FY 1983

### Water

A contract has been negotiated with Wiley Interscience for publication of the Water volume by mid-1984. The book will consist of four sections: inorganic, organic, biological, and physical measurements. Chapter topics include:

*Inorganic*

Major anions
Trace metals
Nutrient elements
Dissolved gases
Strong oxidizing agents
Alkalinity and pH

*Organic*

Organic carbon
Phenolics
Pesticides
Oil and grease
Halogenated hydrocarbons
Surfactants

*Biological*

Biomass indicators
Microbiological constituents
Biological oxygen demand

*Physical*

Temperature
Turbidity
Solids
Asbestos
Color, taste, and odor
Radiation

A new section on biomass indicators such as chlorophylls, phaeophytins, and adenosine triphosphate is in preparation. This is important because biomass indicators can provide important information on the effects that effluents from facilities such as petroleum refineries and nuclear power plants have on the water into which they are released. A new section on turbidity is planned, and new sections are being prepared on strong oxidizing agents and on color, taste, and odor.

Instrument notes will be completely revised and expanded to include all the current manufacturers in this field.

### Radiation

The Radiation volume is scheduled to be published in April 1983.

### Air

Contingent on funding, this volume will be updated and edited for publication.

## REFERENCE

1. Environmental Instrumentation Survey, Lawrence Berkeley Laboratory (1983), *Instrumentation for Environmental Monitoring: Vol. 1, Radiation*, 2nd ed., John Wiley and Sons, New York.

# CURRENT STATUS OF THE IMPACT THEORY OF MASS EXTINCTION

*H.V. Michel, F. Asaro, W. Alvarez, and L.W. Alvarez*

Two geological boundaries, the Permian-Triassic and the Cretaceous-Tertiary, and a more recent boundary between the Eocene and Oligocene stages are being investigated for geochemical anomalies associated with impacts and extinctions.

## ACCOMPLISHMENTS DURING FY 1982

### Eocene-Oligocene Boundary

Five new iridium anomalies in deep-sea cores associated with microtektites (34 million years old) from the North American strewn tektite field have been discovered. The site locations and the excess Ir

*This work was supported by the Department of Energy under Contract No. DE-AC03-76SF00098, the California Space Institute under Award CS24-81, and the NASA Ames Research Center under Contract A-71683 B.

abundances (expressed in nanograms per $cm^2$) were Deep-Sea Drilling Project sites 167 (>0.8), 166 (2), and 69A (29) in the Central Pacific, DSDP 94 (~45) in the Gulf of Mexico, and DSDP 216 (4) in the Indian Ocean. These data, together with two earlier Ir anomalies[1,2] found in the Caribbean Sea (one by ourselves and the other by another group) and associated with extinctions of radiolaria, indicate an equatorial distribution over halfway around the world (Fig. 1). The ratios of iridium, chromium, and nickel in DSDP 69A are close to the values expected for chondritic meteorites. This work reinforces the association of microtektites, impacts, iridium anomalies, and extinctions.

## Permian-Triassic Boundary

Sensitive measurements of Ir and other elements were made on a suite of samples from near the Permian-Triassic boundary (about 230 million years old) in five locations in China. There were two sites near Nanking, two near Changsingh, and one near Kweiyang, a span of 1300 kilometers. The boundary should have either a volcanic or an extraterrestrial-impact source, since clay minerology studies indicated it was an altered glass. No Ir was detected in any of the five samples within an overall upper limit of 0.008 parts per billion. At present, the best explanation for the origin of the boundary is volcanic.[2]

## Cretaceous-Tertiary Boundary

New Ir anomalies in the Cretaceous-Tertiary (C-T) boundary (about 65 million years old) were identified in deep-sea cores from DSDP sites 530A, 527, 528, and 529 in the South Atlantic Ocean. About 30 elements were measured in suites of samples from each site. This work demonstrated that, almost without exception, every continuously deposited Cretaceous-Tertiary boundary contains an Ir anomaly.

Correlation of data on plankton, brachiopods, ammonites, bivalves, and cheilostome bryozoans show that they (as well as nannoplankton and foraminifera) became extinct suddenly at the C-T boundary.

In a collaboration with W. Clemens, a new continental Ir anomaly at Lance Creek near Lusk, Wyoming, was identified. This anomaly is close (within 20 cm) to the geological C-T boundary, i.e., the base of

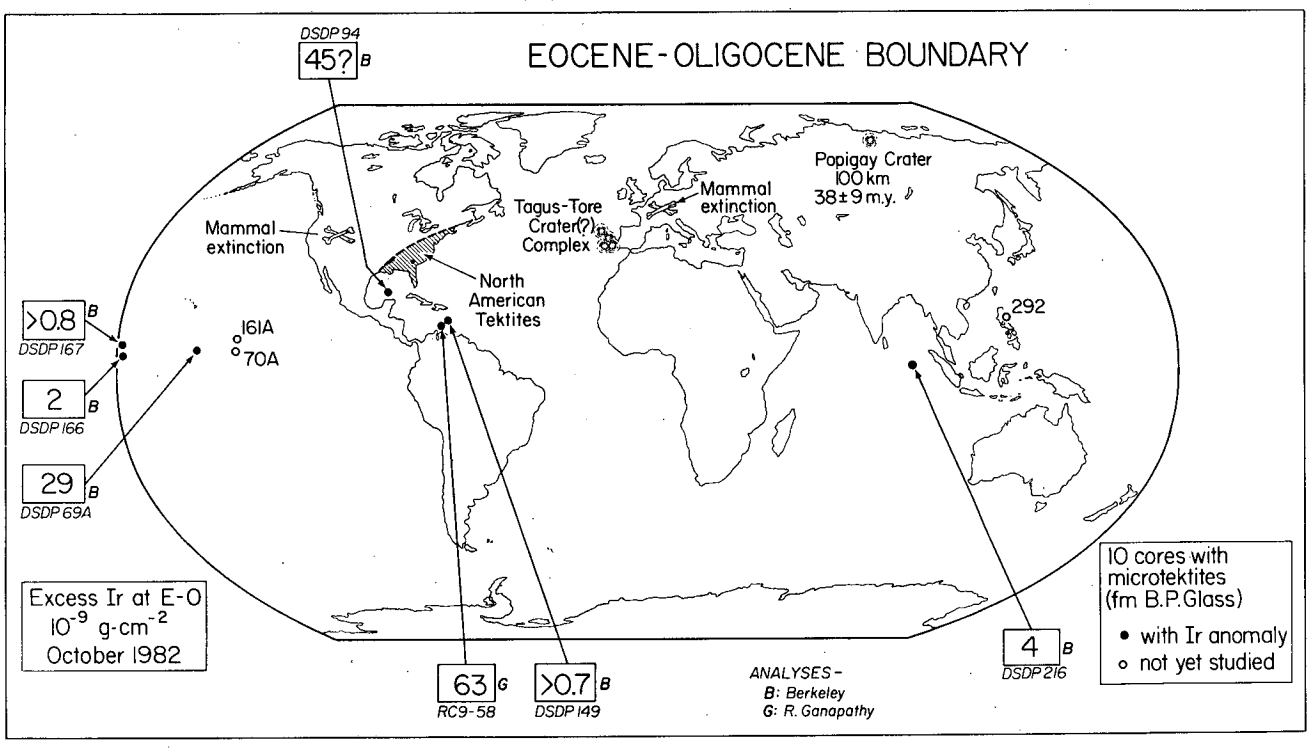


Figure 1. Sites of iridium anomalies at the Eocene-Oligocene boundary, by Deep-Sea Drilling Project (DSDP) site number (known as of October 1982). Boxes indicate excess Ir abundances in nanograms per square centimeter. (XBL 8210-2946)

the lowest Tertiary coal layer. Continental Ir anomalies which are in agreement with the geological boundary have been found in Montana and Wyoming by us and in New Mexico and Colorado by others. Since all C-T Ir anomalies following an extraterrestrial impact would have been deposited at the same time, such anomalies could be used as precise relative time markers.

Statistical analysis of most of the pertinent dinosaur stratigraphic data has shown that the dinosaurs became extinct in western North America suddenly at the C-T boundary. Because of the small number of dinosaur fossils compared to the much more numerous smaller fossils of marine organisms, there is an uncertainty of about 30,000 years in the estimated time of extinction of the dinosaurs. Because of our work, more precise characterizations of dinosaur stratigraphic positions are being made, and more precise data will be forthcoming.

Fourteen black shales from three deep-sea cores were studied, but no Ir was detected in any sample. This demonstrated that highly organic reducing environments do not automatically produce Ir anomalies.

A detailed stratigraphic profile was measured for ~30 elements in the Stevns Klint C-T sediments in Denmark. There was an obvious shift in position of the various elements (on the order of a few centimeters) in the boundary layer. The work strongly suggests that Ir (a very noble element) is, nonetheless, mobile in deep sea sediments. Previous work of ours had shown that the Au/Ir and Pt/Ir ratios in bulk samples from the center of the boundary agreed exactly with comparable data on Type I carbonaceous chondrites, but that the Ni/Ir ratio was ~20% too low in the C-T material. The present work, however, shows that there is no Ni deficit in the boundary and that the Ni has only been shifted in position with respect to the Ir (Fig. 2).

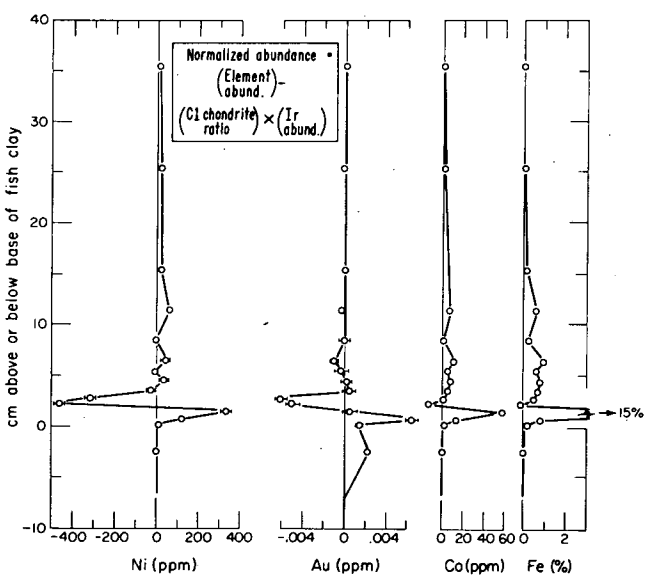


Figure 2. Deviations of siderophile abundances in Stevns Klint section from C1 chondrite expectations (normalized by iridium). (XBL 827-943)

Studies of many elements in mineral fractions have shown that Cretaceous-Tertiary Ir is not particularly concentrated by pyrite or glauconite, although it is associated with pyrite-bearing clays. In collaboration with A. Montanari, however, we found that Ir is concentrated strongly in magnetite from one Italian C-T section.[3] It is preferentially found in the fine clay fractions; it is also found in the silt-size silicate fractions, but not in silt-size quartz fractions. Iridium anomalies associated with 13 new marine C-T sections in Italy were found. In the sand fraction of these and other C-T clay layers containing the Ir anomaly, evidence of diagenetically altered microtektites,[3,4] i.e., impact debris, was found. Thus, the impact source of the C-T Ir anomaly is again confirmed.

## Summary

Over 43 C-T Ir anomalies (Fig. 3) have now been detected throughout the world, 30 of these by the present researchers and their collaborators. The worldwide distribution of the C-T Ir anomaly has thus been amply confirmed, as has its extraterrestrial-impact origin. The correlation of Ir anomalies (and hence impacts) with the C-T extinctions has also been confirmed.

The repetitive nature of the Ir anomaly has also been confirmed in at least one other geological layer (from the Eocene-Oligocene Ir anomaly). Not all major mass extinctions, however, are necessarily due to impacts: no Ir was associated with the biggest of all (the Permian-Triassic).

## PLANNED ACTIVITIES FOR FY 1983

The iridium and other geochemical anomalies will be searched for in Eocene-Oligocene boundary sediments from the Apennines in Italy. The intention is to

establish a precise time marker for relating marine taxa extinctions in that region to those already studied in seven equatorial sites. Extensive studies will also be made of geochemical anomalies associated with the Cretaceous-Tertiary boundary (65 million years ago) in Montana, Wyoming, and Canada in order to precisely relate the times of extinction of different land taxa.

## REFERENCES


1. Alvarez, W., Asaro, F., Michel, H.V., and Alvarez, L.W. (1982), "Iridium Anomaly Approximately Synchronous with Terminal Eocene Extinctions," *Science 216*, p. 286.
2. Asaro, F., Alvarez, L.W., Alvarez, W., and Michel, H.V. (1982), "Geochemical Anomalies Near the Eocene/Oligocene and Permian/Triassic Boundaries," Geological Society of America Special Paper 190, p. 517.
3. Montanari, A., et al. (1983), "Spheroids at the Cretaceous-Tertiary Boundary: Probable Origin as Authigenically Altered Microtektites," submitted to *Geology*.
4. Montanari, A., et al. (1982), "Micropaleontological, Mineralogic and Chemical Analysis of C-T Boundary Clay in the Northern Apennines," *GSA Abstracts with Program 14*(7), p. 569.


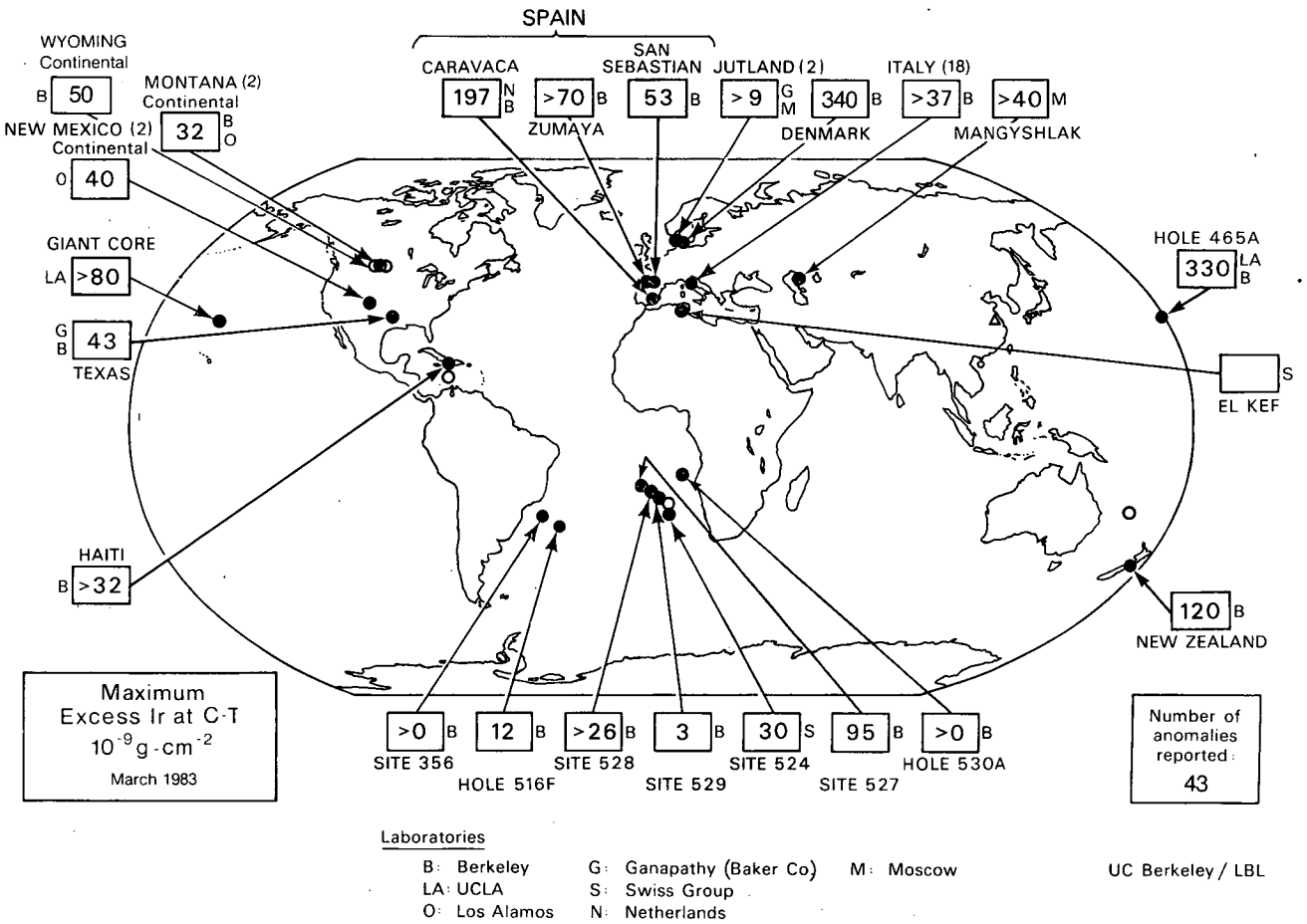


Figure 3. Sites of Cretaceous-Tertiary iridium anomalies known as of March 1983 (43 in all). Boxes indicate maximum excess Ir abundances in nanograms/cm$^2$. Laboratories performing the analyses are also indicated. (XBL 833-94)

# ENERGY ANALYSIS PROGRAM

## INTRODUCTION

The Energy Analysis Program is engaged in interdisciplinary activities in which analysts representing many different fields work together on issues of national significance. The program's emphasis on economics, public policy, and social issues and behavior distinguish it from other LBL activities. At the same time, however, engineering and technical analyses underlie its economic and policy studies, a foundation that distinguishes its work from that of most other analysis groups working on these issues. Virtually all of the research and analysis of the program is quantitative, and a large portion of the program research staff is engaged in developing and applying large-scale computer simulation models.

The primary emphasis of the Energy Analysis Program at present is the study of energy use in buildings. This subject has been stressed for a number of reasons; one of the most important is the strong research effort within the Energy and Environment Division on energy conservation in buildings (especially the Energy Efficient Buildings and the Solar Energy Programs). The Energy Analysis Program provides a rigorous and extensive analytical capability to complement the more specialized pursuits of other groups in the Division involved in building energy research. The program will continue to emphasize analysis of energy use and efficiency in buildings, and it will also extend and apply the analysis techniques to other important national and international energy policy issues.

The work of the program during fiscal year 1982 can best be divided into the following groups of projects:

(1) Engineering and technical residential energy studies, including simulation studies and analysis of results of program survey data.

(2) Economic analyses, including studies of regulatory policies to reduce energy use of appliances and of heating and cooling equipment; studies of market behavior; development of models to evaluate hourly and peak effects of conservation programs for residences; residential energy demand forecasting; and analysis of the effects of energy conservation programs on electric and gas utilities.

(3) Commercial building energy analysis, involving computer simulation studies and a preliminary effort to develop a simplified approach to understanding effects of conservation measures on commercial office buildings.

(4) International studies treating aspects of energy demand in member countries of the Organization for Economic Cooperation and Development (OECD) and in less developed countries.

The following describes some of the most interesting and important studies in these four research areas. The first two are in group (1), residential energy studies; the second two, in group (2), economic analysis; the fifth, in group (3), commercial building energy analysis; and the sixth, in group (4), international studies. They are meant to be illustrative of the research of the Energy Analysis Program in FY 1982; others could equally well have been chosen.

## BUILDING ENERGY SIMULATION STUDIES

Simulations were performed for five house prototypes in 45 locations in the United States. The simulation, using the DOE-2 computer code developed at LBL, involved about 20 sets of measures to improve the thermal integrity of the prototype houses in each location. The results will be available during the next fiscal year as part of a guide to energy conservation for homebuilders and as the underpinnings of a simple slide rule for builders and others to estimate the effects of efficiency measures for all locations in the country. The research results will be useful for (1) providing a quantitative understanding of energy savings of the most important conservation measures, (2) improving considerably our understanding of the effects of weather on residential energy use, (3) providing the basis for a comprehensive economic analysis of residential energy conservation (to be conducted during FY 1983), (4) providing a comprehensive data base for energy demand forecasting

(currently used in the economic studies of the program), (5) evaluating the behavior of the market in the absence of policy interventions (used in the economic and policy studies of the program), and (6) providing information for the development of simplified analysis tools for residential energy audits, for example.

## OCCUPANT BEHAVIOR STUDIES

This research was aimed at assessing the relationship between physical characteristics of houses (especially thermal integrity), occupant behavior, and cooling energy use. The approach involved gathering data on electricity use in about 300 residential buildings (from utility bills), occupant attitudes and behavior (from a one-hour survey developed by the project team), and, for a subsample of houses, measured data on air infiltration and temperature settings. The study produced a number of outputs: (1) a statistical model of cooling energy use for the houses in the sample, (2) a deterministic model of energy use against which the measured data were compared, and (3) a partial evaluation of a utility load management program that took place during the period in which the data were gathered. Three papers have recently been published on the findings of the study. Follow-up work now addresses (1) analysis of data collected for the heating season in Davis, California; (2) analysis of data collected in Lodi, California; and (3) a new study using submetered data, an analysis that will significantly refine our statistical models and help us better understand the effects of attitudes and behavior on energy use in houses.

## MARKET PENETRATION OF HEAT PUMPS

This effort was aimed at improving an important element of the residential energy demand forecasting model used in the program. (The model was originally developed at the Oak Ridge National Laboratory; LBL has improved and extended it in several ways). The improvement in this work was in the projection of the market penetration of heat pumps. This is an important issue in energy forecasts, because heat pumps are considerably more efficient than alternative electric heating options.

The study noted that heat pumps do not at first sight enjoy an economic advantage over other systems in most parts of the nation. This was surprising because, in the past decade, heat pumps have increased their market share from very small percentages to about half of the residential electric heating market (about 25% of the total new heating market). The analysis of this problem (to understand and quantitatively characterize factors leading to market penetration of heat pumps) involved: (1) case studies of heat pump penetration in a number of regions of the United States; (2) use of the results of the case studies to formulate and apply a discrete-choice model to fully describe market penetration; and (3) use of results of the first two tasks to refine the energy demand forecasting model. During FY 1982, the first task was completed, with several interesting findings: if one defines the economics more broadly than as the first and operating cost of a system, heat pumps are economic in many regions. There are several reasons for this. Because of the natural-gas shortages of the 1970s, suburbs in some regions expanded without gas lines, and gas hookups are consequently expensive; because of the peak-power benefits of heat pumps, some utilities have offered preferential rates to heat-pump owners; and sometimes there is concern that natural gas will not be available in the future. A complex real-world situation revealed by these case studies provides an interesting challenge for the quantitative modeling of heat-pump market penetration (tasks 2 and 3, planned for FY 1984).

## MARKET BEHAVIOR STUDIES

An important issue for energy conservation policy studies is the degree to which the market would achieve cost-effective conservation measures in the absence of policy intervention. This is a particularly relevant issue under the current Administration in Washington, D.C., which supports the belief that the market is likely to achieve many or most energy objectives without federal policies.

As a step toward resolving this issue, an empirical analysis has been performed of energy efficiency investments in the residential sector over the past decade. To our knowledge, this work is one of the few detailed empirical assessments of market behavior in residential energy conservation investments. Two papers are under preparation, one on investments in energy efficiency for residential appliances and heating and cooling equipment, the other on investments in thermal integrity in new houses.

The findings of both studies indicate that there is a

substantial underinvestment in energy efficiency improvements (relative to the behavior of a "free" or "optimal" market) for most residential energy conservation measures and that the market has *not* improved (relative to the cost-effective level of investment) during the past decade. Some of the reasons for this situation are discussed in the papers; however, much more empirical and theoretical work is needed to advance our understanding of market behavior and energy conservation investments. A continued effort in this area in FY 1983 is expected to make some progress in this direction.

## COMMERCIAL BUILDING ENERGY ANALYSIS

The research in commercial building energy analysis was directed at performing a "proof of concept" test of a new idea for understanding the effects of conservation measures (including their interactions) on energy use in a commercial office building. The basic approach involved performing a set of DOE-2 computer simulations, fitting these results to equations, and using the equations to "predict" results of other DOE-2 simulations. The approach was modeled on the simulation work on residential buildings, with the difference that interactions among measures, which are very important for commercial buildings, were included. The long-term objective is to develop a new approach to energy analysis of commercial buildings that will greatly simplify the procedure for architects and engineers designing new buildings.

The work showed that the technique proposed is highly promising. Almost all predictions of DOE-2 energy simulations were within a few percent of the actual results. If work in this area continues, there is considerable potential for building a simplified microcomputer model that will permit building designers to perform energy analysis with little investment of time and money.

## OECD RESIDENTIAL ENERGY STUDY

This work represents the first comprehensive assessment of residential energy use in nine OECD countries. It has produced (1) an extensive and consistent residential energy data base disaggregated to end uses, (2) an econometric study of residential energy use among the nine countries, and (3) as assessment of key factors that influence or determine the nature of residential energy demand in the OECD countries. One interesting observation is that heating energy use per square foot per degree-day in Sweden and Great Britain is roughly equal even though Swedish buildings are much more energy efficient than British buildings. The explanation is that the Swedes are able to maintain much higher (and presumably more comfortable) indoor temperatures than the British. One of several important findings is that econometric relations have considerable predictive power within the countries, in large part because the econometric studies were performed on data disaggregated to energy end uses.

Continuing research addresses energy use in commercial buildings in the OECD countries.

## FUTURE DIRECTIONS ON THE ENERGY ANALYSIS PROGRAM

These projects (and others omitted for the sake of brevity) represent a good beginning to a systematic analysis of the issues studied. Most of these projects will continue and can be expected to deepen our understanding of the issues of energy use and energy conservation in buildings. In addition, the program is striving to expand its work to encompass other key energy policy issues. In particular, international energy issues, critical energy price and supply questions, key resource and environmental issues, and electric utility analyses are likely to constitute some of the new initiatives of the next few years for the program.

# RESIDENTIAL ENERGY CONSERVATION: DEVELOPING A GUIDE FOR HOMEBUILDERS*

*R.L. Ritschard, Y.J. Huang, J.G. Ingersoll, M.D. Levine, R.A. Boschen, L. Chang, C. Hsui, and D. Wilson*

Rising fuel costs have focused attention on the need to improve energy efficiency in residential houses. In recent years, numerous energy strategies have been advocated, ranging from conventional measures such as improving the thermal integrity of the building shell or using more efficient heating and cooling systems to less conventional measures such as employing passive solar designs or experimental mechanical systems.

The Building Energy Analysis Project at LBL has included considerable work over the past several years in analyzing the energy benefits of conservation measures for numerous locations throughout the United States, using state-of-the-art computer simulation programs. Our research effort has resulted in a comprehensive data base that enables us to estimate the amount of energy use for typical houses located anywhere in the country. The ability to quantify energy budgets for various conservation measures is particularly vital to a housing market that traditionally has been sensitive to costs. The comprehensivenesss of our analytical effort is also important because of the strong relationship that exists between a building's energy use and its geographical location. Conservation strategies that are applicable to one location or building type may be ineffectual or even counterproductive when applied indiscriminately elsewhere.

## ACCOMPLISHMENTS DURING FY 1982

The primary emphasis of the Building Energy Analysis Project in FY 1982 was on disseminating the valuable information gained from our previous and ongoing work to the general public. Part of this effort included ongoing research into technical issues such as building energy performance, energy analysis techniques, and evaluation of analysis results. However, FY 1982's work also involved a major effort to translate technical information into a format that will be understandable and relevant to homebuilders and others in the building industry.

To insure that this technical information reaches the homebuilder audience, we have been working closely with a consultant firm, Steven Winter Associates, to produce a guidebook on the energy use of new residential buildings. This book, referred to as the Homebuilders' Guide, will include information from our analysis effort on projected energy use, presented through simplified graphic techniques acceptable to the intended audience. In addition, corollary information will be presented on energy-efficient construction practices, design principles, and usable methods for doing economic analyses. The end product will be a document with solid technical background but that is attractive and understandable to those who will make a major impact on future residential energy use.

The primary objective is thus to provide, in simple format, information for homebuilders on the selection of conservation measures for new houses. The guide will permit homebuilders to calculate easily the energy savings and economics of numerous sets of conservation measures in various house designs.

### Methodology

LBL has developed a comprehensive data base on the predicted energy consumption of typical residential homes in various U.S. weather locations. This data base was assembled from a series of simulations using the DOE-2.1A computer program for five building prototypes: one-story, two-story, split-level, mid-townhouse, and end-townhouse, in 45 weather locations. Significant research was also done on climate to develop a simple method for extrapolating results from the 45 base locations to more than 3000 intermediate locations. (See Y.J. Huang, "Climate Analysis in Support of the Homebuilders' Guide," this

*This work was supported by the Assistant Secretary for Conservation and Renewable Energy, Office of Conservation, Building Systems Division, U.S. Department of Energy under Contract No. DE-AC03-76SF00098.

annual report.) For each building prototype in any weather location, 16 to 19 effective combinations of energy conservation measures such as insulation (ceiling, floor, and walls), window glazings, and infiltration levels were simulated. Three types of building foundations (slab-on-grade, crawl space, or basement) were also simulated, depending on the weather location. Table 1 shows a matrix of base-case runs according to location, building prototype, and foundation type. This comprehensive data base of nearly 5000 DOE-2.1A runs is designed to cover the range in new residential construction in all U.S. climate regions and serves as the technical basis of the Homebuilders' Guide.

A sensitivity analysis of the effects on building energy use of variations in building design and operation was also done. This analysis was used to extend the base-case results to account for differences between individual buildings and to give accurate values for differences between conservation measures as applied to specific buildings. Sensitivity studies were conducted in up to 11 locations for the following topics: building area, equipment efficiencies, window size and location, thermostat setback, internal loads, levels of air infiltration, and enhanced solar design (direct-gain and attached-sunspace configurations). More than 1500 computer simulations were done for these sensitivity studies.

Table 1. Matrix of base-case simulations by city, prototype, and foundation type.

| | Ranch | | | Two-story | | | Split level | | | Mid townhouse | | | End townhouse | | |
|---|---|---|---|---|---|---|---|---|---|---|---|---|---|---|---|
| City | Slab | Bsmt | Crawl | Slab | Bsmt | Crawl | Slab | Bsmt | Crawl | Slab | Bsmt | Crawl | Slab | Bsmt | Crawl |
| 1. Albuquerque, NM | X | | | X | | | X | | | X | | | X | | |
| 2. Atlanta, GA | X | X | X | X | X | X | X | X | X | | X | X | X | X | X |
| 3. Birmingham, AL | X | X | | X | X | | X | X | | X | X | | X | X | |
| 4. Bismarck, ND | | X | | | X | | | X | | | X | | | X | |
| 5. Boise, ID | | X | X | | X | X | | X | X | | X | X | | X | X |
| 6. Boston, MA | | X | | | X | | | X | | | X | | | X | |
| 7. Brownsville, TX | X | | | X | | | X | | | X | | | X | | |
| 8. Buffalo, NY | | X | | | X | | | X | | | X | | | X | |
| 9. Burlington, VT | | X | | | X | | | X | | | X | | | X | |
| 10. Charleston, SC | X | | X | X | | X | X | | X | X | | X | X | | X |
| 11. Cheyenne, WY | | X | | | X | | | X | | | X | | | X | |
| 12. Chicago, IL | X | X | | X | X | | X | X | | X | X | | X | X | |
| 13. Cincinnati, OH | X | X | X | X | X | X | X | X | X | X | X | X | X | X | X |
| 14. Denver, CO | | X | | | X | | | X | | | X | | | X | |
| 15. El Paso, TX | X | | | X | | | X | | | X | | | X | | |
| 16. Fort Worth, TX | X | | | X | | | X | | | X | | | X | | |
| 17. Fresno, CA | X | | X | X | | X | X | | X | X | | X | X | | X |
| 18. Great Falls, MO | | X | | | X | | | X | | | X | | | X | |
| 19. Honolulu, HI | X | | | X | | | X | | | X | | | X | | |
| 20. Jacksonville, FL | X | | | X | | | X | | | X | | | X | | |
| 21. Juneau, AK | | X | | | X | | | X | | | X | | | X | |
| 22. Kansas City, MO | | X | | | X | | | X | | | X | | | X | |
| 23. Lake Charles, LA | X | | | X | | | X | | | X | | | X | | |
| 24. Las Vegas, NV | X | | X | X | | X | X | | X | X | | X | X | | X |
| 25. Los Angeles, CA | X | | X | X | | X | X | | X | X | | X | X | | X |
| 26. Medford, OR | | X | X | | X | X | | X | X | | X | X | X | X | |
| 27. Memphis, TN | X | X | X | X | X | X | X | X | X | X | X | X | X | X | X |
| 28. Miami, FL | X | | | X | | | X | | | X | | | X | | |
| 29. Minneapolis, MN | | X | | | X | | | X | | | X | | | X | |
| 30. Nashville, TN | X | X | X | X | X | X | X | X | X | X | X | X | X | X | X |
| 31. New York, NY | X | X | | X | X | | X | X | | X | X | | X | X | |
| 32. Oklahoma City, OK | X | | | X | | | X | | | X | | | X | | |
| 33. Omaha, NB | | X | | | X | | | X | | | X | | | X | |
| 34. Philadelphia, PA | | X | | | X | | | X | | | X | | | X | |
| 35. Phoenix, AZ | X | | | X | | | X | | | X | | | X | | |
| 36. Pittsburg, PA | | X | | | X | | | X | | | X | | | X | |
| 37. Portland, ME | | X | | | X | | | X | | | X | | | X | |
| 38. Portland, OR | | X | X | | X | X | | X | X | | X | X | | X | X |
| 39. Reno, NV | X | X | | X | X | | X | X | | X | X | | X | X | |
| 40. Salt Lake City, UT | | X | | | X | | | X | | | X | | | X | |
| 41. San Antonio, TX | X | | X | X | | X | X | | X | X | | X | X | | X |
| 42. San Diego, CA | X | | X | X | | X | X | | X | X | | X | X | | X |
| 43. San Francisco, CA | X | | X | X | | X | X | | X | X | | X | X | | X |
| 44. Seattle, WA | | X | X | | X | X | | X | X | | X | X | | X | X |
| 45. Washington, DC | | X | | | X | | | X | | | X | | | X | |

A more detailed discussion of the methodology and assumptions used in this research is presented elsewhere.[1] In addition, heat-pump and window sensitivities are described in separate articles in this annual report.

## Results

The results of this project are being provided in both tablular and graphic formats to facilitate future analysis by internal users (LBL research staff) and outside researchers as well as those involved in the residential construction industry. Samples of such output are given in Tables 2 and 3, which summarize heating and cooling energy requirements for New York City and Phoenix, respectively. Figures 1 and 2 display some of this same information graphically.

Table 2. Energy requirements for a one-story ranch house (with basement) in New York City.

| Option | RC RW Flr In Gls | Heating load (million Btu's) | Cooling load (million Btu's) | Heating energy (million Btu's) | Cooling energy (kWh) | No. of hours heated | No. of hours heated |
|---|---|---|---|---|---|---|---|
| A01 | 00-00-FMO-HI-1 | 106.453 | 16.092 | 152.078 | 2207.8 | 4589 | 1233 |
| B01 | 11-00-FMO-HI-1 | 76.098 | 11.528 | 108.714 | 1702.1 | 4281 | 1240 |
| C02 | 11-11-FMO-HI-1 | 60.722 | 10.539 | 86.747 | 1589.7 | 4018 | 1290 |
| E01 | 19-11-FM1-HI-1 | 52.682 | 9.694 | 75.261 | 1490.6 | 3843 | 1271 |
| F02 | 19-11-FM1-HI-2 | 43.766 | 9.337 | 62.525 | 1449.1 | 3611 | 1313 |
| I05 | 19-19-FM3-HI-2 | 37.977 | 8.945 | 54.254 | 1403.2 | 3426 | 1315 |
| I03 | 30-11-FM3-HI-2 | 38.765 | 8.838 | 55.380 | 1390.1 | 3452 | 1302 |
| J03 | 30-19-FM3-HI-2 | 35.274 | 8.666 | 50.393 | 1369.9 | 3347 | 1318 |
| K03 | 30-19-FM3-HI-3 | 32.800 | 8.419 | 46.858 | 1340.4 | 3273 | 1334 |
| L04 | 38-19-FM3-HI-3 | 31.820 | 8.342 | 45.459 | 1331.2 | 3247 | 1339 |
| M01 | 38-19-FM4-HI-3 | 29.077 | 7.999 | 41.540 | 1290.4 | 3113 | 1300 |
| NO2 | 38-27-FM4-HI-3 | 27.194 | 7.939 | 38.849 | 1283.5 | 3053 | 1309 |
| NO5 | 49-19-FM4-HI-3 | 28.242 | 7.954 | 40.346 | 1285.0 | 3091 | 1313 |
| 002 | 49-27-FM4-HI-3 | 26.361 | 7.911 | 37.659 | 1279.9 | 3032 | 1326 |
| P01 | 60-27-FM4-HI-3 | 25.822 | 7.833 | 36.889 | 1270.5 | 3014 | 1327 |
| P02 | 49-27-FM5-HI-3 | 25.377 | 8.408 | 36.253 | 1340.8 | 3017 | 1398 |
| M51 | 38-19-FM4-LO-3 | 21.044 | 8.004 | 30.064 | 1291.7 | 2820 | 1403 |
| 052 | 49-27-FM4-LO-3 | 18.380 | 7.794 | 26.258 | 1266.4 | 2683 | 1402 |

RC = Ceiling R value; RW = Wall R value; Flr = Floor insulation; In = Insulation level; Gls = Number of glazings.

Table 3. Energy requirements for a one-story ranch house (slab foundation) in Phoenix, Arizona.

| Option | RC RW Flr In Gls | Heating load (million Btu's) | Cooling load (million Btu's) | Heating energy (million Btu's) | Cooling energy (kWh) | No. of hours heated | No. of hours heated |
|---|---|---|---|---|---|---|---|
| A01 | 00-00-FM0-HI-1 | 30.375 | 81.977 | 43.394 | 10216.6 | 1981 | 3607 |
| B01 | 11-00-FM0-HI-1 | 19.789 | 66.393 | 28.270 | 8499.1 | 1735 | 3557 |
| C02 | 11-11-FM0-HI-1 | 15.443 | 59.759 | 22.062 | 7762.9 | 1589 | 3549 |
| D01 | 19-11-FM0-HI-1 | 14.194 | 56.987 | 20.278 | 7449.3 | 1553 | 3539 |
| E01 | 19-11-FM1-HI-1 | 11.026 | 48.515 | 15.752 | 6477.0 | 1312 | 3472 |
| F02 | 19-11-FM1-HI-2 | 8.842 | 45.139 | 12.632 | 6083.1 | 1161 | 3479 |
| G05 | 19-19-FM1-HI-2 | 7.851 | 43.228 | 11.216 | 5858.2 | 1098 | 3473 |
| G01 | 30-11-FM1-HI-2 | 7.993 | 43.045 | 11.418 | 5835.1 | 1096 | 3480 |
| H04 | 30-19-FM1-HI-2 | 7.017 | 41.128 | 10.024 | 5607.1 | 1032 | 3471 |
| I07 | 30-19-FM1-HI-3 | 6.396 | 39.621 | 9.137 | 5425.1 | 982 | 3477 |
| I06 | 38-19-FM1-HI-2 | 6.706 | 40.358 | 9.580 | 5514.2 | 1007 | 3480 |
| J06 | 38-19-FM1-HI-3 | 6.092 | 38.826 | 8.704 | 5328.2 | 954 | 3481 |
| K03 | 30-19-FM3-HI-3 | 5.945 | 38.347 | 8.494 | 5271.5 | 921 | 3469 |
| K01 | 38-19-FM3-HI-2 | 6.255 | 39.088 | 8.935 | 5361.4 | 946 | 3471 |
| L04 | 38-19-FM3-HI-3 | 5.646 | 37.545 | 8.065 | 5173.2 | 895 | 3473 |
| M03 | 38-27-FM3-HI-3 | 5.178 | 36.626 | 7.398 | 5061.6 | 846 | 3475 |
| H54 | 30-19-FM1-LO-2 | 4.180 | 37.951 | 5.971 | 5216.4 | 741 | 3556 |

RC = Ceiling R value; RW = Wall R value; Flr = Floor insulation; In = Insulation level; Gls = Number of glazings.

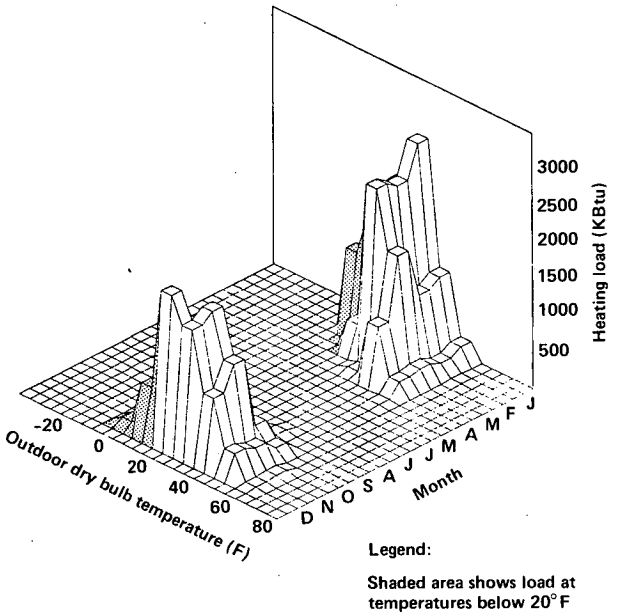


Figure 1. Calculated heating load: Three-dimensional graph shows relationship between monthly heating loads and outdoor temperatures for a one-story ranch house in New York City. Shaded area shows load at temperatures below 20°F. (XBL 824-8868)

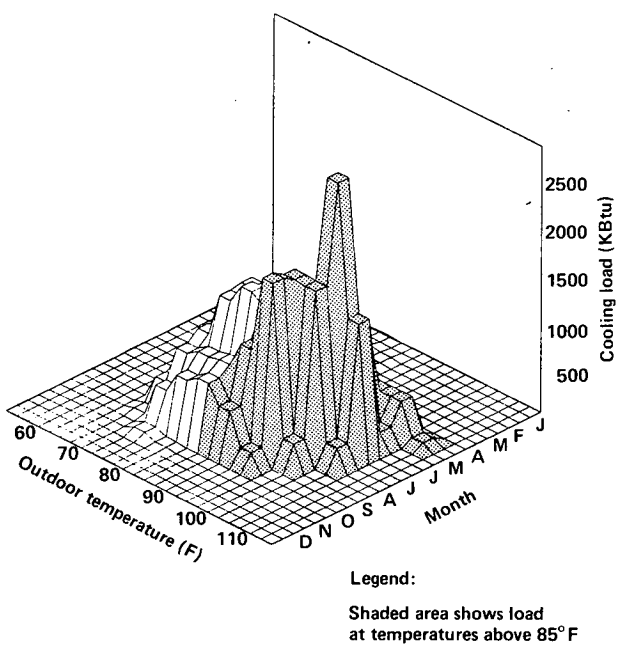


Figure 2. Calculated cooling load: three-dimensional graph shows relationship between monthly cooling loads and outdoor temperatures for a one-story ranch house in Phoenix, Arizona. Shaded area shows load at temperatures above 85°F. (XBL 824-8870)

## PLANNED ACTIVITIES FOR FY 1983

This work will continue during FY 1983 with the major emphasis on the final completion of the Homebuilders' Guide and the preparation of various technical documents (LBL reports and journal articles) that support the research effort.

## REFERENCE


1. J. Ingersoll, et al. (1982), *Methodology and Assumptions for the Evaluation of Heating and Cooling Energy Requirements in New Residential Buildings.* Lawrence Berkeley Laboratory Report LBL-13767.


# THE EFFECT OF WINDOW SIZE AND ORIENTATION ON HEATING AND COOLING LOADS IN RESIDENTIAL HOUSES*


*Y.J. Huang and R.L. Ritschard*


A major objective for the Homebuilder's Guide (see preceding article) is to quantify the effects of various window configurations and control strategies on residential building energy use for various U.S. locations. To maintain consistency with the original data base, the DOE 2.1 computer program was used for the window sensitivity studies. Eleven representative cities were selected out of the original 45 after climate analysis and test runs. (How the cities performed is described in the next article.)

Results from these studies will appear in the Homebuilders' Guide as tables showing the estimated change in heating and cooling loads for various window configurations. The data base will also be studied more analytically in the future, and conclusions will be presented as technical reports.

## ACCOMPLISHMENTS DURING FY 1982

Repetitive computer simulations were done using DOE-2.1 to determine the impact of window size, orientation, and control strategies on residential building energy use. More than 100 different glazing conditions were modeled, including both conventional construction practices and conservation strategies such as adding thermal mass and night insulation. ("Thermal mass") refers to the use of the concrete floor slab to store solar gains, "night insulation" to the use of R5 shutters at night.) These simulations were performed on a prototype 1540-ft$^2$ ranch house in all locations. In addition, attached sunspaces were modeled in two sizes (12-ft and 24-ft lengths) and in two configurations (opaque and glass roofs) for the same 11 cities.

### Methodology

A DOE-2 master file was created, enabling parametric simulations for the following variations in window size, orientation, and control strategies:

(1) Window sizes and orientations:

(a) 154 ft$^2$ (10% of floor area)
- — equally distributed (2.5% each side)
- — 5% each on the north and south
- — 5% each on the east and west
- — 7.5% on the south and 2.5% on the north.

(b) 231 ft$^2$ (15% of floor area)
- — equally distributed (3.75% each side)
- — 7.5% each on the north and south
- — 7.5% each on the east and west
- — 5% on the east, 10% on the west
- — 10% on the north, 5% on the south
- — 10% on the east, 5% on the west
- — 10% on the south, 2.5% on the east and west
- — 10% on the south, 5% on the north
- — 12.5% on the south and 2.5% on the north.

(c) 308 ft$^2$ (20% of floor area)
- — equally distributed (5% on each side)
- — 15% on the south, 2.5% on the east and west
- — 15% on the south, 5% on the north.

(d) conditioned sunspace configuration, attached to the south wall
- — 96 ft$^2$ (12 ft by 8 ft), glass or opaque roof
- — 192 ft$^2$ (24 ft by 8 ft), glass or opaque roof.

(2) Glass types
- (a) single, double, and triple pane
- (b) single pane on the south, double pane elsewhere
- (c) double pane on the south, triple pane elsewhere


*This work was supported by the Assistant Secretary for Conservation and Renewable Energy, Office of Conservation, Building Systems Division, U.S. Department of Energy under Contract No. DE-AC03-76SF00098.

(d) reflective glass
(e) absorptive glass

(3) Conservation and control strategies
(a) night insulation
(b) light and heavy thermal mass
(c) night insulation plus light and heavy thermal mass.

## Results

These window configurations and glass types, as well as appropriate combinations of the conservation and control strategies, were modeled for the following base cities: Albuquerque, Atlanta, Chicago, Denver, Lake Charles (Louisiana), Miami, Minneapolis, New York, Phoenix, San Francisco, and Seattle.

The results of these window simulations have been post-processed to produce a set of tables showing differences in annual heating and cooling loads or energies for different glazing conditions as compared to the base case of 10% glazing equally distributed. An example of the data is shown in Table 1.

## PLANNED ACTIVITIES FOR FY 1983

More than 1000 simulations were performed on DOE-2 to analyze the impact of windows on residential energy use. The resulting data base represents a

Table 1. Results of parametric analysis of the impact of window configurations and control strategies on residential building energy use.[a]

| | | Equal Distribution | | | | Different Window Orientations | | | | | | | South Window Orientation With Added Conservation Measures | | |
|---|---|---|---|---|---|---|---|---|---|---|---|---|---|---|---|
| Standard | | Ref.Gl | Abs.Gl | N.Ins | T.Mass | 7.5N 7.5S | 7.5E 7.5W | 5.0E 10.0W | 10.0N 5.0S | 10.0E 5.0W | 2.5E+W 10.0S | 2.5N 12.5S | 10.0S 5.0N | N.Ins | N.Ins+ T.Mass |
| Single-Glaze | | | | | | | | | | | | | | | |
| H | 0. | 5.41 | 5.05 | -12.88 | -.28 | 0. | -1.27 | 2.87 | 1.76 | 2.01 | 3.23 | -6.69 | -6.58 | -4.46 | -17.34 |
| C | 0. | -2.12 | -1.96 | 0. | -1.81 | -1.41 | .44 | 1.12 | -1.67 | .09 | .31 | -.75 | -.97 | -.97 | -2.76 |
| | | | | | | | | | | | | Double-Glaze, Single on South | | | |
| | | | | | | | | | | | | .50 Inch Gap | | | |
| | | | | | | | | | | | | H | 2.90 | -7.23 | -7.85 |
| | | | | | | | | | | | | C | -.31 | -.31 | -2.08 |
| | | | | | | | | | | | | .25 Inch Gap | | | |
| | | | | | | | | | | | | H | 3.45 | -6.78 | -7.41 |
| | | | | | | | | | | | | C | -.25 | -.25 | -2.04 |
| Double-Glaze | | | | | | | | | | | | | | | |
| .50 Inch Gap | | | | | | | | | | | | | | | |
| H | 0. | 4.64 | 5.25 | -7.37 | -.04 | -1.23 | 2.57 | 1.61 | 1.64 | 2.90 | -5.88 | -5.87 | -4.01 | -11.38 | -13.21 |
| C | 0. | -1.90 | -2.12 | 0. | -1.68 | -1.26 | .41 | 1.04 | -1.50 | .09 | .28 | -.67 | -.89 | -.89 | -2.53 |
| .25 Inch Gap | | | | | | | | | | | | | | | |
| H | 1.84 | 6.66 | 7.29 | -5.80 | 1.81 | .57 | 4.51 | 3.52 | 3.55 | 4.85 | -4.25 | -4.24 | -2.31 | -9.96 | -11.85 |
| C | .23 | -1.74 | -1.96 | 0. | -1.51 | -1.08 | .66 | 1.31 | -1.32 | .33 | .52 | -.46 | -.69 | -.69 | -2.39 |
| | | | | | | | | | | | | Triple-Glaze, Double on South | | | |
| | | | | | | | | | | | | .50 Inch Gap | | | |
| | | | | | | | | | | | | H | -2.24 | -8.68 | -9.44 |
| | | | | | | | | | | | | C | -.51 | -.51 | -2.00 |
| | | | | | | | | | | | | .25 Inch Gap | | | |
| | | | | | | | | | | | | H | -.90 | -7.64 | -8.43 |
| | | | | | | | | | | | | C | -.31 | -.31 | -1.87 |
| Triple-Glaze | | | | | | | | | | | | | | | |
| .50 Inch Gap | | | | | | | | | | | | | | | |
| H | 0. | 3.99 | 4.94 | -5.51 | .05 | -1.20 | 2.30 | 1.46 | 1.34 | 2.61 | -5.15 | -5.26 | -3.62 | -9.13 | -10.61 |
| C | 0. | -1.73 | -2.07 | 0. | -1.48 | -1.16 | .38 | .99 | -1.39 | 0.5 | .24 | -.64 | -.80 | -.80 | -2.23 |
| .25 Inch Gap | | | | | | | | | | | | | | | |
| H | 1.42 | 5.59 | 6.59 | -4.34 | 1.48 | .17 | 3.83 | 2.95 | 2.83 | 4.15 | -3.96 | -4.07 | -2.36 | -8.12 | -9.67 |
| C | .22 | -1.59 | -1.94 | 0. | -1.32 | -.99 | .61 | 1.25 | -1.23 | .28 | .47 | -.45 | -.62 | -.62 | -2.11 |

[a]Figures are MBtu differences in heating and cooling loads from a base-case house (Denver ranch house with basement), with standard windows (15% of floor area) equally distributed and (1) single-glazed, (2) double-glazed, and (3) triple-glazed. Ref.Gl=reflective glass, Abs.Fl=absorptive glass, N.Ins=R-3 night insulation, T.Mass=thermal mass (4-in. concrete slab).

valuable resource for further research and analysis. In addition to producing a technical paper documenting the methodology of this study, the Residential Energy Analysis Group intends to investigate further the energy relationships between windows and building types, and between windows and climate parameters.

## CLIMATE ANALYSIS IN SUPPORT OF THE HOMEBUILDERS' GUIDE*

*Y.J. Huang*

The following climate analysis was done during FY 1982 as part of the technical support for the Homebuilder's Guide project. There were three major goals for this work: (1) to determine the number of cities for "base case" thermal integrity simulations, (2) to devise a simple technique for interpolating energy values from base city locations to other areas, and (3) to determine the number of cities for window sensitivity studies.

Major determinants in the analysis effort were the need to incorporate a large existing data base of DOE-2 simulations done in FY 1981 and the requirement that the techniques developed be comprehensible to the intended homebuilder audience.

### ACCOMPLISHMENTS DURING FY 1982

Climate data and the existing DOE-2 data base for 52 cities showed that the relationship of building to climate in most of these locations was divergent enough to keep them as base cities. Nine cities were eliminated as redundant while two new ones were added, resulting in a final list of 45 base cities for thermal integrity studies (Table 1). Thirty-year average heating and cooling degree-day totals at various base temperatures were compiled for more than 3000 National Oceanic and Atmospheric Administration (NOAA) cooperative stations, as were average summer wet-bulb temperatures and insolation values for more than 300 locations. These climate parameters were used to define regions within which DOE-2 values for a base city could be used for extrapolation to other locations, using ratios of heating degree-days at 57°F base (for heating) and cooling degree-days at 65°F base (for cooling).

DOE-2 runs were done for all 45 base locations to determine geographical variations in the impact on building energy use of varying window sizes and orientations. Following analysis of results, 11 cities were selected as base cities for comprehensive window sensitivity studies (Table 1).

Table 1. Base cities for the Homebuilders' Guide.[a]

| | | | | | |
|---|---|---|---|---|---|
| 1. | Albuquerque, NM | ( H*) | 24. | Las Vegas, NV | ( D ) |
| 2. | Atlanta, GA | ( D*) | 25. | Los Angeles, CA | ( J ) |
| 3. | Birmingham, AL | ( D ) | 26. | Medford, OR | ( C ) |
| 4. | Bismarck, ND | ( A ) | 27. | Memphis, TN | ( D ) |
| 5. | Boise, ID | ( B ) | 28. | Miami, FL | ( F*) |
| 6. | Boston, MA | ( B ) | 29. | Minneapolis, MN | ( A*) |
| 7. | Brownsville, TX | ( F ) | 30. | Nashville, TN | ( D ) |
| 8. | Buffalo, NY | ( A ) | 31. | New York, NY | ( C*) |
| 9. | Burlington, VT | ( A ) | 32. | Oklahoma City, OK | ( D ) |
| 10. | Cheyenne, WY | ( G ) | 33. | Omaha, NB | ( B ) |
| 11. | Chicago, IL | ( B*) | 34. | Philadelphia, PA | ( C ) |
| 12. | Charleston, SC | ( D ) | 35. | Phoenix, AZ | ( K*) |
| 13. | Cincinnati, OH | ( C ) | 36. | Pittsburgh, PA | ( B ) |
| 14. | Denver, CO | ( G*) | 37. | Portland, ME | ( B ) |
| 15. | El Paso, TX | ( H ) | 38. | Portland, OR | ( I ) |
| 16. | Fort Worth, TX | ( E ) | 39. | Reno, NV[b] | ( C ) |
| 17. | Fresno, CA | ( D ) | 40. | Salt Lake City, UT | ( B ) |
| 18. | Great Falls, MO | ( A ) | 41. | San Antonio, TX[b] | ( E ) |
| 19. | Honolulu, HA | ( F ) | 42. | San Diego, CA | ( J ) |
| 20. | Jacksonville, FL | ( E ) | 43. | San Francisco, CA | ( J*) |
| 21. | Juneau, AK | ( A ) | 44. | Seattle, CA | ( I*) |
| 22. | Kansas City, MO | ( C ) | 45. | Washington, DC | ( C ) |
| 23. | Lake Charles, LA | ( E ) | | | |

[a]Window zones are shown in parentheses (see Fig. 7); base cities selected for window sensitivity studies are indicated by asterisks.

[b]Reno, Nevada, and San Antonio, Texas, were added to complete national coverage. Cities for which DOE-2.1 runs were done but which had heating and cooling energy deltas within 5% of other cities were eliminated. They are: Raleigh, North Carolina; Tulsa, Oklahoma; Lake Charles, Louisiana; St. Louis, Missouri; and Richmond, Virginia.

#### Determination of Base Cities

A DOE-2 data base of over 3000 computer simulations was analyzed to determine the absolute as well as relative changes in heating and cooling energies for a prototype ranch house with varying thermal

*This work was supported by the Assistant Secretary for Conservation and Renewable Energy, Office of Conservation, Building Systems Division, U.S. Department of Energy under Contract No. DE-AC03-76SF00098.

integrity levels in 52 locations. (Figure 1 shows a typical plot of cooling energies for 16 levels of thermal integrity in 22 locations.) The original locations had been selected partly for climate differences and partly for population distribution. However, nine locations showed less than 5% difference in heating and cooling energies from that of other cities for the entire range of thermal integrity; these cities were therefore eliminated. Two new cities were added to differentiate between coastal and inland climates in the West and South, bringing the final number of base locations to 45.

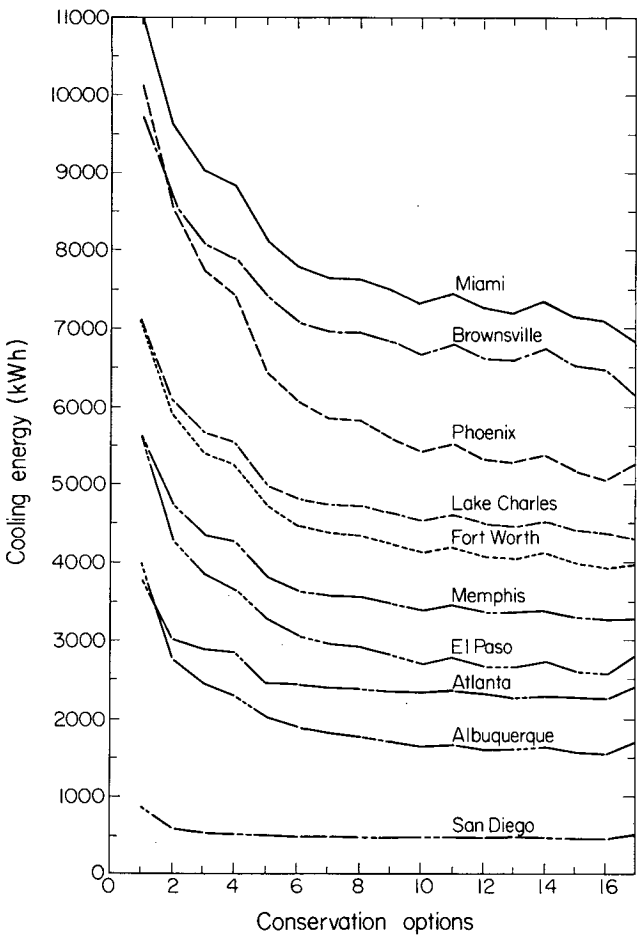


Figure 1. Cooling energies in 22 cities (slab foundations, up to 16 options). (XBL 831-1087)

## Development of Interpolation Technique

To develop the interpolation technique, climate data were compared with energy values from the original DOE-2 data base to establish those climate parameters useful for interpolating heating and cooling energies. Four parameters were selected as first-order indicators for residential building energy values:

(1) 57°F base heating degree-days for absolute heating energies.

(2) The ratio of base 65°F heating degree-days to base 57°F heating degree days for the delta (relative) change in heating energies due to varying thermal integrities. (Since a tight house has a lower balance point temperature than a loose one, this ratio will reflect the relative change in heating energies).

(3) Base 65°F cooling degree-days for absolute cooling energies.

(4) Latent enthalpy hours for the delta change in cooling energies due to varying thermal integrities. (Since latent heat is unaffected by changes in thermal integrity, locations with high latent enthalpy hours will show little change in cooling energies due to improvements in thermal integrity).

To keep the interpolation method simple, regional boundaries are drawn around each base city in such a way that the only interpolation necessary will be for heating and cooling degree-day differences. These will appear in the Homebuilders' Guide as tables of "location multipliers" and are actually the ratio of heating and cooling degree-days between secondary locations and the base city.

Thirty-year averages of heating and cooling degree-days to various temperature bases for over 3000 NOAA cooperative stations and Test Reference Year (TRY) data on latent enthalpy hours for 300 stations were used for drawing boundaries around the base cities. Figure 2 shows a sample of the NOAA degree-day data compiled for this work. Figures 3 and 4 show sample computer maps of heating degree-days and the ratio of heating degree-days to different base temperatures.

Since the one-step interpolation will take care of degree-day differences, more weight has been placed on keeping the relative changes in energies as uniform as possible within each region. A three-tiered system was devised for drawing boundaries between base cities; if no significant variation between cities were found under the first-level criteria, the second-level criteria were used; if neither varied, then the third-level criteria were used. These criteria are as follows:

*Heating Boundaries*

(1) Equal differences in the ratio between heating degree-days base 65 to heating degree-days base 57 between base cities.

(2) Equal differences in heating degree-days.

(3) Equal geographical distance between base cities.

*Cooling Boundaries*

(1) Equal differences in latent enthalphy hours between base cities.

(2) Equal differences in cooling degree-days.

(3) Equal geographical distance between base cities.

Figure 5 shows the resulting boundaries for the 45 cities. These boundaries will not appear in the Homebuilders' Guide, although they can be inferred by the selection of base cities and the "location multipliers" given for secondary locations.

## Determination of Window Sensitivities for Base Cities

The following set of sensitivity runs were done using DOE-2 for all 45 base cities to determine variations in relative heating and cooling energies due to changes in window size and orientation (the base case has 10% glazing equally distributed):

(a) 15% glazing equally distributed, loose thermal integrity

(b) 15% glazing equally distributed, tight thermal integrity

(c) 15% glazing, 12.5% on the south, loose thermal integrity

(d) 15% glazing, 12.5% on the south, tight thermal integrity

The equally distributed sensitivities indicate the combination of solar transmission gain and conduction losses as window size increases, while the

| Station name | Station number | Zone no. | Lat-titude | Longi-tude | HDD 50 | HDD 55 | HDD 57 | HDD 60 | HDD 65 | CDD 55 | CDD 60 | CDD 65 | CDD 70 |
|---|---|---|---|---|---|---|---|---|---|---|---|---|---|
| ANDALUSIA 1 NW | 010252 | 12 | 31.19 | 86.30 | 573 | 975 | 1177 | 1535 | 2305 | 4498 | 3237 | 2181 | 1295 |
| ANNISTON FAA AP | 010272 | 2 | 33.35 | 85.51 | 812 | 1319 | 1567 | 1999 | 2872 | 3912 | 2771 | 1809 | 1043 |
| AUBURN AGRONOMY FARM | 010430 | 3 | 32.36 | 85.30 | 691 | 1153 | 1382 | 1783 | 2611 | 4109 | 2914 | 1921 | 1096 |
| BAY MINETTE | 010583 | 20 | 30.53 | 87.47 | 333 | 620 | 770 | 1061 | 1688 | 5028 | 3644 | 2447 | 1463 |
| BELLE MINA 2 N | 010655 | 3 | 34.42 | 86.53 | 1075 | 1630 | 1898 | 2371 | 3273 | 3684 | 2600 | 1680 | 971 |
| BIRMINGHAM WSO CITY | 010829 | 3 | 33.28 | 86.50 | 851 | 1368 | 1619 | 2066 | 2943 | 3965 | 2839 | 1891 | 1138 |
| BIRMINGHAM WSO | 010831 | 3 | 33.34 | 86.45 | 817 | 1318 | 1563 | 2002 | 2863 | 3987 | 2845 | 1881 | 1114 |
| BREWTON 3 SSE | 011084 | 12 | 31.04 | 87.03 | 430 | 770 | 945 | 1268 | 1970 | 4659 | 3332 | 2212 | 1283 |
| CHATOM 3 N | 011566 | 12 | 31.30 | 88.15 | 438 | 773 | 963 | 1287 | 2001 | 4624 | 3306 | 2193 | 1276 |
| CLANTON | 011694 | 3 | 32.51 | 86.38 | 823 | 1342 | 1592 | 2038 | 2896 | 3872 | 2746 | 1781 | 1025 |
| DAYTON | 012188 | 3 | 32.21 | 87.39 | 648 | 1069 | 1279 | 1646 | 2431 | 4462 | 3215 | 2177 | 1297 |
| DEMOPOLIS LOCK AND D | 012245 | 3 | 32.31 | 87.50 | 727 | 1190 | 1417 | 1813 | 2640 | 4230 | 3034 | 2033 | 1205 |
| EUFAULA | 012730 | 12 | 31.59 | 85.06 | 559 | 942 | 1144 | 1498 | 2266 | 4474 | 3202 | 2145 | 1274 |
| EVERGREEN | 012758 | 12 | 31.26 | 86.56 | 556 | 935 | 1136 | 1485 | 2241 | 4531 | 3253 | 2184 | 1292 |
| FAIRHOPE 2 NE | 012813 | 20 | 30.33 | 87.53 | 326 | 599 | 742 | 1017 | 1618 | 5155 | 3748 | 2524 | 1525 |
| FAYETTE | 012883 | 3 | 33.41 | 87.49 | 895 | 1435 | 1699 | 2149 | 3042 | 3830 | 2720 | 1786 | 1033 |
| FRISCO CITY | 013105 | 12 | 31.26 | 87.24 | 516 | 884 | 1082 | 1417 | 2144 | 4669 | 3373 | 2276 | 1352 |
| GADSDEN STEAM PLANT | 013154 | 3 | 34.02 | 86.00 | 956 | 1512 | 1782 | 2250 | 3160 | 3673 | 2587 | 1671 | 958 |
| GREENSBORO | 013511 | 3 | 32.42 | 87.36 | 597 | 1010 | 1223 | 1587 | 2361 | 4491 | 3240 | 2190 | 1319 |
| HALEYVILLE | 013620 | 3 | 34.14 | 87.37 | 1158 | 1750 | 2036 | 2527 | 3454 | 3470 | 2422 | 1528 | 845 |
| HEADLAND | 013761 | 12 | 31.21 | 85.20 | 506 | 852 | 1041 | 1367 | 2068 | 4699 | 3389 | 2269 | 1332 |
| HIGHLAND HOME | 013816 | 12 | 31.57 | 86.19 | 602 | 989 | 1193 | 1541 | 2302 | 4433 | 3155 | 2090 | 1216 |
| HUNTSVILLE WSO | 014064 | 3 | 34.39 | 86.46 | 1083 | 1636 | 1906 | 2379 | 3279 | 3716 | 2634 | 1708 | 995 |
| LAFAYETTE | 014502 | 3 | 32.54 | 85.24 | 707 | 1166 | 1395 | 1797 | 2637 | 3989 | 2798 | 1806 | 1010 |
| MARION JUNCTION 2 NE | 015121 | 3 | 32.28 | 87.13 | 678 | 1117 | 1335 | 1716 | 2518 | 4318 | 3095 | 2073 | 1229 |
| MOBILE WSO | 015478 | 20 | 30.41 | 88.15 | 347 | 633 | 787 | 1073 | 1695 | 5232 | 3848 | 2643 | 1647 |
| MONTGOMERY WSO | 015550 | 12 | 32.18 | 86.24 | 568 | 960 | 1167 | 1519 | 2277 | 4608 | 3238 | 2274 | 1387 |
| MUSCLE SHOALS FAA AP | 015749 | 27 | 34.45 | 87.37 | 1098 | 1663 | 1943 | 2414 | 3315 | 3783 | 2709 | 1788 | 1067 |
| ONEONTA | 016121 | 3 | 33.57 | 86.29 | 1105 | 1694 | 1984 | 2469 | 3406 | 3487 | 2437 | 1554 | 870 |
| OZARK 6 NNW | 016218 | 12 | 31.31 | 85.41 | 436 | 762 | 937 | 1249 | 1928 | 4778 | 3439 | 2293 | 1358 |
| ROBERTSDALE 1 E | 016988 | 20 | 30.32 | 87.40 | 362 | 655 | 809 | 1104 | 1738 | 4940 | 3563 | 2373 | 1398 |
| ROCK MILLS | 017025 | 3 | 33.09 | 85.18 | 880 | 1399 | 1655 | 2108 | 2996 | 3725 | 2609 | 1672 | 937 |
| SAINT BERNARD | 017157 | 12 | 34.12 | 86.47 | 1201 | 1817 | 2120 | 2612 | 3570 | 3402 | 2375 | 1508 | 836 |
| SAND MT SUBSTA AU | 017207 | 2 | 34.17 | 85.58 | 1114 | 1695 | 1985 | 2478 | 3411 | 3385 | 2338 | 1452 | 786 |
| SCOTTSBORO | 017304 | 2 | 34.41 | 86.03 | 1178 | 1783 | 2082 | 2587 | 3534 | 3431 | 2402 | 1531 | 854 |
| SELMA | 017366 | 3 | 32.25 | 87.00 | 469 | 819 | 1004 | 1334 | 2040 | 4858 | 3546 | 2433 | 1498 |
| TALLADEGA | 018024 | 3 | 33.27 | 86.06 | 816 | 1312 | 1556 | 2001 | 2878 | 3786 | 2649 | 1703 | 968 |
| THOMASVILLE | 018178 | 12 | 31.55 | 87.44 | 653 | 1064 | 1275 | 1636 | 2413 | 4438 | 3180 | 2132 | 1267 |
| TROY | 018323 | 12 | 31.49 | 85.59 | 466 | 811 | 1004 | 1333 | 2052 | 4633 | 3326 | 2219 | 1305 |
| TUSCALOOSA FAA AP | 018380 | 3 | 33.14 | 87.37 | 738 | 1208 | 1439 | 1842 | 2675 | 4289 | 3101 | 2102 | 1278 |
| UNION SPRINGS | 018438 | 12 | 32.08 | 85.43 | 642 | 1055 | 1268 | 1639 | 2433 | 4356 | 3113 | 2080 | 1225 |
| VALLEY HEAD | 018469 | 2 | 34.34 | 85.37 | 1413 | 2078 | 2403 | 2929 | 3958 | 3034 | 2058 | 1262 | 667 |

Figure 2. Sample page of heating (HDD) and cooling (CDD) degree-day data to different base temperatures (°F), from 3000 National Oceanic and Atmospheric Administration cooperative stations.

south-oriented sensitivities indicate the amount of solar transmission gain possible.

The results were then mapped to clarify the geographical differences. Figure 6 shows the change in heating energy for a tight house when window area is increased from 10% to 15% of floor area (gradient lines represent 1 MBtu difference in heating energy). Figure 7 shows the grouping of cities that resulted. There are six zones in the eastern half of the country running basically east-west (zones A,B,C,D,E,F). Zones G and H have been separated because of the large solar heat gains in the Rockies, as have Zones I and J because of the low solar heat gains along the Pacific coast. Finally, zone K in the southwest has been separated because of its extreme increase in cooling energies.

## PLANNED ACTIVITIES FOR FY 1983

A large amount of climate data has been gathered and analyzed in the course of this work. This information is extremely useful for continued research into the relationship between climate and building energy use. More comprehensive analysis, particularly in correlating climate parameters to cooling energy use, will make it possible to reduce the DOE-2 data base to a set of mathematical equations.

The analysis so far has covered only single-family detached houses. Additional research will be necessary to extend the analysis to cover other residential buildings such as multi-family units and condominiums.

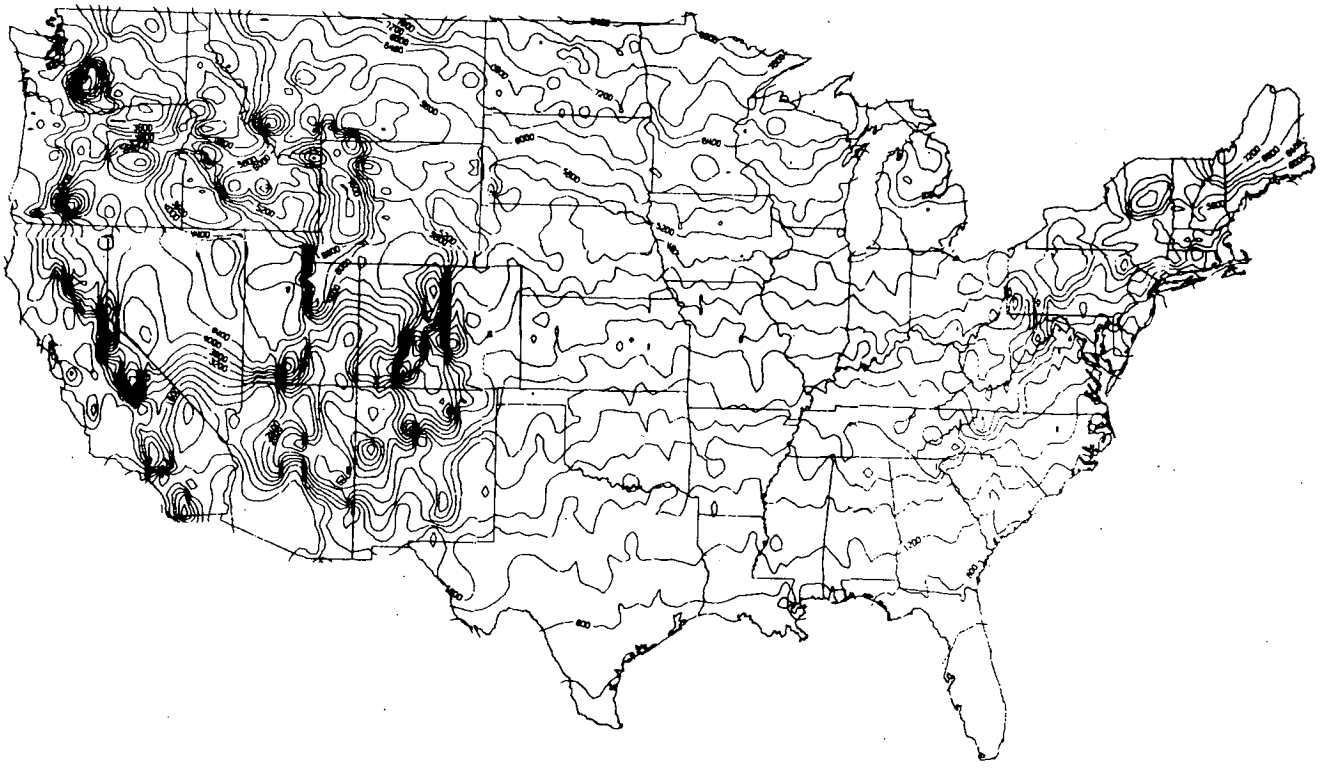

Figure 3. Heating degree-days (3118 Stations) at base 57°F. (XBL 831-1081)

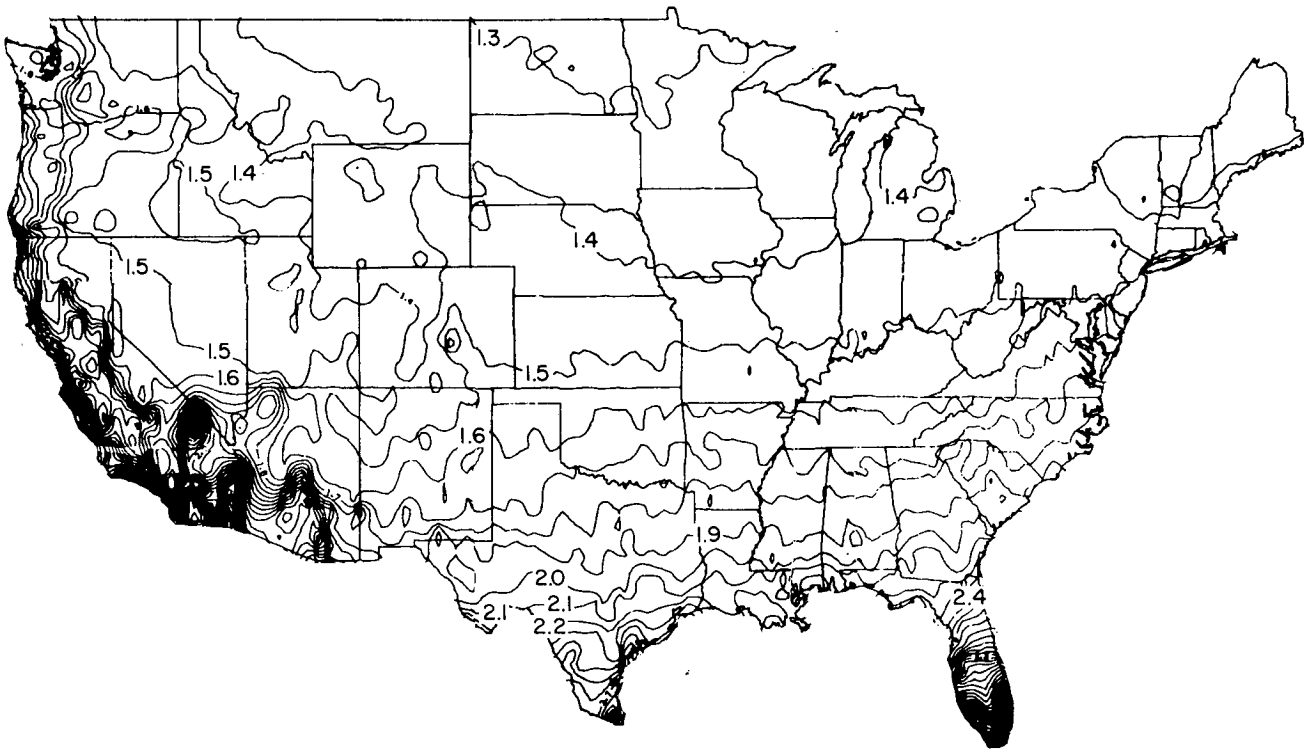


Figure 4. Heating degree-day ratios (HDD base 65/HDD base 57), in °F. (XBL 831-1082)

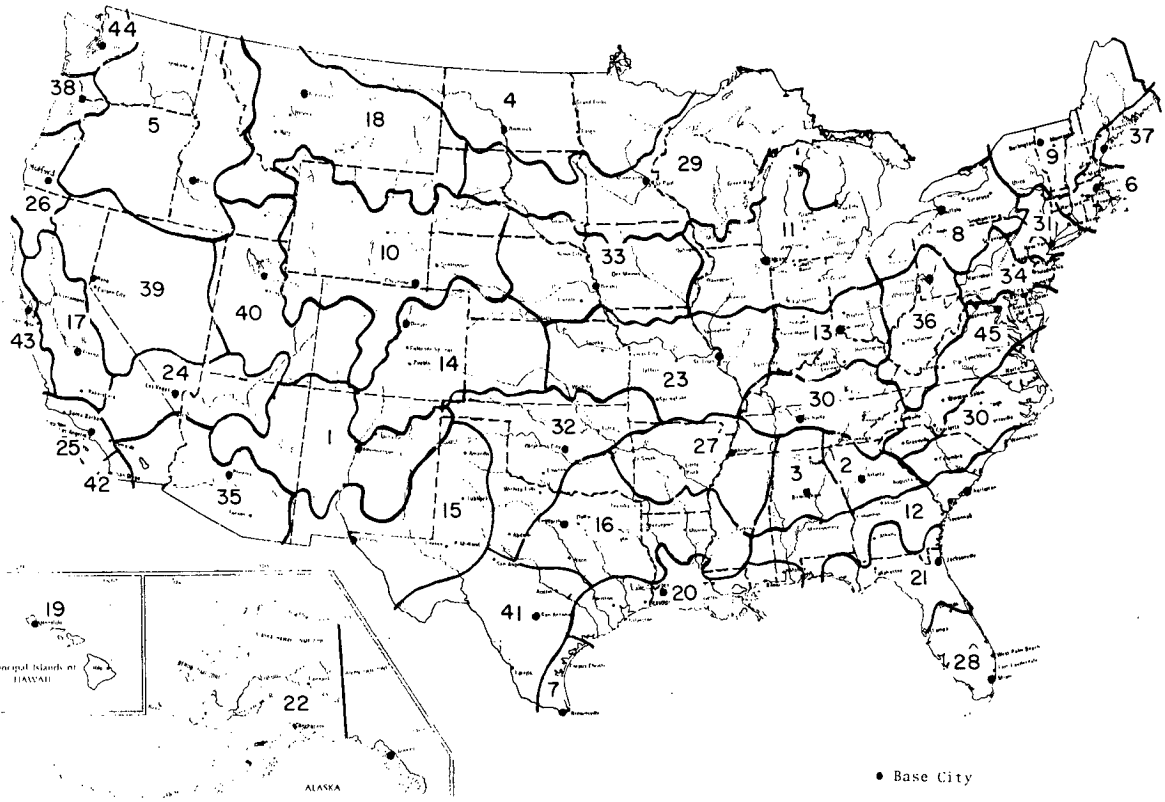


Figure 5. Base cities and boundaries for Homebuilders' Guide. (see Table 1 for numbered list of base cities.) (XBL 831-1083)

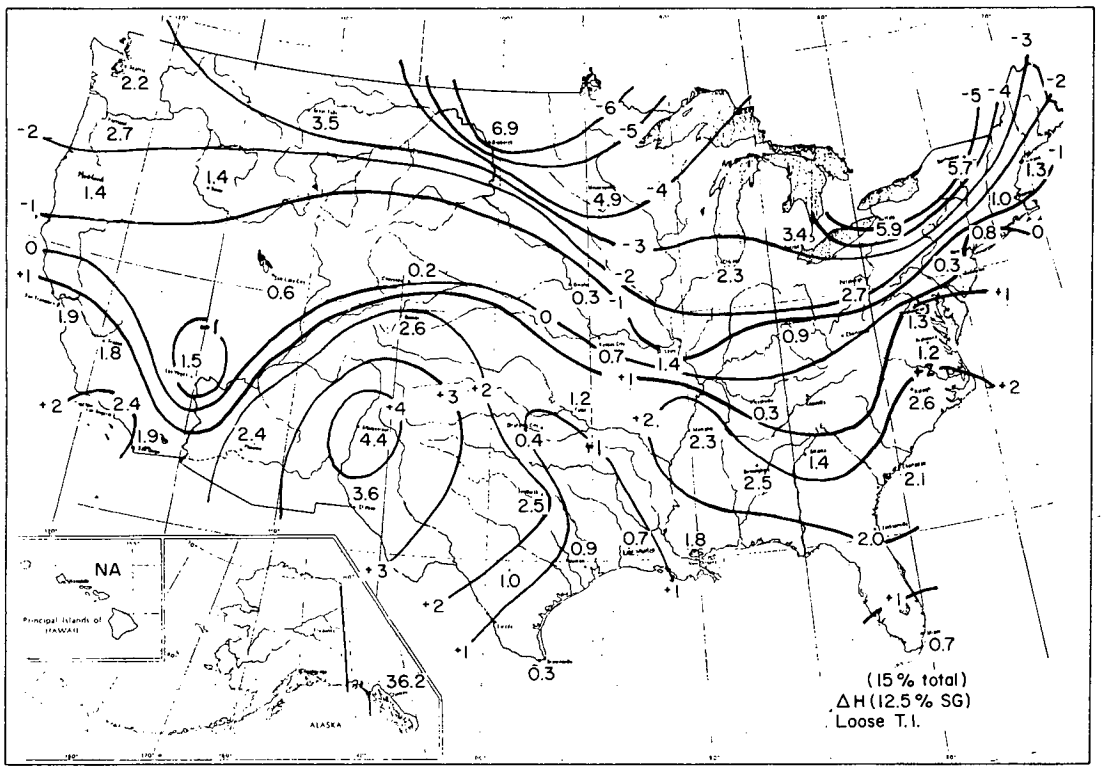


Figure 6. Relative heating energies for a loose house when window area is increased from 10% equally distributed to 15% (12.5% on the south, and 2.5% on the north). (XBL 831-1084)

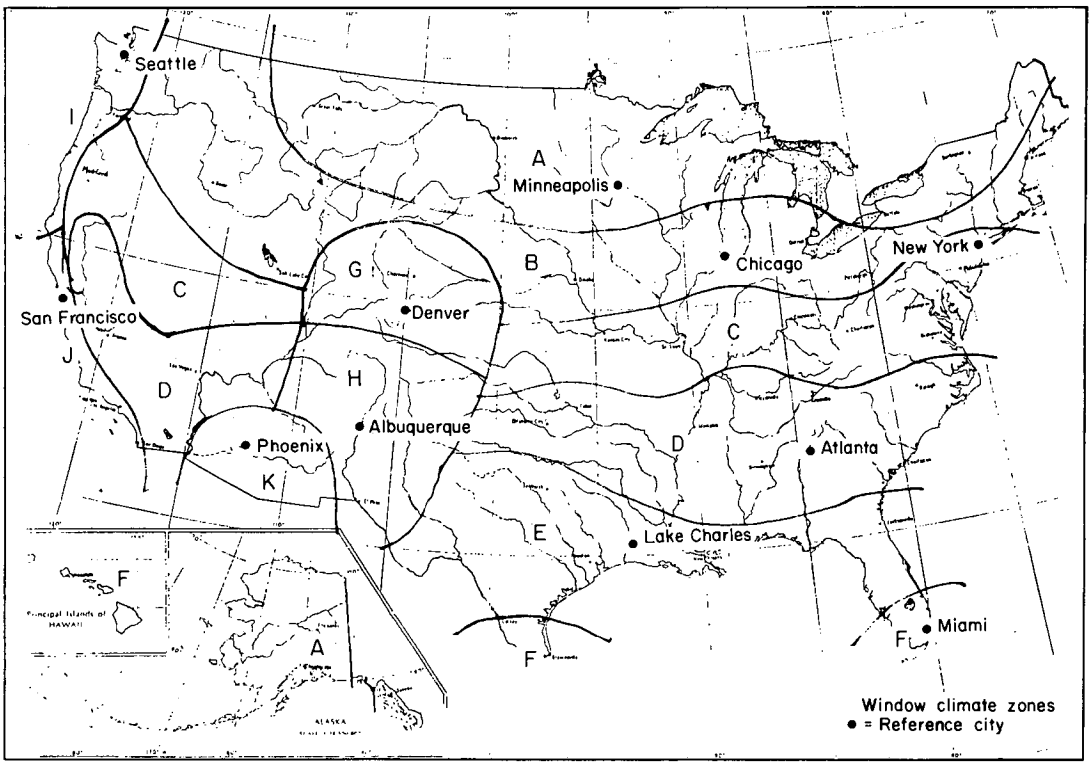


Figure 7. Base cities and zones for window sensitivity studies. (XBL 831-1080)

# DETERMINATION OF THE SEASONAL COEFFICIENT OF PERFORMANCE OF CONVENTIONAL AIR SOURCE HEAT PUMPS IN RESIDENTIAL BUILDINGS*

*J.G. Ingersoll and D.K. Arasteh*

The steady-state coefficient of performance (COP) of a heat pump as given by the manufacturer does not provide adequate information to determine its seasonal (actual) coefficient (SCOP) as installed in a building. (The seasonal cooling COP is also the device's energy efficiency rating.) The diurnal and seasonal weather variability specific to any location coupled with the particular characteristics of the building and the heat pump will degrade any device's performance. Existing rules used to infer a seasonal COP from manufacturers' data and weather information are not detailed enough to provide accurate results.

The DOE-2 computer code has been applied, with proper adjustments, to the heat-pump parameters in order to match measured performance data. A SCOP has thus been determined for 44 locations in the United States for single-family one-story, two-story, and townhouse prototypical buildings. The results are universal in that they apply to any heat pump whose steady-state COP is known, that is, when the SCOP is expressed as directly proportional to the steady-state COP at the American Refrigeration Institute (ARI) established points for heating (47°F) and cooling (95°F). This constitutes a significant improvement over previous determinations of the SCOP, which appear limited to specific devices. Empirical equations have been derived expressing the SCOP for heating and for cooling as functions of the respective steady state heating and cooling COPs as well as heating and cooling degree-days.

## ACCOMPLISHMENTS DURING FY 1982

### Methodology

Four designs representative of current construction have been analyzed: a one-story, 1540 $ft^2$ house with 154 $ft^2$ of glass area; a two-story, 2240-$ft^2$ house with 224 $ft^2$ of glass area; a split-level 1905-$ft^2$ house with 210 $ft^2$ of glass area; and a two-story 1200-$ft^2$ attached townhouse with 144 $ft^2$ of glass area.[1] The window area is assumed to be equally distributed on all four sides so as to take into account the random orientation of buildings. Each prototype is assumed to be well-insulated with R30 to R38 (very cold climates) ceiling insulation; R19 wall insulation; R5 perimeter insulation up to 2 feet deep for a slab-on-grade foundation and 8 feet for a basement foundation, or R11 underfloor insulation for a vented crawl-space foundation; double or triple (very cold climates) glazings with 1/2-inch air gaps; and an average infiltration of 0.7 ach for the five winter months from November to March, including air changes due to building operation.

Each building is kept at 70°F during the heating season and at 78°F during the cooling season. The heat pump is assumed to have a 3-ton capacity, which is adequate for the heating and cooling of all prototypical buildings when they are well-insulated and have no temperature setbacks. A 3-kW electric resistance heater supplies any additional heating capacity that the heat pump may be unable to provide during very cold hours. It is also assumed that the electric resistance heater is thermostatically controlled and is automatically turned on when the ambient air temperature is below 30°F. Since the heat pump modeled here is a split system with the compressor located outdoors, it is assumed that a 50-W crankcase heater is activated whenever necessary.[2]

Taking into account the outdoor (climatic) and indoor (thermostat setting, internal load) conditions for each hour as well as those of the previous hours, DOE-2 calculates the building's heating/cooling load for that hour. The energy required to meet the load is then calculated from the capacity of the heat pump at the hour's outdoor dry-bulb temperature (full-load COP) and the ratio of the building load to the equipment capacity in that hour (partial-load COP). In our analysis, we had to determine the proper full-load and partial-load COP curves according to manufacturer's data and measured heat pump performance data in buildings.

*This work was supported by the Assistant Secretary for Conservation and Renewable Energy, Office of Buildings and Community Systems, Buildings Division of the U.S. Department of Energy, under Contract No. DE-AC03-76SF00098.

The full-load COP curve, as supplied by the heat-pump manufacturer, has to be modified for the heating mode to include the effect of performance degradation caused by the accumulation of frost on the system's evaporator coils. The build-up of frost, which commences at about 50°F and becomes rather significant below 40°F, reduces the net heat transfer from the outside air to the refrigerant fluid, resulting in a lower system performance. Unpublished performance data for these conditions were obtained from a manufacturer of relatively efficient heat pumps.[3] These data agree with experiments, as yet unpublished, by the National Bureau of Standards (NBS), which show approximately a 15% decrease in performance at 35°F.[4] In the cooling mode, no such degradation takes place. However, the heat-pump performance in the cooling mode depends on the outdoor and indoor wet-bulb temperatures. The coil by-pass factor is furthermore assumed to be fixed at 0.1.

Heat-pump performance degradation due to cycling on and off has also been incorporated in the analysis. The resulting partial-load factor is defined as the ratio of the building's load (heating or cooling) at a given ambient temperature to the heat pump's capacity at the same temperature. Since DOE-2.1A performs only hourly calculations, a partial load is defined for every hour of the year. The partial-load curves are based on data taken at NBS and assume an average cycling rate of one cycle per hour (1.0 cph)—typical of new buildings with relatively long thermal constants due to high thermal integrities.

The curves for full load with defrost degrade and partial load were adjusted so as to be able to reproduce—using DOE-2.A—the measured seasonal COPs of specific heat pumps operated in buildings over a period of 2 years.[5] This adjustment provides a certain degree of confidence that our empirical heat-pump model is satisfactory for performance simulations and that the obtained seasonal COPs are therefore on the right track. Additional validation will be required, however, to further test both the model and the values of its parameters and to improve on either or both of them if necessary.

## Results

The seasonal COPs for heating and cooling for each of the four prototypical buildings have been calculated for 44 locations representing all the major population centers and climatic regions of the country. Since an Oak Ridge National Laboratory (ORNL) study has indicated that the relative seasonal degradation of the COP is independent of the steady-state COP itself at the ARI points,[5] we have expressed all the seasonal COPs in a normalized form that makes them applicable to any heat-pump model, not just the one used here. This normalization has been achieved by dividing the heating and cooling seasonal COPs obtained through the DOE-2 simulations with the respective steady-state COPs supplied by the manufacturer for the ARI rating points.

The resulting COPS are presented in Table 1. Sensitivity studies have been performed to determine the effect on these COPs of a number of parameters. These parameters included: full-load curves from other manufacturers of heat pumps; buildings of

Table 1. Normalized seasonal heating and cooling COPs for four prototypical single-family houses in 44 locations in the U.S.[a]

| | Heating (SHCOP/HCOP) | | | | Cooling (SCCOP/CCOP) | | | |
|---|---|---|---|---|---|---|---|---|
| Location | 1-S | 2-S | S-L | T-H | 1-S | 2-S | S-L | T-H |
| Albuquerque, NM | 0.62 | 0.63 | 0.62 | 0.59 | 0.71 | 0.72 | 0.72 | 0.69 |
| Atlanta, GA | 0.64 | 0.66 | 0.65 | 0.60 | 0.81 | 0.81 | 0.81 | 0.80 |
| Birmingham, AL | 0.64 | 0.65 | 0.65 | 0.60 | 0.83 | 0.82 | 0.82 | 0.81 |
| Bismark, ND | 0.51 | 0.49 | 0.50 | 0.52 | 0.66 | 0.69 | 0.69 | 0.63 |
| Boise, ID | 0.64 | 0.65 | 0.64 | 0.59 | 0.69 | 0.69 | 0.68 | 0.64 |
| Boston, MA | 0.65 | 0.66 | 0.65 | 0.60 | 0.64 | 0.67 | 0.67 | 0.61 |
| Brownsville, TX | 0.66 | 0.68 | 0.67 | 0.63 | 0.86 | 0.84 | 0.84 | 0.85 |
| Buffalo, NY | 0.63 | 0.62 | 0.62 | 0.60 | 0.52 | 0.58 | 0.58 | 0.51 |
| Burlington, VT | 0.57 | 0.55 | 0.56 | 0.57 | 0.55 | 0.59 | 0.60 | 0.52 |
| Charleston, SC | 0.66 | 0.67 | 0.66 | 0.61 | 0.85 | 0.83 | 0.83 | 0.83 |
| Cheyenne, WY | 0.60 | 0.59 | 0.59 | 0.57 | 0.44 | 0.49 | 0.51 | 0.44 |
| Chicago, IL | 0.62 | 0.61 | 0.61 | 0.59 | 0.68 | 0.70 | 0.70 | 0.64 |
| Cincinnati, OH | 0.64 | 0.64 | 0.63 | 0.60 | 0.77 | 0.78 | 0.77 | 0.74 |
| Denver, CO | 0.62 | 0.62 | 0.62 | 0.59 | 0.58 | 0.58 | 0.59 | 0.52 |
| El Paso, TX | 0.63 | 0.65 | 0.64 | 0.59 | 0.78 | 0.78 | 0.78 | 0.77 |
| Fort Worth,TX | 0.64 | 0.66 | 0.65 | 0.60 | 0.83 | 0.82 | 0.82 | 0.81 |
| Fresno, CA | 0.65 | 0.67 | 0.66 | 0.61 | 0.74 | 0.74 | 0.74 | 0.74 |
| Great Falls, MT | 0.57 | 0.56 | 0.56 | 0.55 | 0.44 | 0.49 | 0.51 | 0.44 |
| Honolulu, HI | .... | .... | .... | .... | 0.89 | 0.88 | 0.84 | 0.84 |
| Jacksonville, FL | 0.66 | 0.68 | 0.67 | 0.62 | 0.85 | 0.84 | 0.84 | 0.84 |
| Juneau, AL | 0.62 | 0.62 | 0.62 | 0.68 | .... | .... | .... | .... |
| Kansas City, MO | 0.61 | 0.60 | 0.60 | 0.59 | 0.80 | 0.80 | 0.79 | 0.77 |
| Lake Charles, LA | 0.65 | 0.67 | 0.66 | 0.62 | 0.85 | 0.84 | 0.83 | 0.84 |
| Las Vegas, NV | 0.66 | 0.68 | 0.67 | 0.62 | 0.77 | 0.75 | 0.75 | 0.75 |
| Los Angeles, CA | 0.71 | 0.72 | 0.71 | 0.67 | 0.24 | 0.28 | 0.30 | 0.27 |
| Medford, OR | 0.65 | 0.66 | 0.65 | 0.60 | 0.32 | 0.62 | 0.64 | 0.56 |
| Memphis, TN | 0.65 | 0.66 | 0.66 | 0.61 | 0.83 | 0.82 | 0.80 | 0.81 |
| Miami, FL | 0.66 | 0.68 | 0.67 | 0.62 | 0.88 | 0.86 | 0.86 | 0.87 |
| Minneapolis, MN | 0.53 | 0.51 | 0.52 | 0.53 | 0.75 | 0.76 | 0.76 | 0.72 |
| Nashville, TN | 0.64 | 0.64 | 0.64 | 0.60 | 0.81 | 0.80 | 0.80 | 0.79 |
| New York, NY | 0.65 | 0.66 | 0.65 | 0.61 | 0.73 | 0.74 | 0.74 | 0.70 |
| Oklahoma City, OK | 0.62 | 0.62 | 0.62 | 0.60 | 0.80 | 0.80 | 0.79 | 0.66 |
| Omaha, NB | 0.59 | 0.57 | 0.57 | 0.58 | 0.77 | 0.78 | 0.77 | 0.74 |
| Philadelphia, PA | 0.65 | 0.66 | 0.65 | 0.60 | 0.78 | 0.78 | 0.78 | 0.75 |
| Phoenix, AZ | 0.64 | 0.66 | 0.65 | 0.61 | 0.80 | 0.78 | 0.78 | 0.78 |
| Pittsburgh, PA | 0.63 | 0.63 | 0.63 | 0.60 | 0.70 | 0.72 | 0.72 | 0.68 |
| Portland,ME | 0.61 | 0.60 | 0.60 | 0.61 | 0.46 | 0.53 | 0.54 | 0.41 |
| Portland, OR | 0.66 | 0.67 | 0.66 | 0.66 | 0.47 | 0.47 | 0.47 | 0.47 |
| Salt Lake City, UT | 0.63 | 0.63 | 0.63 | 0.59 | 0.68 | 0.70 | 0.70 | 0.85 |
| San Diego, CA | 0.71 | 0.72 | 0.71 | 0.68 | 0.38 | 0.39 | 0.43 | 0.40 |
| San Francisco, CA | 0.68 | 0.69 | 0.68 | 0.65 | 0.09 | 0.10 | 0.12 | 0.11 |
| San Antonio, TX | 0.65 | 0.67 | 0.66 | 0.61 | 0.84 | 0.82 | 0.82 | 0.82 |
| Seattle, WA | 0.66 | 0.67 | 0.66 | 0.60 | 0.34 | 0.35 | 0.34 | 0.28 |
| Washington, DC | 0.65 | 0.66 | 0.65 | 0.61 | 0.79 | 0.79 | 0.78 | 0.76 |

[a]1-S = One-story; 2-S = Two-story; S-P = Split-level; T-H = Townhouse.

different thermal integrity than those used in this analysis; and different size (capacity) for the heat pump. The resulting sensitivities will only be summarized here. The effect of full-load or steady-state curves of other manufacturers is small, i.e., within a few percent. This is because heat-pump curves tend to be very similar in shape. The effect of different building thermal integrities is also within a few percentage points as long as the building has roughly R19 ceiling insulation, R11 wall insulation, double-glazed windows, no foundation insulation for a slab, R5 for a basement or R11 for a vented crawl space, and an infiltration rate of 0.7 ach or less.

These insulation levels are already typical of new construction in every part of the country[1] and are such that a typical building of every climate in the United States would not need a heating or cooling heat-pump system in excess of 3 tons capacity. For some climates and a higher level of thermal integrity, a smaller system—one as low as 1.5 tons capacity—could be acceptable, but this is true for cooling rather than heating. The hourly demand for heating is nearly as high in a heating climate as it is in a cooling climate, albeit for many fewer hours in the latter. The converse is true for cooling. The difference is that the hourly demand for heating is higher than that for cooling in all climates, although the duration of each changes with climate. Consequently, while a 3-ton heat pump will be needed for heating in both New York and Phoenix, a 1.5-ton heat pump will be adequate for cooling in both locations, at least in new construction or in buildings with better levels of thermal integrity. Heat pumps with a smaller capacity for cooling than for heating can be expected to perform a little better overall than heat pumps with equal heating and cooling capacities. This improvement of the seasonal COP in the cooling mode is nevertheless no more than 5%.

### Conclusions

The results presented in Table 1 indicate clearly that in almost all climates the seasonal heating COP is degraded from the manufacturer's steady state COP anywhere between 35 and 45%; and the seasonal cooling COP is degraded between 20 and 30%. We can also discern a rather characteristic trend in both the heating and cooling seasonal COPs. In the heating seasonal COPs a broad maximum exists for climates with 2000 to 4000 heating degree-days, base 65°F. The seasonal heating COP is less for climates with fewer heating degree-days because of cycling or partial-load degradation and also for climates with more degree-days because of degradation from use of the auxiliary resistance heater. The seasonal cooling COP, on the other hand, appears to improve as the cooling degree-days increase. For any location with fewer than 1000 cooling degree-days, base 65°F, degradation due to cycling is substantial. Between 1000 and 3000 degree-days, the seasonal COP increases significantly, and, above 3000 degree-days, it remains virtually unchanged. Also, for all cooling degree-days, the seasonal COP rises with higher humidity, presumably because of a better utilization of the latent capacity of the device.

## PLANNED ACTIVITIES FOR FY 1983

Although this task—determining the seasonal coefficient of performance of heat pumps—was concluded in FY 1982, the information gathered and the methods developed will be used to support other Building Energy Analysis Projects.

## REFERENCES


1. National Association of Home Builders Research Foundation, Inc. (1980), *Single-Family Detached and Attached Construction Practices—1979*, Rockville, MD.
2. Dossat, R.J. (1978), *Principles of Refrigeration*, 2nd Ed., pp. 460-461, John Wiley and Sons, New York.
3. Hurle, G., The Coleman Company (1980), private communication.
4. Didion, D., National Bureau of Standards (1982), private communication.
5. Baxter, V.D., et al. (1982), "Comparison of Field Performance to Steady-State Performance for Two Dealer-Installed Air-to-Air Heat Pumps," Oak Ridge National Laboratory, Oak Ridge, TN (unpublished).

# ENERGY EFFICIENCY IN CHINESE BUILDINGS*

*Y.J. Huang, A. Canha de Piedade, A.H. Rosenfeld, and D. Tseng*

Energy analysis of conservation measures for Chinese buildings is intriguing because there are large differences in construction, use patterns, and space conditioning demands in comparison with the United States. Since the construction industry in China is one of the largest in the world, its adoption of conservation measures could have a significant impact on world energy consumption. Furthermore, insights gained from this study may be applied to formulating conservation strategies for other developing nations.

## ACCOMPLISHMENTS DURING FY 1982

A cost-benefit analysis of energy conservation measures for typical Chinese residential buildings was done using the DOE-2 energy analysis program and simple economic calculations. Through the help of a visiting Chinese architect as well as sources in China, fairly detailed information was gathered on building designs, construction practices, operating conditions, and building costs in the People's Republic of China. Weather tapes were also obtained for the two largest Chinese cities, Beijing and Shanghai.

Results from this preliminary study showed that simple conservation measures would conserve coal in Beijing at a cost below the international price, even without additional savings from infiltration reduction and possible downsizing of the central heating system. For Shanghai, similar conservation measures in unheated buildings would raise winter indoor temperatures to within the comfort zone.

### Methodology

A DOE-2 input file was created for a "typical design" low-rise multi-family residential building representative of current Chinese construction. ("Typical design" is a term used in China to refer to standardized building designs that are mass-produced to meet urban housing needs.) For simplicity, only a middle floor unit with three apartment units and a stairwell was simulated (Fig. 1). The following input was used for internal loads: occupants at 1 person/12 $m^2$ of floor area, plus lights and cooling at 1 $W/m^2$. Since we were unable to find data on infiltration rates for Chinese houses, simulations were done using two rates—a "leaky" rate averaging 1 ach, and a "medium" rate averaging 0.5 ach. For Beijing, the building was modeled with a central heating system (coal-fired, circulating hot water); for Shanghai, the building was modeled both with and without a central heating system. No cooling system was simulated for either city.

Parametric analysis for Beijing and Shanghai included envelope conditions ranging from the current Chinese practice of using brick walls (37 cm thick on the north and 24 cm on the south) and single-glazed windows to options such as cavity brick walls, cavity walls with perlite, aerated concrete infill walls, insulated sandwich panels, and double-glazed windows.

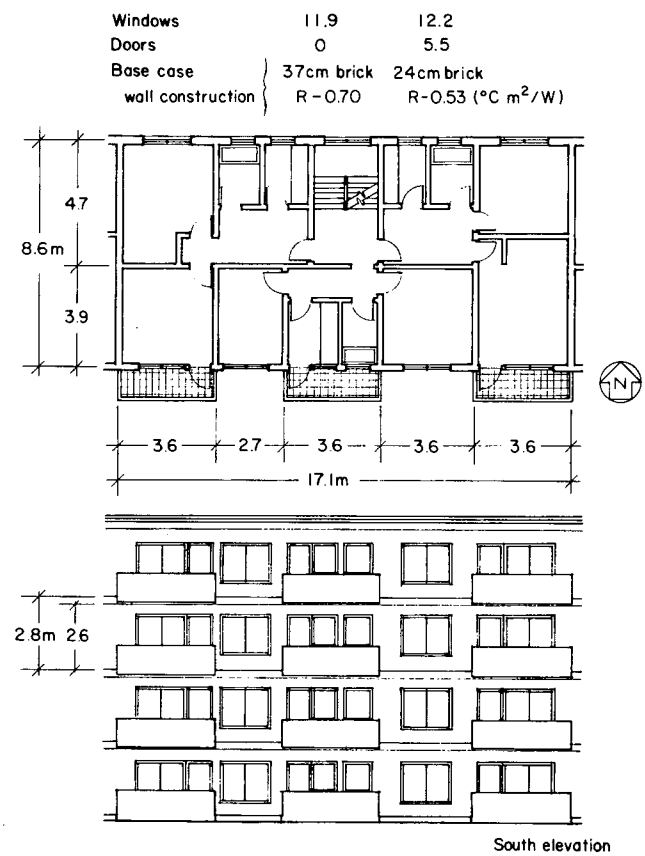


Figure 1. Typical design for three-apartment middle unit. For the base case, the north wall (37 cm brick) has a conductance $k$ = 1.42 $W/m^2K$. When a 10-cm cavity filled with expanded perlite is introduced between the same 37 cm of bricks, $k$ drops to 0.45 $W/m^2K$. (XBL 8210-4864)

*This work was supported by the Assistant Secretary of Conservation and Renewable Energy, Office of Conservation, Building Systems Division, U.S. Department of Energy under Contract No. DE-AC03-SF00098.

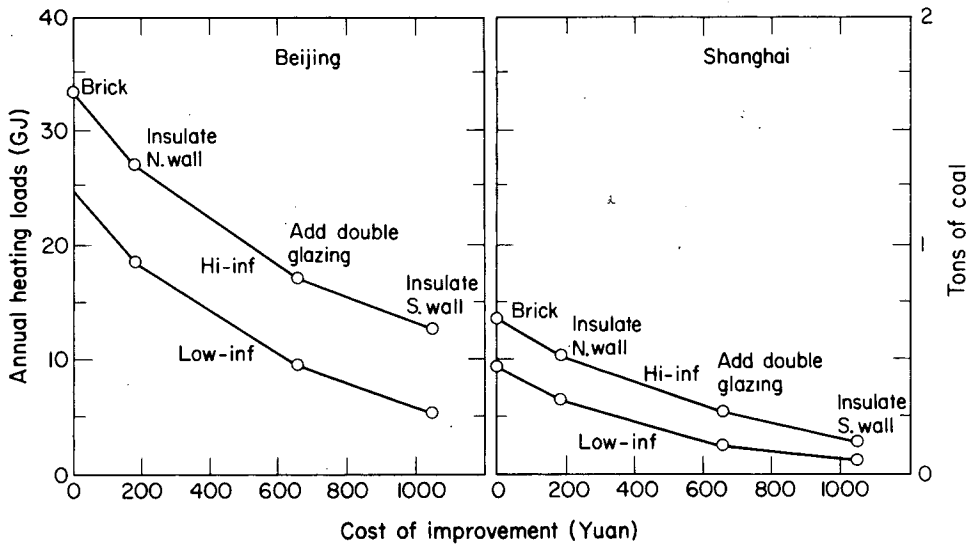


Figure 2. Annual heating load decreases as a series of conservation measures is applied to a three-apartment middle unit in Beijing and Shanghai. (XBL 8210-4865)

Economic analysis of the energy savings was based on Chinese domestic prices and used the two concepts of simple payback time and the cost of conserved coal. International coal prices were used because of uncertainties regarding the domestic pricing of coal in China. Since the heating system efficiency was assumed to be 70%, these economic estimates will be on the conservative side.

## Results

Analysis of the DOE-2 results show that three simple conservation options have attractive payback periods in Beijing—insulating the north wall (7 years), adding double glazing (13 years), and insulating the south wall (22 years). The payback periods would be even shorter if we make the reasonable assumptions that infiltration is also reduced and the heating systems could be downsized. For heated Shanghai apartment buildings, the payback periods for the same options are nearly double because of the milder climate (Fig. 2). Figure 3 shows the heating loads for the same three options in Beijing separated into building components and clarifies the effects of each of the conservation measures.

The first option—adding insulation to the north wall—is particularly attractive since the only costs are for a slight modification of the wall construction to create a cavity, plus the cost of the perlite insulation.

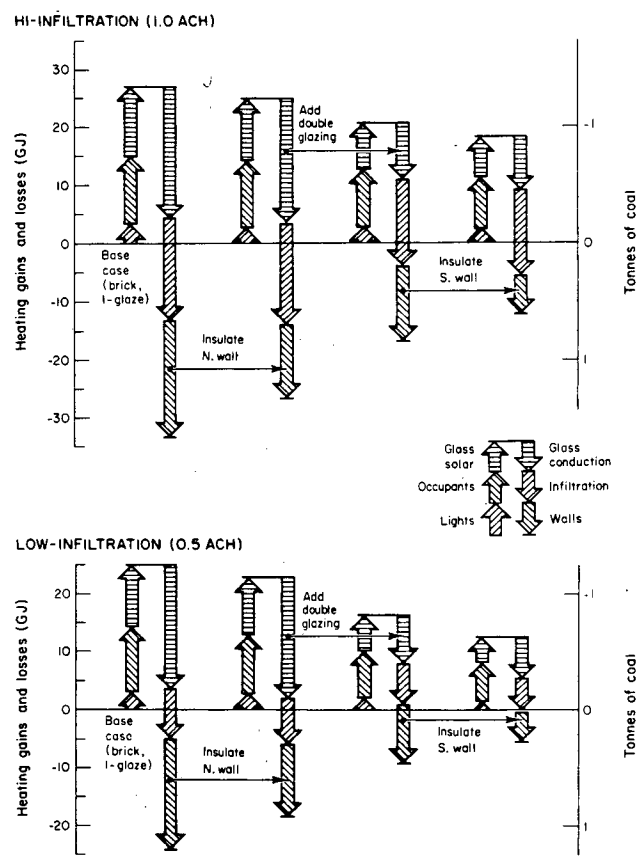


Figure 3. Heating gains and losses for a typical Beijing apartment building (base case) and seven energy conservation options. In each case, the effects are separated for various components of the building. (XBL 8210-4866)

For unheated residential buildings in Shanghai, the benefits from these same options are not in fuel savings, but in improving conditions within the living spaces. Figure 4 shows the differences in floating indoor temperatures between a typical brick building in Shanghai and buildings with insulation or both insulation and reduced infiltration. While the temperatures in the brick building never rise above 16°C (60°F), those for the insulated building with reduced infiltration are within the comfort zone during the daytime hours, reaching as high as 21°C (70°).

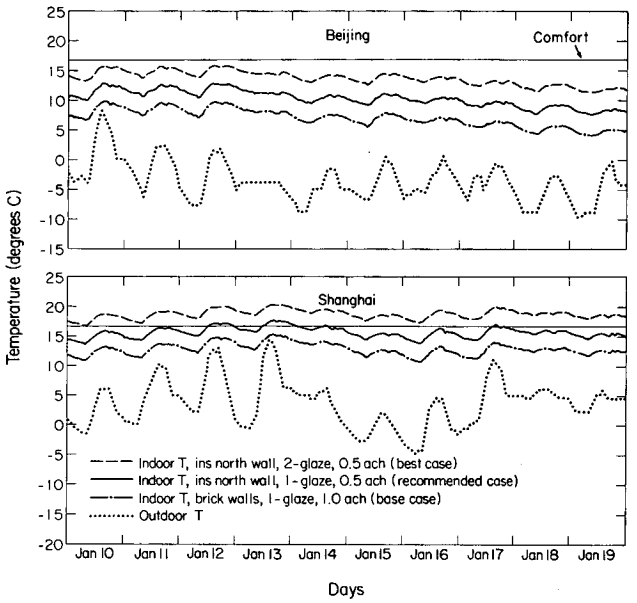


Figure 4. Floating indoor temperatures in winter for a typical building in Beijing and Shanghai with standard brick walls only, with insulation, and with both insulation and double glazing. (XBL 831-1085)

## PLANNED ACTIVITES FOR FY 1983

More detailed information concerning this research effort will be available shortly as LBL report LBL-15183.

The results of this paper were presented by one of the co-authors, Professor A. Rosenfeld, at the First U.S.-China Conference on Energy Resources and Environment held in Beijing in November 1982. Further analysis is contemplated following review of comments from Chinese researchers, incorporation of more detailed data on Chinese buildings and climate conditions, and formulation of a research agenda.

# OCCUPANT BEHAVIOR AND RESIDENTIAL ENERGY USE*

*P.P. Craig, J.C. Cramer, T.M. Dietz, B. Hackett, D.J. Kowalczyk, M.D. Levine, and E.L. Vine*

Lawrence Berkeley Laboratory, in conjunction with a number of cosponsoring organizations,† has been investigating the effects of occupant behavior on residential energy use for the last several years. Occupant behavior has been examined in three interrelated projects using household data collected in the California cities of Davis and Lodi: (1) comparison of estimated and actual summer electricity consumption using the U.S. Department of Energy's DOE-2.1A building energy analysis model; (2) the construction of a multiple regression model that combines structural-physical characteristics of a residence with appliance and behavioral data of occupants for explaining the variation in summer electricity use; and (3) the evaluation of utility-sponsored and locally run community electricity management programs in Davis and Lodi. The conclusions and issues resulting from this work have laid the foundation for continued work in the study of occupant behavior and energy use in other communities in the country for FY 1983.

## ACCOMPLISHMENTS DURING FY 1982

Principal activities were the analysis of survey data previously collected in Davis and the collection of survey data in Lodi, California. The methods used in collecting the Davis data are described elsewhere[1] and are briefly summarized below.

During the summer of 1980, a random sample of 241 Davis households was surveyed. A questionnaire was developed and administered to the building occupants that contained over 200 questions covering a wide variety of energy use attitudes and behaviors and the background characteristics of the residents. The interviewers also obtained other data, such as building area and orientation, building shading, window area and orientation, appliance inventory, and

*This work was supported by the Assistant Secretary of Conservation and Renewable Energy, Office of Buildings and Community Systems, Systems Analysis Division of the U.S. Department of Energy under Contract No. DE-AC03-76SF00098.

†Kellogg Public Research Program, University of California, Davis; Pacific Gas and Electric Company, San Francisco, Calif.; Center for Environmental and Energy Policy Research, University of California, Davis; and the California Energy Commission, Sacramento, Calif.

insulation characteristics for the wall and ceiling, all of which affect energy loads. Additional information was collected on energy efficiencies of key appliances, and, for a selected subsample, air infiltration rates and internal building temperatures were recorded. Hourly weather data were collected on solar radiation, dry-bulb temperature, air pressure, wind speed, and wind direction. Monthly energy use data for the survey respondents for 1979 and 1980 were provided by the local utility, the Pacific Gas and Electric Company (PG&E).

During the summer of 1981, 291 households were surveyed in Lodi, using a questionnaire similar to that in Davis. The interviewers also obtained data on appliance and housing characteristics and internal building temperatures. Monthly energy-use data for the survey respondents for 1980 and 1981 were provided by the municipal utility and PG&E.

## Comparison of Estimated and Measured Electricity Use

Total electricity use and cooling loads for a three-month cooling season (July-September, 1980) in 74 single-family detached houses in Davis were estimated and compared with measured data. Total electricity use for the summer was estimated by predicting cooling loads and appliance-related electricity demand. Appliance electricity use was derived from manufacturers' data, and patterns of appliance use were elicited from occupants through the household survey. Cooling loads were estimated by using an interpolation model to simplify application of the DOE-2.1A energy use computer model. The starting point for the interpolation model was the parametrization of a baseline house, representative of typical single-family detached residences in Davis. This baseline house was run on the DOE-2.1A program using Davis weather tapes for three summer months of 1980. The interpolation model was then developed, using a sensitivity analysis in which all the major house characteristics and occupant behavior patterns that affect cooling loads were varied singly, and sometimes jointly, in the DOE-2.1A model. The equations in the interpolation model (Table 1) represent the DOE-2.1A runs to within approximately 5%. The model was constructed in such a way that values from the questionnaire and building audit could be inserted into the model to predict cooling electricity use. The form was chosen to ensure that when base case values were inserted into the equations, total cooling use would equal the cooling load required by the base house.

Table 1. The interpolation model.

$$\text{Cooling electricity} = (7.1/\text{EER}) \times (\text{House area}/1975) \times (E1 + E2 + E3 + E4 + E5 + E6 + E7)$$

where

EER = Energy efficiency ratio of air conditioner

$E1 = \{[55 \times (\text{Sch-3})] - 138\} \times (\text{Temp-79}) + [-505 \times (\text{Sch-3})] + 1745$

$E2 = [350 \times (11 - \text{Wall insulation})]/11$

$E3 = \{[-10 \times (\text{Sch-3})] + 9\} \times (19 - \text{Ceiling insulation}$

$E4 = [-1.3 \times (\text{Sch-3}) + 1.6] \times (\text{Area of south glazing} - 75)$

$E5 = [3.5 \times (\text{Sch-3}) - 7.4] \times (\text{Shaded glazing percentage} - 50)$

$E6 = [0.9 \times (\text{Sch-3})] \times (\text{Area of north glazing} - 225)$

$E7 = (-180 \times \text{Venting})$

where

Temp refers to occupant-reported indoor room temperature

Venting refers to night venting (on = 1, off = 0)

Sch refers to occupant-reported air conditioning use with the following codes:

| | |
|---|---|
| Almost always | Sch = 2 |
| Often | Sch = 3 |
| Sometimes or almost never | Sch = 4 |
| Never | Cooling electricity = 0 |

Predicted total electricity use was calculated for each house by adding the cooling load from the interpolation model to the appliance load. After attempting several other forms of the model, the final interpolation model, using occupant-reported air conditioning schedules and indoor temperatures, was run on the 74 single-family detached houses. Analysis of the means of measured and predicted total electricity use showed that this procedure overestimated the electricity use of single-family detached homes during the cooling season by 499 kWh, or 18% of average use.

We next examined the accuracy of our estimates of total electricity use for each house (instead of the entire sample), by using multiple regression analysis. This analysis showed that our procedure explained 31% of the variation in measured energy use (Fig. 1). When cooling loads were examined by subtracting the appliance load from total electricity use for both measured and predicted values, regression analysis indicated that only 12% of the variation in measured cooling electricity use could be explained by our method (Fig. 2).

Thus, while the procedure used in this project is helpful in predicting the mean total electricity use for a large sample of single-family detached houses, it is

very unlikely that precise forecasting of individual house electricity use is possible, even when there are no changes in occupancy, unless expensive monitoring techniques are utilized. (In FY 1983, we plan to examine households that have been submetered to see if we can increase the predictive capability of our models for individual homes.) Accordingly, conservation planners should be extremely careful to limit their promises for cooling-season electricity reduction and should emphasize average as opposed to individual benefits.

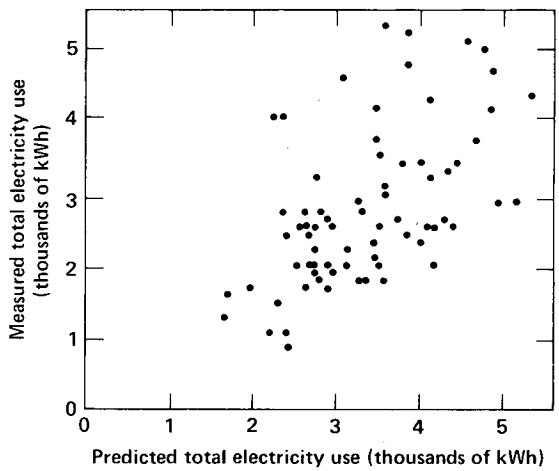


Figure 1. Predicted vs. measured total electricity use, using LBL's appliance saturation index as an indicator of appliance energy use and the DOE-2.1A model for cooling energy use. (XBL 824-8887)

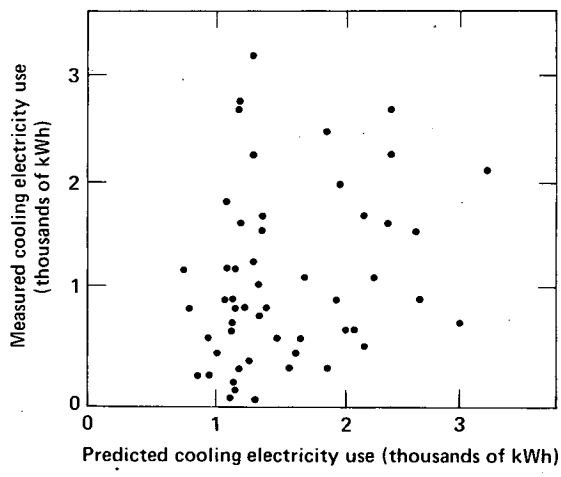


Figure 2. Predicted vs. measured cooling electricity use, using LBL's appliance saturation index as an indicator of appliance energy use and the DOE-2.1A model for cooling energy use. (XBL 824-8886)

## Multiple Regression Models of Residential Energy Use[2]

The purpose of this project is to discover and understand the structural-physical, behavioral, attitudinal, and demographic determinants of residential energy consumption in order to identify where programs to promote energy efficiency should be directed. Using multiple regression analysis, we construct models that attempt to explain the variation in energy use among Davis and Lodi households.

Several regression models are being developed in this project. A model incorporating structural-physical and behavioral determinants has been constructed and run on all the building types in the Davis sample during the cooling season and is discussed in this report. Similar models will be constructed for analyzing the heating season and total energy use in Davis. In addition, other models will include demographic and attitudinal determinants and will be used for analyzing the cooling and heating seasons, as well as for the entire year. All these models will be run with the Lodi data in order to determine the generalizability of our results.

In this project, several structural-physical and behavioral variables important in influencing electricity use were selected from the survey and energy audit for statistical analysis. These variables included wall and ceiling insulation levels, floor and glazing areas, number of rooms, orientation of house, frequency of air conditioner use, venting, shaded glazing areas, air conditioner settings and schedules, and a constructed conductivity measure. Multiple regression analysis (using the least squares method) was conducted with total electricity use as the dependent variable and with the above variables as the selected independent variables. Hierarchical regression was used, and many combinations of variables were tested to find the best equation. The models were run separately on single-family detached homes, on all other types of residence (e.g., apartments, duplexes, single-family attached houses, condominiums, duplexes, triplexes, and fourplexes), and on all residences to discover which independent variables were statistically significant and which models explained the most variation in household electricity use (i.e., high $R^2$).

After testing for interaction effects and nonlinearity and examining the problem of multicollinearity, where independent variables are highly correlated with one

another, a final structural-behavioral regression model was constructed for all households as follows:

Total electricity use (kWh) =

-701.11 + 87.90 (Frequency of air conditioner use)

+ 0.36 (Appliance saturation index) + 0.52 (Floor area)

+ 0.06 [(Appliance use) × (Number of people home)]

+ 0.11 [(Floor area) × (Air conditioning use)]

+ 408.37 (Building type)

where

- Frequency of air conditioner use was coded from 0 (never) to 4 (always)
- Appliance saturation index was composed of the following electrical appliances: water heater, clothes dryer, clothes washer, oven, refrigerator, freezer, dishwasher, and swimming pool filter/pump
- Building type was coded (1) single family-detached and (0) for all other building types.

This model explained 75% of the variation ($R^2$ = 0.75) in electricity use in the cooling season for all the households in the Davis sample (Fig. 3); for single-family detached households and for all other households, $R^2$ was 0.51 and 0.60, respectively.

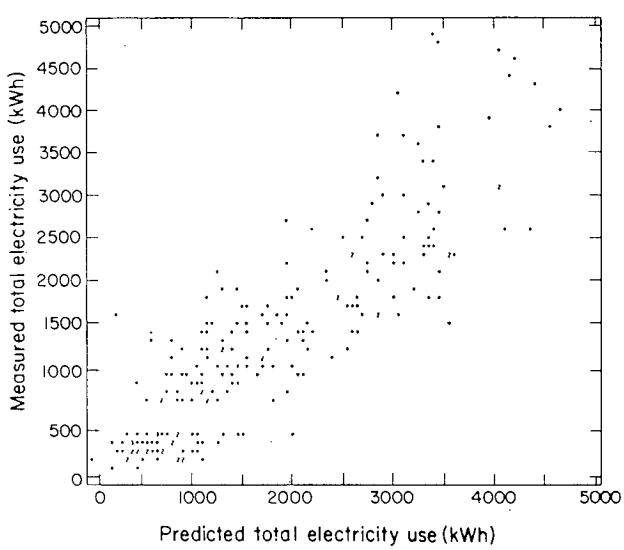


Figure 3. Predicted vs. measured total electricity use, using multiple regression analysis. (XBL 8211-7358)

Thus, it appears that information on selected key variables is sufficient for explaining more than three-quarters of the variation in total electricity use for all households, although our ability to explain energy use was diminished for specific housing types. This research therefore strongly supports the theory that occupant behavior is a significant determinant of residential electricity use after controlling for structural-physical characteristics of dwellings. Accordingly, the education of the residential energy consumer should be an important focus of public policy in reducing energy use, as exemplified in the project described below.

Despite our success in predicting household electricity use, there is still a large amount of variance unexplained by both the structural-behavioral regression model and the procedure used in the first project. Some of the likely reasons for the differences in values between predicted and measured electricity use are:

1. Self-reported behavior (e.g., occupants' reports of air conditioning use) was sometimes wrong.
2. Some major building characteristics (e.g., percentage of window shading) were very difficult to measure.
3. Appliance loads were not accurately estimated for individual homes (e.g., we sometimes relied on national appliance energy efficiencies when household-specific data were missing).
4. Cooling electricity use was calculated from weather data for one local site instead of site-specific weather information, thereby neglecting important microclimatic conditions.
5. Some household behaviors affecting cooling energy use are only partially captured in regression models (e.g., night venting).
6. Some household behaviors affecting cooling energy use are not represented at all in regression models (e.g., microclimatic effects of exterior vegetation).
7. Responses to the survey were elicited from one household member while energy use is a composite of all household members.

## Evaluation of Peak Load[3]

During the summer of 1980, the City of Davis and PG&E implemented the first year of a two-year experi-

mental peak-electricity load-management program named Prime Time. The program was based on the principle of inducing peak electricity use reduction via goal-setting, community and individual financial incentives, and feedback. A similar program was implemented in Lodi during the summer of 1981.

In these programs, residents were asked to reduce their weekday use of electricity during a specified afternoon time period (in Davis, from noon to 6 p.m.). Throughout the program, literature drops, newspaper, radio, and television reports, and a wide variety of special community events organized by citizen activists and civic leaders brought the message of peak-load management to the public. The Prime Time program made reductions voluntary and offered as a reward a portion of the utility's cost savings resulting from the program: $10,000 would be awarded the city for every 1% reduction in peak electricity use compared to the use of the previous summer. The maximum amount PG&E would pay was $100,000. The target of the program in Davis was primarily the residential sector, especially persons who lived in single-family detached houses.

The index used by PG&E and the City of Davis for estimating changes in peak electricity use was 100 $K(C-D)/C$, where $C$ was the peak electricity use for 1979 measured on summer weekdays from noon to 6 p.m., $D$ was the peak electricity use measured over the same time period in 1980, and $K$ was an adjustment for the difference in the number of summer weekdays and number of customers in 1979 and 1980. According to this index, the Prime Time program resulted in a total peak load reduction of 22%. Davis earned the maximum reward of $100,000, which was spent on capital improvement projects oriented toward conservation, such as planting more trees along streets.

Because the index did not take into account changes in weather, fuel prices, and conservation behavior, we conducted an evaluation of the Prime Time program using data collected from our survey of Davis residents and other data sources. We found that although 80% of our sample had heard of the Prime Time program, very few respondents stated that they had recently shifted appliance use from the afternoon to some other time period. In addition, respondents also indicated that there was very little opportunity to shift appliance use away from peak hours. This was particularly true for air conditioning, a major target of the program. Moreover, program participants reported significantly less air conditioning use than nonparticipants by setting their air conditioner at higher temperatures and by greater reliance on night venting, which was promoted by the Prime Time program. In sum, many people responded to the program by reducing their total consumption of electricity, rather than by shifting the timing of electricity consumption.

A comparison of average electricity consumption per customer in the residential sector between Davis and a group of 50 cities (all being served by the same utility, receiving the same electricity rates, and having similar weather) showed that electricity consumption in Davis declined by about 6.9% over that in the control group. If, as we believe, the 50 cities are comparable to Davis, then the 6.9% reduction can be attributed to the Prime Time program. The survey data, combined with PG&E's figures on household electricity consumption, also provide support for the aggregate results. Using multiple regression analysis, we constructed a model that contained as variables pre-program electricity consumption, floor area, percentage of shaded glazing, type of dwelling unit, health need for air conditioning, and participation in the Prime Time program. By comparing participants and nonparticipants, we found that the average household savings of electricity due to the Prime Time program was about 8.4%. Since 54% of our sample said they participated in the program, overall conservation in the residential sector would have been about 4.5%. Given that 4.5% is an underestimate because of increased participation after the interview and spillover effects not consciously attributed to the program, this estimate is consistent with the aggregate estimate of 6.9% residential conservation. This estimate represents about 34% of the reduction in total residential electricity consumption (a reduction of 20%). If we assume that this share applies to peak load as well as to total consumption, then of the observed 22% reduction in peak load, approximately 7.5% would have been due to Prime Time (after controlling for weather, prices, etc.).

We intend to examine the electricity load management program in Lodi in the near future. Preliminary evidence indicates that participants in this program have saved energy compared to nonparticipants.

## PLANNED ACTIVITIES IN FY 1983

We intend to analyze the heating season and total energy use in Davis as was done for the cooling season in the first two projects. The models will also

include attitudinal and demographic data. We also expect to analyze the Lodi data (including the electricity load management program) in the same fashion as the Davis data. We also plan to continue our evaluation of the effects of occupant behavior on residential energy use by analyzing households that have had key appliances submetered.

## REFERENCES


1. Vine, E., et al. (1982), "The Applicability of Energy Models to Occupied Houses: Summer Electric Use in Davis," *Energy*, in press.
2. Vine, E., et al. (unpublished, 1982), "Structural-Physical and Behavioral Determinants of Residential Energy Use: Summer Electric Use in Davis."
3. Kowalczyk, D., et al. (1982), "Evaluation of a Community-Based Electricity Load Management Program," *Energy*, in press.


# ENERGY CONSERVATION IN PUBLIC HOUSING*


*R.L. Ritschard and D.F. Dickey*


Building energy efficiency will demand increasing attention by public housing officials in this decade. Rising energy costs during the past several years have created an ever-widening gap between the allowable expenses of a local public housing authority and the income that it obtains from rents. The difference between these is made up by federal public-housing operating subsidies, which increased from $12.6 million in 1968 to $685 million in 1978.[1]

A large and growing proportion of a local public authority's expenditures consists of utility costs, which have risen primarily as a result of increasing prices rather than increased consumption. Preliminary surveys indicate that energy consumption for a sample of large public housing authorities actually decreased slightly during the last three years.[2] The energy costs for public housing nationwide have climbed from $185 million in 1970 to an estimated $740 million in 1980 (an increase of over 400%).[1] This cost varies widely between building types, climates, and user characteristics. Most of this increase has occurred during the last few years and will probably continue: fuel costs are expected to rise over general inflation for many years to come. Public housing not only has many of the financial problems that face private market rental housing, but, as in multi-family rentals, tenants have few incentives to conserve energy. In addition, there is a proposal by the federal government to shift financial and management responsibilities to state and local agencies.

The federal agency charged with overseeing the energy characteristics of public housing is the Department of Housing and Urban Development.[3] In the bygone days of cheap energy, HUD's involvement in energy efficiency was limited.

Before 1973, consideration of thermal integrity was "suggested" by HUD to local housing authorities at the time of construction, but no mandatory standards existed.[4] As a result, perhaps 75% of the existing public housing stock was constructed without regard to effective thermal insulation.[4] Compliance with HUD's early guidelines resulted in very little thermal integrity. Application of the 1963 standard to San Francisco's climate, for example, meant that no insulation of *any* type was recommended in any component of either a low-rise or high-rise building.[4]

Mandatory insulation standards were finally promulgated in 1973.[4] HUD's new conservation requirements had little impact on the public housing stock, however, because a moratorium on new public housing construction was imposed during that same year and lasted until 1977. HUD has required cost-benefit analyses of energy conservation improvements in public housing projects. These conservation decisions are targeted for completion by 1983 and must favor measures with the shortest payback periods (rather than the lowest life-cycle costs).[9] Local public housing authorities have also begun to make energy efficiency improvements in existing stock in an attempt to reduce rising energy expenditures. A significant source of funds for energy conservation retrofit has been modernization money provided by HUD.


*This work was sponsored by the Assistant Secretary of Conservation and Renewable Energy, Office of Conservation, Building Systems Division, U.S. Department of Energy under Contract No. DE-AC03-76SF00098.

## ACCOMPLISHMENTS DURING FY 1982

### National Perspective on Public Housing Characteristics

*Physical Condition*

Public housing provides about one-fifth of the low-income rental housing in the nation. A recent report commissioned by HUD evaluated the physical condition of the public housing stock and estimated that there are approximately 1.2 million dwelling units (9900 projects managed by 2700 local housing authorities) with more than 3.4 million occupants.[1] The average single project was built before 1965 and contains 119 units. More than half of the units are classified as family low-rise apartments, which means the buildings are predominately four stories or less (Table 1). A surprising finding is that many of the projects conform to key points in the minimum property standards and are well-built.

Table 1. National public housing characteristics.

| | Total units (percent) | Avg. age (years) | Number of dwelling units |
|---|---|---|---|
| Family low-rise[a] | 30.8 | 23 | Greater than 200 |
| Family low-rise | 26.2 | 18 | Less than 200 |
| Elderly | 23.8 | 12 | |
| Family high-rise[b] | 17.1 | 20 | Greater than 200 |
| Family high-rise | 2.1 | 14 | Less than 200 |

[a]Low-rise buildings predominately four stories high or less.
[b]High-rise buildings predominately five or more stories (also those with combinations of high and low-rise buildings).
*Source*: Reference 1, p.11.

*Energy Use*

Public housing annually uses an estimated 146 million Btu per dwelling unit, or 175 trillion Btu for the entire stock.[1] Of this annual total amount, 65% is used for space heating, 22% for domestic hot water heating, and the remainder for lighting and appliances. The average annual energy use by fuel type (Btu) is as follows: natural gas—64%, oil—25%, and electricity—11%. Since the per-unit cost is greater for electricity than for the other sources, electrical costs account for nearly one-third of the average annual energy bill. The average cost per dwelling unit is estimated at $673 (in 1980 dollars).[1]

*Potential for Energy Conservation Investment*

Energy efficiency retrofit of the nation's public housing inventory was the subject of a study recently completed for HUD. Four hundred public housing projects were surveyed, and the cost of bringing each project up to three separate energy efficiency standards was calculated. The results were then weighted so that estimates for all projects could be computed.

An average investment of $1347 per dwelling unit is estimated by the study to yield average annual savings of $324 per unit (for an average payback of 4.2 years).[3] Nationwide costs for this level of investment would be $1.5 billion. A wide range of levels of investments would be necessary to accommodate different types of projects. High-rise housing projects with over 200 units and vacancy rates above 10% were found to require an average of $2680 to meet the standard. Low-rise projects designed exclusively for elderly tenants were estimated to require only $600.[6] Regardless of how the estimates are disaggregated, however, the total investment needed (some $1.5 billion) is certainly substantial. On the other hand, this investment would reduce the average per-unit energy consumption from 146 million Btu to 68 million Btu, which is comparable to typical, private-sector housing adapted for energy conservation.[1] Since HUD currently provides the bulk of the public housing subsidies to local housing authorities, the federal government will be the major benefactor of any investments it makes today. In addition, the comfort level and well-being of the low income tenants can also be enhanced if the physical condition of the public housing stock is improved to some minimum level.

### Examples of Energy Conservation

To gain an understanding of how energy conservation has been addressed in the public housing sector, we review three examples of local energy-saving strategies. These examples are not an exhaustive listing, but instead cover some of the major activities that public housing authorities are pursuing. Data on specific energy measures, their costs and savings, and implementation processes are not readily available because most local housing authorities have not yet reached this stage in the energy retrofit process.

*Window Retrofits*

The New York City Housing Authority, which ini-

tiated an energy conservation program in 1974, is deeply committed to energy conservation. One particularly successful strategy has been the replacement of over 22,000 steel casement windows with energy-efficient, double-hung, double-glazed aluminum windows (including thermal breaks) at the Cypress Hills and Brownsville Houses. The costs of the windows, which were funded by a Department of Energy (DOE) weatherization grant, amounted to approximately $3.3 million.[7] The prior steel casement windows were subject to excessive air infiltration and frequent glass breakage during windy weather and sharp fluctuations in outside temperature. As shown in Table 2, the energy savings, as measured by fuel oil consumption per degree-day before and after installation of the energy-efficient windows, were significant. If domestic hot water usage is excluded by subtracting a constant hot water factor per year for each project (calculated from summer-season fuel consumption), estimated savings for space heating are only 21.1 gallons/degree-day (16.1%) for Cypress Hills Houses and 18.1 gallons/degree-day (14.5%) for the Brownsville Houses. This method presents a more accurate picture of the effects of window replacement on fuel consumption because neither the number of degree days nor the type of windows affects hot water consumption.

Table 2. Window retrofit data for two New York City housing projects.

| | Cypress Hills | Brownsville |
|---|---|---|
| No. of apartments | 1,444 | 1,338 |
| Windows replaced | 10,980 | 11,548 |
| Total cost (including insulation) | $1,524,447 | $1,774,447 |
| Gallons fuel oil/degree-day (1978-1979) | 182.6 | 167.7 |
| Gallons fuel oil/degree-day (1980-1981) | 159.7 | 148.5 |
| Savings (gal/degree day) | 22.9 | 19.2 |
| Percent energy savings (including domestic hot water) | 12.5 | 11.4 |
| Gallons fuel oil (space heating)/ degree day (1973-74) | 131.1 | 124.8 |
| Gallons fuel oil-(space heating)/ degree day (1980-81) | 110.0 | 106.7 |
| Savings (gal/degree-day) | 21.1 | 18.1 |
| Percent energy savings (space heating) | 16.1 | 14.5 |

*Source*: New York City Housing Authority memorandum from John Kelleher, February 22, 1982.

Another significant benefit of the double-glazed windows is a reduction in glass breakage and in routine maintenance (cycle painting of frames). It is estimated that, for an average 1000-unit project, this saves about $20,000 per year in maintenance costs.[8] With an additional grant, another 2266 apartments are being retrofitted at Highbridge Houses and St. Nicholas Houses; however, energy-use data are not yet available.

Even though the initial cost for window replacements is significant and the payback period involved is relatively long (probably 10 years), the potential energy savings from such an option are appreciable. These are especially significant if we consider that as much as 65% of a public housing unit's average energy consumption is attributed to space heating.

*Computerized Energy Management System*

An innovative approach to energy conservation was taken by the Trenton Public Housing Authority in New Jersey. At the Page Homes complex—six 3-story brick buildings totaling 159 units and constructed in 1954—a computerized energy management system was installed with federal funds.[9]

The heating system consists of a central plant, located in a separate building, that circulates hot water through underground pipes to the six project buildings. The operation of the energy management system is straightforward. A number of indoor temperature sensors are placed in selected apartments (72 throughout the complex). The main program reads apartment temperatures, outside temperatures, and time of day on a 15-minute cycle and operates pumps and boilers to regulate the amount of heat delivered to the apartments. The system was activated on January 27, 1981, when outdoor temperatures were between 20° and 30°F. At that time, inside temperatures were generally in excess of 82°F. By mid-February, average building temperatures were being maintained at approximately 74°F daytime and 72°F at night.

Significant reductions in fuel-oil consumption were achieved with this system (Table 3). For the seven months of 1981 in which the computer system operated and for which heat was supplied (excluding the months of June through September), oil consumption was reduced by about 53% from the previous year. If weather adjustments are considered, the savings were approximately 48%. After the first full year of operation, consumption was roughly cut in half

from the previous year, making Page Homes one of the most fuel-efficient old apartment complexes in New Jersey, even though apartment temperatures were held at a relatively balmy 72° to 75°. It is estimated that fuel oil savings in the past winter exceeded $60,000.[10]

*Meter Conversions*

A major emphasis of HUD's energy conservation efforts in public housing has been the active promotion of conversion from master metering of tenants' utilities to either submetering or individual metering. In rules first promulgated in May 1976, HUD required public housing authorities (PHA's) to perform benefit/cost analyses regarding metering conservation.[11] Empirical evidence indicates that when a single master meter is used to record energy consumption for an entire multi-family building and utility bills are included as part of the monthly rent, tenants have little incentive to save energy and will therefore consume more than when individually metered. A report on this topic estimates an average savings in electricity use of 15 to 20% and in natural gas of 5 to 7% after converting from master to individual meters.[12] These results, however, are for multi-family dwellings where tenants are made financially responsible for the energy they use, but not specifically for public housing occupants. HUD's regulations established a presumption that conversion to either individual metering or submetering would automatically conserve 25 to 35% of PHA heating energy, regardless of significant variables such as the condition of the project, amount of insulation, or types of tenants.[13]

As a result of litigation brought by tenant groups, HUD has been required to temper somewhat its preference for meter conversion over other conservation retrofit measures.[14] New regulations promulgated in May 1980 require that meter conversion must be considered against 20 other conservation and solar measures as part of energy audits of public housing.[15] Additionally, until HUD can substantiate its presumption of 24-35% savings from meter conversion, a nationwide injunction prohibits further conversion.[16]

Table 3. Page Homes fuel-oil consumption (gallons of #4 oil).

| Month | 1978 | 1979 | 1980 | 1981 |
|---|---|---|---|---|
| Jan. | 31,000 | 30,300 | 26,100 | 24,100 |
| Feb. | 27,200 | 26,700 | 24,900 | 10,800[a] |
| Mar. | 22,200 | 19,000 | 20,800 | 9,600 |
| Apr. | 15,900 | 17,600 | 10,200 | 5,600 |
| May | 12,000 | 4,000 | 4,200 | 3,500 |
| June-Sept. | (No heat supplied to apartments) | | | |
| Oct. | 12,000 | 10,600 | 8,400 | 4,500 |
| Nov. | 18,600 | 14,400 | 17,500 | 6,400 |
| Dec. | 19,600 | 22,600 | 18,600 | 8,650 |

[a]First full month of operation of the computer system.

*Source*: Page Homes Demonstration Project for the Application of Computers to Energy Conservation in Public Housing Projects, Trenton Housing Authority, Trenton, New Jersey, February 1982.

## Conclusions

Our assessment of energy conservation efforts in public housing leads to the conclusion that there is substantial potential for saving energy in public housing projects. Because HUD plays a substantial portion of the costs of tenant energy consumption under any billing option, it is in HUD's long-term economic interest to invest in cost-effective weatherization and retrofit measures.

Since data on energy-saving strategies that have been successful for public housing are virtually nonexistent, local authorities are forced to make decisions about conservation investment strategies in a void of technical information. The federal government, which has been a major funding source in other energy conservation research, has not fully addressed this sector. With assistance from the Department of Energy and/or the Department of Housing and Urban Development, the technical research community can provide high quality documentation of effective energy conservation measures in public housing.

## PLANNED ACTIVITIES IN FY 1983

This work will continue in 1983 if funding is available. In particular, an analysis of the San Francisco public housing stock will be concluded to determine the effect of utility-financed retrofit on energy-use patterns.

## REFERENCES

1. Perkins & Will Inc. and Ehrenkrantz Group (1980), *An Evaluation of the Physical Condition of Public Housing Stock: Final Report, Volume I*, HUD Report H2850.

2. Patten, C. (1981). *National Trends in Fuel Prices and Their Relationship to Public Housing Operating Subsidies,* CLPHA Research Report #82-1, Council of Large Public Housing Authorities, Boston.
3. 42 USC § 1437 (d), 3535 (d).
4. Ferrey, S. (1977), "The Ghosts of Cold November: An Examination of HUD's Energy Conservaton Policy for the Poor," *Clearinghouse Review,* May, p. 5.
5 24 CFR 865.301 et seq.
6. Strunk, R.J. (1980), "Public Housing Modernization Program: An Analysis of Problems and Prospects," *Journal of Housing,* October, pp. 492-496.
7. Research and Policy Development Department, New York Housing Authority (1981), *Status of Fuel Oil-Related Experiments and Initiatives, 1977–Present.*
8. Taleisnik, B, Director, Energy Control and Conservation, New York City Housing Authority (May 28, 1982), personal communication.
9. Trenton Housing Authority (1982), *Page Homes Demonstration Project for the Application of Computers to Energy Conservation in Public Housing Projects*, Trenton, N.J.
10. 24 CFR 865.5400 *et seq.*
11. Booz, Allen Hamilton (1979), *Alternative Metering Practices: Implication of Conservation in Multi-Family Residences*, prepared for the U.S. Department of Energy (HCP/M 1693-03).
12. 24 CFR § 865.404.
13. *Massachusetts Union of Public Housing Tenants et al. v. Landrieu et al.* (April 7, 1981), in U.S. Court of Appeals for the District of Columbia, Docket No. 78-1895, 80-1332.
14. *Fed. Reg.* 30347 *et seq.* (May 7, 1980).
15. *Mass. Union, op. cit.* (March 31, 1982). Injunction issued prohibiting further meter conversion pending remand to HUD for substantiation of meter conversion presumptions by August 1, 1982. HUD did not supply further substantiation by that deadline. Injunction remains in effect, pending district court review. It should be noted that HUD did not issue instructions to its regional offices prohibiting conversion until early June 1982, after a motion for contempt had been filed against HUD for continuing to convert meters in violation of the injunction.

# SIMPLIFIED ENERGY ANALYSIS METHODOLOGY FOR COMMERCIAL BUILDINGS*

*I. Turiel, R.A. Boschen, M. Seedall, and M.D. Levine*

Energy analyses of commercial buildings may be used for new building design, energy end-use forecasting, and energy audit calculations. Most methods of energy analysis are expensive and require long training to be used properly. There are two ways to reduce this time and expense. One is to write a faster-running computer program with simplified algorithms having fewer options and less accuracy than a complex building simulation program such as DOE-2.1[1] or BLAST, for example. Kusuda and Sud used this approach in developing a modified bin method for commercial building energy analysis.[2] A second method is to create a data base by performing a large number of DOE-2.1 runs for the building parameters relevant to energy-use impact and then use this data base to predict the outcome of other energy-conservation measures. This paper discusses our approach to the latter method.

## ACCOMPLISHMENTS DURING FY 1982

We have performed a parametric energy analysis using the DOE-2.1A version of the DOE computer program for an office building in one climatic region, Denver, Colorado. An equation based on this analysis was developed that predicts heating, cooling, and total building energy use as a function of 11 building-envelope and systems-control parameters. These parameters are the key ones for determining energy use-impact in the Denver climate. The equation takes into account both single-parameter changes and the interactions that occur when two parameters are changed simultaneously.

With this methodology, a microcomputer can be used to predict energy consumption in commercial buildings in various climates very cheaply and with high accuracy, as the results will be based on previously performed DOE-2.1 runs. Our initial work indicates, that, at least for the climate studied, this technique indeed predicts energy use very accurately.

*This work was supported by the Assistant Secretary of Conservation and Renewable Energy, Office for Conservation, Building Systems Division, U.S. Department of Energy, under Contract No. DE-AC03-76SF00098.

## Base-Case Building Characteristics and Operating Conditions

Many assumptions must be made concerning the operating conditions and characteristics of the base-case building before its interaction with the appropriate climate and its operation can be simulated with DOE-2.1A. The office building we modeled was selected as typical and studied during Phase II of the Department of Energy (DOE) Building Energy Performance Standards (BEPS) project.[3] The building has been altered slightly to make its construction characteristics internally more uniform throughout.

The base-case building is a 100,000 $ft^2$ (72 ft × 232 ft), six-story office building in Denver, Colorado. Denver has a climate with 6000 heating degree-days (base 65°F) and with 667 hours when the outdoor dry-bulb temperature is greater than or equal to 80°F. Weather information was obtained from a Test Reference Year (TRY) tape for 1976.

The composition of walls, roof, and floors is described under the materials heading in Table 1. The total R-value of the external walls and roof varies with the R-value of the insulation in each assembly. We have not studied the effect of varying the R-value of the underground floors, since heat transfer to the ground is not well enough understood to be properly modeled. All interior floors have a fixed R-value of 9.

Each of the four exposures has the same window-to-wall ratio (22%), and the windows have the same solar transmission (40%) and glass conductance (0.574 Btu/hr·$ft^2$°F). We have studied the effect of fixed shading by varying the window setback. Lighting is provided by fluorescent lamps recessed in a suspended ceiling. The average lighting power density is 2.5 W/$ft.^2$, and 50% of the heat of lights is assumed to enter each space according to its installed wattage. The remaining 50% is exhausted to the outside through the ventilation system.

Three types of HVAC systems have been studied. The first is composed of a number of water-to-air unitary heat pumps for both heating and cooling, with a circulating water loop. A 300-kW electric boiler provides back-up heat generation if the water temperature of the loop falls below 60°F. The other two are double-duct constant-volume and double-duct variable-volume systems. Both have a gas-fired hot water boiler and centrifugal chiller.

Table 1. Base-case values for large office building.

LOCATION AND ORIENTATION

City: Denver
Size: 72 ft × 232 ft (6 stories)
Orientation: Long axis points 60° east of north
Ground reflectance: 0.20

MATERIALS

Average Mass Density: 62 lb/$ft^2$

| | |
|---|---|
| External Walls: | 4″ heavyweight concrete, R9 polystyrene insulation, 5/8″ gypsum board. Total R=9.5. |
| Internal Walls: | 5/8″ gypsum board, 4″ air layer, 5/8″ gypsum board. Total R=2.7. |
| Roof: | 0.5″ roof gravel, 3/8″ built-up roofing, R15 polystyrene insulation, 6″ heavyweight concrete, 4″ air layer, 0.5″ acoustic title. Total R=19. |
| Ground floor: | R24 fiberglass batt insulation, 6″ heavyweight concrete, 3-1/4″ lightweight concrete, carpet with fibrous pad. Total R=30. |

Solar Absorptivity:

Walls: 0.65
Roof: 0.30

WINDOWS AND LIGHTING

Glass solar transmission: 0.40
Glass conductance: 0.574 Btu/hr · $ft^2$ °F (double glazing)
Window-to-wall ratio: 22
Window shading setback/window height: 0.125 (1-foot setback)
Heat of lights to space: 0.50
Lighting power: 2.5 W/$ft^2$
Infiltration: 0.6 air changes/hour

SYSTEMS

Outside air/person: 7 cfm/person
Thermostat setpoints:

Heating: 72°F
Cooling: 78°F

Night Setback:

Heating: 60°F
Cooling: 99°F

Economizer: None

## Base-Case Building Results

We have performed parametric energy analyses for 16 building parameters and the three HVAC system types. Here, we report only the results for the heat-pump system. Five variables—orientation, ground reflectance, window setback ratio, roof absorptance, and wall absorptance—have very small effects (<2% change) on total energy use in Denver's climate. For the other 11 parameters, curves were fit to the DOE-2.1 simulation results.

Of these 11 parameters, only six cause a 10% or greater change in total energy use. These parameters are wall insulation, glass conductance, window-to-wall ratio, lighting power, amount of outside ventilation air, and nighttime heating setback temperature. A 10% change in total energy use is quite large when we realize that, except for lighting power, the variations in each parameter do not affect lighting, hot water, and elevator energy use, which total 60% of the total base-case energy use. A 25% change in space conditioning energy use is required to obtain a 10% change in total energy use.

It is important to note that a change in the HVAC system can have a greater impact on energy use than a change in the value of a building-envelope or system-control parameter. For example, at a 50% window-to-wall ratio, a heat-pump system may use 33% less energy than a dual-duct constant-volume system, whereas a change in the window-to-wall ratio from 75% to 25% reduces energy use by only 15% (Fig. 1). Table 2 lists the functional relationship between heating and cooling energy use and each of the 11 parameters studied.

When the interaction matrix element is small, multiple measures may be treated by adding the results of single measures taken one at a time. The parametric equations developed for changes in a single parameter can be used for these cases. For large interactions, a different methodology must be used to estimate energy use accurately. When heating and cooling energy use are separately estimated, the errors resulting from not considering interactions between multiple simultaneous conservation measures are, in general, larger than the errors for the total energy use estimation.

## Energy-Use Prediction Methodology

Our single-parameter energy analysis indicated that total energy use (in Denver's climate) can be accurately expressed as an analytic function of each of 11 building parameters, while all others were held constant. When the interaction between two parameters is small, simple addition of energy savings from multiple measures will provide reliable estimates of the combined total energy savings. To determine heating, cooling, or total energy use as a function of two simultaneously varying parameters, where the interaction between parameters is large, we performed a Taylor series expansion of energy use as a function of two variables, $P_i$ and $P_j$. $P_i$ and $P_j$ represent any two building parameters. Equation (1) is the second-order expression used.

$$E\,(P_{i1},P_{j1}) = E_o + \frac{\partial E}{\partial P_i}\,\Delta P_i + \frac{\partial E}{\partial P_j}\,\Delta P_j + \partial^2\frac{E}{\partial P_i^2}\,\frac{\Delta P_i^2}{2} + \partial^2\frac{E}{\partial P_j^2}\,\frac{\Delta P_j^2}{2} + \frac{\partial^2 E}{\partial P_i \partial P_j}\,\Delta P_i \cdot \Delta P_j \qquad (1)$$

In Eq. (1), $E_o$ is the base-case energy use and $E(P_i,P_j)$ is the energy use when the parameters $P_i$ and $P_j$ have values $P_{i1}$ and $P_{j1}$ respectively. All derivatives are evaluated at $(P_{io}, P_{jo})$, the base-case values of parameters $P_i$ and $P_j$. $\Delta P_i$ equals $(P_{i1} - P_{io})$, and $\Delta P_j$ is defined similarly.

All five partial derivatives were evaluated by using actual DOE-2.1 runs.

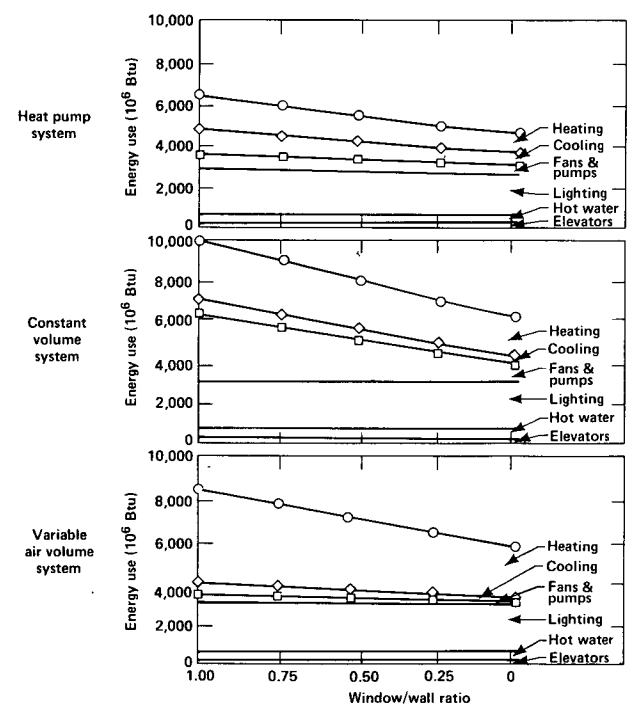


Figure 1. Annual total energy use with varying window-to-wall ratios in a large office building, Denver, Colorado. (XBL 824-8924)

Table 2. Parametric equations for heating and cooling.

| Parameter | Functional Form | Fitted equation |
|---|---|---|
| Roof Insulation Heating | Asymptotic | $E_H = 1507.65(3.22 + R)^{-1} + 800.63$ |
| Roof Insulation Cooling | Linear | $E_C = 6(RR + 3.22)/5 + 621.14$ |
| Wall Insulation[a] Heating | Asymptotic | $E_H = 2682/(1.52 + RW) + 609.3$ |
| Wall Insulation Cooling | Linear | $E_C = 618 + 4.26(RW)$ |
| Window to Wall Ratio—Heating | Linear | $E_H = 755.16 + 671.65(WWR)$ |
| Window to Wall Ratio—Cooling | Linear | $E_C = 536.16 + 611.65(WWR)$ |
| Glass Solar Transmission—Heating | Linear | $E_H = 1110.8 - 468.1(GST)$ |
| Glass Solar Transmission—Cooling | Linear | $E_C = 448.8 + 607.7(GST)$ |
| Glass Conductance Heating | Quadratic | $E_H = 487.6 + 791.2(GC) - 132(GC)^2$ |
| Glass Conductance Cooling | Quadratic | $E_C = 789.4 - 280.3(GC) + 98.9(GC)^2$ |
| Lighting—Heating | Linear | $E_H = 1732 - 347.1(LIT)$ |
| Lighting | Linear | $E_{Light} = +979.4(LIT)$ |
| Lighting—Cooling | Linear | $E_C = 217.35 + 169.8(LIT)$ |
| Outside Air—Heating | Quadratic | $E_H + 374.4 + 58.4(OA) + 2.4(OA)^2$ |
| Outside Air—Cooling | Quadratic | $E_C = 1042.5 - 76.2(OA) + 3.1(OA)^2$ |
| Heat of Lights to Space—Heating | 3rd order polynomial | $E_H = 1764 - 2874.2(LS) + 2731.3(LS)^2 - 892.5(LS)^3$ |
| Heat of Lights to Space—Cooling | 3rd degree polynomial | $E_C = 234.66 + 816.40(LS) + 313.6(LS)^2 - 516.9(LS)^3$ |
| Heating Setpoint Heating | Linear | $E_H = -997.0 + 26.4(TH)$ |
| Heating Setpoint Cooling | Linear | $E_C = 138.2 + 7.3(TH)$ |
| Cooling Setpoint Heating | Linear | $E_H = 743.6 + 2.05(TC)$ |
| Cooling Setpoint Cooling | Quadratic | $E_C = 10{,}941 - 219.55(TC) + 1.12(TC)^2$ |
| Night Thermostat Setback—Heating | 3rd degree polynomial | $E_H = -3853.6 + 275.3(THS) - 5.95(THS)^2 + 0.0447(THS)^3$ |
| Night Thermostat Setback—Cooling | 2nd degree polynomial | $E_C = 1440.8 - 29.1(THS) + 0.268(THS)^2$ |

[a]R3 to R19 only.

## Model Testing

After all coefficients needed for the Taylor series expansion were determined for all combinations of parameter pairs, a FORTRAN program was written to facilitate energy analysis with a microcomputer. We tested our simplified energy analysis methodology by using the computer program to predict energy use for combinations of parameters (two at a time) not previously studied. Table 3 shows the results of this comparison between the DOE-2.1 simulations and the simplified-model predictions.

The predictive capability of the simplified model is very good for both heating and cooling energy use, except where the parametric deviation from the base-case values is both large and in a direction opposite from that originally taken when the derivatives used in the Taylor series expansion were calculated. As can be seen from Table 3, as we move closer to the base-case values for glass solar transmission (GST) and window-to-wall ratio (WWR), there is a dramatic improvement in the accuracy with which heating and cooling energy use is predicted. For most test runs, the model prediction and the DOE-2 model simulations differ by less than ±5% for both heating and cooling energy use.

Aside from the test results shown in Table 3, we also compared DOE-2 runs to model predictions for the 55 two-at-a-time simulations that were used to obtain the mixed partial derivatives in Eq. (1). The DOE-2 simulations and the model predictions differed by less than 15% in all cases for both heating and cooling energy use. In 51 out of 55 cases, the heating energy use differed from the DOE-2 runs by less than 10%, and in only one case did the cooling energy use differ from the DOE-2 runs by more than 10%. The accuracy of our model can be improved by reducing the region of application of each pair of conservation measures. This requires applying the Taylor series expansions to several regions rather than only one and thus entails additional DOE-2 runs.

To perform our analyses, 200 DOE-2 were required. This includes both the single-parameter and two-parameter simulations that were necessary to complete the interaction matrix and calculate the Taylor series expansion coefficients.

## PLANNED ACTIVITIES FOR FY 1983

The simplified methodology described in this paper worked well in the case tested, a mid-sized office building in Denver. A FORTRAN program that is easy to use and fast running can be used to accurately predict (if one takes DOE-2.1 results as a measure of accuracy) heating, cooling, and total energy use as a function of 11 major building parameters. We plan to test the sensitivity of our results to changes in building base case assumptions and in HVAC system type.

Table 3. Summary of predictive capability of simplified energy use model.

| Parametric Values (two at a time) | | Total energy use | | | Heating energy use | | | Cooling energy use | | |
|---|---|---|---|---|---|---|---|---|---|---|
| | | DOE-2.1A results (MBtu) | Model prediction | % diff. | DOE-2.1A results (MBtu) | Model prediction | % diff. | DOE-2.1A results (MBtu) | Model prediction | % diff. |
| LIT = 0.25 | LS = 0.75 | 3124 | 3172 | 1.5 | 1632 | 1687 | 3.4 | 275 | 267 | 3 |
| WWR = 0.16 | GC = 0.43 | 4809 | 4819 | <1 | 787 | 784 | <1 | 639 | 647 | 1 |
| GST = 0.25 | GC = 0.23 | 4741 | 4761 | <1 | 734 | 713 | 3 | 632 | 655 | 5 |
| RW = 3 | WWR = 0.24 | 5281 | 5094 | 3.5 | 1203 | 1020 | 15 | 639 | 666 | 4 |
| WWR = 0.16 | LIT = 2.1 | 4417 | 4460 | 1 | 993 | 1018 | 2.5 | 518 | 531 | 2.5 |
| GST = 0.75 | RW = 11 | 5054 | 5024 | 1 | 684 | 679 | <1 | 919 | 868 | 5.5 |
| LIT = 0.5 | GC = 0.23 | 3032 | 3157 | 4.1 | 1265 | 1307 | 3.3 | 327 | 403 | 23 |
| WWR = 0.10 | GST = 0.25 | 4804 | 4833 | <1 | 859 | 863 | <1 | 557 | 564 | 1 |
| WWR = 0.60 | GST = 0.45 | 5673 | 5665 | <1 | 1110 | 1135 | 2.2 | 996 | 987 | 1 |
| WWR = 0.50 | GST = 0.50 | 5552 | 5469 | 1.5 | 1011 | 1001 | 1.0 | 993 | 963 | 3 |
| WWR = 0.75 | GST = 0.75 | 6516 | 6194 | 5 | 947 | 761 | 20 | 1754 | 1676 | 4.5 |
| RW = 11 | OA = 9 | 5047 | 5053 | 1 | 1021 | 1040 | 2.0 | 624 | 608 | 2.5 |
| THS = 57 | TH = 70 | 4752 | 4784 | 2 | 724 | 749 | 3.5 | 641 | 645 | <1 |
| RW = 19 | TC = 80 | 4734 | 4772 | <1 | 737 | 808 | 9.6 | 608 | 593 | 2.5 |
| LIT = 2.0 | TC = 80 | 4433 | 4469 | <1 | 1038 | 1060 | 2.0 | 478 | 499 | 4.4 |

*Notes:* LIT = lighting, WWR = window-to-wall ratio, GST = glass solar transmission, RW = wall insulation rating, THS = night thermostat setback, LS = heat of lights to space, GC = glass conductance, OA = outside air, TH = heating setpoint, TC = cooling setpoint.

In addition, we expect to determine the validity of this approach for other climate regions and building types. Finally, we need to compare the results obtained from our model, which uses a prototypical base-case building, to the results of a DOE-2 simulation for a specific building.

## REFERENCES


1. Lokmanhekim, M., et al. (1979), *DOE-2: A New State of the Art Computer Program for the Energy Utilization Analysis of Buildings*, Lawrence Berkeley Laboratory Report LBL-8974.
2. Kusuda, T., and Sud, I., (1982), "Update: ASHRAE TC4.7 Simplified Energy Analysis Procedures," *ASHRAE Journal*, July.
3. American Institute of Architects (AIA) (1979), *Life-Cycle Cost Study of Commercial Buildings*, Final Report by AIR Research Corporation, for Department of Energy, Office of Conservation and Solar Energy, Office of Buildings and Community Systems, Washington, D.C.
4. W.S. Fleming and Associates, Inc. (1981), *Draft Recommendations for the Standard Evaluation Techniques (SET) of the Building Energy Performance Standards (BEPS)*, Landover, Maryland.


# ECONOMIC STUDIES

## ESTIMATES OF RESIDENTIAL ENERGY SAVINGS FROM PROPOSED FEDERAL POLICIES FOR APPLIANCES*


*J.E. McMahon and M.D. Levine*


Energy conservation was the goal of legislation passed by Congress in the 1970s. The U.S. Department of Energy has subsequently considered several alternative policies that could save energy. This study focuses on the residential sector of the United States and uses the ORNL/LBL Residential Energy Model to assess the consequences of these potential policies. The objectives of this study were:

(1) to estimate the energy savings from specific policies;
(2) to estimate the monetary savings or costs to the nation's consumers from specific policies;
(3) to define the range of values of energy and economic savings using different assumptions about the future; and
(4) to compare the expected effects of several alternative federal policies.

Two measures of the policies' effects were selected as useful indicators: energy savings and economic savings. All policies considered that save energy have also shown overall economic savings. Some policies have negative economic effects for specific products. The major policies considered were:

(1) proposed mandatory efficiency standards for eight products;
(2) four alternative levels of mandatory efficiency standards;
(3) four alternative labeling programs, differing in the assumed fraction of consumers that would respond;
(4) a 5-year delay in the proposed mandatory efficiency standards;
(5) a 25% tax credit to consumers for the incremental cost of more efficient appliances.

### ACCOMPLISHMENTS DURING FY 1982

#### Method

The ORNL/LBL Residential Energy Model simulates energy consumption over the period 1977-2005. Among the results from the model, four elements were considered:

(1) annual energy consumed (by end use);
(2) annual cost of energy (using average, not marginal cost);
(3) annual cost of equipment; and
(4) the number of each appliance type sold annually.


*This work was supported by the Standards Branch, Consumer Products Division, Office of Buildings and Community Systems, U.S. Department of Energy under Contract No. DE-AC03-76SF00098.

Energy was expressed in source units, including losses in generating and transmitting electricity (1 kWh = 11,500 Btu). All costs were expressed in 1980 dollars.

A 19-year period was considered, from 1987 to 2005. Policy effects were determined by comparing the results of two runs of the model, one for the base (no policy) case, and one for each policy. Input assumptions used in the LBL/ORNL model are fully described elsewhere.[1] The same base case was used for comparing all policies.

Sensitivity analyses were performed only for the proposed mandatory efficiency standards policy. Each sensitivity analysis involved two runs, a base case and a policy case. The key variables altered in the sensitivity analyses were energy costs, equipment costs, and efficiency trends.

Energy savings were defined as the difference between the energy consumed in the base case by a particular end use and the energy consumed in the policy case. Thus any changes caused by the policy—whether in investments in the thermal integrity of buildings, appliance purchases (e.g., to those using a different fuel), efficiency choice, or usage behavior—are included. The eight end uses analyzed were: central space heaters, room air conditioners, central air conditioners, water heaters, refrigerator/freezers, freezers, ranges/ovens, and clothes dryers. Only the results for the three major end uses (central space heating, central air conditioning, and water heaters) and the total for all eight products are presented here.

## Sensitivity Analysis

The energy savings calculated for proposed mandatory efficiency standards are presented in Fig. 1, under a variety of assumptions. The first row is the reference policy, using energy costs from the National Energy Policy Plan ("mid" scenario), equipment costs from DOE's engineering analysis,[2] and base-case efficiencies as calculated by the ORNL/LBL model. The efficiency standards proposed for furnaces achieve no energy savings under these assumptions. Significant energy savings are expected for central air conditioners and water heaters, together accounting for 85% of the total energy savings of the policy.

The reliability of these results was tested by altering the key assumptions. First, future energy-cost assumptions were varied to the upper and lower bounds in the National Energy Policy Plan. The high and low NEPP energy-cost scenarios produce energy savings similar to those obtained with the original assumptions. The total energy savings were 1% lower when high fuel prices were assumed, and 11% higher when low fuel prices were used. Less investment in efficient equipment occurs in the no-policy case when fuel prices are lower.

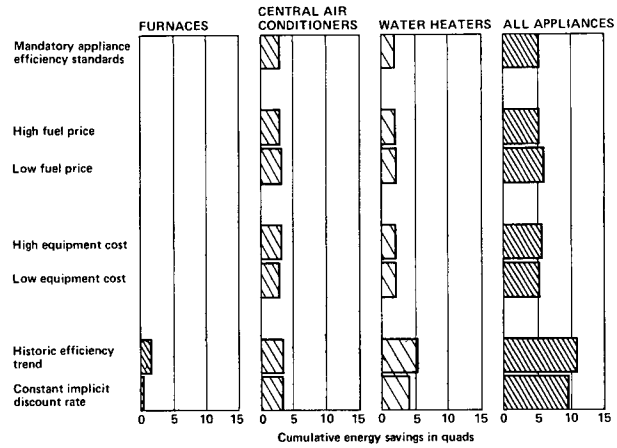


Figure 1. National energy savings, 1987-2005, from proposed DOE consumer product efficiency standards.
(XBL 824-8932)

Next, the purchase cost of equipment was varied. In the high equipment cost case, the purchase costs of all equipment were increased 10%. With higher equipment costs, less efficient appliances are purchased in the no-policy case. Thus the policy mandating a minimum efficiency saves more energy. In this sensitivity case, 10% higher equipment costs would mean 4% additional energy savings. Conversely, 10% lower equipment costs would mean 4% less energy savings attributable to the policy.

The original scenario included projections of significant improvements in equipment efficiencies in the no-policy case. The "historic efficiency trend" case assumes instead that the trend in efficiencies seen from 1972 to 1978 is carried on indefinitely into the future. This produces a more gradual transition to higher efficiency products in the no-policy case and an energy savings estimate due to mandatory efficiency standards nearly twice that obtained from the original assumptions. Water heaters and furnaces both show substantially increased energy savings.

Another alternative assumption about efficiency trends is that purchasers of appliances will continue to apply the same relative weight to operating costs, compared to purchase costs, when buying appliances in the future as they applied in 1978. That is, the

implicit discount rate will be constant in the future at the value observed in 1978. Consumers in this case would buy less efficient appliances than in the original no-policy case. The energy savings are nearly 82% higher than in the original estimate, with noticeable increases for water heaters and for refrigerators (not shown).

The implication of these last two sensitivities is that the ORNL/LBL model assumes a more rapid move toward more efficient products in the future than has been observed historically, or than would be expected if purchasers continued to discount operating costs as much as they have until the present.

The net present benefit of the proposed standards for the eight products is $5.5 billion, with more than 72% of that amount due to water heaters and central air conditioners. All future costs are discounted to 1980, assuming a real discount rate of 10%. The different energy cost assumptions have little effect on the net present benefit, since the differences occur in future years, where the values will be greatly discounted. High equipment costs, since they apply in all years, have a greater but still moderate effect. The efficiency-trend assumptions cause the greatest variation in the energy-savings results with both the historic efficiency case and the constant discount rate case showing substantially higher net present benefit than the original assumptions ($10.9 billion and $10.7 billion, respectively).

### Alternative Federal Policies

National energy savings were calculated for a variety of Federal policies, including: (1) mandatory appliance efficiency standards; (2) four levels of alternative mandatory standards; (3) four alternative labeling programs; (4) mandatory standards, delayed 5 years before implementation; and (5) a 25% tax credit toward the incremental cost of more efficient products.

The proposed mandatory standards would save 5.2 quads (source energy), most of which can be attributed to central air conditioners and water heaters. This set of standards is composed of different levels for different products. Four efficiency levels were analyzed for each product, with energy savings ranging from 2.74 Q (level 1) to 7.80 Q (level 4). The higher efficiency levels provide greater energy savings, as expected.

Each product is affected somewhat differently by the standards. Furnaces show no energy savings for any level considered. Central air conditioners and water heaters show increasing energy savings at higher efficiency levels. (The efficiency assumed for levels 3 and 4 was the same for water heaters.)

The labeling programs were assumed to reduce the implicit discount rate of the average consumer by 50% for most products, but only 20% for furnaces, central air conditioners, and water heaters. (This is consistent with the strong influence that third-party purchasers, such as builders and landlords, have on efficiency choices for the latter three products.) The four alternative labeling programs differ only in the fraction of appliance purchases expected to be affected. The four levels correspond to 10, 25, 50, and 75% of appliance purchases having the desired decrease in the implicit discount rate. None of the labeling programs achieve the energy savings accomplished by the mandatory standards.

The mandatory standards under consideration would save $5.5 billion (1980 dollars), almost half attributable to water heaters. The four standard levels show increasing savings from level 1 to level 3, but decreased savings for level 4. This result is due to the high purchase cost when very efficient air conditioners are mandated. While the economic savings still amount to over $4 billion, this is only slighter higher than the $3.86 billion saved at level 2.

The economic savings of all other programs considered are less than the level 2 savings. Increasing fractions of consumers influenced by labeling show increasing economic savings, up to $3.6 billion when 75% of the appliance purchasers are affected. The 5-year delay in mandatory standards would reduce the savings by almost half, from $5.5 billion to $2.8 billion. Finally, the tax credit program would save $2.3 billion.

## PLANNED ACTIVITIES FOR FY 1983

The greatest uncertainty in simulating future energy consumption seems to lie in the rate of penetration of efficient appliances into the marketplace in the absence of governmental intervention. Therefore, research effort should be directed at characterizing the elements upon which such penetration depends. Particular attention should be paid to separating the effects of various components of the marketplace such as manufacturers, wholesalers/retailers, homebuilders, landlords, and consumers.

Second, the range of uncertainty in all the input parameters and formulations should be ascertained,

so that the absolute range of variation in the results can be quantified.

## REFERENCES


1. U.S. Department of Energy (1982), *Consumer Products Efficiency Standards Economic Analysis Document,* Office of Conservation and Renewable Energy, DOE/CE-0029, Washington, D.C.
2. U.S. Department of Energy (1982), *Consumer Products Efficiency Standards Engineering Analysis Document,* Office of Conservation and Renewable Energy, DOE/CE-0030, Washington, D.C.


# COST/EFFICIENCY TRADEOFFS IN THE RESIDENTIAL APPLIANCE MARKETPLACE*


*J.E. McMahon and M.D. Levine*


Manufacturers' decisions to manufacture and market certain products from the universe of technically possible designs interact with purchasers' decisions to purchase a particular set of products from the range of alternatives perceived to be available. The marketplace which results does not offer perfect freedom of choice. Manufacturers' decisions determine the set of products available, and purchasers have imperfect knowledge of these products, at least with regard to energy efficiency. Policy analysis must rely on some estimate of how the marketplace will behave both with and without a given policy.

We need to understand the historical performance of the marketplace to make reliable estimates of its future behavior. In fact, multiple marketplaces exist, at least one for each type of product—refrigerators, furnaces, water heaters, air conditioners, etc.—and for each type of consumer, such as homeowners, landlords, rich and poor. The marketplace is shaped not only by consumers, but by manufacturers, who limit the choice of designs by their decisions on which products to manufacture and the efficiencies of those products. While there is a considerable body of literature on the theory of consumer decision-making,[1] this theory does not encompass all the problems of market analysis. There has been no analysis of the quantitative relationship of all the determinants of decision-making in the marketplace, including the role of appliance manufacturers. In particular, data on the efficiency of particular products may be available, but it is not known to whom they are sold.

Data on the average efficiency of products purchased in the United States have recently become available.[2] This article describes the use of such aggregate data as a starting point from which aggregate measures of market behavior can be inferred. Results are expressed as "aggregate implicit discount rates" for each product and fuel type. These discount rates, as defined here, serve as a single parameter that describes market behavior with respect to energy efficiency investments. Their value depends on the set of design options available; equipment purchase cost as a function of energy efficiency; energy consumption per unit; energy prices and assumed fuel escalation rates; appliance lifetimes; and, for space conditioning end uses, the thermal integrity of the building.

## ACCOMPLISHMENTS DURING FY 1982

### Method

The analysis, by using implicit discount rates, assumes that behavior in the marketplace can be characterized as if individuals made some type of life-cycle cost decision. (Whether or not this is actually the case, the implicit discount rates may nonetheless be revealing.[3]) No competition among alternative fuels is considered here. The formulation looks at decision-making for products of different efficiencies but same fuel type. For a given product type and fuel, the life-cycle cost formulation quantifies the marketplace decision process for selecting the efficiency purchased. The method, as presently applied, does not account for other factors, such as special features, which might influence efficiency choice. (Extensions of the method, using hedonic approaches,[4] could be applied if sufficient data were available.) The observed average efficiency choice is characterized by an aggregate implicit discount rate. This measure is the discount rate


*This work was supported by the Standards Branch, Consumer Products Division, Office of Buildings and Community Systems, U.S. Department of Energy under Contract No. DE-AC03-76SF00098.

which, if used to achieve a minimum life-cycle cost, would produce the observed efficiency choice of the marketplace.

Shipment-weighted energy factors for each product and fuel type were obtained from the U.S. Department of Energy Survey of Manufacturers.[2] Table 1 shows the numerical values for the products purchased in 1972 and 1978, and manufacturers' estimates for 1980 and 1985.

Table 1. Efficiency improvements since 1972 in residential appliances.

| Product/Fuel | Shipment-weighted energy factors[a] 1972 | 1978 | 1980 (est.) | 1985 (est.) |
|---|---|---|---|---|
| Room Air Conditioner | 6.22 | 6.75 | 6.97 | 7.24 |
| Central Air Conditioner | 6.66 | 6.99 | 7.41 | 8.44 |
| Water Heater - Electric | 79.80 | 80.67 | 81.33 | N.A.[b] |
| Water Heater - Gas | 47.35 | 48.17 | 51.18 | N.A.[b] |
| Refrigerator/Freezer | 4.22 | 5.09 | 5.67 | 6.26 |
| Freezer | 8.08 | 10.07 | 10.73 | 11.68 |
| Range/Oven - Electric | 35.79 | 41.41 | 42.98 | 43.81 |
| Range/Oven - Gas | 13.81 | 17.66 | 20.55 | 25.13 |
| Dryer - Electric | 2.61 | 2.59 | 2.70 | 2.70 |
| Dryer - Gas | 2.10 | 2.38 | 2.41 | 2.42 |
| Furnaces - Gas | 62.68[c] | 63.58 | 65.86 | 72.06 |
| Furnaces - Oil | 73.64[c] | 75.20 | 76.0 | 77.66 |

[a]The shipment-weighted energy factor is the product of the energy factor (e.g., efficiency, energy efficiency ratio, etc.) of a particular model times the number of units of that model shipped in the year indicated summed over all models reported to DOE, divided by the total shipments.

[b]N.A. - Not available.

[c]For 1975.

The cost-versus-efficiency data were obtained from the engineering analysis performed for the March 1982 DOE Consumer Product Efficiency Standards Analysis.[5] The cost-versus-energy consumption data were aggregated and a curve-fitting approach was applied to obtain a continuous relationship between purchase cost and energy consumption. The specific formulation adopted was taken from the Oak Ridge National Laboratory Engineering-Economic Model of Residential Energy Use.[6]

## Results

Table 2 presents the results of the analysis of the aggregate implicit discount rates in the purchase of residential equipment using the life-cycle-cost methodology described above. The results are for 1978, the last year for which complete data are available. (Data on shipments, equipment usage, purchase price versus energy efficiency, and average fuel price are compiled in Ref. 2.) The aggregate implicit rates are for returns in real dollars (i.e., they should be increased by the annual inflation rate if the analysis is done in current dollars). An annual real fuel escalation rate of zero percent is assumed for all fuels. (If higher fuel escalation rates are assumed, then the results in Table 2 would increase.)

Table 2. Aggregate implicit discount rates in 1978 for existing single-family homes.[a]

| Appliance/Fuel | | Assumed lifetime (years) | %[b] |
|---|---|---|---|
| Central space heat | - Electric | 23 | 50 |
| | - Gas | 23 | 40 |
| | - Oil | 23 | 40 |
| | - Other | 23 | 60 |
| Room heaters | - Electric | 23 | 270 |
| | - Gas | 23 | 170 |
| | - Oil | 23 | 530 |
| | - Other | 23 | 280 |
| Air conditioners | - Room | 15 | 50 |
| | - Central | 12 | 10 |
| Water heater | - Electric | 13 | 160 |
| | - Gas | 13 | 450 |
| | - Oil | 13 | 60 |
| | - Other | 13 | 670 |
| Refrigerator | - Electric | 19 | 80 |
| Freezer | - Electric | 21 | 100 |
| Range/oven | - Electric | 18 | 80 |
| | - Gas | 18 | 60 |
| | - Other | 18 | 10 |
| Clothes dryer | - Electric | 18.5 | 10 |
| | - Gas | 18.5 | 30 |

[a]*Source*: DOE Consumer Product Efficiency Standards base-case data (September 1981).

[b]Values rounded to nearest 10%.

Overall, the high values of the aggregate implicit discount rates in Table 2 indicate that the average appliance or heating and cooling system purchased

does not include energy efficiency measures that yield very high returns on investment. For example, an investment of $21 in a refrigerator to include increased door insulation, a higher compressor efficiency, a double door gasket, and an anti-sweat heater switch in a refrigerator would save $22/year at 1978 fuel prices, an annual return of 100% on the investment. Yet the average refrigerator purchased in 1978 did not have these features. For those appliances with aggregate implicit discount rates higher than the 80% calculated for refrigerators (freezers, electric and gas water heaters, room heaters), efficiency measures with even greater returns were not included in the average product purchased in 1978.

It is widely believed that products purchased by parties other than the homeowner will be less energy efficient than those purchased directly. This seems reasonable because the homeowner pays the bill and thus has an incentive for investing in equipment of higher efficiency. However, the results in Table 2 do not support the perception that second-party purchasers are less willing to invest in products of higher energy efficiency. Central air conditioners are usually purchased by the homebuilder; room air conditioners, by the homeowner. The aggregate implicit discount rate for the purchase of room air conditioners is much greater than for central air conditioners. (Efficiency improvements with payback periods of 2 years are excluded from the average new room air conditioner purchased in 1978, while improvements with payoffs in about 10 years are included in the average central air conditioner.) Similar central space heating systems (generally purchased by the builder) have much lower aggregate implicit discount rates than room heaters (purchased by homeowners in most cases). The only products with unusually high discount rates that are mostly purchased by second parties are electric and gas water heaters.

That most of the products purchased by second parties (generally builders) appear to have *lower* discount rates associated with the investment in energy efficiency is a suprising finding. Most studies have assumed that the greatest incentive to invest in energy efficiency would occur when the purchaser and the person paying fuel costs were the same. However, the results presented in Table 2 are not unreasonable. The builder or contractor who purchases a central air conditioner is likely to be much more sophisticated than a homeowner who, often on a very hot or humid day, decides to buy a room air conditioner. Furthermore, the manufacturers of room and central air conditioners, knowing their respective markets, are more likely to design more efficient products for purchasers who can discriminate among different models on the basis of energy efficiency.

## PLANNED ACTIVITIES FOR FY 1983

Further analysis of these phenomena is needed to confirm or reject these hypotheses. In particular, we intend to compare more carefully the efficiencies of products sold primarily to builders with those of products sold to homeowners, to better understand the range of choices in the marketplace. Further, manufacturers might be willing to discuss some of the considerations relating to the market that strongly influence their decisions about energy efficiency of product lines. Finally, considerable information about decisions in the marketplace (including manufacturers' decisions) could be gained by applying our analysis techniques to derive aggregate implicit discount rates for room and central air conditioners and heating systems on a regional basis. The difficulty in extending the analysis in this way is that a breakdown of regional sales data by product efficiency is not available, to the best of our knowledge.

An important general conclusion of this work is that the aggregate implicit discount rate obtained by our approach is much higher than the cost of capital or the average return on investments available to homeowners (personal or business investments) for most products. (Central air conditioners appear to be a major exception to this rule in many parts of the nation.) For example, improvements in gas furnaces can yield a return of 40% per year, in real dollars. Furthermore, since the returns are in the form of a reduced fuel bill rather than higher earnings, the return is not taxed. More efficient refrigerators can yield, on average, an 80% after-tax return on investment. However, our results indicate that, in 1978, these efficiency investments were not made in most purchases.

Additional research will focus on understanding better some of the reasons for this apparent market failure. We hope to do time series studies to understand how discount rates have changed over the past decade. We are also conducting research to improve and make more sophisticated the methodology by

which the implicit discount rates are calculated. (For example, a forthcoming paper by R. Scott, M. Levine, and P. Back[3] considers such factors as demand and usage elasticities in deriving implicit discount rates.) Because we are still developing methodology and scrutinizing data, the numbers in Table 2 may change somewhat; however, we believe the general conclusions of this article are unlikely to be altered.

## REFERENCES


1. Amemiya, T. (1981), "Qualitative Response Models; A Survey," *Journal of Economic Literature, 19*, pp. 1483-1536.
2. U.S. Department of Energy, Office of Conservation and Renewable Energy (1982), *Consumer Products Efficiency Standards Economic Analysis Document,* DOE/CE-0029.
3. Scott, R.E., Levine, M.D., and Back, P. (1982), *Estimates for an Economic Model Incorporating Price and Usage Elasticity Adjustments for Consumer Decision-Making Over Energy Efficiency Options in the Purchase of New Single-Family Housing,* Lawrence Berkeley Laboratory report (in preparation).
4. Rosen, S. (1974), "Hedonic Prices and Implicit Markets: Product Differentiation in Pure Competition," *Journal of Political Economy 82* (1), pp. 34-55, January/February.
5. U.S. Department of Energy, Office of Conservation and Renewable Ennergy (1982). *Consumer Products Efficiency Standards, Economic Analysis Document*, DOE/CE-0030.
6. Hirst, E., and Carney, J. (1978). *The ORNL Engineering-Economic Model of Residential Energy Use,* Oak Ridge National Laboratory Report ORNL/CON-24.


# HEAT-PUMP ENERGY DEMAND ANALYSIS*


*J.A. Sathaye, H. Ruderman, and S. Ng*


Sales of heat pumps for heating and cooling homes have increased dramatically in the past 7 years, replacing gas, oil, and electric heaters. Growing future use of heat pumps could significantly increase the demand for electricity relative to gas and oil. Electric and gas utilities are concerned about the impact that heat pumps could have on their peak loads during summer and winter. Heat pumps can add to winter electricity loads if they replace oil or gas furnaces. They can increase summer load if the demand for air conditioning is higher. Electric utilities that have little capital may face difficulties in financing new generating plants to meet the increased demand. Some utilities, however, are encouraging the purchase of heat pumps to replace electric resistance heaters because they use less electricity. Heat pumps can also change load characteristics, thus having an impact on utility system planning.

This study will help determine changes in energy demand due to heat pumps and will provide a tool for analysis for a region or a utility-service area. In forecasting heat-pump sales and energy demand, we have adopted a unique mixed estimation approach in which traditional econometric analysis is performed along with case studies to determine the reasons for heat-pump penetration. The two approaches are then combined to arrive at demand elasticities for our residential model of energy demand. The approach can be adapted to other end-use studies in specific utility-service areas. Preliminary results were presented at the 1982 Santa Cruz conference of the American Council for an Energy Efficient Economy.[1]

## ACCOMPLISHMENTS DURING FY 1982

Our investigation of heat pumps started by examining the historical and geographical variation in market penetration. The history of heat-pump penetration (Fig. 1),[2,4] may be divided into two periods, before and after 1975. Prior to 1975, heat pumps comprised


*This work was supported by the Assistant Secretary for Conservation and Renewable Energy, Office of Building Energy Research and Development, Building Equipment Division of the U.S. Department of Energy under Contract Number DE-AC03-76SF00098.

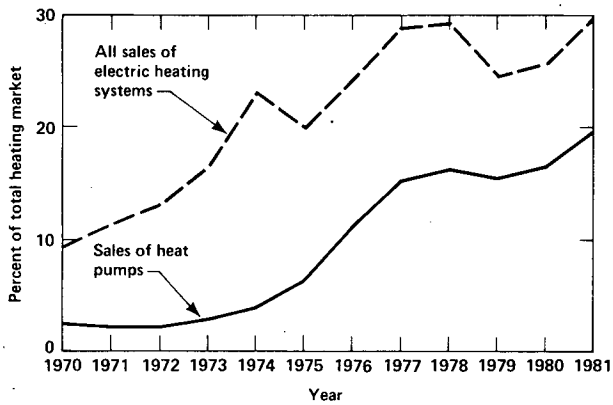


Figure 1. Sales of electric heating systems as percent of space heating market. Sources: Data for 1970-1978 are from Ref. 2; data for 1979 are from Ref. 3; and data for 1980-1981 are from Ref. 4. (XBL 824-8903)

3-5% of the total sales of central heating equipment. Sales of heat pumps increased rapidly after 1975; by 1981, they accounted for 20% of total sales. An important reason for this increase was the restriction on new natural-gas hookups that prevailed from 1976 to 1979 and still continues in some areas.

Figure 2 maps heat-pump penetration in 1979, the last year for which data are available.[5] The variation from state to state is large, ranging from little or no penetration in the Northeast and Northern Rocky Mountain states to nearly complete penetration in Arizona and South Carolina. Sales of heat pumps have been high in states with relatively high electricity prices as well as those with low prices. In most states, gas restrictions were an important factor in determining sales. However, there were some exceptions, such as Colorado. Even in Nevada and Iowa, states where natural gas has been widely used, heat-pump saturation was high. Our examination of the heat-pump sales data indicates that their penetration is not easily explainable on the basis of a few simple variables such as price or gas restrictions.

The second phase of the study was to make an economic comparison of space conditioning alternatives. During the 1970s, heat pumps were more expensive than natural gas systems on both first and life-cycle cost bases in most parts of the country. There are three important components to consider in comparing the costs of alternative systems: first costs, fuel costs, and maintenance costs. Estimates of these costs from three studies (including ours) are shown in Table 1.[6,7] The Oak Ridge National Laboratory (ORNL) study[6] concluded that in some areas of the country, such as Knoxville, the first cost and life-cycle cost of heat pumps are lower than those of natural-gas systems. Our analysis of these costs suggests that, although the equipment costs may be very different from those assumed in the other studies, the life-cycle costs of most systems fall within the uncer-

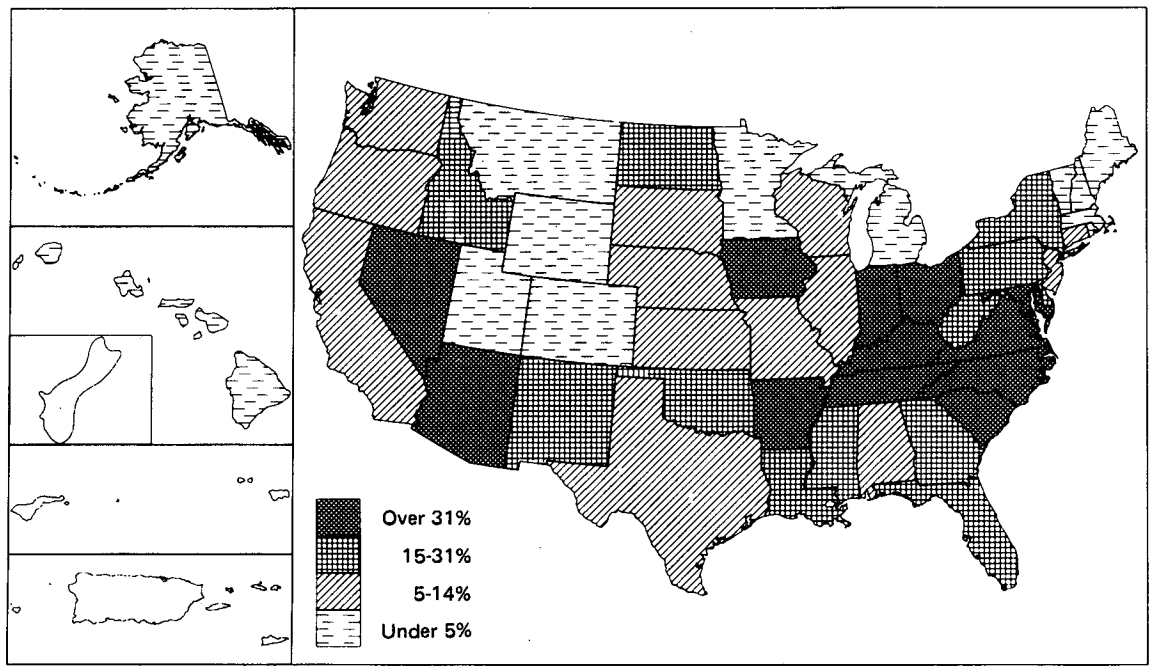


Figure 2. Heat-pump saturation in new single-family units, 1979. Source: Ref. 5. (XBL 823-8678)

tainties associated in making such comparisons. Oil systems are definitely more expensive in all three studies.

Table 1. Cost comparison of central heating and cooling equipment.

| Study | | Heat pump | Gas furnace, central A/C | Electric furnace, central A/C | Oil furnace, central A/C | central A/C |
|---|---|---|---|---|---|---|
| LBL[a] | Equipment cost | 1,640 | 1,435 | 1,179 | 1,479 | 749 |
| | Life-cycle cost | 15,302 | 14,887 | 15,583 | 21,609 | |
| ORNL[b] | Equipment cost | 1,199 | 2,024 | 1,559 | 1,969 | 1,279 |
| | Life-cycle cost | 14,861 | 15,476 | 15,963 | 22,099 | |
| AGA[c] | Equipment cost | 1,869 | 1,808 | -- | 1,919 | 1,019 |
| | Life-cycle cost | 15,531 | 15,260 | -- | 22,049 | |

Note: Life-cycle cost includes other equipment costs, installation cost, maintenance cost, and energy cost. These costs are from an ORNL report[3] and were added to the equipment cost to estimate comparable life-cycle costs for the three studies. Energy costs are based on prices in the Knoxville, Tennesee area and the following present-worth factors: electricity, 18.59; fuel oil, 25.25; natural gas, 31.17.

[a] Ref. 1.

[b] Ref. 6.

[c] American Gas Association, Ref. 7.

Our analysis of historical penetration data and the present cost of space-conditioning systems suggested that heat-pump penetration should decline after 1979, the last year with widespread restrictions on new gas hookups. However, the data indicate otherwise. By 1981, heat pump penetration had increased to 20% of all sales of central heating equipment. To understand this increase, we conducted an informal survey in several places that had high penetration in 1979. The results, summarized in Table 2, indicate that local factors are important considerations.

Another part of our approach is to construct a discrete-choice model of market penetration of space-conditioning equipment. This is an econometric model that simulates consumer decision-making when faced with mutually exclusive choices. In this study, the choice is the initial investment in the type of residential space heating and cooling system, e.g., gas furnace with central air conditioning vs. electric resistance heating with room air conditioning vs. a heat pump. The decision is assumed to depend on the initial capital and long-term operating costs of the equipment, as well as on income, family size, dwelling size, and location. The capital and operating costs depend the climate, energy prices, and thermal integrity of the structure, and on the type, efficiency, and size of the appliance.

Parameters of the model were estimated from data on newly constructed residential units between 1975 and 1979 in the Census Bureau's *Annual Housing Survey.*[8] Additional data on climate, energy prices, and natural-gas restrictions were from other sources. Numerous statistical and consistency tests were conducted to confirm the goodness of fit and the significance of the key parameters. Preliminary results on the parameters were obtained during FY 1982.

Table 2. Regional factors affecting heat-pump market penetration.

| Region | Gas permit moratorium | Cost of gas distribution | Other factors |
|---|---|---|---|
| Phoenix, AZ | Recent | High | Hook-up charges |
| Philadelphia, PA | Current | Low | Utility incentives for installation |
| Tennessee Valley | Recent | High | Utility incentives for installation |
| Iowa | Recent | High | Displacing propane heaters |
| Kentucky (except Owensboro) | Recent | High | Consumer preference, lower operating cost |
| Maryland | Recent | High | Operating cost expected to be competitive with gas |
| Southern and Central Indiana | Recent | High | Non-availability of gas |
| Cincinnati, Ohio | Recent | Low | Consumer preference, lower operating cost |
| Northeast Ohio | Recent | Low | Used as a back-up system for gas |

## PLANNED ACTIVITIES FOR FY 1983

Besides investigating the reasons for the large market penetration of heat-pump in additional regions of the country, the main emphasis during FY 1983 will be to improve and apply the discrete choice model. Results from simulations with the model will be used to calculate market share and usage elasticities for

heat-pump and other heating and cooling appliances. These elasticities will be used directly in the ORNL/LBL Residential Energy Demand Model. We are investigating the possibility of incorporating technical efficiency elasticities in the simulation. The discrete choice model will also provide estimates of implicit discount rates and project market saturation for these appliances.

To date, the ORNL/LBL Residential Energy Demand Model has treated space heating and cooling as independent end uses, linked only through common characteristics of the housing shell. The model will be substantially improved by combining these two end uses into one—space conditioning. Heat pumps will be allowed as an explicit option, where previously heat-pump saturation was buried in electric central space heating systems along with electric warm-air furnaces.

The results of the discrete-choice-model estimation will be used directly in the ORNL/LBL model. Specifically, the market share and usage elasticities will be input into the new space conditioning methodology. The result will be a more realistic and complete treatment of space conditioning system choice.

When completed, this change will provide an improved methodology for simulating future energy consumption in the residential sector, with explicit treatment of heat pumps. The treatment will better reflect the interrelationship between heating and cooling systems.

## REFERENCES


1. Sathaye, J.A., Ruderman, H., and McMahon, J. (1982), "Heat Pump Energy Demand Analysis," presented at the ACEEE Santa Cruz Conference, August 1982, Lawrence Berkeley Laboratory Report LBL-14422.
2. Fiechtel, R.B., Novicky, E.R., and Wusterbarth, A.R. (1980), *Energy Capital in the U.S. Economy,* MTSC, Inc., Bethesda, Maryland.
3. U.S. Department of Commerce, Bureau of the Census (1980), *Current Industrial Reports,* MA-35-M.
4. *Air Conditioning, Heating, and Refrigeration News* (1981), December.
5. National Association of Home Builders (1980), Survey Data, Washington, D.C.
6. Abbatiello, L.A., Nephew, E.A., and Ballou, M.L. (1981), *Performance and Economics of the ACES and Alternative Residential Heating and Air Conditioning Systems in 115 U.S. Cities,* Oak Ridge National Laboratory Report ORNL/CON-52.
7. American Gas Association (1982), *An Economic, Efficiency and Environmental Comparison of Current Home Heating and Cooling Systems,* Washington, D.C.
8. U.S. Department of Commerce, Bureau of the Census (1974-1979), *Annual Housing Survey.*


# UTILITY CONSERVATION PROGRAMS: THEORY AND PRACTICE*


*E.P. Kahn*


In this project, large-scale conservation programs sponsored by regulated utilities are examined on both a theoretical and case-study basis. Utilities have increased the scope and scale of their conservation activities substantially over the last several years. Experimental or demonstration programs have been upgraded and, in many cases, currently involve substantial expenditures. To understand long-range incentives for utilities to continue and expand these efforts, a theoretical model is employed. The model is complemented by a case study.

This research continues previous work devoted to analysis of utility programs to promote solar water-heating,[1] and consideration of the role played by current utility construction projects on the evaluation of conservation programs.[2]

## ACCOMPLISHMENTS DURING FY 1982

The principal problem facing utility planners is the pervasive uncertainty surrounding estimates of the supply and demand functions in their markets. However, conventional engineering economics of alternative projects assumes that all relevant information is known. Choices in such a framework are reduced to relatively straightforward optimization; thus risk and uncertainty play no major role in analysis. This traditional framework is not well-suited to current conditions. To address the essential problem of uncer-


*This work was supported by the Assistant Secretary for Conservation and Renewable Energy, Office of Conservation, Building Systems Division of the U.S. Department of Energy under Contract No. DE-AC03-76SF00098.

tainty, economic models developed to understand commodity price stabilization[3] are adapted to the context of regulated utilities.

## Theory

Energy prices in unregulated markets turn out to exhibit as much instability as the prices of widely traded agricultural commodities. Stabilization theory addresses the benefit to consumers and producers of reducing this instability by regulatory or investment policy. Stabilization benefits are of two kinds: (1) changes in average producer income (positive or negative), called transfer benefits; and (2) changes in producer income variations, called risk benefits. The sign and magnitude of each benefit depends upon a small number of parameters.

Because regulation has stabilized consumer prices substantially more than unregulated energy prices, any transfer benefits from further stabilization come at the expense of producers. Conservation programs tend to reduce these producer losses to some degree by increasing price elasticity. This effect is less beneficial to producers than a partial price destabilization.

Stabilization produces different risk benefits for different utility projects. Three generic projects are compared: (1) traditional regulated production, (2) utility conservation programs, and (3) unregulated supply projects. The latter promises the greatest producer benefits, although the non-traditional nature of this alternative raises questions of regulatory policy. Conservation programs compete favorably with traditional regulated production provided that their output and scale can be controlled sufficiently. If conservation programs do not have less output variability than supply projects, they are less attractive to utility shareholders.

The theoretical model is formulated at such a great level of generality that many details of practical utility conservation programs are suppressed. The case study explores such neglected dimensions.

## Case Study

The proposed conservation and load management programs of Southern California Edison Company (SCE) are analyzed in detail. Cost/benefit analysis of the SCE program indicates substantial differences between the high productivity of conservation programs and the lower value of load management. In spite of these differences, however, SCE allocates a large share of its budget to the less valuable load management activities. Table 1 characterizes the SCE program. A variety of factors explains the allocation decision.

Table 1. Total 1983 SCE proposed program—utility perspective (millions of 1983 dollars).

| Program Segment | Cost | Benefit |
|---|---|---|
| 1. Commercial & Industrial | | |
| (a) Conservation (Audit + Incentives) | 28 | 696 |
| (b) Load Management | 18 | 32 |
| Total | 46 | 728 |
| 2. Residential | | |
| (a) Conservation | | |
| (1) ZIP/CIP | 18 | 54 |
| (2) Rate Case | 17 | 58 (?) |
| (b) Load Management | 28 | 68 |
| Total | 63 | 180 |

| Total Budget Commitment | Cost | Benefit | Benefit/Cost Ratio |
|---|---|---|---|
| Complete Program | 109 | 908 | 8.3 |
| without 1a | 81 | 212 | 2.7 |
| without 1a, +2a2 fails | 81 | 154 | 1.9 |
| Total Load Management | 46 | 100 | 2.2 |
| ZIP/CIP Refrigerators | 1.5 | 23 | 15.3 |
| C & I Audits (=1a) | 28 | 696 | 24.9 |

The value of load management is in reduced future kilowatt capacity requirements. SCE uses gas turbine and oil-fired station refurbishment costs as a proxy for this value. These costs are considerably more stable than the oil costs avoided by conservation programs, the savings from which are primarily in kilowatt-hours.

Regulatory policy also favors load management. Fuel-adjustment clauses—whereby fuel price increases are automatically passed through to utility customers—reduce the incentive to save kilowatt-hours, since no earnings risk is attached to energy. Only the fixed capacity cost component of rates is related to shareholder earnings.

Other factors distinguishing the SCE program are the magnitude of incentives offered to participating customers, and the decision to expense rather than capitalize program costs.

Utility conservation programs involve potential conflicts of interest between participants and non-participants. Such conflicts are most clear when large financial incentives are offered for participation. Figure 1 shows the relationship between participant incentives (horizontal axis) and indirect benefits to non-participants for various elements of SCE's ZIP/CIP programs (standing for zero-interest and cash-incentive programs, respectively). In general, greater participant incentives mean smaller non-participant benefits. Mandatory programs such as air-conditioner cycling are necessary to keep the whole program from injuring nonparticipant interests.

Finally, the costs identified in Table 1 are revenues SCE proposed to collect without any effect on shareholder earnings. This treatment concentrates costs at the onset of the program and typically does not match the benefit stream. If SCE had a long-range interest in conservation and load management, one would expect a capitalization treatment that spread costs out over time and contributed to earnings.

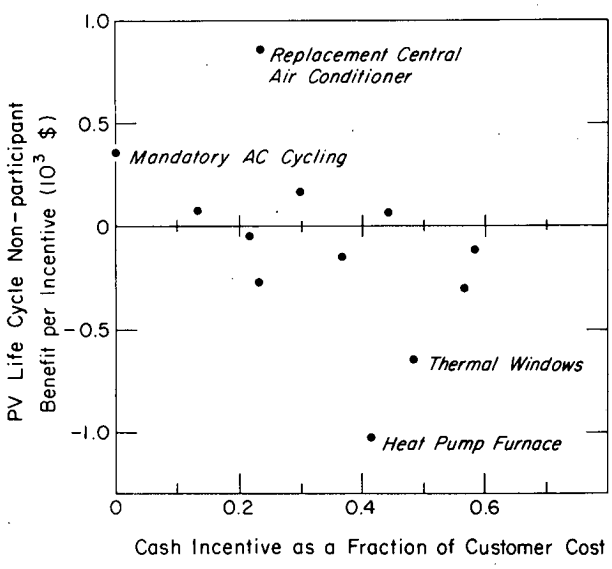


Figure 1. Participant incentives (horizontal axis) and benefits to nonparticipants (vertical axis) in Southern California Edison's ZIP/CIP (zero interest/cash-incentive) programs. (XBL 827-913)

## PLANNED ACTIVITIES FOR FY 1983

The theoretical model of utility behavior will be expanded to account for the capitalization-versus-expensing-question, and to treat the conflict of interest among various groups of consumers. Practical programs will be examined to develop evidence on the critical issue of controllability. Factors contributing to conservation output flexibility will be identified.

## REFERENCES


1. Kahn, E., Benensen, P., and Brown, B. (1981), "Commercialization of Solar Energy by Regulated Utilities," *Energy and Environment Division Annual Report 1980,* Lawrence Berkeley Laboratory Report LBL-11990.
2. Kahn, E., (1983), "Electric Utility Conservation Programs and the Decision to Abandon Partially Completed Supply Projects," *Energy: The International Journal* (in press).
3. Newbery, D., and Stiglitz, J. (1981), *The Theory of Commodity Price Stabilization.* Oxford University Press, Oxford.


# RESIDENTIAL HOURLY AND PEAK DEMAND MODEL*†


*G. Verzhbinsky, E.L. Vine, and M.D. Levine*


We have continued to develop a computer model that simulates the hourly electricity demand for electric utility service areas. This model is integrated with the Oak Ridge National Laboratory (ORNL)/ Lawrence Berkeley Laboratory (LBL) Residential Energy Demand Model. The most important new feature of the hourly demand model is that it is disaggregated to 12 end uses. This disaggregation, in addition to its extensive time-of-use and engineering/econometric data base, makes possible the evaluation of specific electric utility conservation programs and various energy conservation policies.


*This work was supported by the Assistant Secretary for Conservation and Renewable Energy, Office of Buildings and Community Development, Buildings Division of the U.S. Department of Energy under Contract No. DE-AC03-76SF00098.


†A more detailed description of this work is found in the report "LBL Residential Hourly and Peak Demand: Description and Preliminary Validation" by G. Verzhbinsky, E.L. Vine, and M.D. Levine (unpublished, 1982).

## ACCOMPLISHMENTS IN FY 1982

### Key Issues

Electric utility systems design, capacity projections, financial impacts of alternative supply and demand management strategies, rate setting, and energy conservation and load management programs are all important facets of the electric utility industry. Each raises key issues confronting electric utilities today. Many issues relating to energy conservation and load management are assuming increasing importance to utilities in the current economic climate because of the difficulty in raising capital for new power plants.

In an effort to understand these issues and to provide a quantitative evaluation of some of them, we have developed a computer model that forecasts hourly electricity demands for the residential sector. A key feature of this model is its disaggregation into each of 12 major end uses. The model is based on both econometric and engineering/economic data, as well as measured data on time of use of energy demand by end use. The high degree of detail about hourly demand by end use, combined with economic information and a specification of the average efficiency of each appliance type in the thermal integrity of the house, make possible the evaluation of the potential impact of specific energy conservation and load management activities within an electric utility service area. The model has been applied to the evaluation of the likely impacts of the proposed Building Energy Performance Standards and the Consumer Products Efficiency programs of the U.S. Department of Energy.

The residential hourly demand model is currently integrated with the ORNL/LBL Residential Energy Demand Model.[1,2] To achieve this integration, selected changes were made in the ORNL/LBL model, especially in the characterization of the thermal integrity of new houses and the addition of a utility-specific data base.[2,3] This approach of incorporating the hourly and average energy demand forecasting models takes advantage of the key features of the ORNL/LBL model: its treatment of socio-economic determinants of energy demand growth, its engineering/economic data, and its analysis of residential end-use efficiency choices. At the same time, including hourly demand data and appropriate algorithms substantially increases the analytical capabilities of the ORNL/LBL model.

### Overview of Residential Hourly Demand Model

The disaggregated residential hourly demand model was developed by LBL with the assistance of Hittman Associates, Inc. (HAI).[4] The model:

- Projects the hourly and peak electricity demand for the residential sector of an electric utility service area.
- Estimates the impact of different energy conservation policies on the hourly demand curve (load shape, including peak demand in the residential sector).
- Estimates reductions in the fuels and capacity for electric generation, by fuel type, resulting from residential energy conservation programs.

The model considers 12 end uses, divided into two groups: temperature sensitive (central space heating, room space heating, heat pumps, room air conditioning and central air conditioning) and temperature insensitive (water heating, refrigerating, freezing, cooking, clothes drying, lighting, miscellaneous). The model deals with three housing types: single-family, multi-family, and mobile homes. Also, it disaggregates the total housing stock into three groups by age of the house (and hence, by average, its thermal integrity): houses built before 1974, those built from 1974 to the present, and homes built after the start of the U.S. Department of Energy Building Energy Performance Standards program, assumed to have its initial impact in 1982. The model can handle as many as five climate zones within a utility service area. It simulates hourly electricity demand for each year from 1977 to 2005 (8760 hours each year). The total hourly demand curve is transformed into the load duration curve, which presents the number of hours where load exceeds any fixed value.

The model is part of a larger modeling effort to assess conservation impacts on utilities. This effort has the following objectives:

- Computing hourly electricity demand profiles under a wide range of economic conditions
- Evaluating and projecting hourly load profiles by climate region within a service area, by building type (single-family detached house, single-family attached house, mobile home), and by building thermal integrity
- Evaluating the likely impacts of energy conservation programs on the hourly and peak demands of an electric utility

- Quantifying the costs and benefits of energy conservation programs to the consumer
- Evaluating the effect of utility conservation programs on the cost of delivered electricity and on the financial performance of electric utilities
- Estimating the degree to which energy conservation will reduce demands for oil and gas to generate peak and intermediate electricity
- Evaluating a range of potential load management strategies to reduce peak demand in the residential sector
- Providing a quantitative basis for comparing costs and effects of investments in energy conservation programs and in increased generating capacity (including expansion of transmission and distribution systems, if required) in specific electric utility service areas.

## Input Data

The model is extremely data intensive. Estimates of time of use of each end use are the most important and most difficult data to obtain. For the five weather-dependent end uses (central space heating, room space heating, heat pump, room air conditioning, and central air conditioning), time of use is a function of temperature and humidity, as well as time of day.

To keep track of the data, we have followed the NEPOOL model[5] procedure of defining time-of-use matrices. Initial matrices of relative fraction of capacity of individual appliances in use, as a function of temperature and hour of day, are input into the model. Adjustments are applied for service area, climate zone, house type, house vintage, and day type (weekday or weekend). Specification of the hourly temperature profile permits selection of relative use values from the adjusted matrices. The final set of values is normalized to the annual demand obtained from the ORNL/LBL residential energy use demand model.

All calculations of hourly electricity demand for temperature-sensitive end uses are based on appliance-use matrices.[5] Each element of these matrices gives the fraction of the connected appliance that is operating at any specified temperature and time-of-day conditions. In other words, these matrices show the shape of hourly demand for any given hourly temperature curve.

For temperature-insensitive appliances, the corresponding appliance-use matrices do not depend on temperature conditions and house vintage but instead depend on housing type (single-family, multi-family, and mobile homes), day type (weekday/weekend), season (winter/summer), and hour of day. The load shapes for these appliances are considered to be the same for all service areas. These matrices are provided by a California Energy Commission study (1979).[6,7]

## Results

Three types of analyses have been performed using the LBL residential hourly and peak demand model: (1) comparison between diversified demand predicted by the model and aggregation of computer simulation results of undiversified hourly energy use of individual houses using the DOE-2 energy analysis model, (2) analysis of data for a test utility (Detroit Edison) to partially validate and refine the model inputs, and (3) parametric studies to evaluate impacts of energy conservation programs on the hourly load profiles of electric utilities. The first two analyses have been completed during the past year and the third is presently under way.

Figure 1 presents the comparison between the hourly model results and the energy simulations on a typical residential building in the New England area. The simulations are compared for different temperatures, ranging between 9°F and 60°F at 8 a.m. Below 27°F, the simulations on an individual house (using the DOE-2 computer code) were generally 15 to 20% higher than the diversified demand predicted by the LBL model. Above 27°F, the estimated total demands from the hourly model and from the simulation of individual houses approach each other until they are essentially identical above 40°F.

The significance of these results derives from two major differences between models: (1) DOE-2 estimates the hourly heating (and cooling) energy of a building from weather data and building characteristics. As such, it can provide estimates of undiversified residential heating energy demand. (2) The heating load inputs to the hourly model are based on interpolations and extrapolations from measured diversified demand. Thus, if both models were completely accurate, one could conclude from Fig. 1 that (1) undiversified demand appears to be about 20% higher than diversified demand at temperatures below 27°F, leading to an estimated diversity

factor of about 0.8 during cold weather in New England; and (2) at higher temperatures, where space heating is required a smaller fraction of the time, the diversity factor appears to approach 1.0. These results are probably less meaningful as a measure of the diversity factor of residential heating demand than they are as a measure of the reasonableness of the model results. Since the diversity factors and the comparison of diversified demand (from the hourly load model based on measured data) with undiversified demand (from DOE-2) are both reasonable, we conclude that the hourly model is operating in a generally acceptable manner. This is a necessary but not sufficient condition for gaining full confidence in the model results.

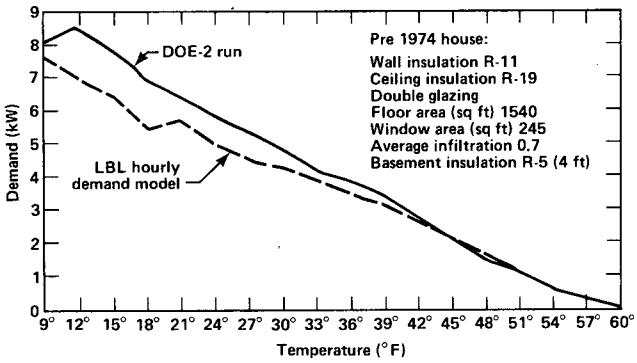


Figure 1. Hourly consumption for heating (New England, 8 a.m.) by temperature in pre-1974 single-family houses. (XBL 824-8955)

The second application of the model provides additional information on the accuracy and meaningfulness of the model results. Figure 2 shows a comparison between utility data and model estimates of residential peak demand for the period 1978 to 1982; the estimates reflect three different approaches to peak demand. In the TEMP approach, dry-bulb temperature was used to construct the room air conditioning fraction-in-use matrix. In the THI approach, the matrix was based on the temperature-humidity index. And in the diversified THI approach, these matrices were additionally adjusted by a "flattening" procedure; demand was apportioned to other hours of the day by multiplying the elements of the THI matrices that are less than 0.3 by 3, an arbitrary number. This flattening procedure is intented to simulate the diversity in hourly demands due to differences in customer behaviors.

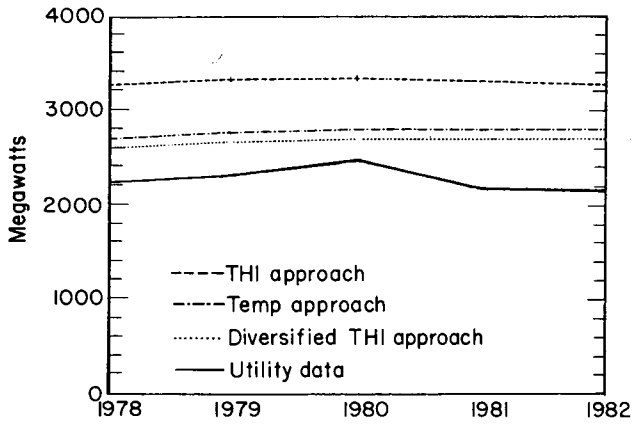


Figure 2. Residential electricity peak demand comparisons, 1978-1982. (Sources: Detroit Edison, Load Research Department, 1982; and residential hourly and peak demand model, LBL.) (XBL 831-1092)

We expect the diversified THI approach to yield the best results, as it contains the most complete and realistic data set. This is borne out by the results in Fig. 2. However, agreement between measured and predicted residential peak demand is only within about 20% for this case. At the present stage of model development, this degree of difference is not surprising. It can be accounted for by any one or more of the following:

- The utility data are low because of the methods employed by Detroit Edison to calculate residential peak load.
- The hourly weather data run on the peak load model are not suitable for detailed comparisons, since only a "typical" year was run and adjustments for the real weather conditions were not made.
- Additional improvements in the model and the data in the model are needed.

Future work will attempt to identify the sources of discrepancies between model results and utility data for Detroit Edison and other utilities, in order to refine the model.

The third area of analysis involves parametric studies to estimate the hourly and peak load impacts of residential energy conservation measures. This work is just beginning and will be pursued after additional research has been completed to improve the model.

## PLANNED ACTIVITIES FOR FY 1983

The main activities projected for FY 1983 involve:

- Completing the comparisons between utility data and model estimates
- Performing sensitivity studies on major residential energy conservation measures and programs

- Carrying out selected model improvements
- Working with utilities to begin the process of adoption of the model in the electric utility planning process
- If resources permit, initiation of research on a model of hourly demand in commercial buildings.

## REFERENCES


1. Hirst, E., and Garvey, J. (1978), *The ORNL Engineering-Economic Model of Residential Energy Use,* Oak Ridge National Laboratory Report ORNL/CON-24.
2. McMahon J.E. (1981), *Residential End Use Demand Modeling: Improvements to the ORNL Model.* Lawrence Berkeley Laboratory Report LBL-12860.
3. Herring, H., and McMahon, J.E. (1981), *Applications of the ORNL/LBL Residential Energy Demand Model to Utility Service Areas.*
4. Hittman Associates, Inc. (1980), *An Analysis of Energy Efficiency Standards on Electric Utility Peak Loads, Task 5 Final Report.*
5. NEPOOL Load Forecasting Task Force and Battelle Columbus Laboratories (1977), *Report on Model for Long-Range Forecasting of Electric Energy and Demand to the New England Power Pool,* Columbus, Ohio.
6. California Energy Commission (1979), *Technical Alterations of the Residential Sales Forecasting Model: Electricity and Natural Gas,* Sacramento, CA.
7. California Energy Commission (1979), *Technical Documentation of the Peak Load Forecasting Model,* Sacramento, CA.


# INTERNATIONAL RESEARCH

## INTERNATIONAL PROGRESS IN RESIDENTIAL ENERGY EFFICIENCY*


*L.J. Schipper, A.N. Ketoff, S.P. Meyers, S. Rosse, and W. Chern*


In 1979, the Lawrence Berkeley Laboratory (LBL) was asked by the Energy Information Administration of the Department of Energy (DOE) to gather demographic, economic, and energy data for the residential sectors of a variety of countries in the Organization for Economic Cooperation and Development (OECD). It was discovered that neither the OECD nor most of its member countries kept such statistics for the residential sector in one place. For the first two years, therefore, this work was primarily directed toward data collection.

The research focused on nine OECD countries: the United States, Canada, Denmark, France, West Germany, Italy, Japan, Sweden, and the United Kingdom. The data collected included information about incomes and expenditures, size of households and dwelling characteristics, household equipment, and actual consumption of fuels, often by purpose and dwelling type. The output of the study includes a data base covering energy use from 1960 through 1980 and several analyses of consumption patterns and their evolution, including comparisons of consumption patterns among countries and within a country over time. Finally, an econometric analysis of the energy consumption data is under way.


*This work was supported by the Assistant Secretary for Conservation and Renewable Energy, Office of Building Energy Research and Development of the U.S. Department of Energy under Contract No. DE-AC03-76SF00098.


## ACCOMPLISHMENTS IN FY 1982

### Major Factors Affecting Consumption

We examined many factors to study the determinants of energy demand, including dwelling and family size, climate, income and prices, central heating penetration, appliance size and use frequency, efficiency, habits, and "culture." Many of these are highly intertwined, so a statistical and econometric investigation was performed to estimate their importance and their correlation.

Factors such as climate and number of people per dwelling vary widely across the sample and over time. To explain some of the important differences, we stu-

died a range of *structural* indicators of energy use:

- *Energy prices and disposable income* influence the choice of systems and fuels, the marginal cost of using systems, and the economic attractiveness of conservation investments. In this study, we have examined real energy prices for each fuel, as well as for heating and non-heating, where possible. Currencies were compared using purchasing-power parities.
- *Outdoor climate,* measured in degree-days (adjusted throughout the study to the same base, 18°C) affects the amount of heat required to keep a given structure at a given indoor temperature. For each day of the heating season, the difference between the outdoor temperature and an indoor reference temperature is noted, and the sum of these over the season indicates the severity of the climate.
- *Indoor temperature* strongly affects energy demand for space heating and cooling. Differences among countries are influenced by the cost and physics of heating.
- *Dwelling characteristics* include type (detached, semi-detached, farmhouse, attached, etc.), size, vintage, and construction materials. Homes have become larger in nearly every country studied. It is worth noting that large houses have less outside surface per unit of floor area than smaller homes, which reduces heat losses per unit of floor area. This fact has certainly contributed to reductions in heating per unit area in some countries over long periods of time.
- *Demographic characteristics* such as household size, age distribution, and number of people at home during heating hours all influence energy use. Households have become smaller in every country. Smaller households mean more wall area per person, which increases heating needs per capita. On the other hand, lower density decreases per-dwelling use of cooking, hot water, and appliances, though not in proportion to the number of people. Therefore, energy intensities should be examined on both per-dwelling and per-capita bases.

## Econometric Findings

Because so many factors influence consumption, it is clear that no simple, linear form would describe residential energy use. Therefore, in our econometric study we used a multinomial logit model (a specialized statistical model for econometric analysis) to analyze aggregate residential consumption and space heating consumption as well as their fuel shares, over the 1960-1978 period. Heat was converted to "useful energy" by assuming conversion efficiencies of 45-65% for different fuels. Prices and incomes were converted to U.S. dollars, using 1970 purchasing power parities, and then deflated, using respective consumer price indices. Explanatory factors tested include climate, people per dwelling, size and type of dwellings, central heat penetration, energy prices, and incomes. Obviously, there may be multicollinearity—for example, between income and central heating penetration, between climate and central heating penetration, or between energy prices and the persistence of noncentral heat.

Currently, we are validating our model and updating calculations to 1980. Highlights of the analysis to date include the following:

1. Energy price, central heat saturation, income per dwelling, and dwelling size are all important in explaining energy use.
2. Climate, measured in heating degree-days (base 18°C) shows only weak explanatory power for total energy, but was far more important for heating.
3. The economic and structural variables explain most of the variations in energy use per dwelling, but the European countries still exhibit consumption that is lower than is explained by the model.
4. Fuel shares for heating depend on price, but at the same time, increased incomes led to the use of less solid fuels, an increase in the use of oil, and a growth in electricity relative to oil use.
5. Our results gave lower aggregate price elasticity (−0.2 for total demand, −0.3 for space heating) and income elasticity (+0.3 for total demand, +0.4 for space heating) than most other studies we reviewed. These results may be interpreted as both long-term, because of the cross-sectional nature of our

study, or as short- to mid-term, because of its time-series nature. Long-term effects cause changes in fuel, equipment, and weatherization; short-term effects mean reductions in heating, hot-water, and appliance use.

## Conclusions of OECD Study

- Increases in equipment ownership (central heat, running hot water, and major appliances), driven by higher incomes, were responsible for the great increases (4-8%/annum) in residential energy use through 1973 and for the sustained growth rates that continued through the late 1970s, although after 1973 these growth rates slowed considerably relative to income growth. Increased equipment penetration absorbed some of the gains from conservation between 1973 and 1978.
- Great variations in equipment ownership, lifestyle, and energy intensity occur even at roughly similar income levels. Differences in prices, climate, housing stocks, heating, bathing and cooking habits, and engineering efficiency account for these variations, but in differing proportions.
- Increased energy prices since 1973 have induced reductions in energy-use intensities and have more recently caused shifts away from oil heating systems where alternatives existed. Heating energy use has been reduced considerably in centrally-heated homes since 1972.

When all factors are counted, there are still significant differences in efficiency of heating and appliance systems among countries. The best techniques used in one country may allow significant energy savings through their introduction elsewhere. Information programs have probably played an important role in informing consumers of options for conserving energy. Energy conservation programs have promoted investments in energy-saving equipment that otherwise might not have been undertaken. Still, the effects of these programs on total energy saved appear to be less than the short-term actions taken by consumers in response to higher prices or other motivating factors.

*Cross-Country Differences*

A major portion of the variability in energy use can be explained by prices, incomes, climate, etc., but a residual fraction that is not accounted for by the model still remains. Other countries use less energy per dwelling, adjusted for climates, than the United States as shown in Fig. 1. When the heating component of energy use is examined separately, and each country's consumption is divided by the number of degree-days (Fig. 2), the United States still consumes more energy than the other countries, though the difference is due in part to the larger size of U.S. housing. Stock vintage, building codes, and government housing policies may play a role here. The Japanese space-heating data contain a large residual fraction that we believe is accounted for by lifestyle and culture. Finally, the growth in the structural component continued after the oil embargo, largely obscuring the real conservation achievements.

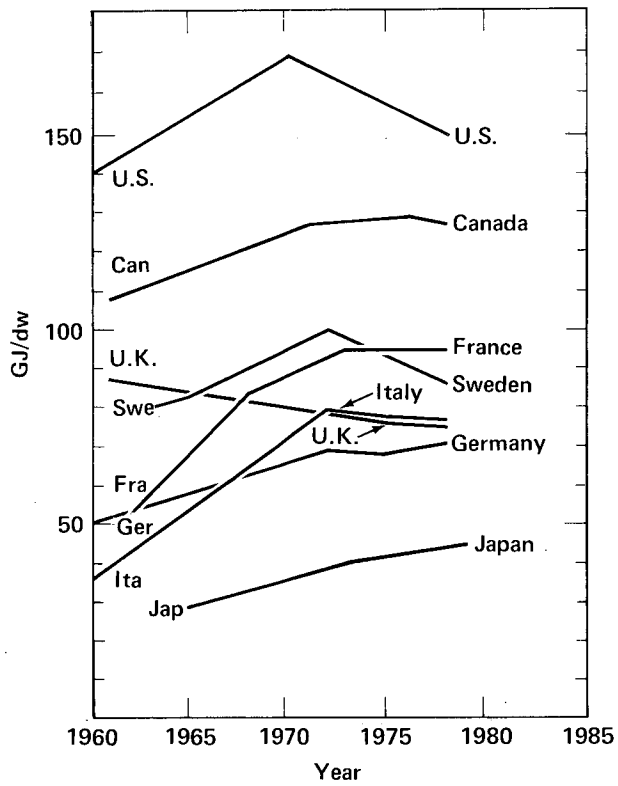


Figure 1. Energy consumed per dwelling (heat adjusted at U.S. climate). (XBL 824-8882)

*Conservation*

All countries showed a decrease in the growth rate of energy use after the 1973–74 oil shock, but some of the decrease was only temporary. Most showed

more permanent decreases in heating energy use during the period between 1978 and 1980. Higher prices have primarily brought on low-cost conservation measures such as additional insulation or lower indoor temperatures, and incremental improvements in new systems.

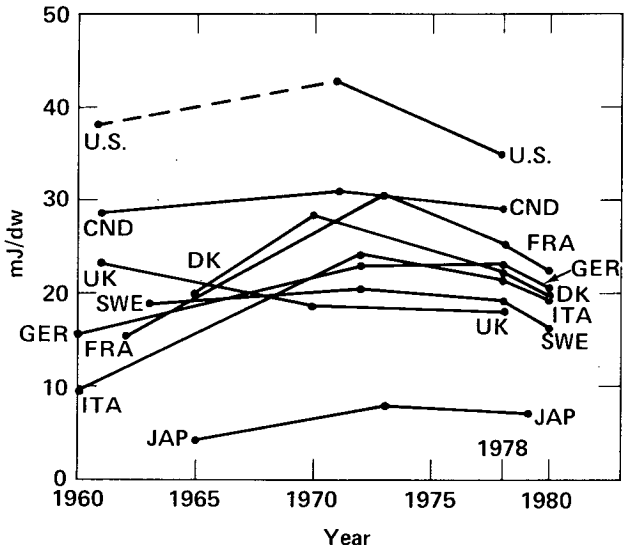


Figure 2. Space heating energy use per degree-day. (XBL 824-8893)

*District Heating*

District heating—heat piped to many buildings from a central system—is rapidly approaching saturation in Sweden and Denmark in multi-family dwellings; its cost savings, however, are questionable, particularly in single-family dwellings. In new multi-family dwellings in the densest areas, and in older, leaky multi-family dwellings, there is still a small advantage. Much lower penetration occurred in Germany and France. Although district heating often recycles "waste heat," it should not be seen as "free"; only a fraction of the heat delivered is really "waste heat" that would otherwise have been lost. For most of the United States, it appears that weatherization and tightening will save far more energy at less cost than district heat.

*Electric Heating*

Electric heating received a boost from the 1973–74 oil-supply disruption, as its share in new homes (principally single-family dwellings) and in conversions from non-central heating increased. However, it fell back somewhat as gas advanced. In 1979, gas gained most from oil price increases. Therefore, electric heating's competition with gas is crucial. In Sweden, where gas is non-existent and electricity is as cheap as oil, electricity has made significant gains.

Comparisons with gas- and oil-fueled homes for purposes of estimating relative economics are difficult. The best data we have (from Sweden) show that for homes of the same kind (SFD), of the same vintage, and in similar climate regions, the consumption of oil per unit area is 1.6–2.1 times greater than that of electricity, measured at the building boundary, for central or baseboard heat and hot water. This difference is smaller than others have claimed.

Increasing penetration of electric heating is occurring primarily in Sweden and Canada, where prices are lowest and are close to parity with oil. Homes in Sweden, however, are so tight that the cost difference between electricity and oil would be minimal, and either fuel is less costly than district heat for single-family dwellings. Heat pumps have had some success in Sweden and Germany, but their greatest penetration has been in the U.S.

*Policy*

Market forces are necessary for improved energy efficiency, but not sufficient for complete adjustment to higher costs. In virtually every country, consumers are willing to make simple investments but need help to make larger long-term investments. Renters always fare worse than owners. Government research, demonstration, and direct support are important for the development and testing of new ideas and major products. Demonstration and testing of components in whole houses are important research areas.

Governments have an important role in sponsoring research and development in long-term conservation investments as well as in encouraging construction practices that would result in far better building shells. Codes affecting building practices in Sweden, Denmark, and France appear to have been effective in stimulating technological advances resulting in improved building shells. Standards appear to have been most significant in Denmark; in Sweden, they are tighter, but building practices at the time of implementation were closer to what the codes called for. Ultimately, however, the Swedish standard will result in significantly tighter homes, and will demand more of homes heated with electric-resistance heating. In addition, the southern areas of Sweden, which

had the least demanding codes, are now following the stricter requirements of the north.

## U.S. Residential Energy Use and Conservation

The National Interim Energy Consumption Survey (NIECS) conducted by the Energy Information Administration provided the opportunity to estimate residential energy use in the United States by energy source and end use from comprehensive household and utility survey data. By carefully comparing groups of households for equipment ownership and factors affecting energy consumption for particular uses, it was possible to estimate average household energy consumption for the main end uses (Table 1). Using these averages and data from the Annual Housing Survey on equipment ownership, a portrait of residential energy use was assembled (Fig. 3).

Table 1. Average household energy consumption by end-use and fuel, April 1978 - March 1979 (in gigajoules).

| | Gas | Oil | Electricity | LPG |
|---|---|---|---|---|
| Space heating | 95 | 127 | 35 | 65 |
| Water heating | 26 | 38 | 14 | 17 |
| Cooking | 10 | - | [a] | 9 |
| Air-conditioning | - | - | 9 | - |
| Other appliances | - | - | 16 | - |

[a]Average electricity consumption for cooking could not be accurately derived by the method used in this study.

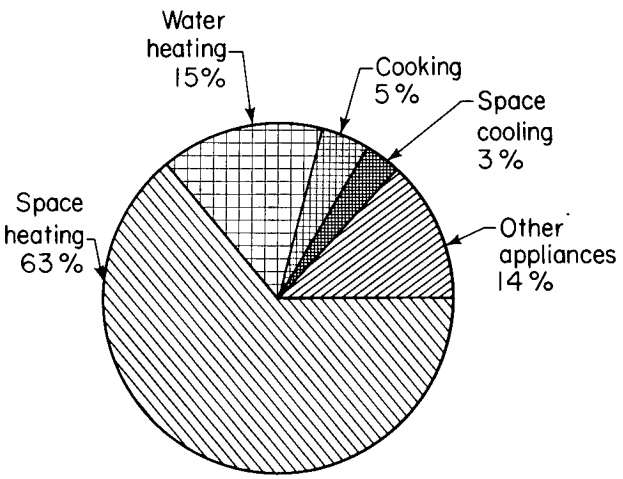


Figure 3. U.S. residential energy use, 1978-1979 (site energy). (XBL 831-1078)

Space heating is by far the most important residential energy end-use. Statistics indicating the average intensity of oil, gas, and electricity use were developed both for all households and for households in single-family structures (which constitute two-thirds of the U.S. housing stock). As can be seen in Table 2, after accounting for climate and dwelling size (estimated from NIECS data), oil and gas in single-family structures have roughly the same energy intensity, and it is about twice that of electricity (measured as site energy). This difference is attributable to furnace losses with oil and gas, the higher level of insulation in electrically heated homes, climatic factors other than temperature (i.e., solar gains), and, perhaps, differences in heating habits.

Table 2. Average energy consumption for space heating in single-family[a] structures.

| | Oil | Gas | Electricity |
|---|---|---|---|
| Single-family (GJ) | 124 | 109 | 46 |
| per C-degree-day (MJ) | 43.0 | 39.1 | 20.6 |
| per C-degree-day and per square meter (KJ) | 270 | 268 | 129 |

[a]Single refers to households in detached and attached structures.

The decline in average energy residential use from 142 million Btu per household in 1973 to 117 million Btu in 1980 (site energy, excluding wood) indicates that decreases in the energy intensity of various end uses have occurred. Part of this decline is due to the increasing penetration of electricity in space heating (from 10% of all households in 1973 to 18% in 1980), since electricity is roughly twice as efficient in terms of site energy as oil or gas. Part is due to the increased use of wood, particularly since 1979. Such factors make interpretation of changes in aggregate energy use difficult. Reliable data on changes in energy intensity for particular energy sources and end uses are unfortunately scarce. The best indicator of energy conservation is gas space heating: average consumption per degree-day fell 16% from 1970 to 1978, and has fallen further since then. An even greater drop, probably in the range of 25-30%, has occurred in oil space heating. With respect to other end uses, assessment of changes in energy intensity is difficult, though it seems clear that the stock of appliances is more efficient in 1980 than in 1973.

## PLANNED ACTIVITIES FOR FY 1983

Activities planned for FY 1983 include completing the econometric analysis of residential energy use, using 1980 data, and beginning an investigation of commercial-sector energy use in the OECD countries.

This report was done with support from the Department of Energy. Any conclusions or opinions expressed in this report represent solely those of the author(s) and not necessarily those of The Regents of the University of California, the Lawrence Berkeley Laboratory or the Department of Energy.

Reference to a company or product name does not imply approval or recommendation of the product by the University of California or the U.S. Department of Energy to the exclusion of others that may be suitable.

TECHNICAL INFORMATION DEPARTMENT
LAWRENCE BERKELEY LABORATORY
UNIVERSITY OF CALIFORNIA
BERKELEY, CALIFORNIA 94720